HE 20.3160: 60/12

cancer treatment reports

RECEIVED
MIAMI UNIVERSITY
LIBRARIES
MAY -9 1977
DEPOSITORY
DOCUMENTS DEPARTMENT

Proceedings of the Symposium on Cell Kinetics and Cancer Chemotherapy

Subject and Author Indexes: 1976

Volume 60
Number 12
December 1976
Pages 1697-2021

U.S. DEPARTMENT OF HEALTH, EDUCATION, AND WELFARE
Public Health Service National Institutes of Health

cancer treatment reports

National Cancer Institute, Frank J. Rauscher, Jr., *Director*

Division of Cancer Treatment, Vincent T. DeVita, Jr., *Director*

Editorial Board

Bruce A. Chabner, *Editor-in-Chief*
Associate Editors:
David A. Cooney
David G. Johns
John S. Macdonald
Stephen C. Schimpff
Susan M. Sieber
John M. Venditti
John L. Ziegler

Editorial Staff

Pamela W. Hutchins, *Managing Editor*
Jean M. Griffin, *Assistant Editor*
Editorial Assistants:
Virginia T. Ascosi
Elaine P. Beck

Advisory Board

Bernard Fisher
Emil J Freireich
Lewis W. Guiss
Simon Kramer
Faith H. Kung
LaSalle D. Leffall, Jr.
John A. Montgomery
David G. Nathan
Paul E. Neiman
Stanley E. Order
Theodore L. Phillips
Philip Rubin
Edward F. Scanlon
Samuel Silverman
Joseph V. Simone

RECEIVED
MIAMI UNIVERSITY
LIBRARIES
MAY - 9 1977
DEPOSITORY
DOCUMENTS DEPARTMENT

Editorial Policy

The Editorial Board will consider manuscripts dealing with all aspects of preclinical and clinical cancer treatment. These may include such topics as surgery, radiotherapy, chemotherapy, immunotherapy, supportive care, pharmacology, cell biology and kinetics, mechanisms of drug action, and medicinal chemistry.

The journal will consist of two parts. One part will consider previously unpublished manuscripts of original work under four main categories:

1. Clinical or preclinical research.
2. Correspondence regarding manuscripts previously published in *Cancer Treatment Reports.* Letters on other topics will be published at the discretion of the Editorial Board.
3. Invited guest editorials and reviews. Unsolicited contributions will be considered on their individual merits.
4. Brief communications. Under this category the Editorial Board will consider short contributions which should not exceed five typewritten pages. Four types of communication will be considered in this category.
   (a) Ideas relating to cancer treatment.
   (b) Preliminary research reports.
   (c) Clinical case reports.
   (d) Brief clinical trials of novel treatments.

All material submitted for consideration in the journal will be subject to review when appropriate by at least two outside reviewers and one member of the Editorial Board. The decision to publish a manuscript is solely the responsibility of the Editorial Board.

The second part of this journal will consist of supplements (published bimonthly) which may include proceedings of meetings and symposia and program information from the Division of Cancer Treatment, National Cancer Institute. Requests to publish information in *Cancer Treatment Reports* supplement will be considered by the Editorial Board.

INSTRUCTIONS TO AUTHORS

Summary
Begin the article with a short summary.

Text
Submit an original and three copies of the manuscript, typed double spaced. Each page should begin with a new paragraph. Use accepted spelling, abbreviation, and hyphenation found in *Webster's New International Dictionary*. Footnotes should be typed at the bottom of the page on which they appear.

Tables
Submit each table on a separate page, typed double spaced. Please use standard abbreviations; otherwise spell out.

References
Submit references typed double spaced. Follow the standard form of *Index Medicus:* author, title, name of journal, volume number, page or inclusive pages, and year. In book references give author, title of book, edition (if more than one), city, name of publisher, date of book, volume number, and pages cited. References in text should begin with number 1 and continue consecutively. References to papers presented at meetings should include author; title of paper; title, city, and date of meeting; city and name of publisher; date of publication; volume number; and pages. Papers presented at meetings but not published should be cited in a footnote rather than in the reference section.

Illustrations
Photographs and graphs preferably should be clear, glossy prints. Original art work should be done in black ink for good reproduction. Please send 2 copies of each print.

Nomenclature
Names of compounds should conform to American usage. See *Chemical Abstracts* for proper nomenclature.

Abbreviations
Only standard abbreviations are acceptable. If a new or coined abbreviation is used, it must be defined when first mentioned.

Brief Reports
Manuscripts published in the Brief Reports section can be no longer than 5 double-spaced pages including references and tables. Summaries and figures are usually omitted.

Symposia
Requests to publish the proceedings of symposia should be addressed to the Managing Editor. A copy of the agenda and a list of speakers should accompany such requests.

Submission of Manuscripts
Manuscripts and all inquiries concerning the status of manuscripts should be addressed to: Managing Editor, Cancer Treatment Reports, National Cancer Institute, 8300 Colesville Rd, Rm 3A05, Blair Bldg, Silver Spring Md 20910. We invite all authors to submit with their manuscripts a short list of possible reviewers. The editorial board will take these names into consideration in selecting those who will be asked to evaluate your manuscript.

Reprints
Supplied free of charge: 250 reprints will be sent to the senior author about three weeks after publication of the article.

SUBSCRIPTIONS

Cancer Treatment Reports is for sale by the Superintendent of Documents, US Government Printing Office, Washington, DC 20402. The yearly subscription rate is $38.35 domestic, with an additional $9.60 for foreign mailing. The prices vary for individual issues. Payment is required in advance; check or money order should be made payable to the Superintendent of Documents. Please specify List ID "CAN" (the identifying code for this journal) when requesting a subscription.

Contents

Cancer Treatment Reports
Vol. 60, No. 12
December 1976

Proceedings of the Symposium on Cell Kinetics and Cancer Chemotherapy (Annapolis, Maryland, November 4–6, 1975)

Page

Introduction 1697
Stanley E. Shackney
National Cancer Institute, Bethesda, Maryland

Cell Kinetics and Cancer Therapy: History, Present Status, and Challenges 1699
Seymour Perry
National Institutes of Health, Bethesda, Maryland

Session I: Population Age-Dependent Responses to Therapy—In Vitro

Introduction 1705
George M. Hahn
Stanford University School of Medicine, California

Age-Dependent Survival and Cell-Cycle Progression of Cultured Cells Exposed to Chemotherapeutic Drugs 1707
Benjamin Drewinko and Barthel Barlogie
University of Texas System Cancer Center, M. D. Anderson Hospital and Tumor Institute, Houston

Comparative Chemosensitivity of Exponential- Versus Plateau-Phase Cells in Both In Vitro and In Vivo Model Systems 1719
P. R. Twentyman
Clinical Oncology and Radiotherapeutics Unit, The Medical School, Cambridge, England

Computer Simulation of Leukemia Therapy: Combined Pharmacokinetics, Intracellular Enzyme Kinetics, and Cell Kinetics of the Treatment of L1210 Leukemia by Cytosine Arabinoside 1723
T. Lincoln, P. Morrison, J. Aroesty, and G. Carter
The Rand Corporation, Santa Monica, California

Session II: Population Age-Dependent Responses to Therapy—In Vivo

Introduction 1741
L. F. Lamerton
Institute of Cancer Research, Surrey, England

Page

Size Dependence of the Response of Lewis Lung Tumors to BCNU 1743
G. Gordon Steel, Kay Adams, and Judith Stanley
Institute of Cancer Research, Surrey, England

Effects of Surgery on the Cell Kinetics of Residual Tumor 1749
Linda Simpson-Herren, Audrey H. Sanford, and James P. Holmquist
Southern Research Institute, Birmingham, Alabama

Proliferative Character and Growth Modes of Neoplastic Disease as Determinants of Chemotherapeutic Efficacy 1761
Larry L. Schenken
Allegheny General Hospital, Pittsburgh, Pennsylvania

Session III: Drug Lethality and Sublethal Damage

Introduction: Cytotoxic Damage and Repair 1777
M. M. Elkind
Division of Biological and Medical Research, Argonne National Laboratory, Illinois

Effects of Tumor Bearing on the Dynamics of Host Hemopoietic Cells 1781
P. K. Lala
McGill University, Montreal, Canada

Recovery of Cells From Induced, Potentially Lethal Damage 1791
George M. Hahn
Stanford University School of Medicine, California

In Vitro Responses of Mammalian Cells to Drug-Induced Potentially Lethal and Sublethal Damage 1799
S. C. Barranco
University of Texas Medical Branch, Galveston

Session IV: Recruitment and Synchrony—In Vitro

Introduction 1811
Renato Baserga
Temple University Health Sciences Center, Philadelphia, Pennsylvania

Use of Cell-Cycle Information in the Preparation of Drug Combinations: Results With Cytosine Arabinoside Plus Actinomycin D 1813
B. K. Bhuyan, T. J. Fraser, and K. J. Day
The Upjohn Company, Kalamazoo, Michigan

Physical-Chemical Characterization of Living Cells by Laser-Flow Microfluorometry 1819
C. Nicolini, F. Kendall, C. Desaive, R. Baserga, B. Clarkson, and J. Fried
Temple University Health Science Center, Philadelphia, Pennsylvania

Arrested and Cycling CHO Cells as a Kinetic Model: Studies With Adriamycin 1829
Robert A. Tobey, Harry A. Crissman, and Melvin S. Oka
Los Alamos Scientific Laboratory, University of California, New Mexico

Session V: Recruitment and Synchrony—In Vivo

Page

Introduction 1839
Sven-Aage Killmann
University Hospital of Copenhagen, Denmark

Evidence for Recruitment and Synchronization in Leukemia and Solid Tumors 1841
Alvin M. Mauer, Sharon B. Murphy, and F. Ann Hayes
St. Jude Children's Research Hospital, Memphis, Tennessee

Synchronization With Phase-Specific Agents in Leukemia and Correlation With Clinical Response to Chemotherapy 1845
William R. Vogler, William B. Kremer, William H. Knospe, George A. Omura, and Karl Tornyos
Emory University School of Medicine, Atlanta, Georgia

Resting Cells in L1210 and JB-1 Ascites Tumors With Special Emphasis on Recycling 1861
N. R. Hartmann, P. Dombernowsky, and P. Bichel
Finsen Institute, Copenhagen, Denmark

Session VI: Status of Human Tumor Cell Kinetics

Introduction 1871
E. P. Cronkite
Brookhaven National Laboratory, Upton, New York

Role of Radioautographic Studies in Clinical Investigative Oncology and Chemotherapy 1873
Stanley E. Shackney
National Cancer Institute, Bethesda, Maryland

Comparison of Cell Proliferation Kinetics in Human and Experimental Tumors: Response to Irradiation 1887
M. Tubiana and E. Malaise
Institut Gustave-Roussy, Villejuif, France

Session VII: Drug Scheduling—Experimental Studies

Introduction 1897
L. M. van Putten
Radiobiological Institute TNO, Rijswijk, The Netherlands

Mathematic Models of Cell Synchrony and Drug Scheduling 1899
A.-j. Valleron
Institut Gustave-Roussy, Villejuif, France

Page

Rapid Methods for Utilizing Cell Kinetics for Treatment in the C3H/He Spontaneous Mammary Tumor: Effects of Vincristine 1913
Lewis M. Schiffer, Paul G. Braunschweiger, and Lawrence Poulakos
Allegheny General Hospital, Pittsburgh, Pennsylvania

Combined Effect of Cytosine Arabinoside and Thiopurines 1925
Fred Valeriote, Teresa Vietti, and Mark Edelstein
Washington University School of Medicine, St. Louis, Missouri

Session VIII: Drug Scheduling—Clinical Studies

Introduction 1935
Emil Frei
Sidney Farber Cancer Center, Boston, Massachusetts

Kinetic Response of Human Leukemic and Lymphoma Cells In Vivo to Combination Chemotherapy Using Flow Microfluorometry 1937
Jerrold Fried, Zalmen Arlin, Agnes Alikpala, Charlotte T. C. Tan, and Bayard Clarkson
Memorial Sloan-Kettering Cancer Center, New York

Kinetic Aids to Proper Chemotherapeutic Scheduling: Labeled Nucleoside Incorporation Studies In Vivo 1947
Robert C. Young
National Cancer Institute, Bethesda, Maryland

Investigations on Pharmacologic Induction of Partial Synchronization of Tumor Cell Proliferation: Its Relevance for Cytostatic Therapy 1959
H. O. Klein, D. Adler, M. Doering, P. J. Klein, and K. J. Lennartz
University of Cologne, West Germany

Abstracts: Flow Microfluorometry Workshop

In Vivo Effects of Cyclophosphamide and Adriamycin on Mouse Tumor Cell Cycle Parameters Using Flow Microfluorometry Analysis 1981
David S. Alberts and Joe Gray

Perturbation of Cell Cycle Progression With Melphalan In Vitro 1981
B. Barlogie and B. Drewinko

Determination of Sensitivity and Resistance of L1210 Leukemia to Cytosine Arabinoside, In Vivo, Using Flow Microfluorometric Cell-Cycle Analysis 1981
Oliver Alabaster and Bill Bunnag

Flow Microfluorometric Determinations of DNA, Protein, and Cell Volume: Analysis of Tumor Cell Kinetics 1982
H. A. Crissman, P. L. Wanek, and J. A. Steinkamp

Page

Study of In Vivo Tumor State and Response to Therapy by Analysis of DNA Distribution 1982
Yosh Maruyama, M. R. Raju, Elvira Bain, and James H. Jett

Dissociation of Mammary Tumors and the Characterization of Cells by Electronic Volume Analysis, Velocity Sedimentation, Density Gradients, Morphology, and Chemotherapy 1982
R. M. Zucker, J. Harari, J. Finley, and J. Noel

Quantitative Comparison of Measurements With Different Fluorochromes of DNA 1983
Walfried A. Linden and Heinz Baisch

Evaluation of Two-Parameter Pulse-Cytophotometric Data From Cells Stained With DNA- and Protein-Specific Dyes 1983
Heinz Baisch

Flow-Microfluorometric Analysis of Nuclei Isolated From Brain and Brain Tumors 1984
T. Hoshino, K. T. Wheeler, J. W. Gray, and K. Nomura

Cell Cycle Studies of Isoproterenol-Stimulated Transplantable Salivary Gland Carcinoma of the BALB/c Mouse 1984
W. E. Delaney, I. R. Toth, P. Basuk, E. C. Wu, D. Lehane, and P. J. McKenna

Differential Effects of Chemotherapeutic Agents on Labeling Index, Incorporation of Radiolabeled DNA-Precursors, and Colony Formation of Human Lymphoma Cells 1984
Pamela Roper

Double-Emulsion Autoradiography for Analysis of a Possible G_0 Phase in Rat Epidermis 1985
Fredric J. Burns

Thymidine Incorporation During Aging of Normal Human Diploid Cell Cultures: Quantitative Autoradiographic Analysis Using Scanning Microdensitometry 1985
G. L. Grove, E. D. Kress, and V. J. Cristofalo

Studies on the Kinetics of "Nonproliferating" Cells in Solid Tumors Aided by Autoradiography 1985
Milan Potmesil and Anna Goldfeder

Semi-Automated Cell and Grain Counting 1986
P. A. Bunn, S. S. Ford, and S. E. Shackney

Lymphocyte PHA and PPD Stimulation as an In Vitro Model for Recruitment: Proliferation Kinetics of the System 1986
J. L. Bernheim, R. Dorian, M. Djobadze, and J. Mendelsohn

	Page
Subject Index: Volume 60	1989
Author Index: Volume 60	2009
Reviewers: 1976	2017

The Secretary of Health, Education, and Welfare has determined that the publication of this periodical is necessary in the transaction of the public business required by law of this Department. Use of funds for printing this periodical has been approved by the Director of the Office of Management and Budget through November 30, 1976.

Proceedings of the Symposium on Cell Kinetics and Cancer Chemotherapy

Division of Cancer Treatment
National Cancer Institute

Editor: Stanley E. Shackney

November 4–6, 1975
Annapolis, Maryland

Introduction

The purpose of this conference is to bring together the clinician, the experimentalist, and the mathematician in order to focus on the role of cell kinetics in cancer chemotherapy. Cell kinetics represents many things to many people. At the outset, it might be worthwhile to establish what we mean by cell kinetics. Some think of cell kinetics as the measurement of the durations of the phases of the cell cycle. Others consider cell kinetics to be synonymous with certain techniques, such as tritiated thymidine studies or stem cell assay studies. I would like to suggest that we consider cell kinetics not as a set of measurements and not as a technique or group of techniques, but as a scientific field which concerns itself with the quantitative aspects of the growth behavior of proliferating cell populations and their responses to perturbation by chemical and physical agents.

Given this definition, I think we would agree that the field of cell kinetics should, and undoubtedly will, play an important role in the development of a rational, scientifically grounded approach to cancer therapy. We know that there are kinetic differences between human tumor cell populations and critical normal host tissues. It is not too much to hope that some day we will learn to exploit these differences therapeutically in a systematic fashion.

The problems involved are formidable ones both on conceptual and technical grounds, and the search for their solution must always be associated with ongoing patient care of the highest standards. It would seem that there is much to be gained from developing strong interdisciplinary ties among clinicians, experimentalists, and mathematicians in order to mount an integrated effort to achieve the goal of cancer therapy optimization.

Stanley E. Shackney

Cell Kinetics and Cancer Therapy: History, Present Status, and Challenges

Seymour Perry [1,*]

In assessing the state-of-the-art in any area of research it is of interest to look back and determine the progress achieved and what has been learned, but it is also essential, for purposes of perspective, that we look ahead; we must decide on our goals, what new technology needs to be developed, and what new knowledge must be acquired. This will by no means be a comprehensive review, but only a citation of a few of the highlights in cell kinetics through the years.

The earliest study in cell kinetics of which I am aware was in 1925 by Minot and Isaacs (1) who reported the transfusion of blood from a patient with chronic lymphocytic leukemia and a high wbc count into a patient with lymphosarcoma and a normal peripheral blood count. The next 20 years saw frequent reports of studies which utilized the technique of cross-circulation. A typical example was the study by Lawrence and co-workers (2) who cross-circulated the blood from an irradiated leukopenic cat into a normal cat. They observed a survival time of 16–24 hours for the cross-circulated leukocytes in the blood of the irradiated animals. In 1933, an important observation was made by Yoffey (3) who found that in dogs there were two to three times as many lymphocytes entering the blood daily from the thoracic duct as were present in the blood, suggesting that lymphocyte survival in the vascular tree was only a few hours. Through the years, these studies led many others to examine the question of lymphocyte recirculation. The early attempts to determine leukocyte intravascular survival times were followed by studies utilizing supravital stains or natural markers so that transfused cells could be distinguished in the circulation of a recipient. White (4) and Lissac et al (5) transfused wbcs labeled with quinacrine and monitored the presence of labeled cells by their fluorescence. Brecher and Peden (6) took advantage of a natural marker by transfusing rat granulocytes, which contain alkaline phosphatase, into mice whose granulocytes are devoid of this material.

At about this time radioisotopic labels were introduced and shortly thereafter Ottesen (7) reported the use of ^{32}P in the study of leukocyte kinetics in animals, and in 1952 Kline and Cliffton (8) reported the use of ^{32}P to study leukocyte kinetics in man. They concluded that leukocytes were confined to the bone marrow for 4 days and were then released into the circulation where the majority remain for about 9 days. Ottesen (9,10) was able to separate granulocytes and lymphocytes and estimated that the mean age of the granulocytes in the blood was approximately 9 days with most of the cells entering the circulation at 6 days. He described two groups of lymphocytes, one group with a mean age of 3–4 days and the other with a mean age of 100–200 days. Craddock et al (11) and Perry and co-workers (12,13) using ^{32}P, leukapheresis, and bacterial endotoxin for granulocyte mobilization developed the concept of the bone marrow reserve. This group also made significant observations in lymphocyte kinetics (14) which amplified the studies reported by Yoffey 2 decades earlier. At about this time, Howard and Pelc (15) first demonstrated, by autoradiographic methods, the various phases of the cell cycle, which has remained a very important concept in cell kinetics.

The introduction of tritiated thymidine in 1955 and its utilization by the group at Brookhaven under Cronkite ushered in a new era in cell kinetics (16–19). Here was a material that was nonexchangeable, provided essentially a pulse label, and because autoradiography could be employed, permitted a qualitative and quantitative assessment in cell kinetics hitherto impossible. Several laboratories in addition to the one at Brookhaven obtained important data on leukocyte kinetics in acute and chronic leukemias, including the demonstration that leukemic cells recycled from the spleen (20–26). Quastler and Sherman (27) made a classic contribution to kinetic analysis by proposing the labeled-mitosis method for the determination of the cell-cycle time.[2]

[1] Office of the Director, National Institutes of Health (NIH), Bethesda, Md.

Reprint requests to: Seymour Perry, MD, OD, Bldg 1, Rm 111, NIH, Bethesda, Md 20014.

[2] Note should be made of a recent report (Shackney SE. The radioautographic transfer function and its implications for radioautographic methodology. *J Natl Cancer Inst* 55:811–820, 1975), which raises serious questions concerning interpretation of the percent-labeled mitosis curve. The observations indicate that the shape of the curve depends on the counting threshold and relative exposure and hence it appears that interpretation of any given curve may be complicated.

Gavosto et al (28,29) and Astaldi (30) dispelled the early hypothesis that leukemic cells were in unrestrained proliferation, established the concept of a block in maturation, and provided evidence for heterogeneity of leukemic cell populations, ie, a proliferating pool of large cells and a nonproliferating compartment of smaller cells. Baserga and Kisieleski (31) and others obtained data revealing that cell-cycle times of tumor cells were often of longer duration compared to their normal counterparts. Lajtha and Oliver (32) proposed the concept of a cell population with nonuniform cell-cycle times including a number of cells in a state of dormancy, ie, the G_0 cells.

Another important development was the introduction of ^{32}P-labeled di-isopropylfluorophosphate. After the report by Leeksma and Cohen (33) in 1956 that this label was taken up by leukocytes, investigators at the University of Utah under Wintrobe (34–36) embarked on a series of studies which went a long way toward elucidating granulocyte intravascular kinetics.

With the availability of these important techniques many studies were reported which vastly expanded knowledge concerning leukocyte kinetics in man and in animals and eventually led within a few years to one of the most important conferences on cell kinetics ever convened. This meeting was held in Salt Lake City, Utah, in January 1959, under the sponsorship of the Hematology Study Section of the National Institutes of Health, which included among its members Drs. Wintrobe, Castle, Cronkite, Stohlman, and Good and was entitled the "Conference on Fundamental Problems and Techniques for the Study of Kinetics of Cellular Proliferation." The proceedings were subsequently published as a book (37), now a classic, edited by the late Fred Stohlman.

This meeting was designed to cover all aspects of cell kinetics and was international in character. Participants included hematologists, biochemists, theoretic chemists, statisticians, mathematicians, electrical engineers, and some of the most famous names in hematology and cell kinetics, eg, Drs. Bessis, Castle, Chargaff, Dameshek, Gowans, Lajtha, Lamerton, Quastler, and Yoffey. It is of interest that the conference was unaware or at least took no notice of the potential relevance of cell kinetics in the treatment of the myeloproliferative disorders. In 1948, aminopterin and methotrexate were introduced by Farber and co-workers (38) who had reported temporary remissions in acute leukemia in children. In succeeding years, as other agents such as 6-mercaptopurine, corticosteroids, cyclophosphamide, and vincristine became available, marked improvements were reported, largely in children with acute lymphocytic leukemia, but very little attention was paid to the possible relevance of cell kinetics.

The potential importance of an understanding of cell kinetics in the management of human acute leukemia was not fully appreciated until Skipper (39), Schabel et al (40), and Simpson-Herren and Lloyd (41), at the Southern Research Institute, Birmingham, Ala, provided the impetus, particularly with their studies of the therapy of experimental leukemia as well as of solid animal tumors and their demonstration of the relationship between growth characteristics and response to treatment.

In 1961, a new era in the study of cell kinetics was opened with the description of the spleen-colony assay method (42), although its usefulness is limited since it can only be applied to experimental animals. Nevertheless, it is important as an assay for the colony forming cell(s), which is thought to give rise to erythrocytic, granulocytic, thrombocytic, or mixed colonies in the spleen of irradiated mice. By combining this technique with cell separation methods, at least one group has claimed the tentative identification of the hemopoietic stem cell in mice (43). Another major advance was the development of the agar-colony assay since this technique could be utilized to assay human normal and leukemic bone marrow (44–46); it has become a useful tool in attempts to identify the elusive hemopoietic cell(s) (47) and to characterize humoral stimulatory factors (48,49). At present, it is generally accepted that the precursor cell in the agar-colony system as currently employed is a committed cell giving rise to both granulocytes and macrophages.

The most recent significant development in the investigation of stem cells has been the ip diffusion-chamber technique (50). This technique makes it possible to grow human marrow and peripheral blood cells in millipore chambers implanted ip and is conducive to stem cell proliferation and differentiation (51). This approach has also led to claims for the detection of pluripotential stem cells (52). By combining this method, density gradient sedimentation, and lymphocyte subpopulation separation techniques, a population of lymphocytes has recently been identified which seems to possess true pluripotentiality (53).

Particularly important for cancer chemotherapy were the classic observations of Bruce et al (54) who described the differential sensitivity of resting hemopoietic stem cells and rapidly proliferating lymphoma cells in mice after treatment with a variety of antitumor drugs. These observations tended to mold the thinking of chemotherapists toward the relevance of cell-cycle specificity or nonspecificity of drugs in designing therapeutic regimens.

Thus far I have briefly sketched the history of

studies in leukocyte kinetics but the path for research in solid tumor kinetics was quite different. One of the earliest reported efforts to quantitate tumor growth was that of Gaylord and Clowes (55) in 1906, who attempted to calculate the volume of mouse tumors. There were many similar attempts in the next 3 decades, but even as late as 1935, Schrek (56) concluded that the "measurement of the size of the tumors in the living animal appears to be the chief difficulty in quantitating studies of tumor growth." He also observed that the smaller the inoculum, the smaller the percent takes and the longer the latent period, but the size of the inoculum had little if any effect on the rate of growth of the resulting tumor.

It is of interest to note that Casey (57), in 1934, suggested that tumor growth could be described by a Gompertzian curve, but felt that his data were not firm enough to permit generalization at the time. In 1935, Mottram (58) described an important study in the induction of tumors in mice by the application of tar which led to the appearance of "epitheliomatous warts." He commented that "the varying latent period of tumors found in different animals is usually said to be directly proportional to their length of life. The present explanation gives an alternative which can be put to test by measuring side by side the rates of growth of tumors and their latent periods." He made a case for the single-cell origin of tumors "for the reason that it takes long periods of time, several months for single cells to grow to visible warts. These periods are comparable to the latent period or the period when no tumor can be detected." He also concluded that the growth rate of tumor cells alone determines the benignity or malignancy of that tumor. In 1939, Brues and co-workers (59) came to the conclusion that the latent period between initial application of a carcinogen and the time when a tumor became palpable could be accounted for by assuming that the neoplasia began with a relatively small number of malignant cells and that the subsequent growth rate was constant.

During the end of the 1950s and early 1960s a large number of reports appeared describing the growth characteristics of both animal and human tumors (60–68). In 1956, one of the early reports was that of Collins et al (60) which dealt with the growth rates of Wilms' tumor and metastatic bronchogenic carcinoma. They proposed the concept that a large portion of the life of a tumor occurs before clinical detection and questioned the value of early diagnosis in treatment since the growth characteristics of the tumor seemed to determine the outcome. In 1951, this skepticism concerning the importance of early diagnosis had been raised by MacDonald (61) who was an advocate of the so-called biologic predeterminism in human cancer, which was considered to reflect the relationship between characteristics of the tumor and reactive influences in the host. Weiss et al (62) reported data in lung cancer suggesting that survival in this tumor is determined by the biologic characteristics, ie, the growth rate of each tumor, and questioned the urgency of resection. Gershon-Cohen and co-workers (63) also supported this concept, claiming that the growth rate in breast cancer determines the ultimate outcome.

In 1959, Brindley et al (64) reported the results of direct observations of the number and size of lesions as a method of following the growth of human tumors. Spratt and Ackerman (65) studied the growth of colon cancer and rate of growth of pulmonary metastases as related to host survival and attempted to correlate the measured rates of growth with the duration of life of the patient. The doubling-time concept was introduced in the early 1960s by Bertalanffy and Lau (66) who provided evidence that in transplanted tumors there was a constant increase in the number of malignant cells each day during the period of active growth until the onset of necrosis.

One of the important milestones in solid tumor cell kinetics came in 1965, when Laird (69) suggested that tumor growth could be described by a Gompertzian curve. She was probably unaware of the fact that 30 years previously Casey, as noted above, had put forth the same hypothesis based on his observations in animal tumors.

As in leukocyte kinetics, a new era began in solid tumor kinetics when investigators began to utilize tritiated thymidine to study animal and human tumor-growth characteristics. One of the early important series of studies were those of Mendelsohn et al (70,71) who, in using the C3H mouse as a model, made some important fundamental observations and proposed the growth-fraction hypothesis.

The group under Professor Lamerton in England with Steel, Tannock, and Barrett have made many valuable observations and provided a number of useful concepts including that of cell loss in tumors (72), the value of mathematic modeling in analysis of cell kinetic data (73), and the relevance of small blood vessels to tumor-growth kinetics (74).

As previously mentioned, the Southern Research Institute group including Skipper, Schabel, Simpson-Herren, and Griswold have made notable contributions to our knowledge of cell-cycle kinetics of animal tumors particularly as related to treatment.

Probably the earliest reported human studies with tritiated thymidine were those in 1960 by Johnson et al (75) at Brookhaven who provided data on several solid tumors, including carcinoma of the breast and testes and glioblastoma multiforme. Ba-

serga et al (76) also reported on the uptake of tritiated thymidine by human tumors after in vivo injection and Wolberg and Brown (77) described the results of their large study of human tumors based on the in vitro uptake of labeled uridine and thymidine.

During the years since those early observations, there have been many in vitro-labeling studies and a large number of in vivo studies (78–87), but technical and ethical considerations often limited the in vivo investigations to single samples and determinations of the labeling index. There have been relatively few reports of in vivo cell-cycle determinations in human solid tumors or in normal tissues. To my knowledge, no studies of the cell cycle in human solid tumors were reported in the literature prior to 1968.

From this very brief historical review, I think it is fair to say we have come a long way and have learned a great deal. We may logically conclude that the kinetics of cell proliferation have relevance to cancer chemotherapy; however, it must also be admitted that the reasons for whatever successes we have had in treatment are not completely understood. If one is a cell kineticist he tends to attribute advances to the observed differences in growth characteristics between normal and neoplastic tissues. If one is a chemotherapist without a commitment to cell kinetics, selective toxicity takes the credit. However, it is difficult to escape the fact that the development of better drug schedules, better combinations of drugs, and the discovery of more effective agents have been largely responsible for the improvements in the prognosis of patients with cancer. As has been pointed out recently (88), it is undoubtedly premature and unjustified on the basis of our present knowledge to expect cell kinetics to provide all the answers. It is difficult at present to give the credit to either the therapist or the kineticist exclusively nor is it a useful exercise to do so. It is far more fruitful to identify the obstacles that confront us in attempting to utilize knowledge in cell kinetics most effectively in the treatment of cancer patients.

Before I list some of these obstacles, I am obliged to provide a footnote to the present role of cell kinetics in cancer therapy. It is obvious that the current, postulated importance of cell kinetics arises in part because of limitations in the types of agents we have available to treat patients with cancer. These drugs generally interfere with cell proliferation in one way or another. If our colleagues in molecular biology were to develop drugs which selectively affect cell structures (ie, the cell membrane or biochemical processes unrelated to cell proliferation), cell kinetics would be less of a consideration than we presently perceive in the management of patients with cancer. Similarly, if tumor angiogenesis turns out to be a critical factor and an antiangiogenesis agent is produced, reliance on conventional antitumor drugs might be unnecessary. These, however, are potential promises. Of more immediate concern are some challenges we need to meet.

(*A*) New techniques are needed to assess cell-cycle times, growth fraction, and other important parameters before and during the course of treatment. Present approaches are either too slow or impractical.

(*B*) We need to be able to quantitate the numbers of tumor stem cells and to determine how they are affected by treatment. We need new technologies to do this rapidly.

(*C*) There is a critical need for efficient techniques to achieve synchronization in human neoplasia in vivo. There is little evidence that the agents now used for synchronization have any *selective* action in vivo or that significant or useful synchronization has been achieved in the treatment of patients with hematologic malignancies or with solid tumors.

(*D*) There is a large gap in our knowledge of growth characteristics of small subclinical metastases. These are the lesions which spell the difference between cure and relapse and present the therapist with his greatest challenge. The technical difficulties are immense and although biochemical markers in the blood or urine may turn out to have sufficient sensitivity for monitoring purposes, this would seem unlikely.

(*E*) Our information concerning resting cells is inadequate and there are no efficient, practical techniques for their recruitment.

(*F*) A beginning has been made in expanding our knowledge of the role of the vasculature in tumors, but we need to know a great deal more about the relationship between the tumor cell population, tumor blood vessels, and tumor architecture in general.

(*G*) Theoretically, computer modeling can be of use in planning a treatment regimen and in changing treatment as warranted. Unfortunately, until the foregoing problems are solved, I am not optimistic that computer modeling will be of great help to the clinician. There is yet to be a demonstration that computer programs can be utilized to design effective or curative treatment regimens even in experimental tumors.

Drs. Shackney and Schiffer have been responsible for organizing this conference and deserve our sincere appreciation. I share their hope that it evolves into more than merely the presentation of a series of papers, but that it develops into a concerted effort

to solve the difficult problems in cell kinetics as related to cancer treatment. I would urge that this conference be considered the forerunner of an annual or semi-annual workshop to deal with these questions.

I look forward to this symposium not because I expect some of the obstacles to be resolved but because, by bringing together this distinguished group of investigators who represent a variety of research areas within cell kinetics, the opportunities for fruitful interchange have been optimized. Therefore, I am confident that out of this meeting will come important progress in cell kinetics which in turn should have an important and beneficial impact on therapy.

REFERENCES

1. MINOT GR, and ISAACS R. Transfusion of lymphocytes: their rapid disappearance from the peripheral circulation of man. JAMA 84:1713–1715, 1925.
2. LAWRENCE JS, ERVIN DM, and WETRICH RM. Life cycle of white blood cells. Am J Physiol 144:284–296, 1945.
3. YOFFEY JM. The quantitative study of lymphocyte production. J Anat 67:250–262, 1932–33.
4. WHITE LP. The intravascular life span of transfused leukocytes tagged with Atabrine. Blood 9:73–82, 1954.
5. LISSAC J, MATHÉ G, and BERNARD J. Etude du "sejour vasculaire" des polynucleaires par une methode utilisant un indicateur fluorescent. Rev Fr Etud Clin Biol 1:631–642, 1956.
6. BRECHER G, and PEDEN JC, JR. Circulation time and fate of naturally (alkaline phosphatase) and fluorescent (Atabrine) labeled granulocytes. *In* The Kinetics of Cellular Proliferation (Stohlman F, ed). New York, Grune and Stratton Inc, 1959, pp 227–230.
7. OTTESEN J. Life span of red and white blood corpuscles of the hen. Nature 162:730–731, 1948.
8. KLINE DL, and CLIFFTON EE. Lifespan of leucocytes in man. J Appl Physiol 5:79–84, 1952.
9. OTTESEN J. On the age of human white cells in peripheral blood. Acta Physiol Scand 32:75–93, 1954.
10. CHRISTENSEN BC, and OTTESEN J. The age of leukocytes in the blood stream of patients with chronic lymphatic leukemia. Acta Haematol 13:289–298, 1955.
11. CRADDOCK CG, JR, PERRY S, and LAWRENCE JS. The dynamics of leukopoiesis and leukocytosis as studied by leukopheresis and isotopic techniques. J Clin Invest 35:285–296, 1956.
12. PERRY S, CRADDOCK CG, JR, and LAWRENCE JS. Rates of appearance and disappearance of white blood cells in normal and in various disease states. J Lab Clin Med 51:501–515, 1958.
13. PERRY S, ET AL. The combined use of typhoid vaccine and P^{32} labeling to assess myelopoiesis. Blood 12:549–558, 1957.
14. PERRY S, ET AL. Rate of production of P^{32}-labeled lymphocytes. Blood 14:50–59, 1959.
15. HOWARD A, and PELC SR. Synthesis of deoxyribonucleic acid in normal and irradiated cells and its relation to chromosome breakage. Heredity 6:261, 1953.
16. TAYLOR JH, WOODS PS, and HUGHES WL. The organization and duplication of chromosomes as revealed by autoradiographic studies using tritium-labeled thymidine. Proc Natl Acad Sci USA 43:122–128, 1957.
17. BOND VP, ET AL. Cell turnover in blood and blood-forming tissues studied with tritiated thymidine. *In* The Kinetics of Cellular Proliferation (Stohlman F, ed). New York, Grune and Stratton Inc, 1959, pp 188–200.
18. RUBINI JR, ET AL. The metabolism and fate of tritiated thymidine in man. J Clin Invest 39:909–918, 1960.
19. CRONKITE EP, and FLIEDNER TM. Granulocytopoiesis. N Engl J Med 270:1347–1352, 1403–1408, 1964.
20. PERRY S, ET AL. Studies of leukocyte kinetics by liquid scintillation counting in normal individuals and in patients with chronic myelocytic leukemia. J Clin Invest 45:1388–1399, 1966.
21. MOXLEY JH III, ET AL. Return of leukocytes to the bone marrow in chronic myelogenous leukaemia. Nature 208:1281, 1965.
22. KILLMANN S-A. Acute leukemia: the kinetics of leukemic blast cells in man. Ser Haematol 1:38–102, 1968.
23. PERRY S, GODWIN HA, and ZIMMERMAN TS. Physiology of the granulocytes. JAMA 203:937–944, 1025–1032, 1968.
24. MAUER AM, and FISHER V. Comparison of the proliferative capacity of acute leukaemia cells in bone marrow and blood. Nature 193:1085–1086, 1962.
25. MAUER AM, and FISHER V. Characteristics of cell proliferation in four patients with untreated acute leukemia. Blood 28:428–445, 1966.
26. CLARKSON B, ET AL. Studies of cellular proliferation in human leukemia. I. Estimation of growth rates of leukemic and normal hematopoietic cells in two adults with acute leukemia given single injections of tritiated thymidine. J Clin Invest 46:506–529, 1967.
27. QUASTLER H, and SHERMAN FG. Cell population kinetics in the intestinal epithelium of the mouse. Exp Cell Res 17:420, 1959.
28. GAVOSTO F, ET AL. Proliferation and maturation defect in acute leukemia cells. Nature 203:92–94, 1964.
29. GAVOSTO F, MARAINI G, and PILERI A. Proliferative capacity of acute leukaemia cells. Nature 187:611–612, 1960.
30. ASTALDI G, and MAURI C. Recherches sur l'activite proliferative de l'hemocytoblast de la leucemie aigue. Rev Belg Path 23:69–82, 1953.
31. BASERGA R, and KISIELESKI WE. Comparative study of the kinetics of cellular proliferation of normal and tumorous tissues with the use of tritiated thymidine. I. Dilution of the label and migration of labeled cells. J Natl Cancer Inst 28:331–339, 1962.
32. LAJTHA LG, and OLIVER R. Cell population kinetics following different regimes of irradiation. Br J Radiol 35:131–140, 1962.
33. LEEKSMA CHW, and COHEN JA. Determination of the life span of human blood platelets using labelled disopropylfluorophosphonate. J Clin Invest 35:964–969, 1956.
34. ATHENS JW, ET AL. Leukokinetic studies. I. A method for labeling leukocytes with diisopropylfluorophosphate (DFP^{32}). Blood 14:303–333, 1959.
35. MAUER AM, ET AL. Leukokinetic studies. II. A method for labeling granulocytes in vitro with radioactive diisopropylfluorophosphate (DFP^{32}). J Clin Invest 39:1481–1486, 1960.
36. CARTWRIGHT GE, ATHENS JW, and WINTROBE MM. The kinetics of granulopoiesis in normal man. Blood 24:780–803, 1964.
37. STOHLMAN F, JR, ed. The Kinetics of Cellular Proliferation. New York, Grune and Stratton Inc, 1959.
38. FARBER S, ET AL. Temporary remissions in acute leukemia in children produced by folic acid antagonist, 4-aminopteroyl glutamic acid. N Engl J Med 238:787–793, 1948.
39. SKIPPER HE. Kinetic behavior versus response to chemotherapy. Prediction of response in cancer chemotherapy. Natl Cancer Inst Monogr 34:2–14, 1971.

40. SCHABEL FM, JR, SKIPPER HE, TRADER MW, ET AL. Experimental evaluation of potential anticancer agents. XIX. Sensitivity of nondividing leukemic cell populations to certain classes of drugs in vivo. Cancer Chemother Rep 48:17–30, 1965.
41. SIMPSON-HERREN L, and LLOYD HH. Kinetic parameters and growth curves for experimental tumor systems. Cancer Chemother Rep 54:143–174, 1970.
42. TILL JE, and MCCULLOCH EA. A direct measurement of the radiation sensitivity of normal mouse bone marrow cells. Radiat Res 14:213–222, 1961.
43. VAN BEKKUM DW, VAN NOORD MJ, MAAT B, ET AL. Attempts at identification of hemopoietic stem cell in mouse. Blood 38:547–558, 1971.
44. PLUZNIK DH, and SACHS L. The cloning of normal mast cells in tissue culture. J Cell Physiol 76:77, 1965.
45. BRADLEY TR, and METCALF D. The growth of mouse bone marrow cells in vitro. Aust J Exp Biol Med Sci 44:287, 1966.
46. PIKE BL, and ROBINSON WA. Human bone marrow colony growth in agar gel. J Cell Physiol 76:77, 1970.
47. DICKE KA, VAN NOORD MJ, MAAT B, ET AL. Identification of cells in primate bone marrow resembling the hemopoietic stem cell in the mouse. Blood 42:195–208, 1973.
48. CHERVENIK PA, and BOGGS DR. Bone marrow colonies: stimulation in vitro by supernatant from incubated human blood cells. Science 169:691, 1970.
49. RICKARD KA, MORLEY A, HOWARD D, ET AL. The in vitro colony forming cell and the response to neutropenia. Blood 37:6–13, 1970.
50. BENESTAD HB. Formation of granulocytes and macrophages in diffusion chamber cultures of mouse blood leukocytes. Scand J Haematol 7:279, 1970.
51. SQUIRES DJP, and LAMERTON LF. The effect of various cytotoxic agents on bone marrow cells as measured by diffusion chamber assays. Br J Haematol 29:31–42, 1975.
52. BOYUM A, and BORGSTROM E. The concentration of granulocytic stem cells in mouse bone marrow determined with a diffusion chamber technique. Scand J Haematol 7:294, 1970.
53. BARR RD, WHANG-PENG J, and PERRY S. Hemopoietic stem cells in human peripheral blood. Science 190:284–285, 1975.
54. BRUCE WR, MEEKER BE, and VALERIOTE FA. Comparison of the sensitivity of normal hematopoietic and transplanted lymphoma colony-forming cells to chemotherapeutic agents administered in vivo. J Natl Cancer Inst 37:233, 1966.
55. GAYLORD HR, and CLOWES GHA. On the spontaneous cure of cancer. Surg Gynecol Obstet 2:633, 1906.
56. SCHREK R. A quantitative study of the growth of the Walker rat tumor and the Flexner-Jobling rat carcinoma. Am J Cancer 24:807–822, 1935.
57. CASEY AE. The experimental alteration of malignancy with a homologous mammalian tumor material. I. Results with intratesticular inoculation. Am J Cancer 21:760–775, 1934.
58. MOTTRAM JC. On origin of tar tumours in mice, whether from single cells or many cells. J Pathol 40:407–414, 1935.
59. BRUES AM, WEINER AE, and ANDERVANT HB. Relation between latent period and growth rate in chemically induced tumors. Proc Soc Exp Biol Med 42:374–377, 1939.
60. COLLINS VP, KOEFFLER RK, and TIVEY H. Observations on growth rates of human tumors. Am J Roentgenol 76:988–1000, 1956.
61. MACDONALD I. Biological predeterminism in human cancer. Surg Gynecol Obstet 92:443–453, 1951.
62. WEISS W, BOUCOT KR, and COOPER DA. The survival of men with measurable proned lung cancer in relation to growth rate. Am J Roentgenol Radium Ther Nucl Med 98:404–415, 1966.
63. GERSHON-COHEN J, BERGER SM, and KLICKSTEIN HS. Roentgenography of breast cancer moderating concept of "biologic predeterminism." Cancer 16:961–964, 1963.
64. BRINDLEY CO, MARKOFF E, and SCHNEIDERMAN MA. Cancer 12:139–146, 1959.
65. SPRATT JS, and ACKERMAN LV. The growth of a colonic adenocarcinoma. Am J Surg 27:23–28, 1961.
66. BERTALANFFY FD, and LAU C. Rates of cell division of transplantable malignant rat tumor. Cancer Res 22:627–631, 1962.
67. BRENNAN MJ, PRYCHODKO W, and HOREGLAD S. Quantitative studies on growth of spontaneous tumors in biology. *In* Interactions in Normal and Neoplastic Growth (Brennan MJ, and Simpson WL, eds). Little Brown and Co, 1962, pp 739–748.
68. SPRATT JS, and SPRATT TL. Rates of growth of pulmonary metastases and host survival. Ann Surg 159:161–171, 1964.
69. LAIRD AK. Dynamics of tumor growth. Br J Cancer 18:490–502, 1964.
70. MENDELSOHN ML, DOHAN FD, JR, and MOORE HA, JR. Autoradiographic analysis of cell proliferation in spontaneous breast cancer of the C3H mouse. I. Typical cell cycle and timing of DNA synthesis. J Natl Cancer Inst 25:477–484, 1960.
71. MENDELSOHN ML. The growth fraction: a new concept applied to tumors. Science 132:1496, 1960.
72. STEEL GG. Cell loss from experimental tumors. Cell Tissue Kinet 1:193–207, 1968.
73. BARRETT JC. A mathematical model of the mitotic cycle and its application to the interpretation of percentage labeled mitoses data. J Natl Cancer Inst 37:443–450, 1966.
74. TANNOCK IF, and STEEL GG. Quantitative techniques for study of the anatomy and function of small blood vessels in tumors. J Natl Cancer Inst 42:771–782, 1969.
75. JOHNSON HA, ET AL. Labeling of human tumor cells in vivo by tritiated thymidine. Lab Invest 9:460–465, 1960.
76. BASERGA R, HENEGAR GC, KISIELESKI WE, ET AL. Uptake of tritiated thymidine by human tumors in vivo. Lab Invest 11:360–364, 1962.
77. WOLBERG WH, and BROWN RR. Autoradiographic studies of in vitro incorporation of uridine and thymidine by human tumor tissue. Cancer Res 22:1113–1119, 1962.
78. IVERSEN U, ET AL. Cell kinetics of African cases of Burkitt's lymphoma. Eur J Cancer 8:305–308, 1972.
79. BELL B, ALMAY TP, and LIPKIN M. Cell proliferation in the gastrointestinal tract of man. J Natl Cancer Inst 38:615–628, 1967.
80. TITUS JL, and SHORTER RG. Labeling of human tumors with tritiated thymidine. Arch Pathol 79:324–328, 1965.
81. REFSUM SB, and BERDAL P. Cell loss in malignant tumors in man. Eur J Cancer 3:235–236, 1967.
82. TRINDEL E, MALAISE E, and TUBIANA M. Cell proliferation kinetics in five human solid tumors. Cancer 22:611–620, 1968.
83. FABRIKANT JI, ET AL. The kinetics of cellular proliferation in normal and malignant tissues. Radiology 92:1309–1320, 1969.
84. YOUNG RC, and DEVITA VT. Cell cycle characteristics of human solid tumors in vivo. Cell Tissue Kinet 3:285–290, 1970.
85. SHIRAKAWA S, LUCE JK, TANNOCK IF, ET AL. Cell proliferation in human melanoma. J Clin Invest 49:1188–1199, 1970.
86. BREUR K. Growth rate and radiosensitivity of human tumours. I. Growth rate of human tumours. Eur J Cancer 2:157–171, 1966.
87. BRESCIANI F. Cell proliferation in cancer. Eur J Cancer 4:343–366, 1968.
88. VAN PUTTEN LM. Are cell kinetic data relevant for the design of tumour chemotherapy schedules? Cell Tissue Kinet 7:493–504, 1974.

Introduction to Session on Population Age-Dependent Responses to Therapy—In Vitro

George M. Hahn [1]

Cell "age" is the theme of this session. The chronologic age of an individual cell is easy enough to define: it is the elapsed time between completion of mitosis by the mother cell and the time of examination. In vitro, at least, this age can be measured by time-lapse cinematography. However, to a therapist such a definition is quite useless. The response of a cell to a therapeutic agent depends not on chronologic age but on "maturation" variables. Of these, total DNA or DNA synthesis is most frequently used, probably because of its measurement via autoradiography or cytofluorometry. Only under very restricted conditions are chronologic and maturation variables simply related. The most interesting and important of these is that of an undisturbed, untreated cell population growing without any nutrient or density inhibitions. Then the probability of survival of an individual cell of known chronologic age exposed to a single treatment can be characterized by an age-response function, ie, a plot of measure of survival versus chronologic age. Furthermore, because the distribution of cell number versus chronologic age ("age distribution") is predictable on theoretic grounds, the fraction of cells surviving the treatment can be determined.

However, after the first (and subsequent) treatment two changes occur. First, the simple exponential age distribution for viable cells becomes modified. For example, an antimetabolite may have killed essentially all the S-phase cells. Second, the rate at which a cell acquires maturation age becomes modified. Another perhaps more conventional way of saying this is that the cell population becomes parasynchronized and that the cells' traverse of the cell cycle is changed. It is these points which are covered in the first paper in this session by Dr. Benjamin Drewinko.

Dr. Peter Twentyman then addresses himself to another problem, equally important in tumor therapy. Once the cells' proliferative pattern becomes modified by density and nutritional (oxygen?) limitations, their response to drugs also changes. Cells are no longer freely "cycling." They may become "blocked" in a particular part of the cell cycle and the response of such cells to agents may be different entirely from that of cells in any part of the normal cell cycle. A useful system here is that of plateau phase cells, and Dr. Twentyman compares the in vitro behavior of plateau phase cells with that of tumor cells in vivo. Finally, Dr. Thomas Lincoln discusses the way one can combine both types of in vitro survival results and pharmacokinetic concepts to attempt to predict the overall response of tumors to chemotherapeutic agents.

[1]Stanford University Medical Center, Calif.

Age-Dependent Survival and Cell-Cycle Progression of Cultured Cells Exposed to Chemotherapeutic Drugs [1]

Benjamin Drewinko* and Barthel Barlogie [2]

Studies on the effects of antitumor agents at the cellular level provide useful information which may guide the development of improved treatment regimens. Antitumor agents produce two types of responses on treated cells: lethality and delay in the normal transit through the mitotic cycle. Since these responses are the result of an interplay between the type, extent, and duration of the injury caused by drugs to critical biosynthetic pathways or subcellular structures and the capacity of cells to bypass or repair such damage, these effects cannot be investigated in cell-free systems. One or several major biochemical modes of action have been defined for most drugs, but no definite causal relationship has ever been demonstrated with respect to cell lethality. Most major molecular effects are usually elicited at concentrations far below those required to induce cell killing or progression delay. Furthermore, distinct biochemical changes can take place at different dose levels which may or may not be within the range of concentrations that induce cellular effects. Therefore, studies at the cellular level provide not only practical information applicable to the development of chemotherapeutic protocols, but generate new insights into drug-induced biologic and biochemical changes which open new avenues of research concerning the mode of action of antitumor agents.

One method of approach is the investigation of the cellular response at different stages of the mitotic cycle performed on synchronized cells. Three considerations should be mentioned with respect to the technical limitations of obtaining synchronized populations. (*a*) Synchronization does not imply the phasing of all cellular processes, but refers to the simultaneous manifestation of some distinct marker such as the synthesis of DNA, the mitotic apparatus, etc. While the population may appear completely phased with respect to one biochemical process, other biochemical activities which should normally occur in subsequent stages may have already taken place during the interval required to obtain the synchronous population. (*b*) No technique provides more than partial synchrony. Although cells in one stage of the cycle may predominate, the population is spread at various points throughout that stage and even in other stages of the cycle. (*c*) Synchronization is an ephemeral event since the cells have random rates of transit through the cycle stages; this decay in synchrony prevents clear-cut interpretation of results obtained after the release of the synchrony induction.

With these considerations in mind, we will now describe some results obtained on synchronized populations derived from a long-term culture of human lymphoma cells (T_1 cells) (1) treated with various chemotherapeutic drugs. Culture conditions, morphologic and biologic properties, and kinetic parameters have already been extensively described (2–6). We synchronize T_1 cells with a single treatment of 3 mM TdR of a 24-hour duration (7). The degree of synchrony is monitored by the labeling and mitotic indices and by DNA histograms obtained by pulse cytophotometry (8). Figure 1 demonstrates the degree of synchrony obtained in a typical experiment. At the end of the synchronization procedure (0 hour), 85%–90% of the cells are in S phase. This level is maintained for the next 6 hours after which the proportion of S-phase cells declines rapidly; at 13 hours about 78% of the cells are in G_2 phase. A mitotic peak ranging from 5% to 12% occurs between 15 and 17 hours and cells subsequently enter G_1 phase composing 84% of the population at 28 hours. Replicate cultures are exposed for 1 hour to increasing concentrations of drugs at 2-hour intervals throughout the length of the cell cycle. The colony-formation technique is used to assess survival of treated cells with respect to untreated controls obtained at each time point; cell-progression delay is monitored by pulse cytophotometry.

Figure 2 shows cell cycle-dependent killing of four

[1]Supported by contracts N01-CM-61156 and N01-CM-43801 from the Division of Cancer Treatment, National Cancer Institute, National Institutes of Health, Department of Health, Education, and Welfare.

[2]Departments of Laboratory Medicine (Dr. Drewinko) and Developmental Therapeutics (Dr. Barlogie), University of Texas System Cancer Center, M. D. Anderson Hospital and Tumor Institute, Houston.

**Reprint requests to:* Benjamin Drewinko, MD, PhD, Department of Laboratory Medicine, University of Texas System Cancer Center, M. D. Anderson Hospital and Tumor Institute, 6723 Bertner Dr, Houston, Tex 77030.

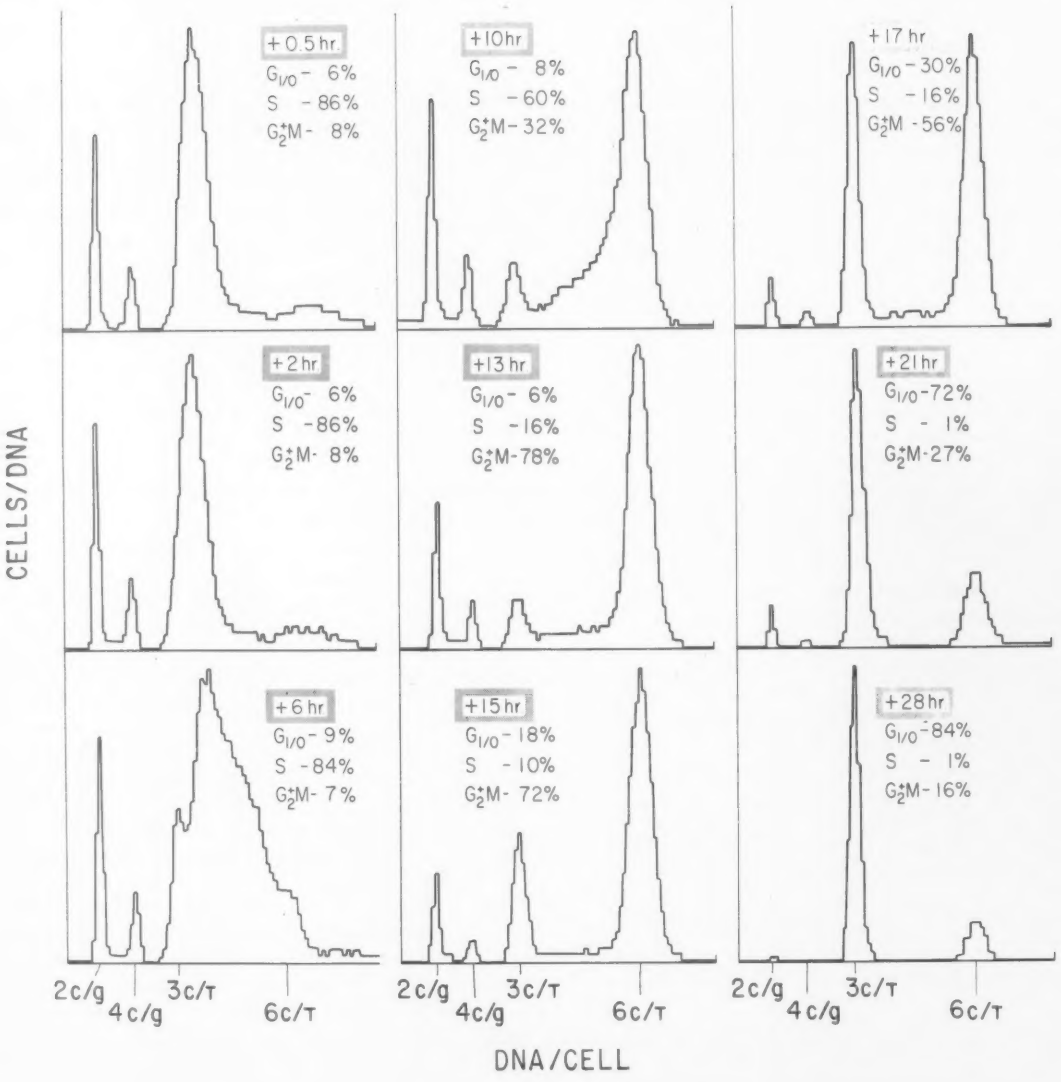

FIGURE 1.—DNA histograms of synchronized T_1 cells obtained at regular intervals after release of a single TdR block (3 mM for 24 hrs). G_1 and (G_2 + M) peaks of T_1 cells appear at 3 and 6 C/T_1, and the corresponding peaks of concurrently measured avian cells (for quality control) appear at 2 and 4 C/g. Ethanol-fixed cells were stained with mithramycin at a dose of 50 μg/ml (+ 7.5 mM $MgCl_2$) for 5 mins. 50,000–100,000 cells were measured for each DNA histogram (*From* ref 8.)

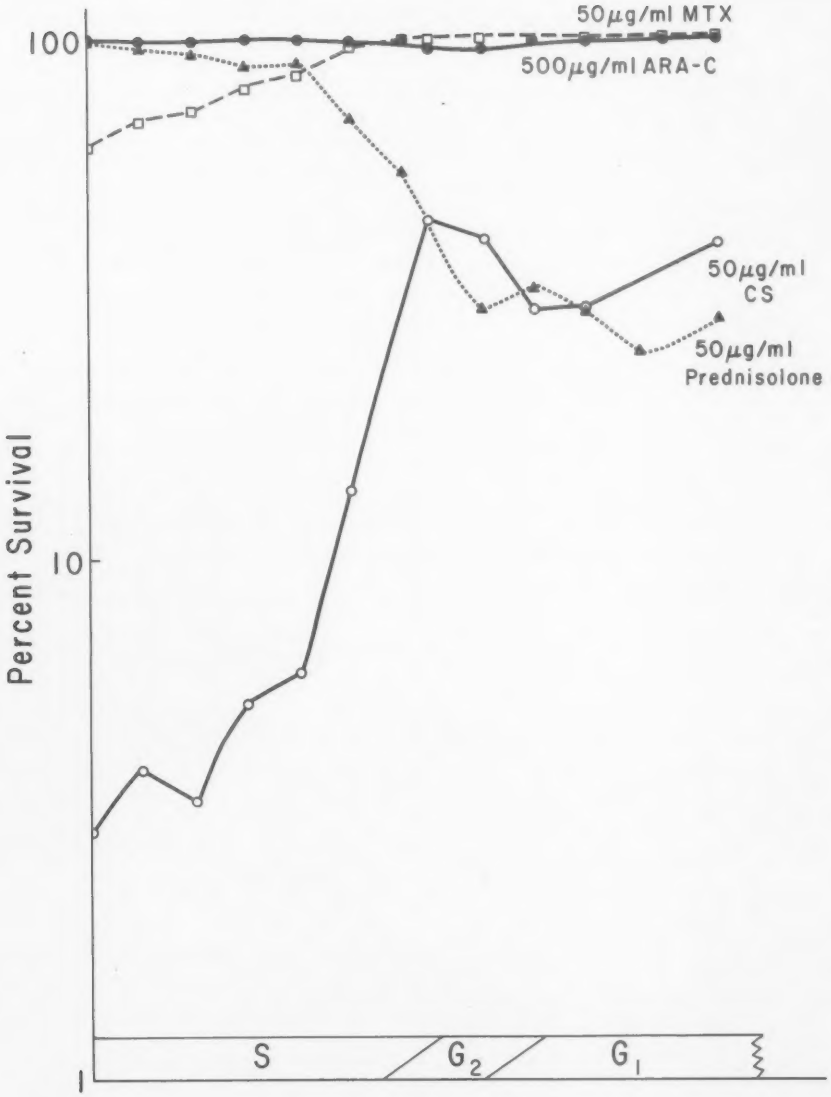

FIGURE 2.—Survival of synchronized T_1 cells exposed to a single concentration of phase-sensitive drugs for 1 hr at regular intervals throughout the cell cycle. (*From* Drewinko B. Cancer Chemotherapy—Fundamental Concepts and Recent Advances. Year Book Medical Publishers, 1975.)

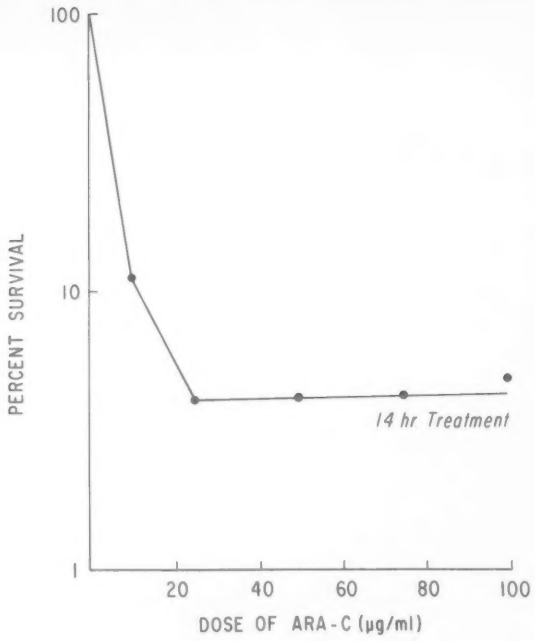

FIGURE 3.—Effect of increasing concentrations of cytosine arabinoside on synchronized S-phase cells. (*From* Drewinko B, et al. Cancer Res 32:2737–2742, 1972.)

phase-sensitive drugs (methotrexate, cytosine arabinoside, prednisolone, and camptothecin). As expected, methotrexate was effective only in S phase, although the degree of killing was relatively poor. Camptothecin, although much more efficacious in S phase, also killed cells in G_1 and G_2. Prednisolone was completely ineffective in S phase at all concentrations, killing cells only in G_1 and G_2 phase. Cytosine arabinoside failed to exert any lethal effect for concentrations up to 1 mg/ml. However, treatment of synchronized cells for the entire length of S phase produced > 95% killing (fig 3). These results suggest that: (*a*) all cells in the purported sensitive stage are not equally susceptible to the lethal effects of a phase-sensitive drug such as methotrexate; some possible causes which are worthy of exploration could be differential drug uptake and metabolism, distinct intracellular concentrations of susceptible enzymes, etc; (*b*) even if cells in the sensitive stage are all equally susceptible, for rapidly degradable drugs such as cytosine arabinoside, continuous incubation is necessary to achieve irreversible damage by the mechanism of "unbalanced growth" ascribed to this agent (9); (*c*) phase-sensitive drugs that exert the greatest killing effect in one stage of the cycle (ie, camptothecin) may also kill cells in other phases; this could be accomplished by different lethal mechanisms or by differential efficacies caused by fluctuations in target availability or increased effi-

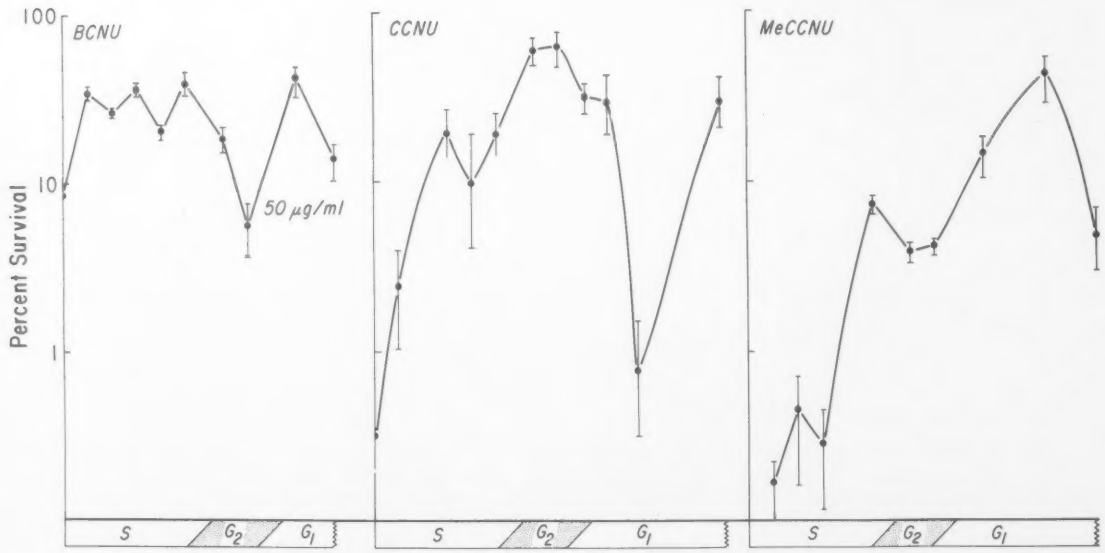

FIGURE 4.—Survival of synchronized cells exposed to a single concentration of nitrosourea derivative (50 µg/ml) for 1 hr at regular intervals throughout the cell cycle. (*From* Drewinko B, et al. Cancer Res 36:511–515, 1976.)

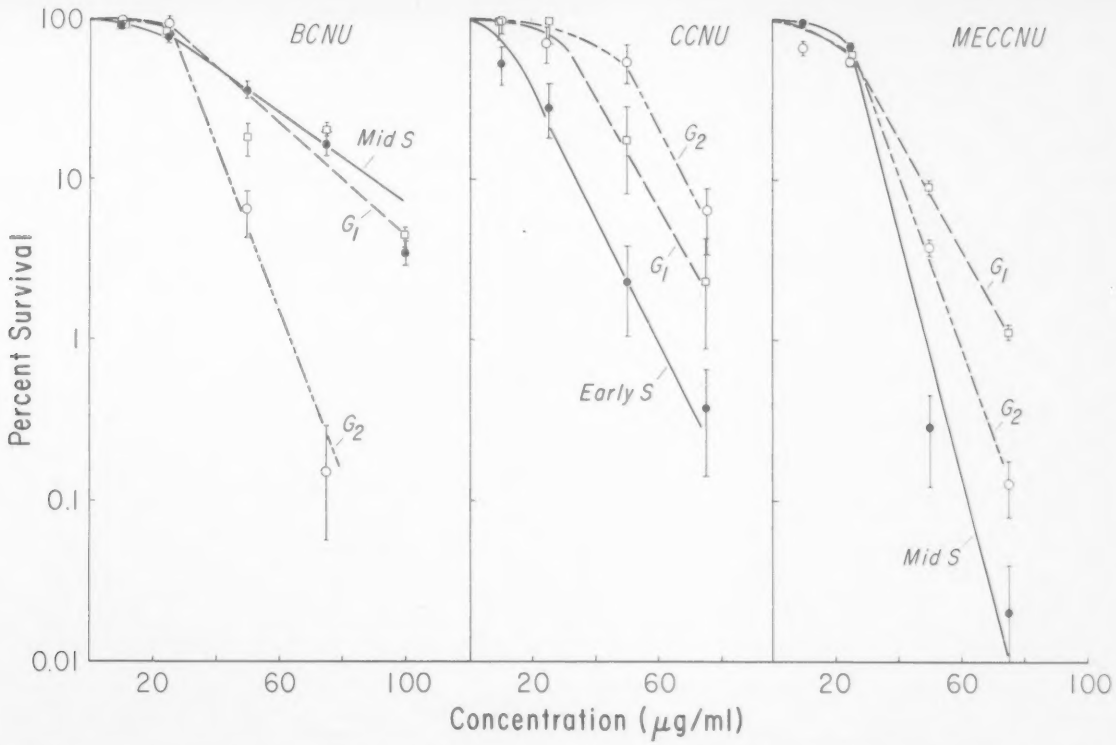

FIGURE 5.—Survival of synchronized cells exposed to increased concentrations of nitrosourea derivatives at selected points of the cell cycle. (*From* Drewinko B, et al. Cancer Res 36:511–515, 1976.)

ciency in repair mechanisms; and (*d*) cells in the stage of DNA synthesis may be insensitive to the lethal action of steroids; this phenomenon may be independent of the actual synthesis of nucleic acid and possibly related to different biochemical processes that take place simultaneously, since steroid effects on DNA synthesis are secondary to their interference with protein and glucose metabolism (10).

Survival of T_1 cells treated with three nitrosourea derivatives is shown in figure 4. BCNU appears more effective in G_2 phase, while both CCNU and methyl-CCNU are more efficacious in early S. In addition, CCNU kills cells in G_1 to a considerable extent. Furthermore, survival curves obtained as a function of increasing concentrations of the three drugs at various stages of the cell cycle show independent differences in both the capacity to absorb damage (expressed by the extent of the shoulder region) and the sensitivity of the critical target (reflected by the incline of the slope of the exponential part of the curve) (fig 5). Cell cycle-dependent survival of cells exposed to another alkylating agent, Yoshi 864, is shown in figure 6; the greatest cell killing is observed in early S and in G_1 phase. Survival curves obtained at each stage of the cycle are shown in figure 7 which demonstrates that fluctuation in killing effects is largely the result of cycle-dependent differential capacities to absorb lethal damage. These results suggest that even though all of these alkylating agents may have a similar radiomimetic mechanism of action, the mode, and probably the target molecule by which the lethal effect comes about, differs in each.

Figure 8 demonstrates cell cycle-related killing effects of bleomycin, *cis*-dichlorodiammine-platinum(II) [*cis*-DDP(II)], and adriamycin. The three drugs kill cells in all stages of the cell cycle, although they exert relatively greater effects at specific phases: G_2 for *cis*-DDP(II) and bleomycin and late S for adriamycin. All three drugs allegedly kill cells by affecting DNA chains. Bleomycin produced strand breaks (11), *cis*-DDP(II) produced cross-linking and strand breaks (12), and adriamycin produced intercalation (13). Again, it is appealing to speculate that for these drugs killing is

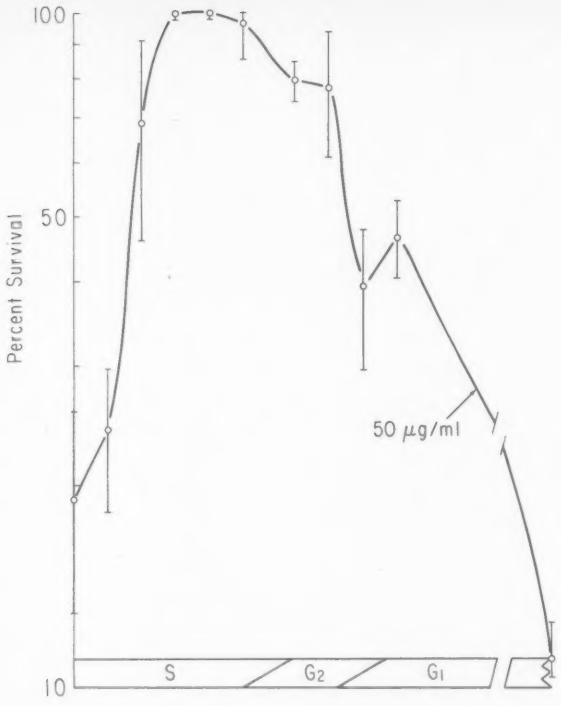

FIGURE 6.—Effect of a single concentration of Yoshi 864 (50 μg/ml) incubated for 1 hr with synchronized T_1 cells at different points of the cell cycle. (*From* Drewinko B, et al. Cancer Treat Rep. In press, Nov 1976.)

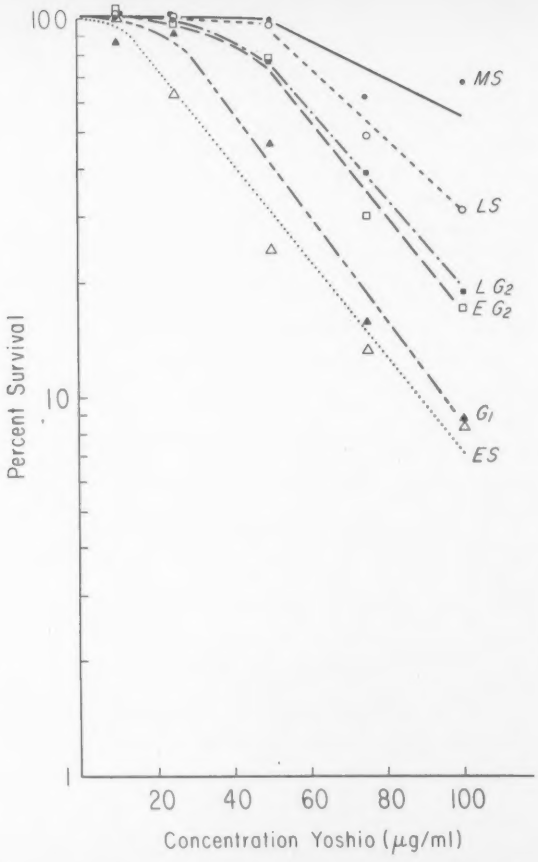

FIGURE 7.—Survival of synchronized T_1 cells treated with increasing concentrations of Yoshi 864 at selected stages of the cell cycle. (*From* Drewinko B, et al. Cancer Treat Rep. In press, Nov 1976.)

effected at each stage by either different modes of action or by different degrees of efficacy of a single mode. Conversely, the sensitive target may be completely unrelated to DNA and variations in degree of killing may represent fluctuations of its availability during the mitotic cycle.

Figure 9 demonstrates cell cycle-dependent survival of lymphoma cells treated with VP-16-213, a semi-synthetic derivative of podophyllotoxin. Almost a tenfold difference in killing efficiency is noted from the lowest survival point in G_2 to the highest survival in mid G_1. Thus, the pattern of cell killing induced by VP-16-213 is similar to the cell cycle-dependent effects on macromolecular synthesis and induction of chromosomal aberrations noted by other investigators for this agent (14,15).

Cell cycle-dependent induction of cell-progression delay was investigated by exposing synchronized cells in different stages of the cell cycle to increasing concentrations of bleomycin, adriamycin, VP-16-213, and Yoshi 864 for 1 hour or longer and observing the subsequent transit through the cycle by means of pulse cytophotometry. All of these agents produced delay in G_2 phase; the degree and reversibility of this delay depended on the particular drug, the concentration used, and the length of incubation. Delay in G_2 could be induced by short-term treatment in different stages of the cycle; the most sensitive stage varied for each drug. Table 1 shows results for cells at various points of the cycle incubated for 1 hour with 100 μg/ml of bleomycin. There was a transitory increase in the subsequent G_2 fraction, mainly at the expense of cells in G_1. This effect, noted 19 hours after TdR release, was somewhat more pronounced when bleomycin was dispensed in late S or early G_2. Cells treated in G_1 showed no alterations in the subsequent distribution of the various compartments of the cell cycle. By 80 hours after TdR release, the distribution of all treated cells returned to control values. When the

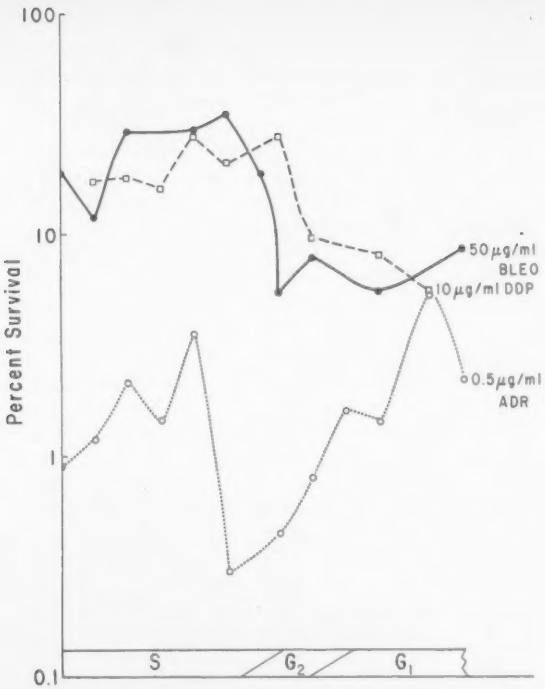

FIGURE 8.—Survival of synchronized T_1 cells exposed to a single concentration of bleomycin, *cis*-DDP(II), and adriamycin. (*From* Drewinko B. Cancer Chemotherapy—Fundamental Concepts and Recent Advances. Year Book Medical Publishers, 1975.)

distribution of cells was measured 15 hours after starting continuous incubation on different synchronized populations, we observed a pattern of decreasing G_2 accumulation from treatment initiated in early S to treatment begun in late G_2 (table 2). These results indicate that the sensitive target responsible for the transit delay in G_2 phase is

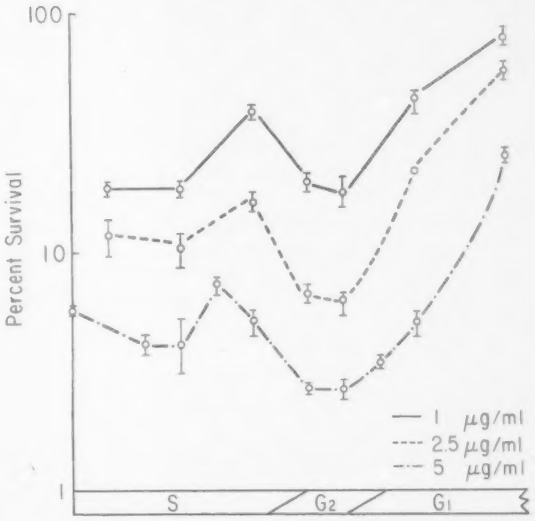

FIGURE 9.—Survival of synchronized T_1 cells exposed for 1 hr to VP-16-213 at selected stages of the cell cycle.

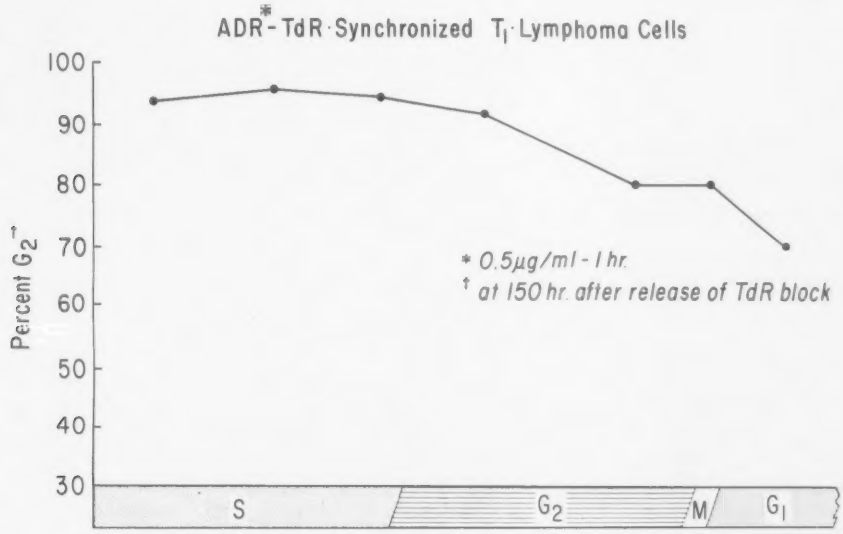

FIGURE 10.—Degree of subsequent G_2 accumulation after a 1-hr treatment with 0.5 μg/ml of adriamycin at selected stages of the cell cycle measured 150 hrs after synchrony release.

largely present in S phase, and although its damage by bleomycin will not interfere with the synthesis of DNA, it will eventually be expressed as a delay in the premitotic stage. For bleomycin, survival assessed by colony-formation was unrelated to cell-progression delay both in the stage of the cycle where maximum effect was noted and in the degree of effect caused by a given concentration; this suggests independent mechanisms of killing and blocking and indicates the unreliability of using the cytokinetic changes induced by bleomycin to predict its lethal effects.

Cells treated for 1 hour with 0.5 μg/ml of adriamycin were effectively blocked in G_2 regardless of the stage of the cycle where treatment was applied (fig 10). This block was largely irreversible and its degree corresponded to the level of cell killing assessed by colony-formation, indicating the usefulness of cytokinetic changes as predictors of adriamycin-induced lethality.

Cytokinetic effects induced by 100 μg/ml of Yoshi 864 for 1 hour are shown in figure 11. Cells treated in G_1 and early- and mid-S phase had a prolonged G_2 transit within the lifespan of the treated cells. When treatment was initiated in late-S or G_2 phase the rate of progression into mitosis was not affected, but when monitored for the subsequent life cycle the amplitude and duration of the G_2 wave were considerably greater compared to that of control cells. Thus, the G_2 delay is an obligatory event for cells treated with Yoshi 864 that will result independent of the position in the cell cycle where treatment with the drug is applied. However, development of this effect necessitates a given period of time and, therefore, manifestation of this response may occur either within the same cell cycle of cells treated in G_1 and early- or mid-S phase or the delay is evidenced in the immediate progeny of cells treated in late S and G_2. This kinetic effect is short-lived since after nearly complete recovery from the G_2 block no second G_2 wave is observed in the progeny of the perturbed cells. Although the stages of the cell cycle most sensitive to the lethal effect of Yoshi 864 (G_1 and early S) were also those in which the subsequent G_2 block was manifested during the lifespan of the treated cells, neither the extent of the G_2 block nor the fraction of cells irreversibly arrested in G_2 correlated with degree of cell killing assessed by colony-formation.

Cytokinetic effects on synchronized cells treated

TABLE 1.—Distribution of synchronized cells in the various phases of the cell cycle after 1-hr incubation with bleomycin (100 μg/ml)* (*From* Barlogie B, et al. Cancer Res 36:1182–1187, 1976.)

Phase of bleomycin addition	G_1			S			G_2		
	19 hrs	31 hrs	80 hrs	19 hrs	31 hrs	80 hrs	19 hrs	31 hrs	80 hrs
Control†	37‡	78	69	23(21)	6(7)	12(13)	40	16	19
ES	31	66	68	19	9(8)	12(11)	50	25	20
MS	24	64	67	26	6(8)	12(11)	50	30	21
LS	22	63	67	24(24)	5(3)	12(12)	54	32	21
EG_2	23	65	60	21(19)	6(5)	16(15)	56	29	24
LG_2	26	63	57	25(22)	8(7)	19(18)	49	29	24
EG_1			62			18(14)			20
LG_1			69			12(12)			19

*Nos. in parentheses = labeling index.
†No drug added.
‡Values expressed as % of total population.

TABLE 2.—Effect of continuous incubation with bleomycin (100 μg/ml) on synchronized T_1 cells observed 15 hrs after drug addition (*From* Barlogie B, et al. Cancer Res 36:1182–1187, 1976.)

Phase of bleomycin addition	G_1		S		G_2	
	Control*	Bleomycin*	Control	Bleomycin	Control	Bleomycin
ES	30†	5	14	9	56	86
MS	72	9	1	9	27	82
LS	89	31	1	7	10	62
EG_2	82	45	1	8	17	47
LG_2	82	62	1	1	17	37

*Measured 15 hrs after initiation of bleomycin treatment on replicate cultures.
†Values expressed as % of the total population.

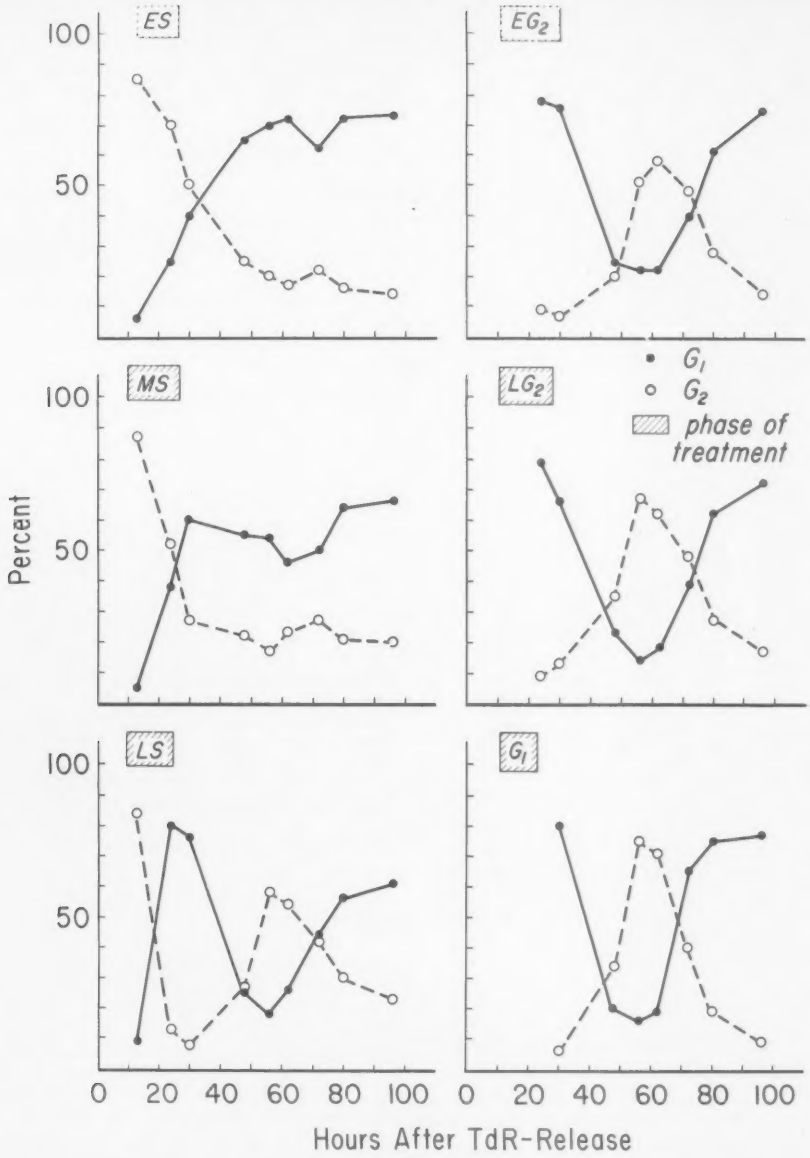

FIGURE 11.—Effect of a 1-hr treatment with 100 μg/ml of Yoshi 864 on the distribution of synchronized T_1 cells in G_1 and G_2 phase. The drug was added 2 hrs (ES), 6 hrs (MS), 10 hrs (LS), 13 hrs (EG_2), 15 hrs (LG_2), and 24 hrs (G_1) after release of a 24-hr TdR block (3 mM). (*From* Drewinko B, et al. Cancer Treat Rep. In press, Nov 1976.)

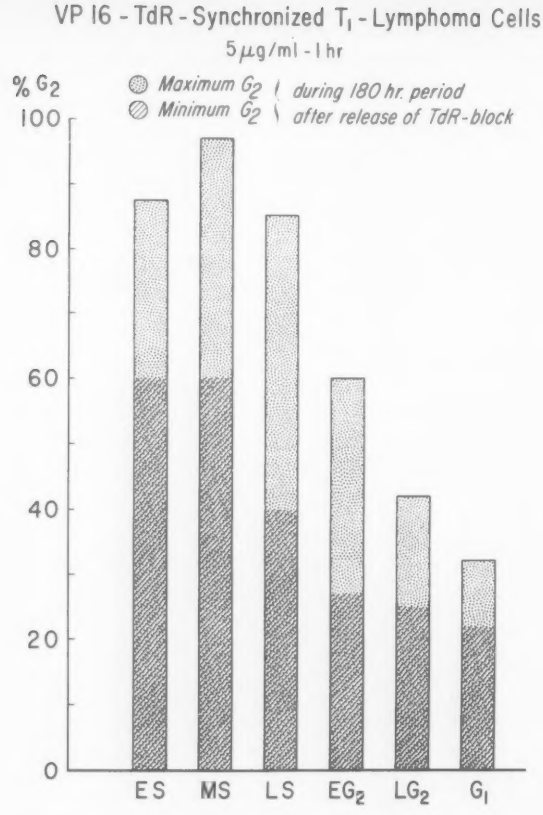

FIGURE 12.—Degree of G_2 accumulation induced by a 1-hr treatment with 5 μg/ml of VP-16-213 at selected stages of the cell cycle. The height of the bars represents the maximum degree of accumulation achieved during the 180-hr interval of the experiment. The dotted segment demonstrates the level of subsequent decrease of G_2 accumulation.

for 1 hour with 5 μg/ml of VP-16-213 were followed for 180 hours as shown in figure 12. The maximum degree of accumulation in G_2 achieved during this period is represented by the height of the bars. Cells treated throughout S phase demonstrated the greatest magnitude of G_2 block. The proportion of subsequent recovery, indicated by the dotted segment, was similar for cells treated in all stages. Again, no correlation between the degree of G_2 block and the magnitude of cell killing was observed for VP-16-213.

In conclusion, it appears that cell-progression delay in G_2 phase is a common effect induced by several drugs, but not necessarily the result of an attack on the same target. With the possible exception of adriamycin, there seems to be no definite causal relation between cell killing and cell-progression delay and recovery from the G_2 block on the first cell generation. Our studies also suggest that bleomycin and Yoshi 864 may represent useful synchronizing agents. Although these drugs induce a considerable degree of irreversible G_2 block with subsequent cell death, cells able to escape this block will emerge partially synchronized. A fraction of these cells (or their progeny) will subsequently die from the inherited damage, but those cells which escape the G_2 block with intact reproductive capacities will be amenable to complete sterilization by the scheduling of a second phase-sensitive drug at full cytocidal dose employed after the adequate time interval.

LIST OF COMPOUNDS

Adriamycin: NSC-123127; CAS reg. No. 23214-92-8

BCNU: NSC-409962; CAS reg. No. 154-93-8; urea, 1,3-bis(2-chloroethyl)-1-nitroso-

Bleomycin: NSC-125066; CAS reg. No. 11056-06-7; [2,4'-bithiazole]-4-carboxylic acid, 2'-(2-aminoethyl)-, monohydrate

Camptothecin: NSC-100880; CAS reg. No. 25387-67-1

CCNU: NSC-79037; CAS reg. No. 13010-47-4; urea, 1-(2-chloroethyl)-3-cyclohexyl-1-nitroso-

Cytosine arabinoside: NSC-63878; CAS reg. No. 69-74-9; cytosine, 1-β-D-arabinofuranosyl-, monohydrochloride

Methotrexate: NSC-740; CAS reg. No. 59-05-2; glutamic acid, *N*-[*p*-[[(2,4-diamino-6-pteridinyl)methyl]methylamino]benzoyl]-

Methyl-CCNU: NSC-95441; CAS reg. No. 33073-59-5; urea, 1-(2-chloroethyl)-3-(4-methylcyclohexyl)-1-nitroso-

Prednisolone: NSC-9900; CAS reg. No. 50-24-8; pregna-1,4-diene-3,20-dione, 11β,17,21-trihydroxy-

VP-16-213: NSC-141540; 4'-demethylepipodophyllotoxin 9-(4,6-*O*-ethylidene-β-D-glucopyranoside)

Yoshi 864: NSC-102627; CAS reg. No. 3458-22-8; 1-propanol, 3,3'-iminodi-, dimethanesulfonate (ester), hydrochloride

REFERENCES

1. TRUJILLO JM, DREWINKO B, and AHEARN MJ. The ability of tumor cells of the lymphoreticular system to grow in vitro. Cancer Res 32:1057-1065, 1972.
2. DREWINKO B, TRUJILLO JM, and GONZALEZ-DIDDI M. Harvesting methods of immunoglobulin producing cells. Eur J Clin Biol Res 16:494-497, 1971.
3. DREWINKO B, and TRUJILLO JM. Morphological aspects of human lymphoid cells grown in vitro. In Vitro 7:344-358, 1972.
4. DREWINKO B, LICHTIGER B, and WELCH JE. Biological characteristics of an established human immunoglobulin producing lymphoid cell line. Medicina 33:59-67, 1973.
5. DREWINKO B, MAVLIGIT GM, AMBUS U, ET AL. Inhibition of human lymphoma cell-line colony formation by lymphocytes from patients with lymphoma and cancer hospital employees. Cancer 37:2929-2937, 1976.
6. DREWINKO B, TRUJILLO JM, BARRANCO SC, ET AL. Kinetics of a human immunoglobulin producing cell line grown in vitro. Eur J Clin Biol Res 14:906-911, 1971.
7. DREWINKO B, LICHTIGER B, and TRUJILLO JM. Synchronization of cultured human lymphoid cells. Eur J Clin Biol Res 18:30-37, 1973.

8. BARLOGIE B, DREWINKO B, BÜCHNER T, ET AL. Pulse cytophotometric analysis of synchronized cells in vitro. Cancer Res 36:1176–1181, 1976.
9. KIM JH, EIDINOFF ML, and FOX JJ. Action of 1-β-D-arabinofuranosylcytosine on the nucleic acid metabolism and viability of HeLa cells. Cancer Res 25:698–702, 1965.
10. ROSEN JM, FINA JJ, MILHOLLAND RJ, ET AL. Inhibition of glucose uptake in lymphosarcoma 1798 by cortisol and its relationship to the biosynthesis of deoxyribonucleic acid. J Biol Chem 245:2074, 1970.
11. SUZUKI H, HAGAI K, YAMAKI H, ET AL. On the mechanism of action of bleomycin. Scission of DNA strands in vitro and in vivo. J Antibiot 22:446–448, 1969.
12. CONNORS TA, and ROBERTS JJ. Platinum coordination complexes in cancer chemotherapy. Berlin, Springer-Verlag, 1974.
13. CALENDI E, DIMARCO A, REGIANI M, ET AL. On physicochemical interactions between daunomycin and nucleic acids. Biochim Biophys Acta 103:25–49, 1965.
14. GRIEDER A, MAURER R, and STÄHELIN H. Effect of an epipodophyllotoxin derivative (VP 16-213) on macromolecular synthesis and mitosis in mastocytoma cells in vitro. Cancer Res 34:1788–1793, 1974.
15. HUANG CC, HOU Y, and WANG JJ. Effects of a new antitumor agent, epipodophyllotoxin, on growth and chromosomes in human hematopoietic cell lines. Cancer Res 33:3123–3129, 1973.

Comparative Chemosensitivity of Exponential- Versus Plateau-Phase Cells in Both In Vitro and In Vivo Model Systems

P. R. Twentyman [1,*]

The work in our laboratory on the chemotherapeutic response of plateau-phase cultures of mammalian cells has been inspired largely by the kinetic analysis of such cultures carried out between 1967 and 1972 in the laboratories of Hahn and Little (1). These two groups were able to suggest that, from a kinetic viewpoint, plateau-phase cultures may represent a better model of in vivo populations of tumor cells than do cultures in the exponential phase of growth. Over the last few years several laboratories including those of Hahn et al (2,3), Barranco et al in Galveston, Texas (4,5), and our own in England (6,7) have examined the relative response to chemotherapy of exponential- and plateau-phase cultures. The results have been confusing in that, at least for some drugs, conflicting results have been obtained by these groups without any obvious kinetic basis for the discrepancies. Whereas the other two groups have used lines of Chinese hamster cells in their work, we have used a continuous culture subline of the EMT6 mouse tumor, and this has the considerable advantage that we may compare our in vitro results with data obtained for the same cell line in vivo. In this paper I will compare our in vitro results with new data obtained for two modes of growth in vivo and discuss the validity of the in vitro model.

METHODS AND MATERIALS

In Vitro

The growth conditions of our continuous culture subline EMT6/M/CC have been published previously (6). The kinetic pattern occurring during the life of the cultures is summarized in figure 1. When 10^5 cells are inoculated into flasks, a short lag period is followed by 3 days of exponential growth with a population doubling time of 11–12 hours. If the medium is not changed, a rapid death of the population occurs. With daily medium change, however, the cell number can be kept constant for many days after reaching the plateau value. Cell numbers eventually begin to fall at about Day 18. The plating efficiency remains > 60% up until this time. In figure 1(b) the pulse ^{3}HTdR labeling index is shown. The exponential phase value of 55%–60% falls to around 25% upon approaching plateau numbers in fed cultures. This is maintained for 4 days at which time a further fall to < 2% is seen. The cell loss from the monolayer into the medium in the period between medium changes is shown in figure 1(c). The low value during the exponential phase rises to about 20% per day during the first 4 days after attaining plateau numbers but then falls to about 2% per day. The system may therefore be regarded as exhibiting three distinct phases: an exponential phase, with all cells in the cell cycle having a cycle time of 11–12 hours, an early-plateau phase where the proliferation rate is reduced and cell production is balanced by cell loss, and a late-plateau phase where proliferation has virtually ceased. The full kinetic analysis of the three phases has been published elsewhere (8).

Drugs are added in volume of < 0.2 ml directly into the medium in which the cells are growing. After 1 hour (except in the bleomycin[2] experiments where an exposure time of 2 hours was used) the medium is removed, the cells are trypsinized from the surface, a cell suspension is prepared, and the surviving fraction is assayed using a cloning technique (6).

In Vivo

Following intradermal inoculation of 4×10^4 cells of our subline EMT6/VJ/AC (9) into the flanks of Balb/c mice, solid tumors become palpable by about Day 5 or 6. By Days 9–10, the tumor-volume doubling time is about 46 hours. The EMT6 tumor may also be grown as lung nodules.[3] If 10^5 cells are inoculated iv at Day 0, cells lodge in the lungs and

[1]Medical Research Council, Clinical Oncology and Radiotherapeutics Unit, The Medical School, Cambridge, England.

Reprint requests to: Dr. Peter R. Twentyman, Medical Research Council, Clinical Oncology and Radiotherapeutics Unit, The Medical School, Hills Rd, Cambridge, CB2 2QH, England.

[2]Bleomycin: NSC-125066; CAS reg. No. 11056-06-7; [2,4'-bithiazole]-4-carboxylic acid, 2'-(2-aminoethyl)-, monohydrate.

[3]Brown JM. Radiosensitization of pulmonary metastases with intravenous infusion of pyrimidine analogs. Presented at the 5th International Congress of Radiation Research, Seattle, Wash, 1974.

the number of tumor cells in the lung increases exponentially with a doubling time of around 17 hours over a period of 12–13 days. This doubling time is very similar to the reported cell cycle time measured in the EMT6 solid tumor (10,11).

Drugs are injected ip into tumor-bearing mice and later, at the appropriate time, the mice are killed and cell suspensions prepared from either solid tumors or from complete sets of lungs. Cells are then assayed for surviving fractions using a cloning technique as previously described (12).

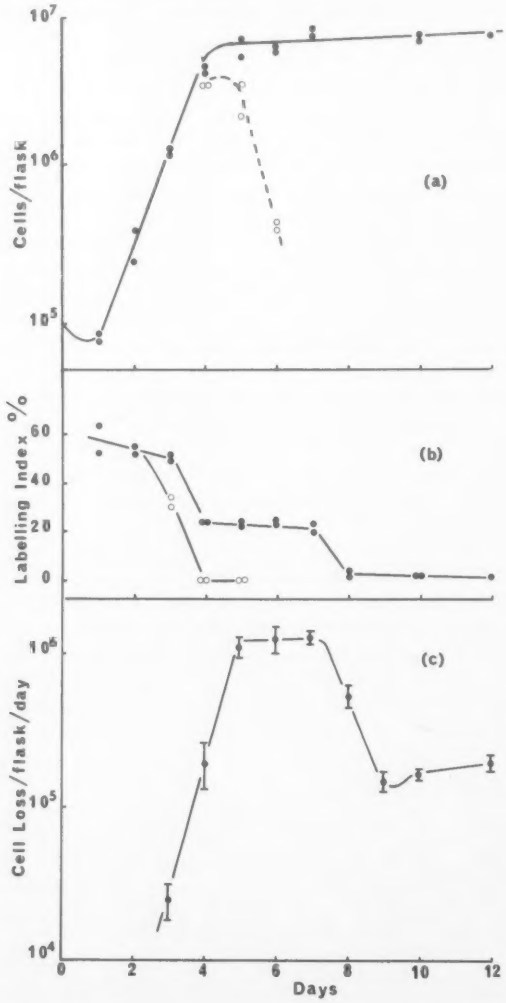

FIGURE 1.—Change in: (*a*) No. of cells/flask; (*b*) pulse ^{3}HTdR labeling index; (*c*) cell loss/flask/day with age of culture after inoculation of 10^5 cells at Day 0. ○ = unfed cultures; ● = cultures with daily medium change starting on Day 2. In (*c*), error bars show ± 2 SEs of the mean of 4 flasks. [Reprinted from ref 8.]

RESULTS

In Vitro

Bleomycin (BLM) (fig 2A).—The biphasic dose-response curve seen during the exponential phase is lost and the cells become less sensitive to this agent during the early-plateau phase. In late-plateau phase, however, the sensitivity is increased again beyond that seen in exponential phase.

Adriamycin[4] *(ADM) (fig 2B).*—During exponential phase, the dose-response curve is biphasic with an extremely rapid fall to a surviving fraction of 10^{-3} at 2 μg/ml. This initial rapid fall is not seen in either early- or late-plateau phases when the cells are very much less sensitive.

BCNU and CCNU[5] *(figs 2C and 2D).*—For both of these agents, the surviving fractions obtained during the various growth phases may be equally well fitted by the same lines, indicating little change in sensitivity between the phases.

In Vivo

The results of our in vivo experiments are to be published shortly (13) and will be only briefly summarized here.

BLM.—Because the "repair of potentially lethal damage" phenomenon is very important for this agent (9,14), we determined the time-response curve for solid tumors and lung nodules using a dose of 4 mg/kg which is on the plateau of the dose-response curve for solid tumors (12). The initial (30 minutes) response was greater in solid tumors than in lung nodules. If, however, assay was delayed until 6 hours after drug administration, then the measured surviving fraction was about 20% for lung nodules but had recovered to almost 100% for the solid tumor.

ADM.—Although the cells in lung nodules showed a little more sensitivity, very little response to this agent was seen in either the solid tumor or lung nodules at 2 hours after very high doses of this agent.

BCNU and CCNU.—There was little difference in sensitivity measured 2 hours after drug administration between cells in lung colonies and in solid tumors.

---

[4]Adriamycin: NSC-123127; CAS reg. No. 23214-92-8.

[5]BCNU: NSC-409962; CAS reg. No. 154-93-8; urea, 1,3-bis(2-chloroethyl)-1-nitroso-.

CCNU: NSC-79037; CAS reg. No. 13010-47-4; urea, 1-(2-chloroethyl)-3-cyclohexyl-1-nitroso-.

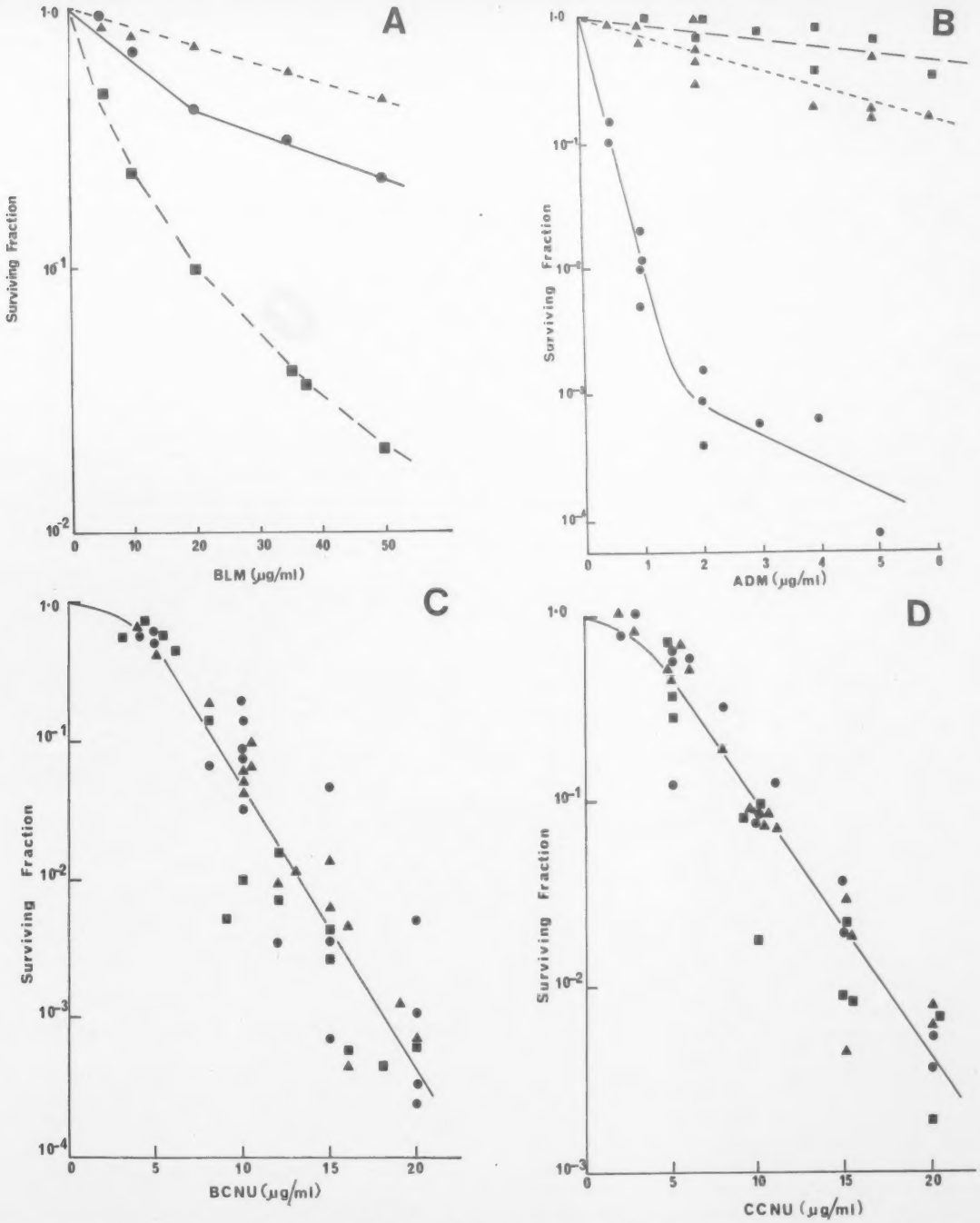

FIGURE 2.—*A*. Change in surviving fraction of EMT6 cells in vitro with dose of BLM; drug exposure time = 2 hrs. *B*. Change in surviving fraction of EMT6 cells in vitro with dose of ADM; drug exposure time = 1 hr. *C*. Change in surviving fraction of EMT6 cells in vitro with dose of BCNU; drug exposure time = 1 hr. *D*. Change in surviving fraction of EMT6 cells in vitro with dose of CCNU; drug exposure time = 1 hr. ● = exponential-phase cells; ▲ = early plateau-phase cells; ■ = late plateau-phase cells. [*B*, *C*, and *D* are reprinted from ref 7.]

DISCUSSION

BLM.—We have previously summarized the results of various workers for the response of cells in vitro to BLM and have been unable to find any consistent factor which explains the different relative responses of exponential- and plateau-phase cells (6). It is clear, however, that plateau-phase cells may in some circumstances be very much more sensitive to BLM than are exponential-phase cells (3,4). Our in vivo results indicate that cells in lung nodules may initially be less sensitive than cells in solid tumors, but that this trend may be reversed when the "repair of potentially lethal damage" phenomenon has operated. It therefore seems likely that any preferential action of BLM against slowly proliferating cells can only be exploited if a method of inhibiting "repair of potentially lethal damage" can be found.

ADM.—Both our own in vitro results and those of Barranco and Novak (5) indicate that rapidly dividing cells are much more sensitive than slowly dividing cells to this agent. Our in vivo results, however, show no such large differential. It has been recently shown that the sensitivity of cells in the EMT6 solid tumor is greatly increased if the tumor is heated, due to increased access of drug into the cell (15). It may be, therefore, that the high sensitivity of exponential cells in vitro is caused by high membrane permeability during the prevalent growth conditions rather than by the state of proliferation per se.

BCNU and CCNU.—Our in vitro results showing no change in sensitivity between the various growth phases are in disagreement with the results of other workers (3,4,16) who have shown exponential-phase cells to be less sensitive than plateau-phase cells to these agents. The data from our in vivo system, however, are in accordance with our in vitro findings for this cell line.

There does, therefore, appear to be a considerable degree of agreement between our in vitro and in vivo results, although in one instance, the in vitro result appears to be positively misleading. The plateau-phase model may therefore be a useful one for obtaining preliminary data, so long as the in vitro results are applied to the same cell line in vivo and are not taken to have any universal validity.

REFERENCES

1. HAHN GM, and LITTLE JB. Plateau phase cultures of mammalian cells: an in vitro model for human cancer. Curr Top Radiat Res 8:39–83, 1972.
2. RAY GR, HAHN GM, BAGSHAW MA, ET AL. Cell survival and repair of plateau-phase cultures after chemotherapy—relevance to tumor therapy and to the in vitro screening of new agents. Cancer Chemother Rep 57:473–475, 1973.
3. HAHN GM, GORDON LF, and KURKJIAN SD. Responses of cycling and noncycling cells to 1,3-bis(2-chloroethyl)-1-nitrosourea and to bleomycin. Cancer Res 34:2373–2377, 1974.
4. BARRANCO SC, NOVAK JK, and HUMPHREY RM. Response of mammalian cells following treatment with bleomycin and 1,3-bis(2-chloroethyl)-1-nitrosourea during plateau phase. Cancer Res 33:691–694, 1973.
5. BARRANCO SC, and NOVAK JK. Survival responses of dividing and nondividing mammalian cells after treatment with hydroxyurea, arabinosylcytosine, or adriamycin. Cancer Res 34:1616–1618, 1974.
6. TWENTYMAN PR, and BLEEHEN NM. Changes in sensitivity to radiation and to bleomycin occurring during the life history of monolayer cultures of a mouse tumour cell line. Br J Cancer 31:68–74, 1975.
7. TWENTYMAN PR, and BLEEHEN NM. Changes in sensitivity of cytotoxic agents occurring during the life history of monolayer cultures of a mouse tumour cell line. Br J Cancer 31:417–423, 1975.
8. TWENTYMAN PR, WATSON JV, BLEEHEN NM, ET AL. Changes in cell proliferation kinetics occurring during the life history of monolayer cultures of a mouse tumour cell line. Cell Tissue Kinet 8:41–50, 1975.
9. TWENTYMAN PR, and BLEEHEN NM. Studies of "potentially lethal damage" in EMT6 mouse tumour cells treated with bleomycin either in vitro or in vivo. Br J Cancer 32:491–501, 1975.
10. ROCKWELL SC, KALLMAN RF, and FAJARDO LF. Characteristics of a serially transplanted mouse mammary tumor and its tissue-culture-adapted derivative. J Natl Cancer Inst 49:735–749, 1972.
11. WATSON JV. The cell proliferation kinetics of the EMT6/M/AC mouse tumour at four volumes during unperturbed growth. Cell Tissue Kinet 9:147–156, 1976.
12. TWENTYMAN PR, and BLEEHEN NM. The sensitivity to bleomycin of a solid mouse tumour at different stages of growth. Br J Cancer 30:469–472, 1974.
13. TWENTYMAN PR, and BLEEHEN NM. The sensitivity to cytotoxic agents of the EMT6 tumour in vivo. Comparative response of lung nodules in rapid exponential growth and of the solid flank tumour. Br J Cancer 33:320–328, 1976.
14. HAHN GM, RAY GR, GORDON LF, ET AL. Response of solid tumor cells to chemotherapeutic agents in vivo. Cell survival after 2 and 24 hour exposure. J Natl Cancer Inst 50:529–533, 1973.
15. HAHN GM, BRAUN J, and HAR-KEDAR I. Thermochemotherapy: synergism between hyperthermia (42–43°) and adriamycin (or bleomycin) in mammalian cell inactivation. Proc Natl Acad Sci USA 72:937–940, 1975.
16. HAGEMANN RF, SCHENKEN LL, and LESHER S. Tumor chemotherapy: efficacy dependent on mode of growth. J Natl Cancer Inst 50:467–474, 1973.

Computer Simulation of Leukemia Therapy: Combined Pharmacokinetics, Intracellular Enzyme Kinetics, and Cell Kinetics of the Treatment of L1210 Leukemia by Cytosine Arabinoside [1,2]

T. Lincoln,[3,4,*] P. Morrison,[4] J. Aroesty,[4] and G. Carter [4]

SUMMARY

An integrated mathematic computer-based model of the pharmacokinetics, intracellular enzyme kinetics, and cell kinetics of the treatment of L1210 leukemia by cytosine arabinoside (ara-C) is described. The compartment model of Bischoff and Dedrick is extended to the intracellular level by inclusion of equations describing the phosphorylation, dephosphorylation, and deamination of ara-C with enzymatic feedback control. The activities of kinase, deaminase, and phosphatase are explicitly included in the models and are estimated from relevant data. Cell proliferation is described by a continuous-flow mathematic model in which cellular maturation and cell-to-cell variability in maturation rates are key variables. Cell proliferation is related to intracellular biochemistry through mathematic expressions which relate cell lethality and progression delay to the time course of intracellular ara-CTP. In vitro and in vivo experiments performed in a number of laboratories are compared by simulation. The most sensitive parameters in dose-response and cell-survival simulations are deoxycytidine kinase activity, ara-CTP half-life, renal clearance of ara-C, and cell-kinetic parameters for proliferation and cell killing. Progression delay is vital to the realistic simulation of divided-dose schedules. By comparative simulation we have identified areas of uncertainty which can be classified by a few additional measurements. The applications of simulations combining pharmacokinetic, biochemical, and cell-kinetic data in vitro and in vivo are discussed, exploring consistency among different measurements, and relating experimental protocols to clinical treatment.

[Cancer Treat Rep 60:1723–1739, 1976]

We have undertaken a difficult problem in quantitative biology: to simulate in the mouse the pharmacokinetic distribution of cytosine arabinoside (ara-C) to tissues, to simulate the intracellular biochemical kinetics of ara-C phosphorylation, dephosphorylation, and deamination, and to simulate the detailed effects of this drug on the proliferation cycle of the L1210 in vitro and in vivo. Our interest is in clinical disease, but we have chosen the L1210 tumor because of the richness of the experimental data (Chou et al [1]; Bhuyan et al [2]; Skipper et al [3]; Borsa et al [4]; Dombernowsky and Hartmann [5]; Ho [6]; Bischoff et al [7]; Dedrick et al [8]; and Edelstein et al[5]).

Other experimental tumors with smaller growth fractions would, of course, be more consistent with our objective, but the availability of needed biochemical data and the possibility of in vitro-in vivo correlation for both progression delay and cell lethality made L1210 a natural starting point. Our integrative approach, illustrated in figure 1, poses the following questions: Do we understand these

[1]Supported by Public Health Service grants CA-12369, CA-19663, and CA-14088 from the National Cancer Institute, National Institutes of Health, Department of Health, Education, and Welfare.

[2]Cytosine arabinoside: NSC-63878; CAS reg. No. 69–74–9; cytosine, 1-β-D-arabinofuranosyl-, monohydrochloride.

[3]The University of Southern California Comprehensive Cancer Center, Los Angeles.

[4]The Rand Corporation, Santa Monica, Calif.

*Reprint requests to: Thomas L. Lincoln, MD, Physical Sciences Department, The Rand Corporation, 1700 Main St, Santa Monica, Calif 90406.

[5]Edelstein M. A model for the action of 1-β-D-arabinofuranosylcytosine. PhD dissertation, Washington University, 1975.

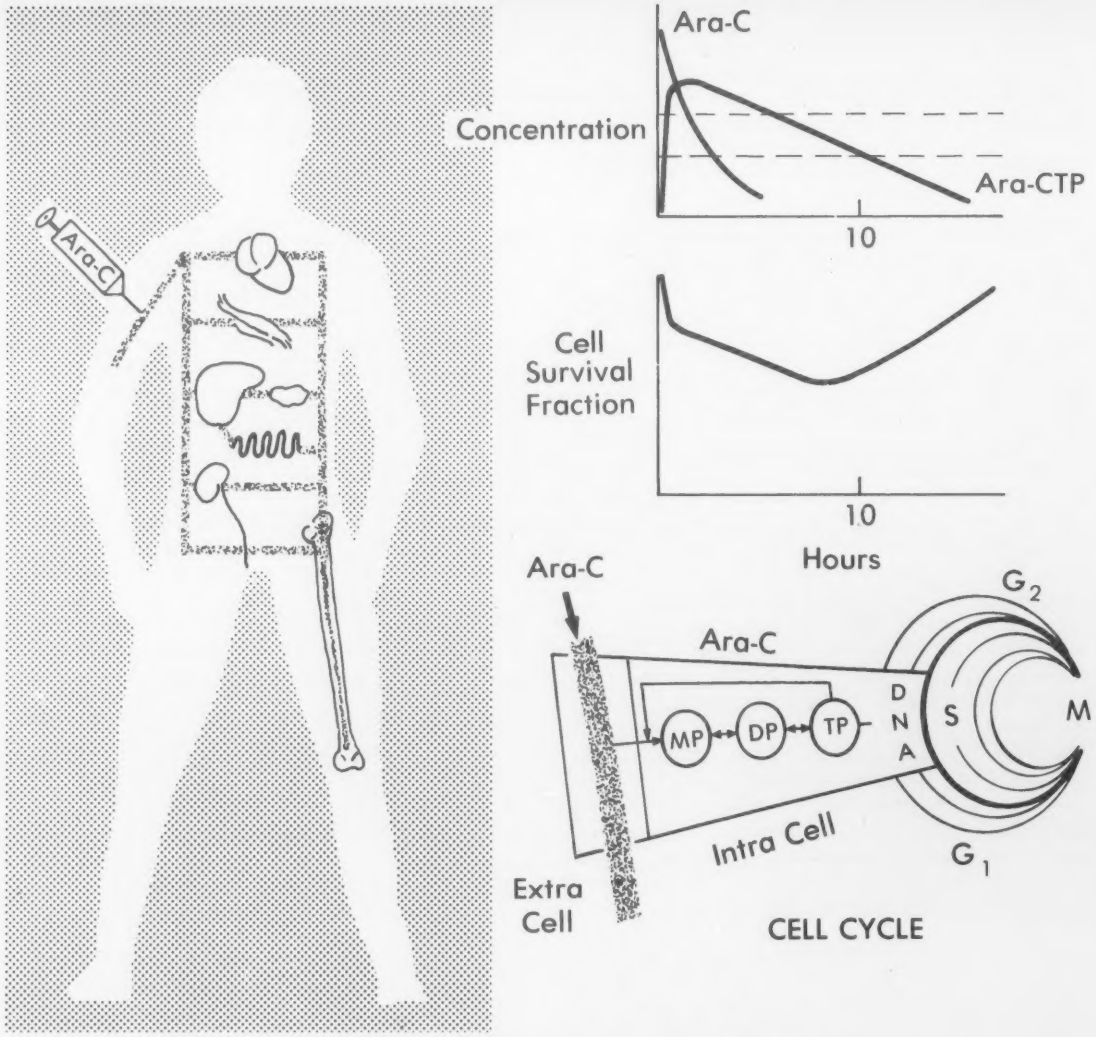

FIGURE 1.—Pharmacokinetics, intracellular enzyme kinetics, and cell proliferation kinetics are simultaneously simulated using mathematic computer-based descriptions of drug distribution; excretion and metabolism; the net conversion of ara-C to its active form within the cell, ara-CTP; and the effect on tumor-cell survival of the time history of ara-CTP.

biologic components well enough to model them individually? And do we understand them well enough to integrate them and to scale them to man?

These questions can be answered with a cautious yes. The questions, however, must be considered on two levels. One level is intimately related to the data at hand: how should data about the same system be compared when the results stem from different laboratories using different methods and different animal or tumor strains, or when investigators take different measurements? The other level poses the problem of extrapolation and biologic generality: how should the specific results of these particular biologic experiments be used to solve the complex problems of clinical treatment?

APPROACH

We use the experimental approach of mathematic simulation and introduce models which follow the biologic process *in detail* to produce *more* than curves that fit. To introduce a precise biochemical

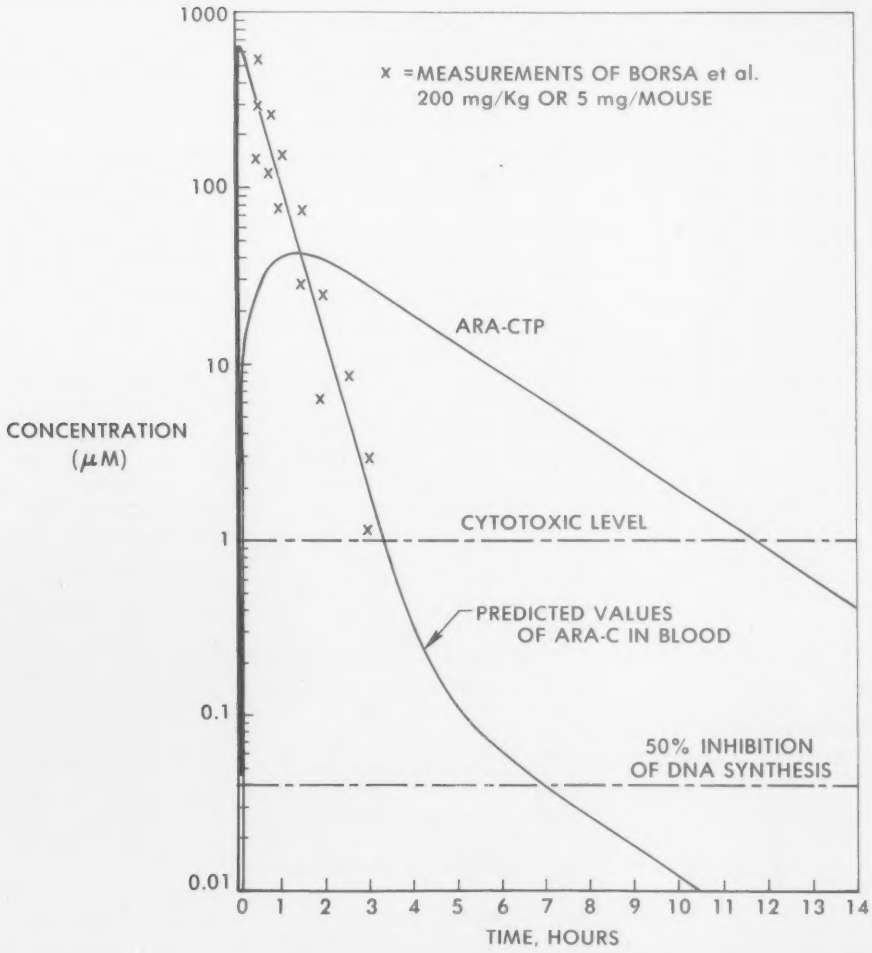

FIGURE 2.—The pharmacokinetic simulation of ara-C and ara-CTP. Note that intracellular levels of ara-CTP which are either cytotoxic or cytostatic persist well after blood levels of ara-C have decayed to insignificance.

mechanism, we have extended the models of Bischoff et al (7) at the intracellular level to include the mixed inhibition enzyme kinetics of Dixon and Webb (9). The parameters of these models are physiologic and biochemical so that procedural and species differences can be introduced by changes in coefficients (Dedrick et al [8] and Lincoln [10]). These models have then been recalibrated using the tissue-specific data of Chou et al (1) as described elsewhere (Morrison et al [11]). Figure 2 summarizes these results. The most significant new finding by experiment and by our calibration simulations is the ara-CTP level in tissues which decays much more slowly than the ara-C levels in blood. For example, at a dose of 5 mg/mouse, ara-CTP levels in the spleen are at cytotoxic levels for 11 hours and can appreciably inhibit the synthesis of DNA for ~ 15 hours. This is contrasted with negligible blood levels of ara-C after 5 hours. Because of the rapid phosphorylation of ara-C and the long half-life of ara-CTP, ara-CTP levels are closely related to peak ara-C levels in tissues. Here we integrate these results with cell kinetics.

The cell kinetic formulation describes the process

of cell maturation from cell division through DNA synthesis to mitosis in such a way that variations in rates of DNA synthesis or labeled nucleotide incorporation are explicitly modeled. The cell-kinetic model must also interpret modern kinetic measurements of DNA content which divide a cell population according to maturity.

To do this we assume maturation to be a continuous process and individual cells to differ in their rate of maturation. To interpret the perturbation of cell-kinetic systems, the distribution of cells over cycle times and the distribution of cells according to the proliferative maturity must be explicitly represented and followed as a function of time. The explicit inclusion of biologic processes related to progression delay extends the earlier work of Shackney (12) and Himmelstein and Bischoff (13).

Rubinow's maturity-time representation (14) has been extended (Aroesty et al [15]) as a continuous-flow maturation model to represent cell proliferation as summarized in figure 3. Intercellular variability in maturation rate is explicitly included in this description.

The rate of cell maturation is related to the elapsed time since cell birth or age, a, according to the equation

$$d\mu = \frac{da}{\left[\frac{T}{\alpha(\mu,t)}\right]} \qquad [1]$$

where $\alpha(\mu,t)/T$ is the rate of maturation in the presence of drug effects. If no drug effect is present, then $d\mu = da/T$, and T is the cell-cycle transit time.

The fundamental equation for the cell-density function $n(t,\mu,T)$ in figure 3 becomes

$$\frac{\partial n}{\partial t}(t,\mu,T) + \frac{\partial}{\partial \mu}\left\{\frac{\alpha(\mu,t)n(t,\mu,T)}{T}\right\} = -\lambda(t,\mu,T)n(t,\mu,T) \qquad [2]$$

where λ is the cell-death function and represents both drug effects and natural tumor attrition.

The basic cellular conservation law for describing cell proliferation is:

[the time rate of change in the number of cells of a given maturity] = [the difference between the number of cells which, as they age, mature into and out of this maturity level] − [the number of cells of this maturity level which are killed]

While the continuous maturity variable, μ, and the maturation rate, $\alpha(t,\mu)/T$, are appropriate conceptual variables for describing this model, it is sometimes more convenient to replace μ by its equivalent in age.

In figure 3 the volume bounded by the cell-density function corresponds to the total number of cells, N(t), and the phases of the cell cycle, G_1, S, G_2, and M, are shown as wedge-like regions. However, the latter is a simplification and is not vital to our approach. One consequence of this is that the durations of the individual phases of the cell cycle are highly correlated.

In the present simulations, possible correlations between parents and offspring have been neglected. The simplest version of the kernel function boundary condition consistent with observations on the distribution of maturation rates is

$$\frac{n(t,0,T)}{T} = \beta\, G(T) \int_{T_{min}}^{T_{max}} n(t,1,T')\,\frac{dT'}{T'}. \qquad [3]$$

G(T) was chosen to be a displaced γ distribution, described by a mean cycle time $\overline{T}$, a minimum cycle time T_{min}, and a coefficient of variation.

As cell populations become more dense, there are changes in cell-cycle time distributions and in the proportion of cells which do not cycle or which die. These phenomena are among those which are most indirectly measured and incompletely understood. Here, we consider only rapidly growing cell populations which may exhibit cycle prolongation and increased cell death but for which it appears unnecessary to make added assumptions about a G_0 phase to account for a change in growth fraction.

Our models consider natural attrition, the accumulation of nonviable cells, and changes in the attrition rate due to ara-CTP. Thus, we are prepared to analyze differences in cell loss in early, rapidly growing tumors and in older ascites tumors where the cells are denser and the behavior exhibits relatively slow net growth.

We have calibrated this model against the labeled mitosis data of Dombernowsky and Hartmann (5) for the L1210 and the JB1. A single model formulation was developed which could reproduce the percent labeled mitosis (PLM) curves and the instantaneous and continuous labeling indices (LI and CLI) for data taken at three sample points along the Gompertzian growth curves for these tumors. To match the CLI we assumed a subgroup of cells which are "sterile," ie, which mature to the point of division, but are unable to divide successfully and die. The changes observed with increasing cell density could be obtained by making the mean and minimal cycle times a function of N(t). Simulations could be obtained for the two tumors which differed only in the coefficients assigned to each without alteration of the model structure.

To include the effects of ara-C, we developed a cell death function $\lambda(t,\mu,T)$ which is related to ara-CTP

$$N(t) = \int_{T_{min}}^{T_{max}} \int_{0}^{1} n(t, \mu, T)\, d\mu dT \quad \text{(Total Number of Cells)}$$

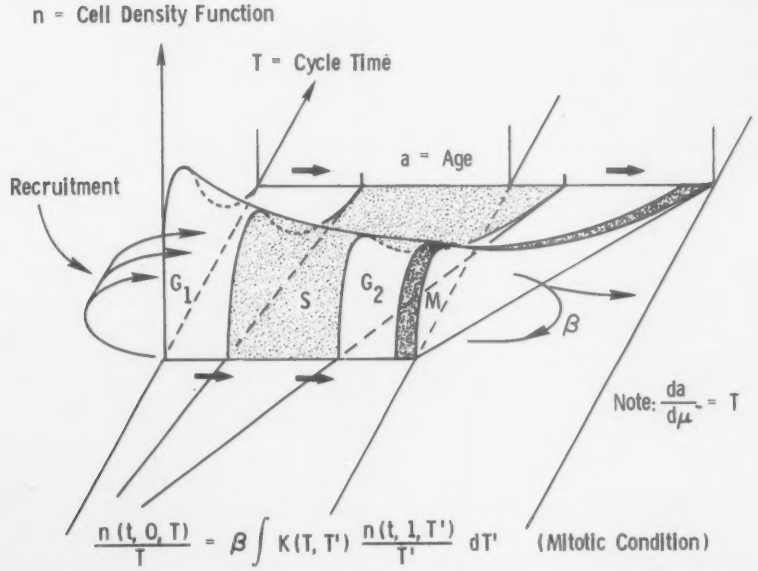

FIGURE 3.—The domain of the cell-density function, a 3-dimensional representation of the dependence of the cell-density function on cell age and cycle time. The total No. of cells is related to the volume covered by the curved surface. When the age, a, equals the cycle time, T, then cells divide resulting in β-daughter cells per division. T_{min} and T_{max} correspond to the minimum and maximum cell-cycle times. The maturity variable μ relates to continuous landmarks in the cell cycle, ie, $\mu = 0$ corresponds to newly divided cells, and $\mu = 1$ corresponds to initiation of mitosis. β is the average No. of daughter cells per division and K(T,T') is a kernel function which relates the maturation rate of a daughter cell to that of its parent.

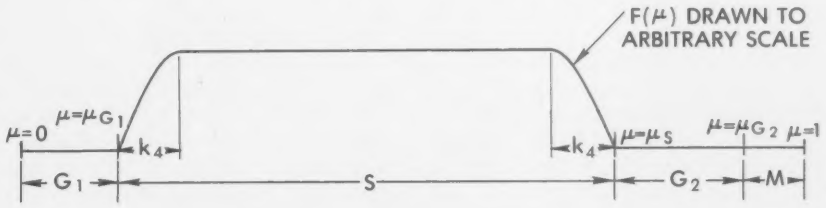

FIGURE 4.—The shape of the ara-CTP sensitivity function $F(\mu)$, in maturity space. $F(\mu)$ is zero in G_1, G_2, and M, gradually rises to its maximum in S, and then decays symmetrically.

concentration over time and to proliferative kinetics. The exact means by which ara-CTP exerts its lethal effect are not known. One suggestion (Karon et al [16]) is that ara-CTP is incorporated into DNA to produce lethal events. In the presence of ara-C, DNA synthesis is largely blocked by the inhibition of DNA polymerase by ara-CTP. Nevertheless, some ara-CTP residues are incorporated into newly formed sections of DNA (Silagi [17]; Graham and Whitmore [18]). This would eventually result either in the inability of a cell to produce correctly sequenced mRNA or in chain termination. Presumably, when the cell could not cope with either of these occurrences very long they would constitute lethal events. Another suggested mechanism is unbalanced growth: a lethal event due to the inhibition of DNA synthesis by ara-CTP while protein and RNA synthesis continues unaffected. In our model, death is determined uniquely by the concentration history of ara-CTP. Significant differences between cells lie in their varying abilities to synthesize or degrade ara-CTP and their cell-kinetic state. If this assumption is valid, only these differences must be taken into account to provide simulation of cell death which is consistent with either incorporation or unbalanced growth modes of action. The simplest way to represent the cumulative effect of ara-CTP is an integral over time. If cells did not progress through the cycle, an appropriate form would be

$$\frac{d\lambda(t,\mu,T)}{dt} = \frac{F(\mu)(ap_3)^{k_1}}{K_2 + (ap_3)^{k_1}} - k_3\lambda. \qquad [4]$$

However, since some cells do progress through the cycle in the presence of ara-CTP, the appropriate generalization is

$$\frac{\partial\lambda}{\partial t} + \frac{\alpha^{(t,\mu)}}{T}\frac{\partial\lambda}{\partial\mu} = \frac{F(\mu)(ap_3)^{k_1}}{K_2 + (ap_3)^{k_1}} - k_3\lambda. \qquad [5]$$

This extension of equation [4] reflects the requirement that λ be an intrinsic cell property, dependent on intracellular events. $F(\mu)$ is a maturity-dependent sensitivity function, k_1, K_2, and k_3 are constant parameters, and ap_3 is the intracellular concentration of ara-CTP.

The first term on the right-hand side of equation [5] is positive and always leads to an increase in the cell-death function. Cells can be exposed to high levels of drugs for a short time without toxicity, thus the second term, $k_3\lambda$, which always decreases the cell-kill function, allows cells to recover from low-level damage caused by ara-CTP. If ara-CTP is removed, the cell-kill function approaches zero with a half-life which varies inversely with k_3.

The sensitivity factor $F(\mu)$ has been introduced to account for the S-phase specificity of ara-CTP. Kim et al (19), for example, have shown that HeLa cells treated with ara-C in mid-S phase are at greater risk than cells at the beginning or end of S phase. $F(\mu)$ is non-zero only during S phase, thus allowing $\lambda(\mu,t)$ to increase in value only during this phase. It is assumed that $F(\mu)$ rises from zero at the beginning of DNA synthesis, is nearly constant over most of S phase, and then decays symmetrically to zero at the end of the synthetic period.

If the maturity at the beginning of S phase is defined as μ_{G_1} and at the end of S phase as μ_S, then $\mu_S - \mu_{G_1}$ is the maturity interval corresponding to DNA synthesis. The sensitivity function rises and falls as a Gaussian curve, maintaining a constant value over a central region, and is graphically represented by figure 4. This general shape is required to allow cells blocked in early S phase due to the inhibition of DNA polymerase to remain there at a reduced risk of death relative to mid-S phase cells. The present model (equations [2] and [5]) eventually permits these blocked cells to be killed, but only after they have progressed into the more sensitive part of S phase.

The equation for $\lambda(\mu,t)$ is most easily interpreted in the case where the primary lethal event is the incorporation of ara-CTP into DNA. This term, $\lambda(\mu,t)$, is assumed proportional to the amount of ara-CTP incorporated into potentially lethal sections of DNA at any instant of time, and $F(\mu)$ is identified with the maturity-dependent probability of incorporating an ara-CTP molecule into such a lethal gene. The term $(ap_3)^{k_1}/[K_2+(ap_3)^{k_1}]$ represents the kinetics of incorporation generalized to include the case of allosterism, and $k_3\lambda$ represents the effects of excisional repair. The parameter k_3 does not depend on ara-CTP because it has been shown (Rama Reddy et al [20]) that the repair enzyme, at least in *E. coli*, is not inhibited by ara-CTP.

The representation of ara-C-induced progression delay is highly simplified. The rate of maturation in S phase is assumed to be reduced from the normal value (1/T) by an amount proportional to the percent inhibition of DNA synthesis which has been determined experimentally by Chou et al (1) as a function of ara-CTP concentration. Thus, $\alpha(\mu,t)$ is determined by the line drawn through Chou's data shown in figure 5 for S phase and is unity outside of S phase.

ESTIMATION OF PARAMETERS

The most difficult area is the estimation of constants and parameters for the various model components. This is an exercise in consistency and plausibility, requiring careful comparison of conflicting and often incomplete data obtained from different

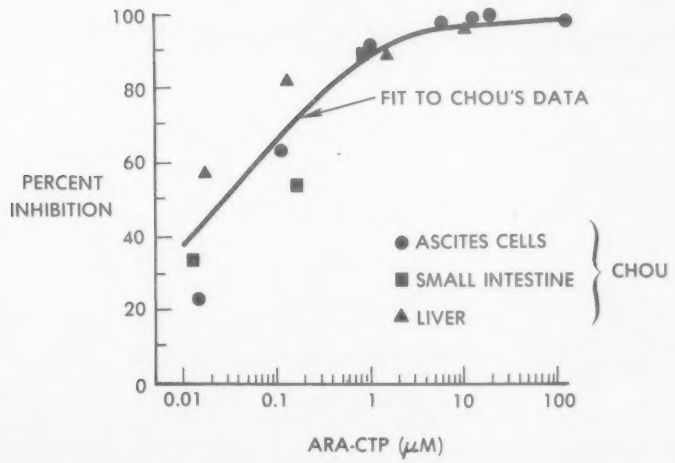

FIGURE 5.—The relationship between progression delay and ara-CTP levels in mice using Chou's (ref 1) data. The fit to Chou's data, which was based on thymidine incorporation, is used to determine $\alpha(\mu,t)$ in equation [6].

laboratories under differing experimental conditions.

To model the effect of ara-C on the L1210, we examined the in vitro experiments of Bhuyan et al (2), the survival curves for L-cells of Graham and Whitmore (18), and the L1210 in vivo measurements by Chou et al (1) and Edelstein et al.[6]

Enzyme activities appear explicitly in the equations governing the time history of ara-CTP, but the requisite activity data have not yet been gathered for these particular L1210 strains which are used in survival and progression-delay studies. A sensitivity analysis of these equations (Morrison et al [11]) indicated that deaminase activity could be estimated from ara-C/ara-U ratios in plasma; kinase activity could be estimated from short-term (1 hour) measurements of ara-CTP and the insensitivity of predicted values to phosphatase levels; and phosphatase activities could be estimated from the measured ara-CTP half-life at longer times (8 hours). It was found that consistency across different laboratories and different L1210 strains could be established by permitting kinase activity to assume different numerical values for each laboratory.

This must be considered a provisional resolution of the problem of inadequate enzyme activity data. Until such data are available, it is supported by the observation that salvage enzymes such as deoxycytidine kinase are suppressed in different cell lines. The original extract values of Ho (6) had been shown earlier (Morrison et al [11]) to lead to accurate simulations of ara-CTP levels in normal murine tissues, but it was necessary to increase the Ho-Schrecker (21) value for L1210 cells (V_k = 16.6 μM/minute) by a factor of four to accurately simulate Chou's measurements (1) on ascites L1210 cells.

Chou's measured relationship between DNA synthesis rate and ara-CTP levels is the quantitative basis for the representation of progression delay (fig 5). Bhuyan's (2) measurements of cellular survival and dose response in vitro are the quantitative basis for the representation of the cell-kill function (equation [5]). The expression is in terms of ara-CTP concentration, a quantity not measured by Bhuyan. Bhuyan did however measure DNA synthesis inhibition as a function of ara-C levels at 1 hour. If ara-CTP is responsible for inhibition of DNA synthesis, then the correspondence between Chou's and Bhuyan's measurements, combined with an enzyme-kinetic simulation of Bhuyan's experience, could be used to establish kinase activity for Bhuyan's culture. The kinase activity (V_k = 2.67 μM/minute) required to maintain correspondence between Chou's and Bhuyan's measurements was far less than our estimate of Chou's value, or even the extract value measured by Ho and Schrecker.

Measurements by Edelstein et al[6] represent a physiologically relevant in vivo model for the treat-

[6]See footnote 5.

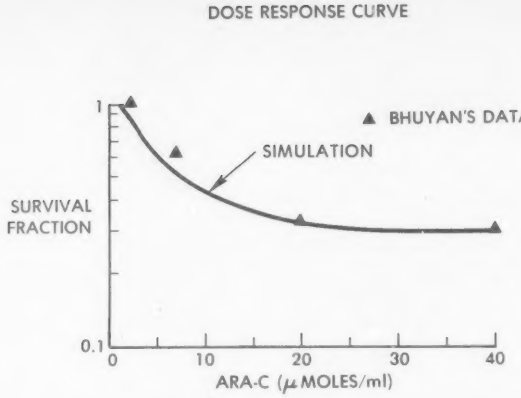

FIGURE 6.—Simulation of Bhuyan's (ref 2) measurements in vitro. Exposure of L1210 cells to ara-C for 1 hr followed by washing and plating of cells.

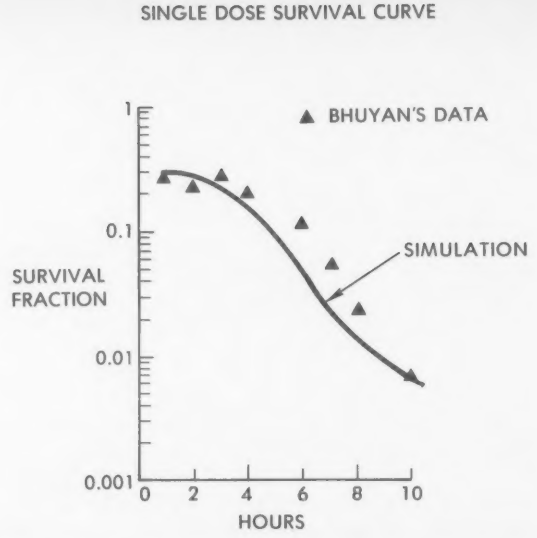

FIGURE 7.—Ara-C single-dose survival curve in vitro. Simulation of Bhuyan's (ref 2) measurements. 20 μM ara-C concentration for different times of exposure followed by washing and plating of cells.

ment of L1210. Tumor cells growing in the femoral cavity of the mouse are treated with ara-C and then transplanted to assess viability by means of the spleen colony assay. Simulations of these experiments were performed by using numerical values for organ sizes, blood flows, clearance rates, and enzyme activities of normal murine tissue taken for our earlier study (Morrison et al [11]). Consistency between Edelstein's survival data at 1 mg/mouse and the in vitro data of Bhuyan were then established by simulation, using a kinase value of V_K = 16.67 μM/minute, intermediate to the Chou and Bhuyan values.

The intracellular half-life of ara-CTP determines total length of exposure to cytotoxic effects and progression delay. We employed a half-life of about 2 hours, a value consistent with our earlier pharmacokinetic simulations. While this is twice the ara-CTP half-life measured in HeLa cells (Momparler et al [22]), this larger value coupled with the kinase value of 67 μM/minute for ascites cells and the Ho extract value for liver tissue, simulated Chou's measurements on both normal and tumor cells. The combination of greater kinase activity and shorter ara-CTP half-life (phosphatase) could perhaps account for the percent inhibition of DNA synthesis remaining at 8 hours; such parameters would overpredict ara-CTP tissue levels after 1 hour of exposure.

Cell-cycle coefficients for L1210 were obtained from simulation and comparison with data of Dombernowsky and Hartmann (5). For both L1210 and JB1, we found (and will present in future reports) that a distribution of cycle times corresponding to a displaced γ distribution characterized by three parameters—minimum cycle time, mean cycle time, and coefficient of variation—was appropriate for simulation. The coefficient of variation, the fraction of cycle time spent in each phase of the cell cycle, the difference between the mean time of transit and the minimum cycle time, and the sterilization rate (to be discussed below) were all independent of tumor size. The mean cycle time increased with increasing tumor burden in a way which was consistent with damped (Gompertzian) growth. The maturity intervals corresponding to the different phases of cycle could be approximated by constants, μ_{G_1}, μ_S, μ_M, independent of individual cell-cycle time. Thus, the phase durations are highly correlated.

The average cycle time of L1210 cells (5-day tumor) of 12 hours and a coefficient of variation of the cycle time distribution of 0.3 were obtained from simulation and comparison with data of Dombernowsky and Hartmann (5). The S phase interval in maturity space is defined by μ_{G_1} = 0.2 and μ_S = 0.92.

RESULTS

Our detailed comparisons of simulations to data impose a hypothetic consistency on the data from many laboratories and focus on those parameters which appear inconsistent. Of necessity, these are the parameters to which the simulations are sensitive: (*a*) the deoxycytidine kinase activity, (*b*) the

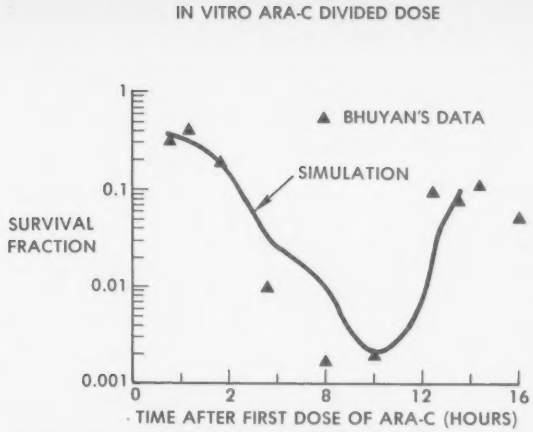

FIGURE 8.—Ara-C divided dose in vitro. Simulation of Bhuyan's (ref 2) measurements. L1210 cells in vitro are exposed to 1 hr of ara-C at a concentration of 20 μM and then exposed, after various time intervals, to a second dose at the same level; the cells are then washed and plated. The simulation, in this instance, is very sensitive to both ara-CTP level and progression delay.

ara-CTP half-life, (*c*) the renal clearance of ara-C, (*d*) the shape of the ara-CTP kill function, and (*e*) the distribution of cells in the cell cycle perturbed by cell kill and progression delay.

The simulation of Bhuyan's in vitro measurements of ara-C cytotoxicity is shown in figures 6–8. Figure 6 shows our simulation and the dose response obtained by Bhuyan when cells were exposed for ara-C for 1 hour, washed, and then subjected to a plating assay to determine cell survival. But, because of the long half-life for decay of ara-CTP, and because the nucleotide must be dephosphorylated before it leaves the cell, cell washing does not terminate the effect of the intracellular levels of ara-CTP. This is a consistent theme of our simulations. A 1-hour in vitro exposure to ara-C is equivalent to a much longer exposure to ara-CTP, the exact length depending on kinase levels and ara-C levels.

Figure 7 compares the simulated survival curve for a continuous exposure to 20 μM ara-C with the data of Bhuyan. The set of biochemical/cell-kinetic

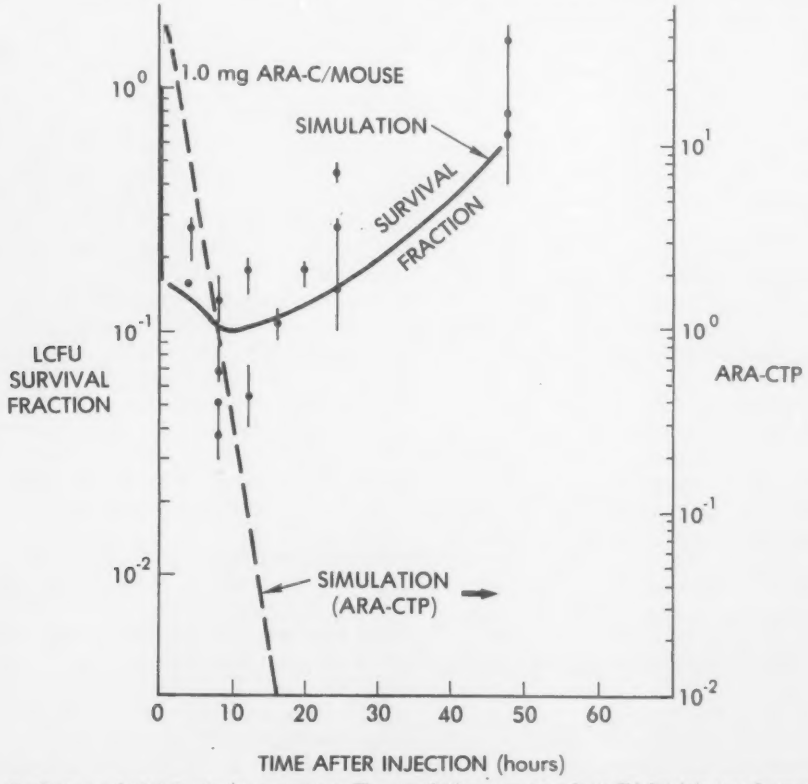

FIGURE 9.—Ara-C effects on L1210 in vivo, 1 mg/mouse. The simulation corresponds to Edelstein's (*see* footnote 5) measurements, where 2×10^6 L1210 cells are inoculated iv into $C3D2F_1$ mice, and a single iv injection of ara-C is given on Day 4. At various times after the ara-C injection, the femoral marrow of the mice is removed, and the number of leukemic colony-forming units are determined using the spleen colony assay. Simulated levels of ara-CTP are also shown. Significant inhibition of DNA synthesis exists for 14 hrs, by comparison with fig 6.

coupling parameters, described in equation [5] and figure 4, is chosen on the basis of the simulations shown in figures 6 and 7.

Figure 8 presents the results of Bhuyan's split-dose experiments and our corresponding simulation. Cell kill due to the second dose is sensitive to the intracellular half-life of ara-CTP. If the half-life is long, the L1210 cells remain blocked in the very early part of S phase where the values of the sensitivity function, $F(\mu)$, are low (*see* fig 4). They do not progress into the more lethal mid-S phase until much too late to account for the position of the first minimum in figure 8 (the time of maximum kill due to the second dose). The simulation reproduces the data of Bhuyan relatively well but shows a slight delay in the onset of maximum kill. A higher deoxycytidine kinase activity and a 50-minute ara-CTP half-life could also account for this split-dose data but such a short half-life would be inconsistent with the DNA synthesis-recovery data of Chou.

The response of L1210 cells growing in the femoral marrow of leukemic mice to single injections of ara-C was simulated and compared with the experiments by Edelstein et al.[7] Figure 9 shows the simulation of a dose of 1 mg/mouse, roughly equivalent to the in vitro work of Bhuyan. The simulations were performed in two steps. First, the ara-CTP concentration in mouse marrow infiltrated with L1210 cells was simulated after two modifications to our earlier work: (*a*) the competition of 1 mM AMP for the 5'-nucleotidase enzyme is included in the kinetic expression for the phosphatase, and (*b*) the nucleotide ratios of ara-CTP and ara-CDP to ara-CMP are reassigned to equal 7.1 and 1.6, respectively, agreeing with Chou's (1) measurements for the L1210 system. These two changes appear to be self-cancelling, since the computed half-life of ara-CTP is unchanged.

The ara-CTP profiles were then used in equations [2] and [5] to predict cellular surviving fraction, in order to compare with the measurements employing the spleen colony assay. We note again that the numerical parameters in those equations were based on Chou's and Bhuyan's data, and the required consistency between the Edelstein in vivo measurements and the others was achieved by choosing the appropriate kinase value. Our additional simulations of other doses are shown in figures 10 and 11. Figure 10 shows that additional cellular lethality after the initial killing of S-phase cells is negligible at a low dose of 0.1 mg/mouse. Cellular progression is delayed for 15 hours, blocked cells rapidly desynchronize, and the growth rate quickly assumes its exponential (asynchronous) value. It is difficult to compare the simulation with the scattered data in this instance. Qualitatively, there is similarity but the experiments show slight but pronounced reduction in viability until the time of significant regrowth. These are the levels which roughly correspond to clinical doses of ara-C.

The high-dose simulation, figure 11, is for 10 mg of ara-C per mouse. Again, there is reasonable agreement between predicted simulation and experimental measurement. An interesting feature of this simulation, and the data, is that the effect of a high dose of ara-C, even at very short times of exposure, is to kill many more cells than are in S phase. For example, our predicted value of short-exposure surviving fraction is $< 7\%$ of the cells. This suggests that most of the cells which were in cell-kinetic sanctuary at the time of injection (G_1 and G_2 phases of cycle) were ultimately killed by the lethal amounts of ara-CTP remaining within the cell, even after the L1210 cells had been removed from the host animal, consistent with the data. This dose level approximates the exposure of L1210 cells to ara-C using the ip route in Skipper's best pulse-dose protocol.

DISCUSSION

Our simulation results point to measurements which would clarify remaining uncertainties. These include: the measurement of enzyme activities which control ara-CTP level and half-life; deoxycytidine kinase and phosphatase; the ara-CTP levels over time in tumor cells as a function of ara-C exposure; and renal excretion of ara-C and ara-U in the treated tumor-bearing mouse. Observations on changes in clearance as a function of water load corresponding to the volumes of saline used as a vehicle for ara-C injection would clarify the comparison of in vivo experiments. Cell-kinetic measurements which give total cell number as well as surviving fraction together with measures of metabolic viability would differentiate between the loss of replicative ability, cell death, and reversible quiescence.

The simulations show the importance of the enzyme activities which determine the level and the half-life of ara-CTP. We can show by simulation that if the half-life of ara-CTP is held constant for all experimental L1210 data as well as the cell-kinetic parameters, and if the cells are exposed to the appropriate measured or pharmacokinetically calculated dose of ara-C, then only the deoxycytidine kinase activity has to be varied according to the laboratory source of the L1210 cells in order to accurately reproduce and predict the experimental survival data.

[7] *See* footnote 5.

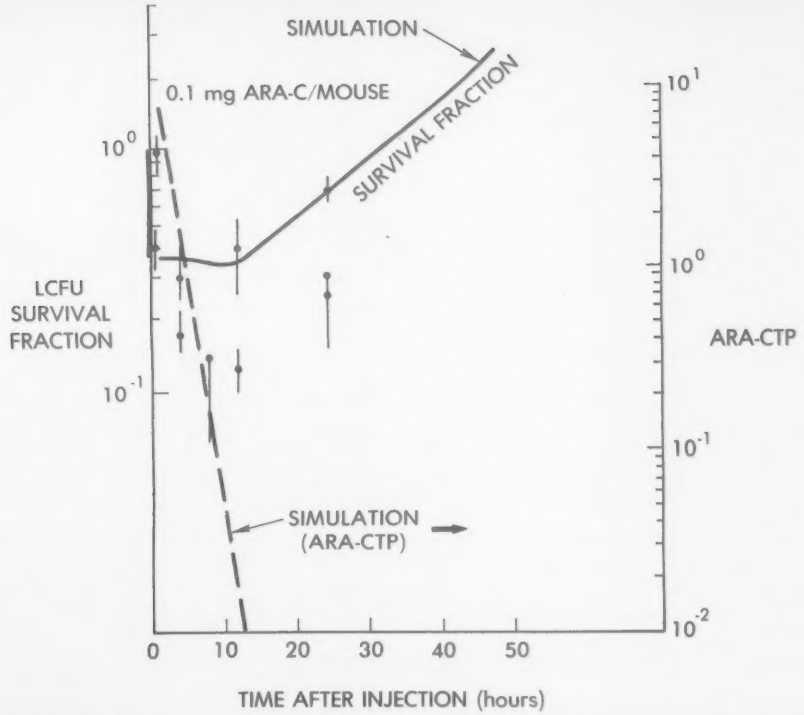

FIGURE 10.—Ara-C effects on L1210 in vivo, 0.1 mg/mouse. The simulation corresponds to Edelstein's (*see* footnote 5) protocol outlined in fig 9. At this dose, which is comparable to levels achieved during clinical treatment of AML, the primary effect after the initial cell killing is to delay regrowth of cell survivors. The simulated levels of ara-CTP suggest that appreciable inhibition of DNA synthesis exists for 12 hrs, by comparison with fig 6.

Thus, the experimental question is raised: do these L1210 cells vary from one to another in their kinase activity? A determination and comparison of the deoxycytidine kinase activity and ara-CTP half-life in the L1210 cells from the laboratories of Bhuyan, Chou, and Valeriote would resolve this question. The ara-CMP phosphatase enzyme has not been found to change its activity even in cells grown in ara-C-containing medium (Schrecker [21]). Thus the activity of this enzyme is a less likely candidate for variations among laboratories.

If differences in enzyme activities (or renal clearance) do not account for the differences between tissue culture and in vivo results, then the *hostility* of the tumor-cell environment must be taken into account. Host defense mechanisms could enhance the cytotoxic effect of a given level of ara-CTP so that the impact of the drug would be greater in vivo than in vitro. For example, macrophages might attack and remove sublethally damaged cells before they had a chance to recover,[8] or a balance between tumor growth and tumor-cell immunity might be tipped in favor of the host by increased cycle times due to progression delay.

At the more general level, these simulations of particular experiments shed light on some of the broad issues of cell kinetics and chemotherapy. As a matter of convenience, we label these issues with the name of the investigator who has posed the problem most clearly:

1. Steel's Dilemma[9]
   Why is it that cell-kinetic arguments derived from thymidine-labeling experiments do not predict the chemotherapeutic effects of cycle-sensitive agents?
2. Hartmann's Puzzle (Dombernowsky et al [5,23])
   How should the changing cell kinetics of grow-

[8]In vitro experiments to clarify the effect of activated macrophages on ara-C dose response could be performed using a modification of techniques of Holtermann OA, Lisafeld BA, Klein E, et al. Nature 257:229, 1975.

[9]Steel GG. Descriptive and operational cytokinetics. *In* Proceedings of the Symposium on Clinical Pharmacology, Jacksonville, Fla, Mar 1973.

Steel GG. Heterogeneity of tumor cell populations. *In* Proceedings of the Workshop on Clinical Usefulness of Cell Kinetic Information for Tumor Chemotherapy, Rijswijk, Netherlands, Oct 1974.

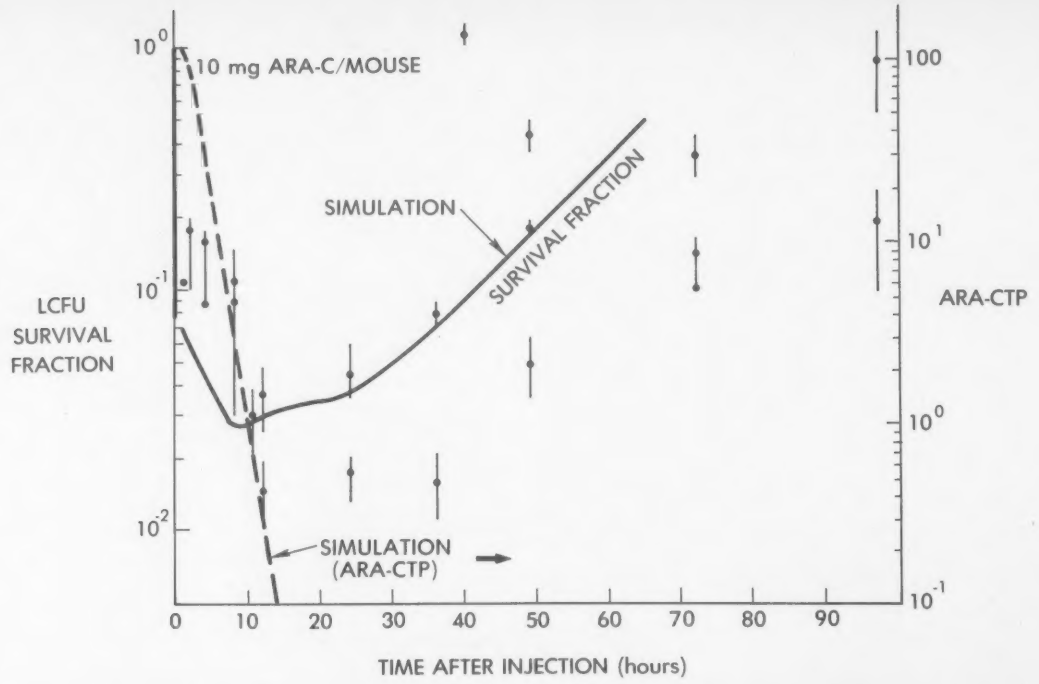

FIGURE 11.—Ara-C effects on L1210 in vivo, 10 mg/mouse. The simulation corresponds to Edelstein's (*see* footnote 5) experiments outlined in fig 9. At this high dose, the simulation predicts that the short-exposure surviving fraction is < 10%. Cells which were in G_1 and G_2 during initial exposure progress into a sensitive phase while ara-CTP levels are still high. The peak ara-CTP level with L1210 cells growing in marrow is comparable to that achieved by Skipper during his effective single ip injection treatment of L1210 ascites cells growing in mouse peritoneum.

ing tumor populations be modeled to consistently account for all of the data?

3. Rubinow's Paradox (Rubinow [14]; Aroesty et al [15])
   How should the cell-kinetic relatedness of daughter cells to parent cells be introduced so as to satisfy both the short- and long-term experimental results of synchronized cultures?
4. Skipper's Hypothesis (Skipper et al [3,24,25])
   How can the experimental success of pulse-dose ara-C therapy in an L1210-bearing mouse and the partial clinical success of the parallel therapy for acute myelogenous leukemia (AML) in man be compared now that it is known that the rates of tumor growth are not comparable and that the mechanisms of action of ara-C are significantly different from those assumed by Skipper's explanation?

It will be seen that all of these issues are more or less inter-related. All depend upon the capacity of the model to interpret one set of data, to be extended systematically to interpret additional kinds of experiments, and to be corrected for changes in mechanism as experiments improve.

STEEL'S DILEMMA

Steel challenges the premise that the passage through S phase as defined by continuous labeling with tritiated thymidine is equivalent to the lethal effects of high concentrations of ara-C on DNA synthesis. If these were equivalent, then the curve for all survivors as a fraction of the total time of exposure to ara-C would be the same as the curve of unlabeled cells after an equivalent exposure to tritiated thymidine. This is not the case. More cells are killed than are labeled, which does not lend itself to easy explanation. A second inconsistency pointed out by Steel concerns the extension of models which are designed to interpret PLM curves to include the phenomenon of continuous labeling.

Steel presents data on the same cell systems which demonstrate that his cell-cycle models (SAB1, SAB2, and SAB3), based on PLM data taken from

flash-labeling experiments (Steel [26]), do not predict the cumulative labeling with ^{3}H-TdR nor the cumulative cytotoxic effect of ara-C. The models underestimate both labeling and cytotoxicity in example after example. The failure of all three models, which offer different hypotheses for nonproliferating pools and cell death, underlines the observation that these concepts are not sufficiently flexible to "correct" his model.

He concludes that "the thymidine labeling data poorly predict the response of clonogenic tumor cells [to ara-C], and that the [SAB] models are even less 'useful.' "[10]

Our models resolve in large measure the inconsistency between ^{3}H-TdR labeling and ara-C cytotoxicity for the L1210 system by noting that the intracellular phosphorylation of ara-C forms a pool of ara-CTP which is dephosphorylated with a half-life of ≥ 90 minutes. Survival fractions in vivo and in vitro are measured at the time of transfer of cells to an ara-C-free medium after exposure. Cells exposed to sufficiently high doses of ara-C will contain lethal amounts of ara-CTP after transfer which will continue to kill cells as they enter S. We have shown that the ara-CTP pool can extend the effective exposure time by several hours; this is sufficient time to re-establish consistency between thymidine labeling and cytotoxicity, at least for the rapidly growing L1210.

Steel's inconsistency may in fact be associated with clonogenicity in other systems; however, our results suggest that pharmacokinetics and intracellular biochemistry must be considered in its resolution.

HARTMANN'S PUZZLE

Dombernowsky and Hartmann (5,23) and Jansson (27,28) have set themselves a complex modeling task which we call Hartmann's Puzzle. They consider a cell population growing in a limited environment. As the population density increases, overall growth slows down and the cell-cycle kinetics of the population changes. These investigators utilize four kinds of data at three different cell densities: (*a*) an LI, (*b*) a PLM curve, (*c*) a CLI, and (*d*) a distribution of DNA content.

The puzzle is to construct a model which will be consistent with the above data not only at one cell density but throughout the growth of the population. We complicate the puzzle by the additional caveat that the same model structure (with different parameter values) should be applicable to different cell types. Data on L1210, JB1, and Sarcoma 180 are available.

For these three tumors, Dombernowsky and Hartmann propose three separate models patterned after those of Steel. As in Steel's experience, the CLI gives a poor fit to each tumor, unless quiescent cells are introduced to improve it. The same model structure does not apply to all tumors. This inconclusive attempt adds further weight to the observed limitations of Steel's modeling approach. Steel's approach and ours may both be used to interpret PLM curves. However, as in Hartmann's Puzzle, where the consistency of more and more data is demanded, differences in the detailed description of cellular flow become important. We have obtained a reasonable fit to the data in Hartmann's Puzzle while still maintaining a structure which is consistent with intracellular enzyme chemistry.

An intriguing hypothesis from our explanation of Hartmann's Puzzle is a simple assumption about cell death which appears valid for the systems tested: some proportion of cells are presumed to be "sterilized" as a function of time, the proportion being a characteristic of the cell type and its environment. These sterilized cells (similar to Steel's doomed cells in concept) live to maturity, when they die instead of dividing. The sterilization rate independent of cycle time may be interpreted as an external influence measuring the "hostility" of the environment. In vivo, a proportion of that hostility may be the immune response. This hypothesis is susceptible to test by repeating a Hartmann's Puzzle experiment in a set of animals which are partially immunized against a particular tumor and comparing these results to a parallel set which is not immunized. The model parameters for these two cases should differ in one term only—the term for cell sterilization. Increased sterilization should represent increased immunologic resistance. Janik and Steel's (29) results for immunologically perturbed tumors support this position. It was shown that immunologic stimulation had little effect on PLM measurements, but showed more considerable effects on growth rate, implying the primary dependency of the sterilization rate on natural hostility.

Our use of Hartmann's Puzzle is designed to uncover a common cell-kinetic model structure which will fit a broad class of cell types. Differences in cell types should be representable by different sets of parameter values without ad hoc revisions to the structure itself. Thus we would expect to describe acute leukemic cell growth in a kinetic structure which is compatible with that used to describe the L1210, but with parameters appropriate to its slower growth rate and extensions to account for the observed degree of differentiation. Changing

[10] *See* footnote 9, 1974.

growth characteristics which are a function of cell density provide the framework for describing the competition between normal marrow and leukemic marrow.

RUBINOW'S PARADOX

This so-called paradox bears on the question of how the inheritance of cycle times by daughter cells contributes to neoplastic selection and tumor cell resistance. The problem also appears when one attempts to model PLM curves which show waves that extend beyond two cycles.

The paradox can be clearly demonstrated by attempting to interpret the decay of synchrony in a group of synchronized tetrahymena (Rubinow [14]; Aroesty et al [15]). In perfectly synchronized cells with the same cycle times, the population would grow in a large series of steps, each step marking a division and each step twice as large as the last. Where there is a distribution of cycle times, these steps appear as waves which damp out to an exponential curve as the cycle times are redistributed. The problem arises when one attempts to model the desynchronization which damps out these steps. Like ourselves, Rubinow has investigated the class of models which implies a certain biologic consistency in the rate of progression through the cell cycle. A cell is born with a given maturation rate which it keeps until division. A growing cell population is distributed over a range of maturation asynchronously.

At the time of mitosis, cells are reborn with new maturation rates which are chosen to yield a steady-state distribution comparable with experiment. New maturation rates may be assigned in many ways. At one extreme, daughter cells are assigned to maturation rates for a probability distribution which is independent of the parent cell. In this way a steady-state distribution can be continually maintained. At the other extreme of perfect heredity, each daughter cell can be assigned a maturation rate exactly like that of the parent. In this situation, rapidly dividing cells outgrow the slow ones after many generation times, and the maturation rate distribution becomes a δ-function centered at the shortest T.

When the decay of synchrony for tetrahymena is simulated using Rubinow's model and a random redistribution maintains the steady state for tetrahymena cycle times, the measured waves and the simulated waves do not match. Only in the long run, does the growth rate reach the appropriate steady-state value. However, if perfect heredity is assumed, the short-term match between the growth wave and the simulation is excellent, but in the long run the steady-state growth rate is that of the shortest cycle time.

Rubinow's paradoxic result shows that the von Foerster-type of mathematic model poses difficulties which cannot be overcome by a simple boundary condition. The problem is hardly approachable using the compartment-model system, but using the flow-model approach the problem can be resolved. The paradox appears when one is restricted to the two extreme cases of perfect heredity and random redistribution. It is also not solved by making simple proportional combinations of these two functions. An appropriate match requires a more complex set of assumptions: a form of heredity which incorporates a variance from a parent cell to daughter cell plus a bias to account for the drift of the mean and the maintenance of the steady-state distribution.

Our simulations confirm that PLM data can usually be interpreted neglecting heredity. Valleron's work (30) described at this conference suggests that there are other instances where heredity can play a significant role even during the short times associated with labeled mitoses data. Long-term exposure to chemotherapy can select cells with more rapid cycle times but the possible interplay between heredity and enzyme kinetics has not yet been examined either experimentally or by simulation.

SKIPPER'S HYPOTHESIS

Skipper's Hypothesis is that the treatment of L1210 in the mouse with ara-C is a good pharmacokinetic and cell-kinetic animal model for the treatment of acute leukemia in man (Skipper et al [3]). He observed that it took a very large single dose of ara-C to achieve a significant level of toxicity (LD10) in the mouse, but that a total dose less than one seventh as large as one ip injection distributed evenly over 16 days produced the same toxicity. The daily-dose regimen suppressed the tumor, but did not eradicate it. This same lower total dose distributed in smaller increments every 3 hours for 24 hours and repeated every fourth day yielded the same host toxicity. This pulse dose regimen "cured" the mice.

Skipper sketched a rationale for these results: the every 3 hours $\times$ eight-pulse-dose regimen kept the level of ara-C high enough for about 30 hours so that $> 99.9\%$ of the L1210 cells had entered the DNA synthesis and were exposed to lethal cytotoxic effects. Thirty hours included all but the tail of the distribution of L1210 cycle times while the host tissues were protected by the survival of low-growth fraction cells present in normal tissues. These cells passed through a drug-free window in the 3 days between courses. (In the daily regimen, a drug-free

window occupying a portion of each day was equally good for the host, but also provided a window for relatively short-cycle-time tumor cells.) The 3-day interval was too short for the L1210 cells to recover their previous population so that in a sequence of courses, all tumor cells were destroyed by the stepwise application to cell kill. This rationale suggested pulse-dose treatment schedules for AML chemotherapy in man, typified by the pulse-dose COAP regimens (Hart et al [31]). These were remarkably successful in achieving remission, but unlike the mouse have not eradicated the last proliferating cells in the human leukemias Freireich [32]). Moreover, in man, continuous iv ara-C at 100 mg/m^2 for 5–7 days has proved to be as effective as pulse-dose therapy every 8 hours at the same dose per day without increased toxicity (Freireich[11]). Clarkson et al (33) showed by classic labeling experiments that AML cells in man grow more slowly than normal cells. Thus, Skipper's formal argument as applied to man is undermined from both sides. Differential kill based on rapid growth was not a valid rationale, and the rationale for host toxicity could also not be supported.

As more information about the pharmacokinetics and metabolism of ara-C in mice and L1210 has been obtained, it has become clear that the reasons for Skipper's initial success are considerably more complex than originally supposed. Ara-C is converted within cells to a longer-acting active form, ara-CTP, which is cytotoxic at high intracellular levels and cytostatic at lower levels. These lower cytostatic levels "block" DNA synthesis causing progression delay (Chou et al [1]; Bhuyan et al [2]). The effect of multiple doses of ara-C on cells in the proliferative cycle can only be quantified if these features are taken into account. The fruitfulness of Skipper's Hypothesis needs no defense. The depth of our present understanding of ara-C both in the clinic and in the laboratory is in large measure the result of his proposal and the work which it engendered.

It is clear from the work of Bhuyan and Edelstein that a high dose of ara-C causes a limited cell synchrony. First, cells in S phase are killed. Cells entering S phase continue to be killed until the concentration of ara-CTP falls to a level where there is only progression delay. For an additional period of time, cells pile up at the beginning of S phase so that after this block is released there is an increased proportion of cells in the S phase and an increased susceptibility to a second dose. Divided-dose experiments quantify this result. These phenomena are important in explaining the Skipper L1210 experiment.

High dose alone has a very exaggerated effect on transplanted tumors. Our simulations of the Edelstein experiments[12] on L1210 growing in murine femoral marrow predict that 80% of those cells which are not in S phase at the time of exposure die when the animal is injected with a 10-mg dose, even if they are removed from host marrow within an hour.

For ip injection of ara-C into animals bearing ip L1210 cells, this effect is more pronounced. The initial high levels of ara-C in the cavity are rapidly phosphorylated to higher levels of intracellular ara-CTP within ascites cells than if the same dose is given iv or sc, so that even more tumor cells are killed. This results in an even greater therapeutic advantage.

The success of Skipper's protocol in the main would appear to depend largely on pharmacokinetic advantages achieved by route of administration and the long-term presence of ara-CTP. A cell-kinetic enhancement of these progression delays can also be demonstrated.

Although the same biologic processes are operative in AML, the situation is so different that the same explanation cannot hold. In Skipper's initial hypothesis he compared low cell densities in mice to high cell densities in man. Pulse-dose therapy with ara-C is effective in mice against the proliferation of L1210 at both high and low cell densities. In man, pulse-dose therapy appears to be effective only in the overt AML where the density of leukemia cells is high and the cell population is growing slowly, probably due to a lengthening of cycle times and to an increase in the death rate.

Thus the paramount question becomes: how does ara-C in pulse or continuous dose exhibit its effectiveness in the slow growing AML in relapse? Here results are measured by a striking loss in tumor mass, but there is a diminution of therapeutic advantage in the tumor-cell density decrease so that no more than a marrow remission is possible. We can at least propose an answer to this question which lies within the scope of our simulations. It places much more weight on the differential advantage of progression delay than on that of cell kill.

In man there appears to be little pharmacokinetic advantage. We have shown elsewhere (Lincoln et al [34]) that ara-C iv push offers an advantage in tissue distribution due to flow considerations, but that this advantage is virtually lost when the drug is given as a 15-minute infusion. There is no significant difference between these modalities, or indeed between pulse-dose push and continuous 5-day infusion. Normal hematopoietic tissue would appear to

[11]Freireich EJ. Personal communication, 1974.

[12]*See* footnote 5.

contain sufficiently high values of kinase (Ho and Frei [35]) to offer no protection. Differences in the level of deaminase do not appear to be as significant as was once supposed.

The simplest cell-kinetic proposal states that while both normal cells and tumor cells are killed by the drug, the more rapidly growing normal cells outgrow the slower growing tumor cells and re-establish a marrow remission. This advantage may be lost as the cell density of tumor cells falls and their cycle-kinetic times grow shorter to approximate those of normal cells. Rubinow has proposed a model which incorporates this instability in a hematopoietic control system.

Our models point to an additional factor which depends upon cell loss. Moore et al (36) have pointed out that the effectiveness of cycle-sensitive drugs in inducing remission in AML appears to be related to a high instability in the tumor population characterized by a high cell-loss rate in agar culture. If there is a cell loss via death or end-stage cells which is independent of maturation rate, then this loss will be enhanced by progression delay which will significantly slow the passage through the cell cycle. Such a cell loss might depend upon the inherent fragility of a tumor population, but it might also depend upon the hostility of the tumor environment. This hostility might be nothing more than a lack of nutritional components or the presence of certain toxic metabolites, or it might be the exposure to other drugs such as cyclophosphamide or vincristine, or it might involve host reactions including host-tissue immunity. For any of the above cases, the immediate result of progression delay would be a loss of tumor mass with the re-establishment of a new equilibrium at a lower level.

Only in the case of tissue immunity might a permanent advantage be gained. An enhanced immune response would increase the difference in loss rate between tumor cells and normal cells, facilitating remission and leading, in some cases at least, to the elimination of the last tumor cell. Only if a tissue-immune response against leukemic cells were present would an advantage be retained when the cell cycle is short. This response would be enhanced if the cycle time is prolonged by cytostatic doses of ara-C in the patient in remission. This may be the key to remission maintenance, which can be sustained with *bacillus* Calmette-Guérin-immune enhancement or with intermittent doses of agents such as ara-C as long as the patient exhibits tissue immunity (Gutterman et al [37]). Moreover, in patients treated with chemotherapy and immunotherapy who subsequently relapse, limited experience indicates (Freireich[13]) that a second remission is easier to achieve than in those cases which had received no immune enhancement.

The interaction among these mechanisms and their detailed relation to cell kinetics has not yet been modeled for lack of experimental data, although Janik and Steel's (29) work is highly suggestive.

Our approach to cell-cycle kinetics has been to include the variation in maturation rates associated with different cells, which will allow us to consider most of the above phenomena. However, we still neglect any intercellular variation in enzyme kinetics or nucleotide values. This is primarily because variation in maturation rate is the key to understanding labeling mitosis data, while biochemical and pharmacologic measurements are given as mean values, in the main. Experimental or clinical protocols involving synchronization or recruitment strategies may be sensitive to such variations. Presently, our simulations show desynchronization after a period of progression delay which is due to variation in maturation rate (cycle-time distribution). Other mechanisms for desynchronization may in fact be operating.

CONCLUSIONS

To accurately interpret the cell-kinetic in vivo chemotherapy experiments such as those of Skipper or Edelstein and to relate them to man, organ pharmacokinetics, intracellular pharmacology, and the proliferation kinetics of tumor cells must be integrated to expose the underlying biologic processes which are brought into play. This scaffolding appears to be an intricate and complicated way to organize our thoughts. Ultimately, an analysis of sensitivity may lead to simpler formulations, but for the present it is the only way to capture the subtlety needed for prediction and quantitative therapeutic manipulation.

REFERENCES

1. CHOU TC, HUTCHISON DJ, SCHMID F, ET AL. Metabolism and selective effects in 1-β-D-arabinofuranosylcytosine in L1210 and host tissues in vivo. Cancer Res 35:225–236, 1975.
2. BHUYAN BK, FRASER TJ, GRAY LG, ET AL. Cell-kill kinetics of several S-phase-specific drugs. Cancer Res 33:888–894, 1973.
3. SKIPPER HE, SCHABEL FM, JR, MELLETT LB, ET AL. Implications of biochemical, cytokinetic, pharmacologic, and toxicologic relationships in the design of optimal therapeutic schedules. Cancer Chemother Rep 54:431–450, 1970.
4. BORSA J, WHITMORE AF, VALERIOTE F, ET AL. Studies on the persistence of methotrexate, cytosine arabinoside and leukovorin in serum of mice. J Natl Cancer Inst 42:235–242, 1969.

[13]*See* footnote 11.

5. DOMBERNOWSKY P, and HARTMANN NR. Analysis of variations in the cell population kinetics with tumor age in the L1210 ascites tumor. Cancer Res 32:2452–2458, 1972.
6. HO DHW. Distribution of kinase and deaminase of arabinofuranosylcytosine in tissues of man and mouse. Cancer Res 33:2816–2820, 1973.
7. BISCHOFF KB, DEDRICK RL, ZAHARKO D, ET AL. Methotrexate pharmacokinetics. J Pharm Sci 60:1128–1133, 1971.
8. DEDRICK R, FORRESTER DD, and HO DHW. In-vitro in-vivo correlation of drug metabolism—deamination of 1-β-D-arabinofuranosylcytosine. Biochem Pharmacol 21:1–16, 1972.
9. DIXON M, and WEBB EC. Enzymes, 2nd ed. New York, Academic Press, 1964.
10. LINCOLN TL. Pharmacosimulation. *In* Traite de Pharmacologie Clinique (Giroud GP, et al, eds). In press.
11. MORRISON PF, LINCOLN TL, and AROESTY J. Disposition of cytosine arabinoside (NSC-63878) and its metabolites: a pharmacokinetic simulation. Cancer Chemother Rep 59:861–876, 1975.
12. SHACKNEY SE. A computer model for tumor growth and chemotherapy and its application to L1210 leukemia treated with cytosine arabinoside (NSC-63878). Cancer Chemother Rep 54:399–429, 1970.
13. HIMMELSTEIN KJ, and BISCHOFF KB. Models ara-C chemotherapy of L1210 leukemia in mice. J Pharmacol Biopharmacol 1:69–81, 1973.
14. RUBINOW SI. A maturity-time representation for cell populations. Biophys J 8:1055–1073, 1968.
15. AROESTY J, LINCOLN T, SHAPIRO N, ET AL. Tumor growth and chemotherapy: mathematical methods, computer simulations, and experimental foundations. Math Biosci 17:243–300, 1973.
16. KARON M, BENEDICT WF, and RUCKER N. Mechanism of 1-β-D-arabinosylcytosine-induced cell lethality. Cancer Res 32:2612–2615, 1972.
17. SILAGI S. Metabolism of 1-β-arabinofuranosylcytosine in L cells. Cancer Res 25:1446–1453, 1965.
18. GRAHAM FL, and WHITMORE GF. The effect of 1-β-D-arabinofuranosylcytosine on growth, viability, and DNA synthesis of mouse L-cells. Cancer Res 30:2627–2635, 1970.
19. KIM JH, PEREZ AG, and DJORDJEVIC B. Studies on unbalanced growth in synchronized HeLa cells. Cancer Res 28:2443–2447, 1968.
20. RAMA REDDY GV, GOULIAN M, and HENDLER SS. Inhibition of *E. coli* DNA polymerase II by ara-CTP. Nature [New Biol] 234:286–288, 1971.
21. SCHRECKER AW. Metabolism of 1-β-D-arabinofuranosylcytosine in leukemia L1210: nucleoside and nucleotide kinase in cell-free extracts. Cancer Res 30:632–641, 1970.
22. MOMPARLER RL, BRENT TP, LABITAN A, ET AL. Studies on the phosphorylation of cytosine arabinoside in mammalian cells. Mol Pharmacol 7:413–419, 1971.
23. DOMBERNOWSKY P, BICHEL P, and HARTMANN N. Cytokinetic analysis of the JB-1 ascites tumor at different stages of growth. Cell Tissue Kinet 6:347–357, 1973.
24. SKIPPER HE. Perspectives in cancer chemotherapy: therapeutic design. Cancer Res 24:1295–1302, 1964.
25. SKIPPER HE, SCHABEL FM, JR, and WILCOX WS. Experimental evaluation of potential anticancer agents. XIII. On the criteria and kinetics associated with "curability" of experimental leukemia. Cancer Chemother Rep 35:3–111, 1964.
26. STEEL GG, and HANES S. The technique of labelled mitoses: analyses by automatic curve-fitting. Cell Tissue Kinet 4:93–105, 1971.
27. JANSSON B. A dynamic analysis of experimental PLM-curves, etc, for a mouse ascites tumor. Research Institute of National Defense, 104 50, Stockholm, Sweden, Jan 1972.
28. JANSSON B. Mathematical models in cell cycle kinetics. *In* Mathematical Models in Biology and Medicine. Amsterdam, North Holland Publishing Co, 1973, pp 21–39.
29. JANIK P, and STEEL GG. Cell proliferation during immunological perturbation in three transplanted tumours. Br J Cancer 26:108–114, 1972.
30. VALLERON A-J. Mathematic models of cell synchrony and drug scheduling. Cancer Treat Rep 60:1899–1911, 1976.
31. HART JS, SHIRAKAWA S, TRUJILLO J, ET AL. The mechanism of induction of complete remission in acute myeloblastic leukemia in man. Cancer Res 29:2300–2307, 1969.
32. FREIREICH EJ, BODEY GP, and HART JS. Current status of therapy for acute leukemia. *In* Recent Results in Cancer Research, Current Concepts in the Management of Leukemia and Lymphoma (Ultmann JE, et al, eds). New York, Springer-Verlag, 1971, vol 36, pp 119–125.
33. CLARKSON B, FRIED J, STRIFE A, ET AL. Studies of cellular proliferation in human leukemia. Cancer 25:1237–1260, 1970.
34. LINCOLN T, AROESTY J, MEIER G, ET AL. Computer simulation in the service of chemotherapy. Biomedicine 20:9–16, 1974.
35. HO DHW, and FREI E, III. Clinical pharmacology of 1-β-D-arabinofuranosylcytosine. Clin Pharmacol Ther 12:944–954, 1971.
36. MOORE M, SPITZER G, WILLIAMS N, ET AL. Agar culture studies in 127 cases of untreated acute leukemia. Blood 44:1–18, 1974.
37. GUTTERMAN JR, HERSH EM, RODRIGUEZ V, ET AL. Chemoimmunotherapy of adult acute leukemia—prolongation of remission in myeloblastic leukemia with B.C.G. Lancet 2:1405–1409, 1974.

Introduction to Session on Population Age-Dependent Responses to Therapy—In Vivo

L. F. Lamerton [1]

The title of this session can be interpreted in two ways, either as relating to the age structure of the cell population in terms of the various phases of the division cycle or to the age of the tumor. I shall concern myself in this Introduction mainly with the second interpretation because I believe that therapeutic response related to age and size of tumor is one of the most important areas for study at the present time. Clinically, it has been recognized for a long time that, other things being equal, small tumors are more easily curable than large ones, and important innovations in modern radiotherapeutic and chemotherapeutic techniques are based on the assumption that small metastases, at a size below the present level of detectability, may be particularly susceptible. Very relevant to this concept was the work some years ago of Humphreys and Karrer (1) who showed that the sensitivity to certain drugs of tumor nodules produced in the lungs of mice changed markedly with their age and that at diameters > 1 mm the sensitivity dropped substantially. These early observations have led to some very interesting work. I will not attempt to review this work but I thought it might be worthwhile to consider briefly some of the factors that are likely to be of importance in determining variation in therapeutic response with tumor size.

For a homogenous cell population and an agent that kills exponentially, the total number of cells will be a major determinant of the dose required for cure, but if the population is heterogeneous in its response, success may be determined by the response of the most resistant minority. An increase in heterogeneity is one of the characteristics of increasing tumor size, and the change in response with size can, in general, be regarded as a combination of two factors, the increase in total number of cells and the development of less susceptible subpopulations.

One such subpopulation is that of cells with a slow proliferation rate resulting, at least in part, from nutritional deficiencies caused by inadequate vascularity. I say "at least in part" because there is now evidence of humoral factors affecting the rate of cell proliferation in tumors from experiments in which the proliferation rate of cells in one tumor site is affected by the presence of tumor in another site. Evidence about this will be presented in some of the papers in this session.

A problem facing the investigator interested in the development of slowly proliferating subpopulations is that the size of such a population that can affect profoundly the therapeutic response may be too small to be recognized by the classic techniques of cell population kinetics, such as the labeled mitoses curve which gives little information about slowly dividing cells. However, the practically important point is how these populations may be speeded up. There is evidence, from experimental tumors, that this will occur after reduction of tumor size, but how completely and by what mechanisms are important subjects for study. In particular, one would like to know whether different mechanisms are required for speeding up slowly cycling cells and for triggering resting cells into division. If the mechanisms are the same, and come into play by a simple reduction in cell population, then the arguments about the distinction between slowly cycling and resting cells become very academic.

Another subpopulation related to the growth dynamics of the tumor, whose relative resistance is of profound importance in certain types of therapy, is that of severely hypoxic cells. In radiotherapy there is no doubt of the significance of poorly oxygenated cells, but how far it also applies in chemotherapy has been explored only slightly. Again, there will be some discussion of this in the following reports. A further factor that could be of importance in determining change in response with tumor size is a change in the rate of appearance of mutant or enzyme-adapted cells. In addition to the various cellular factors there is, of course, the possible limitation to access of drug resulting from deficiencies in vascular and other transport systems.

I have not mentioned the immunologic problem with regard to small tumors. The situation here is complicated, but this is an area where much more work is required comparing the dose of agent actually required to cure a tumor compared with that calculated from cell dose response data.

[1]Division of Biophysics, Institute of Cancer Research, Surrey, England.

From a practical point of view perhaps the most important question to ask in this area of work is the size at which a tumor begins to show impaired susceptibility to therapeutic agents, and how this varies with site and tumor type. It may well be that the lung is a particularly good site for adequate oxygenation of small tumors, and other sites, eg, the liver, might be less favorable. Is this a possible factor in the difference found clinically in the response of lung and liver secondaries? This is a subject where much work is required and will necessarily involve basic considerations of tumor angiogenesis, in the light of the work done by Folkman (2). The pattern of change of susceptibility with tumor size may also depend to an important extent on the type of tumor and particularly perhaps on its growth rate, and here work on different tumor types including, if at all possible, human tumors would help a great deal towards a more effective therapy of disseminated cancer.

REFERENCES

1. HUMPHREYS SR, and KARRER K. Relationship of dose schedules to the effectiveness of adjuvant chemotherapy. Cancer Chemother Rep 54:379–392, 1970.
2. FOLKMAN J. Tumor angiogenesis factor. Cancer Res 34:2109–2113, 1974.

Size Dependence of the Response of Lewis Lung Tumors to BCNU[1,2]

G. Gordon Steel,* Kay Adams, and Judith Stanley[3,4]

SUMMARY

The survival of Lewis lung tumor cells has been studied after a single ip dose of BCNU. In dissectible subcutaneous and intramuscular tumors and artificial lung metastases survival was measured by colony formation in soft agar and in vivo in the lung. The long-term control of small lung nodules by single doses of BCNU was studied and cell-survival estimates were inferred. The results demonstrate that the cytotoxic action of BCNU shows a strong dependence upon tumor size.

[Cancer Treat Rep 60:1743–1748, 1976]

The cure rate of tumors decreases with increasing tumor size for two main reasons. First, large tumors contain more cells that have to be killed to prevent regrowth; for any treatment that kills the same fraction of cells in different-sized tumors there will be a maximum tumor cell population size that can reliably be cured. Second, there is the possibility that the extent of cell kill decreases with an increase in tumor size. If extent of cell kill is specified in terms of the fraction of cells that survive a given dose of chemotherapeutic agent to the host, then a lower cell kill in large tumors could be the result either of reduced drug access to the cells or to a reduced cellular sensitivity to the agent. In the case of radiation as the therapeutic modality, access is unlikely to be modified by tumor size (and indeed dose reduction can be accurately measured or calculated) and lower cell kill must be due to lower cellular sensitivity.

An in vivo cell-survival curve gives direct information about the relationship between fractional cell kill and dose to the animal. The procedure is to treat tumor-bearing animals with graded doses of radiation or cytotoxic drugs; shortly afterwards single-cell suspensions are prepared and assayed for colony-forming ability in a test environment. A comparison of colony formation from treated and control tumors gives an estimate of surviving fraction.

This procedure has been used in the study of tumor-size dependence of therapeutic response in the Lewis lung tumor by Shipley et al (1) for radiation and by Steel and Adams (2) for cyclophosphamide. It was found that when Lewis lung tumors were irradiated in the subcutaneous site and colony formation was assayed by a soft-agar technique in vitro, the response to γ-rays was consistent with a large hypoxic fraction of about 36%. When small pulmonary colonies of Lewis lung tumor were irradiated in situ in air-breathing mice and colony formation was again assessed in vitro, the hypoxic fraction was found to be below the limits of detection ($< 5 \times 10^{-3}$). When a similar comparison of cell survival in large intramuscular tumors and small lung nodules was made for cyclophosphamide treatment, the level of cell kill was also greater in the small tumors. In this case, however, the difference was not so marked and appeared as an extra 30% cell kill that was probably independent of dose.

The results to be described here are part of a wider study of tumor size dependence of therapeutic response in which we have been using not only cell cloning assays but also an assay based upon tumor cure. This paper is a preliminary report of this experimental approach; it will concentrate on the response of the Lewis lung tumors to BCNU.

[1]Supported in part by contract N01-CM-23717 from the Division of Cancer Treatment, National Cancer Institute, National Institutes of Health, Department of Health, Education, and Welfare.

[2]BCNU: NSC-409962; CAS reg. No. 154-93-8; urea, 1,3-bis(2-chloroethyl)-1-nitroso-.

[3]Radiotherapy Research Department, Divisions of Radiotherapy and Biophysics, Institute of Cancer Research, Belmont, Surrey, England.

[4]We gratefully acknowledge the support and encouragement of Professors L. F. Lamerton and M. J. Peckham.

*Reprint requests to: Dr. G. Gordon Steel, Radiotherapy Research Unit, Institute of Cancer Research, Clifton Ave, Belmont, Surrey, SM2 5PX, England.

MATERIALS AND METHODS

The Lewis lung tumor was passaged im in C57BL mice from the Institute of Cancer Research colony by the injection of small volumes of tumor homogenate. Intramuscular tumors were used for in situ treatment or to make a cell suspension when they reached a leg diameter of about 8–10 mm (a tumor weight of about 0.2–0.4 g). Subcutaneous tumors were prepared in the same way and used when they reached a volume of 500–1000 mm^3. Lung colonies were produced by the iv injection of 5000 viable tumor cells plus lethally irradiated tumor cells and microspheres as described below; the mice were treated at Day 15 after implantation and 1–2-mm lung colonies were then removed. The cell-suspension procedure was to excise the tumor, chop finely using crossed scalpels, and digest with 2.5% trypsin in phosphate-buffered saline. Gentle agitation was used during the digestion and a few hard shakes in trypsin-free medium were used at the end to bring the cells into suspension. Further details of these procedures have been given (2), as well as details of tests which have shown that in our hands the Lewis lung tumor shows a low level of antigenicity.

For the present work, three types of cell-survival assays were used: cell cloning assays in soft agar and in the lung and an assay based upon the eradication of lung colonies. The cell cloning assays required the production of tumor-cell suspensions from both treated and untreated tumors, and in the case of tumors treated with BCNU the animals were killed 16 hours after ip injection of the agent. For the lung colony assay (3) the tumor cells were then mixed with lethally irradiated Lewis lung cells and 15-μm plastic microspheres so that each 0.3-ml injection volume contained 10^6 lethally irradiated cells, 10^6 microspheres, and the number of viable cells that were estimated to give about ten to 20 lung colonies per mouse. In the present experiments the yield was about one colony per 300 viable cells injected, and the colonies were counted at Day 15 after injection. For in vitro assay the cells were plated out in Ham's F-12 medium supplemented with fetal calf serum and thickened with 0.3% Bacto agar. To each dish were added 10^4 lethally irradiated cells and 3×10^8 rat erythrocytes and the dishes were incubated within air-tight plastic boxes gassed with an atmosphere of 5% oxygen (4).

Colony-Cure Assay

An assay by the extinction of lung colonies was based on the method previously used for the extinction of small intramuscular implants of Lewis lung tumor cells (2). The growth of the lung colonies was first studied by killing animals at intervals from 8 to 20 days after the iv injection of cells, removing and fixing the lungs, and then measuring the size of 20 to 80 lung colonies at each interval using a dissecting microscope fitted with a calibrated eyepiece graticule. The results are shown in figure 1 where the median colony volume is plotted against time. The data demonstrate clear growth retardation as has been observed for the growth of transplanted tumors in other anatomic sites. If it is assumed that each lung colony originates from a single cell and that there is no initial lag period before active growth commences, then the growth curve may be extrapolated backwards to the volume of one cell at time zero. The volume of tumor per cell in lung colonies is not accurately known, but on the basis of measurements of DNA content per cell and per milligram of tumor we have taken a value of 10^{-5} mm^3 per cell. By trypsinization of the Lewis lung colonies we have extracted 4×10^4 cells/mg of tissue and the tumor volume per cell cannot therefore be $> 2.5 \times 10^{-5}$ mm^3. If 10^{-5} at zero time is taken as the origin of the growth curve, it is not possible to obtain a good fit to these data using a Gompertz equation (5) without the doubling time of the curve initially being well below 0.5 day. Since the median intermitotic time of the Lewis lung tumor cells has been determined within small lung nodules to be about 16 hours (6), we regard a volume doubling time of about 0.7 days as the minimum that is biologically realistic. We have therefore preferred to fit the growth data using a composite curve which is exponential up to a size of 0.1 mm^3 and Gompertzian thereafter. The theoretic curve drawn in figure 1 has the following parameters: initial doubling time, 0.67 day; maximum volume, 60 mm^3; cells/mm^3, 10^5; and changeover from exponential to Gompertzian at 9 days.

Within any mouse or group of mice there is some variation in the size of lung colonies. For one particular experiment the results are shown in figure 2. A total of 117 colonies in fixed lungs were measured, in this case using precision calipers under a dissecting microscope. We have simulated this distribution of colony diameters using a Monte Carlo computer model in which the growth of 1000 colonies is studied, each following the basic growth curve shown in figure 1. All colonies are assumed to have the same maximum volume, cell density, and changeover point, and the colony-size variation is assumed to arise from variation in the initial growth rate. The broken line in figure 2 was derived on the assumption that the initial growth rates were described by a Gaussian distribution whose coefficient of variation was 0.09. The theoretic and experimental diam-

eter distributions have the same mean (1.9 mm) and the same coefficient of variation (0.16).

Since there may be some variation in the lung colony growth rate from experiment to experiment we have normalized the growth curve within each experiment to the size of the control lung colonies observed at one time after implantation. Within this control group the distribution of diameters was determined, and this distribution was then fitted by manipulating the mean and coefficient of variation of the initial doubling time, again assuming that the other parameters were constant. When this had been done, it was possible to derive from the model a distribution of colony size at some other time after implantation.

The procedure for obtaining an estimate of cell kill after treatment with a cytotoxic drug was as follows. A number of mice were simultaneously injected with untreated Lewis lung cells using a viable cell dose that was judged to give about ten colonies per mouse. The mice were then divided into groups of ten and each group was treated with a standard dose of drug at a different time after implantation. Two control groups were left untreated, one being killed at a time when the colonies were easily countable (usually 15 days). The other group was kept with the treated groups which were observed for a period of 60 days. The survival of the mice was recorded and when any animal died or had to be killed it was dissected and checked for the presence of lung tumors. All untreated control mice died with tumor, and the few treated mice that died early and without lung tumors were regarded as toxic deaths and excluded from the groups. The first of the control groups gave a value for the average number of colonies per mouse and allowed the growth curve to be fitted, as previously described. The survival of mice treated with 15, 20, 30, or 40 mg/kg of BCNU is shown in figure 3. These results came from two separate experiments, one experiment using 15 and 30 mg/kg and the other using 20 and 40 mg/kg. In each case the number of colonies per mouse was somewhat higher than had been

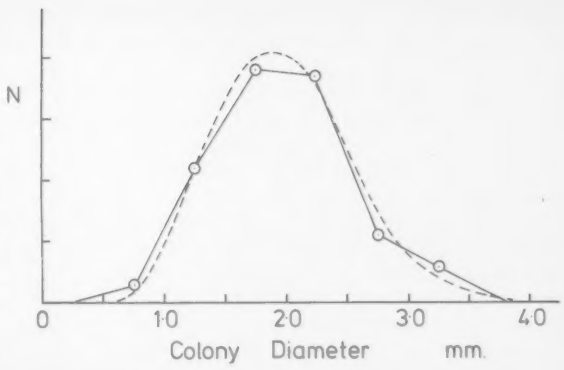

FIGURE 2.—Distribution of lung colony diameters in one experiment. Animals were killed at 15 days after implantation and the diameters were measured on fixed lungs. The broken line is a theoretic distribution (*see* text).

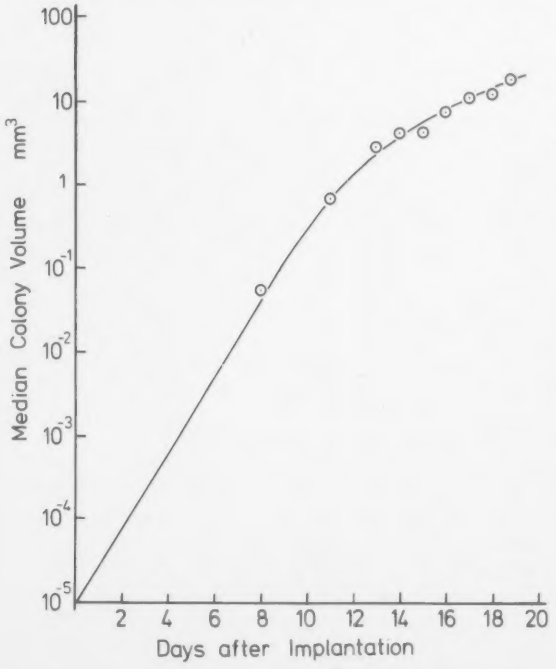

FIGURE 1.—Growth curve for lung colonies of the Lewis lung tumor. The points represent median colony volumes determined on fixed lungs. The full line is a theoretic curve, exponential up to 9 days and Gompertzian thereafter (*see* text).

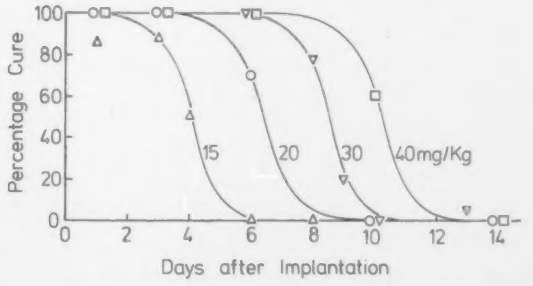

FIGURE 3.—Tumor cure as a function of time after implantation at which treatment was given for 4 dose levels of BCNU. Each experimental point represents the proportion of 60-day survivors from 10 mice treated at one particular time. —△— = 15 mg/kg, —○— = 20 mg/kg, —▽— = 30 mg/kg, —□— = 40 mg/kg.

hoped; the values are given in table 1 together with the estimates of initial doubling time and its spread. The full lines in figure 3 have been drawn by eye to have a similar shape and to fit the experimental data at each dose level. The accuracy of this fit is limited by the relatively wide spacing of the data points. At the present time we are seeking to increase the precision of these data and also to extend the colony-growth model to derive theoretic mouse-cure data. From the curves in figure 3 it is possible to estimate for each BCNU dose the colony age for which mice are cured with 50% probability. These ages are 4, 6.5, 8.5, and 10.3 days successively.

Pending a more rigorous analysis of these data we have estimated the level of cell kill as follows. From the colony-growth model we calculate the theoretic colony-size distributions at 4, 6.5, 8.5, and 10.3 days and determine the mean number of cells per colony. The average number of tumor cells per mouse at these times is obtained by multiplying by the average colonies per mouse. We then make the critical assumption that the cure of a mouse is frustrated by the survival of one or more tumor cells. The number of mice surviving is then a Poisson function of the average number of cells surviving per mouse, and 50% mouse survival occurs when there is an average of 0.7 cells surviving per mouse (7). On this assumption the level of cell kill for any dose of BCNU is obtained by dividing 0.7 by the estimate of the average number of cells per mouse at the time of treatment.

RESULTS

The results are summarized in figure 4 and table 1. Single-dose treatment of large subcutaneous tumors with BCNU and assay by the in vitro colony technique indicated a surviving fraction of about 0.1 at a dose of 40 mg/kg. In two experiments treatment of 1–2-mm diameter lung colonies and assay by the lung colony technique gave results that did not agree well, but had a surviving fraction of about 2×10^{-3} at 20 mg/kg. The two experiments in which the colony-cure assay was used agreed well. The points define a survival curve that is slightly concave upwards, with surviving fractions of 5×10^{-4} at 15 mg/kg and 7×10^{-6} at 30 mg/kg.

DISCUSSION

The cell cloning and colony-cure assays that have been used in the present work provide basically different ways of assessing the extent of tumor cell kill due to BCNU. Each has its own advantages, but each is based on certain distinct assumptions. The cell cloning assays involve removing the tumors

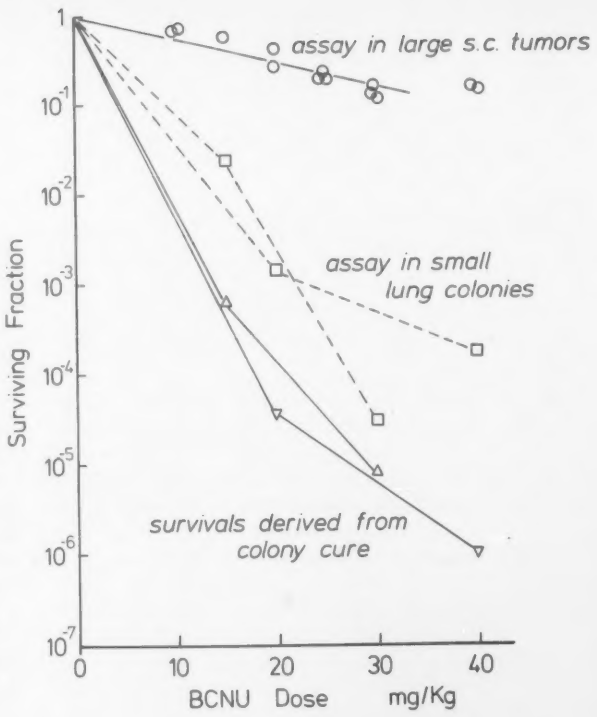

FIGURE 4.—Cell survival after single doses of BCNU. The circles indicate surviving fraction in large subcutaneous tumors determined by the in vitro cloning assay. The square points are the results (in 2 separate experiments) of measuring surviving fraction in 1–2-mm diameter lung colonies by cell cloning assays. The triangles indicate surviving fractions determined by colony-cure assay (*see* table 1).

shortly after treatment, preparing a single-cell suspension, and then allowing the cells to settle and to grow in the lungs of recipient mice or in soft agar. The time of removal of the tumors after BCNU treatment could influence the results, eg, because of prolonged availability of the drug. Our choice of 16 hours as the time at which the animals were killed was based on the observations of Hill and Stanley (8) that the BCNU survival curve for B16 melanoma also treated in C57BL mice was the same whether the assays were performed at 2 or 22 hours after the injection of the drug. The production of a single-cell suspension is also a potential source of artifact. The ability of a cell to recover from sublethal damage and to go on to divide may depend upon its association with the cells among which it had been growing before treatment. Trypsinization destroys these natural cellular contacts and may itself impose additional damage. Thus, although cell cloning assays

TABLE 1.—Colony Nos. and growth-rate parameters: estimates of surviving fraction

	Experiment			
	A		B	
Colonies/mouse	23.3 ± 2.4		26.0 ± 4.0	
Initial doubling time	0.714 day		0.730 day	
Coefficient of variation of growth rate	0.083		0.073	
BCNU dose (mg/kg)	20	40	15	30
Colony age for 50% mouse cure (days)	6.5	10.3	4.0	8.5
Mean cells/colony	6.3×10^2	2.7×10^4	46	3.8×10^3
Surviving fraction	4.8×10^{-5}	1.1×10^{-6}	5.8×10^{-4}	7.1×10^{-6}

are now in widespread use, they are artificial and their validity needs to be confirmed by techniques that do not involve destroying the tumor architecture.

Comparison of the results of cell cloning assays with tumor cure offers a potential check on the validity of the results. Reinhold and De Bree (9) found that the long-term control of experimental rhabdomyosarcoma by radiation was consistent with what would have been expected from in vitro colony-assay results. Rockwell and Kallman (10) found in the EMT6 tumor that cell survival data underestimated the radiation curability and ascribed the discrepancy to host response against a tumor that is known to be somewhat antigenic. Steel and Adams (2) examined cell survival and tumor cure by cyclophosphamide in small intramuscular implants of the present Lewis lung tumor. When allowance was made for a slight increase in cellular sensitivity between large and small tumors, there appeared to be good agreement.

The tumor-cure experiments that have been described here have given plausible results, but the inherent assumptions should not be overlooked. We assume that the growth curve for small lung tumors is as indicated in figure 1. A lag period after implantation before active growth ensues would lead us to overestimate the size of colonies at treatment. Our assumption of a cell density of 10^5 mm^3 in Lewis lung nodules is a figure that is not as yet known with satisfactory precision. The other principal assumption is that a lung colony can regrow as a result of the survival of one or more tumor cells. A tumor clearly cannot grow back from less than one cell but it is not known whether there are local factors that raise the average number of cells required for colony regrowth. The Lewis lung tumor growing in the present strain of mice has been found to be of low antigenicity (2) but it is difficult to rule out the possibility that some extra cell kill in the tumors treated and left in situ may have derived from a host reaction.

One possible factor in the interpretation of the present results is that the level of cell kill in lung tumors is greater than in an intramuscular tumor of the same size, perhaps as a result of better drug availability. This possibility seems unlikely in view of our failure to detect such a site-dependent response with cyclophosphamide, but it is being investigated.

The principal conclusion of this preliminary report is that the cytotoxic action of BCNU against the Lewis lung tumor appears to show a stronger size dependence than we have previously found with cyclophosphamide. At a maximum-tolerated dose of 40 mg/kg the surviving fraction in 0.2–0.4-g intramuscular tumors was about 0.1. At this same dose level the surviving fraction in approximately 2–5-mg lung colonies was about 10^{-4} and the eradication of microscopic lung colonies was consistent with a survival of about 10^{-6}. This, therefore, appears to be a situation in which an agent that is relatively ineffective against palpable intramuscular tumors shows considerable effectiveness against artificial lung metastases.

REFERENCES

1. SHIPLEY WU, STANLEY JA, and STEEL GG. Tumor size dependency in the radiation response of the Lewis lung carcinoma. Cancer Res 35:2488–2493, 1975.
2. STEEL GG, and ADAMS K. Stem-cell survival and tumor control in the Lewis lung carcinoma. Cancer Res 35:1530–1535, 1975.
3. HILL RP, and STANLEY JA. The lung colony assay: extension to the Lewis lung tumour and the B16 melanoma—radiosensitivity of B16 melanoma cells. Int J Radiat Biol 27:377–387, 1975.
4. SHIPLEY WU, STANLEY JA, COURTENAY VD, ET AL. Repair of radiation damage in Lewis lung carcinoma cells following in

situ treatment with fast neutrons and γ-rays. Cancer Res 35:932–938, 1975.
5. McCredie JA, Inch WR, Kruuv J, et al. The rate of growth of tumors in animals. Growth 29:331–347, 1965.
6. Simpson-Herren L, Sanford AH, and Holmquist JP. Cell population kinetics of transplanted and metastatic Lewis lung carcinoma. Cell Tissue Kinet 7:349–361, 1974.
7. Porter EH, Hewitt HB, and Blake ER. The transplantation kinetics of tumour cells. Br J Cancer 27:55–62, 1973.
8. Hill RP, and Stanley JA. The response of hypoxic B16 melanoma cells to in vivo treatment with chemotherapeutic agents. Cancer Res 35:1147–1153, 1975.
9. Reinhold HS, and De Bree C. Tumor cure rate and cell survival of a transplantable rat rhabdomyosarcoma following x-irradiation. Eur J Cancer 4:367–374, 1968.
10. Rockwell S, and Kallman RF. Cellular radiosensitivity and tumor radiation response in the EMT6 tumor cell system. Radiat Res 53:281–294, 1973.

Effects of Surgery on the Cell Kinetics of Residual Tumor [1]

Linda Simpson-Herren,* Audrey H. Sanford, and James P. Holmquist [2,3]

SUMMARY

Noncurative excision of a primary sc Lewis lung tumor performed on Day 7 or later results in an increase in the thymidine index and growth rate with minimal changes in the cell cycle parameters of the lung metastases. The stimulation of the lung nodules is accompanied by a small but consistent decrease in median lifespan. Sham surgery performed on Day 3 or later also results in a decrease in median lifespan and an increase in the thymidine index of the undisturbed primary tumor. Artificial metastases (10^6 cells iv) are inhibited by the presence of a second (sc) implant and the median lifespan of the doubly implanted mice exceeds that of mice bearing iv implants only. In mice bearing widely metastasized Lewis lung carcinoma, surgery alone may have a detrimental effect on life expectancy, but the residual tumor foci, stimulated to more rapid growth, should be appropriate targets for adjuvant chemotherapy.

[Cancer Treat Rep 60:1749–1760, 1976]

Fifty percent or more of malignant tumors in man have metastasized prior to clinical presentation and are beyond the reach of curative surgical or radiologic therapy. Systemic chemotherapy designed to eradicate residual metastatic tumor foci after surgery or radiation therapy provides a feasible approach to curative therapy. The effects of the initial treatment (surgery or radiation) on normal and malignant tissue, the time required for host recovery, and the period of maximum drug sensitivity of the tumor population become major factors in planning adjuvant therapy.

Previously, we investigated the cell population kinetics of primary and metastatic Lewis lung carcinoma in the same hosts (1) and found a higher thymidine index (TdRI), a shorter cell cycle, and a narrower distribution of cell cycle times in the small lung metastases than in the larger, primary tumors. This report describes the cell population kinetics of spontaneous lung metastases after surgical removal of the primary tumor and of artificial metastases (iv implanted cells) in the absence of a primary tumor and in the presence of a second sc implant.

MATERIALS AND METHODS

Biologic Systems

Lewis lung carcinoma was passed by biweekly sc implant of trocar fragments in C57BL/6 mice. For kinetic experiments fragments were passed sc into BDF_1 mice. The hybrid strain is commonly used for chemotherapy trials and was therefore chosen as the host for these studies. One million (10^6) mechanically separated, trypan blue-excluding, mono-dispersed cells were injected into the tail vein of BDF_1 mice to establish artificial lung metastases.

Tumor Growth

Growth of sc tumors was followed by caliper measurements of two perpendicular diameters, and the tumor mass was assumed to approximate a prolate ellipsoid with the volume equal to (length [mm] × width [mm]^2)/2 if the density were equal to 1. Total lung tumor mass was assumed to be equal to the difference in weight of the excised, blotted tumor-bearing lungs and similarly prepared lungs of con-

[1]Supported by contract N01-CM-43756 from the Division of Cancer Treatment, National Cancer Institute, National Institutes of Health, Department of Health, Education, and Welfare.

[2]Kettering-Meyer Laboratory, Southern Research Institute, Birmingham, Ala.

[3]We wish to express our appreciation to Dr. Joseph Mayo and Kay Johnson for supplying the tumor-bearing mice and for performing the surgery. We are grateful to Tommie Lou Barker for her excellent assistance with the animal work.

*_Reprint requests to:_ Mrs. Linda Simpson-Herren, Southern Research Institute, 2000 9th Ave S, Birmingham, Ala 35205.

current, normal controls. Growth data were fitted by a Gompertz function as previously described (1).

Surgical Procedures

Mice were anesthetized with Metofane. Tumors and surrounding skin were removed and the incision was closed with wound clips. Mice were allowed to recover in an atmosphere of 90% oxygen and 10% CO_2 at 32°C. Mortality was usually < 10%. Surgical procedures for the sham groups were identical except that a corresponding area of skin was removed from the side opposite the tumor.

Thymidine Studies

Thymidine-methyl-^{3}H(^{3}H-TdR) at 6.7 curies/mmol, obtained from New England Nuclear Corp, Cambridge, Mass, was used for all studies. ^{3}H-TdR was administered ip at the following doses: 2 microcuries/g of body weight for studies of the cell cycle and associated TdRIs and 10 microcuries/g of body weight for measurement of TdRI as a function of tumor age.

At the designated periods after injection of ^{3}H-TdR, mice were killed in a CO_2 atmosphere and lungs were infused in situ with 10% buffered formalin and preserved in formalin until processed for paraffin embedding. Sagittal sections of the lungs were cut at 3μ–4μ. Slides were treated as previously described (1) and dipped in Ilford K-2 emulsion diluted 1:1 with distilled water. The periods for dark storage of the emulsion-covered slides were 3 or 6 weeks for cell cycle (^{3}H-TdR at 2 microcuries/g of body weight) and 2 or 4 weeks for pulse TdRI (^{3}H-TdR at 10 microcuries/g of body weight). The exposure periods were based upon extensive experience with this tumor system, levels of ^{3}H-TdR, and the particular conditions of autoradiography. These levels of ^{3}H-TdR and periods of emulsion exposure yield heavily labeled cells with sufficient visible cellular detail to identify mitotic figures. Autoradiographs were developed in Kodak D19 developer and stained with hematoxylin and eosin.

Data Acquisition

All tumor nodules found in each sagittal lung section were scanned for measurement of percent labeled cells or mitotic figures. At least 100 mitotic figures were scored when this amount could be found in the small tumor foci. When the lung nodules were extremely small few mitotic figures were evident. In those instances, data from several autoradiographs from the same tissue were pooled. In no instance were the data for lung nodules used unless at least ten mitotic figures per slide were found. For the cell cycle studies, autoradiographs exposed for 3 weeks were used for points on the first wave and those exposed for 6 weeks were used for points on the second wave to compensate for the reduction to one half in grain count/cell that occurs with each cell division.

One to three thousand cells per slide were scored from duplicate slides for each TdRI and autoradiographs from both exposure periods were checked to confirm the adequacy of exposure, ie, that the observed TdRI would not be significantly changed by increasing the duration of emulsion exposure. Background grain density was low on most slides (< 1 grain/cell) and the grain count threshold for each cell was based upon the background in the immediate vicinity.

Computer Analysis of Data

Percent labeled mitosis (PLM) data were analyzed by computer using the mathematic model described by Barrett (2) and Steel and Hanes (3).

RESULTS

Growth Curves

Growth data for lung tumor masses (either spontaneous or artificial) are well-fitted by a Gompertz equation (fig 1). The curves for spontaneous and artificial metastases show minimal evidence of a plateau, probably due to pulmonary failure and host death with massive lung tumor growth. Few mice survive with lung tumor burdens > 1 g. The mass of lung tumor in surgically treated mice appears to approach this burden at a more rapid rate than similar tumor masses in intact (untreated, tumor-bearing) mice (fig 1, table 1).

Cell Cycles

The PLM curve for lung metastases in intact mice at 21 days postimplant of the primary tumor is shown in figure 2 and the calculated parameters are given in table 2. The mean cell cycle time (T_c) was 16.1 hours with a DNA synthesis time (T_s) of 11.5 hours and a TdRI of 0.37. When the primary sc tumor was removed 48 hours prior to the injection of ^{3}H-TdR on the 21st day postimplant, the TdRI appeared to be slightly depressed (0.31) with a slight increase in the T_c (19.1 hours) and no appreciable change in the T_s.

A study was then planned to measure the cell population kinetics at 96 hours after surgery to determine, if possible, whether the reduced TdRI

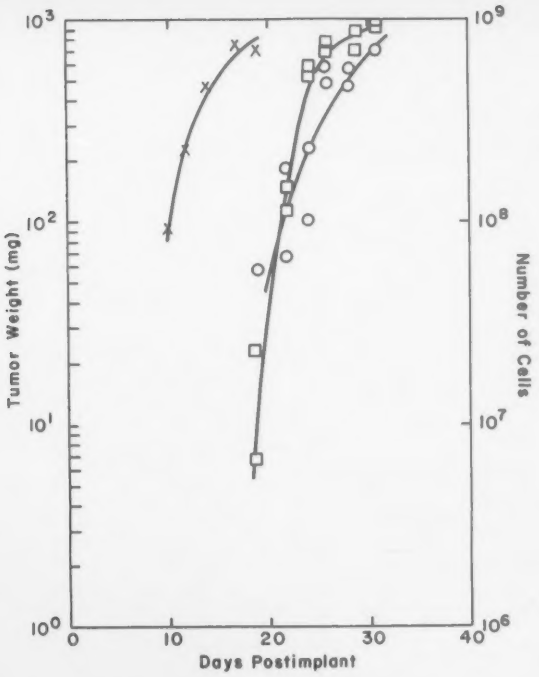

FIGURE 1.—Gompertz-fitted growth curves for the lung tumor mass of spontaneous metastases in untreated mice (○), of spontaneous metastases after surgical removal of the primary tumor on Day 14 (□), and of artificial metastases after 10^6 cells iv (×).

observed at 48 hours was transient, whether it persisted for long periods, or whether it might be attributed to the tumor age (Day 23 postimplant). Technical difficulties related to the removal of large, frequently ulcerated, and invasive tumors encountered in the first study led to the decision to remove primary tumors on Day 14 and begin the PLM study by injection of ^{3}H-TdR on Day 18. The mean TdRI of the lung metastases in this study was 0.46 with cell cycle parameters very similar to those found in lung nodules in the intact mouse at Day 21.

Studies of artificial metastases on Day 15 indicated that the mean T_c was 18.8 hours with an 11.8-hour S phase. The TdRI was 0.48 which agrees well with the value found in spontaneous metastases 96 hours after surgical excision of the primary. The significance of the difference in the length of the cell cycle in spontaneous and artificial metastases is questionable but might be due to the size of tumor nodules and to the total tumor burden found in the lungs on Day 15 of the artificially induced metastases.

Thymidine Indices

To further pursue the kinetics of lung nodules in the absence of a primary tumor, we measured the TdRI of lung metastases as a function of time postimplant for spontaneous lung metastases in intact mice, in mice following surgical removal of the primary tumor, in artificial metastases, and in lungs of mice with both an sc tumor and artificial metastases (fig 3). The latter study was included to determine whether a growing sc tumor had any effect on the growth of unrelated, iv implanted cells. Each set of data was fitted by linear regression analysis.

The TdRIs of lung nodules in intact mice decreased with time postimplant in a near linear manner with mean values ranging from 0.37 on Day 17 to 0.26 on Day 31. When the primary tumors were removed on Day 14 and the TdRIs were measured starting on Day 16, the index was elevated on Day 16 and decreased only to 0.48 by Day 30. Thus, surgical removal of the primary tumor on Day 14 resulted in an increase in the observed TdRIs of residual lung nodules for about a 2-week period. The values for Days 32 and 35 were omitted from the linear regression analysis due to the cachexia of mice surviving at that time and to the obvious break in the line. The best-fit line for TdRIs during the 2-week postsurgery period closely resembles that of artificial metastases.

TdRIs of artificial lung nodules were not related to time postimplant of cells (fig 3). There was essentially no change in the measured values from Day 5, when only a few lung nodules contained sufficient cells to obtain reliable counts, until Day 23, a time when tumor cells essentially replaced normal lung tissue and only a few animals survived. The high proliferative rate was reflected by the rapid increase in lung tumor mass described by the Gompertz fitted curve in figure 1.

When a solid sc tumor was implanted 2 days prior to iv implant of counted cells, the TdRIs of lung nodules decreased with time postimplant as observed in the intact mice. The slopes of the line for both artificial and spontaneous metastases in the presence of growing, sc tumors are nearly identical but the labeling indices are higher in the artificial metastases. There is also greater variability in the latter group and the line does not fit the data as well.

The effects of sham surgery were compared with those of surgical excision on the TdRIs of pulmonary metastases and of the primary tumor, if present (fig 4). In two experiments, sham surgery apparently stimulated the TdRI of the undisturbed primary tumor for a period of 96 hours or longer.

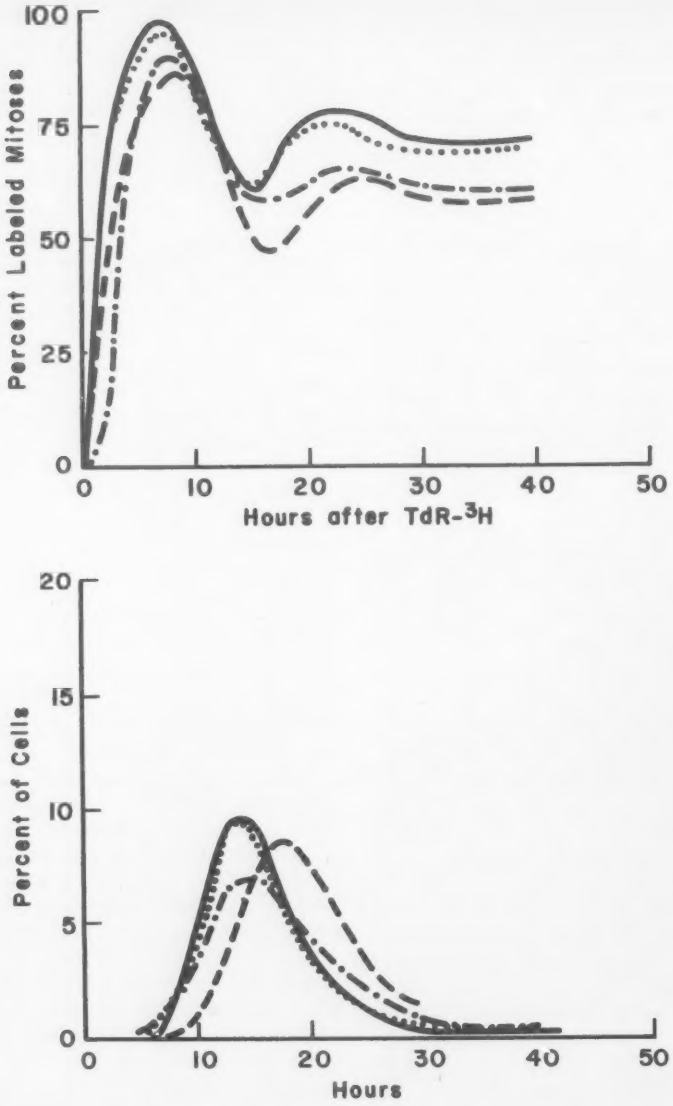

FIGURE 2.—Curves obtained by computer analysis of PLM data (upper) and distributions of intermitotic times from the analyses (lower). —— = spontaneous metastases of untreated mice 21 days postimplant of primary tumors; ---- = spontaneous metastases (Day 21) 48 hrs after surgical excision of primary tumors; ····· = spontaneous metastases (Day 18) 96 hrs after surgical excision of primary tumors; ·-·-· = artificial metastases (10^6 cells iv) 15 days postimplant.

TABLE 1.—Growth data of lung tumor masses in surgically treated mice

Lung tumor mass (mg)	Doubling time (days) of lung metastases		
	Artificial metastases	Spontaneous metastases	Spontaneous metastases after surgery
10	0.5	0.5	0.5
50	0.8	1.0	0.7
100	1.1	1.3	1.0
500	4.1	5.0	2.9
700	10.3	12.9	5.1
Maximum calculated weight (mg)	880	870	1100

TABLE 2.—Measured and calculated kinetic parameters for spontaneous and artificial lung metastases

Metastases	Time postimplant (days)	TdRI	Cell cycle parameters			
			T_c	T_s	T_{G_1}	T_{G_2}
Spontaneous	21	0.37	16.1(14.8)*	11.5 ± 3.7(10.9)	2.3 ± 5.5(0.9)	2.3 ± 1.5(1.9)
Spontaneous (48 hrs after surgery)	21	0.31	19.1(17.4)	11.2 ± 3.3(10.7)	4.1 ± 7.0(2.1)	3.8 ± 4.1(2.5)
Spontaneous (96 hrs after surgery)	18	0.46	15.6(14.6)	11.2 ± 3.8(10.6)	2.1 ± 3.3(1.2)	2.3 ± 2.3(1.6)
Artificial	15	0.48	18.8(16.7)	11.8 ± 6.7(10.3)	2.9 ± 7.5(1.0)	4.1 ± 2.0(3.7)

*Median values given in parentheses.

The TdRIs of lung nodules during the 4-day period after sham surgery were about 0.55 which appears to be the maximum value found in this system under any condition. The limited number of values at 21 and 24 days' postimplant are too variable to determine whether the TdRIs of these nodules were elevated at 7 days or later. However, when the primary sc tumor was excised, the mean TdRI of the residual lung nodules was about 0.50 and remained near this value with little evidence of decline until Day 28 postimplant. These results confirmed the surgical study shown in figure 3.

Effects of Surgery on Lifespan

Surgical excision of primary Lewis lung tumors, if performed on Day 4 or earlier, provides some long-term "cures" and an increase in lifespan over the untreated controls (table 3) (4). However, if the primary tumors are removed on Day 6 or later, the surgically treated mice survive a shorter period of time than the controls. Any deaths occurring within 24 hours after surgery were considered to be related to the surgical procedure and were eliminated from the calculations. Sham surgery, which leaves the primary tumor intact, has a more profound effect on lifespan (table 3) than surgical excision of the tumor. This may result from a stimulation of the growth rate of the primary tumor or to an increased rate of formation of metastases.

Effects of Double Implants on Tumor Growth and Lifespan

The results of an additional study (table 4) indicate that the lifespan of mice bearing artificial metastases is extended by the presence of a growing sc tumor and the magnitude of the effect appears to be a function of the relative time of tumor implant. The maximum increase (+5.5 days) occurred when the sc tumor was implanted 2 days before the iv cells and lesser increases were seen when the sc tumor was implanted at earlier and later times. If two sc tumors were implanted simultaneously, the lifespan was not affected but the total mass of the two tumors was equal to the mass of a single sc implant throughout the growth period (fig 5).

DISCUSSION

"Outbursts" (5) of metastatic growth following surgical excision of a primary tumor is a recognized clinical problem (6) and has been noted, in particular, in osteogenic sarcoma (7). This phenomenon has been attributed to release of viable cells due to manipulation of the tumor during surgery (8–10) or

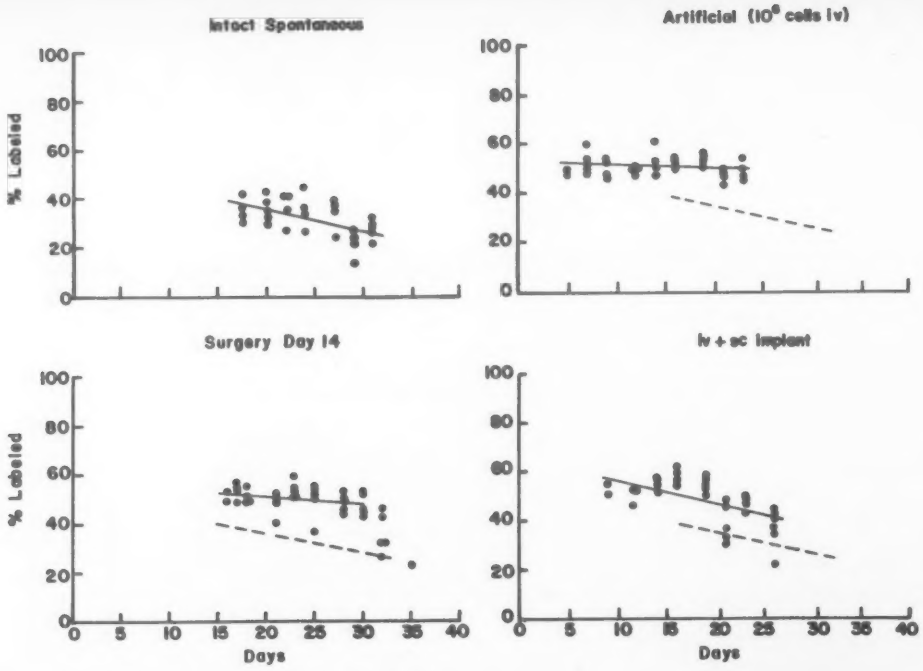

FIGURE 3.—Thymidine indices as a function of days postimplant for spontaneous lung nodules in intact mice, spontaneous lung nodules in mice after removal of the primary tumors on Day 14 (points at Days 31 and 35 were omitted from the analysis), lung nodules after implant of 10^6 cells iv (artificial metastases), and lung nodules of mice with both iv and sc implants. The solid line is the best-fit line from a linear regression analysis and the line for the intact mice is repeated as a dashed line for reference on the other graphs. TdRIs for artificial metastases and spontaneous metastases after surgery are essentially independent of time as shown by a low linear regression correlation coefficient.

to acceleration of growth of metastases that originated before the tumor was recognized (11–20). Outgrowth of existing metastases has been attributed to changes in the immune status of the host due to removal of a major portion of the tumor burden (16,21–23) or to direct or indirect effects of the surgical procedure (17,24–28).

Effects of a Growing Solid Tumor

These studies strongly suggest that a growing solid tumor, whether a primary tumor or a second implant, tends to decrease the TdRI (and proliferative fraction) of the small, metastatic nodules. In the absence of a primary tumor (either following surgical excision of the primary tumor or following iv implant) the mean TdRIs are about 0.50, the same value found in small, growing sc tumors (1). Rate of growth of the sc tumors in the doubly implanted mice is decreased in comparison to the mice bearing single sc implants (and spontaneous lung metastases). Unfortunately, it is not feasible to determine the rate of growth of an sc tumor in the absence of metastases in this system due to the high rate of spontaneous metastases. If mice are given two simultaneous sc implants, the total sc tumor mass increases at approximately the same rate as the mass of single sc implant. Thus, it is evident that in the Lewis lung carcinoma there is interaction between multiple tumor foci and a reduction in growth rate of each foci. An increase in lifespan (ILS) is concomitant with a decrease in the growth rate of the lung tumor mass.

Several investigators (29–31) have demonstrated an interaction between sc and ip implants of Ehrlich carcinoma and an ILS of mice bearing double (sc and ip) implants. Artificial metastases (iv) of line 1 alveolar cell carcinoma inhibit sc growth of the same tumor (32). Goldie et al (33) found that fast-growing tumors (Sarcomas 37 and 180 and lymphosarcoma) promoted secondary peritoneal growth in early stages but inhibited peritoneal growth in advanced stages. Milas et al (34) using a fibrosarcoma in C_3Hf/Bu mice observed a reduction in the number of pulmonary (artificial) metastases in the presence of a growing sc tumor and the degree of reduction

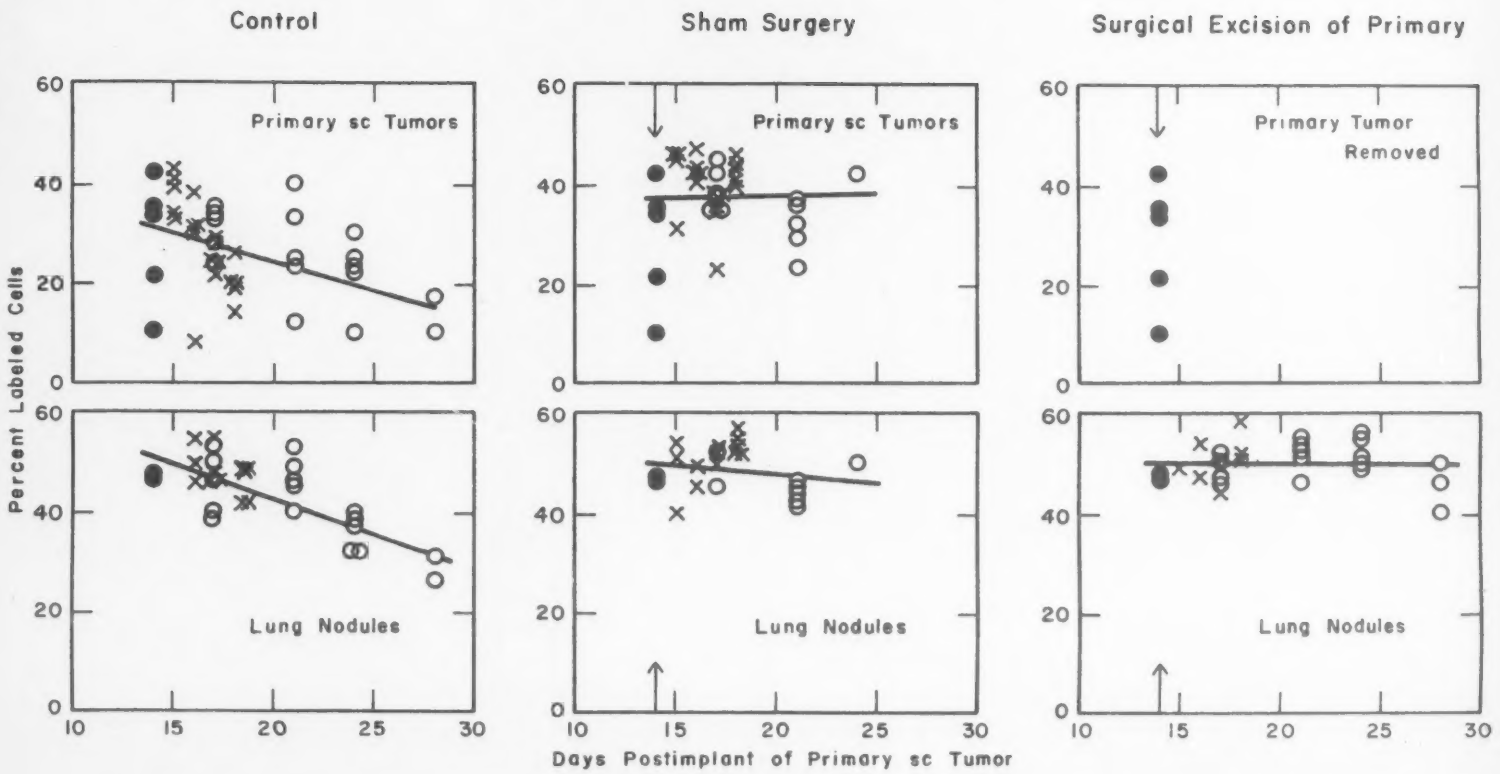

FIGURE 4.—Effects of sham surgery and surgical excision of primary sc Lewis lung tumor on the TdRIs of residual tumor foci. Experiment 1: ● = TdRIs on Day 14 prior to surgical procedures, ○ = samples taken after designated treatment. Experiment 2: × = TdRIs at 24, 48, 72, and 96 hrs after indicated treatment. TdRIs of lung nodules after surgical excision and both primary and lung nodules after sham surgery are essentially independent of time as indicated by a low linear regression correlation coefficient.

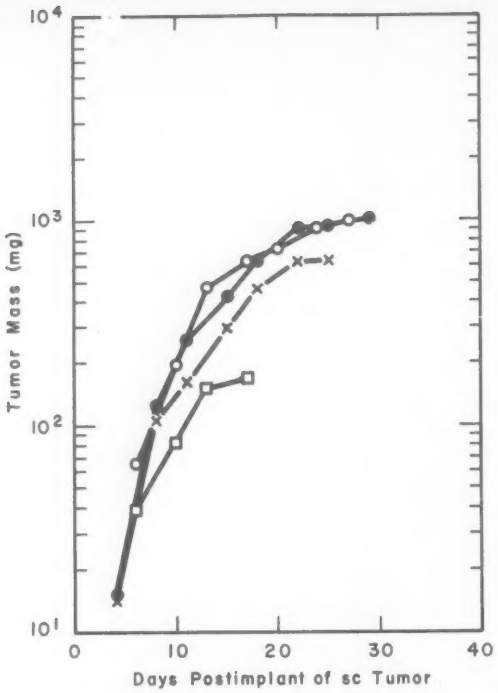

FIGURE 5.—Growth curves for sc tumors in mice bearing 1 sc implant (●), bilateral sc implants (total tumor mass) (○), iv (10^6 cells) and sc tumors implanted simultaneously (×), and iv (10^6 cells) implanted 5 days prior to sc tumors (Day 0) (□). Symbols represent median tumor mass.

was related to the time between implants. The growth rate of spontaneous tumors in C_3H mice depends upon the number of tumors present; the more tumors present, the slower the growth rate of the earliest tumor (35). The total amount of E0771 tumor tissue in C57BL mice at death was similar whether there were single or multiple tumors (36). A similar finding was also reported for spontaneous C3H tumors (36). In contrast, Rockwell and Kallman (37) have reported that both the growth rate and cell population kinetics of single and multiple KHT sarcomas in C3H/Km mice were not significantly different in any respect. It appears that an interaction between multiple tumor foci in transplanted and spontaneous experimental tumor systems is a frequent, but not universal, finding.

Effects of Surgical Excision

An increase in the TdRI and in the growth rate with little change in cell cycle parameters occurs following surgical excision of primary Lewis lung carcinoma. If the primary tumor is removed on Day 6 or later, the lifespan of surgically treated mice is less than the controls. Excision of these Lewis lung sc primary tumors, particularly as they become large and invasive, is often incomplete and local recurrence is observed in some mice. An enhancement of metastatic growth following partial removal of a primary tumor was reported in 1910 by Marie and Clunet (19) and in 1913 by Tyzzer (20). This enhancement has been attributed to shedding of viable cells during manipulation of the tumor during surgery (8–10). However, the changes in the TdRIs of Lewis lung carcinoma in these experiments during the 96-hour period after surgery were observed in tumor foci that were too large to have resulted from viable cells shed at surgery.

The increase in TdRIs would be entirely consistent with outburst or acceleration of growth of existing tumor foci and may be due, in part, to changes in the immune status of the host (16,21–23) after removal of the tumor. A characteristic pattern of cell-mediated immunity has been demonstrated in several tumor systems (23,38–42) where levels of immunity increase during the early phase of tumor growth followed by an "eclipse" when the tumor reaches about 1 g (or > 10% of the body weight depending upon the study). Surgical removal of the primary tumor is frequently followed by a rapid return of immune response (23,42–44). Prehn (45,46) has suggested that a weak immune response to tumor-specific antigens stimulates rather than inhibits tumor growth, and results of studies by Jeejeebhoy (47) are compatible with this hypothesis. A rebound of immune response after surgery with resultant stimulation of residual tumor tissue could well be a contributing factor in the increased TdRIs (and growth rate) of lung nodules and decreased lifespan that we have observed with Lewis lung carcinoma. This tumor has been shown to evoke a weak but consistent immune response in syngeneic mice (48). Antithymocyte globulin reportedly increases the number, size, and rate of appearance of pulmonary metastases of Lewis lung carcinoma in syngeneic mice (49).

Effects of Sham Surgery

A surgical procedure (sham) which is designed to simulate tumor excision but leaves both the primary tumor and its spontaneous metastases undisturbed also results in a slight increase in TdRI of the pulmonary metastases and a decrease in lifespan. In addition, the TdRI of the primary tumors is increased and may account for the more profound effects of sham surgery over surgical excision on the lifespan. Adverse effects related to metastatic

TABLE 3.—Effects of surgery on lifespan of tumor-bearing mice

Experiment No.	Day of surgical procedure†	Changes in median day of death* and No. of long-term survivors after surgical excision of primary tumors or sham surgery: Surgery excision, change in MDD	Tumor-free survivors (Day 70)	Sham surgery, change in MDD	Tumor-free survivors (Day 70)
1‡	2	+11	6/20		
	4	+6.5	8/20		
	6	−1	0/20		
	8	−1.5	0/20		
	10	−3	0/20		
	12	−4	0/20		
2	3	+1	1/10	−4.5	0/10
	7	−5.5	0/10	−7.5	0/10
	10	−2.5	0/10	−8.5	0/10
	13	−1	0/10	−3.5	0/10
	17	−0.5	0/10	+0.5	0/10
3	14	−2	0/20	−4	0/20

*MDD = median day of death. The MDD in experiments 1 and 2 was Day 29. Changes in MDD were calculated with respect to concurrent controls.
†Tumors implanted on Day 0.
‡Reported by Mayo et al (4).

Summary of data on effects of surgical excision on lifespan from 19 experiments

Day of surgical excision	No. of experiments	Changes in MDD (Days)	Long-term survivors
7	4	−2.4	0/40
10	1	−2.0	0/10
12	7	−1.8	0/87
13	1	−2.0	0/20
14	1	0	0/10
15	2	−1.5	0/20
16	2	−2.5	0/18
21	1	+0.5	0/10

TABLE 4.—Effects of double implants on lifespan

Day of iv implant	Day of sc implant	Median day of death after iv implant	ILS (days)
—	0	28.5	—
0	None	20.5	—
0	−5	23.0	+2.5
0	−2	26.0	+5.5
0	0	24.5	+4.0
0	+3	23.0	+2.5
0	+5	22.0	+1.5

growth as either direct or indirect effects of a surgical procedure, trauma, incisional biopsy or stress have been reported in both man and experimental animals (1,8,17,24,26,28,50,51). The stimulatory effect of sham surgery and tumor excision on the TdRI of residual tumor foci is consistent with the observed decrease in lifespan.

Lifespan

Surgical excision of primary Lewis lung carcinoma has a biphasic effect on lifespan. If surgery is performed before Day 7 when tumors are small (< 500 mg) some cures are usually obtained with an ILS of dying mice. If surgery is delayed until tumors are larger and presumably have shed more viable cells (52), there is a detrimental effect on lifespan. This biphasic effect is probably related to the apparently conflicting reports (17,53–56) on the effects of surgery on the number of metastatic foci and on lifespan in various experimental tumor systems. Following early surgery when only a few viable cells remain in the host, the metastatic foci may be stimulated to grow to a large size but the effects are beneficial to the host in terms of lifespan. If surgical excision is performed late when many viable cells have been shed, both nodules that have been growing for a period of time and recently shed viable cells may be stimulated to produce detectable nodules and a detrimental effect on lifespan of the host. The variation in distribution of viable cells remaining after surgery in Lewis lung carcinoma and three other transplanted tumor systems is demonstrated in the data of Skipper (personal communication) shown in table 5. Distribution of viable cells from the primary site occurs rapidly and relatively uniformly from Lewis lung carcinoma in contrast to the B16 melanoma, C3H breast, and Colon 26 tumors. No cures or ILS s are found when any mice have a body burden $> 10^4$ Lewis lung cells after surgery. More than 50% cures (0 viable cells remaining) in Colon 26 are seen when 13% of the mice have a residual burden of 10^7 cells. The times indicated by early and late tumors and the effects of surgery on lifespan appear to be a function of the tumor system, the rate of growth, and its capacity to metastasize.

Implications

The implication of these studies is that a noncurative surgical procedure in Lewis lung carcinoma results in a stimulation of the TdRI and an increase in growth rate of residual tumor foci. Under these conditions, surgery alone may have a detrimental effect on life expectancy; but the residual tumor foci, stimulated to more rapid growth, should be appropriate targets for adjuvant chemotherapy. Consistent with this approach to therapy would be the reports (4,57) that surgery plus adjuvant chemo-

TABLE 5.—Viable cells remaining after surgical excision of primary Lewis lung tumors*

Day of surgery†	Weight of primary tumor (g)	% of mice bearing indicated Nos. of viable cells after surgery									% ILS excluding cures
		10^8 or <	10^7 or <	10^6 or <	10^5 or <	10^4 or <	10^3 or <	10^2 or <	10^1 or <	0 (cures)	
2	<0.06	—	—	—	—	100	95	85	40	30	38
4	<0.06	—	—	—	—	100	85	75	55	40	24
6	0.35	—	—	100	90	60	5	0	0	0	
8	0.60	—	100	95	70	0	0	0	0	0	
10	1.2	—	100	94	22	0	0	0	0	0	
12	1.5	—	100	84	11	0	0	0	0	0	
16	2.0	100	90	50	0	0	0	0	0	0	
21	2.5	100	70	0	0	0	0	0	0	0	

Comparison of viable cells remaining after surgical excision of primary tumors from 4 transplanted lines

Tumor system	Day of surgery†	Size of primary tumor	% of mice bearing indicated Nos. of viable cells after surgery								% ILS excluding cures
			10^7 or <	10^6 or <	10^5 or <	10^4 or <	10^3 or <	10^2 or <	10^1 or <	0 (cures)	
Lewis lung	8	0.60	100	95	70	0	0	0	0	0	—
B16 melanoma	8	0.15–0.18	—	—	—	—	100	85	80	45	122
C3H breast (transplanted)	7–9	0.3	—	100	98	93	87	69	51	36	55
Colon tumor 26	7–9	0.2	100	87	80	71	69	64	64	56	79

*Skipper HE, Southern Research Institute. Personal communication.
†Tumors implanted on Day 0.

therapy yielded cures in advanced Lewis lung carcinoma when neither surgery or chemotherapy alone was effective. Thus, the effectiveness of chemotherapy as a surgical adjuvant in this system may be attributed not only to a reduction in body burden of tumor cells but to an increase in the rate of cell proliferation in residual tumor. The human tumors demonstrating the greatest response to chemotherapy are the rapidly growing malignancies (58), and the concepts provided recently (59) for treatment of micrometastases are reinforced by the results reported here. It would be hazardous to extrapolate the results from one experimental tumor to all experimental systems and more hazardous to extrapolate to man without confirming data, but the multiple effects of surgery discussed here and the indications for adjuvant chemotherapy should be carefully evaluated, particularly in other rapidly growing, highly metastatic tumors.

REFERENCES

1. SIMPSON-HERREN L, SANFORD AH, and HOLMQUIST JP. Cell population kinetics of transplanted and metastatic Lewis lung carcinoma. Cell Tissue Kinet 7:349–361, 1974.
2. BARRETT JC. A mathematical model of the mitotic cycle and its application to the interpretation of percentage labeled mitoses data. J Natl Cancer Inst 37:443–450, 1966.
3. STEEL GG, and HANES S. The technique of labeled mitoses: analyses by automatic curve-fitting. Cell Tissue Kinet 4:93–105, 1971.
4. MAYO JG, LASTER WR, JR, ANDREWS CM, ET AL. Success and failure in the treatment of solid tumors. III. "Cure" of metastatic Lewis lung carcinoma with methyl-CCNU (NSC-95441) and surgery-chemotherapy. Cancer Chemother Rep 56:183–195, 1972.
5. DUNPHY JE. Some observations on the natural behavior of cancer in man. N Engl J Med 242:167–172, 1950.
6. BURNS ER. On the failure of self-inhibition of growth in tumors. Growth 33:25–45, 1969.
7. PRICE CHG, and JEFFREE GM. Metastatic spread of osteosarcoma. Br J Cancer 28:515–524, 1973.
8. RIGGINS RS, and KETCHAM AS. Effect of incisional biopsy on the development of experimental tumor metastases. J Surg Res 5:200–206, 1965.
9. SAKA K, and MARCHETTA FC. Radioautography of in vitro labeled tumor cells in postoperative wound drainage. Cancer 19:735–737, 1966.
10. SPJUT HJ, and MATEO LE. Recurrent and metastatic carcinoma in surgically treated carcinoma of lung. Cancer 18:1462–1466, 1965.
11. CRILE G, JR, and DEODHAR SD. Role of preoperative irradiation in prolonging concomitant immunity and preventing metastases in mice. Cancer 27:629–634, 1971.
12. CRILE GW, JR. Factors influencing the spread of cancer. Postgrad Med 39:331–335, 1966.
13. GARLAND LH, COULSON W, and WOLLIN E. The rate of growth and apparent duration of untreated primary bronchial carcinoma. Cancer 16:694–707, 1963.
14. GERSHON-COHEN J, BERGER SM, and KLICKSTEIN HS. Roentgenography of breast cancer moderating concept of "biologic predeterminism." Cancer 16:961–964, 1963.
15. POTTER JF. Concepts of the mechanisms of tumor metastasis. Med Ann DC 35:463–466, 1966.
16. GERSHON RK, CARTER RL, and KONDO K. Immunologic defenses against metastases: impairment by excision of an allotransplanted lymphoma. Science 159:646–648, 1968.
17. SCHATTEN WE. An experimental study of postoperative tumor metastases. I. Growth of pulmonary metastases following total removal of primary leg tumor. Cancer 11:455–459, 1958.
18. GREENE HSN, and HARVEY EK. The inhibitory influence of a transplanted hamster lymphoma on metastasis. Cancer Res 20:1094–1100, 1960.
19. MARIE P, and CLUNET J. Fréquence des métastases viscérales chez les souris cancéreuses aprés abtalion chirurgicale de leur tumeur. Bull Assoc Fr Etud Cancer 3:19–23, 1910.
20. TYZZER EE. Factors in production and growth of tumor metastases. J. M. Research 28:309–332, 1913.
21. THUNOLD S. Acquired immunity after surgical removal of subcutaneous Ehrlich's ascites carcinoma. Acta Pathol Microbiol Scand 71:564–574, 1967.
22. BELEHRADEK J, JR, BARSKI G, and THONIER M. Evaluation of cell-mediated antitumor immunity in mice bearing a syngeneic chemically induced tumor. Influence of tumor growth, surgical removal and treatment with irradiated tumor cells. Int J Cancer 9:461–469, 1972.
23. WHITNEY RB, LEVY JG, and SMITH AG. Influence of tumor size and surgical resection on cell-mediated immunity in mice. J Natl Cancer Inst 53:111–116, 1974.
24. ROMSDAHL MM. Influence of surgical procedures on development of spontaneous lung metastases. J Surg Res 4:363–370, 1964.
25. RUDENSTAM CM, and IVARSSON L. Effect of surgical trauma on metastasis formation. (Abstr) *In* Proceedings of the 11th International Cancer Congress, 1974, vol 1, pp 63–64.
26. RUDENSTAM CM. Experimental studies on trauma and metastasis formation. Acta Chir Scand (suppl) 391:1–83, 1968.
27. SCHATTEN WE, and KRAMER WM. An experimental study of post-operative tumor metastases. II. Effects of anesthesia, operation and cortisone administration on growth of pulmonary metastases. Cancer 11:460–462, 1958.
28. HOOVER HC, and KETCHAM AS. Techniques for inhibitory tumor metastases. Cancer 35:5–14, 1975.
29. HALLERAKER B, and HARTVEIT F. Interaction between subcutaneous and intraperitoneal transplants of Ehrlich carcinoma: the possible role of antitumor antibody. J Pathol 105:95–103, 1971.
30. HARTVEIT F, and HALLERAKER B. Effect of subcutaneous transplants of Ehrlich carcinoma on the survival time of mice with intraperitoneal transplants of the same tumour. J Pathol 105:85–93, 1971.
31. VINCENT PC, and NICHOLLS A. Comparison of the growth of the Ehrlich ascites tumor in male and female mice. Cancer Res 27:1058–1065, 1967.
32. YUHAS JM, and PAZMIÑO NH. Inhibition of subcutaneously growing line 1 carcinomas due to metastatic spread. Cancer Res 34:2005–2010, 1974.
33. GOLDIE H, WALKER M, KELLEY L, ET AL. Free tumor cell growth in the peritoneal cavity (ascites tumor) of mice bearing subcutaneous tumors. Cancer Res 16:553–558, 1956.
34. MILAS L, HUNTER N, MASON K, ET AL. Immunological resistance to pulmonary metastases in C3HF/Bu mice bearing syngeneic fibrosarcoma of different sizes. Cancer Res 34:61–71, 1974.
35. CHESHIRE PJ. The effect of multiple tumors on mammary tumor growth rate in the C3H mouse. Br J Cancer 24:542–547, 1970.
36. GOODMAN GJ. Effects of one tumor upon the growth of another. Proc Am Assoc Cancer Res 2:207, 1957.
37. ROCKWELL S, and KALLMAN RF. Growth and cell population

kinetics of single and multiple KHT sarcomas. Cell Tissue Kinet 5:449–457, 1972.

38. MIKULSKA ZB, SMITH C, and ALEXANDER P. Evidence for an immunological reaction of the host directed against its own actively growing primary tumor. J Natl Cancer Inst 36:29–35, 1966.
39. VAAGE J. Concomitant immunity and specific depression of immunity by residual or reinjected syngeneic tumor tissue. Cancer Res 31:1655–1662, 1971.
40. CAHPUT B, RELLA W, and VETTERLEIN M. Changes in cell mediated immune functions by growing tumor. Eur J Cancer 10:185–188, 1974.
41. DECKERS PJ, DAVIS RC, PARKER GA, ET AL. The effect of tumor size on concomitant tumor immunity. Cancer Res 33:33–39, 1973.
42. YOUN JK, LEFRANCOIS D, and BARSKI G. In vitro studies on the mechanism of the "eclipse" of cell-mediated immunity in mice bearing advanced tumors. J Natl Cancer Inst 50:921–926, 1973.
43. BARSKI G, and YOUN JK. Evaluation of cell-mediated immunity in mice bearing an antigenic tumor. Influence of tumor growth and surgical removal. J Natl Cancer Inst 43:111–121, 1969.
44. PARANJPE MS, and BOONE CW. Kinetics of the antitumor delayed hypersensitivity response in mice with progressively growing tumors: stimulation followed by specific suppression. Int J Cancer 13:179–186, 1974.
45. PREHN RT. The immune reaction as a stimulator of tumor growth. Science 176:170–171, 1972.
46. ———. Immunological surveillance. *In* Clinical Immunobiology (Bach FH, and Good RA, eds). New York, Academic Press, 1974, pp 191–203.
47. JEEJEEBHOY HF. Stimulation of tumor growth by the immune response. Int J Cancer 13:665–678, 1974.
48. CARNAUD C, HOCK B, and TRAININ N. Influence of immunologic competence of the host on metastases induced by the 3 LL Lewis tumor in mice. J Natl Cancer Inst 52:395–399, 1974.
49. JAMES SE, and SALSBURY AJ. Facilitation of metastasis by antithymocyte globulin. Cancer Res 34:367–370, 1974.
50. PETERS LJ. Enhancement of syngeneic murine tumour transplantability by whole body irradiation—a non-immunological phenomenon. Br J Cancer 31:293–300, 1975.
51. RISCA R, KIRICUTA I, and TODORUTIU C. Conditions of surgery aggression favourizing metastases. *In* Proceedings of the 11th International Cancer Congress, 1974, vol 4, pp 640–641.
52. MARTINEZ C, MIROFF G, and BITTNER JJ. Effect of size and/or rate of growth of a transplantable mouse adenocarcinoma on lung metastases production. Cancer Res 11:1023–1026, 1956.
53. KINSEY DL. Effects of surgery upon cancer metastasis. JAMA 18:734–735, 1961.
54. KETCHAM AS, KINSEY DL, WEXLER H, ET AL. The development of spontaneous metastases after the removal of a "primary" tumor. II. Standardization protocol of 5 animal tumors. Cancer 14:875–882, 1961.
55. KETCHAM AS, WEXLER H, and MANTEL N. Studies on the effects of surgery on transplanted animal tumors and their metastases. J Natl Cancer Inst 27:1311–1319, 1961.
56. WEXLER H, MINTON JP, and KETCHAM AS. A comparison of survival time and extent of tumor metastases in mice with transplanted, induced and spontaneous tumors. Cancer 18:985–994, 1965.
57. KARRER K, HUMPHREYS SR, and GOLDIN A. An experimental model for studying factors which influence metastasis of malignant tumors. Int J Cancer 2:213–223, 1967.
58. ZUBROD CG. The basis for progress in chemotherapy. Cancer 30:1474–1479, 1972.
59. SCHABEL FM, JR. Concepts for systemic treatment of micrometastases. Cancer 35:15–24, 1975.

Proliferative Character and Growth Modes of Neoplastic Disease as Determinants of Chemotherapeutic Efficacy [1]

Larry L. Schenken [2,*]

The concomitant evolution of several conceptual frameworks in oncotherapeutic research has resulted in significant advances in cancer therapy in the last decade. As Carter and Soper (1) have suggested, the optimal utilization of chemotherapeutic agents requires information on the mechanism of drug action, cell cycle specificity, pharmacologic characteristics, toxicologic considerations, and also clinical results. However, central to most treatment-schedule designs is the underlying concept that treatment efficacy hinges on the ability to achieve cytotoxic levels of drugs in as many labile tumor cells as possible.

Since it was discovered that many chemotherapeutic agents selectively kill cells (both tumor and normal) in certain kinetically defined proliferative stages, many investigators have suggested that parameters descriptive of the proliferative state could be used to optimize drug selection and oncotherapeutic schedule design. Skipper (2,3) suggested that the compartmental analysis of a tumor's proliferative state could be used to describe or predict chemotherapeutic responses. DeVita (4) stated that the differential kinetic analysis of normal and tumor tissues coupled with appropriate drug distribution information could lead to optimal dose selection and scheduling. Also, Bono (5) based several biochemical rationales for drug selection on structural-functional changes associated with the proliferative progression of cells. Chuang (6) recently reported a rather elegant number of cell kinetic and pharmacokinetic studies in a highly formalized computer-based prediction scheme for projecting L1210 growth curves during treatment schedules with cytosine arabinoside. Several reviews of the relationships between cell kinetic data and chemotherapeutic responses have been recently published (7–9).

The Cytokinetic Paradigm

In order to more accurately formalize our ways of thinking or patterns of research, we have constructed a cytokinetic paradigm for investigating the effects of oncotherapeutic modalities on proliferative tissue. Three basic precepts provide the underlying framework upon which the paradigm rests: (*a*) that proliferative tissues, be they normal or malignant, grow or renew in an orderly, predictable fashion; (*b*) that a given oncotherapeutic treatment results in a defined level of damage or cell kill; and (*c*) that predictable cytokinetic changes are induced in a given tissue by a given cytotoxic treatment. (The degree of cytokinetic change post-treatment is related to the severity and type of damage caused by the treatment. Such changes may influence the response of a second treatment.)

Although one may utilize a cytokinetic paradigm for investigating responses in both normal and tumor tissues, figure 1 presents some generalities that may be applicable to a number of human neoplasms and experimental tumor systems not significantly influenced by homeostatic or immunologic control. As suggested in figure 1, throughout the observable range of tumor size increased tumor mass is accompanied by increases in observed tumor doubling times, instantaneous doubling times (or logarithmic doubling times [10]), cell loss factor, and mean cell cycle times. But with increased tumor mass, one may also see decreases in tumor-cell clonogenicity, thymidine labeling index (LI), and growth fraction. Although the placement of the curves shown in figure 1 may vary widely from tumor to tumor, the use of the paradigm requires that such data are obtainable for all tumors and that appropriate curves can be constructed for *any* tumor.

The curves in figure 1 suggest how the kinetic parameters of a small, highly proliferative, highly clonogenic tumor may change as the tumor grows. Tumor mass approaches theoretic maximum, instantaneous doubling times increase dramatically, and observed doubling times may increase by a factor of 60 or 70. Cell loss may increase 15-fold. The LI may decrease from 60% to < 0.6%; growth fraction similarly decreases dramatically, and mean cell cycle times can increase to two or three times the

[1] Supported in part by Public Health Service grant CA-10438 and contract N01-CM-43730 from the National Cancer Institute (NCI), National Institutes of Health, Department of Health, Education, and Welfare.

[2] Clinical Radiation Therapy Research Center, Allegheny General Hospital, Pittsburgh, Pa.

[*] *Reprint requests to:* Larry L. Schenken, PhD, Cancer Research Unit, Division of Radiation Oncology, Clinical Radiation Therapy Research Center, Allegheny General Hospital, 320 E North Ave, Pittsburgh, Pa 15212.

initial values. As the tumor grows, successively smaller proportions of cells are in the proliferative compartment and the proportion of nonproliferative (G_0) cells increases. Thus, as a tumor grows, there are changes in cell proportions susceptible to various categories of cytotoxic agents.

The second component of a cytokinetic paradigm for chemotherapy of neoplasia relates specifically to the classification of cell kill elicited by a given type of agent. In figure 2, the relative cell kill resulting from the *minimum* dosage necessary to kill "all" of the most sensitive subpopulation of cells within a tumor is plotted as a function of decreasing growth fraction for several classes of chemotherapeutic agents.

In panel A of figure 2 it may be seen that when the growth fraction is 1.0, cell kill resulting from treatment with a cycle-active, stage-nonspecific agent is maximum; cell kill is minimum when the growth fraction is 0.0. Higher concentrations of this type of drug will not result in enhanced cell kill; lower concentrations will generate curves parallel to and of lesser magnitude than the curve presented.

Cycle-active, stage-specific agents will generate a relative kill curve similar to the one shown in panel

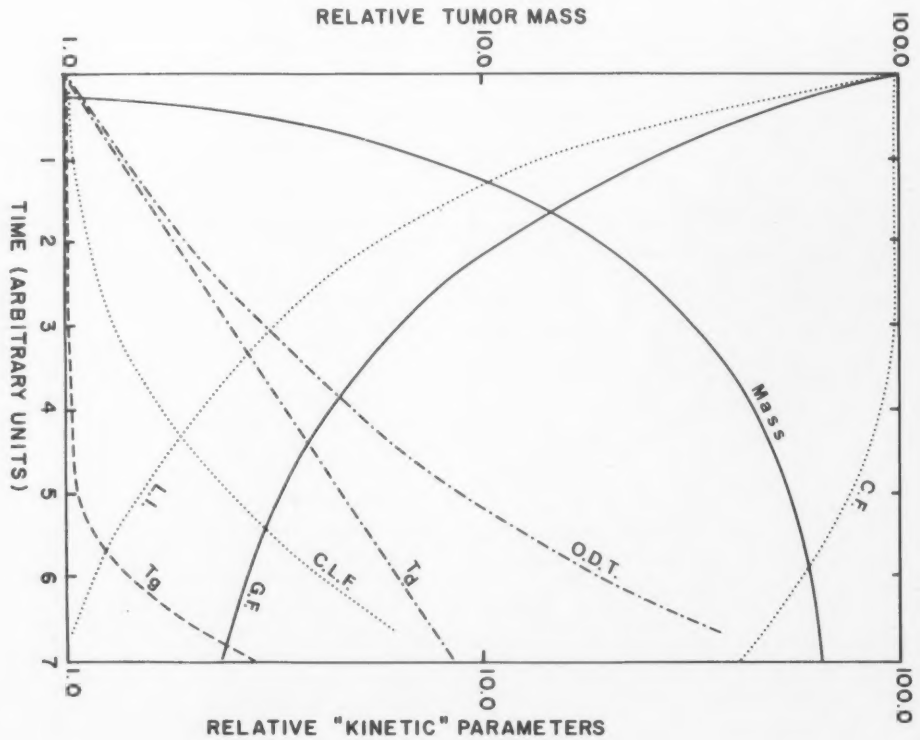

INSERT 105

FIGURE 1.—Cytokinetic paradigm: temporal aspects of cytokinetic changes in tumors of varying ages. C.F. = clonogenic fraction; Mass = tumor mass; O.D.T. = observed doubling time; T_d = instantaneous or logarithmic doubling time; C.L.F. = cell loss factor; G.F. = growth fraction; T_c = mean cell cycle time; L.I. = ^{3}HTdR labeling index.

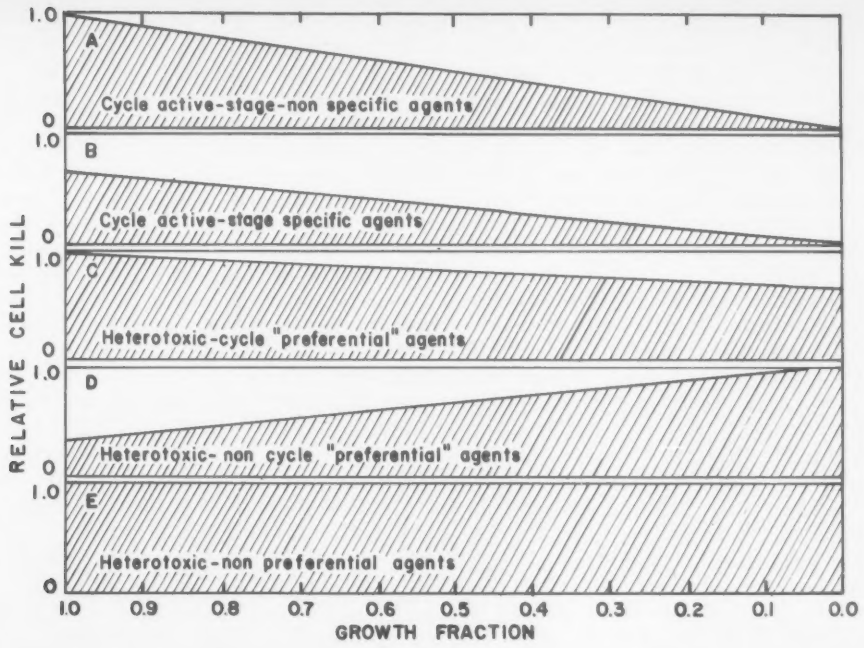

FIGURE 2.—Cytokinetic paradigm: relative cell kill as a function of growth fraction for several descriptive classes of chemotherapeutic agents; classification of agents according to these categories is useful in providing differential cell kill in tumors of varying growth fraction.

B of figure 2. As with cycle-active, stage-nonspecific agents, increasing the dosage of cycle-active, stage-specific agents will not displace the curve upward, and lesser amounts of drug will generate parallel curves displaced downward from the curve plotted. Relative cell kill caused by an agent toxic to any of several phases of the cell cycle can be summed to determine the starting point for such a curve.

The cell kill caused by heterotoxic, cycle-"preferential" agents in populations of differing growth fraction is presented in panel C of figure 2. As contrasted to the first two drug types, increasing the concentration of drug in this classification results in kill curves parallel to and displaced upward from the curve drawn and decreased concentrations of drug will result in curves parallel to and displaced downward from the curve drawn. Panels D and E of figure 2 may be similarly evaluated.

The cytokinetic paradigm thus constructed provides a rational background for investigations relative to the design of chemotherapeutic treatment schedules and for the selection of cytotoxic agents. With added constraints imposed by pharmacokinetic and toxicologic considerations it becomes usable in most tumor treatment situations, whether they be for primary or metastatic lesions.

TUMOR STUDIES

The P815X2 Tumor System

The P815X2 mastocytoma is a murine mast cell tumor of connective tissue origin. The tumor was chemically induced in DBA/2 mice by Dunn and Potter (11), and established as a subline of transplantable neoplastic cells by Schindler et al (12). A particularly advantageous feature of this tumor is the multiplicity of growth modes which may be investigated. In vitro suspension growth may be characterized by an initial log-phase of growth (doubling time, approximately 11 hours) of reasonable duration, a secondary plateau phase of growth, and a third degenerative phase (13). The P815X2 tumor may also be grown in vitro as spheroid clones in semi-solid plasma clot gels. A single viable cell in such cloning media will give rise to a visible (diameter 2–3 mm) clone of cells in approximately 8 days. The P815X2 tumor can also be grown in vivo as an ascites tumor. As such, it exhibits a log doubling time of 14 hours, causes late abdominal plaques, and, eventually, metastasizes to several organs. Tumor growth following an sc inoculation (lower back) of 1×10^6 viable cells proceeds in an ordered fashion.

The mid-range doubling time (1.0–2.0-cm² area) of such tumors is approximately 5 days. Dimensional analysis of the tumor suggests that proportionality exists between diameter² or πr^2 expressions of area, and expressions of volume as defined by the formulas for expanding prolate spheroids. Thus, for convenience, diameter² or πr^2 expressions may be used to express changes in tumor growth pattern, and periodic non-destructive measures of tumor size in animals can be made on a repetitive basis.

Pathologic evaluation[3] of microscopic sections cut from solid tumors of various ages following sc inoculation of 1×10^6 P815X2 cells suggests that there is an orderly transition from young, amorphous, highly proliferative tumors to older tumors with proliferative zoning, internal organization, and low relative-proliferative activity.

The pattern of metastatic spread of the tumor is well defined. Inoculation of dispersed target-organ tissue into recipient animals to measure "takes" or in vitro cloning assays of metastatic cellularity verify that no metastatic involvement can be detected in most tissues prior to Day 6 post-inoculum. By Day 7 (or shortly thereafter), minimal metastatic cellularity can be shown in the lung, thymus, and mediastinal lymph nodes of the animal. Metastatic P815X2 cells can be demonstrated by Day 12 post-inoculum in the spleen, liver, and axillary lymph nodes. By Day 16, small numbers of metastatic cells may be found in brain tissue. As tumor-bearing animals approach death (approximately Day 26) large numbers of tumor cells may be demonstrated in the lungs; also, macroscopically visible colonies of tumor cells are apparent. The tumors' histologic appearance and degree of involvement vary considerably among organ sites, yet are quite predictable within a given site. Thus, the antineoplastic effects of chemotherapeutic agents on the same cell line may be evaluated in different sites (modes) of metastatic growth.

Previous studies in our laboratory have suggested that the responsiveness of the sc P815X2 solid tumors to various therapeutic efforts varies greatly with age of the tumor. Although more or less conventional schedules of radiotherapy are capable of controlling tumor growth, the high D_0s of cell survival curves for young tumors (225 rads) and advanced tumors (425 rads) almost preclude radiation alone as an effective modality (14). Surgical removal of the primary, followed by regional radiotherapy, will virtually eliminate local disease, but animals demonstrate little increased lifespan (ILS); they still die of metastatic disease (15). The tumor is amenable to treatment with many chemotherapeutic agents. Drug studies with adriamycin[4] alone, or in combination with radiotherapy, suggest unencouraging results (16). Although adriamycin is capable of causing high degrees of cell kill when rapidly proliferating cells are exposed in vitro or when metastatic cells are exposed in vivo,[5] the adriamycin-induced control of solid tumors in vivo (with many dosage schedules) has been impossible to achieve due to animal drug toxicity (17).

Studies to date have suggested that although adriamycin is capable of effective P815X2 cell kill in growth modes that are diffuse and reasonably proliferative, the drug is incapable of generating significant cell kill in tumor populations of a low growth fraction. We will present data in this paper illustrative of how utilization of the cytokinetic paradigm may suggest appropriate methods for the effective utilization of adriamycin in combined drug schedules.

METHODS OF INVESTIGATION

Experimental System

As previously stated, the P815X2 mastocytoma-DBA/2 mouse system was used. Animals (6–8-week-old males) were fed Purina Chow and acidified water ad libitum and were maintained in temperature/humidity regulated quarters on a 12-hour photoperiod. Tumors for all experimental groups were established by an sc inoculation of 1×10^6 cells on the lower back. All treatment groups contained a minimum of ten animals each.

Drugs

Adriamycin, BCNU, and cyclophosphamide were solubilized immediately before use in dilutions appropriate for injection of 0.01 ml of solution/g of animal weight.[6] Route of drug administration was ip.

---

[3]Schenken LL, Hagemann RF, Burholt DR, et al. Histopathologic correlates of tumor sensitivity to chemotherapeutic agents. Submitted for publication.

[4]Adriamycin: NSC-123127; CAS reg. No. 23214-92-8. Supplied by Developmental Therapeutics Program (DTP), Division of Cancer Treatment (DCT), NCI, Bethesda, Md.

[5]Hagemann RF, Schenken LL, Burholt DR, et al. Cytocidal action of adriamycin and irradiation on a multimodal growth experimental tumor system. Submitted for publication.

[6]BCNU: NSC-409962; CAS reg. No. 154-93-8; urea, 1,3-bis(2-chloroethyl)-1-nitroso-. Supplied by DTP, DCT, NCI, Bethesda, Md.

Cyclophosphamide: NSC-26271; CAS reg. No. 6055-19-2; 2*H*-1,3,2-oxazaphosphorine, 2-[bis(2-chloroethyl)amino]tetrahydro-, 2-oxide, monohydrate. Supplied by Mead Johnson Laboratories, Evansville, Ind.

Measures

Caliper measures of tumor diameters were used to express tumor area. Areas were calculated by the formula

$$A = \pi\left(\frac{D_1 + D_2}{4}\right)^2.$$

Mean area ± SE was plotted. P815X2 cell survival curves were obtained (as previously described [13]) from tissue excised 60 minutes after in vivo drug administration. Survival was measured in 7-, 14-, and 21-day-old solid tumors, in metastatically involved tissues (spleen, lung, and liver) on Days 14 and 21 post-inoculum, and in ascites tumors on Days 4 and 8 post-inoculum. In other studies, animal survival, integral tumor size (as percent of untreated control), and tumor size at death were monitored. Post-treatment indices of proliferative activity in various tumors were measured by tritiated thymidine (^{3}HTdR) incorporation. Tumors were excised 30 minutes after injection of 50 microcuries of ^{3}HTdR/mouse. Tissue samples were bisected. One subsample was weighed, fixed in Carnoy's solution, solubilized with Soluene, and counted in a liquid scintillation spectrometer to determine ^{3}H activity. Results were expressed as dpm/mg of wet weight. The contralateral sample was used to make tissue imprints on glass slides. These were fixed in Carnoy's to remove unincorporated ^{3}HTdR, and conventional autoradiographs were prepared. Autoradiographs were then scored for percent labeled cells.

RESULTS

Toxicity studies in non-tumor-bearing mice suggested that the LD10/30 for single-dose drug exposures were as follows: BCNU, 40 mg/kg; cyclophosphamide, 305 mg/kg; adriamycin, ≈ 10 mg/kg. Similarly, "maximum" non-lethal doses for weekly (q7d × 4) drug administration were determined: BCNU, 20 mg/kg; cyclophosphamide, 150 mg/kg; adriamycin, ≈ 3.5 mg/kg.

BCNU Alone

The effect of post-inoculum time on efficacy of BCNU administration was investigated. Previous reports of drug mode of action (18) and our "guesstimates" (from the paradigm) of changes in tumor growth fraction suggested that single-dose drug exposures would be more effective if given early in the development of the tumor. The growth inhibitory effects of a 20-mg/kg BCNU treatment given either 2 hours after or 2, 4, 7, 9, or 11 days after tumor inoculum are summarized in figure 3. As the dose of BCNU is delayed, its effect is reduced. Recovery of tumor growth proceeds after initial delays; there is a tendency for the "regrowth" curves following treatment to mimic the growth pattern seen in untreated controls (fig 3, G), but to be displaced temporally. Single doses of 20 mg/kg of BCNU, given either early or late, did not modify animal lifespan. Animals in all treatment groups died at approximately the same time as controls (mean, 26 ± 2.5 days). Even though single-drug treatments result in no increases in animal lifespan, delays in tumor growth are seen. Treatment 2 hours after cell inoculum results in the integral tumor size being reduced to 38% ± 14% of control. Treatment at Day 2 results in a reduction to 51% ± 9% of control: Day 4, 47% ± 7%; Day 7, 64% ± 3%; and Day 11, 83% ± 6%. Thus, post-treatment calculations of integral tumor size also suggest that the best control results from the earliest drug exposure.

The effects of weekly administrations of 20-mg/kg BCNU doses on tumor growth are summarized in figure 4. All drug schedules are 20 mg/kg q7d × 4; the significant variable is the time (from +2 hours to +11 days) of start of treatment. Again, as with single-dose exposures of the drug, delay in start of treatment results in decreased efficacy. Integral tumor size is reduced to < 1% for the A schedule, < 2% for the B schedule, 16% ± 7% for the C schedule, 19% ± 6% for the D schedule, 36% ± 18% for the E schedule, and 47% ± 9% for the very delayed F schedule. Although all schedules resulted in significant reduction in tumor mass, regrowth occurs during the treatments. Such regrowth may be related to changes in drug distributions, the genesis of true drug resistance, or redistribution of sensitive cell populations. We are presently trying to elucidate the reason for such regrowth. The maximum ILS elicited by any weekly BCNU treatment was 68%.

Adriamycin Alone

Although previous studies (16,17) suggested that chemotherapy with adriamycin alone would be relatively ineffective, we thought it necessary to use a "toxicity equivalent" level of adriamycin in these studies. Single doses of either 5 or 3.5 mg/kg were used, and weekly schedules of 3.5 mg/kg were investigated to measure effects on tumor growth and animal lifespan. Single exposures of either 3.5 or 5 mg/kg of adriamycin given 2 hours or 2 days post-inoculum resulted in short-term deviation from control values. Drug given on Day 4 or later had no effect on tumor growth. Similarly, 3.5-mg/kg/week schedules (q7d × 4) caused no statistically signifi-

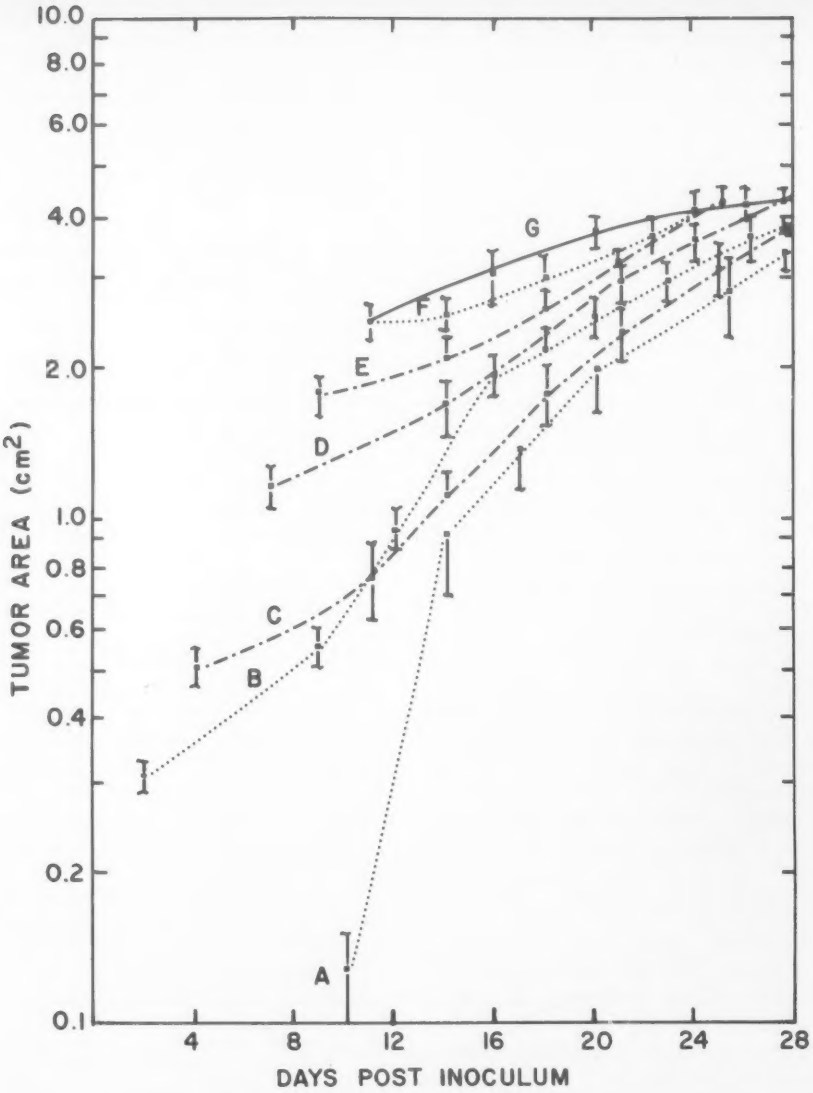

FIGURE 3.—Effects of single-dose BCNU exposure on solid P815X2 tumor growth. Single exposures of drug given at various times following cell inoculation. A = +2 hrs; B = +2 days; C = +4 days; D = +7 days; E = +9 days; F = +11 days; G = late growth of control tumors (mean ± SE).

cant reduction of tumor growth if the start of treatment was delayed to Day 4 or longer. No adriamycin treatments, single or weekly, resulted in increased animal lifespan, or in significantly decreased integral tumor size.

These single-drug studies again verified our feeling that BCNU was capable of generating solid tumor control, and that adriamycin when used alone was a poor therapeutic agent for solid tumors.

Cell Survival Studies

In an attempt to better delineate the differential responses seen following BCNU therapy from those seen following adriamycin therapy, in vivo cell survival studies were performed. The cytokinetically based paradigm for chemotherapy *suggested* that BCNU and adriamycin demonstrated qualitatively differential specificities of sensitive target popula-

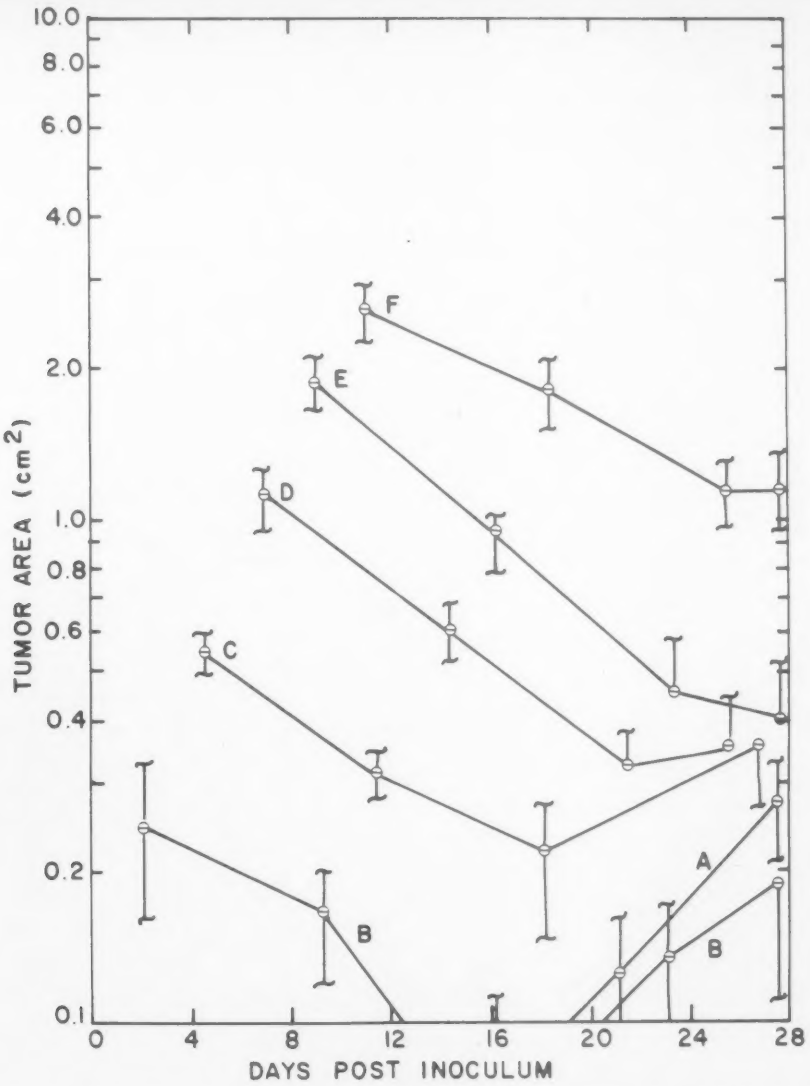

FIGURE 4.—P815X2 tumor growth during weekly BCNU treatment schedules. All schedules = 20 mg/kg of BCNU/wk for 4 wks. Times for schedule starts are same as for fig 3 (mean ± SE).

tions: we knew from previous studies that the LI in solid tumors decreased from 40% in young (3-day) tumors to < 1% in tumors that had grown for 21 days. BCNU was capable of causing tumor size reduction if either young or old tumors were treated, and furthermore, BCNU was more effective if treatment was started early. Therefore, it was hypothesized that BCNU could be classified as a heterotoxic cycle-preferential agent. Adriamycin, on the other hand, exerted no influence on tumors of advanced age, and produced only slight, short-lived suppression of growth of young tumors. Thus adriamycin could be thought of as *either* a cycle-active, stage-specific agent, or as a cycle-active, stage-nonspecific agent (panel A or B of fig 2).

Cloning assays (12) performed on tumor tissues removed 1 hour following in vivo BCNU exposures are summarized in figure 5. Survival data for 7-, 14-, and 21-day tumors have been averaged and plotted in figure 5(A) (mean ± SE). The data thus plotted

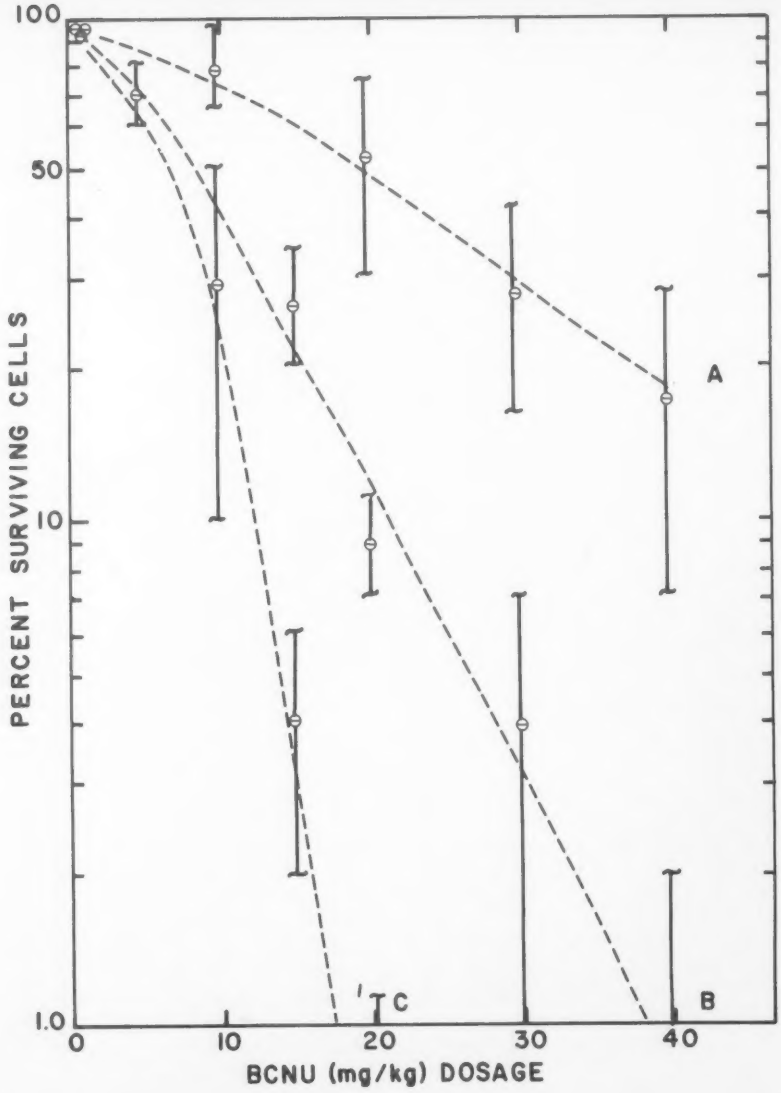

FIGURE 5.—Cell survival curves for P815X2 tumor cells exposed in vivo to varying doses of BCNU. A = solid tumor response range; B = metastatic cell response; C = cells exposed as ascites tumors (mean ± SE).

represent the *range* of kill one could expect to see in solid tumors that have advanced to stages of relatively low growth fraction, ≤ 0.30.[7] The survival curve suggests log kill over the range of concentrations that are acceptably toxic to animals. A similar plot of pooled data from metastatically involved spleen, lung, and liver (14 and 21 days post-inoculum) may be seen in figure 5(B). The range of BCNU kill for metastatic P815X2 cells appears to also decrease logarithmically with increasing drug dosage. The slope of this metastatic cell-kill curve is much greater than the slope of figure 5(A). A similar plot of cell-kill range following in vivo exposure of P815X2 ascites tumors is shown in figure 5(C).

Cell survival curves following in vivo exposure to adriamycin were also obtained and are shown in

[7]Schenken LL, Hagemann RF, Burholt DR, et al. The utilization of growth fraction as a predictor of chemotherapeutic efficacy. Submitted for publication.

figure 6. As in figure 5, ranges of kill (mean ± SE) for pooled data were plotted. Curve A of figure 6 shows the cell survival seen in solid tumors following adriamycin treatment. A trailing off of the survival curve suggests little increase in cell kill as drug concentration is increased from 1.0 to 3.0 mg/kg. The plot of survival in metastatic sites (fig 6[B]) demonstrates an initial log kill to concentrations of 0.5 mg/kg followed by a rapid trailing off of the survival curve. The survival data for cells exposed as ascites tumors demonstrated great age-dependent variability, so it was deemed necessary in this instance to plot data from log ascites growth (fig 6 [D]) separate from early plateau ascites growth (fig 6[C]). Adriamycin-induced cell kill proceeds logarithmically with increasing drug dose in figure 6(C and D).

Inspection of the pooled survival data for solid tumors, metastatic P815X2 cells, and tumor cells growing in ascites summarized in figures 5 and 6

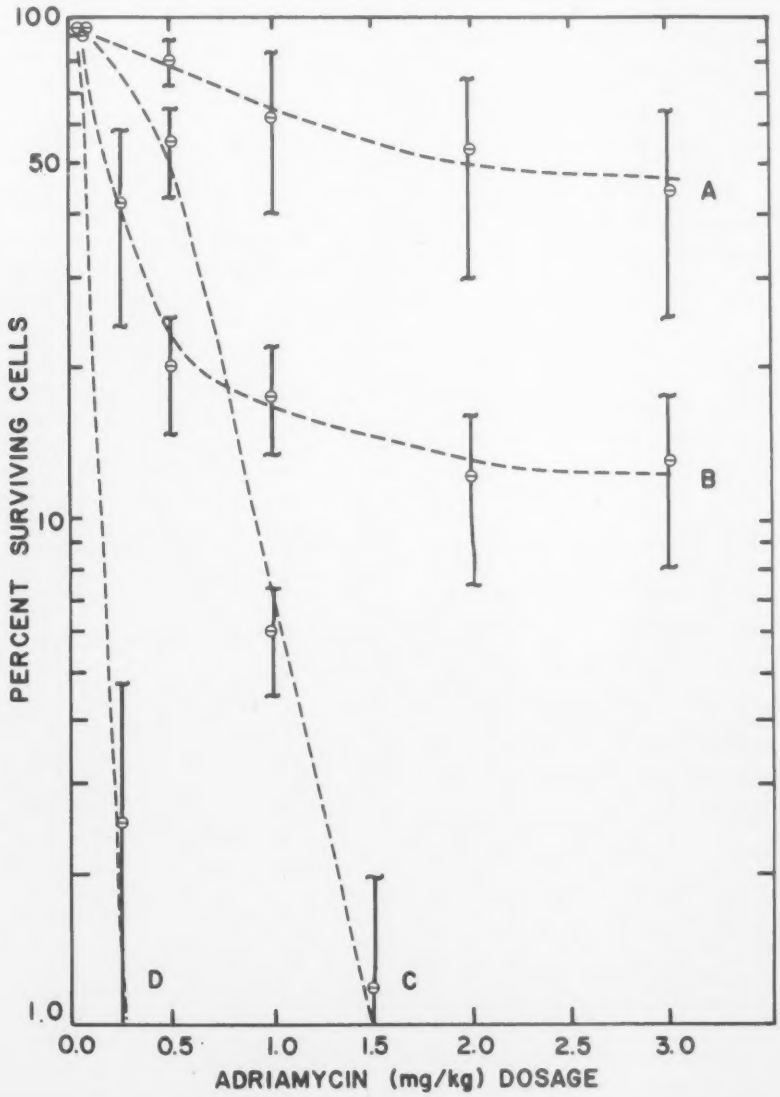

FIGURE 6.—P815X2 survival following in vivo adriamycin exposure. A = solid tumors; B = metastatic cells; C = plateau-phase ascites; D = log phase ascites.

further reinforces the concept that BCNU is quite capable of generating log kill of tumor cells in various growth modes and that adriamycin is capable of eradicating large numbers of highly proliferative cells but becomes more and more ineffective as tumor growth becomes less proliferative. (Previous survival analyses have further shown in solid tumors, as age increases and growth fraction of such tumors decreases, that adriamycin efficacy is proportionately reduced.[5]) Although one is further tempted to conclude that the comparative trailing off of survival curves in solid and metastatic growth modes is reflective of relative differences in growth fraction, appropriate kinetic studies designed to test this hypothesis are in progress. Although definitive answers to the question of adriamycin kill specificity also must be based (at least in part) on drug-distribution studies, it seems reasonable to assume that if log kill does exist to a certain dose level, and that thereafter increased drug administration results in minimal increases in cell kill, then the trailing phenomenon is likely caused by resistant subpopulations.

Proliferative Changes

If it is recalled that the paradigm suggests that a fundamental response elicited in tumors after cytotoxic treatment is proliferative change (ie, decreases in tumor mass result in transient increases in LI, growth fraction, etc), the necessity for obtaining comparative proliferative measures following treatments with BCNU and/or cyclophosphamide (treatments summarized later in this paper) is obvious.

The data summarized in figure 7 show tumor LI and ^{3}HTdR dpm/mg as a function of time following a 20-mg/kg in vivo exposure to BCNU (fig 7[A]) or a 150-mg/kg exposure to cyclophosphamide (fig 7[B]). Animals bearing 7-day-old tumors were given the drug ip in both cases. Both the dpm/mg measures and the ^{3}HTdR LIs changed dramatically following BCNU or cyclophosphamide treatment. Both parameters remained below control limits for approximately 48 hours following the drug treatments and then increased to high levels during the post-treatment time span of 48–96+ hours. This would suggest that the efficacy of a cycle-active agent on tumor cells surviving either the BCNU or the cyclophosphamide treatment would be highest during these delayed times, and that cycle-active drug efficacy would be minimal shortly after BCNU or cyclophosphamide treatment.

[5]See footnote 5.

Combined BCNU-Adriamycin Studies

Although adriamycin alone caused little change in the growth patterns of solid tumors and appeared incapable of significant cell kill in solid tumors, the drug showed promising activity against metastatic P815X2 cellularity at doses as low as 0.5 mg/kg, and could reduce cell survival to approximately 1.0% in log phase ascites (proliferative) tumors with such doses. Also, it was observed that BCNU efficacy in controlling solid tumors was reasonably good, and that following a single BCNU treatment the tumor's relative proliferative activity increased during the post-treatment time period of 24–96+ hours. Therefore, the combination of BCNU plus adriamycin was evaluated.

Adriamycin given qd on Days 8–11, 15–18, 22–25, and 29–32 (0.5 mg/kg) post-inoculum results in no tumor control as seen in figure 8(A). The growth data summarized in figure 8(B) show the effect of 20 mg/kg of BCNU q7d × 4 beginning Day 7 post-inoculum (a time when metastases are already present). The combination of the above schedules results in tumor growth summarized by figure 8(C). It was hoped that the adriamycin fractions given on Days 1–4 after each weekly BCNU dose would temporally bracket the proliferative rebound from the BCNU treatment, and result in enhanced tumor control. Such temporal placement of low adriamycin dosages in a weekly BCNU schedule resulted not only in greatly enhanced control of local tumor, but greatly increased animal ILSs and high cure rates. Comparative data for different treatment schedules with drugs are summarized in table 1.

Combined Cyclophosphamide-Adriamycin Studies

Previous studies with cyclophosphamide and cyclophosphamide-radiation combinations suggested that, like BCNU, cyclophosphamide was capable of controlling local disease, but incapable of curing systemic disease. A dose of 150 mg/kg of cyclophosphamide was selected for combined studies because such drug levels cause approximately the same degree of animal toxicity as 20 mg/kg of BCNU (if given in single-dose or in 150-mg/kg q7d × 4 schedules).

The effect of tumor age on single-dose cyclophosphamide response is summarized in figure 9. The effects of weekly doses of 150 mg/kg of cyclophosphamide are summarized in figure 10. As with BCNU, single doses of cyclophosphamide seemed more efficacious if given early, and, as with BCNU, schedules of cyclophosphamide given weekly caused better tumor control if the schedule was started early.

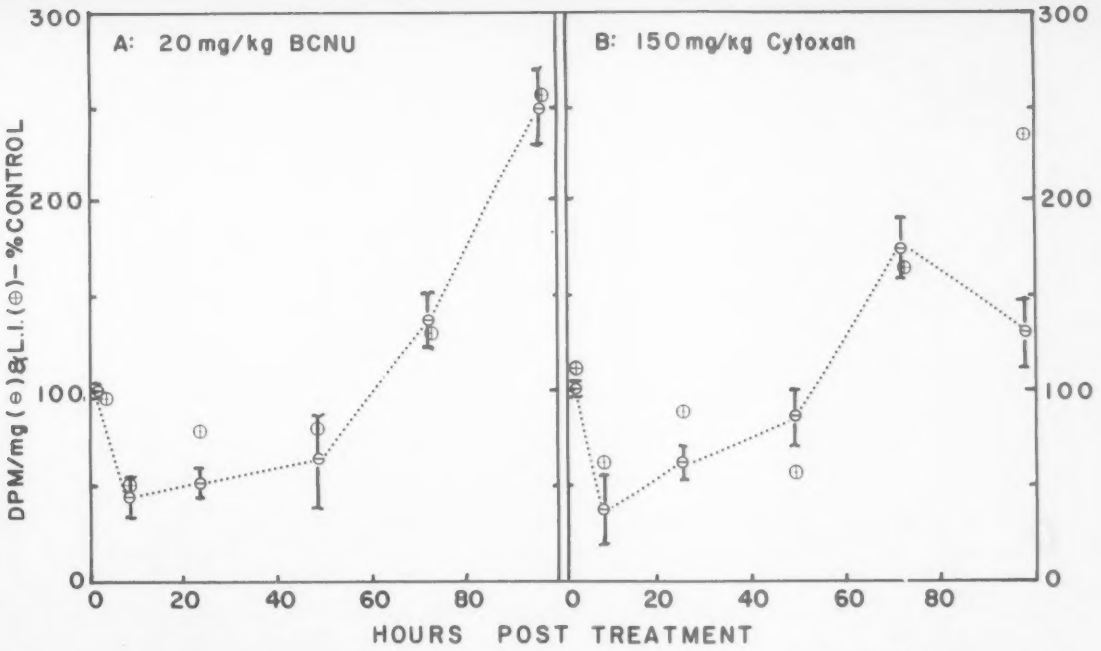

FIGURE 7.—^{3}HTdR dpm/mg P815X2 tumor mass following single in vivo exposure of 20 mg/kg of BCNU (A) and 150 mg/kg of cyclophosphamide (B) (% of control values ± SE). LI expressed as % of control also plotted.

Cyclophosphamide given alone in any of the schedules summarized in figures 9 and 10 resulted in a maximum ILS of 81%; no cures resulted. As summarized in figure 11 and in table 1, the combination of 150 mg/kg of cyclophosphamide q7d + 0.5 mg/kg of adriamycin qd on Days 8–11, 15–18, 22–25, and 29–32 proved much better than the cyclophosphamide-alone schedule. Although weekly schedules of cyclophosphamide alone can eradicate local disease, animals still die of metastatic involvement. The addition of low dose, fractionated adriamycin to the weekly cyclophosphamide schedule results in faster ablation of solid tumors, and greater ILSs and modest cure rates.

DISCUSSION

Although one cannot and should not discount such considerations as differences in drug distributions, microvasculature, intrinsic levels of cellular sensitivities, or changing patterns of host-mediated drug detoxification and elimination, it appears incontrovertible that differential responses seen following chemotherapeutic treatments of tumors with varying degrees of maturation or in varying growth modes may most readily be correlated with the kinetic character of the tissue at the time of treatment.

There have been indications in the literature that alkylating agents exhibit differential responses in tumors of varying growth fraction. DeWys (19) and Mayo (20) have both suggested that the Lewis lung experimental solid tumor was more sensitive to cyclophosphamide in early stages of growth. Straus and Goldin (21) have suggested increased efficacy of loading schedules of cyclophosphamide in the treatment of L1210. Studies with the drug BCNU suggest that anomalous drug-distribution patterns or serum-binding effects may be responsible for the very confusing relationships reported between proliferative state and drug sensitivity. Yet many studies relatively free of drug-distribution considerations such as van Putten's work with hematopoietic stem cells (22) suggest a positive correlation between proliferative activity and the BCNU sensitivity of cell populations.

A number of investigators, including Sandberg and Goldin (23), have reported a lack of effectiveness of adriamycin treatment for management of solid tumors. Sandberg et al (24) have suggested that the most effective schedules for L1210 therapy with adriamycin were q3h (195% ILS) and daily (63%

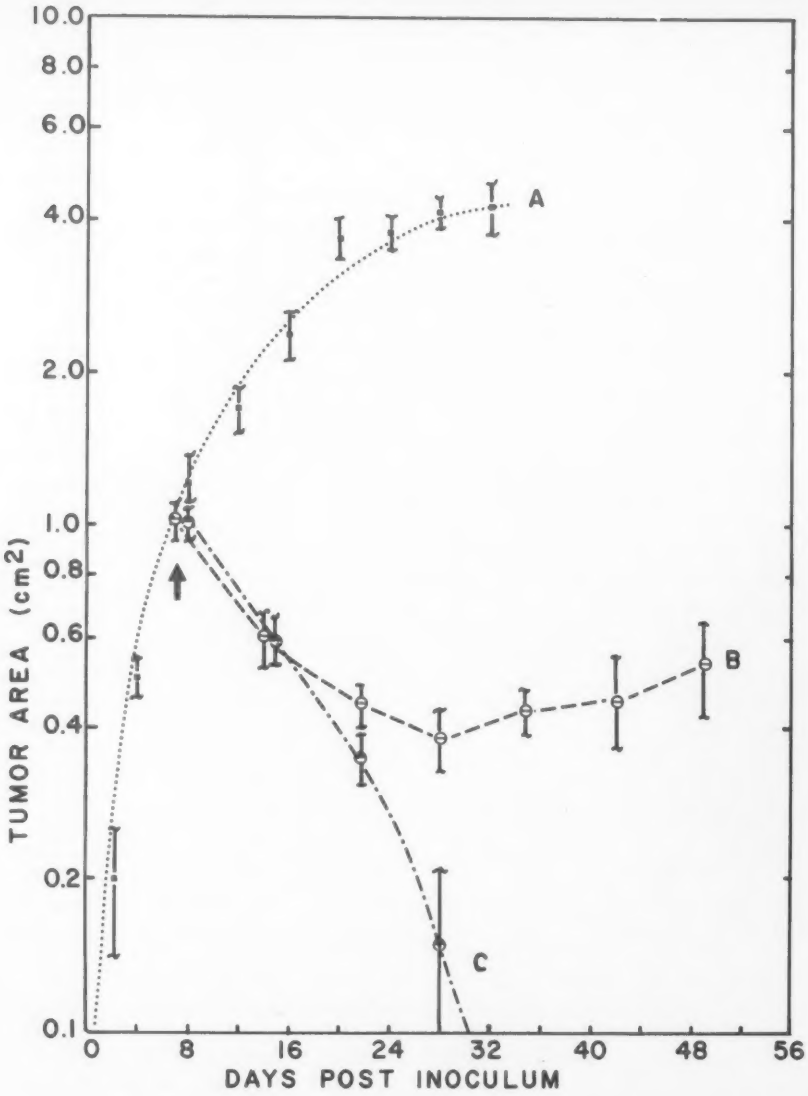

FIGURE 8.—Combination BCNU-adriamycin therapy: A = 0.5 mg/kg of adriamycin on Days 8–11, 15–18, 22–25, 29–32; B = 20 mg/kg of BCNU on Days 7, 14, 21, 28; C = combination of A and B schedules (mean tumor area ± SE).

ILS). This result suggests again that adriamycin exhibits some degree of preferentiality toward kill of cycling cells.

The combination of adriamycin with other chemotherapeutic agents has proven advantageous in many clinical situations and in many studies using experimental tumor systems. Corbett et al (25) found the combination of cyclophosphamide and daily adriamycin most effective after sc implantation of C3H mammary adenocarcinomas. Also, Kopper and Steel (26) found that the combination of cyclophosphamide plus adriamycin given 7 days later was advantageous in treating human tumor lines maintained in immune-suppressed mice. Such studies, and studies summarized in this communication, suggest that adriamycin, although not necessarily effective in controlling solid tumor growth when the proliferative activity of the tissue is low,

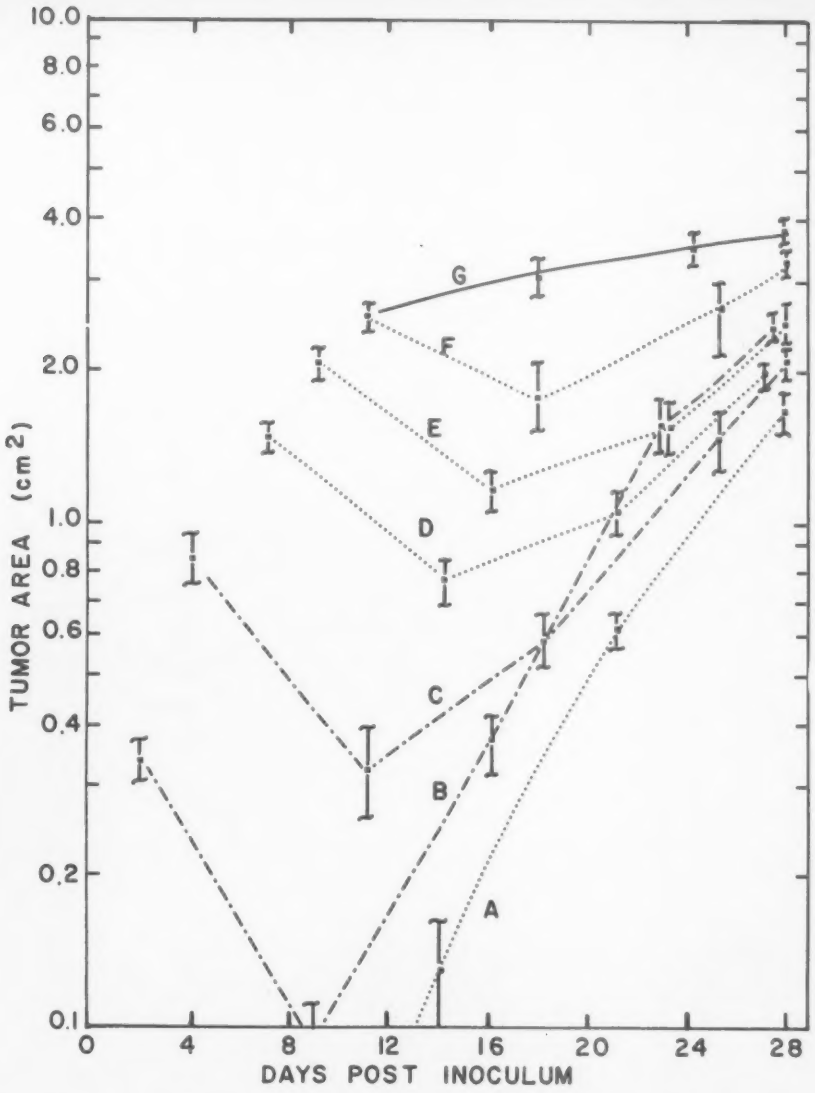

FIGURE 9.—Effects of single-dose cyclophosphamide exposures on P815X2 solid tumor growth. Dosage = 150 mg/kg of cyclophosphamide. Schedule is the same as in fig 3.

may be used with a high degree of efficacy during periods of proliferative rebound induced in such tumors by other drugs.

The use of a cytokinetically based paradigm for planning chemotherapeutic strategies may prove helpful, especially in situations where the efficacy of a therapeutic agent is impaired by the presence of non-proliferative, resistant subpopulations of tumor cells in certain growth modes.

REFERENCES

1. CARTER SK, and SOPER WT. Integration of chemotherapy into combined modality treatment of solid tumors. Cancer Treat Rev 1:1–13, 1974.
2. SKIPPER HE. Improvement of the model systems. Cancer Res 29:2329–2333, 1969.
3. SKIPPER HE. The cell cycle and chemotherapy of cancer. *In* The Cell Cycle and Cancer (Baserga R, ed). New York, Marcel Dekker Inc, 1971.

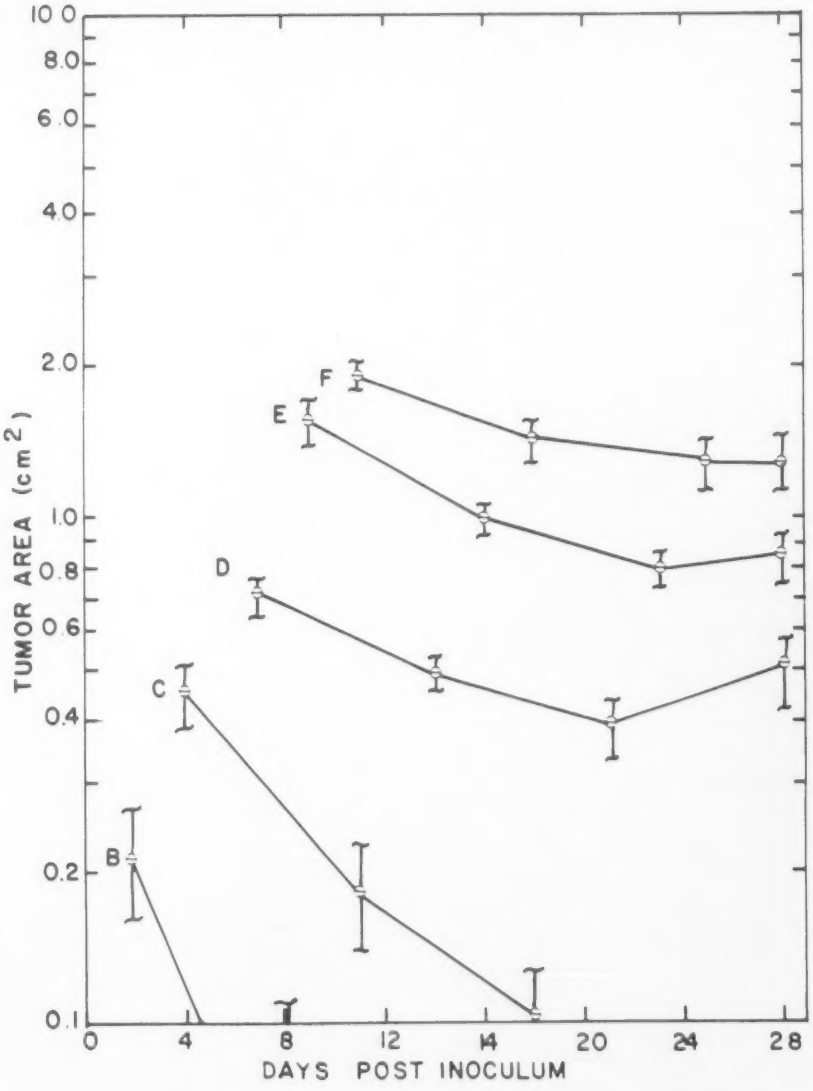

FIGURE 10.—Effects of weekly cyclophosphamide (150 mg/kg q7d × 4 as in fig 4) treatment on P815X2 tumor growth (mean area ± SE). "A" schedule results in total ablation of visible tumor mass for duration of animal lifespan.

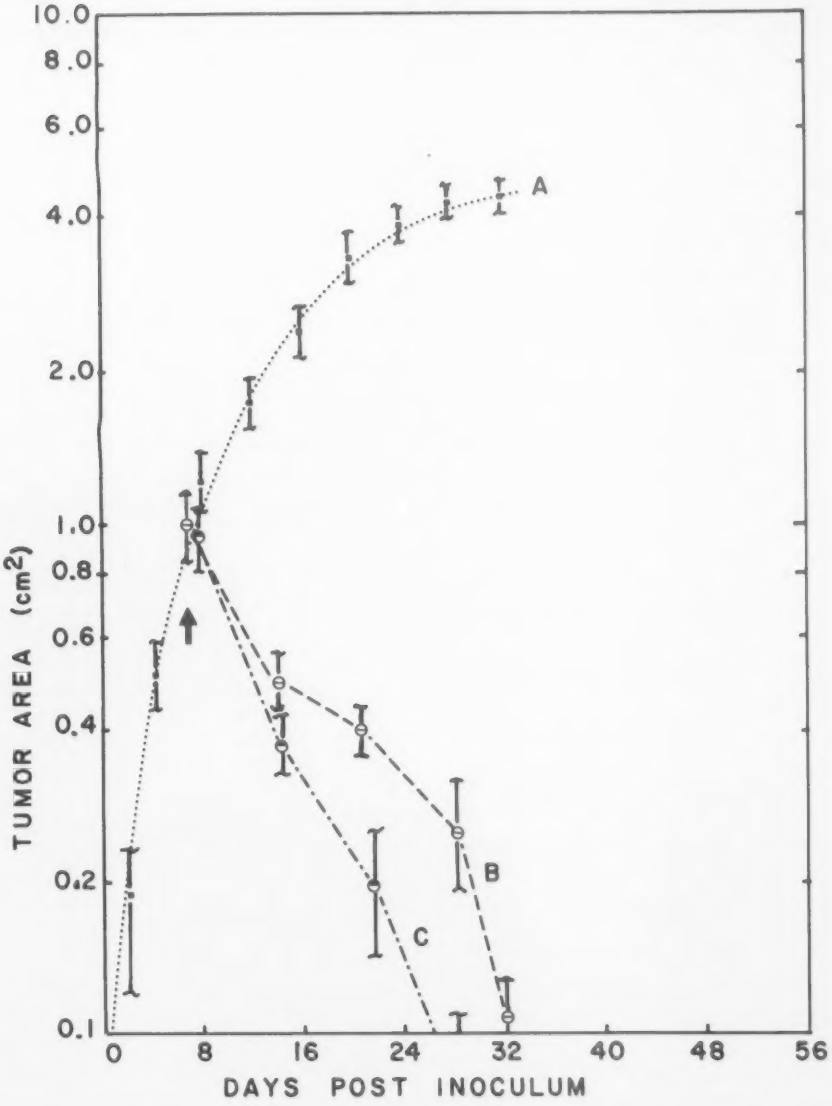

FIGURE 11.—Combination cyclophosphamide-adriamycin therapy: A = 0.5 mg/kg of adriamycin on Days 8–11, 15–18, 22–25, 29–32; B = 150 mg/kg of cyclophosphamide on Days 7, 14, 21, 28; C = combination of A and B schedules (mean tumor area ± SE).

TABLE 1.—Treatment response parameters for BCNU, cyclophosphamide, and adriamycin combinations

Treatment schedule (mg/kg)	Mean tumor size at death (cm^2)	Animal survival time (days)	ILS (%)	Responders (%)	Duration of response* (days)	Cure rate (%)
None	4.25	26	—	—	—	—
Adriamycin, Days 8–11, 15–18, 22–25, 29–32 (0.5)	3.80†	26	0	0	0	0
BCNU, Days 7, 14, 21, 28 (20)	0.40	38	68	60	57	0
Combination of adriamycin + BCNU schedules	0.28	64+	246	90	71	80
Cyclophosphamide, Days 7, 14, 21, 28 (150)	0.30	40	53	60	16.5	0
Combination of cyclophosphamide + adriamycin schedules	0.05	46	77	90	21.5	20

*Response defined as regression of tumor to nonpalpable mass.
†Not statistically different from controls.

4. DEVITA VT. Cell kinetics and the chemotherapy of cancer. Cancer Chemother Rep Part 3, vol 2(1):23–33, 1971.
5. BONO VH, JR. Biochemical rationales for the selection of combinations of chemotherapeutic agents. Cancer Chemother Rep Part 2, vol 4(1):131–136, 1974.
6. CHUANG SN. Mathematic models for cancer chemotherapy: pharmacokinetic and cell kinetic considerations. Cancer Chemother Rep 59:827–842, 1975.
7. WHEELER GP, and SIMPSON-HERREN L. Effects of purines, pyrimidines, nucleotides, and chemically related compounds on the cell cycle. *In* Drugs and the Cell Cycle (Zimmerman AM, Padilla GM, and Cameron IL, eds). New York, Academic Press, 1973, pp 249–306.
8. VAN PUTTEN LM. Are cell kinetic data relevant for the design of tumor chemotherapy schedules? Cell Tissue Kinet 7:493–504, 1974.
9. VALERIOTE F, and VAN PUTTEN L. Proliferative-dependent cytotoxicity of anticancer agents: a review. Cancer Res 35:2619–2630, 1975.
10. SIMPSON-HERREN L, and LLOYD HH. Kinetic parameters and growth curves for experimental tumor systems. Cancer Chemother Rep 54:143–174, 1970.
11. DUNN TB, and POTTER M. A transplantable mast cell neoplasm in the mouse. J Natl Cancer Inst 18:587–596, 1957.
12. SCHINDLER R, DAY M, and FISHER GA. Culture of neoplastic mast cells and their synthesis of 5-hydroxy tryptamine and histamine in vitro. Cancer Res 19:47–51, 1959.
13. HAGEMANN RF, SCHENKEN LL, and LESHER S. Tumor chemotherapy: efficacy dependent on mode of growth. J Natl Cancer Inst 50:467–474, 1973.
14. SCHENKEN LL, POULAKOS L, and HAGEMANN RF. Responses of an experimental solid tumor to irradiation: a comparison of modes of fractionation. Br J Cancer 31:228–236, 1975.
15. SCHENKEN LL, and HAGEMANN RF. Combined modality therapy of solid P815X2 mastocytomas. Proc Am Assoc Cancer Res and ASCO 16:68, 1975.
16. POULAKOS L, SCHENKEN LL, HAGEMANN RF, ET AL. Control of local tumor growth with combined fractionated radiotherapeutic and chemotherapeutic regimens. J Natl Cancer Inst 54:1103–1105, 1975.
17. SCHENKEN LL, POULAKOS L, HAGEMANN RF, ET AL. Treatment of solid P815X2 murine mastocytoma with adriamycin (NSC-123127): toxicity limitations. J Natl Cancer Inst 56: 683–685, 1976.
18. CARTER SK, SCHABEL FM, JR, BRODER LE, ET AL. 1,3-Bis(2 chloroethyl)-1-nitrosourea (BCNU) and other nitrosoureas in cancer treatment: a review. *In* Advances in Cancer Research (Klein G, and Weinhouse S, eds). New York, Academic Press, 1972.
19. DEWYS WD. A quantitative model for the study of the growth and treatment of a tumor and its metastases with correlation between proliferative state and sensitivity to cyclophosphamide. Cancer Res 32:367–373, 1972.
20. MAYO JG. Biologic characterization of the subcutaneously implanted Lewis lung tumor. Cancer Chemother Rep Part 2, vol 3(1):325–330, 1972.
21. STRAUS MJ, and GOLDIN A. Effects of priming dose schedules in Cytoxan treatment of mouse leukemia L1210. Proc Soc Exp Biol Med 145:1132–1138, 1974.
22. VAN PUTTEN LM, LELIEVELD P, and KRAM-IDSENGA LKJ. Cell cycle specificity and therapeutic effectiveness of cytostatic agents. Cancer Chemother Rep 56:691–700, 1972.
23. SANDBERG J, and GOLDIN A. Use of first generation transplants of a slow growing solid tumor for evaluation of new cancer chemotherapeutic agents. Cancer Chemother Rep 55:233–238, 1971.
24. SANDBERG JS, HOWSDEN FL, DIMARCO A, ET AL. Comparison of the antileukemic effect in mice of adriamycin (NSC-123127) with daunomycin (NSC-82151). Cancer Chemother Rep 54:1–7, 1970.
25. CORBETT TH, GRISWOLD DP, MAYO JG, ET AL. Cyclophosphamide-adriamycin combination chemotherapy of transplantable murine tumors. Cancer Res 35:1568–1573, 1975.
26. KOPPER L, and STEEL GG. The therapeutic response of three human tumor lines maintained in immune-suppressed mice. Cancer Res 35:2704–2713, 1975.

Introduction to Session on Drug Lethality and Sublethal Damage: Cytotoxic Damage and Repair [1]

M. M. Elkind [2,*]

In cancer therapy it is now known that there are a number of characteristics of cytotoxic agents that are of importance. Before discussing these, it is useful to note that the term cytotoxic agent, as used here, is meant to include ionizing radiation in addition to chemotherapeutic drugs. It is also worth keeping in mind that adjuvants of one sort or another (eg, hyperthermia) may play a dominant role in modifying the characteristics of a given cytotoxic agent or some combination of them and, as I will discuss further, each of two or more agents may serve to enhance the others' effectiveness.

Cell Determinants

The use of in vitro cell culture systems, or cell systems that permit survival measurements in vitro and in vivo, has been instrumental in the development of basic concepts. Clearly, cells in culture are not entirely adequate for predicting either normal or tumor tissue responses. Nevertheless, the unraveling of the constellation of factors that reflect the basic cell biology is possible to a sufficiently greater degree with in vitro as opposed to in vivo systems as to strongly favor quantitative studies with cells preparatory to tissue measurements. At the least, cell culture studies can help to establish many of the principles needed to understand tissue responses.

Damage Registration

For cells undergoing active growth, cytotoxicity usually varies through the cell cycle. The correlation with the position or the age of a cell in its cycle has come to be called the "age-response function" or "age-response pattern" (1, chapter 2).

To illustrate age-response dependencies, consider the following cytotoxic agents: X-rays, mechlorethamine, and actinomycin D.[3] The age dependencies shown in figure 1 are for V79 Chinese hamster cells. In each case the variation for a small and a large single dose is traced. As one might expect, the shape of the patterns for mechlorethamine is similar to that for X-rays, supporting the long-standing notion that mechlorethamine is a radiomimetic agent. (This point will be discussed again further.) On the other hand, after small doses of actinomycin D, survival is maximal during G_2 as well as S, but after larger doses cells in G_2 are clearly more resistant than those in S. These patterns illustrate: (*a*) age-dependent responses; (*b*) similarities and differences in age responses; and (*c*) age responses, the shapes of which depend upon the level of effect.

Although it is reasonable to expect similarities in response among many types of cells in the case of a given agent, there are some situations which might be expected to be different. These include: noncycling, so-called G_0 cells; neoplastic versus their related normal cells; and cells in various degrees of nutritional sufficiency including oxygenation. Examples of the relevance of these factors are: (*a*) enhanced cell-killing by hyperthermia in neoplastic compared to normal cells; (*b*) enhanced toxicity of electron affinic cell sensitizers in hypoxic compared to euoxic cells; and (*c*) reduced cell killing by radiation of hypoxic tumor cells compared to euoxic tumor cells.

Dose Delivery

Ionizing radiation has the advantage that it is penetrating and directional. Also, for practical reasons, the dose-delivery rate is usually high. With chemicals there are the questions of: (1) penetration; (2) activation (or of a competing deactivation); (3) lesion production after the active material reaches the critical site, or of metabolic imbalance in the instance of a cycle-dependent action; and (4) dose rate since the time constants of these various steps may be comparable to progression rates in the cell cycle. In addition, as with radiation, cell aging of

[1]Supported by the US Energy Research and Development Administration.

[2]Division of Biological and Medical Research, Argonne National Laboratory, Ill.

Reprint requests to: Dr. M. M. Elkind, Division of Biological and Medical Research, Argonne National Laboratory, Argonne, Ill 60439.

[3]Mechlorethamine: NSC-762; CAS reg. No. 55-86-7; diethylamine, 2,2'-dichloro-*N*-methyl-, hydrochloride.

Actinomycin D: NSC-3053.

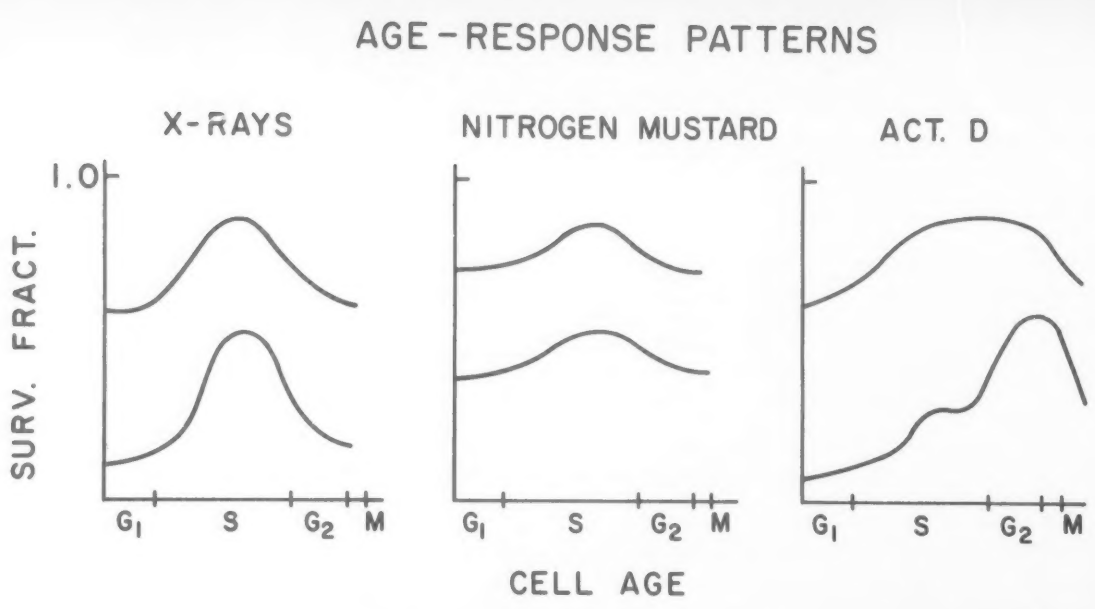

FIGURE 1.—Age-response dependencies for X-rays, mechlorethamine, and actinomycin D. Each line represents the variation of survival through the cell cycle after a fixed dose delivered in a short period of time compared to the length of the cycle (ie, about 1 min for X-rays and about 30 mins for the drugs). For each agent, the lower curve is the age-response pattern after a dose somewhat larger than for the upper curve. These patterns come from data obtained with various sublines of V79 Chinese hamster cells (2,3).

sublethally damaged cells may be affected by drug treatment. The release of still potent drug from lysing cells may be another factor complicating the situation in vitro (4) and in vivo.

Sublethal Damage Repair

When a threshold-type survival curve does not reflect nonlinearities in drug penetration or activation, it may be assumed that surviving cells are sublethally damaged. This is the case for mammalian cells exposed to X-rays (1). When accumulation of sublethal damage plays a significant role in cell killing, the possible repair of sublethal damage must be accounted for in the instance of treatments involving multiple doses. In radiation therapy it is well known that repeated doses of X- or γ-radiation reduce survival less efficiently than single doses (1). In general, those cytotoxic agents whose killing action involves the accumulation of sublethal damage might be expected to reduce survival according to F in figure 2 if damage is completely repaired between dose fractions.

Thus, sublethal damage repair (repair in this context being used in an operational sense) by itself can have a large effect on cell killing. If some amount of repopulation also takes place between dose fractions, the rate of survival decrease with increasing total dose may be even further reduced. With respect to drug action, repair and repopulation can be complicated by drug persistence due to binding in the cell.

Potential Lethal Damage Repair

The physiologic state of cells, their position in their growth cycle, and perhaps metabolic factors as well may all play a role in the expression of cell killing in vitro and in vivo. In contrast to sublethal damage repair, it is not possible to predict the extent, maximum or otherwise, of this form of repair. A few general remarks can be made nevertheless.

When a cell is treated with a cytotoxic agent, usually a considerable amount of potentially lethal damage is registered. An example comes from X-ray cell killing where it is known that cells may survive even after thousands of single strand breaks and hundreds of double strand breaks are registered in their DNA. With rare exceptions, mammalian cells, including xeroderma pigmentosum cells, repair breaks produced by ionizing radiation since the

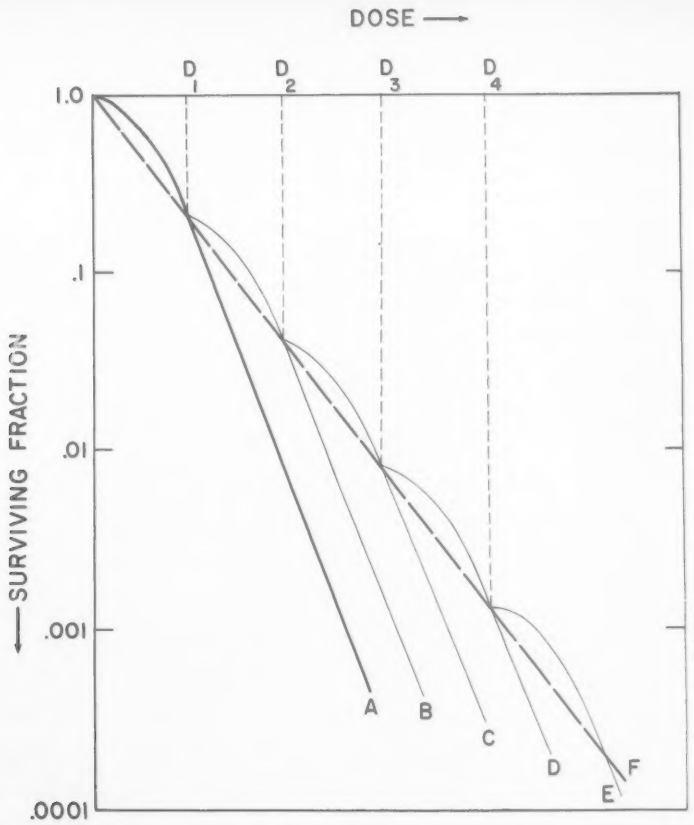

FIGURE 2.—Effect of repair of sublethal damage on cell survival. A = the single dose-survival curve. Repair of sublethal damage after dose D_1 causes the shoulder to reappear (ie, a return of a capacity for sublethal damage) so that B has the same shape as A. If this process is repeated after each dose fraction, F is the next survival curve instead of A (1).

progeny of survivors are like the parental cells. In this sense, most normal and tumor cells are repair competent. Consequently, post-treatment conditions that shift the balance between the amount of repair effected before the damage is fixed can alter the level of survival. In the case of radiation studies, the shifts in the slopes of survival curves are clear, but modest. After some chemotherapeutic agents, however, much larger changes have been observed. Consequently, the control of the repair of potential lethal damage in a given instance can have an important influence on the efficiency of cell killing.

Damage Interaction

In addition to repair processes which may or may not be operative after the treatment with a single agent, the damage produced by two or more agents may interact. This offers the possibility of an enhanced differential response between tumor and normal tissues, particularly if some specificity for the tumor tissue is involved. In view of the directionability of ionizing radiation, in principle radiation in combination with an appropriate drug offers such an advantage.

However, not all chemotherapeutic agents produce damage which interacts with radiation damage. With reference to the examples in figure 1, even though mechlorethamine over the years has been thought to act like radiation, it does not produce damage interactive with radiation damage (2). Actinomycin D does produce such damage (4) although the molecular action of this antibiotic had not been associated with radiation damage. The foregoing serves to illustrate that to utilize damage interaction, a detailed examination of cell-response properties is needed.

Age-Response Complementation

Finally, when two or more agents are used, even in the absence of damage interaction, enhanced net responses may be obtained. These could result when age-response functions complement each other or when advantage is taken of the partial synchronizations which result from each treatment. Using the patterns in figure 1 once again as examples, the sensitivity of S cells after moderate to large doses of actinomycin D would have the effect of appearing to enhance the killing of the population surviving an X-ray exposure (even if there were no damage interaction) because mainly S cells survive the latter. If mechlorethamine was added immediately before or after X-rays, an enhanced net response would not result because S cells are resistant to both treatments. However, if survivors of an X-ray exposure were allowed to age until they reached G_2, at that time an exposure to mechlorethamine would be particularly effective (even though there could be no damage interaction) because G_2 cells are sensitive to this agent.

Thus, complementation of age-response patterns in principle can be used to advantage if, in addition to dose size, appropriate dose scheduling is used. Considerations such as these have been already discussed (5).

As previously noted, cell studies are devoid of the physiologic influences of the host and hence have their limitations. While these should be recognized and while the number of cell-based phenomena of which we are aware may still be incomplete, the information already at hand indicates that in vitro studies have much to recommend them. Indeed, a knowledge of cell responses in the absence of host-mediated factors may help to identify the latter when they are large enough to contribute significantly.

REFERENCES

1. ELKIND MM, and WHITMORE GF. The Radiobiology of Cultured Mammalian Cells. New York, Gordon and Breach Science Publishers, 1967.
2. SAKAMOTO K, and ELKIND MM. X-rays and nitrogen mustard: independent action in Chinese hamster cells. Biophys J 9:1115–1130, 1969.
3. ELKIND MM, KANO E, and SUTTON-GILBERT H. Cell killing by actinomycin D in relation to the growth cycle of Chinese hamster cells. J Cell Biol 42:366–377, 1969.
4. ELKIND MM, SAKAMOTO K, and KAMPER C. Age-dependent toxic properties of actinomycin D and X-rays in cultured Chinese hamster cells. Cell Tissue Kinet 1:209–224, 1968.
5. ELKIND MM. Some principles for a rational, cell-based development of combined radiation-drug therapy. Front Radiat Ther Oncol 4:76–78, 1969.

Effects of Tumor Bearing on the Dynamics of Host Hemopoietic Cells [1]

P. K. Lala [2,3,*]

SUMMARY

Hemopoietic status of the host is an important consideration in any cancer chemotherapy protocol. This paper examines several aspects of the response of the host lymphomyeloid system to tumors transplanted elsewhere: (*a*) characteristics of host leukocytes migrating into the tumor; (*b*) leukocyte dynamics in the marrow and the spleen; and (*c*) dynamics of hemopoietic stem cells. Repeated prelabeling of mice with ^{3}HTdR prior to Ehrlich ascites tumor (EAT) transplantation indicated a large-scale, selective migration and/or retention of newly formed lymphocytes and monocytes within the tumor. Similar observations were also made in sc transplants of strain-specific TA-3(St) tumor. Bone marrow was found to be a major source of these mononuclear cells since their accumulation was suppressed by a prior irradiation of host marrow. Labeling with ^{125}I-antimouse IgM, with or without prior incubation of cells with anti-θ serum, revealed that, within the 7-day-old EAT, about a third of the small lymphocytes were maturing B cells having readily detectable surface IgM, about a third were T cells expressing θ antigen, and the rest had neither marker, possibly including very immature B cells. A high incidence of last cell category was also found in subcutaneous TA-3(St) tumors. Ip transplantation of 10^{6} EAT cells into CBA/HT$_6$ or TA-3(St) cells into A/J mice caused a transient decline in femoral marrow leukocyte level (affecting lymphocytes most) followed by a recovery and an overshoot. In contrast, there was a steady rise in splenic weight or cellularity mostly accountable for by lymphocytes. This was partly due to local lymphoid proliferation and partly due to extraneous migration. Parabiosis of CBA with T$_6$ chromosome-bearing CBA/HT$_6$ mice revealed that a large proportion of cells dividing in the spleen of the CBA host after tumor transplantation had migrated recently from blood. Using partial marrow chimeras (repopulated with T$_6$ chromosome-bearing marrow cells), bone marrow was identified as their major source. Furthermore, host spleens showed an increased incidence of small lymphocytes bearing no detectable surface-IgM nor θ antigen (possibly inclusive of immature B cells), and a low incidence of T cells. Tumor transplantation produced a rapid and substantial decline in the pleuripotent stem cell (CFU-S) content of the femoral marrow followed by a recovery. The converse was true for the CFU content of the spleen, and in addition, there was an initial rise in the blood CFU level, suggesting an early CFU traffic from marrow to spleen. A qualitatively similar pattern was also noted for stem cells committed to granulocyte or macrophage development as evaluated from in vitro colony assays. An early rise in splenic CFU level was also elicited by injecting sonicated tumor cells or their plasma membrane fractions, thus possibly indicating an antigen-driven effect. A high level of colony-stimulating activity (for in vitro colony growth) was found in the tumor fluid. This

[1]Supported by the Medical Research Council of Canada and by Public Health Service research grant CA-1711-01 from the National Cancer Institute, National Institutes of Health, Department of Health, Education, and Welfare.

[2]Department of Anatomy, McGill University, Montreal, Canada.

[3]The author gratefully acknowledges the expert technical assistance of Mrs. D. Hodge and Miss D. Dixon.

*Reprint requests to: Dr. P. K. Lala, Department of Anatomy, McGill University, Montreal, Canada.

was elaborated by tumor cells, and to a minor extent by host leukocytes within the tumor. This finding may be of significance during later stages of CFU rise. A high proportion of the splenic CFUs in the tumor-bearing mice were found to be in the cell cycle since they were vulnerable to high dose-high specific activity ^{3}HTdR. These results demonstrate that tumors can cause a large-scale migration of immature B cells from the marrow into the tumor and the spleen, as well as an early migration of stem cells from the marrow to the spleen where they proliferate. Overall effects of chemotherapy on these phenomena and their consequences on host-tumor balance remain to be clarified.

[Cancer Treat Rep 60:1781–1789, 1976]

An optimal protocol for tumor chemotherapy should aim at inflicting maximal injury to the tumor and minimal injury to the host tissue components that are essential for host functions and survival. To achieve this, a large number of parameters concerning the therapeutic agent, the tumor, and the tumor-bearing host must be understood (1,2). Among the host components, hemopoietic status of the tumor-bearing host represents an important parameter for consideration since injury to the lymphomyeloid system often becomes a limiting factor in chemotherapy. Although considerable information has been gained on the effects of various cytostatic and cytotoxic agents on hemopoiesis under physiologic conditions (3–7), such conditions may not always apply to tumor-bearing hosts. Tumor bearing itself may lead to a significant perturbation in the kinetics of the host lymphomyeloid system. Several studies have examined the hemopoietic status of rodents infected with leukemogenic or polycythemia-inducing viruses to investigate the evolution of these diseases (8–13), and also of hosts bearing these hemopoietic disorders (14–18). Some studies have also been extended to human leukemias (reviewed by McCulloch et al [19]) as well as lymphomas (20). In all these instances the malignant conditions directly involve the hemopoietic tissue. However, this tissue can also be affected by the presence of a tumor at a distant site (21–23). This paper examines several aspects of the response of the host lymphomyeloid system to tumors transplanted elsewhere: (*a*) characteristics of host leukocytes migrating into the tumor; (*b*) leukocyte dynamics in the marrow and the spleen; and (*c*) the dynamics of hemopoietic stem cells. Finally, attempts have been made to correlate the findings.

MATERIALS

Several tumor-host systems were employed in various parts of this study: (*a*) Ehrlich ascites tumor (EAT) maintained in CF_1-strain mice by a weekly ip transfer of 10^6 tumor cells; (*b*) EAT maintained in CBA/HT_6-strain mice on a similar protocol of passage; and (*c*) TA-3(St)-line tumor either maintained as ascites tumors using a similar protocol or grown as solid sc tumors by transplanting 5×10^6 tumor cells from the ascites form of the tumor under the skin on the medial aspect of the left thigh in A/J-strain mice. EAT grows in any mouse strain and is of unknown genetic origin. TA-3(St)-line tumor originated in A-strain mice and is strain-specific. Growth curves for these tumors are presented in figure 1. Despite considerable differences in the tumor load at the plateau phase of growth of the ascites tumors, the median host survival times were reasonably close. It was about 2 weeks for the CF_1 mice with EAT and 2 days shorter for the CBA/HT_6 mice with EAT or A/J mice with TA-3(St) ascites tumors.

METHODS, RESULTS, AND DISCUSSION

Characteristics of Host Leukocytes Migrating Into the Developing Tumor

Infiltration by host leukocytic elements is a significant feature of most tumors whether spontaneous, induced, or transplanted. This study was aimed at understanding (*a*) the kinetics, (*b*) the source, and (*c*) the surface properties of host leukocytes accumulating within the transplanted tumor. Study (a) was undertaken in the CF_1-EAT system. Conclusions from this study (24) have been basically confirmed also in TA-3(St) sc tumors grown in A/J mice. Study (b) was performed in the CF_1-EAT system and study (c) in the CBA/HT_6-EAT system.

Kinetics

There was a marked increase in the number of peritoneal leukocytes (lymphocytes, monocytes, macrophages, and granulocytes) during the growth of EAT. During the plateau phase of tumor growth they comprised, on the average, 7% of the total cell population (fig 2), and about five times the size of the leukocyte population found within the circulating blood volume of a 25-g mouse. This accumulation

could be explained by migration from blood rather than by local proliferation, since none of these cells at any stage of tumor growth incorporated label 1 hour after an injection of ^{3}H-thymidine (^{3}HTdR), with the exception of a very minor labeling of some macrophages.

Kinetics of their accumulation was investigated with a series of 12 injections of ^{3}HTdR (20 microcuries every 8 hours), intended to label the bulk of newly formed host leukocytes at their production sites. Two hours after the last injection, animals were injected ip with saline (control group) or 10^6 tumor cells (experimental group) and then serially killed at intervals up to 6 days. Granulocyte labeling in blood, as well as peritoneal space, was near 100% in both groups at all intervals. Temporal changes in the labeling of lymphocytes (fig 3) or monocytes (fig 4) were identical in the peritoneal space and blood in the control group indicating a free exchange of cells between these compartments. In contrast, higher than normal labeling of these cells was found in the blood of tumor-bearing hosts indicating an increase in their turnover in the circulation. More significantly, labeling indices of lymphocytes or monocytes within the ascites tumor exceeded those for the respective cell types in the blood of the same animals indicating a selective migration and/or retention of newly formed cells within the tumor, in contrast to a random migration into the normal peritoneal space. Furthermore, an identical labeling of macrophages to that of monocytes within the tumor suggested a short monocyte-macrophage transition. Essentially similar results were obtained for the mononuclear cells invading the sc solid TA-3(St) tumors growing in A/J mice: their labeling indices were much higher than those exhibited by the mononuclear cells in the blood of the same animals or control animals (Kaizer L, and Lala PK. Cell Tissue Kinet. In press.). Thus, migration of young mononuclear cells into the tumor appears to be a fairly general phenomenon, at least in the transplanted tumors.

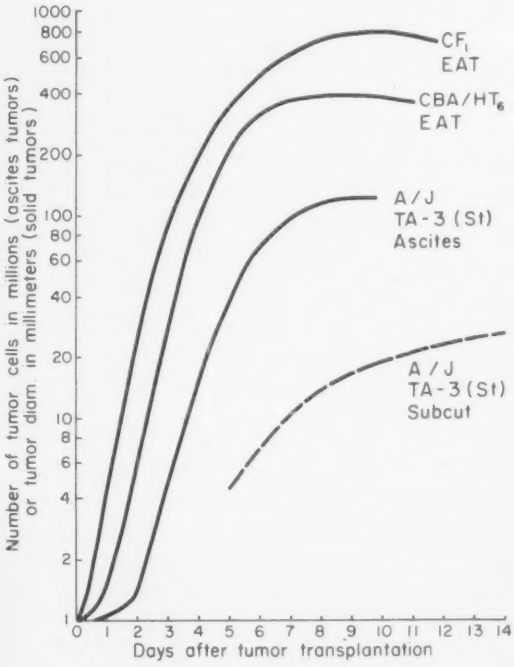

FIGURE 1.—Growth curves for the 3 ascites tumors (after ip transplantation of 10^6 tumor cells) and 1 solid tumor (after sc transplantation of 5×10^6 tumor cells) employed in this study.

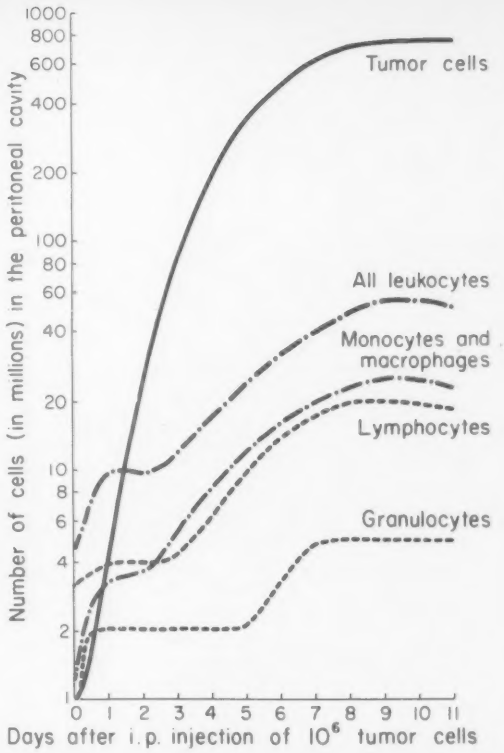

FIGURE 2.—Total No. of tumor cells and various types of host leukocytes observed within the EAT growing in CF_1 mice.

Source of the Young Mononuclear Cells Invading Tumors

Monocytes are unequivocally known to be marrow-derived cells (25), but there are two major primary sources for newly formed lymphocytes in normal animals—bone marrow and thymus (26). The accumulation of young lymphocytes within the tu-

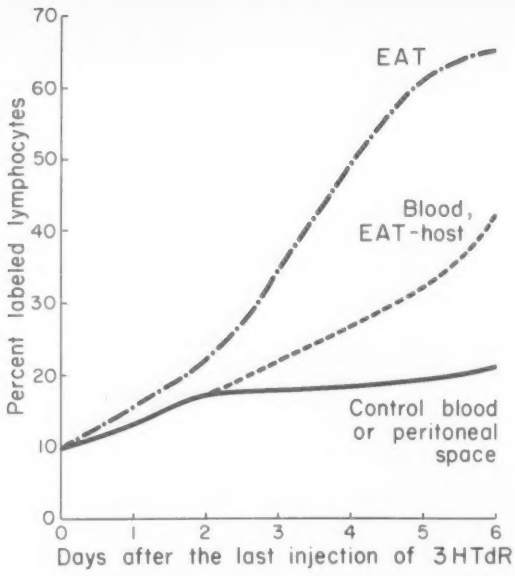

FIGURE 3.—Temporal changes in the labeling index of lymphocytes in the blood and peritoneal space of normal (saline-injected) and ascites tumor-bearing animals injected repeatedly with ^{3}HTdR (prior to injection of saline or tumor cells respectively).

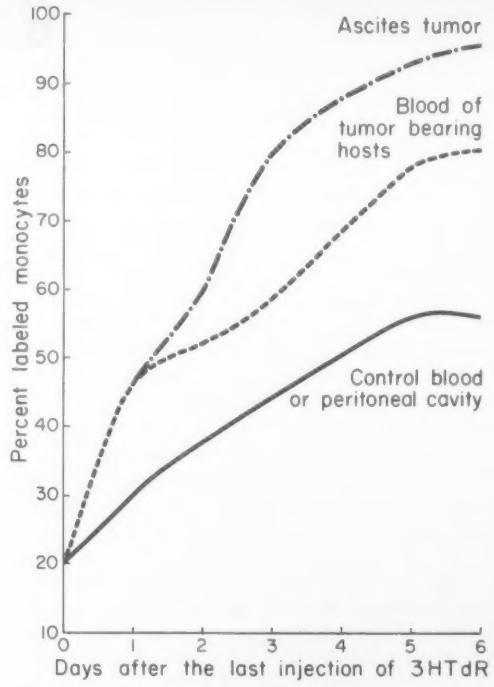
Ascites tumor
Blood of tumor bearing hosts
Control blood or peritoneal cavity
Percent labeled monocytes
Days after the last injection of 3HTdR

FIGURE 4.—Labeling pattern of monocytes in the blood and peritoneal space of normal and ascites tumor-bearing animals after the repeated ^{3}HTdR labeling protocol.

mor was too early, at least at the initial stage, to be explained by immigration of a progeny of lymphocytes activated in a secondary lymphoid organ. For these reasons, the role of marrow and/or thymus as possible sources was examined by blocking production in these organs. Control animals were sham-irradiated and thus had normal lymphopoiesis. Experimental animals were divided into three groups: group I—those given 900 rads of whole-body irradiation to stop lymphopoiesis completely; group II—those given 1000 rads of local irradiation to four limbs alone to block hemopoiesis in about half of the body marrow contained in long bones; group III—those given 1000 rads of whole-body irradiation while the limbs were shielded (this resulted in cessation of cell production in about half of the hemopoietic marrow and in the thymus as well). Four days later, 10^6 EAT cells were transplanted ip into all groups of mice which were then serially killed to quantitate the absolute numbers of various leukocyte types within the developing tumors at different intervals. The 4-day post-irradiation interval for tumor transplantation was selected on the basis of pilot experiments using whole-body irradiation. By this time, all mature leukocytes disappeared from circulation; thus in group I animals, tumors at all ages were virtually leukocyte-free. Moreover, tumor-growth curves were identical in all three

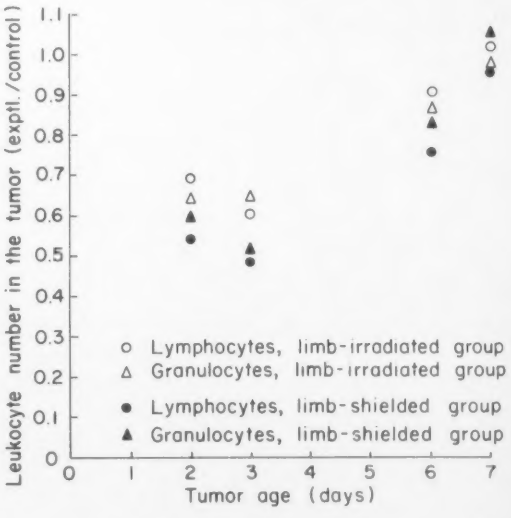

FIGURE 5.—Temporal changes in the absolute No. of lymphocytes and granulocytes within the ascites tumors growing in pre-irradiated hosts relative to the Nos. seen in the tumors growing in sham-irradiated hosts.

groups. Figure 5 shows the ratio of the mean absolute leukocyte numbers for tumors in groups II and III relative to the number seen in control tumors grown in sham-irradiated mice. Both groups showed a significant depletion of all forms of leukocytes at 2–3 days. This was slightly more pronounced in the limb-shielded group. Recovery to near normal levels was attained in both cases at 6–7 days. Early lymphocyte depletion in both experiments suggests bone marrow as an important source of these cells. A recovery at later intervals can best be explained primarily either by a hyperplasia of the unirradiated marrow and/or a regeneration of the irradiated marrow. This is because the second group in which the thymus, spleen, and lymph nodes were also irradiated, in addition to about half of the hemopoietic marrow, showed essentially a similar pattern. However, these findings do not exclude organs other than marrow as minor sources of lymphocytes accumulating in the tumor.

TABLE 1.—Mean labeling index (%) of small lymphocytes incubated with various concentrations of ^{125}I-labeled anti-IgM

	Anti-IgM concentration (μg/ml)			
	1	3	10	20
Normal spleen	35	47	47	46
7-day-old ascites tumor	12.5	17	25	36
Spleen of tumor-bearing host	27	34.5	38	42.5

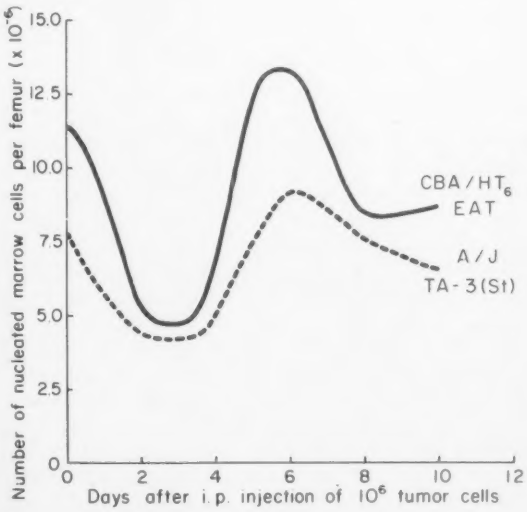

FIGURE 6.—Temporal changes in the absolute No. of nucleated marrow cells per femur at different days of ascites tumor development.

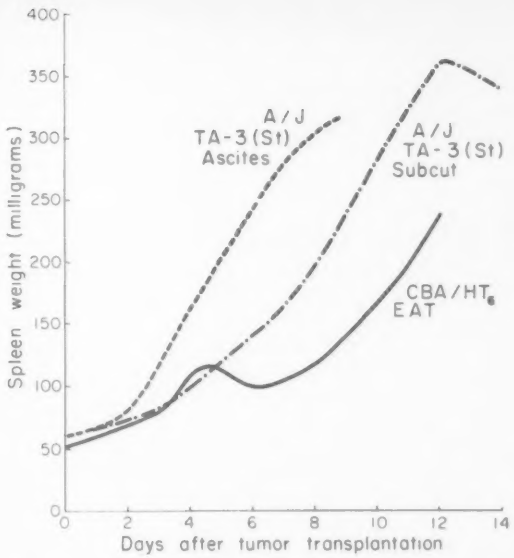

FIGURE 7.—Changes in splenic mass in various hosts during 3 different types of tumor development.

Surface Properties of Lymphocytes Invading the Tumor

Mouse lymphocytes can be broadly subdivided into two categories (27) according to their surface properties: B cells possessing immunoglobulin (Ig) on their cell surface and engaged in humoral immune response, and T cells possessing θ-antigen on the surface and engaged in cellular immunity. Bone marrow and thymus have been identified as the two primary lymphoid organs where these two respective cell types are initially produced (28,29). Thus, it seemed that an examination of the surface properties of lymphocytes accumulating within the tumors might provide a link to their source and functional potentials. Surface IgM on lymphocytes was detected radioautographically according to the technique described by Osmond and Nossal (30). In brief, cell suspensions were incubated with ^{125}I-labeled goat antimouse globulin (anti-IgM) in a wide range of concentrations for 30 minutes at 0°C (Garnis S, and Lala PK, unpublished data). While the labeling index of small lymphocytes in the normal spleen reached a well-defined plateau of 46% with increasing anti-IgM concentrations (table 1), values for small lymphocytes within the tumor increased steadily and were always lower than in the former case. Labeled lymphocytes within the tumor also showed much lower grain counts at equivalent anti-IgM concentrations, indicating lower densities of IgM on the cell surface. Similar phenomena have also been described for bone marrow small lymphocytes (30). In the bone marrow, small lymphocytes

at the initial post-mitotic stage did not show any detectable surface IgM, but then acquired increasing IgM concentrations with increasing maturity (31). Thus, low-IgM density seen in the small lymphocytes within the tumor indicates that they are relatively young B cells. These IgM+ve cells constituted about one third of the small lymphocyte population (table 1). However, cells which did not exhibit detectable IgM could theoretically represent either T cells bearing θ antigen or θ-ve "null" cells. Such "null" cells in the murine bone marrow are known to include post-mitotic lymphocytes at an early stage of B-cell development (31). To distinguish between the two possibilities, we devised a sandwich radio-immune labeling technique (Lala PK, and Garnis S, unpublished data) in which cells were either exposed to heat-inactivated normal serum (control series) or heat-inactivated anti-θ serum (experimental series) prior to incubation with ^{125}I-anti-IgM. The labeling index in the controls was identical to that just described for B-cell labeling without a prior incubation with normal serum, and thus the difference in the labeling indices for small lymphocytes between the experimental and the control series gave a measure of the percentage of θ-antigen-bearing cells. In the normal spleen, at an anti-IgM concentration of 10 μg/ml, the small lymphocyte labeling index in the experimental series reached close to 90%, but within the tumor it was only 64% indicating that about one third of these small lymphocytes were "null" cells and about one third were T cells. Essentially similar findings have also been recorded for TA-3(St) solid tumors (Lala PK, and Kaizer L, J Natl Cancer Inst, in press). Since "null" cells most possibly included lymphocytes at a very early stage in B-cell development, the majority of the lymphocyte population in the tumor was considered to represent B-cell lineage at various stages of maturation.

Leukocyte Dynamics in the Marrow and the Spleen

Ip tumor transplantation (EAT in CBA/HT$_6$ mice or TA-3(St) in A/J mice) caused a rapid decline in the nucleated cell content of the femur (fig 6), reaching a minimum level at 3 days followed by a rapid recovery and overshoot at 5 days. The depletion was mostly accounted for by lymphocytes. A small transient depletion was also noted in saline-injected controls; thus, this response, at least in part, might be due to non-specific stress. In contrast, there was a steady increase in the splenic weight in all tumor-transplanted animals, either bearing ascites or sc tumors (fig 7). There was a parallel rise in the nucleated cell content of the spleen. Saline-injected controls showed only a transient, insignificant increase in splenic mass, which was not contributed by nucleated cells. Possible mechanisms for the increase in splenic cellularity in tumor-bearing hosts were explored (32). This was explained primarily by a rise in the lymphoid-cell content which constituted 92%–97% of all nucleated cells between 1 and 5 days. In CBA/HT$_6$ mice bearing EAT, this increase was explicable partly by local proliferation and partly by cellular immigration. For example, the overall 1-hour ^{3}HTdR (in vivo) labeling index of nucleated cells was 0.7% in control spleens; this rose slowly to 5% at Day 5. Assuming a DNA synthesis time of 5 hours, local proliferation could account for less than one third of the increase in splenic cellularity between 1 and 2 days and about 80% of the increase between Days 4 and 5. It was calculated that there must be a minimal influx of 8.5×10^6 cells per day into the spleen at the former interval, and a minimal influx of 4.1×10^6 cells per day at the latter interval. However, this computation assumed no efflux out of the spleen, and the actual influxes must be much higher.

The local proliferation in the spleen was primarily seen in the large lymphoid and blast-like cells. The incidence of lymphoid cells among all labeled cells increased from 61% at Day 1 to a peak of 79% at Day 2, thereafter declining slowly to about 55% between 4 and 5 days. At that time there was a small rise in the erythroid and monocytic proliferation.

Two different series of experiments using chromosome markers were designed to trace the life history of cells proliferating in the spleen (32). These indicate that a large proportion of these cells are recent migrants from bone marrow via circulation. In the first series, CBA-strain mice were parabiosed with CBA/HT$_6$-strain animals which contain double T$_6$ marker chromosomes in all somatic cells. Six weeks later, when cross circulation was well established, CBA partners were either injected ip with EAT cells or saline that served as the control. Spleens were karyotyped at different intervals to score the incidence of T$_6$+ve metaphases. While the incidence never exceeded 12% in the controls, tumor transplantation resulted in a rapid rise in this incidence to about 36% at Day 4 in the experimental spleens, indicating a rapid influx of blood-borne cells with proliferative potential into the spleen. The second series of experiments examined bone marrow as a possible source of such cells. Partial marrow chimeras were produced by local irradiation of four limbs of CBA mice followed by a repopulation by transfusing 10^7 T$_6$-chromosome-bearing marrow cells from CBA/HT$_6$ mice. When chimerism was well established, animals were injected with tumor cells

or saline. While T_6+ve metaphases did not exceed 12% in the control spleens, tumor transplantation caused a fast rise in the incidence of T_6+ve cells to 37% at 3 days, or about 25% above the control level. Since possibly only about 40%–50% of the total marrow was chromosomally marked, ≥ 50% of the cells dividing in the spleen at this interval or their immediate precursors must be recent migrants from marrow.

To characterize further the lymphocytes in the spleen of tumor-bearing animals, their surface properties were examined with techniques mentioned earlier. Results (table 1) indicate that in the tumor-bearing animals the incidence of IgM+ve small lymphocytes was slightly less than that in the control spleens at all anti-IgM concentrations; however their absolute number were higher because of an increase in the splenic size. These cells also showed slightly lower than normal IgM density possibly indicative of their low maturity. When labeling was done (at an anti-IgM concentration of 10 μg/ml) following prior exposure to anti-θ serum, about a third of the splenic lymphocytes in the EAT as well as the TA-3(St) tumor-bearing hosts remained unlabeled, and were thus considered as "null" cells—possibly inclusive of very young B cells. Furthermore, these spleens showed a marked increase in the incidence of cells capable of producing B lymphoid colonies in vitro in the presence of 2-mercaptoethanol (Keeb G, and Lala PK, unpublished data). Thus, tumor transplantation produced a rapid immigration of marrow-derived cells in the spleen, a large majority of which were B cells at various stages of maturation.

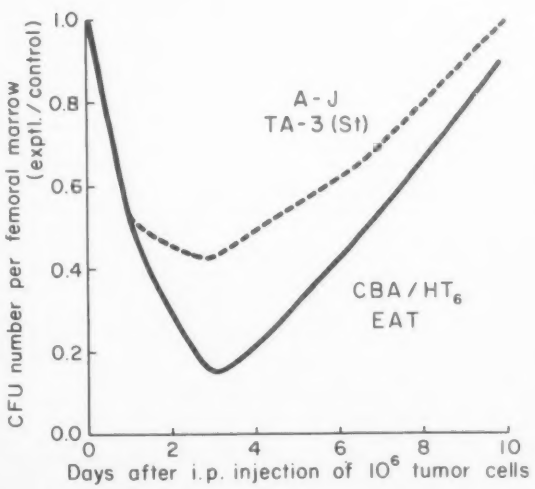

FIGURE 8.—Marrow-CFU content per femur at different days of tumor development, expressed as a fraction of the No. observed in saline-injected control animals.

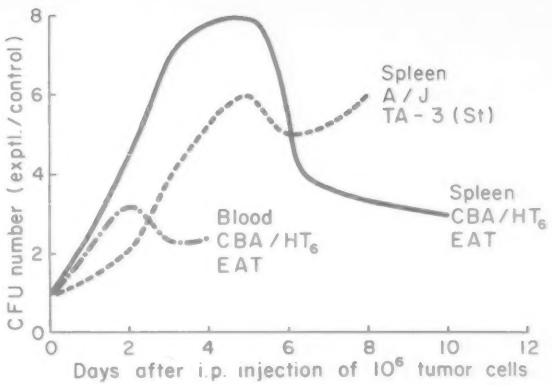

FIGURE 9.—CFU content of the spleen (whole organ) or blood (per unit vol) at different days of tumor development, relative to the respective CFU Nos. observed in saline-injected control animals.

Dynamics of Hemopoietic Stem Cells

The distribution of hemopoietic stem cells (CFUs) in host organs at different stages of tumor development was evaluated with Till and McCulloch's spleen colony technique (33). The data for the whole organ (spleen or femur) or per unit volume of blood were expressed as a ratio relative to the CFU number in the respective tissues of tumor-free, saline-injected control animals of same strain, age, and sex (34). Results are shown in figures 8 and 9. CFU content of femoral marrow declined rapidly, reaching a minimal level (15% of control level in EAT hosts and 41% of control level in TA-3[St] tumor-bearing hosts) at Day 3 following ip tumor transplantation. This was followed by a recovery, reaching a near normal level by Day 10. In contrast, splenic CFU content increased steadily, reaching a peak of eightfold normal in EAT hosts and sixfold normal in TA-3(St) hosts on Day 5. In the former host, a decline followed, but the levels were always supranormal; in the latter host, subsequent changes were not significant up to 8 days. Nearly mirror-image relationships in CFU changes between femoral marrow and the spleen may be indicative of some marrow→spleen CFU traffic. This view was supported by an early rise in the blood CFU content to two- to three-fold control level between 1 and 4 days after EAT transplantation (fig 9). Our recent studies using soft agar colony assays (35) have revealed that similar conclusions would also apply to stem cells committed to granulocyte/macrophage

development (Keeb G, and Lala PK, unpublished data).

The very early CFU response in the spleen cannot be regarded as a simple kinetic consequence of the increased demand created by a large-scale influx of newly formed mononuclear cells into the tumor. Lymphocytes within the tumor did not increase before the third day (fig 2) while the CFU rise in the spleen was seen as early as Day 1 (fig 9). This may have been initiated by the same stimulus that caused migration of young B lymphocytes into the tumor and the spleen. A two- to three-fold increase in the splenic CFU content was also found 2–3 days following an ip injection of 10^6 sonicated EAT cells or the purified plasma membrane fraction from 10^7 EAT cells, indicating that this response may have been caused by some plasma membrane-associated components of the tumor.

The CFU migration was followed by a local CFU proliferation in the spleen. Most of the CFUs were found to be in the cell cycle at 4–5 days of splenic enlargement after EAT transplantation. Incubation of splenic-cell suspensions from tumor-bearing hosts in vitro for 30 minutes with high-dose (300–500 microcuries/ml), high-specific activity (40 millicuries/mM) ^{3}HTdR prior to transplantation into irradiated recipients resulted in a reduction of the CFU number to 30%–40%, reminiscent of the picture found during post-irradiation regeneration (19). Such treatment of the control spleens lowered the CFU number to 76%–90% of the values obtained with untreated cells. The stimulus for CFU proliferation may have been derived directly from the tumor cells or from an increase in the number of host cells elaborating some stimulating factors. Factors stimulating in vitro colony formation are considered to act on the committed rather than the pleuripotent stem cells. In our recent studies (Keeb G, and Lala PK, unpublished data), using the semi-solid agar culture technique (35), we found a high colony-stimulating activity in the cell-free fluid component of the EAT. This activity originated from the tumor cells themselves and, to a minor extent, host mononuclear cells present within the tumor, as indicated by the stimulation provided by feeder layers of these cells fractionated from the EAT.

The dynamics of stem cells in hemopoietic organs of the present tumor-bearing hosts is in many respects qualitatively similar to that found after infection with leukemogenic or polycythemia-inducing or anemia-inducing viruses in mice (8,9,11–13) or treatment with *Bordella pertussis* vaccine (36). Various other agents, antigenic in nature, are also known to enhance the CFU number in the spleen (37). Thus, present findings may also represent antigen-driven effects. A temporary CFU depletion in the femoral marrow observed in the present study may be characteristic of a very early response; it may not be sustained in hosts with long-established tumors where there may be an actual elevation in the marrow stem cell level measured either with in vivo (21) or in vitro (22) colony assay. In our preliminary studies (Lala PK, and Terrin M, unpublished data), we also found a moderate increase in the marrow CFU content in C3H mice bearing spontaneous mammary tumors.

CONCLUSIONS

Tumors at distant sites can profoundly influence the dynamics of host hemopoietic cells. In the present studies using several transplanted tumors in ascites and/or solid form, it was observed that the tumors caused large-scale migration of newly formed mononuclear cells from the marrow into the tumor. Among these cells, the lymphocytes were found to be largely young, bone marrow-derived B lymphocytes at various stages of maturation. An influx of similar cells, or their precursors including hemopoietic stem cells, also occurred from the bone marrow to the spleen where these cells subsequently proliferated. The precise relationship of these cell-migration streams to host-tumor balance must be understood for an exploitation of chemotherapy to the maximal benefit of the host.

REFERENCES

1. VALERIOTE FA. *In* The Cell Cycle in Malignancy and Immunity (Proceedings of the 13th Annual Hanford Biology Symposium at Richland, Wash, Oct 1–3, 1973). Published by the Technical Information Center, Office of Public Affairs, US Energy Research and Development Administration (ERDA). ERDA Symposium Series, Conf-73 1005, 1975, pp 387–427.
2. LALA PK. *In* Proceedings of the 11th International Cancer Congress. Amsterdam, Excerpta Medica, 1974, pp 29–35.
3. FRINDEL E. *In* The Cell Cycle in Malignancy and Immunity (Proceedings of the 13th Annual Hanford Biology Symposium at Richland, Wash, Oct 1–3, 1973). Published by the Technical Information Center, Office of Public Affairs, US Energy Research and Development Administration (ERDA). ERDA Symposium Series, Conf-73 1005, 1975, pp 156–181.
4. BLACKETT NM, and ADAMS K. Cell proliferation and the action of cytotoxic agents on haemopoietic tissue. Br J Haematol 23:751–758, 1972.
5. DUNN CDR. Cell proliferation and drug resistance in the response of colony forming units of rat bone marrow to repeated doses of cytotoxic agents. J Natl Cancer Inst 48:639–649, 1972.
6. DUNN CDR. Effect with time of melphalan on hemopoietic stem cells proliferating at different rates. J Natl Cancer Inst 52:173–180, 1974.
7. DUNN CDR. The chemical and biological properties of busulphan ('Myleran'). Exp Hematol 2:101–117, 1974.
8. OKUNEWICK JP, PHILLIPS EL, and ERHARD P. Increase in number of splenic transplantable colony-forming units in the SJL/J mice after infection with Rauscher leukemia virus. J Natl Cancer Inst 49:1101–1106, 1972.

9. SEIDEL HJ. Hemopoietic stem cells in murine virus induced leukemia. I. Spleen colony assays in CBA mice after Rauscher virus infection. Z Krebsforsch 79:123–134, 1973.
10. SEIDEL HJ. Hemopoietic stem cells in mice with virus-induced leukemia. II. Studies in C3H mice after Rauscher virus infection. Z Krebsforsch 80:229–237, 1973.
11. ITURIZZA RG, and SEIDEL HJ. Stem cell growth and production of colony stimulating factor in Rauscher virus infected CBA/J mice. J Natl Cancer Inst 53:487–492, 1974.
12. WENDLING F, TAMBOURIN PE, and JULLIEN P. Hemopoietic CFU in mice infected by the polycythemia-inducing Friend virus. I. Number of CFU and differentiation pattern in the spleen colonies. Int J Cancer 9:554–566, 1972.
13. WENDLING F, TAMBOURIN P, GALLIEN-LARTIGUE P, ET AL. Comparative differentiation and numeration of CFUs from mice infected either by the anemia or polycythemia-inducing strains of Friend viruses. Int J Cancer 13:454–462, 1974.
14. HOELZER D, HARRISS EB, and JAGER C. Stem cell kinetics in the L5222 rat leukemia. Cell Tissue Kinet 7:567–576, 1974.
15. CHEVALIER C, GAILLARD N, and FRINDEL E. The number of in vitro stem cells in AKR leukemic mice. Blood 44:743–750, 1974.
16. GORDON MY. Quantitation of haemopoietic cells from normal leukaemic RFM mice using an in vivo colony assay. Br J Cancer 30:421–428, 1974.
17. GORDON MY, and COGGLE JE. CFU-C yields from the haemopoietic tissues of normal and leukemic RFM mice. Cell Tissue Kinet 7:61–68, 1974.
18. BROMMER EJP, and BENTVELSEN P. The haematopoietic stem cells in Rauscher virus-induced erythroblastosis of BALB/C mice. Eur J Cancer 10:827–833, 1974.
19. MCCULLOCH EA, MAK TW, PRICE GB, ET AL. Organization and communication in populations of normal and leukemic hemopoietic cells. Biochim Biophys Acta 355:260–299, 1974.
20. BULL JM, DEVITA VT, and CARBONE PP. In vitro granulocyte production in patients with Hodgkin's disease and lymphocytic, histiocytic, and mixed lymphomas. Blood 45:833–842, 1975.
21. MILAS L, and TOMLJANOVIC M. Spleen colony forming capacity of bone marrow from mice bearing fibrosarcoma. Rev Eur Etud Clin Biol 16:462–465, 1971.
22. HIBBERD AD, and METCALF D. *In* Immunological parameters of host-tumor relationships. New York, Academic Press, 1971, pp 202–210.
23. DELMONTE L, LIEBELT AG, and LIEBELT RA. Granulopoiesis and thrombopoiesis in mice bearing transplanted mammary cancer. Cancer Res 26:149–159, 1966.
24. LALA PK. Dynamics of leukocyte migration into the mouse ascites tumor. Cell Tissue Kinet 7:293–304, 1974.
25. VAN FURTH R. *In* Mononuclear Phagocytes. Oxford, Blackwell, 1970, pp 151–165.
26. OSMOND DG. *In* Proceedings of the 6th Annual Leucocyte Culture Conference. New York, Academic Press, 1972, pp 3–32.
27. RAFF MC. Surface antigenic markers for distinguishing T and B lymphocytes in mice. Transplant Rev 6:52, 1971.
28. GRIEVES MF, OWEN JJT, and RAFF MC. T and B lymphocytes. Origins, properties and roles in immune responses. Amsterdam, Excerpta Medica, 1974.
29. OSMOND DG. Formation and maturation of bone marrow lymphocytes. J Reticuloendothel Soc 17:99–114, 1975.
30. OSMOND DG, and NOSSAL GJV. Differentiation of lymphocytes in mouse bone marrow. I. Quantitative radioautographic studies of antiglobulin binding by lymphocytes in bone marrow and lymphoid tissue. Cell Immunol 13:117–131, 1974.
31. OSMOND DG, and NOSSAL GJV. Differentiation of lymphocytes in mouse bone marrow. II. Kinetics of maturation and renewal of antiglobulin-binding cells studied by double-labeling. Cell Immunol 13:132–145, 1974.
32. LALA PK, and LIND C. Cell kinetics in the spleen of tumor-bearing hosts. Anat Rec 181:403, 1975.
33. TILL JE, and MCCULLOCH EA. A direct measurement of the radiation sensitivity of normal bone marrow cells. Radiat Res 14:213–222, 1961.
34. LALA PK, and TERRIN M. Migration of cells with proliferative potential from bone marrow to the spleen of tumor bearing hosts. (Abstr) *In* Proceedings of the 3rd Annual Meeting of the International Society of Experimental Haematology, 1974, p 32.
35. BRADLEY TR, and METCALF D. The growth of mouse bone marrow cells in vitro. Aust J Exp Biol Med Sci 44:287–299, 1966.
36. MONETTE FC, MORSE BS, HOWARD D, ET AL. Hemopoietic stem cell proliferation and migration after *Bordella pertussis* vaccine. Cell Tissue Kinet 5:121–129, 1972.
37. METCALF D, and MOORE MAS. *In* Haemopoietic Cells. Amsterdam, North Holland Publishing Co, 1971, pp 107–108.

Recovery of Cells From Induced, Potentially Lethal Damage [1]

George M. Hahn [2,3,*]

SUMMARY

The recovery of mammalian cells after a variety of treatments is, in part, governed by the cells' ability to deal with repairable, but potentially lethal, lesions. Kinetics of such recovery show a T_i of 10–20 hours after ultraviolet (UV) irradiation and 1.5–2.5 hours after X-irradiation. Recovery after exposure to mechlorethamine and bleomycin (BLM) is similar to X-ray recovery; after methylmethane sulfonate, recovery has components similar to X-ray and UV recovery. The sequential treatments of cells with 43°C hyperthermia and X-rays (or reverse order) modify both the immediate survival after treatments as well as the subsequent recovery kinetics. Very similar results are found after BLM and hyperthermia treatments, suggesting strongly that after exposure to that drug a real repair system is operative. However, although recovery after X-irradiation is similar in vitro and in vivo, after BLM the site of treatment and of recovery strongly influences the magnitude and kinetics of recovery.

[Cancer Treat Rep 60:1791–1798, 1976]

It is well known that the sterilization with drugs of solid tumors involves difficult tasks. In spite of considerable scientific effort to overcome the problems involved, the clinical use of cancer chemotherapeutic agents is still largely palliative and frequently ineffective. Many of the reasons for this unfortunate state of affairs are discussed in this issue. I want to deal with one specific aspect, namely the ability of cells to cope with a wide variety of damages that we inflict upon them in our attempts to halt their proliferative ability. The recovery processes which will be discussed are currently only defined in an operational fashion: after treatment, cell survival increases with time if the post-exposure environment is appropriate. This increase in survival is said to result from "repair of potentially lethal damage" (1). The term repair tends to have a mechanistic connotation, therefore, the term recovery will be used to emphasize our ignorance about specific targets or lesions involved. Recovery takes place in vitro and in vivo. Non-cycling cells in culture and in tumors seem to be particularly able to deal with damage which would be lethal to many actively growing cells. Hence, the study of recovery processes, and particularly studies relating to their inhibition, are of considerable interest.

MATERIALS AND METHODS

Cells and culture conditions have been described in detail (2,3). X-irradiation was at 85 KEV, 9.6 mA, approximately 120 rads/minute with 0.05 Al filtration. The ultraviolet (UV) irradiations were carried out in open Petri dishes without medium; to insure uniform dosimetry (750 ergs/mm²/minute) cells were removed from the edge of the dishes and the cleared areas sterilized with an alcohol swabbing after irradiation. Growth of cells in bromodeoxycytidine (BCdR) to yield cells with bromodeoxyuridine (BUdR)-substituted DNA and visible light irradiation were as described by Yang et al (4). Drug exposure was according to the protocol by Ray et al (5). Heating was in a specially controlled hot-water bath kept to within ±0.1°C (6). For all cases the

[1]Supported by Public Health Service grants CA-04542 and CA-10372 from the National Cancer Institute, National Institutes of Health, Department of Health, Education, and Welfare.

[2]Department of Radiology, Stanford University School of Medicine, Calif.

[3]I would like to thank Drs. Peter Twentyman and Norman Bleehen for making some of their results available to me prior to publication. Dr. Gloria C. Li, Louise F. Gordon, and Jonathan Braun were involved in many of the experiments.

*_Reprint requests to:_ Dr. George M. Hahn, Department of Radiology, Stanford University School of Medicine, Stanford, Calif 94305.

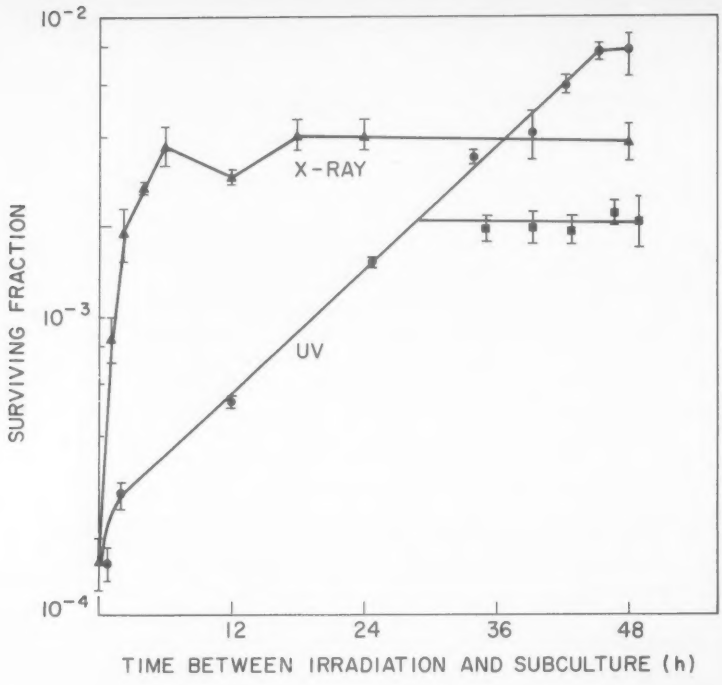

FIGURE 1.—Recovery of plateau-phase cells after exposure to 1500 rads of X-irradiation or to 1000 ergs/mm² of UV irradiation. Twenty-four hrs after UV irradiation the No. of cells per dish starts decreasing. The upper curve assumes that all cells, UV-inactivated or not, have equal probability of lysing. The lower curve assumes that cell lysis occurs only among the UV-inactivated cells. There is little or no cell lysis after X-irradiation, hence only 1 curve is shown. (*From* ref 9 and Hahn GM, and Braun J, unpublished data.)

assay for survival was the Puck cloning technique. The EMT-6 tumor system was described by Rockwell and Kallman (7); its application to chemotherapy was described by Hahn et al (8).

RESULTS

Kinetics of recovery from potentially lethal damage after X-irradiation or after UV irradiation are shown in figure 1. The most obvious difference between the two curves is that of rate of recovery. After X-irradiation the $T_{\frac{1}{2}}$ is 2 ± 0.5 hours; after UV irradiation the $T_{\frac{1}{2}}$ is 20 ± 5 hours if it is assumed that lysed cells may come from clonogenic or from nonclonogenic compartments with equal probability; it is 10 ± 2 hours if it is assumed that essentially only UV-sterilized cells are subject to lysis (9) (Braun J, and Hahn GM; in preparation).

Figure 2 illustrates results from similar experiments performed with cells which had been exposed to a variety of drugs. In these experiments the 0 time point corresponds to the end of treatment. Survival in most cases was 10^{-3}, except for methylmethane sulfonate (MMS)[4] where several curves were combined into a composite result (9) and for bleomycin (BLM)[5] where the shape of the survival curve precluded killing below a level of about 10^{-1}. BLM and mechlorethamine (HN_2)[6] appear to mimic the X-ray case while MMS and BCdR plus visible light appear to have components similar to X-ray, BCdR, and UV. Survival of adriamycin (ADM)[7]-treated cells was corrected for cell killing because of the persistence of ADM attached to plastic or glass dishes (Hahn GM, and Strande D; in preparation). Other drugs for which no repair was found included the nitrosoureas and actinomycin D (data not shown).

The effect on recovery from X-ray damage of a 1-hour pulse of 43°C hyperthermia is shown in figure 3. The top curve shows survival of controls irradi-

[4]Methylmethane sulfonate: NSC-50256; CAS reg. No. 66-27-3.

[5]Bleomycin: NSC-125066; CAS reg. No. 11056-06-7; [2,4'-bithiazole]-4-carboxylic acid, 2'-(2-aminoethyl)-, monohydrate.

[6]Mechlorethamine: NSC-762; CAS reg. No. 55-86-7; diethylamine, 2,2'-dichloro-*N*-methyl-, hydrochloride.

[7]Adriamycin: NSC-123127; CAS reg. No. 23214-92-8.

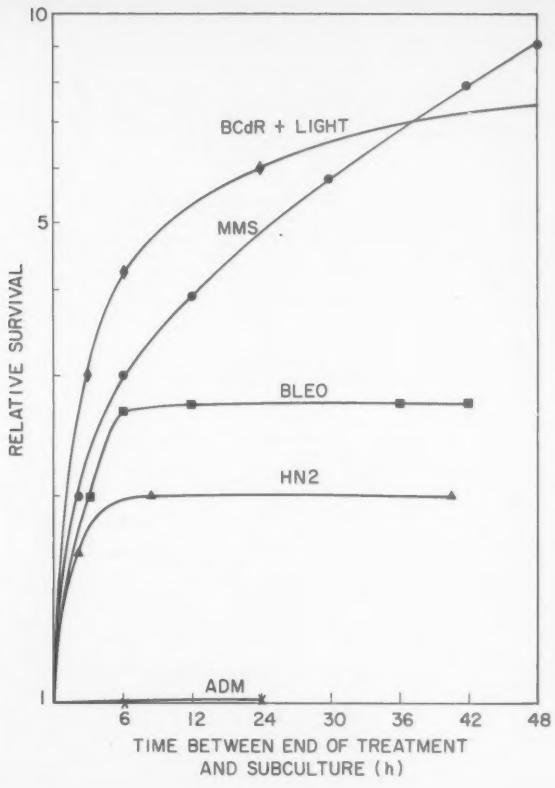

FIGURE 2.—Recovery of plateau-phase cells after exposure to chemotherapeutic agents. All curves normalized to MMS curve (which shows maximum recovery). ADM (1.2 μg/ml, 1 hr); HN_2 (3 μg/ml, 1 hr); MMS (1–5 μg/ml, 1 hr [ref 8]); BLM (20 μg/ml, 1 hr [ref 10]); BCdR and visible light (5×10^{-5} M BCdR; 8 mins of irradiation [ref 4]). (For discussion *see* ref No. 15.)

ated with 1000 rads and then allowed to recover. The squares represent data from an experiment in which cells were similarly irradiated and then exposed to heat. Finally, the triangles are survival values from cells in which that sequence was reversed (ie, heat preceded X-irradiation). In these experiments the 0 time point corresponds to the end of the final treatment.[*]

Figure 4 shows results from a similar set of experiments in which a 1-hour exposure of 20 μg/ml of BLM replaced the X-irradiation (10). Again, the top curve shows recovery by unheated controls, the triangles represent data from cells heated and then treated with drugs, and the squares show data from cells in which the sequence was reversed.

Finally, figures 5 and 6 compare recovery in vivo and in vitro. After X-irradiation the kinetics of recovery of Chinese hamster cells in culture are very similar to those seen in EMT-6 cells in tumors left in situ after exposure (fig 5) (11). However, quite a different story is seen after BLM, where different rates and magnitudes of recovery are observed depending upon the exposure (and recovery) of EMT-6 cells in vivo or in vitro.

[*]Li GC, Evans RG, and Hahn GM. Recovery from potentially lethal X-ray damage: modification and inhibition by elevated temperatures. *Radiat Res.* In press.

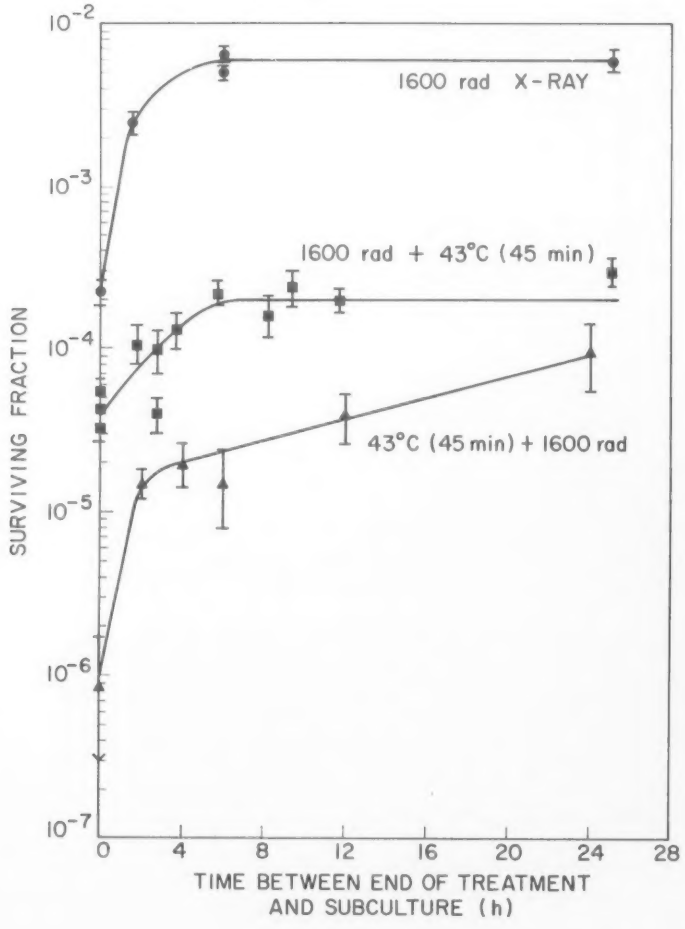

FIGURE 3.—Recovery of cells after X-irradiation and 43°C hyperthermia. Solid symbols = 1000 rads of X-irradiation, control. ■ = 1000 rads, followed by 1 hr of 43°C hyperthermia. ▲ = 1 hr of 43°C hyperthermia, followed by 1000 rads of X-irradiation. Zero of time scale corresponds to end of combined treatment. (Data *from* footnote 8.)

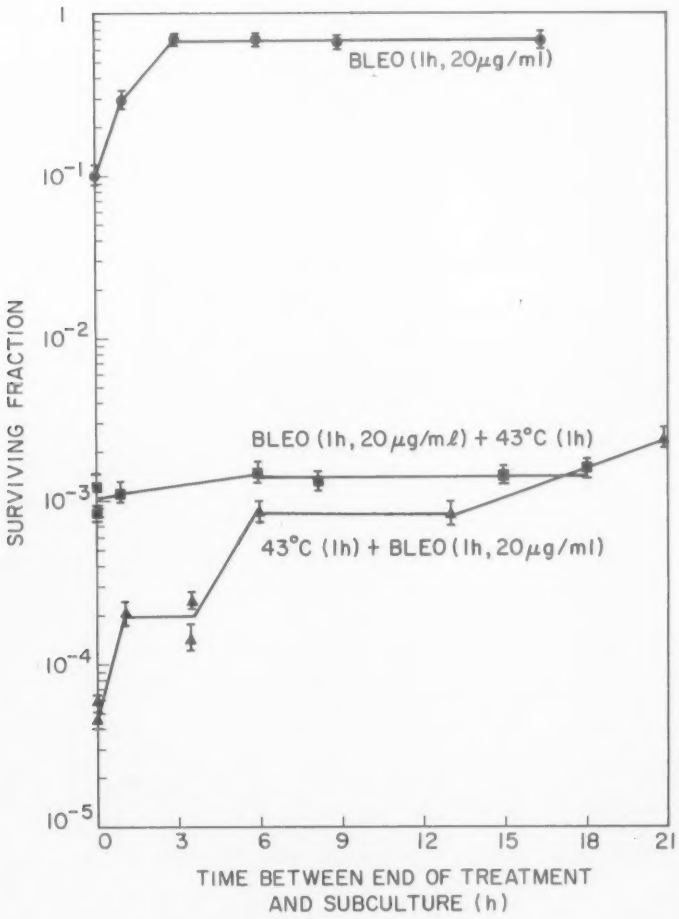

FIGURE 4.—Recovery of cells after BLM and 43°C hyperthermia. Solid symbols = 1 hr BLM (20 μg/ml) at 37°C. ■ = 1 hr BLM (20 μg/ml) a 37°C, followed by 1 hr of 43°C (no BLM). ▲ = 1 hr of 43°C (no BLM) followed by 1 hr of BLM (20 μg/ml) at 37°C. Note the similarities of the results shown here and in fig 3. (*From* ref 10.)

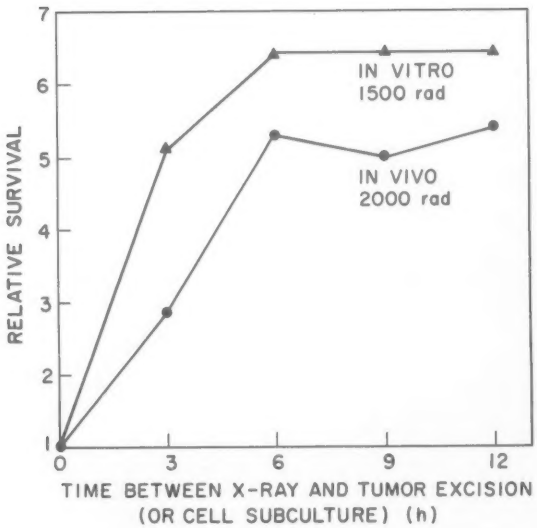

FIGURE 5.—Comparison of recovery of cells from X-irradiation in vivo or in vitro. Solid line = recovery of EMT-6 cells irradiated as solid tumors in vivo (2500 rads X-rays) and permitted to recover in situ. Dashed line = recovery of HA1 cells exposed to X-irradiation (1000 rads) in vitro and permitted to recover in vitro.

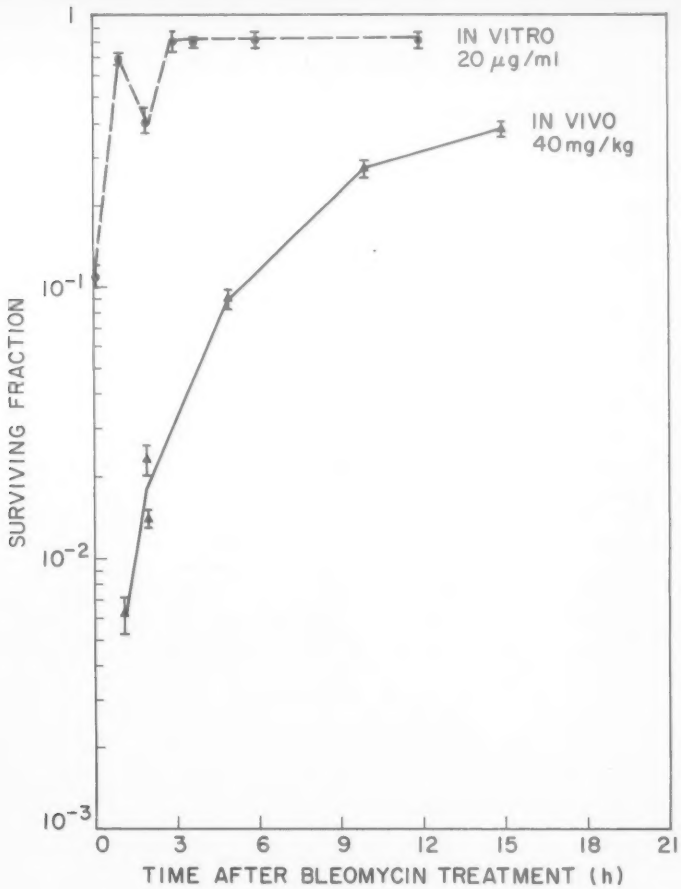

FIGURE 6.—Comparison of recovery of cells from BLM exposure in vivo or in vitro. Solid line = recovery of EMT-6 cells (solid tumors) exposed to BLM in vivo (40 mg/kg) and permitted to recover in situ. Dashed line = recovery of EMT-6 cells (tissue culture monolayers) exposed to BLM (20 μg/ml) in vitro and permitted to recover in vitro.

DISCUSSION

Recovery by cells after a variety of insults can be discussed in terms of X-ray- or UV-like behavior, or in terms of a combination of these (9). Furthermore, repair of DNA can also be analyzed in similar terms (12), although the correspondence between the recovery discussed here and the repair (12) is not complete (9).

Of greatest interest of the X-ray-like drugs, from the point of view of clinical therapy, is perhaps BLM (other drugs inducing X-ray-like recovery patterns are HN_2, other bifunctional alkylating agents, and neocarzinostatin). This agent has shown considerable effectiveness against a variety of solid tumors, and for that reason we have examined its recovery patterns in some detail. Thus, we showed that the drug appeared to be quite effective against the EMT-6 tumor in vivo if the assay for cell survival was made 2 hours after drug administration. However, this conclusion had to be modified; 22 hours later most of the cells had regained their colony-forming ability (8). Twentyman and Bleehen (13) suggested that perhaps some aspect of the subculturing procedure permitted more BLM to enter the cell and hence the increase in survival was an artifact of the assay procedure, rather than a manifestation of a repair process. However, a careful search by these investigators did not isolate the particular step in the procedure which might have given rise to the artifact. The data in figures 4 and 5 make the artifact hypothesis highly unlikely. First,

in the X-ray case permeability is not an issue and subculture techniques can be equalized by using step-up techniques (9). Thus, recovery after X-irradiation is most likely related to specific repair, and here the evidence favors repair of DNA (9).

Second, the results of figure 3 show that heating cells to 43°C for 1 hour prior to or after X-ray has specific effects on immediate survival as well as on the kinetics of subsequent recovery.[8] Figure 4 shows that the interaction of BLM and 43°C hyperthermia is similar to the X-ray interaction in all essential aspects. Thus, it is very likely that recovery after BLM is also a manifestation of repair of DNA. However, Twentyman and Bleehen also point to another puzzle: in their hands exponentially growing cells seem to show as much recovery as do plateau-phase non-cycling cells (14). Furthermore, there is a profound difference between X-ray and BLM exposure when in vitro results are compared with those found in vivo. After X-irradiation, kinetics and magnitude of recovery in vivo or in vitro are quite similar (fig 5) (8). However, our data for BLM (fig 6) as well as those of Twentyman and Bleehen (13) show quite marked differences between the in vitro and in vivo observations.

REFERENCES

1. PHILLIPS RA, and TOLMACH LJ. Repair of potentially lethal damage in X-irradiated HeLa cells. Radiat Res 29:413–432, 1966.
2. YANG S-J, HAHN GM, and BAGSHAW MA. Chromosome aberrations induced by thymidine. Exp Cell Res 42:130–135, 1966.
3. HAHN GM, STEWART JR, YANG S-J, ET AL. Chinese hamster cell monolayer cultures. I. Changes in cell dynamics and modifications of the cell cycle with the period of growth. Exp Cell Res 49:285–292, 1968.
4. YANG S-J, HAHN GM, and VAN KERSEN-BAX I. Effects of light on viability and DNA synthesis of mammalian cells preincubated in media containing brominated pyrimidines. Photochem Photobiol 11:131–136, 1970.
5. RAY GR, HAHN GM, BAGSHAW MA, ET AL. Cell survival and repair of plateau-phase cultures after chemotherapy—relevance to tumor therapy and to the in vitro screening of new agents. Cancer Chemother Rep 57:473–475, 1973.
6. HAHN GM. Metabolic aspects of the role of hyperthermia in mammalian cell inactivation and their possible relevance to cancer treatments. Cancer Res 34:3117–3123, 1974.
7. ROCKWELL S, and KALLMAN RF. Cellular radiosensitivity and tumor radiation response in the EMT-6 tumor system. Radiat Res 53:281–293, 1973.
8. HAHN GM, RAY GR, GORDON LF, ET AL. Response of solid tumor cells exposed to chemotherapeutic agents in vivo: cell survival after 2- and 24-hour exposure. J Natl Cancer Inst 50:529–533, 1973.
9. HAHN GM. Radiation and chemically induced potentially lethal lesions in non-cycling mammalian cells. Radiat Res. In press.
10. BRAUN JB, and HAHN GM. Enhanced cell killing by bleomycin and 43 C hyperthermia and the inhibition of potentially lethal damage. Cancer Res. In press.
11. HAHN GM, ROCKWELL S, KALLMAN RF, ET AL. Repair of potentially lethal damage in vivo in solid tumor cells after X-irradiation. Cancer Res 34:351–354, 1974.
12. REGAN JD, and SETLOW RB. Two forms of repair in the DNA of human cells damaged by chemical carcinogens and mutagens. Cancer Res 34:3318–3325, 1974.
13. TWENTYMAN PR, and BLEEHEN NM. Studies of potentially lethal damage in EMT-6 mouse tumor cells treated with bleomycin either in vitro or in vivo. Br J Cancer. In press.
14. TWENTYMAN PR. Comparative chemosensitivity of exponential- versus plateau-phase cells in both in vitro and in vivo model systems. Cancer Treat Rep 60:1719–1722, 1976.
15. HAHN GM. Repair (or recovery) effects in quiescent Chinese hamster cells. *In* Repair of DNA (Hanawalt PC, ed). Stanford University Press, 1975. In press.

In Vitro Responses of Mammalian Cells to Drug-Induced Potentially Lethal and Sublethal Damage [1]

S. C. Barranco [2,3,*]

SUMMARY

The survival of plateau-phase or nondividing Chinese hamster ovary (CHO) cells (in vitro) was reduced to a greater extent by treatments with nitrosourea compounds than were cells treated in the exponential phase of growth. The greatest decrease in the survival fraction occurred following treatments with methyl-CCNU where approximately 128 times more cells were killed in the plateau phase than in the dividing state (at a dose of 10 μg/ml/hr). Only five times more cells were killed in plateau phase than in exponential growth when cells were treated with CCNU. Cells treated with either nitrosourea compound failed to recover from potentially lethal damage (PLD) and sublethal damage (SLD) even though the survival curves contained shoulder regions. The breakdown products of the nitrosourea compounds are known to inhibit DNA repair and may explain the failure of mammalian cells to recover from SLD and PLD induced by these chemicals. Nondividing CHO cells in vitro were less sensitive to actinomycin D (AMD) than were exponentially growing cells. The proliferating and the nonproliferating cells did not recover from AMD-induced PLD or SLD, and experienced further reductions in survival when they were maintained under the conditions of their respective growth states; however, when dividing cells were placed in conditions suboptimal for growth (incubated in depleted plateau medium) after treatment with AMD they did exhibit increased survival, indicating an ability to recover from PLD and SLD. It was shown that under these conditions recovery from PLD occurred simultaneously with recovery from SLD. The PLD recovery was so great that it masked the true response of the cells to SLD. When adjustments were made for the PLD recovery, the resulting data indicated a slight, but measurable increase in survival. Since AMD inhibits cell progression in all stages of the cell cycle, this increase in survival observed with fractionated doses of AMD *may* be due to recovery from SLD and not to the movement of cells into less sensitive stages of the cell cycle between treatments. Adriamycin was extremely toxic to dividing and nondividing CHO cells in relatively low drug concentrations. The survival response of dividing and nondividing cell populations was biphasic. Adriamycin did not appear to produce PLD. Both dividing and nondividing cells experienced a 1.5-fold to three-fold greater reduction in survival when adriamycin was administered as two small dose fractions (separated by 1–4 hours) than when the same total dose was given at one time. The fractionated-dose technique may represent a means of producing a greater cell-kill with lower doses of the drug, while reducing the toxic side effects to the patient.

[Cancer Treat Rep 60:1799–1810, 1976]

---

[1]Supported by Public Health Service grant CA-15397 from the National Cancer Institute, National Institutes of Health, Department of Health, Education, and Welfare.

[2] Department of Human Biological Chemistry and Genetics, Division of Cell Biology, University of Texas Medical Branch, Galveston.

[3]I wish to acknowledge the excellent assistance of Judy K. Novak, Denise Flournoy, and Peggy Anderson in the preparation of this manuscript.

Reprint requests to: Dr. S. C. Barranco, Department of Human Biological Chemistry and Genetics, Division of Cell Biology, University of Texas Medical Branch, Galveston, Tex 77550.

Recovery from sublethal damage (SLD) is measured by the increase in survival observed as the time interval is increased between two dose fractions of irradiation or drugs (1–4). During the interval between the dose fractions, SLD from the first dose may be repaired and is thus unavailable to interact with SLD from the second dose (3). Thus, the resulting survival may be higher after a fractionated-dose schedule than when the total dose is administered as a single treatment.

Recovery from potentially lethal damage (PLD) is measured by the increase in survival observed when cells are exposed to various growth conditions after single-drug or irradiation treatments (1,5). Conditions which are suboptimal for growth such as low temperature, inhibition of protein synthesis, and maintenance of cells in nutritionally deficient medium have been reported as favoring recovery from PLD (1,5–9). Recovery from PLD occurs in vivo and in vitro (1,10,11), in dividing and nondividing mammalian cells (1,8,12), in oxic and hypoxic cells (7), and independently of recovery from SLD (1,7,8). Conversely, the expression of PLD is measured by a decrease in survival, usually under conditions which inhibit DNA synthesis (5). Although PLD or recovery from it can be measured under various experimental post-treatment conditions, Winans et al (13) have presented evidence that suggests that sublethal and potentially lethal lesions are similar, involving alterations in the same structures. If this is the case then the term PLD should be used only operationally to explain post-treatment changes in survival.

Irradiation studies on mammalian cells in vitro have led to the description and testing of current ideas on repair of DNA in higher organisms related to irradiation sensitivity, carcinogenesis, and mutagenesis. It is equally important that such recovery studies be carried out in detail on mammalian cells following exposure to various chemical agents. Such recovery studies may help to explain the differences in mutation rates or in drug sensitivities of dividing and nondividing cells. The clinical implications of such studies are important since cells that recover from chemical damage and survive may be able to contribute to the regrowth of a tumor.

We have asked several questions relative to the design and interpretation of such drug recovery studies in our in vitro Chinese hamster ovary (CHO) cell system. First, since recovery from SLD after X-ray treatment is associated with the size of the shoulder region of the dose-response survival curve, does the same relationship exist for treatments with chemicals? Second, how does one consider drug concentration and duration of treatment when planning fractionated dose schedules? Third, since recovery from more than one type of damage may occur simultaneously, can the recovery from one type of damage be so great as to mask the response of the cells to another type of damage? Fourth, can the presence or absence of a repair process always explain the differences in sensitivity observed between dividing and nondividing cells?

The experiments described in this paper were designed and performed in an effort to provide answers to some of these questions. Four chemicals were used in these studies. Treatment of dividing or nondividing cells with adriamycin[4] results in biphasic survival curves with no shoulders (14,15). Exposure to actinomycin D (AMD)[5] results in a biphasic (no shoulder) survival curve with dividing cells; however, there is a shoulder region associated with the survival response of nondividing cells.[6] Dividing cells were more sensitive to both of these drugs; however, a significant fraction of nondividing cells were also killed (15).[6] The other two chemicals used in this study were the nitrosourea compounds, CCNU and methyl-CCNU (meCCNU).[7] Treatment of mammalian cells with either of these chemicals results in threshold- or shoulder-type survival curves (1,16) with nondividing cells being more sensitive than dividing cells. In this report we examine the survival responses to drug-induced PLD and SLD by these chemicals in dividing and nondividing populations of mammalian cells.

MATERIALS AND METHODS

Cell and culture techniques.—The CHO cell stocks were maintained in monolayer cultures in Hsu's modified McCoy's 5A medium, supplemented with 20% fetal calf serum in a 5% CO_2, 95% air, humidified incubator at 37°C. At least 19 hours before treatment 10^6 cells were placed into replicate 60 × 15-mm Petri dishes containing medium and 20% fetal calf serum for experiments on exponentially growing populations.

Induction of plateau phase.—Our plateau-phase system has been described previously (1,17). To obtain plateau-phase or nondividing cell populations, 5×10^5 exponentially growing CHO cells were placed into each 60 × 15-mm Petri dish containing 5 ml

[4]Adriamycin: NSC-123127; CAS reg. No. 23214-92-8.

[5]Actinomycin D: NSC-3053.

[6]Barranco SC, and Flournoy DR. Modification of the response to actinomycin D-induced sublethal damage by simultaneous recovery from potentially lethal damage in mammalian cells. Cancer Res 36:1634–1640, 1976.

[7]Methyl-CCNU: NSC-95441; CAS reg. No. 33073-59-5; urea, 1-(2-chloroethyl)-3-(4-methylcyclohexyl)-1-nitroso-.

CCNU: NSC-70037; CAS reg. No. 13010-47-4; urea, 1-(2-chloroethyl)-3-cyclohexyl-1-nitroso.

of medium with 20% fetal calf serum. The cells were never fed again until the experiments were performed 115–120 hours later. Total cell counts were obtained at various intervals; the cell number increased exponentially then plateaued around 8–10 × 10^6 cells/dish after 72 hours. Survival was measured only on cells which had been in plateau phase for an additional 48 hours. At this time the labeling index was < 2% and essentially all of the cells were blocked in a G_0-like compartment. The re-entry of plateau-phase cells back into the cell cycle was followed on cells that had been resuspended (10^6/dish) in fresh medium. At 3-hour intervals cells were pulse labeled with 1 microcurie/ml of tritiated thymidine (specific activity 1.9 curies/mmol) and total cell counts were performed. The cells re-entered the cell cycle in a partially synchronized manner and progressed from G_1 into S phase at 5–10 hours after subculturing. The cell number began increasing at 18–22 hours and doubled by 30 hours after the plateau cells were subcultured (17).

Survival determinations.—The effects of drugs on survival were determined on exponentially growing cells and on cells that had been maintained in plateau phase for at least 48 hours. Cells were treated with drug dilutions made in depleted plateau medium (for plateau-phase cells) or in fresh medium (for exponentially growing cells). The depleted plateau medium was collected from plates of plateau-phase cells, filtered to remove cells and debris, and then used for drug dilutions or incubations after treatment for recovery tests. (The depleted plateau medium has been tested and will not support further growth.) Replicate plates were used in each survival study and each experiment was performed at least three times. In all cases survival was determined by the ability of the treated cells to form colonies. After the treatments the cell monolayers were washed twice with Puck's solution A and trypsinized (0.025% for 5 minutes), and known numbers of single cells were plated into Petri dishes and incubated 6–8 days for colony formation (17,18). Colonies were stained and counted. A cell was considered to have retained reproductive capacity (viability) if it gave rise to a colony of ≥ 50 cells.

Recovery from PLD.—In the experiments reported here, suboptimal growth conditions were achieved by holding plateau phase or exponentially growing cells in depleted plateau medium after treatment with a drug. Following the treatment one group of cells was plated immediately for colony formation while other groups were washed and incubated at 37°C in fresh or depleted medium for 1–4 hours before being plated for colony formation.

Response to SLD.—To test for recovery from SLD, fractionated doses of a drug were used in treatments of dividing and nondividing cells. The treatments were fractionated using the integral-dose concept of drug concentration and duration of treatment C × t; the sum of the integral fractionated doses received by the cells was kept constant during any one experiment (1). For example, the sum of two fractionated doses of 5 μg/ml for 30 minutes 2(5 × 30) equals the same integral dose of 300 as a single treatment with 5 μg/ml for 60 minutes. All cells received one half of the integral dose at 0 hour. At the end of the first treatment, one group of cells was re-treated immediately with the same integral dose, thus allowing no time between treatments for recovery. The other groups of cells were washed and reincubated in the appropriate incubation medium, and received their second integral dose of drug 1–4 hours later. All cells were plated for colony formation immediately after receiving the second drug dose.

Chemical solutions.—The treatment solutions were always prepared immediately before use to ensure against loss of activity. AMD was dissolved in sterile water and diluted to the various treatment concentrations in fresh or depleted plateau medium. Because AMD is known to bind to cells and Petri dishes, all treated populations were extensively washed to remove extracellular AMD before further studies were performed on the cells. The adriamycin solutions were always made immediately prior to use by dissolving adriamycin in sterile 0.9% NaCl solution and diluting into the growth medium. CCNU and meCCNU were dissolved in 95% ethanol and diluted to treatment concentrations in Hanks' balanced salt solution (BSS). Appropriate Hanks' BSS and ethanol controls were included in the experiments and at no time did the plating efficiencies fall below control levels.

Method for calculating recovery ratios.—The data in figure 1 are survival data from PLD and SLD experiments plotted as recovery ratios. The survival values for cells incubated for various times in either fresh or depleted plateau media are compared to survival at 0 hour. The recovery ratios are calculated from the expression, S/S_0-1, where S_0 is the survival fraction for cells given 0 interval for recovery. S is the survival fraction that is being compared to S_0. For example, the survival fraction for cells given 5 μg/ml of AMD for 30 minutes and plated immediately at 0 hour was 0.086 (PLD curve, fig 2). This is S_0. The amount of recovery at that dose (without a recovery period) was 0.086/0.086–1 or 0. Likewise, the survival fraction was 0.155 1 hour later (PLD curve, fig 2). This represents a 0.8-fold increase in survival (ie, 0.155/0.086–1 = 0.8). In situations where survival decreased as a result of post-treatment incubation conditions the recovery ratio becomes a negative value.

RESULTS

Dose response to meCCNU and CCNU.—The effects of meCCNU on survival of CHO cells treated in plateau or exponential phases of growth are presented in figure 3. The dashed line represents the sensitivity of dividing cells to meCCNU prepared in medium containing 20% fetal calf serum and is included for comparison with the other two curves for drug prepared in Hanks' BSS. At the 10-μg/ml/hr dose points, the nondividing or plateau-phase cells are 128 times more sensitive to meCCNU than are cells treated in the exponential phase of growth. The curve for the nondividing cells has a small shoulder followed by an exponential decrease in survival (n = 1.2 and D_0 = 1.2 μg/ml/hr). The survival curve for the dividing cells treated with meCCNU has a much larger shoulder, n = 6 and D_0 = 1.7 μg/ml/hr. The effects of CCNU on survival of CHO cells treated in plateau or exponential phases of growth are presented in figure 4. When measured at the 10-μg/ml dose points there are 5.3 times more plateau-phase cells killed than exponentially growing cells. Once again the curve for the nondividing cells has a much smaller shoulder region than the curve for dividing cells, n = 1.5 and 10.5 respectively. The D_0 for both curves is 1.4 μg/ml/hr.

The cellular response to meCCNU-induced PLD and SLD.—In the experiments reported here, suboptimal growth conditions were achieved by holding

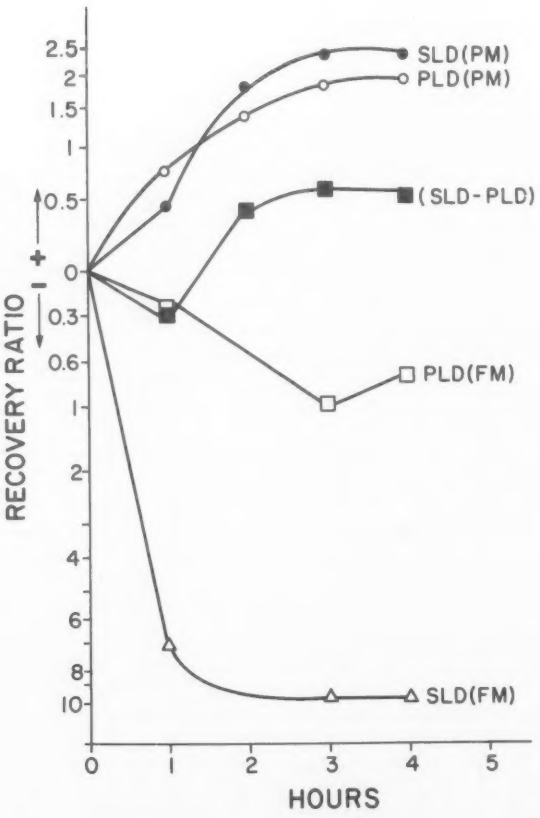

FIGURE 1.—Comparative responses of dividing cells to PLD and SLD when incubated in either fresh (FM) or depleted plateau-phase medium (PM). The SLD-PLD curve represents the response to SLD(PM) once the contribution made by simultaneous recovery from PLD(PM) has been subtracted. (*From* footnote 7.)

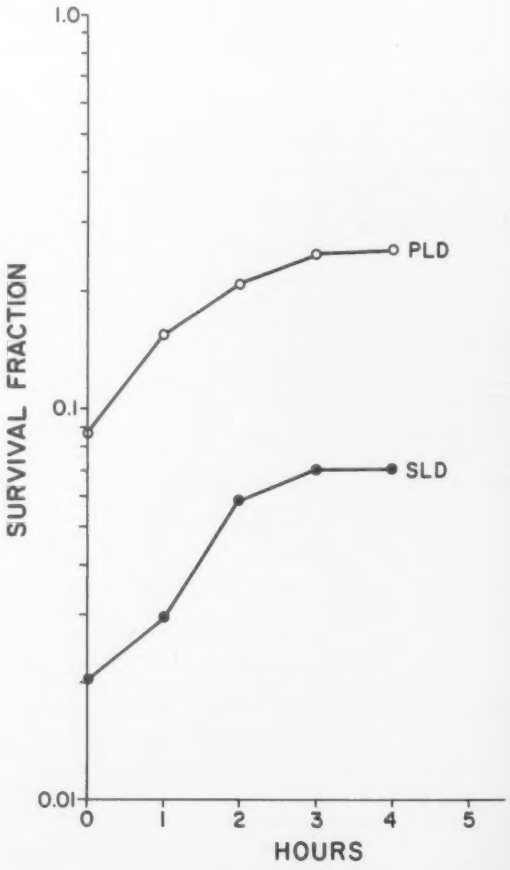

FIGURE 2.—Responses of dividing CHO cells to AMD-induced PLD or SLD while being incubated in depleted plateau medium. The cells received either a single 5-μg/ml dose for 30 mins (PLD) or 2 fractionated doses of 5 μg/ml for 30 mins each (SLD). (*From* footnote 7.)

plateau-phase or exponentially growing cells in depleted plateau medium after treatment with the chemical agents. When dividing and nondividing CHO cells were treated for 1 hour with 7 μg/ml of meCCNU and then incubated in depleted plateau-phase medium, survival decreased with longer holding periods in depleted plateau medium (fig 5). Dividing cells plated for colony formation immediately after the 1-hour treatment with meCCNU had a survival fraction of 0.1. With continued incubation in depleted plateau medium, the survival fraction decreased to 0.02 after 1 hour and ultimately to 0.007 by the end of the fourth hour of post-treatment incubation. Qualitatively similar results were obtained for the nondividing cells (fig 5). The effects of fractionated doses of meCCNU on survival are shown in figure 6. In figure 6A it can be seen that dividing cells treated with two doses of 3.5 μg/ml of meCCNU for 30 minutes exhibited no recovery from SLD. In fact, dividing cells treated with doses near the LD90 level (two fractions of 7 μg/ml for 30 minutes each) actually experienced a threefold reduction in survival when the two doses were separated by 1–4 hours. The response of nondividing cells treated with fractionated doses of meCCNU (near the LD90) is described in figure 6B. Following two doses of 3.5 μg/ml for 30 minutes (separated by the times indicated on the graph) a 12-fold decrease in survival was observed. Therefore, the reduction in survival in plateau-phase cells following fractionated doses (LD90) is four times greater than in exponentially growing cells. Qualitatively similar results were obtained with CCNU (1).

Dose response to AMD.—The effects of AMD on

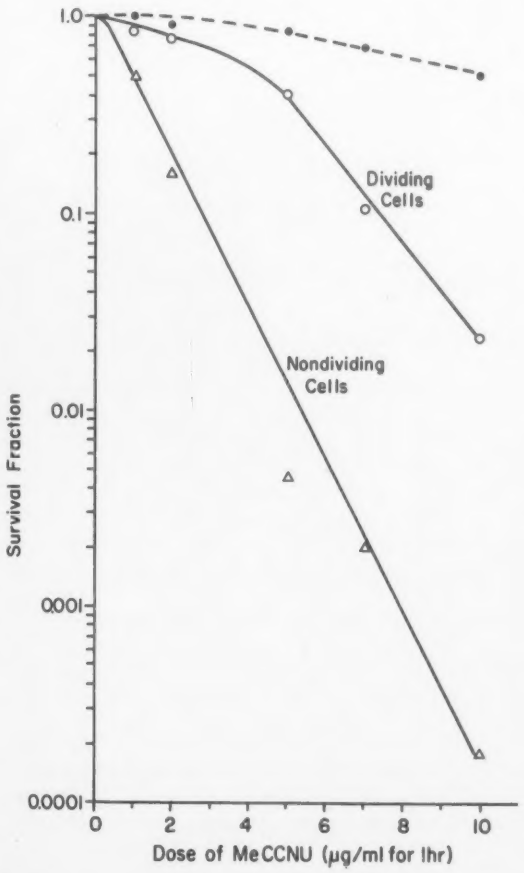

FIGURE 3.—Effects of meCCNU on survival of CHO cells treated in the plateau or exponential phases of growth. --- = sensitivity of dividing cells to meCCNU prepared in medium containing 20% fetal calf serum. (*From* ref No. 1.)

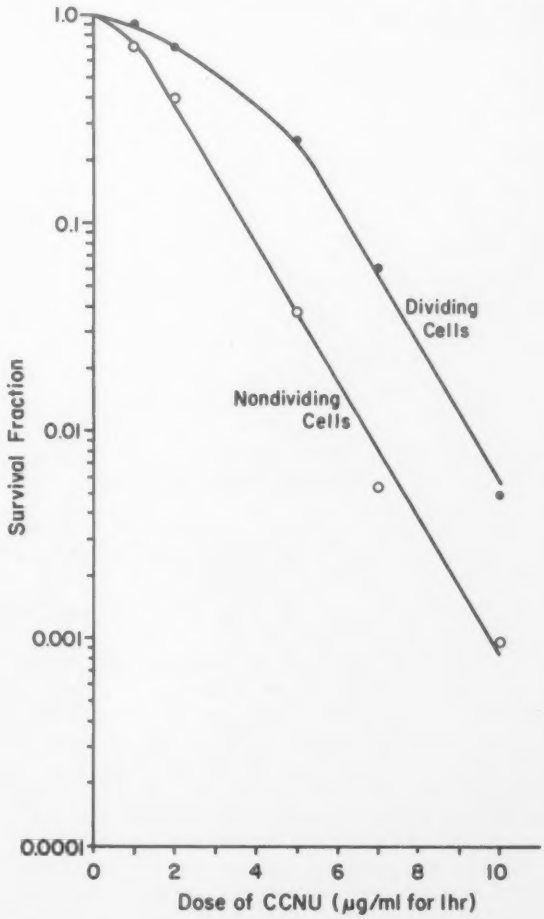

FIGURE 4.—Effects of CCNU on survival of CHO cells treated in the plateau or exponential phases of growth. (*From* ref No. 1.)

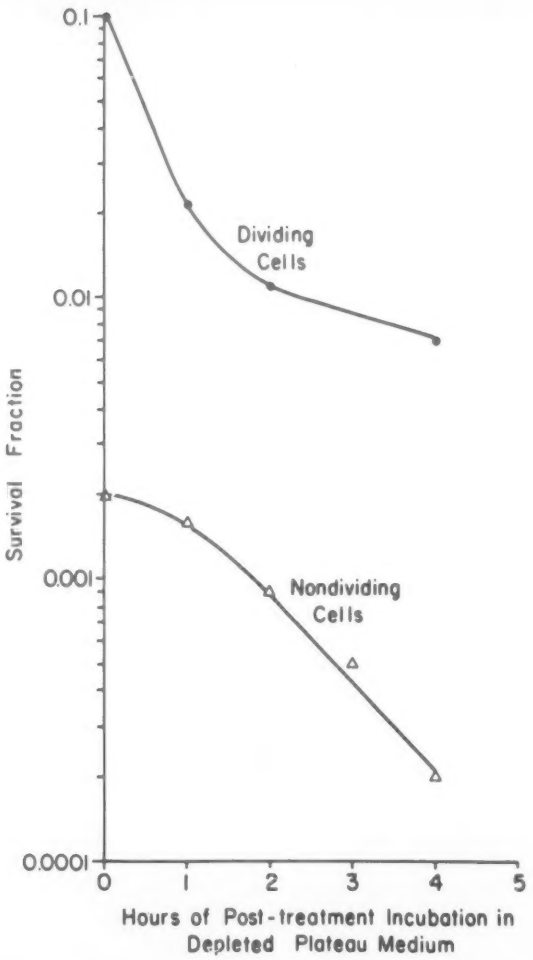

FIGURE 5.—Response of dividing or nondividing CHO cells to incubation in depleted plateau-phase medium after a 1-hr treatment with 7 μg/ml of meCCNU. (*From* ref No. 1.)

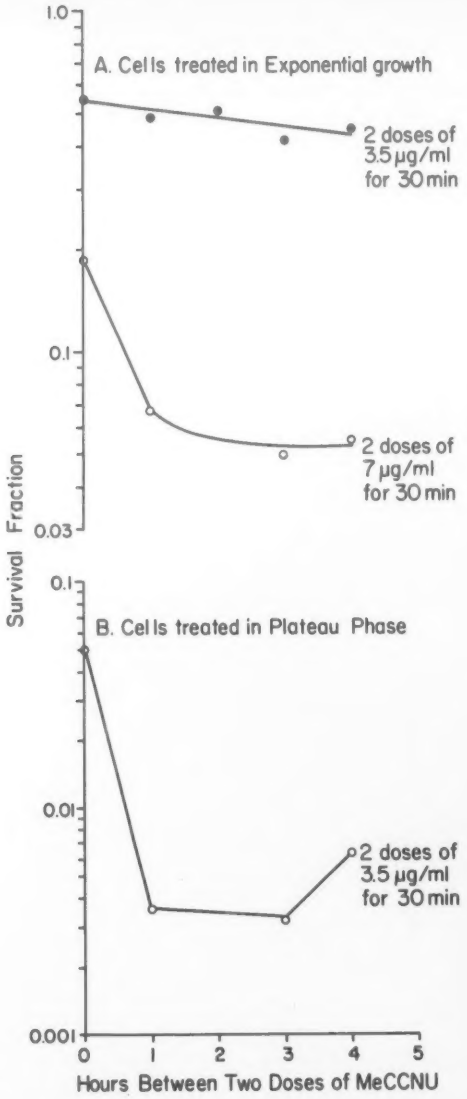

FIGURE 6.—Responses of dividing and plateau-phase CHO cells to fractionated doses of meCCNU. (*From* ref No. 1.)

survival of CHO cells treated in plateau or exponential phases of growth are presented in figure 7. Dividing cells were more sensitive than nondividing cells and their survival curve was slightly biphasic with the inflection point at the 2-μg/ml dose point. The survival curve for dividing cells is characterized as having no shoulder region with D_0's of 0.9 and 1.7 μg/ml (1-hour treatment) for the sensitive and less sensitive slopes of the curve respectively (n = 1). The survival curve for nondividing cells is also biphasic and contains a slight shoulder region with n = 1.5 and D_0's for the sensitive and less sensitive slopes of 1.3 and 5.8 μg/ml (1-hour treatment) respectively.

The cellular responses to AMD-induced PLD and SLD.—The nondividing or plateau-phase cells in these studies were incubated in depleted plateau medium (instead of fresh medium). In this way the test for response to AMD-induced damage could be made in the same environment that the cells were in prior to drug treatment. In addition, incubation in the nutritionally deficient medium may also mimic the extracellular environment of G_0 tumor cells in vivo (19). The nondividing cells were unable

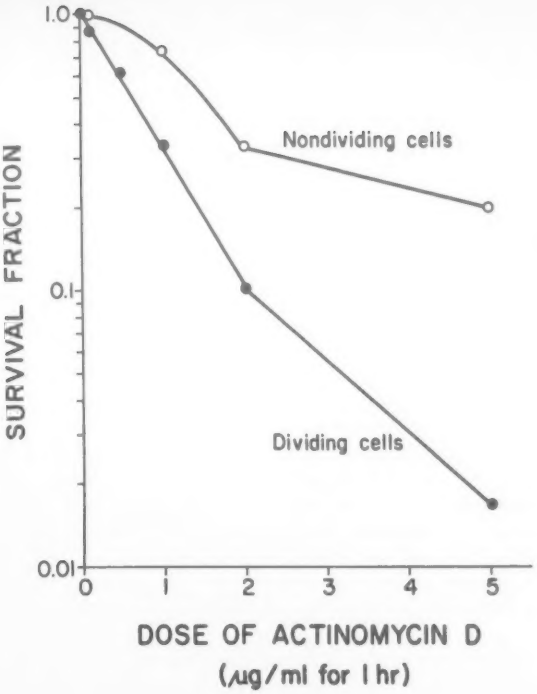

FIGURE 7.—Effects of AMD on survival of CHO cells treated in the plateau and exponential stages of growth. (*From* footnote 7.)

to recover from either type of damage under these conditions.[8] AMD-treated dividing cells incubated in fresh medium (to mimic the extracellular environment of dividing cells in vivo) did not exhibit the ability to recover from PLD or SLD. In fact, an eightfold to tenfold reduction in survival was observed when the LD99 dose was given in two parts (fig 1).[8] However, dividing cells incubated in nutritionally deficient medium did show recovery. In figure 2 it can be seen that dividing cells treated with 5 μg/ml of AMD for 30 minutes and then plated immediately (PLD curve) had survival fractions of 0.086 (0-hour survival fraction); cells held 1–4 hours in depleted medium had up to twofold higher survival values indicating recovery from PLD under these conditions. Dividing cells held in depleted plateau medium between the two 5-μg/ml dose fractions of AMD (SLD curve, fig 2) also exhibited increased survival values. The survival fraction increased from 0.02 (0-time interval between doses) to 0.07 when cells were held 3–4 hours in the nutritionally deficient medium between drug-dose fractions. These same data are presented in figure 1 as a function of recovery ratios (*see* Methods for calculations). It can be seen in figure 1 that AMD-treated cells could not recover from PLD or SLD when they were incubated in fresh medium (PLD-FM and SLD-FM curves). These curves are included in figure 1 for comparison with curves depicting the increased survival observed when dividing cells were incubated in depleted plateau medium (PM) after treatment (SLD-PM and PLD-PM curves). The SLD-PLD curve was obtained by reducing the SLD survival points by the fraction due to recovery from PLD. These data suggest that part of the observed recovery from SLD during incubation in depleted medium was due to recovery from PLD.

Survival responses to adriamycin.—The survival of dividing CHO cells following a 1-hour treatment with varying doses of adriamycin is shown in figure 8. The survival curve is without a shoulder and the response to this drug is biphasic (n = 1, D_0 = 0.2 μg/

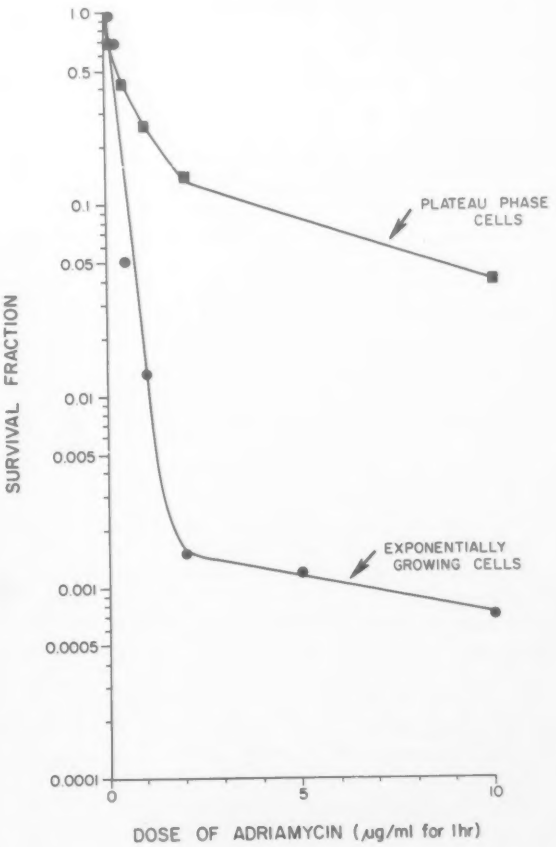

FIGURE 8.—Survival responses of dividing and nondividing CHO cells to adriamycin (20).

[8]*See* footnote 6.

ml for 1 hour in about 99% of the population and D_0 = 9.4 μg/ml for 1 hour in the more resistant group of cells). The survival fraction was reduced to < 0.002 with a dose of 2 μg/ml of adriamycin. At doses > 5 μg/ml the survival response of the remaining resistant 0.1% of the population assumed a shallow slope through a dose of 25 μg/ml (14). The survival fraction in plateau-phase cells decreased to 0.15 after exposure to 2 μg/ml for 1 hour and decreased to 0.04 after exposure to 10 μg/ml for 1 hour.

Cellular response to adriamycin-induced SLD and PLD.—Neither the dividing nor the plateau-phase cells showed any response to PLD. There was neither increased survival nor reduction in survival when the cells were incubated under suboptimal growth conditions after treatment. However, the cells did exhibit a dose-dependent response to fractionated doses of adriamycin. In figure 9 it can be seen that dividing cells treated with two dose fractions of 1 μg/ml for 30 minutes experienced a twofold reduction in survival if the treatments were 1–3 hours apart; survival increased, however, when there was a 4-hour interval between doses, possibly due to cells progressing into less sensitive stages of the cell cycle by the time the second dose was given at the fourth hour. Dividing cells treated with two dose fractions of 5 μg/ml for 30 minutes exhibited a slight reduction in survival if the treatments were 1 hour apart. A threefold decrease in survival was observed when the interval between doses was increased to 3 or 4 hours. Nondividing cells given two large dose fractions (5 μg/ml for 30 minutes or 10 μg/ml for 30 minutes) exhibited 1.6-fold to 2.3-fold reductions in survival when the treatments were given 1–4 hours apart (20).

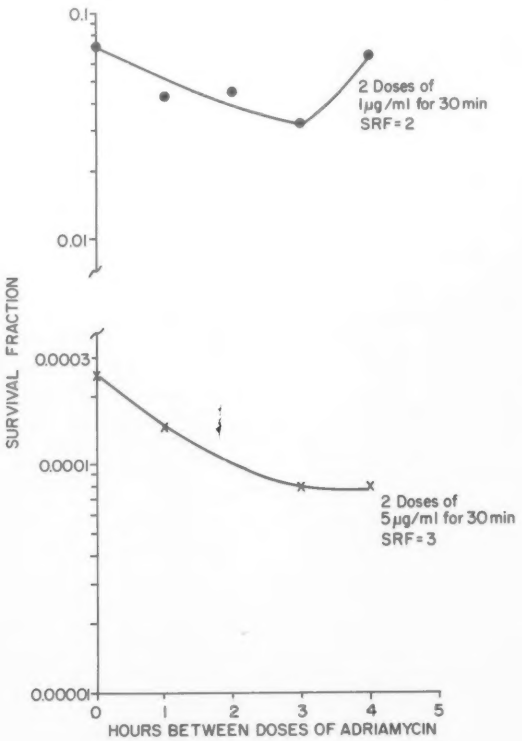

FIGURE 9.—Responses of dividing CHO cells to fractionated doses of adriamycin. The cells were held in fresh medium between treatments. (*From* ref No. 20.)

DISCUSSION

Dose responses of dividing and plateau-phase cells.—The data presented in figures 3 and 4 show that plateau-phase or nondividing cells were more sensitive (relative to survival) to the nitrosourea compounds, CCNU and meCCNU, than were exponentially growing cells. The greatest difference in sensitivity occurred with meCCNU (at the 10-μg/ml dose point) where approximately 128 times more cells were killed in plateau phase than during exponential growth. Nondividing cells were only five times more sensitive than dividing cells when treated with CCNU. These data are in excellent agreement with and support the in vitro data on the nitrosoureas reported by Tobey and Crissman (16) and others (17,21,22). However, in an in vivo mouse bone marrow system (23), resting hematopoietic stem cells were found to be less sensitive to the nitrosourea compounds than were the rapidly proliferating stem cells. (The rapid division of bone marrow stem cells was induced by irradiation depletion of the marrow.) The reasons why the sensitivities of dividing and nondividing cells in vitro (16,17,21,22) differ from the in vivo data (21,23) are not clear, but this could be due to failure of the drug to gain access to the cells in vivo. Dividing cells were more sensitive to AMD than were nondividing cells.[8] The exponentially growing cells were 1.5–3.4 times more sensitive than the nondividing cells (calculated from the D_0's of the survival curves in fig 7). These data are in agreement with recent reports by Wilkoff et al (24), Valeriote et al (25), and Djordjevic and Kim (26). Proliferating cells in S phase of their cell cycle are most sensitive to AMD (26,27). AMD inhibits DNA-directed RNA synthesis through its ability to complex with DNA (28,29). It is this ability to complex DNA which possibly accounts for the activity of AMD against both proliferating and nonproliferating mammalian cells. As with AMD, dividing cells exposed to adriamycin were more sensitive than were nondividing cells (fig 8) (15,20). However, with both of these drugs, and especially with the nitrosoureas,

large fractions of nondividing cells were also killed. We are aware of the limitations inherent in comparing plateau-phase cells in vitro with G_0 cells in vivo. However, these results do suggest a possibility that considerable killing in the G_0 compartment in vivo may be observed. A better understanding of the effects of anticancer drugs on these viable, but nondividing cell populations has potential clinical significance. Since the plateau or G_0 cells generally are not killed by the cell cycle-specific drugs, these cells probably contribute to the repopulation or regrowth of the tumor. Therefore, it is extremely important to identify and characterize drugs that will specifically influence the survival, repair, and repopulation kinetics of G_0 or plateau-phase cells.

Response to PLD.—Phillips and Tolmach (5) have suggested that the response of cells to irradiation may be modified by various post-treatment conditions that interfere with processes that normally result in either repair or expression of damage. For example, irradiation of G_1 cells followed by incubation of the cells in the DNA synthesis inhibitors fluorodeoxyuridine or hydroxyurea resulted in lower survival (5). This suggested that DNA synthesis (unscheduled) may be required for repair of the PLD. This idea was further substantiated by post-irradiation treatment with cycloheximide at doses that primarily inhibited protein synthesis, without altering the repair process, and resulted in higher survival than in cells receiving only irradiation. Therefore, an extremely important parameter to consider in the chemotherapy of tumors is the possibility that the tumor cells may recover from damage caused by the chemical treatment. The recovered cells, therefore, would be able to contribute to the regrowth of the tumor. Experiments were designed to measure recovery from drug-induced PLD, ie, damage that would become lethal to the cell if time and post-treatment conditions are not suitable for repair (5). An increase in survival may be observed after treated cells are held for several hours under conditions that prohibit protein synthesis and cell progression and, therefore, allow time for recovery (5). The recovery from PLD can also be expressed as a change in the slope (D_0) of the survival curve (30). Dividing cells treated with AMD and then incubated 2–4 hours in nutritionally deficient medium showed an approximate twofold increase in survival (fig 1). Plateau-phase cells were unable to recover. That the increased survival observed in dividing cells was related to incubation in depleted medium is supported by the observations that survival decreased when dividing cells were incubated in fresh medium after AMD treatment (fig 1). These data suggest the dividing cells can recover from AMD-induced PLD. We have presented other in vitro evidence that bleomycin-treated cells can also recover from PLD. The recovery ratios of nondividing cells were two times greater than those for dividing cells. These data are consistent with other in vitro and in vivo results (11,12,31).[9] There was neither increased survival (recovery) nor reduction in survival (expression of PLD) when adriamycin-treated dividing and plateau cells were incubated under suboptimal growth conditions. These data suggest that damage of a potentially lethal nature was not produced by adriamycin since no change in the survival response could be measured. In contrast to the data for adriamycin and AMD, dividing and nondividing cells treated with CCNU or meCCNU experienced reductions in survival when they were incubated in depleted plateau medium. It is possible that a degradation step is involved in the repair of alkylation damage (6). We have preliminary evidence that shows that by incubating the nitrosourea-treated cells in depleted plateau medium at 4°C, reduction in survival is prevented. The nitrosoureas are alkylating agents (32) and have been shown to alkylate nucleic acids and proteins (33) in intact cells. However, several reports indicate that more than alkylation is involved in the antitumor effects of these drugs. The nitrosourea compounds are very unstable and the breakdown products are highly reactive (33–35). Among the breakdown products are isocyanates that do not possess antitumor activity; however, Kann et al (34) have shown that 2-chloroethyl isocyanate (a breakdown product of BCNU) inhibits both DNA synthesis and the repair of single strand breaks in DNA. Therefore, since the nitrosoureas are known to cause DNA damage, the isocyanates generated by them may be responsible for the inhibition of repair of DNA damaged by the alkylating agents, thereby resulting in the reduction in survival.

Response to fractionated drug doses (SLD).—Since the size of the shoulder on survival curves is related to recovery from X-ray-induced SLD (3), experiments were performed to determine whether this phenomenon held true for chemically induced damage. Treatment of dividing and nondividing cells with the nitrosourea compounds also resulted in threshold- or shoulder-type survival curves, suggesting that the cells might accumulate and recover from SLD. Furthermore, extrapolation numbers of 10.5 and six for dividing cells compared to 1.5 and 1.2 in plateau-phase cells resulting from treatments with CCNU or meCCNU indicated that the dividing cells might show a greater ability for recovery from SLD. If this were true, it could explain the reason for the

[9]Twentyman PR, and Bleehen NM. Personal communication.

greater sensitivity of nondividing cells to these chemicals (figs 3 and 4) (1,16). The results in figure 6 show that not only do the cells fail to recover from SLD, but the fractionated treatment results in sensitization. When doses near the LD90 survival level were used, the dividing cells were 1.5 to three times more sensitive to the fractionated-dose schedules than to single-dose treatments. However, the plateau-phase cells were 12–14 times more sensitive to the fractionated-dose treatments (fig 6) (1). In other words, the plateau-phase cells were four times more sensitive to fractionated LD90 doses of the nitrosoureas than were the dividing cells. In contrast to the nitrosoureas, adriamycin survival curves were biphasic and had no shoulder regions (fig 8). The dividing and nondividing cells exhibited increased sensitivities to fractionated doses of the drug (fig 9) (20). The response to fractionated treatments was dose-dependent and the reduction in survival was greater in dividing cells than in plateau cells when measured at the same LDs (20). The survival fraction in dividing cells after two dose fractions of 5 μg/ml of adriamycin for 30 minutes (fig 8) was equivalent to that resulting from a single treatment with 25 μg/ml for 1 hour (20). Similar results were obtained with dividing cells incubated in fresh medium between two doses of AMD (fig 7). An eightfold to tenfold reduction in survival was obtained with two dose fractions of 5 μg/ml of AMD for 30 minutes. The survival fraction (0.001) was equivalent to that resulting from a single treatment with 15 μg/ml of AMD for 1 hour (unpublished results). Qualitatively similar effects were produced by fractionated doses of the nitrosoureas. Since the side effects of most cancer chemotherapy drugs appear to be dose-dependent, these results may be clinically relevant in that it may be possible to reduce the total drug doses and toxicity while achieving the same amount of cell-kill through the use of fractionated-dose treatments. Note, however, that these dose fractions are given 1–4 hours apart instead of the usual 24–72-hour schedule used in most clinical protocols.

The effects of recovery from PLD on SLD measurements.—Little (8) has reported that, in addition to recovery from SLD, recovery from PLD can also occur between fractionated doses of irradiation. The CHO cells in our system express the same ability when exposed to bleomycin (1). However, when the recovery from PLD was accounted for, little if any recovery could be observed from bleomycin-induced SLD (1). A similar phenomenon exists with AMD. As long as dividing cells were held in fresh medium (to mimic the in vivo cellular environment) between fractionated dose treatments, no PLD or SLD recovery was observed (fig 1). However, incubation of the dividing-cell population in suboptimal growth conditions (depleted plateau medium) between dose fractionation resulted in a twofold increase in survival. The cells also recovered from PLD under these conditions (fig 1). When the SLD(PM) survival curve was adjusted for the contribution made by recovery from PLD(PM), the resulting SLD-PLD curve suggested that at least part of the observed recovery from SLD was due to the simultaneous recovery from PLD. The 0.5 recovery ratio observed in the SLD-PLD curve may be due to the progression of cells into more resistant phases of the cell cycle by the time the second dose was given (36). However, it has been shown that AMD inhibits cell progression in all phases of the cell cycle (37–39) at dose levels much lower than those used here. It is possible, therefore, that under certain culture conditions cells can recover from AMD-induced SLD.

CONCLUSIONS

From the data presented in this paper the following responses can be made to the questions asked at the beginning of the text.

1. The results of these experiments do not resolve the question concerning the relationship between a shoulder on the survival curve and the ability to accumulate or recover from drug-induced SLD. AMD-treated cells gave rise to survival curves without shoulders and proliferating and nonproliferating cells could not recover from PLD or SLD when the cells were incubated under the conditions of their respective growth states after treatment. In fact, increased cell killing was observed with longer incubation times, possibly because of the effect of DNA-bound AMD on repair. However, recovery from PLD and SLD did occur when treated dividing cells were held under conditions which were unfavorable for growth (ie, depleted plateau medium). When adjustments were made for the PLD recovery, a small but measurable increase in survival was seen and may represent recovery from SLD. Adriamycin-treated cells also gave rise to survival curves without shoulders, and dividing and nondividing cells could not recover from PLD or SLD. In contrast to AMD and adriamycin, treatment with the nitrosourea compounds resulted in survival curves with shoulders; however, not only were the cells unable to recover from SLD, they also seemed to be sensitized by the first drug dose so that the second dose caused up to a 14-fold reduction in survival. The possible existence of nitrosourea breakdown products that inhibit DNA repair may account for this response (34). It is also possible that the presence of a shoulder on the survival curves does not have the same meaning for chemically induced damage as it does for irradiation-induced

damage. The presence of a shoulder on a drug-treatment survival curve may reflect more about drug concentrations and the time required for entry of the drug into the cell and interaction with a target molecule than it does about the accumulation and repair of SLD. In addition, the target size or number may be quite different in plateau-phase cells with a G_1 quantity of DNA (40) than in an exponentially growing cell population where a large fraction of the cells have completed or are in the process of completing DNA replication.

2. In reference to the question of how one considers drug concentration and length of treatment when planning fractionated-dose schedules, the data presented in this paper do not give clear evidence for the proper choice. This subject will be handled in a forthcoming publication. However, we feel that it is important that the integral-dose concept of $C \times t$ be used in fractionated-dose studies and that survival comparisons be made between cells receiving identical integral doses, whether administered alone or in two fractions.

3. Recovery from one type of damage (eg, AMD-induced PLD) can be so great that it may mask the true response of the cells to another type of damage (SLD). This suggests that a test for the response to PLD and SLD be performed for each drug studied. However, more important than the relevance of PLD to SLD measurements is the question of whether PLD really exists. As Winans et al (13) suggest, PLD and SLD may be very similar and involve alterations in the same structures. This phenomenon needs to be thoroughly studied relative to drug effects before this question can be satisfactorily answered.

4. The survival responses to PLD or SLD in these studies do not explain the widely different sensitivities observed between dividing and nondividing cells to AMD, adriamycin, or the nitrosoureas. Other studies dealing with mechanisms of drug action, target size and number, drug sensitization, reactive drug breakdown products, resistance, cell membrane changes, cell surface components, cell progression effects, etc, are necessary.

It is clear from these studies that interpretation of recovery data from drug-induced damage in mammalian cell systems is far more complicated and will take longer than thought at first. However, early clinical benefit may be realized in that information may be gained that would be of value in the planning of dose fractionations or drug combination treatments. Repair and recovery studies are of additional clinical significance since the cells that recover from chemical damage and survive will contribute to the regrowth of the tumor.

REFERENCES

1. BARRANCO SC, NOVAK JK, and HUMPHREY RM. Studies on recovery from chemically induced damage in mammalian cells. Cancer Res 35:1194–1204, 1975.
2. DEWYS WC, and KIGHT N. Kinetics of cyclophosphamide damage-sublethal damage repair and cell-cycle-related sensitivity. J Natl Cancer Inst 42:155–163, 1969.
3. ELKIND MM, and SUTTON H. Radiation response of mammalian cells grown in culture. 1. Repair of X-ray damage in surviving Chinese hamster cells. Radiat Res 13:556–593, 1960.
4. MAURO F, and ELKIND MM. Comparison of repair of sublethal damage in culture Chinese hamster cells exposed to sulfur mustard and X-rays. Cancer Res 28:1156–1161, 1968.
5. PHILLIPS RA, and TOLMACH LJ. Repair of potentially lethal damage in X-irradiated HeLa cells. Radiat Res 29:413–432, 1966.
6. BELLI JA, and SHELTON M. Potentially lethal radiation damage: repair by mammalian cells in culture. Science 165:490–492, 1969.
7. HAHN GM, BAGSHAW MA, EVANS RG, ET AL. Repair of potentially lethal lesions in X-irradiated, density-inhibited Chinese hamster cells: metabolic effects and hypoxia. Radiat Res 55:280–290, 1973.
8. LITTLE JB. Repair of sublethal and potentially lethal radiation damage in plateau phase cultures of human cells. Nature 224:804–806, 1969.
9. WHITMORE GF, and GULYAS S. Studies on recovery processes in mouse L cells. Natl Cancer Inst Monogr 24:141–156, 1967.
10. HAHN GM, RAY GR, GORDON LF, ET AL. Response of solid tumor cells exposed to chemotherapeutic agents in vivo: cell survival after 2- and 24-hour exposure. J Natl Cancer Inst 50:529–533, 1973.
11. RAY GR, HAHN GM, BAGSHAW MA, ET AL. Cell survival and repair of plateau-phase cultures after chemotherapy—relevance to tumor therapy and to the in vitro screening of new agents. Cancer Chemother Rep 57:473–475, 1973.
12. HAHN GM, GORDON LF, and KURKJIAN SD. Responses of cycling and non-cycling cells to 1,3-bis(2-chloroethyl)-1-nitrosourea and to bleomycin. Cancer Res 34:2373–2377, 1974.
13. WINANS LF, DEWEY WC, and DETTOR CM. Repair of sublethal and potentially lethal X-ray damage in synchronous Chinese hamster cells. Radiat Res 52:333–351, 1972.
14. BARRANCO SC, GERNER EW, BURK KH, ET AL. Survival and cell kinetics effects of adriamycin on mammalian cells. Cancer Res 33:11–16, 1973.
15. BARRANCO SC, and NOVAK JK. Survival responses of dividing and nondividing mammalian cells after treatment with hydroxyurea, arabinosylcytosine, or adriamycin. Cancer Res 34:1616–1618, 1974.
16. TOBEY RA, and CRISSMAN HA. Comparative effects of three nitrosourea derivatives on mammalian cell cycle progression. Cancer Res 35:460–470, 1975.
17. BARRANCO SC, NOVAK JK, and HUMPHREY RM. Response of mammalian cells following treatment with bleomycin and 1,3-bis(2-chloroethyl)-1-nitrosourea during plateau phase. Cancer Res 33:691–694, 1973.
18. DEWEY WC, HUMPHREY RM, and CORK A. Comparison of cell-multiplication and colony-formation as criteria for radiation damage in cells grown in vitro. Int J Radiat Biol 6:463–471, 1963.
19. TANNOCK IF. A comparison of cell proliferation parameters in solid and ascites Ehrlich tumors. Cancer Res 29:1527–1534, 1969.
20. BARRANCO SC. A review of the survival and cell kinetics effects of adriamycin on mammalian cells. Cancer Chemother Rep Part 3, vol 6(2):267–272, 1975.

21. HAGEMANN RF, SCHENKEN LL, and LESHER S. Tumor chemotherapy: efficacy dependent on mode of growth. J Natl Cancer Inst 50:467–474, 1973.
22. TWENTYMAN PR, and BLEEHEN NM. The sensitivity of cells in exponential and stationary phases of growth to bleomycin and to 1,3-bis(2-chloroethyl)-1-nitrosourea. Br J Cancer 28:500–507, 1973.
23. VAN PUTTEN LM, LELIEVELD P, and KRAM-IDSENGA LKJ. Cell-cycle specificity and therapeutic effectiveness of cytostatic agents. Cancer Chemother Rep 56:691–700, 1972.
24. WILKOFF LJ, LLOYD HH, and DULMADGE EA. Kinetic evaluation of the effect of actinomycin D, daunomycin, and mitomycin C on proliferating cultured Leukemia L1210 cells. Chemotherapy 16:44–60, 1971.
25. VALERIOTE F, VIETTI T, and TOLEN S. Kinetics of the lethal effect of actinomycin D on normal and leukemic cells. Cancer Res 33:2658–2661, 1973.
26. DJORDJEVIC B, and KIM JH. Different lethal effects of mitomycin C and actinomycin D during the division cycle of HeLa cells. J Cell Biol 38:477–482, 1968.
27. ELKIND MM, KANO E, and SUTTON-GILBERT H. Cell killing by actinomycin D in relation to the growth cycle of Chinese hamster cells. J Cell Biol 42:366–377, 1969.
28. KIRK J. The mode of action of actinomycin D. Biochim Biophys Acta 42:167–169, 1960.
29. REICH E, CERAMI A, and WARD DC. Actinomycin. *In* Antibiotics (Gottlieb D, and Shaw PD, eds). New York, Springer, vol 1, 1967, pp 714–725.
30. LITTLE JB. Repair of potentially lethal radiation damage in mammalian cells: enhancement by conditioned medium from stationary cultures. Int J Radiat Biol 20:87–92, 1971.
31. TAKABE Y, WATANABE M, MIYAMOTO T, ET AL. Demonstration of repair of potentially lethal damage in plateau phase cells of Ehrlich ascites tumor after exposure to bleomycin. Gann 65:559–560, 1974.
32. WHEELER GP, BOWDEN BJ, GRIMSLEY J, ET AL. Interrelationships of some chemical physiochemical and biological activities of several 1-(2-haloethyl)-1-nitrosoureas. Cancer Res 34:194–200, 1974.
33. CHENG CJ, FUJIMURA S, GRUNBERGER D, ET AL. Interaction of 1-(2-chloroethyl)-3-cyclohexyl-1-nitrosourea (NSC 79037) with nucleic acids and proteins in vivo and in vitro. Cancer Res 32:22–27, 1972.
34. KANN HE, JR, KOHN KW, and LYLES JM. Inhibition of DNA repair by the 1,3-bis(2-chloroethyl)-1-nitrosourea breakdown product, 2-chloroethyl isocyanate. Cancer Res 34:398–402, 1974.
35. YOUNG RC, and DEVITA VT. The effect of chemotherapy on the growth characteristics and cellular kinetics of leukemia L1210. Cancer Res 30:1789–1794, 1970.
36. ELKIND MM, and KANO E. Actinomycin D and radiation fractionation studies in asynchronous and synchronized Chinese hamster cells. Radiat Res 44:484–497, 1970.
37. BARRANCO SC, and HUMPHREY RM. A time-specific effect of UV-irradiation on cells progressing from G_2 into metaphase. Mutat Res 9:524–526, 1970.
38. BASERGA R, ESTENSEN RD, and PETERSEN RO. Inhibition of DNA synthesis in Ehrlich ascites cells by actinomycin D. II. The presynthetic block in the cell cycle. Proc Natl Acad Sci USA 54:1141–1148, 1965.
39. KIM JH, GELBARD AS, and PEREZ AG. Inhibition of DNA synthesis by actinomycin D and cycloheximide in synchronized HeLa cells. Exp Cell Res 53:478–487, 1968.
40. TOBEY RA, and LEY KD. Regulation of initiation of DNA synthesis in Chinese hamster cells. I. Production of stable, reversible G_1-arrested populations in suspension culture. J Cell Biol 46:151–157, 1970.

Introduction to Session on Recruitment and Synchrony—In Vitro

Renato Baserga [1]

The title of this session, "Recruitment and Synchrony—In Vitro," may at first seem to have nothing to do with the chemotherapy of tumors. After all, the use of tissue cultures for the screening of anticancer agents has become, I understand, a thing of the past, and deservedly so. The decline and fall of tissue cultures as a model system for screening drugs is a source of modest satisfaction to me since, for years, I have been preaching its obvious pitfall to friends and colleagues: drugs are not catabolized in vitro as they are in vivo. The same objection, of course, applies to those close relatives of tissue culture, the ip ascitic tumors of rodents. Screening of anticancer agents can now be done more intelligently in in vivo systems, especially: (*a*) experimental animals in which cells have been synchronized in vivo by a variety of manipulations (1); (*b*) nude mice (2); and (*c*) metastatic models, in which chemotherapy is directed not against huge primary tumors but against metastatic seeds before they are grossly visible.

Disqualified as a practical screening method, tissue culture remains the method of choice for basic studies to which the motto can be applied: *In Vitro Veritas*. In the field of chemotherapy tissue culture can offer inestimable advantages for studying the G_0 state of cells. Two questions are in order at this point: (*a*) does the G_0 state really exist, and (*b*) if it does, why is it important in the chemotherapy of cancer?

The answer to the first question is, or ought to be by now, simple. I have already reviewed the evidence, elsewhere, that G_0 cells are biochemically different from G_1 cells (3,4) and I will not discuss that evidence in detail again. Briefly, there are differences in chromatin structure and function, in nonhistone chromosomal proteins, in the amount of cytoplasmic ribosomes, and in membrane function. This is in addition to kinetic (5) and theoretic (6) considerations. As an illustration, the reported changes in nuclei and chromatin that occur when G_0 cells are stimulated to enter into G_1 are as follows (4):

Chromatin—(*a*) template activity, (*b*) circular dichroism spectra, and (*c*) ethidium bromide binding.

Nuclei—(*a*) template activity, (*b*) circular dichroism spectra, (*c*) ethidium bromide binding, (*d*) acridine orange binding, and (*e*) thermal stability (decreased).

These changes have been described in several cell populations of human or rodent origin, but not in chick fibroblasts which apparently lack a G_0 (7). Thus, the choice of cells is important if we wish to study the mechanism of the transition from a cycling to a G_0 state. Incidentally, it is not too difficult to see that the entrance of eukaryotic cells into G_0 has many similarities to the sporulation of bacteria.

If G_0 exists (and two of the participants in this session will present further evidence for it), why is it important in cancer therapy? A couple of years ago we suggested that transformed cells find it more difficult to enter G_0 than normal cells (3). It is now confirmed that although normal cells in culture can enter G_0 and remain there in a viable state, transformed cells are unable to respond to nutritional restrictions with a balanced growth arrest (8). Indeed, when the nutritional restriction is severe, transformed cells die rapidly. Suppose now that these findings could be extended to in vivo situations. Two tempting speculations promptly come to our mind; first, that the G_0 state may be a fundamental difference between normal and neoplastic cells; and second, that it may be possible to cause unbalanced growth (and death) in neoplastic cells with little effect on normal cells. In any case, there are very good reasons for studying, in vitro, the basic biochemical mechanisms that regulate the entrance of cells into G_0.

[1]Department of Pathology and Fels Research Institute, Temple University Health Sciences Center, Philadelphia, Pa.

REFERENCES

1. NICOLINI C, and BASERGA R. Cell synchrony in the lining epithelium of the intestinal tract of mice. *In* Proceedings of the 2nd Symposium on Pulse-Cytophotometry, Munster, European Press, 1975.
2. POVLSEN CO, and JACOBSEN GK. Chemotherapy of a human malignant melanoma transplanted in the nude mouse. Cancer Res 35:2790–2796, 1975.
3. BASERGA R, COSTLOW M, and ROVERA G. Changes in membrane function and chromatin template activity in diploid and transformed cells in culture. Fed Proc 32:2115–2118, 1973.
4. BASERGA R. Non-histone chromosomal proteins in normal and abnormal growth. Life Sci 15:1057–1071, 1974.
5. EPIFANOVA OI, and TERSKIKH V. Review article on the rest-

ing periods in the cell life cycle. Cell Tissue Kinet 2:75–93, 1969.
6. SMITH JA, and MARTIN L. Do cells cycle? Proc Natl Acad Sci USA 70:1263–1267, 1973.
7. RUBIN H, and STEINER R. Reversible alterations in the mitotic cycle of chick embryo cells in various states of growth regulation. J Cell Physiol 85:261–270, 1975.
8. BURSTIN SJ, and BASILICO C. Transformation by polyoma virus alters expression of a cell mutation affecting cycle traverse. Proc Natl Acad Sci USA 72:2540–2544, 1975.

Use of Cell-Cycle Information in the Preparation of Drug Combinations: Results With Cytosine Arabinoside Plus Actinomycin D [1,2]

B. K. Bhuyan,* T. J. Fraser, and K. J. Day [3]

SUMMARY

Cytosine arabinoside (ara-C) plus actinomycin D acted synergistically in killing L1210 and DON cells. The time course of cell-kill by the combination was different from that seen for either drug alone. The results obtained (both with L1210 and synchronous DON cells) suggest that cells blocked in G_1/S with continuing unbalanced growth are particularly sensitive to the combined action of ara-C and actinomycin D.

[Cancer Treat Rep 60:1813–1818, 1976]

Based on our knowledge of the effects of drugs on the cell cycle (1–5), the following types of combinations could be prepared:

(*A*) A phase- and cycle-specific drug such as cytosine arabinoside (ara-C) (6) with a non-cycle-specific drug such as BCNU.

(*B*) Drugs with different phase-specific cytotoxicities. For example, ellipticine or neocarzinostatin (maximum toxicity in M and G_1) could be combined with ara-C, hydroxyurea, or vincristine (S-phase-specific drugs) (2).

(*C*) Drugs that act on the same phase but cause their cytotoxic effects through different biochemical mechanisms. For example, the S-phase-specific inhibitor ara-C (DNA polymerase inhibitor) (2) could be combined with other S-phase-specific drugs such as hydroxyurea or 5-hydroxypicolinaldehyde thiosemicarbazone (both of which inhibit ribonucleotide reductase).

(*D*) Sequential combinations in which the first drug accumulates cells in a particular phase, for example, vincristine or colcemid which accumulates cells in mitosis. The block is then released and the second drug such as ara-C (S-phase specific) is given when the cells reach S phase (7).

(*E*) A combination of drugs in which the first drug blocks cell progression in one phase of the cell cycle, for example, ara-C which blocks cells at the G_1/S border. The second drug (eg, actinomycin D) is chosen on the basis of maximum cytotoxicity to cells in G_1/S. This was the rationale on which the ara-C and actinomycin D combination was chosen.

MATERIALS AND METHODS

L1210 cell methods.—L1210 cells were maintained in culture in RPMI 1634 medium (Grand Island Biological Co, Grand Island, NY) supplemented with fetal calf serum (5%), $NaHCO_3$ (0.075% wt/vol), penicillin G (0.1 mg/ml), and streptomycin (0.05 mg/ml).

Determination of survival of L1210 cells.—Cell survival after drug exposure was determined by cloning in soft-agar medium as previously described (8). The plating efficiency of L1210 cells in these experiments ranged between 60% and 80%. The coefficient of variation in determining cell survival was about 15%, the coefficient of variation being the standard deviation expressed as a percentage of the mean. In these experiments the cell survival expected, after exposure to a combination of two drugs which acted additively and independently, was calculated by multiplying the fractional survival obtained with each drug. Synergism for a combination was defined as cell-kill greater than expected if the drugs acted additively and independently (9).

DON cell methods.—DON cells, a Chinese hamster fibroblast line (American Type Culture Collection CCL 16), were grown at 37°C in McCoy's 5A medium supplemented with lactalbumin hydrolysate (0.8 g/

[1]Supported in part by contract N01-CM-33707 from the Division of Cancer Treatment, National Cancer Institute, National Institutes of Health, Department of Health, Education, and Welfare.

[2]Cytosine arabinoside: NSC-63878; CAS reg. No. 69-74-9; cytosine, 1-β-D-arabinofuranosyl-, monohydrochloride.

Actinomycin D: NSC-3053.

[3]The Upjohn Company, Kalamazoo, Mich.

**Reprint requests to:* Dr. B. K. Bhuyan, The Upjohn Company, Kalamazoo, Mich 49001.

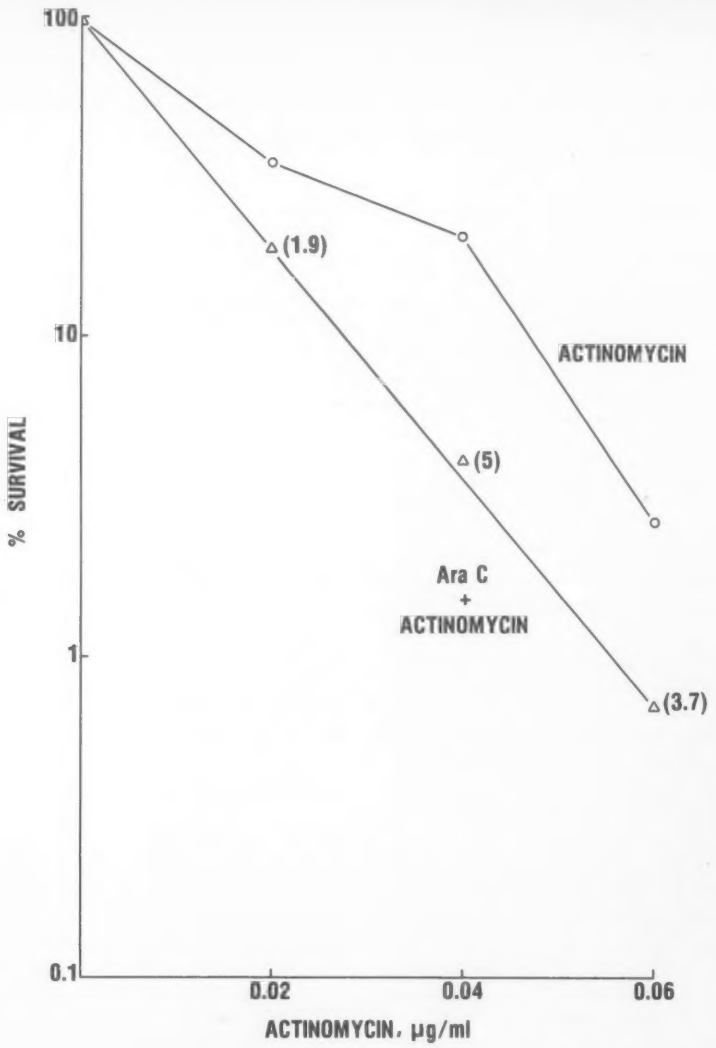

FIGURE 1.—Survival of L1210 cells exposed for 2 hrs to ara-C and actinomycin D alone or in combination. Ara-C was used at 1.2 µg/ml and was nonlethal within the 2-hr exposure. The expected survival was calculated by multiplying the fractional survival obtained with each compound. The numbers within parentheses are the ratios of expected to observed survival values and are measures of synergism.

liter) and fetal calf serum (200 ml/liter). Details of culture maintenance, cell synchronization, and determination of cell survival have been described (2). The plating efficiencies were about 50% for synchronous cells and 70%–80% for asynchronous cells. In the calculation of survival percentages the control samples were normalized to 100% survival. The coefficient of variation in determining cell survival was about 15%. Almost all cell-survival experiments were repeated and the results were found to be reproducible.

Determination of macromolecule synthesis.—Five-ml samples of L1210 cells (about 5×10^5/ml) were incubated with drug and radioactive precursor for 2 hours. After 2 hours, radioactive precursor incorporation was stopped by addition of excess unlabeled precursor. The amount of precursor incorporated was determined by filtering 2-ml aliquots of the cell suspension through Whatman glass fiber paper. The filter was washed four times with 10% cold trichloroacetic acid and once with ethanol. The filter was then placed in a scintillation vial and incubated for

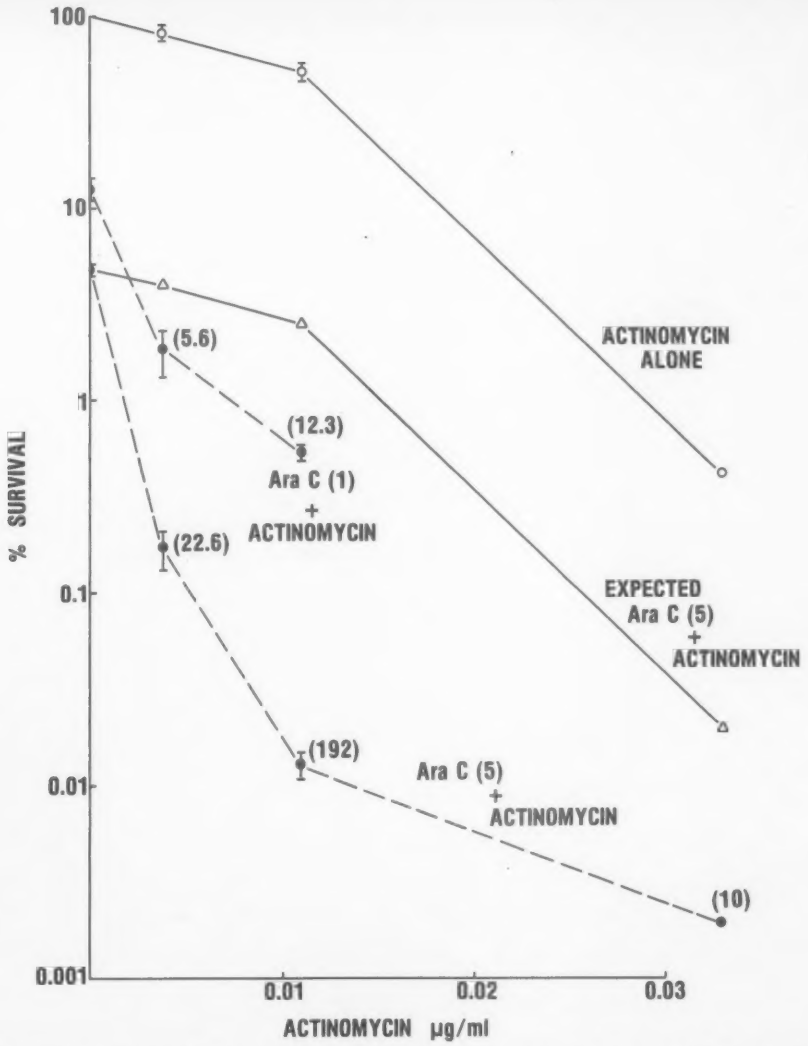

FIGURE 2.—Survival of L1210 cells exposed for 8 hrs to ara-C (5 and 1 μg/ml) and actinomycin D alone or in combination. After 8 hrs' exposure to 1 and 5 μg/ml of ara-C respectively, 12.7% and 4.9% of the cells survived. The expected (additive) survival for ara-C (5 μg/ml) plus actinomycin D was calculated (fig 1) and is a curve parallel to the dose-response curve of actinomycin D alone. The numbers within parentheses are the ratios of expected (additive) to observed survival values.

1 hour with 0.5 ml of 0.5 N perchloric acid at 70°C. Diotol (15 ml) was added and the filter was counted in a scintillation counter. The cell number was determined by counting in the Coulter Counter and the incorporation was expressed as cpm/10^6 cells.

Drug samples.—Ara-C was obtained from The Upjohn Company and was dissolved in medium prior to use. Actinomycin D was dissolved in acetone at 1 mg/ml and diluted with medium prior to use.

RESULTS

Synergistic effect of the combination on L1210 cells.—The synergistic effect of a combination can be shown most easily when one of the drugs is used at a nonlethal concentration. The results obtained when L1210 cells were exposed to a nonlethal concentration of ara-C (1.2 μg/ml) and varying concentrations of actinomycin D for 2 hours are shown in

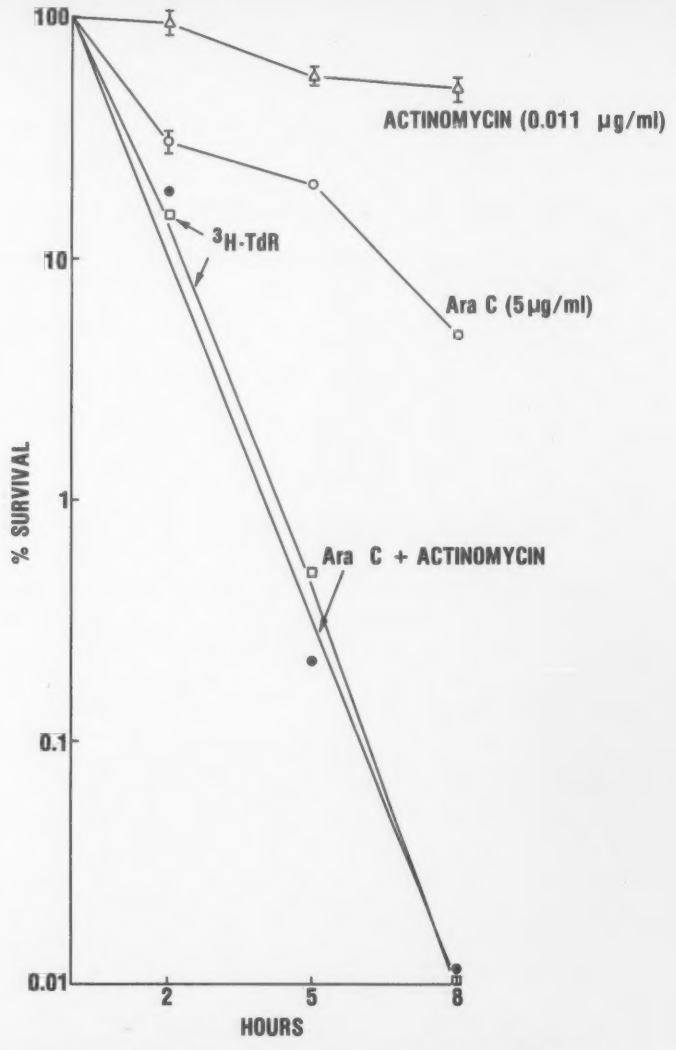

FIGURE 3.—Time-course of survival of L1210 cells exposed to ara-C (5 µg/ml) and actinomycin D alone or in combination. The survival values were compared to those obtained when cells were exposed to ^{3}H-TdR (18 curies/mmol, 10 microcuries/ml).

figure 1. These results clearly show that the cell-kill with this combination was twofold to fivefold greater than that obtained with actinomycin D alone. The results obtained when cells were exposed to a lethal concentration of ara-C (5 µg/ml) in combination with varying concentrations of actinomycin D for 8 hours are shown in figure 2. The cell-kill obtained with the combination was tenfold to 192-fold greater than that expected if the drugs had acted additively. The expected cell-kill, if the drugs act additively and independently, was obtained by multiplying the fractional survival obtained with each drug alone. Figure 3 shows the time-course of cell survival with ara-C, actinomycin D, and both drugs in combination. With ara-C the cell survival decreased rapidly during the first 2 hours due to specific killing of the S-phase cells. After that the cell-survival curve flattened out because the non-S-phase cells were blocked at the G_1/S border and therefore were not killed. After 5 hours the cells

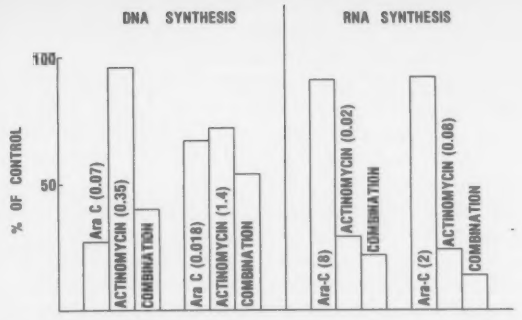

FIGURE 4.—Inhibition of DNA and RNA syntheses in L1210 cells by ara-C and actinomycin D alone and in combination. The values in parentheses show the concentration of the compounds in μg/ml. Combination refers to the combination of ara-C + actinomycin D at concentrations used in that group. The labeled compounds were added at the following levels per ml medium: ^{3}H-TdR (methyl labeled) (12.5 microcuries, 12.5 μg); 5-^{3}H-uridine (1.25 microcuries, 12.5 μg). The control cells incorporated ^{3}H-TdR into DNA and 5-^{3}H-uridine into RNA to give 5.55×10^4 and 4.97×10^4 cpm/10^6 cells respectively.

started dying rapidly again, either because of unbalanced growth or because the cells blocked at G_1/S started entering S phase and were killed. A similar effect of ara-C on cell progression has been reported using other cell lines (4,8,10). The rate of cell-kill with ara-C plus actinomycin D was the same as that seen with ^{3}H-thymidine (^{3}H-TdR) and was much greater than that for ara-C or actinomycin D alone. The rate of cell-kill with ^{3}H-TdR is a measure of the rate of progression of non-S-phase cells into S. The similar rate of cell-kill seen with ^{3}H-TdR and ara-C plus actinomycin D suggests several possibilities which are considered in the Discussion section.

Synergistic effect of the combination on DON cells.—The cell-kill of asynchronous DON cells obtained with ara-C plus actinomycin D is shown in table 1. This combination killed up to fivefold more cells than if the agents had acted additively.

Effect of the combination on synchronous DON cells.—The results obtained when ara-C or actinomycin D was added alone or when the drugs were added in combination to synchronous DON cells are shown in table 2. Ara-C and actinomycin D did not act synergistically when added to cells in G_1 or S.

TABLE 1.—Synergistic cell-kill of DON cells with ara-C + actinomycin D

Drug	Dose (μg/ml)	% survival 2 hrs	5 hrs	8 hrs
Ara-C	100	37.4	27.3	13.3
Actinomycin D	0.02	91.5	76.8	53.8
Actinomycin D	0.005	104	96.2	89.4
Ara-C + actinomycin D	100 + 0.02	18.4 (34.2,1.9)*	5.3 (21,4)*	1.4 (7.1,5.1)*
Ara-C + actinomycin D	100 + 0.005	32.9 (39.9,1.2)*	12.7 (26.3,2.1)*	3.3 (11.9,3.7)*

*The 2 numbers within parentheses are the expected % survival and the ratio of expected to observed survival. The latter value is a measure of the synergistic effect. The expected % survival is equal to the survival obtained if the drugs acted additively and independently.

TABLE 2.—Cell-kill by ara-C + actinomycin D of synchronous* DON cells

Drug	% survival during cell phase— G_1, 1–2 hrs†	G_1/S, 2–3 hrs†	S, 4–5 hrs†	G_1/S block, unbalanced growth, 0–5 hrs†
Ara-C	89	55	47	70
Actinomycin D	80	101	98	86
Ara-C + actinomycin D	79	50	45	21 (60)‡

*A synchronous culture of DON cells was obtained by planting mitotic cells (2).

†Hrs from mitosis. For example, 1–2 hrs means the drugs were added to cells at 1 hr after planting mitotic cells and the % survival was determined after a 1-hr exposure to drugs. For 0–5-hr samples the drugs were added to mitotic cells (0 hr) and exposed to drugs for 5 hrs.

‡% survival expected if the drugs acted additively.

Thus, ara-C plus actinomycin D killed approximately a similar percentage of cells as killed by ara-C alone when they were added to cells in G_1 or S. Ara-C and actinomycin D acted synergistically when they were added for 5 hours (ie, from 0 to 5 hours) to mitotic cells. When ara-C is added at 0 hour to mitotic DON cells, the cells are blocked in G_1/S and do not enter S (8). This results in a 70% survival in cells exposed to ara-C from 0 to 5 hours (ie, ara-C added to mitotic cells) compared to a 47% survival in cells exposed to ara-C for only 1 hour from 4 to 5 hours (ie, ara-C added at 4 hours to cells already in S). When the combination of ara-C and actinomycin D is added from 0 to 5 hours we see much greater cell-kill than with either drug alone. The results suggest that cells blocked in G_1/S (by ara-C added at 0 hour to mitotic cells) with continuing unbalanced growth are particularly sensitive to the combined action of ara-C and actinomycin D.

Effect on DNA and RNA synthesis.—Ara-C specifically inhibits DNA synthesis whereas actinomycin D (11) inhibits RNA synthesis to a much greater extent than DNA synthesis. We investigated whether the synergistic cell-kill by the combination would be reflected in a synergistic inhibition of DNA and RNA synthesis. The results (fig 4) show that ara-C plus actinomycin D did not inhibit total DNA and RNA synthesis to a much greater extent than the more active of the two drugs.

DISCUSSION

Our results clearly show that ara-C and actinomycin D act synergistically in killing L1210 cells. This synergistic effect was seen when either nonlethal (1.2 μg/ml of ara-C for 2 hours) or lethal (5 μg/ml of ara-C for 8 hours) levels of ara-C were combined with different concentrations of actinomycin D.

The time-course of cell-kill with ara-C plus actinomycin D was completely different from that seen with either drug alone. We are unable to explain this yet but offer the following suggestions. Cells blocked in G_1/S by ara-C undergo unbalanced growth (12). This renders the cells particularly sensitive to actinomycin D alone or combined with ara-C. The results with synchronous DON cells corroborate this possibility. Synchronous DON cells undergoing unbalanced growth (when ara-C and actinomycin D were added to mitotic cells for 5 hours) were more sensitive to the combination than to either ara-C or actinomycin D alone. Another possibility could be that, unlike ara-C alone, the combination of ara-C plus actinomycin D did not block cells at the G_1/S border. The cells proceeded normally into S and were killed by ara-C. However, other possible explanations for this synergistic effect can not be excluded. Further studies are in progress to understand this effect.

Ara-C and actinomycin D did not inhibit DNA or RNA synthesis to a much greater extent than the more effective of the two drugs. However, the correlation between inhibition of total DNA synthesis and the lethal effect of ara-C is not clear. Graham and Whitmore (10) reported that DNA synthesis could be inhibited for 14 hours by ara-C without any lethal effect. We observed similar effects with L1210 and DON cells. Chu (13) suggested that the lethality of ara-C could be correlated with its incorporation into low molecular weight RNA fractions. We have not investigated the effect of the combination on the incorporation of ara-C into RNA or DNA.

REFERENCES

1. MADOC-JONES H, and MAURO F. Site of action of cytotoxic agents in the cell life cycle. *In* Antineoplastic and Immunosuppressive Agents. Heidelberg, Springer-Verlag, 1974, vol 1, pp 205–219.
2. BHUYAN BK, SCHEIDT LG, and FRASER TJ. Cell cycle phase specificity of antitumor agents. Cancer Res 32:398–407, 1972.
3. BHUYAN BK, and FRASER TJ. Cytotoxicity of antitumor agents in a synchronous mammalian cell system. Cancer Chemother Rep 58:149–155, 1974.
4. TOBEY RA, and CRISSMAN HA. Use of flow microfluorometry in detailed analysis of effects of chemical agents on cell cycle progression. Cancer Res 32:2726–2732, 1972.
5. WHEELER GP, BOWDON BJ, ADAMSON DJ, ET AL. Comparison of effects of several inhibitors of the synthesis of nucleic acids upon the viability and progression through the cell cycle of cultured H. Ep. No. 2 cells. Cancer Res 32:2661–2669, 1972.
6. CREASEY WA. Arabinosyl cytosine. *In* Antineoplastic and Immunosuppressive Agents. Heidelberg, Springer-Verlag, 1974, vol 2, pp 232–249.
7. VADLAMUDI S, and GOLDIN A. Influence of mitotic cycle inhibitors on the antileukemic activity of cytosine arabinoside (NSC-63878) in mice bearing Leukemia L1210. Cancer Chemother Rep 55:547–555, 1971.
8. BHUYAN BK, FRASER TJ, GRAY LG, ET AL. Cell-kill kinetics of several S-phase specific drugs. Cancer Res 33:888–894, 1973.
9. VALERIOTE F, and LIN H. Synergistic interaction of anticancer agents: a cellular perspective. Cancer Chemother Rep 59:895–900, 1975.
10. GRAHAM FL, and WHITMORE G. The effect of 1-β-D-arabinofuranosyl cytosine on growth, viability and DNA synthesis of mouse cells. Cancer Res 30:2627–2635, 1970.
11. GOLDBERG IH. Actinomycin D. *In* Antineoplastic and Immunosuppressive Agents. Heidelberg, Springer-Verlag, 1974, vol 2, pp 582–589.
12. KIM JH, PEREZ AG, and DJORDJEVIC B. Studies on unbalanced growth in synchronized HeLa cells. Cancer Res 28:2443–2447, 1968.
13. CHU M. Incorporation of arabinosyl cytosine into 2–7S ribonucleic acid and cell death. Biochem Pharmacol 20:2057–2063, 1971.

Physical-Chemical Characterization of Living Cells by Laser-Flow Microfluorometry [1]

C. Nicolini,[2,*] F. Kendall,[2] C. Desaive,[2] R. Baserga,[3] B. Clarkson,[4] and J. Fried [4]

SUMMARY

A rapid method for the laser-flow microfluorometry determination of nucleic-acid content per cell is presented. A frequency distribution of fluorescence is obtained from suspensions of living cells treated with ethidium bromide directly in their own medium (or calcium-magnesium-free Hanks' balanced solution). For a fixed number of cells, a frequency distribution of fluorescence is obtained as a function of the amount of ethidium bromide progressively added to the suspension until saturation. At any ratio of added dye per unit of DNA, histograms generated from cells stained with this method give results similar to those generated after fixation and staining by the Feulgen technique, both in terms of cell-cycle phases and ploidy-level determination. The present technique requires a minimal amount of material, is instantaneous, and is conducted directly on living cells. Furthermore, dye concentration-dependence studies of mean fluorescence per cell allow determination of association constant and binding process (primary and secondary) between the intact cell and ethidium bromide. Cells which have the same amount of DNA but vary in the amount of RNA and/or chromatin conformation (like G_0 and G_1) can then be distinguished.

[Cancer Treat Rep 60:1819–1827, 1976]

The cell cycle includes a series of metabolic events which progress through four distinct phases, operationally defined as G_1, S, G_2, and M. Since the mitotic phase is the only one visually distinguishable in the cycle, until recently most of our knowledge about the cell cycle was obtained by indirect means such as autoradiography (1).

The development of flow microfluorometric techniques (2,3) for the measurement of DNA content of single cells at a high rate (> 40,000/minute) has permitted a statistical precision and sensitivity not obtainable previously. Ordinarily in these flow cytofluorographs the optical interaction of a laser beam with a single cell includes scatter and fluorescence. This has opened a new approach to cell characterization in general, and to the study of the cell cycle in particular. Computer-based mathematic techniques (4) have allowed a further and independent identification of G_1-, S-, and G_2 + M-phase cells, analyzing the fluorometric spectra of DNA distribution. However, the various methods reported to date do not go beyond the acquisition of patterns of DNA-content distribution. Detection of growth fraction, the all-or-none phenomenon of DNA synthesis (G_1-S boundary), the significance of G_0 cells, and phase-segment specificity to a given antimetabolite (with consequent effects on progression through the cycle) are a few points which are extremely important in planning chemotherapy. Determination of cell-cycle kinetics is becoming more and more important in cancer research, medical diagnosis, and therapy of malignant tumors (5,6). This communication reports the development of a new technique which can characterize, by laser-flow microfluorometry, living cells in terms not only of DNA content but also in terms of dye affinity (specifically ethidium

[1]Supported by Public Health Service grants CA-18258 and CA-12923 from the National Cancer Institute, National Institutes of Health, Department of Health, Education, and Welfare.

[2]Division of Biophysics, Department of Biophysics and Physiology, Temple University Health Science Center, Philadelphia, Pa.

[3]Department of Pathology, Temple University School of Medicine, Philadelphia, Pa.

[4]Sloan-Kettering Institute, New York, NY.

*_Reprint requests to:_ Dr. C. Nicolini, Professor of Biophysics, Department of Physiology and Biophysics, Temple University Health Science Center, Philadelphia, Pa 19140.

bromide) and of the differential binding process with the intact cell.

Differences in the chromatin of M, G_1, S, and G_2 cells have been reported both with respect to the amount of actinomycin D bound per unit of DNA (7) and to the sensitivity of chromatin to digestion by DNAse (8). These differences in the "chromosome cycle," which are visualized by light microscopy (without pulse autoradiography) only during mitosis, are resolved during interphase and the transition G_0-G_1 as well, by circular dichroism spectra and by spectropolarimetric binding studies of ethidium bromide (9–11).

A recent review (12) indicates that significant correlations exist between the structure of chromatin and the extent of cell proliferation (aging, serum stimulation, virus transformation, cell-cycle phases, etc). Chromatin, of course, refers to the diffuse interphase form of chromosome isolated from eukaryotic cells and the question remains open as to whether observed chromatin changes are reflected in the intact cell.

The technique described in this report, by studying the dye-concentration dependence of mean fluorescence per cell, is intended to detect these differences as fast and as physiologically as possible, opening new approaches to the utilization of laser-flow microfluorometry.

MATERIALS AND METHODS

Cell Lines

WI-38 cultured human diploid fibroblasts.—These cells were purchased from Flow Laboratories (Rockville, Md) and were plated in 1-liter Blake bottles (surface of 210 cm) containing 75 ml of Basal Medium Eagle supplemented with 10% calf serum, 2-mM glutamine, and 50 mg/ml of streptomycin (13). The experiments were performed when the monolayers reached confluence, 7 or 8 days after plating. Stimulation to proliferate was obtained by the addition of fresh medium containing 10% serum (9). In both cases, the medium was discarded and the cells were then removed with a rubber policeman and suspended in 10 ml of calcium-magnesium (Ca-Mg)-free Hanks' balanced solution.

HeLa cells.—These cells were cultured in suspension in Joklik-modified Eagle's Minimum Essential Spinner Medium (11) supplemented with 3.5% each of calf serum and fetal calf serum, 2-mM glutamine, and 50 mg/ml of streptomycin. They were utilized in log-phase growth and analyzed directly in the same medium in which they were growing.

Duck erythrocytes.—Heparin-treated blood of one duck provides nucleated rbcs (courtesy of G. Vidali, Rockefeller Institute, NY). Two drops of these erythrocytes were suspended in Ca-Mg-free Hanks' balanced solution.

Liver cells.—A 1-year-old albino rat was killed by ether anesthesia. The liver was perfused with cold sodium citrate (14) and then cut in several small pieces. Twenty grams of wet liver, mixed with 20 ml of 0.25-M sucrose, was transferred to a Dounce homogenizer and ten strokes of the pestle were given. The suspension was filtered once to remove clumps of cells and centrifuged twice at a low speed (200 and 100 g) for 2 minutes. The supernatant was a suspension of nuclei and intact cells.

Laser-Flow Microfluorometer

Cell fluorescence was measured on a Cytofluorograf, Model 4802 (Bio/Physics Systems, Inc, Mahopac, NY) using an argon ion laser at 488 nm. Data were stored on a Northern Model NS-602 512-channel pulse height analyzer (Tracor-Norther Scientific, Inc, Middleton, Wis) recorded on tape on a Teletype printer, Model ASR 33, and analyzed both on IBM 1800 and on CDC-6400 digital computers.

Cell Counting and DNA Content Per Cell

Cell counts were carried out with the cytofluorograph and systematically cross-checked against a standard hemocytometer. DNA content per cell was obtained from the Handbook of Biochemistry (1975). The pg/cell was consistent with the value obtained by the method of Scott et al (15), divided by the number of cells.

Modified Feulgen Staining

Preparation of cells for laser-flow microfluorometry was described by Yataganas et al (16). Cells were fixed overnight or longer in 50% methanol, hydrolyzed in 4-N HCl at room temperature, washed, stained in a 0.02% acriflavine hydrochloride solution (Allied Chemical Co, Morristown, NJ) containing 0.05-N HCl and 0.5% potassium metabisulfite, and washed twice in acid alcohol containing 0.12-N HCl in 70% ethanol. Cells were resuspended in distilled water prior to flow microfluorometry.

Our Staining

Living cells were suspended directly in the medium in which they were growing or in Ca-Mg-free Hanks' balanced solution. Ethidium bromide was then added directly to the suspension, and the cell was fed into the flow microfluorometer 5 minutes

later. The concentration of ethidium bromide was then progressively increased and, at every ratio R (μmols of added dye/μmols of total DNA present in the cell suspension), a frequency distribution of both fluorescence and light scattering was obtained. The ethidium bromide concentration was purchased from Sigma Chemical Corp (St. Louis, Mo). Solutions were prepared in distilled water at 2 mg/ml and stored at 4°C. The molar extinction coefficient of the drug was found to be 5600 at 480 nm (17).

Computer Fitting of Laser-Flow Microfluorometry Data From Log-Phased HeLa Cells

A brief description is given of the method utilized for estimating the distribution of cells among the phases of the mitotic cycle of the HeLa log phase using data from the flow microfluorometer. The method can be applied to asynchronous- or synchronous-cell populations, and is not limited to systems with low coefficients of variation of fluorescence intensity.[5] It is based on a mathematic model of the cell population having the following properties: (*a*) the population is separated into compartments, one consisting of G_1 cells, another of G_2 and M cells, and several of S-phase cells which have synthesized different specified fractions of their DNA; (*b*) the fluorescence intensity of cells in each compartment is normally distributed with the mean of the G_2+M compartment having a channel location twice that of the G_1 compartment; the S phase compartments have means at intermediate values. Coefficients of variation are the same for all compartments. The sizes of the compartments are determined by a least-squares fitting procedure utilizing the observed data.

RESULTS

Determination of Ploidy Level

Figure 1 shows the mean fluorescence per cell for a suspension of rat liver cells stained directly with ethidium bromide, as a function of the added dye per unit of DNA (R). Each fluorescence-frequency histogram from which the mean is computed (at every R) was obtained immediately after suspending the rat liver cells in Hanks' balanced solution with the given concentration of ethidium bromide. The total amount of DNA was obtained by multiplying the number of cells in suspension by the amount of DNA per cell in our rat liver cell suspension.

Identification of the diploidy (7 pg of DNA/cell) and the tetraploidy (14 pg/cell) level was obtained by fractionation of the rat liver with sucrose gradient and microphotometric analysis of each fraction (16).

Figure 2 shows the comparison between Feulgen staining and our method (at R = 1.3) on the same rat liver cell suspension. The frequency distribution of fluorescence directly from the cathodic ray tube shows the same number of cells under each peak in both methods. Even without RNase digestion and without fixation, the ploidy level can be quickly (minutes) determined in the intact cell. At any ratio of added dye per unit of DNA (R), the mean fluorescence differs by a factor of two between the two peaks (fig 1) while their separation increases with an increasing amount of dye per unit of DNA until saturation (R = 6). Our method actually shows better separation between the two ploidy levels than with the Feulgen technique.

Determination of Cell-Cycle Phases

The second question that can be raised is the capability of our method of staining the intact living cell (ie, both DNA and RNA) with ethidium bromide in determining the cell-cycle phases. In our method, HeLa S3 cells were taken from the flask in which they were exponentially growing and, after the addition of ethidium bromide (R = 1.3) they were directly fed into the laser-flow microfluorometer in their own suspension medium.

In a second case, identical amounts of HeLa cells from the same flask were treated by a modified Feulgen method (36 hours of fixation with 50% methanol).

Figure 3 shows the frequency distribution of fluorescence intensity per cell as obtained directly from the pulse height analyzer with our method (A) and with the modified Feulgen method (B). The same illustration shows the theoretic curve representing the least-squares fit of the model to the data (*see* Materials and Methods) and corresponding distribution of fluorescence intensities of the G_1 and G_2+M compartment, shown as symmetric (Gaussian) curves. The distribution of fluorescence intensities of the S-phase cell, shown in the upper portion of each diagram, is equal to the difference between the curve representing the total population and the G_1 and G_2+M components. The CV values (computed from the data) and run number are also shown for both our method (A) and the Feulgen method (B). Several runs have been carried out both by varying the fit of the model to the same set of data or by the

[5]Fried J. Presented in part at the 9th Annual Meeting of the Association for the Advancement of Medical Instrumentation, New Orleans, Apr 20, 1974. Submitted for publication.

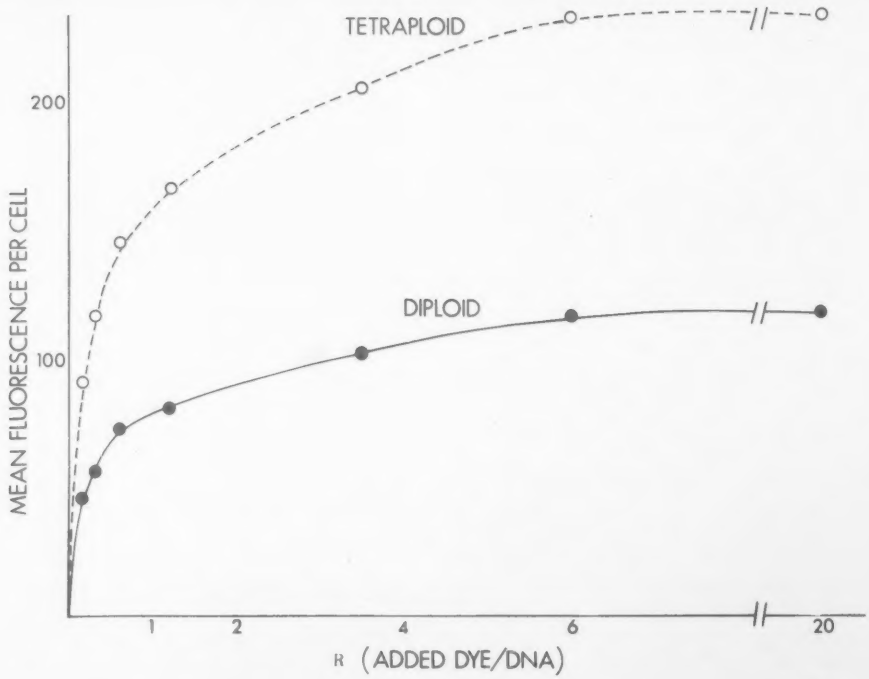

FIGURE 1.—Mean fluorescence/cell for the diploid (●——●) and the tetraploid (○---○) rat liver cells as a function of R (μmols of added ethidium bromide/μmols of DNA).

same fit to different samples from the HeLa S3 cell suspension.

Table 1 shows a comparison of the results obtained with our method and the Feulgen technique as compared with the data obtained by high-resolution autoradiography (1,11) on the same HeLa S3 cells growing in log phase; mean value and relative standard direction of each cell-cycle phase are shown (*see* table 1).

Dye-Concentration Dependence Studies

Ethidium bromide is a specific intercalating dye for nucleic acid, but while, at saturation, the number of binding sites for both DNA and double-stranded RNA are similar, the association constants are substantially different; specifically, they are much smaller for RNA (Parodi S, and Nicolini C, manuscript in preparation).

This circumstance could be used in attempting to discriminate between the two binding processes with the two macromolecules by evaluating the mean fluorescence per cell as a function of added dye. This could allow us to determine the amount of bound and free dye at any concentration of ethidium bromide. By analogy with the Scatchard plot analysis (18) we can then determine the association constant and the number of primary binding sites in the intact cell. The analysis is obviously complicated in the intact cell by the presence of fluorescence (even if reduced) arising also from outside weakly binding process of the dye with the DNA molecule itself and from the presence of mitochondrial DNA.

For this reason, we are presenting the data obtained with the laser-flow microfluorometer from a population varying both in the extent of cell proliferation and the amount of DNA and RNA.

Figure 4 shows the mean fluorescence per cell as a function of the ratio R of added dye per unit of DNA from WI-38 human fibroblasts confluent (G_0), mature duck erythrocytes (G_0), and HeLa S3 cells in G_1 and G_2 phase. These curves show that, at saturation, the mean fluorescence per cell reaches a plateau value which is directly related to the amount of DNA per cell: 7.0 pg for WI-38 human fibroblasts, 10.3 pg for G_1 HeLa cells, and 20.6 pg for G_2 HeLa cells.

The exception is constituted by mature duck erythrocytes (2.65 pg/cell) which do not have any sizable amount of RNA: (*a*) the saturation occurs at

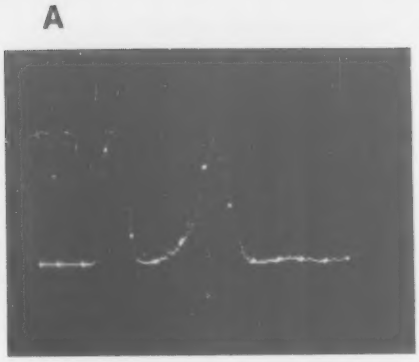

FIGURE 2.—Frequency distribution of fluorescence intensity/cell as obtained directly from pulse height analyzer with: (A) upper panel.—intact rat liver cell (1 year old) suspended directly with ethidium bromide, at R (added dye/DNA) = 1.3, and fed directly into the cytofluorograph (our method). (B) lower panel.—same rat liver cell population treated with the Feulgen method (mixed with 50% methanol for 36 hrs and stained with acriflavine).

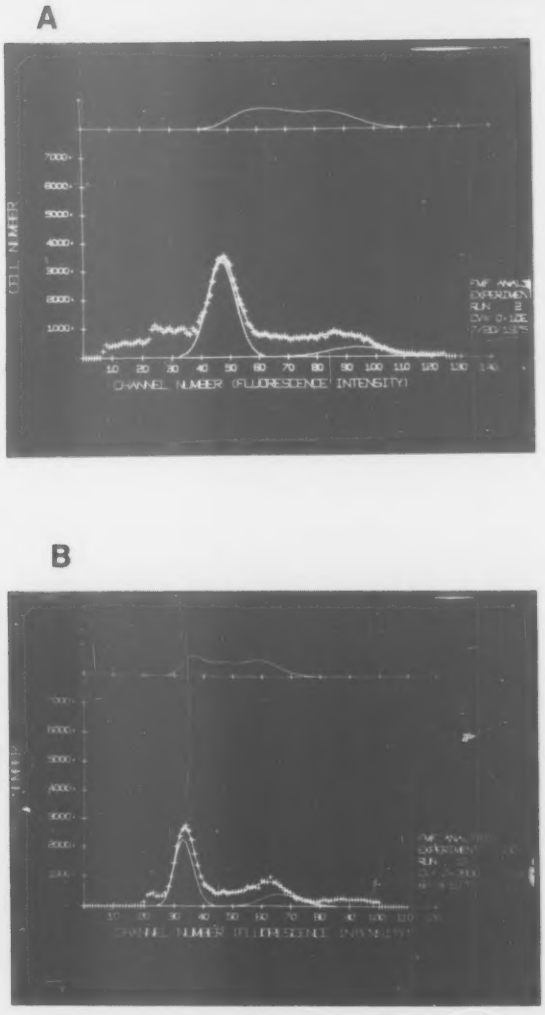

FIGURE 3.—Frequency distribution of fluorescence intensity/cell (++) as obtained directly from the pulse height analyzer with: (A) living HeLa cell suspension dyed with ethidium bromide at R = 1.3. Amount of DNA was computed by multiplying the No. of cells in suspension (> 200,000) by the mean amount of DNA HeLa cell in log phase (14 pg/cell). (B) same HeLa S3 population fixed for 36 hrs in 50% methanol, stained with 0.02% acriflavine hydrochloride, and suspended in distilled water (16). Other details are given in the text regarding the best fitted cell-cycle phases distribution (——).

TABLE 1.—Fraction of cells in each phase of the cell cycle for HeLa S3 cells (means and SDs)

Phase	Autoradiography (%)	Laser microfluorometer: Feulgen (%)	Laser microfluorometer: our method (%)
G_1	46.3±10	44.0±4	50.1±4
S	37.7±5	40.1±7	38.0±4
G_2+M	16.0±4	16.0±4	11.9±5

a lower R (0.5–0.6), and (*b*) the ratio of the mean fluorescence per WI-38/erythrocytes (or HeLa/erythrocytes) is, at saturation ($R \geq 3.0$), larger than what would be expected from a pure DNA content ratio.

In all other cell lines, the ratio of observed mean fluorescence, at saturation, corresponds closely to the expected value from pure DNA content per cell, perhaps because in these examples the increase in RNA closely parallels the increase in DNA content per cell.

Under our experimental conditions, the chromosomes maintain their conformation intact, such that mainly at low R (< 1.0), a variation in conformation could be reflected in variation of fluorescence per cell. This further complicates the interpretation of the results which are already complex because of the presence of RNA and outside weak binding process, but enhances the potentiality of the method in detecting differences otherwise undetectable in terms of pure DNA content.

By analogy with Scatchard plot analysis (18), we attempted to evaluate the association constant between the dye and the intact cell, and the relative number of binding sites available to the dye in the intact cell (both primary and secondary with DNA and RNA). Utilizing the observed intensity of mean fluorescence at very low dye concentrations ($R \leq 0.20$) where all ethidium bromide added can be considered bound, we obtained for each given cell a function which gives the expected value (E) for the

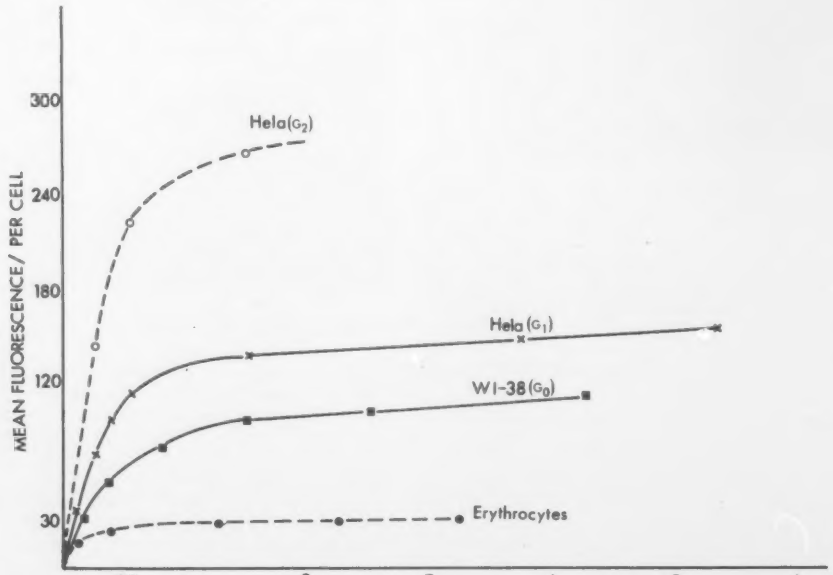

FIGURE 4.—Mean fluorescence/cell as a function of R (added dye/DNA) from duck erythrocytes (●---●) and WI-38 human fibroblasts confluent (■——■). HeLa cells in G_1 (×——×) and G_2 phase (○---○). The assignment of cell-cycle phase for HeLa cells was obtained from the frequency distribution of fluorescence/cell from a log phase growing in suspension. The so-called "G_2" cell population also presumably contains M-phase cells.

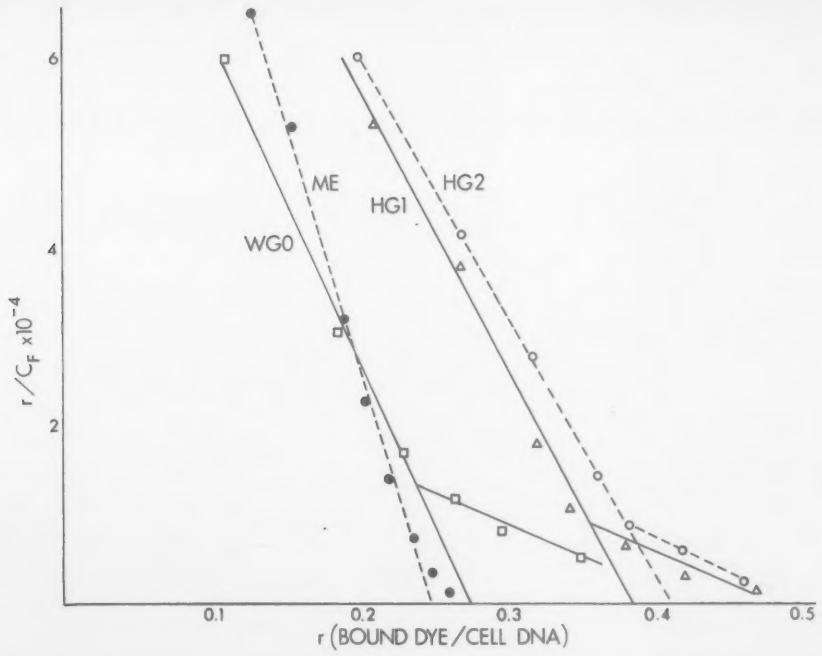

FIGURE 5.—r/C_F vs r (bound dye/DNA) for the binding process between the intact living cell and the ethidium bromide from mature duck erythrocytes (ME, ●---●), WI-38 confluent (G_0, □---□), HeLa in G_1 phase (HG_1, △---△) and G_2 phase (HG_2, ○---○).

mean fluorescence per cell versus the μmols of added dye/μmols of DNA (in a given cell), if all dyes added should bind to the nucleic acid. These functions are:

E_E = 100 R for duck mature erythrocytes.
E_W = 240 R for WI-38 human fibroblasts.
E_{HG_1} = 331 R for HeLa cells in G_1 phase.
E_{HG_2} = 652 R for HeLa cells in G_2 phase.

The ratio (r) of μmols of bound dye/μmols of DNA (in a given cell) is obtained by

$$r = R\,(OB/E)$$

where OB and E are respectively the observed and expected mean fluorescence per cell at a given R (*added* dye/DNA).

The amount (μmols) of free dye (C_F) per DNA, normalized to 100 μmols of DNA for a given cell population, is then given by

$$C_F = \frac{(E - OB)}{E} \times 100\ R.$$

Figure 5 shows the plot of r/C_F vs r (bound dye/DNA), computed as previously indicated, for the same cell lines (erythrocytes, WI-38 in G_0, HeLa in G_1, HeLa in G_2) whose mean fluorescence per cell as a function of R (added dye/DNA) is shown in figure 4.

Figure 5 shows that mature duck erythrocytes and confluent WI-38 human fibroblasts have approximately the same number of primary binding sites available (even if the amount of DNA per cell differs by a factor of 2.6), while the number of primary binding sites for HeLa G_1 and HeLa G_2 cells are also very similar (regardless of the two-factor difference in DNA content), but are substantially increased with respect to the WI-38 (G_0) and mature duck erythrocytes. The relative association constant K can be obtained by

$$\frac{r}{C_F} = K\,(n-r)$$

where (n) is the abscissa intercept and represents the number of binding sites (in the intact cell) per DNA phosphate, (r) is the ratio of bound dye per DNA phosphate, and C_F is the concentration of free dye in μmols.

It seems important to emphasize that mature duck erythrocytes, which have little RNA, present only two minor deviations (maybe due to outside

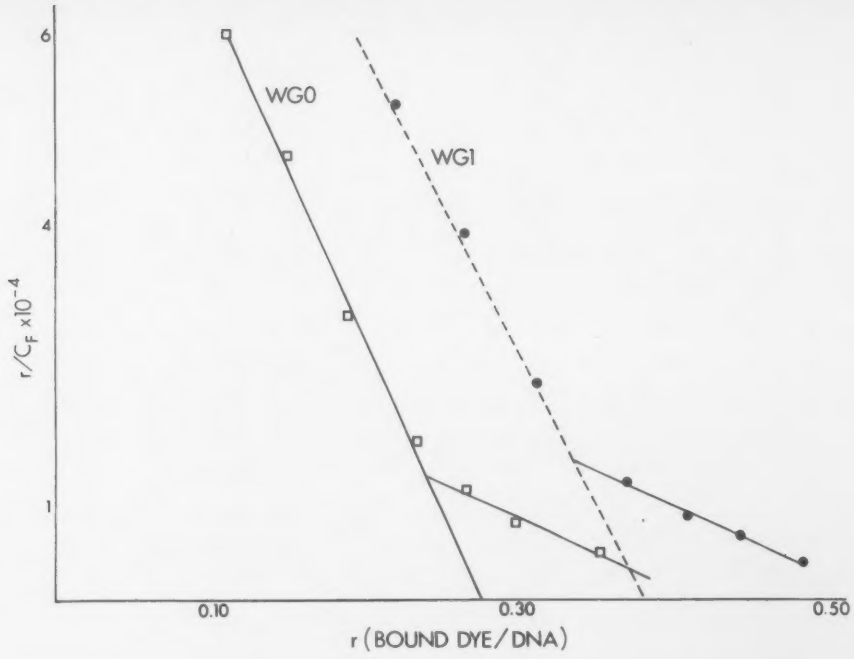

FIGURE 6.—Same as fig 5 except for WI-38 confluent (G_0, □---□) and stimulated to proliferate (WG_1, ●---●).

weakly bound dye to the DNA) from the primary binding process at high concentrations of free dye, but lack the clear secondary binding process otherwise present with similar slopes in WI-38 (G_0) and HeLa (G_1 and G_2) cells.

G_0-G_1 Transition

Experiments conducted with living-cell suspensions of WI-38 stimulated to proliferate (G_1) by the laser-flow microfluorometric method show analogous results (*see* fig 6) in terms of the association constant and number of primary binding sites, like HeLa cells in G_1 phase. Details about the four experiments conducted with WI-38 confluent (G_0) and stimulated to proliferate (G_1) are given in table 2 and in a separate communication (19).

DISCUSSION

Several methods are available in the literature for pulse cytophotometric characterization of cells in addition to the common Feulgen technique, but most of them rely on cell fixation and RNase digestion (20). While this work was in progress, a direct-staining method with propidium iodide which considerably reduces the previous lengthy procedures has appeared in the literature (21). However, incubation of cells in hypotonic solution of propidium iodide, containing citrate, has been considered by

TABLE 2.—Mean fluorescence/cell 2 hrs after stimulation of WI-38 at R = 0.75 (added dye/DNA)

Experiment No.	Phase*		
	G_0	G_0+G_1	G_1
I	100	—	249 (65)
II	100	144	172 (58)
III	100	142	173 (56)
IV	100	115	141 (36)

*Nos. in parentheses indicate % of WI-38 cells which undergo the transition G_0-G_1 in each separate experiment; mean fluorescence is expressed in normalized arbitrary units.

the investigators to be an essential preliminary step for the loss of the structural ability of the plasma membrane for dye exclusion (21). Our present method further speeds up the procedure by immediate direct staining of living cells in the same medium in which they are growing (or in Hanks' balanced solution). It allows, at any fixed ratio of added dye per unit of DNA, determination with good accuracy of both ploidy level and cell-cycle phases.

Furthermore, the concentration-dependence study and the computation of free and bound ethidium bromide per DNA (for a given cell) permit analytic characterization of the various binding processes occurring between the dye and the intact cell, taking advantage of the difference in chromatin conformation and RNA synthesis, like those occurring during the G_0–G_1 transition (9,10,19).

The choice of ethidium bromide in our method is simply dictated by our previous experience with this dye at the molecular level and with isolated DNA, chromatin, and nuclei from various cell lines (9–12); other dyes could be utilized more profitably, depending on the laser-excitation wavelength.

Determination of DNA content distribution by pulse cytophotometry represents a quantitative improvement in speed and accuracy with respect to the determination of the tritiated thymidine specific activity in DNA, but qualitatively, no new parameters of the cell-cycle phase have been introduced. The G_0 phase still remains indistinguishable from G_1 phase and G_1 remains indistinguishable from early S, as does the late-S phase from G_2 and M.

A better description of the cell cycle (a finer subdivision of phases) could allow a substantial improvement in the understanding of the mechanisms of action of drugs and their effects upon cell kinetics.

The most important conceptual advance in the chemotherapy of cancer was the discovery that the biologic determinant dictating susceptibility to a given drug is the growth fraction of tumor cells, ie, the percentage of cells initiating DNA synthesis per unit of time (22,23). No methods have been available until now for the direct identification of the fraction of cells in a nonproliferative state.

Our technique, which takes advantage of changes in chromatin conformation and RNA synthesis during cell proliferation, could shed new light on cell kinetics and cancer chemotherapy in addition to performing the traditional DNA content and cell-cycle phase determination as fast and as physiologically as possible.

REFERENCES

1. BASERGA R, and MALAMUD D. Autoradiography Techniques and Application. New York, Harper and Row, 1968.
2. KAMENTSKY L. Cytology automation. *In* Advances in Biophysics and Medical Physics. New York, Academic Press, 1973, pp 83–142.
3. VANDILLA MA, TRUJILLO TT, and MULLANEY PP. Cell microfluorimetry: a method for rapid fluorescence measurement. Science 163:1213–1214, 1969.
4. DEAN A, and JETT J. Mathematical analysis of DNA distribution derived from flow microfluorometry. J Cell Biol 40:523–527, 1972.
5. TUBIANA M. The kinetics of tumor cell proliferation and radiotherapy. Br J Radiol 44:325–347, 1971.
6. BASERGA R. The Cell Cycle and Cancer. New York, Marcel Dekker, Inc, vol 1, 1971.
7. PEDERSON T, and ROBBINS E. Chromatin structure and the cell division cycle. J Cell Biol 55:322–327, 1972.
8. PEDERSON T. Chromatin structure and the cell cycle. Proc Natl Acad Sci USA 69:2224–2228, 1972.
9. NICOLINI C, and BASERGA R. Circular dichroism and ethidium bromide binding studies of chromatin from WI-38 fibroblasts stimulated to proliferate. Chem-Biol Interact 11:101–116, 1975.
10. NICOLINI C, SALLY NG, and BASERGA R. Effect of chromosomal proteins extractable with low concentrations of NaCl on chromatin structure of resting and proliferating cells. Proc Natl Acad Sci USA 72:3383–3385, 1975.
11. NICOLINI C, AJIRO K, BORUN T, ET AL. Chromatin changes during the cell cycle of HeLa cells. J Biol Chem 250:3381–3385, 1975.
12. BASERGA R, and NICOLINI C. Chromatin structure and function in proliferating cells. Biophys Biochem Acta Rev Cancer 458:109–134, 1976.
13. WIEBEL B, and BASERGA R. Early alteration in amino acid pools and protein synthesis of diploid fibroblast stimulated to synthesize DNA by addition of cells. J Cell Physiol 74:191–202, 1969.
14. JACOB ST, and BHARGAVA PNN. A new method for the preparation of liver cell suspensions. Exp Cell Res 27:453–467, 1962.
15. SCOTT JF, FRACCASTORO AP, and TAFT EB. Studies in histochemistry. I. Determination of nucleic acids in microgram amounts of tissue. J Histochem Cytochem 4:1–10, 1956.
16. YATAGANAS X, MITOMO Y, TRAGANOS F, ET AL. Evaluation of a Feulgen-type reaction in suspension using flow microfluorometry and a cell separation technique. Acta Cytol 19:71–79, 1975.
17. WARING MJ. Complex formation between ethidium bromide and nucleic acids. J Mol Biol 13:269–282, 1965.
18. SCATCHARD G. The attractions of proteins for small molecules and ions. Ann NY Acad Sci 51:660–671, 1949.
19. NICOLINI C, KENDALL F, DESAIVE C, ET AL. The G_0–G_1 transition in WI-38 cells. I. Laser flow microfluorometric studies. Exp Cell Res. In press.
20. TOBEY RA, and CRISSMAN HA. Unique technique for cell cycle analysis utilizing mithramycin and flow microfluorometry. Exp Cell Res 93:235–239, 1975.
21. KRISHAN A. Rapid flow cytofluorometric analysis of mammalian cell cycle by propidium iodide staining. J Cell Biol 66:188–193, 1975.
22. SKIPPER HE. Cancer chemotherapy is many things: G. H. A. Clowes Memorial Lecture. Cancer Res 31:1173–1180, 1971.
23. NICOLINI C. The principles and methods of cell synchronization in cancer chemotherapy. Biochem Biophys Acta 458:243–282, 1976.

Arrested and Cycling CHO Cells as a Kinetic Model: Studies With Adriamycin [1]

Robert A. Tobey,* Harry A. Crissman, and Melvin S. Oka [2,3]

SUMMARY

Adriamycin was examined for effects on survival and cell-cycle progression in exponentially growing (cycling) populations of line CHO Chinese hamster cells and in isoleucine-deficient G_1-arrested (non-cycling) cells. Cell analysis involved a technique combining flow microfluorometry, ^{3}H-thymidine autoradiography, and cell-number enumeration. On a weight basis, adriamycin was approximately 30 times more toxic for cycling cells than for non-cycling cells. Non-cycling cells which were treated for 2 hours with adriamycin and then resuspended in drug-free medium, traversed G_1 at a normal rate and were only slightly delayed in completing S and G_2; in addition, cell division capacity was only slightly affected. However, in cycling populations treated for 2 hours with adriamycin and then resuspended in drug-free medium, the cells initially in S and G_2 suffered a gross impairment in cell-cycle traverse capacity, leading to an accumulation of cells in G_2; a subpopulation of cells initially in G_1 progressed through S phase at a normal rate and were impaired in traversing G_2. Drug-treated cycling cells did not resume dividing until 16 hours after the return to drug-free medium. Polyploid cells were observed in treated, cycling cell cultures but not in treated, non-cycling populations. Cells in exponentially growing cultures exposed to adriamycin were blocked at a stage of G_2 located 72 minutes prior to prophase. Thus, from a kinetic and survival standpoint, cycling cells are far more sensitive to the effects of adriamycin than are non-cycling cells.

[Cancer Treat Rep 60:1829–1837, 1976]

Among the factors to be considered when designing therapeutic regimens is the kinetic response of surviving tumor cells following exposure of susceptible populations to one or more agents. Subsequent administration of appropriate agents which are maximally effective against the types of cells encountered in the surviving population should result in increased cell killing. We have designed a model system employing cultured cells which allows us to monitor in vitro the cell-kinetic responses of cycling and non-cycling cell populations following treatment with toxic agents (1,2). Among the advantages of our in vitro system are the ease and speed of operation along with low cost and complete cell accountability. The value of any such system obviously depends upon whether the results obtained can be utilized as predictive indicators of tumor-cell response in vivo. Although we have not yet determined unequivocally the general predictive reliability of our system, information obtained with a limited number of test compounds for which corresponding clinical data were available indicated that our system yielded results generally comparable to those obtained by others for susceptible tumor-cell populations in vivo (1,2).

In this report, we describe in detail the type of information obtainable with our system, emphasizing the response of cells to treatment with adriamycin. Adriamycin, an anthracycline antibiotic, is an interesting compound for study since it has been shown to be effective against a variety of human

[1]Supported by contract Y01-CM-10056 from the Division of Cancer Treatment (DCT), National Cancer Institute (NCI), National Institutes of Health, Department of Health, Education, and Welfare, under an interagency agreement with the US Energy Research and Development Administration.

[2]Cellular and Molecular Biology Group (Dr. Tobey) and Biophysics and Instrumentation Group (Drs. Crissman and Oka), Los Alamos Scientific Laboratory, University of California, NM.

[3]We gratefully acknowledge the excellent technical assistance of Linda Ferzoco.

*Reprint requests to: Robert A. Tobey, PhD, Los Alamos Scientific Laboratory (MS886), Los Alamos, NM 87545.

solid tumors, including adenocarcinoma of the breast, bronchogenic carcinoma, malignant sarcoma, and neuroblastoma (3).

METHODS

Line CHO Chinese hamster cells were maintained in suspension culture free of contamination with *Mycoplasma* in F-10 medium supplemented with 15% newborn calf serum, penicillin, and streptomycin. Cycling populations were derived from CHO cultures in exponential growth. Arrested populations were prepared by maintaining cells from exponentially growing cultures for 36 hours in isoleucine-deficient medium (4); such cells accumulate in G_1, remain viable, and continue synthesizing a variety of macromolecules without entering a state of gross biochemical imbalance (5). The G_1-arrested cells resumed proliferation following return to complete medium (4,5).

Survival measurements were carried out as described previously (1). Briefly, known numbers of either cycling or non-cycling cells from suspension cultures were plated in plastic tissue-culture dishes, and after 1.5 hours (to allow cells to attach) drug solutions were added. After a 2-hour exposure period, drug solutions were removed and replaced with drug-free complete medium. Plates were incubated for 7 days and were then washed, fixed, and stained (1) prior to determination of surviving colonies ($\geq$ 50 cells). Results presented represent the average of three experiments.

Cell-cycle traverse measurements were run as described previously (1). Suspension cultures of either cycling or non-cycling cells were treated with drug for 2 hours, after which the cells were placed in drug-free medium. The cell number was determined at this time (t = 0), along with an analysis of population DNA distribution by means of flow microfluorometry (FMF). The cultures were again counted 30 hours later, a sample was removed for FMF analysis, and an aliquot was pulse-labeled for 15 minutes with 2 microcuries/ml of ^{3}H-thymidine to determine the fraction of labeled cells, scored by autoradiography (ie, fraction in S phase).

Cells analyzed by FMF were resuspended directly in 25% ethanol containing 15-mM $MgCl_2$ and 100 μg/ml of the fluorescent antibiotic, mithramycin (6,7). DNA content measurements were made with the Los Alamos flow microfluorometer (8) utilizing a laser wavelength setting of 457 nm in the manner described previously (6).

Adriamycin solutions were prepared immediately prior to use by dissolving the drug in 0.9% NaCl. Methyl-^{3}H-thymidine (6 curies/mmol) was purchased from Schwarz/Mann (Orangeburg, NY). Supplies of mithramycin were generously provided by Pfizer Laboratories Division (New York, NY).

RESULTS

Figure 1 describes the survival properties of initially arrested and cycling populations following a 2-hour period of exposure to adriamycin. It is readily apparent that the initially non-cycling cells are far more resistant (approximately 30 times more resistant on a weight basis) to the toxic effects of adriamycin than are cycling cells. The order of magnitude difference in sensitivity between non-cycling and cycling cultures cannot be explained merely on the basis of the greater number of G_1 cells in the

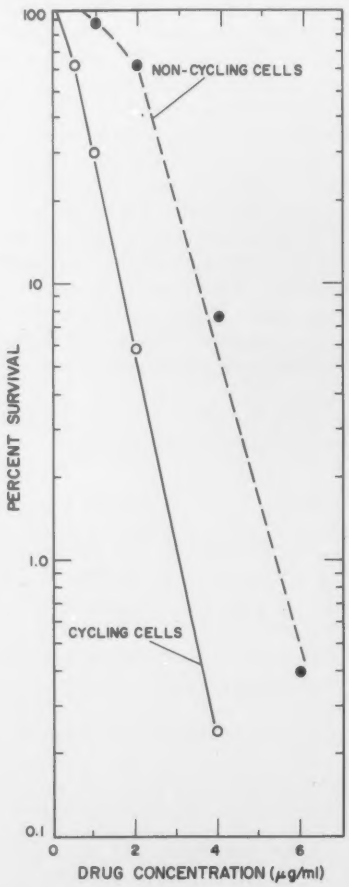

FIGURE 1.—Effects of adriamycin on survival of cycling CHO cells (–○–) and on non-cycling (G_1-arrested) cells returned to cycle following drug removal (–●–). Cells were exposed to drug for 2 hrs after which fresh drug-free medium was added back and the plates were incubated for 7 days prior to scoring the surviving colonies.

arrested population. (The studies of Kim and Kim [9], Barranco et al [10], and Drewinko and Gottlieb [11] have shown that cultured cells in G_1 are more resistant to the lethal effects of adriamycin than are cells in S phase.) As will be shown (table 1), the proportion of CHO cells in G_1 in our non-cycling cultures was approximately 95%, while the fraction of G_1 cells in our cycling populations was approximately 60%. Thus, only a twofold or less difference in survival could be attributable to the relative proportion of G_1 cells in the two populations. (The preceding argument assumes equivalent survival capacity of cells *in all parts of* G_1 which may not be the case, as will be discussed later.)

In addition to the survival measurements, the effects of adriamycin on cell-cycle progression capacity were measured (table 1). In these experiments, cells from either cycling or initially arrested cultures were treated with adriamycin for 2 hours and then restored to drug-free medium for an additional 30 hours. At that time, the cell-cycle distribution and fraction of divided cells were determined.

Examining the cycling cell populations first, it is readily apparent that, in the cultures receiving the highest doses of drug, the cell number did not increase between the time of drug removal and 30 hours later. Furthermore, there was a tendency for cells to accumulate in G_2, primarily at the expense of the complement of cells in G_1. The simplest interpretation of these results is that cell division capacity was inhibited but that ability for a portion of cells initially in G_1 to traverse to G_2 was not totally impaired. Alternatively, during the 30-hour post-treatment period with the drug, cells initially in S could have moved into G_2, with cells initially in G_1 progressing into S phase. Either of these mechanisms would result in a population enriched in the number of cells in late interphase.

In contrast, initially arrested cells exhibited a different kinetic response to treatment with adriamycin. The divided fraction relative to control was far greater than in the cycling cultures, indicating a less dramatic effect on division capacity. Furthermore, the cell-cycle redistributions were less pronounced in the treated, initially arrested cultures. Consideration of these parameters suggests that the primary effect of adriamycin on initially arrested populations is the induction of a slightly reduced capacity for cell-cycle traverse, but not a total inhibition.

To obtain a detailed picture of kinetic response, a culture of isoleucine-deficient, G_1-arrested cells was treated with 4 μg/ml of adriamycin for 2 hours; the cells were then resuspended in fresh, complete medium lacking drug. A drug-free culture served as control. At 2-hour intervals after resuspension in complete medium, aliquots were removed and the cell-cycle distributions measured via FMF analysis (fig 2). It is readily apparent that the rate of traverse of G_1 was similar in the two cultures (fig 2A)

TABLE 1.—Effect of adriamycin on CHO cell-cycle progression capacity*

Drug concentration (μg/ml)	% of cells in—				Cells dividing (%)	Cells dividing (% of control)
	G_1	S	G_2	M		
Cycling cells						
Control (t = 0)	57	26	16	1	—	—
Control (30 hrs)	62	25	10	3	160	—
1	50	25	22	3	89	56
2	42	36	20	2	36	23
4	37	36	24	3	33	21
6	24	22	52	2	31	19
8	23	24	50	3	1	1
10	21	25	52	2	1	1
Non-cycling cells						
Control (t = 0)	95	1	4	0	—	—
Control (30 hrs)	45	40	14	1	121	—
1	51	28	20	1	108	89
2	42	31	23	4	66	55
4	30	38	27	5	64	53
6	23	49	26	2	37	31
8	16	47	36	1	30	25
10	20	47	31	2	24	20

*Cultures of cycling or non-cycling cells were exposed for 2-hr periods to different concentrations of adriamycin and then resuspended in complete drug-free medium for 30 hrs. The cell No. and % of cells in each phase of the cell cycle were determined at the start and end of the experiment. Cell-cycle distributions were determined by FMF analysis utilizing the mithramycin technique (refs 6,7). (Details are given in the Methods section.)

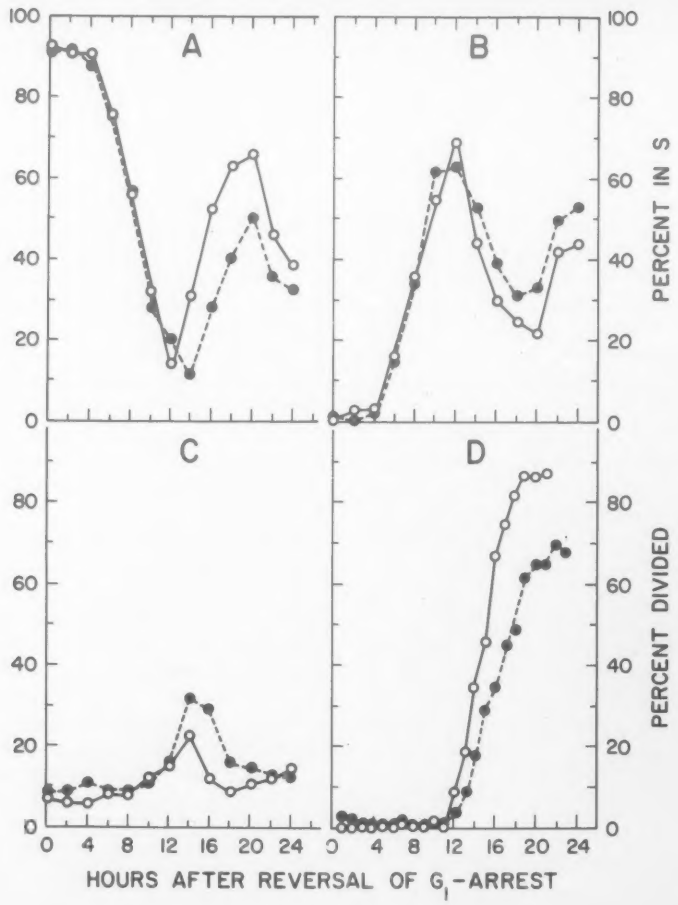

FIGURE 2.—Progression of synchronized CHO cells through the cell cycle following treatment with adriamycin. Cells arrested in G_1 by cultivation in isoleucine-deficient medium for 36 hrs (refs 4,5) were treated for a 2-hr period with 4 μg/ml of adriamycin and then returned to cycle by resuspension in fresh complete medium (–●–). An untreated culture served as control (–○–). Following return to complete medium, samples were removed for determination of the fraction of cells in each phase of the cell cycle by means of combined FMF analysis employing mithramycin (refs 6,7) and ^{3}H-thymidine autoradiography. Cell No. determinations were made with an electronic cell counter.

although the time required to complete S phase was slightly increased in the adriamycin-treated culture (fig 2B). Progression of cells through G_2 (fig 2C) introduced a further delay in the drug-treated culture, which was reflected both as a delay in the time at which the drug-treated cells divided and a reduction in the number of cells which divided during the period of analysis (fig 2D). Thus, as suggested above, only a slight impairment of cell-cycle progression capacity is introduced following treatment of G_1-arrested cells with adriamycin.

A similar experiment involving the kinetic response of exponentially growing cells treated with adriamycin, then resuspended in drug-free medium, was performed and the results are presented in figure 3. The fraction of cells in G_1 dropped rapidly during the first 4 hours, then remained essentially constant over the ensuing 12 hours (fig 3A). At t = 16 hours, the G_1 fraction slowly increased as a result of limited cell division (fig 3D). As cells moved out of G_1, the fraction of cells in S continued to increase for 4 hours, then remained constant for another 6 hours (fig 3B). Concomitantly, the fraction of G_2 cells remained essentially constant over that 10-hour time

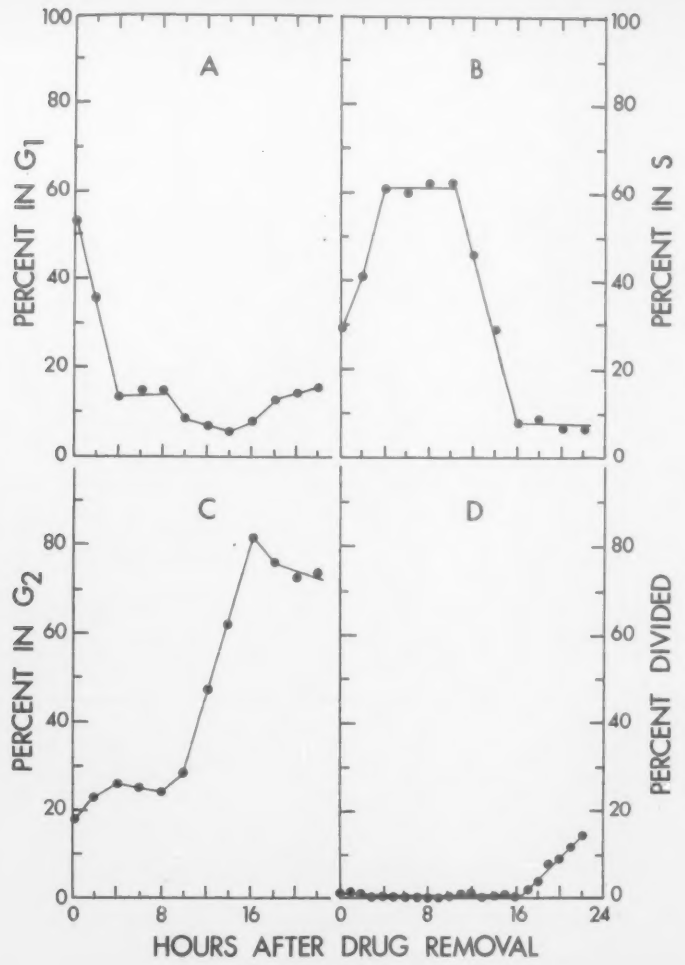

FIGURE 3.—Progression of asynchronous CHO cells through the cell cycle following treatment with adriamycin. Exponentially growing cells were treated for a 2-hr period with 2 μg/ml of adriamycin and then resuspended in fresh complete medium. Aliquots were removed and analyzed by FMF analysis and ^{3}H-thymidine autoradiography as in fig 2. The cell-cycle distributions obtained from a drug-free control culture run in parallel remained unchanged throughout the experiment (data not shown).

period (fig 3C). These results suggest the transfer of cells from G_1 into S in the absence of normal progression of S cells into G_2. After 10 hours, the S fraction declined, yielding an increase in the fraction of cells in G_2 (fig 3C). Only when the cells began dividing, commencing at t = 16 hours (fig 3D), did the G_2 fraction begin to decrease. Thus, the kinetic data suggest that cells in S and G_2 at the time of drug removal were grossly impaired in their ability to progress through the cell cycle and to divide, whereas a subfraction initially in G_1 was less strongly affected.

Examination of the primary FMF data from the experiment illustrated in figure 3 further supports the notion that a subpopulation of cells initially in G_1 was less strongly affected by adriamycin than cells in mid to late interphase. In figure 4 are presented FMF-derived population DNA distributions of exponentially growing cultures immediately after drug removal, t = 0 (fig 4A), and the same culture at different times thereafter. At t = 0 (fig 4A), the DNA distribution is similar to that of an exponentially growing culture, with the first peak (approximate scale value of 21) representing cells

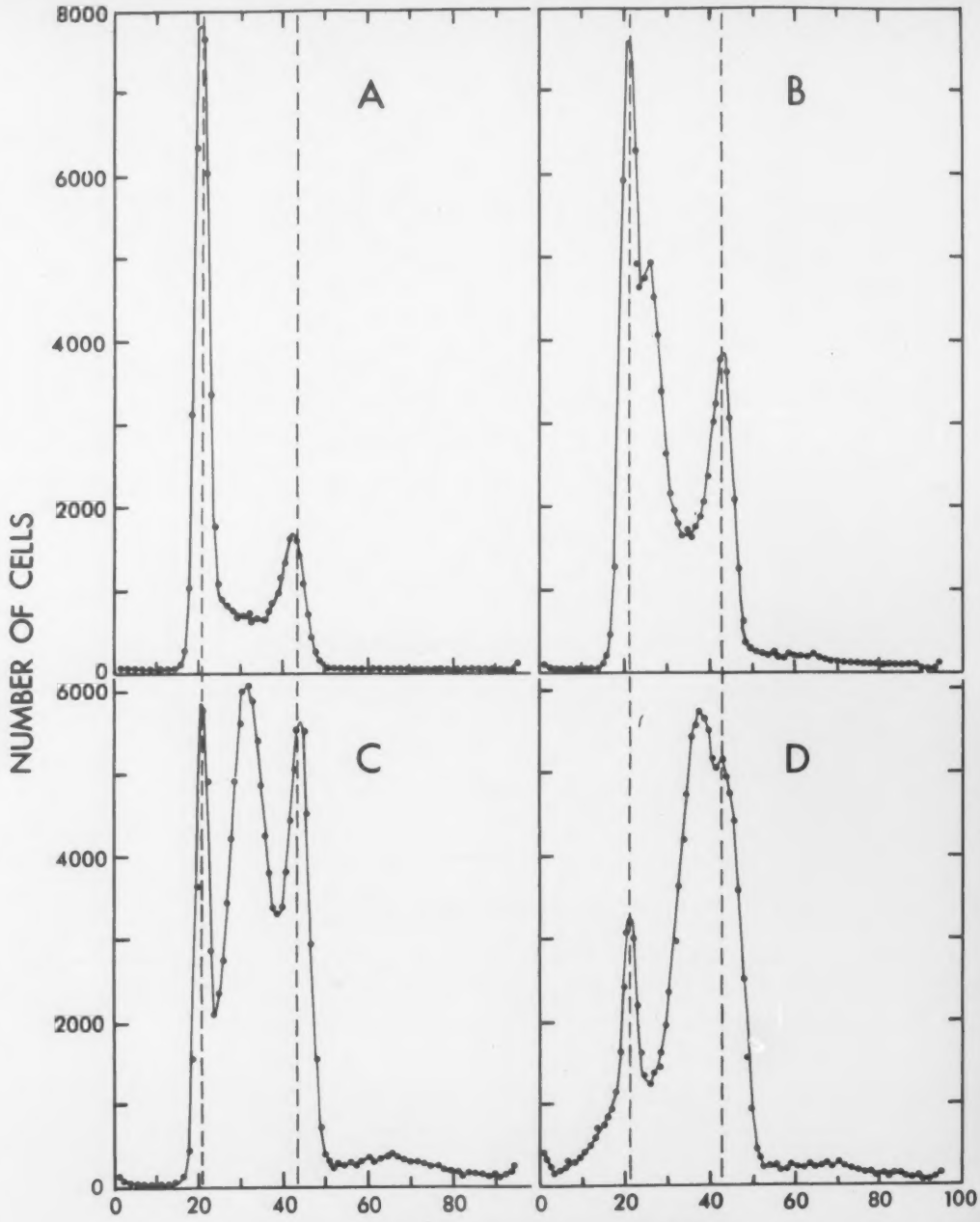

FIGURE 4.—FMF-derived DNA distributions for cultures of asynchronous CHO cells recovering from the effects of treatment with adriamycin. The culture was that described in fig 3. The FMF patterns were prepared from samples taken immediately after drug removal or t = 0 (A), and at 4 (B), 6 (C), and 8 (D) hrs after resuspension of cells in drug-free medium. The dotted line located at an approximate scale value of 21 represents the 2C (G_1) DNA content, and the line located at an approximate scale value of 42 represents the 4C (G_2 + M) DNA content. The cell-cycle distributions obtained from a drug-free control culture run in parallel (data not shown) remained unchanged throughout the entire experiment, similar in appearance to the pattern shown in (A) above.

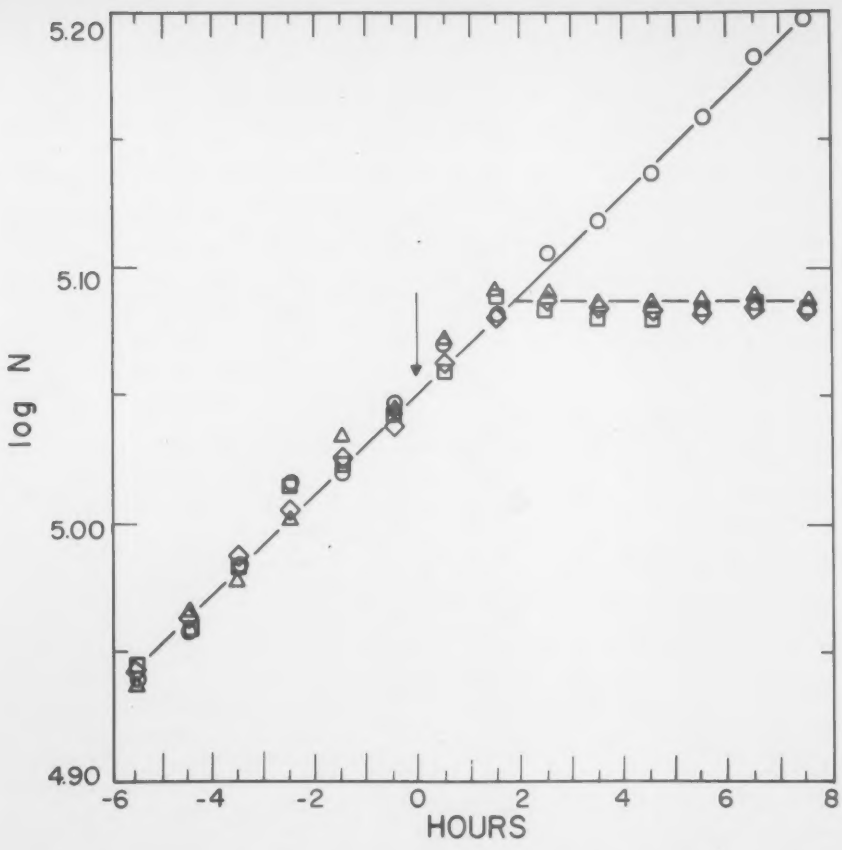

FIGURE 5.—Effect of adriamycin on cell division. An aliquot of exponentially growing CHO cells was split into 4 cultures; at t = 0, 1 of the cultures received 0.5 μg/ml of adriamycin (–◇–), another received 1.0 μg/ml of adriamycin (–□–), and a third received 2.0 μg/ml of adriamycin (–△–). The fourth culture served as the untreated control (–○–). Cell No. determinations were made with an electronic cell counter.

with a 2C or G_1 DNA content, while the second peak (approximate scale value of 42) represents cells in G_2 and M with a 4C DNA content; cells in S phase are represented by intermediate values between the major peaks. By 4 hours (fig 4B), a subpopulation of cells was seen in early S phase, detected as a shoulder on the G_1 peak. At t = 6 hours (fig 4C), the subpopulation was centered in mid-S phase, and by 8 hours (fig 4D), the moving subpopulation had progressed to late-S phase. Thus, even though the subpopulation was superimposed on the more slowly progressing remainder of cells in the culture, FMF analysis allowed visualization of progression of the interesting subpopulation through the cell cycle.

However, note that the subpopulation cells did not continue progressing through G_2 and M at the normal rate, since the first cells in the culture to divide were delayed until after t = 16 hours (fig 3D). Had the subpopulation cells experienced no delays, they should have begun dividing by t = 12 hours. Thus, cells in all stages of interphase from exponentially growing cultures treated with adriamycin exhibited at least a transitory delay in completing the final stages of the cell cycle.

Additional information is obtainable from the primary FMF data in figure 4. A small but reproducible cell fraction in populations with DNA content in excess of 4C was observed in the populations examined in figures 4B–4D. Similar results were never observed in drug-free control cultures. This phenomenon, production of polyploid cells, presumably resulted from a drug-induced inhibition of cytokinesis, but not karyokinesis. Polyploid cells were not observed in adriamycin-treated and released non-cycling populations.

The data presented in figures 3 and 4 suggest that

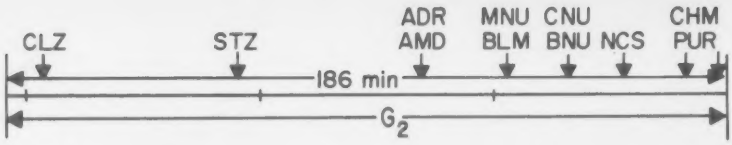

FIGURE 6.—Drug-specific arrest of progression at different stages within the G_2 phase of the cell cycle in asynchronous cultures of CHO cells. The terminal point of action was determined as in fig 5 for the following agents: CLZ = chlorozotocin; STZ = streptozotocin; ADR = adriamycin; AMD = actinomycin D; MNU = methyl-CCNU; BLM = bleomycin; CNU = CCNU; BNU = BCNU; NCS = neocarzinostatin; CHM = cycloheximide; and PUR = puromycin.

one result of treatment of exponentially growing cultures with adriamycin is an accumulation of cells somewhere in G_2. Precise localization of the terminal point of accumulation of cells in G_2 may be determined in the following manner. If adriamycin is added to an exponentially growing culture, the time between drug addition and change in growth rate is a measure of the time back in the cell cycle preceding M/G_1 (ie, cell division) at which adriamycin exerted its terminal effect. Cells beyond the terminal marker will divide in the presence of the drug, while cells at earlier stages in the cell cycle will be unable to progress at the normal rate. Figure 5 presents data obtained by treating an exponentially growing culture with different concentrations of adriamycin. Following drug addition, the cells continued dividing at the normal rate for 1.85 ± 0.1 hours, after which cell division ceased.[4]

Localization of the terminal point of action of adriamycin in G_2, along with similar values for a variety of drugs studied previously (12), are presented in figure 6. The adriamycin temporal marker is situated approximately 77 minutes before prophase, a value essentially identical to that obtained for actinomycin D.

DISCUSSION

Previous studies of both synchronous and asynchronous cycling cultures indicated that cells in S phase were most readily killed by adriamycin, with cells in G_1 much less sensitive (9–11,13). Although we have not determined the cell-cycle-specific survival kinetics, the gross reduction in cycle traverse capacity of cells in S (and early G_2), relative to those in G_1, from exponentially growing cultures of CHO cells treated with adriamycin (figs 3 and 4) supports the concept that S and G_2 cells are more severely damaged than G_1 cells.

In a recent study, Hittelman and Rao (14) reported that adriamycin treatment of cycling cell populations failed to affect progression of cells from G_1 into S phase but caused a prolongation of both S and G_2, precisely as we have found (fig 3). Barranco et al (10) found that adriamycin produced a progression delay in all stages of interphase, although the magnitude of the delay was least in the G_1/S region of the cell cycle. Therefore, the results obtained with our asynchronous populations are in generally good agreement with similar studies performed in other laboratories.

A simple mechanistic explanation for these observations may be formulated if one assumes that maximum cell damage accrues in those cells *attempting to replicate DNA while adriamycin is present in the medium.* Cells in late G_2, M, and early G_1 at the *start* of the drug treatment period will have traversed to an area of the cell cycle encompassing early to mid G_1 by the *end* of the drug exposure period; none of those cells will have passed through S phase during the period that adriamycin remained in the medium.

If one further assumes that, following drug removal, the intercalated adriamycin is removed from the genome on a time-dependent basis, then the cells situated farthest from S phase should have the greatest probability of reducing the level of intercalated adriamycin to a sub-toxic level prior to replication of DNA.

In the event that the above model is correct, the cells least damaged and, therefore, the ones posing the greatest threat as survivors are those located in very early G_1 at the time of removal of adriamycin from a cycling culture. Cells in early G_1 would represent only a very small fraction of the total cycling population at the end of the drug treatment period. In contrast, essentially all cells in the treated non-cycling culture are arrested in early G_1. The relative fraction of early-G_1 cells in treated, arrested populations might be approximately 30 times greater than the fraction found in treated, cycling cultures, thereby explaining the 30-fold difference in survival capacity between the two types of populations (fig 1). Therefore, cells in the arrested populations and cells in late G_2, M, and early G_1 from cycling populations appear to pose the greatest threat as survivors capable of bringing about tumor

[4]The cell-division data in table 1 represent observed increases in cell number after a 2-hour exposure to adriamycin, ie, the clearing out of late G_2 seen in figure 5 has already occurred before the start of the experiments described in table 1.

repopulation. On the basis of kinetic considerations, we support the suggestion by Drewinko and Gottlieb (11) that adequately spaced, multiple low-dose/short-exposure periods should yield a superior adriamycin clinical therapeutic index.

Finally, we would like to comment on the general usefulness of cultured cell systems. A useful model system must allow a variety of responses, characteristic of the manifold responses of tumor cells in vivo, if it is to be of value as a predictive guide. Consequently, in our early studies (1,2,15), we have attempted to "calibrate" our model system through use of agents with a common mode of action, as well as compounds with very dissimilar biochemical effects. For instance, the three nitrosourea derivatives, BCNU, CCNU, and methyl-CCNU, produced generally similar results (1) which were different than results obtained with streptozotocin and chlorozotocin (2) and strikingly different than results obtained with adriamycin in this report. Whereas the cycling cell populations were more resistant to the lethal effects of nitrosourea derivatives than were the arrested populations (1), the reverse was true for adriamycin-treated populations. In terms of kinetic response, non-cycling cells treated with adriamycin were only slightly affected (fig 2) while the same class of cells treated with nitrosourea derivatives accumulated in a state of G_2 arrest (1).

Comparison of the results obtained with the agents examined in our system to date suggests the possibility that different agents (or classes of agents) produce highly specific patterns of kinetic response and survival properties. Thus, *classification* of agents, as well as suggestions for *enhancing cell kill*, could conceivably arise from the type of study outlined in this report. However, much additional information must be accumulated before the value (positive or negative) of such model systems can be accurately determined. The early results, while inconclusive, encourage us to extend these studies to other agents.

LIST OF COMPOUNDS

Actinomycin D: NSC-3053
Adriamycin: NSC-123127; CAS reg. No. 23214-92-8 (supplied by Drug Research and Development Program, DCT, NCI)
BCNU: NSC-409962; CAS reg. No. 154–93–8; urea, 1,3-bis(2-chloroethyl)-1-nitroso-
Bleomycin: NSC-125066; CAS reg. No. 11056–06–7; [2,4'-bithiazole]-4-carboxylic acid, 2'-(2-aminoethyl)-, monohydrate
CCNU: NSC-79037; CAS reg. No. 13010–47–4; urea, 1-(2-chloroethyl)-3-cyclohexyl-1-nitroso-
Chlorozotocin: NSC-178248; D-glucopyranose, 2-[[[(2-chloroethyl)nitrosoamino]carbonyl]amino]-2-deoxy-
Cycloheximide: NSC-185; CAS reg. No. 7006–21–5; glutarimide, 3-[2-(3,5-dimethyl-2-oxocyclohexyl)-2-hydroxyethyl]-
Methyl-CCNU: NSC-95441; CAS reg. No. 33073–59–5; urea, 1-(2-chloroethyl)-3-(4-methylcyclohexyl)-1-nitroso-
Neocarzinostatin: NSC-157365; CAS reg. No. 4507–13–5
Puromycin: NSC-3055; CAS reg. No. 58–58–2; puromycin, dihydrochloride
Streptozotocin: NSC-85998

REFERENCES

1. TOBEY RA, and CRISSMAN HA. Comparative effects of three nitrosourea derivatives on mammalian cell cycle progression. Cancer Res 35:460–470, 1975.
2. TOBEY RA, OKA MS, and CRISSMAN HA. Differential effects of two chemotherapeutic agents, streptozotocin and chlorozotocin, on the mammalian cell cycle. Eur J Cancer 11:433–441, 1975.
3. BLUM RH, and CARTER SK. Adriamycin. A new anticancer drug with significant clinical activity. Ann Intern Med 80:249–259, 1974.
4. TOBEY RA, and LEY KD. Isoleucine-mediated regulation of genome replication in various mammalian cell lines. Cancer Res 31:46–51, 1971.
5. ENGER MD, and TOBEY RA. Effects of isoleucine deficiency on nucleic acid and protein metabolism in cultured Chinese hamster cells. Continued ribonucleic acid and protein synthesis in the absence of deoxyribonucleic acid synthesis. Biochemistry 11:269–277, 1972.
6. CRISSMAN HA, and TOBEY RA. Cell-cycle analysis in 20 minutes. Science 184:1297–1298, 1974.
7. TOBEY RA, and CRISSMAN HA. Unique techniques for cell cycle analysis utilizing mithramycin and flow microfluorometry. Exp Cell Res 93:235–239, 1975.
8. HOLM DM, and CRAM LS. An improved flow microfluorometer for rapid measurement of cell fluorescence. Exp Cell Res 80:105–110, 1973.
9. KIM SH, and KIM JH. Lethal effect of adriamycin on the division cycle of HeLa cells. Cancer Res 32:323–325, 1972.
10. BARRANCO SC, GERNER EW, BURK KH, ET AL. Survival and cell kinetics effects of adriamycin on mammalian cells. Cancer Res 33:11–16, 1973.
11. DREWINKO B, and GOTTLIEB JA. Survival kinetics of cultured human lymphoma cells exposed to adriamycin. Cancer Res 33:1141–1145, 1973.
12. TOBEY RA. Different drugs arrest cells at a number of distinct stages in G_2. Nature 254:245–247, 1975.
13. BARRANCO SC, and NOVAK JK. Survival responses of dividing and non-dividing mammalian cells after treatment with hydroxyurea, arabinosyl cytosine, or adriamycin. Cancer Res 34:1616–1618, 1974.
14. HITTELMAN WN, and RAO PN. The nature of adriamycin-induced cytotoxicity in Chinese hamster cells as revealed by premature chromosome condensation. Cancer Res 35:3027–3035, 1975.
15. TOBEY RA, and CRISSMAN HA. Use of flow microfluorometry in detailed analysis of effects of chemical agents on cell cycle progression. Cancer Res 32:2726–2732, 1972.

UNIVERSITY OF CALIFORNIA LIBRARY

Introduction to Session on Recruitment and Synchrony—In Vivo

Sven-Aage Killmann [1]

If neoplastic cells proliferated much more quickly than normal cells and had a growth fraction of 1, as in some animal systems, cytocidal therapy should be easy, expedient, and without many side effects on normal proliferating tissues. However, growth of human neoplasms differs radically from these premises, and in fact it is surprising that some progress has been made in cancer chemotherapy, considering that the basic philosophy behind the treatment is wrong. In fact, and based on rather good arguments, it has rather recently emphatically been stated that cell kinetics has nothing to do with the strategy of cancer chemotherapy (1). Kineticists, on the other hand, have been well aware that cell kinetics is only one aspect of the problem but have warned that cytokinetically determined drug-to-drug interaction must be considered in multiple-drug treatment (2) after the kinetic effects of single, pharmacologic doses of drugs were made known.

Several drugs arrest cells in S phase, and a starting point for some workers has been whether the ^{3}H-thymidine labeling index (LI) or thymidine incorporation had any predictive value in acute leukemia with respect to remission induction. Some workers (3–6) have demonstrated a relationship between the height of the initial LI or total thymidine incorporation and clinical response, whereas others have not observed this (6–9). In other reports, two parameters (LI plus cytosine arabinoside[2] [ara-C] uptake) were found necessary to predict with some certainty the clinical outcome of regimens including ara-C therapy (10). It has also been suggested that alterations of the LI or thymidine incorporation shortly (3,6–8) or as late as 3 weeks after the start of treatment (11) were correlated with clinical response. In general, the series are too small and treatment schedules are too varied to allow any definite conclusions at this time, although it appears that the LI is far from being the alpha or omega in this matter.

A main stumbling block in the treatment of human neoplasia is the large fraction of the tumor cell population which is in a resting phase (G_0 or very long G_1) but may re-enter active cycle; while they are in the quiescent state they may be quite or totally insensitive to several of the most efficient cell-cycle-active drugs available. Attempts have been made to induce these cells to re-enter active cell cycle (recruitment) and thus make them sensitive to our most potent drugs. Recruitment and synchronization are rather easily achieved in vitro (12); in this session, it will be demonstrated by Hartmann et al (13) that such resting cells which re-enter cycle may be positioned both in G_1 and in G_2. Recruitment is more difficult to prove in vivo, eg, suggestive but not definite evidence in acute lymphocytic leukemia has been presented (14,15). Mauer (9) presents more data along this line in his report, whereas the data of Vogler et al (7) are not very encouraging.

Synchronization is often defined as a shift of cells from one part of the cell cycle to another. In fact, this only means an accumulation of cells in a certain phase, perhaps even with a wider time distribution of cells in that phase than in the unmanipulated state. This may not be of much practical importance. The approach becomes practically interesting only if cells are "telescoped" within a phase and then released as a quasi-cohort to a subsequent phase where they can be hit by another drug which is active in that phase. If cells die in the accumulation phase one has just plain cell death, and in that case the word "synchronization" may be misleading at least for the purpose of therapy aimed at hitting cells in subsequent cycle phases. The proof of synchronization is that after a possible release from the arrested phase, the cell flux through the following phase increases above baseline values. This is often difficult to demonstrate in man.

Synchronization has been obtained in vivo (eg, by hydroxyurea, vincristine [VCR],[3] and ara-C) both in animals where it may increase therapeutic efficiency (16–20) and in man (14–16), but often the degree of synchronization in man is marginal (14,15). Cells may behave differently towards synchronization attempts, thus lymphoblasts seem more manipulable than myeloblasts (14,21) and normal red cell precursors appear very sensitive, in contrast to normal neutrophil precursors (14). This

[1]Division of Hematology, Department of Medicine A, Rigshospitalet, University Hospital of Copenhagen, Denmark.

[2]Cytosine arabinoside: NSC-63878; CAS reg. No. 69–74–9; cytosine, 1-β-D-arabinofuranosyl-, monohydrochloride.

[3]Hydroxyurea: NSC-32065; CAS reg. No. 127–07–1.

Vincristine: NSC-67574; CAS reg. No. 2068–78–2; leurocristine, sulfate (1:1).

touches upon another important point although it is self-explanatory: possible recruitment and synchronization of neoplastic cells are only helpful if normal target cells are not affected to the same degree (2,22).

I would next like to direct your attention to how recruitment and synchronization are usually measured: this is largely done by determining LI and mitotic index (MI) before and after a drug has been applied to a cell system. However, these are basically static parameters. If t_S or t_M change, the corresponding index may become misleading. As already stated, the real criteria must be measures of cell fluxes. A simple but crude way which can be used in man is an injection of VCR and an estimation of cell flux into M phase if one wants to study release from G_2 and/or S (23). Other methods may also prove to be useful (16). An even simpler but maybe still useful way when studying synchronization in S is to follow the MI. If this index rises above the baseline value it is an argument in favor of a rather sudden release from G_2/S, assuming t_M has not been prolonged. Average t_M may be prolonged after several ara-C doses (24). A marked rise in LI with an unchanged MI suggests cell death between S and M. This is the situation encountered in chronic myelocytic leukemia myeloblasts after repeated ara-C doses (25).

Finally, I would like to draw attention to what might be called "uptake phase" and "effector phase" of a cytocidal drug. This is probably realized for a drug like VCR but also holds true for other agents. Thus, ara-C is generally referred to as a pure S-blocking agent. Although this is true, it is probably often not recognized that ara-C is taken up by many pre-S cells and may reveal its damage to the cell only later as shown by reduced leucine incorporation 96 hours after a single dose of ara-C (21) and the late depression of the growth of acute myelocytic leukemia cells in agar.[4]

REFERENCES

1. HALL TC. Limited role of cell kinetics in clinical cancer chemotherapy. Natl Cancer Inst Monogr 34:15–17, 1971.
2. KILLMANN S-A, and ERNST P. An analysis of the relationship of leukemic cell kinetics to chemotherapy. *In* Unifying Concepts of Leukemia (Dutcher RM, and Chieco-Bianchi L, eds). Basel, Karger, 1973, p 1037.
3. ZITTOUN R, BOUCHARD M, FACQUET-DANIS J, ET AL. Incorporation "in vitro" de la thymidine tritiée dans la leucémie aiguë et résponse a la chimiothérapie. Nouv Rev Fr Hematol 15:19–30, 1975.
4. HUBER H, HUBER C, MICHLMAYR G, ET AL. In-vitro proliferation leukämischer Blasten und Ansprechen aug Daunorubidomyzin/Cytosin-Arabinosid. Schweiz Med Wochenschr 101:1785–1787, 1971.
5. SCHMID JR, KIELY JM, TAUXE WN, ET AL. Cell proliferation during relapse and remission. I. DNA and RNA synthesis of leukemic cells in the bone marrow in vitro. Acta Haematol 36:312–322, 1966.
6. VOGLER WR, COOPER LE, and GROTH DP. Correlation of cytosine arabinoside-induced increment in growth fraction of leukemic blast cells with clinical response. Cancer 33:603–610, 1974.
7. VOGLER WR, KREMER WB, KNOSPE WH, ET AL. Synchronization with phase-specific agents in leukemia and correlation with clinical response to chemotherapy. Cancer Treat Rep 60:1845–1859, 1976.
8. BURNS CP, ARMENTROUT SA, and STJERNHOLM RL. Prediction of the response of patients with acute non-lymphocytic leukemia to cytosine arabinoside (NSC-63878) therapy. Cancer Chemother Rep 56:527–534, 1972.
9. MAUER AM. Evidence for recruitment and synchronization in leukemia and solid tumors. Cancer Treat Rep 60:000–000, 1976.
10. BURKE PJ, and OWENS AH. Attempted recruitment of leukemic myeloblasts to proliferative activity by sequential drug treatment. Cancer 28:830–836, 1971.
11. CHEUNG WH, RAI KR, and SAWITSKY A. Characteristics of cell proliferation in acute leukemia. Cancer Res 32:939–942, 1972.
12. NIAS AHW, and FOX M. Synchronization of mammalian cells with respect to the mitotic cycle. Cell Tissue Kinet 4:375–398, 1971.
13. HARTMANN NR, DOMBERNOWSKY P, and BICHEL P. Resting cells in L1210 and JB-1 ascites tumors with special emphasis on recycling. Cancer Treat Rep 60:1861–1870, 1976.
14. LAMPKIN BC, NAGAO T, and MAUER AM. Synchronization and recruitment in acute leukemia. J Clin Invest 50:2204–2214, 1971.
15. LAMPKIN BC, MCWILLIAMS NB, and MAUER AM. Cell kinetics and chemotherapy in acute leukemia. Semin Hematol 9:211–223, 1972.
16. KLEIN HO, LENNARTZ KJ, GROSS R, ET AL. In-vivo- und in-vitro Untersuchungen zur Zellkinetik und Synchronisation menschlicher Tumorzellen. Dtsch Med Wochenschr 97:1273–1282, 1972.
17. KLEIN HO. Synchronization of tumor cell proliferation and the timing of cytostatic drugs. Rev Eur Etudes Clin Biol 17:835–838, 1972.
18. KLEIN HO, and LENNARTZ KJ. Chemotherapy after synchronization of tumor cells. Semin Hematol 11:203–227, 1974.
19. KLEIN HO, LENNARTZ KJ, HABICHT W, ET AL. Synchronisation con Ehrlich-Ascites-Tumorzellen und ihre Bedeutung bei der Anwendung eines alkylierenden Cytostaticum. Klin Wochenschr 48:1001–1005, 1970.
20. RAJEWSKY MF. Influence of drugs on the metabolism of normal and leukemic leukocytes. *In* Erythrocytes (Gerlach et al, eds) (Proceedings of the 2nd International Symposium, Vienna, 1972). Stuttgart, E. Deutsch, 1973, p 460.
21. LANGE WANTZIN G, KARLE H, and KILLMANN S-A. Cell proliferation and protein synthesis parameters of human leukaemic myeloblasts after cytosine arabinoside. Br J Haematol 32:283–289, 1976.
22. VAN PUTTEN LM. Are cell kinetics data relevant for the design of tumour chemotherapy schedules? Cell Tissue Kinet 7:493–504, 1974.
23. ERNST P, and KILLMANN S-A. Perturbation of generation cycle of human leukemic myeloblasts in vivo by methotrexate. Blood 38:689–705, 1971.
24. BACCARANI M, ET AL. Leukemia Res, 1977. In press.
25. BACCARANI M, SANTUCCI AM, TURA S, ET AL. Arabinosyl cytosine in chronic myeloid leukemia: evidence for high cytokinetic sensitivity of myeloblasts. Scand J Haematol 16:335–352, 1976.

[4]Müller-Bérat CN. Effects of cytosine arabinoside on growth of human leukemic myeloblasts in agar. Manuscript in preparation.

Evidence for Recruitment and Synchronization in Leukemia and Solid Tumors [1]

Alvin M. Mauer,* Sharon B. Murphy, and F. Ann Hayes [2]

SUMMARY

In malignant cell populations which are sensitive to drug therapy it does not seem necessary to potentiate treatment with perturbation of the proliferative characteristics. However, in some relatively drug-resistant populations significant advantages can be obtained by recruiting resting cells into the drug-sensitive cell cycle. Further studies of growth-regulatory mechanisms for malignant cell populations may help a great deal in designing better methods of recruiting the resting cells back into active cell division. Synchronization of the dividing cells in a specifically drug-sensitive phase of the cell cycle is another method of potentiating chemotherapeutic effectiveness in relatively drug-resistant cell populations. The biochemical changes induced by sequential drug administration may be equally important in sensitizing the malignant cell to subsequent drug administration.

[Cancer Treat Rep 60:1841–1844, 1976]

A chemotherapeutic advantage for the treatment of leukemia and other forms of cancer has been proposed for recruitment and synchronization of the malignant cell populations. The proposal is based on several assumptions. First, most chemotherapeutic agents are maximally effective during some phase of the cell cycle; therefore, resting cells not in the malignant cell growth fraction would be relatively resistant to drug effect. Second, it is important to demonstrate that the resting cells indeed retain their capacity for returning to active cell division and are, therefore, important to the therapeutic strategy. And third, the resting cells must be demonstrably perturbable by some method so that their return to active cell division, where they will be more drug sensitive, can be assured. Finally, all of this perturbation of the malignant cell population must be done in a manner that will not increase the sensitivity of the normal cells to the drug effect.

Recruitment is defined here as an accelerated return of resting cells into cell division. Synchronization will be the increase of the proportion of cells in cell division in one phase of the cell cycle. In the steady state, cells in the cell cycle are distributed in various phases according to the proportional length of the phase in relationship to the total cell-cycle time. Increase in the proportion of cells in one phase is usually accomplished in the patient by a drug-induced temporary delay in passage through one phase or another of cell division. The usual purpose of synchronization is to accumulate an increased number of cells in a specific drug-sensitive phase of the cell cycle for subsequent administration of another active drug.

FUNCTIONAL SIGNIFICANCE OF THE RESTING CELL

A critical question which arose early in the studies of proliferative activity in human acute leukemia was the nature of the cell in the leukemic population which was apparently out of cycle and not participating in cell division. The essence of the question about this cell, which was characterized morphologically by being small with dense nuclear chromatin, was whether it was an end-stage cell destined to die and, therefore, of no significance, or

[1]Supported by Public Health Service grants CA-08480, CA-05176, CA-08151, and CA-15956 (National Cancer Institute) and a General Research Support grant RR-05584 from the National Institutes of Health, Department of Health, Education, and Welfare, and by the ALSAC.

[2]St. Jude Children's Research Hospital, Memphis, Tenn.

Reprint requests to: Alvin M. Mauer, MD, Medical Director, St. Jude Children's Research Hospital, PO Box 318, Memphis, Tenn 38101.

if this cell was simply temporarily out of phase (in G_0) and under appropriate conditions could return to active cell division.

This question was answered under two conditions in publications appearing in 1969 (1,2). In the first study (1), it was demonstrated that under steady state conditions there was a continued flow of cells between the proliferating and resting compartments in acute lymphoblastic leukemia. In the second study, it was demonstrated that, by chemotherapeutic perturbation, resting cells could be recalled into active cell division (2). These studies were a foundation for further attempts at potentiating chemotherapeutic effectiveness by increasing the proportion of cells in the relatively more drug-sensitive phase of cell division.

RELATIONSHIP OF INITIAL GROWTH FRACTION TO PROGNOSIS

A preliminary consideration to attempts at cell recruitment would be the relationship of the initial size of the growth fraction to therapeutic responsiveness. If the dividing cell is more responsive to treatment, then it might be assumed that the larger the initial growth fraction at the time of starting therapy, the better the response to treatment. Preliminary observations are available in 96 children with acute leukemia (76 acute lymphoblastic leukemia and 20 acute myeloblastic leukemia) in whom initial determinations of bone marrow labeling and mitotic indices were obtained for the leukemic cell population.[3] These studies have not been underway for a sufficient period of time for complete correlations of initial proliferative activity and subsequent clinical course. However, at this time there have been as yet no significant correlations between the initial proliferative activity of the bone marrow leukemic population and subsequent response to therapy.

As has been mentioned, the resting-cell population is characterized by the morphologic appearance of a small cell with dense nuclear chromatin. Therefore, another measure of the size of the growth fraction is the proportion of larger cells with finer nuclear chromatin (3). Recently, evidence has been published that a correlation between the proportion of large leukemic blast cells and subsequent response to therapy can be demonstrated (4). The series of patients, however, was small and not treated in similar fashion. Because of the possible implications of this study for a correlation between treatment response and initial proliferative activity, a similar study was undertaken at the St. Jude Children's Research Hospital (5). In this study, patients were all treated similarly and were divided into two groups based on the proportion of larger leukemic cells in the bone marrow at the time of diagnosis. No relationship between the initial proportion of larger cells and subsequent clinical course could be demonstrated.

Perhaps one reason that there is not a good relationship between the initial proliferative activity and chemotherapy responsiveness in acute lymphoblastic leukemia is because of the relative sensitivity of the whole population to available drugs. Another reason, however, might be that the size of the growth fraction is not static and variability can be demonstrated in the same patient during different phases of his disease (3). In fact, the evidence suggests that the leukemic cell population is under growth-regulatory mechanisms similar to those governing a population of cells growing in tissue culture (6). Therefore, the greater the density of a malignant cell population, the smaller the growth fraction that would be expected.

RECRUITMENT OF RESTING CELLS BY CYTOREDUCTION

If the size of the growth fraction is determined by the total mass of malignant cells or cell density, then it might be anticipated that reduction of the cell mass would result in an increasing proportion of cells in the cell cycle. In order to test this possibility, studies have been done in children who have had neuroblastoma with bone marrow metastases (7). The protocol was designed to reduce the number of neuroblastoma cells by the administration of cyclophosphamide for 7 days. Cyclophosphamide is an effective agent for treatment of neuroblastoma and is relatively independent of the cell cycle for its effectiveness. Bone marrow samples were obtained in 11 patients before and after the administration of cyclophosphamide. In nine of these patients a significant increase in the labeling and mitotic indices occurred. At the time of maximal increase in the growth fraction, an agent which is maximally effective on the cell cycle, adriamycin, was given. Potentiation of the adriamycin effect on cells in DNA synthesis was achieved by this effective recruitment of resting cells into the cell cycle. Furthermore, it was found that there was a good correlation between the apparent effectiveness of the drugs in perturbing the balance of dividing and resting cells and the subsequent clinical response. Thus, the in vivo observations of cell kinetic patterns were predictive for clinical drug responsiveness.

[3]Murphy S. Unpublished observations.

This method of potentiating the effectiveness of cycle-dependent agents by prior cytoreduction with a cycle-independent agent would seem to have applicability to other relatively drug-resistant tumors. Of particular value in this study of neuroblastoma is the availability of tumor cells in the bone marrow which allowed for repeated sampling of the cell population. Similar studies in other solid tumors would obviously be limited if accessibility of the cells for study was lacking.

SYNCHRONIZATION OF DIVIDING CELL POPULATIONS

The simplest method of synchronizing a cell population in vivo is to temporarily delay passage through one phase of the cell cycle. Such delay has been achieved with cytosine arabinoside (8), methotrexate (8,9), and vincristine (10). Administration of a second agent at the time of the maximal increase of cells in the drug-sensitive phase of the cell cycle should provide for potentiation of the effectiveness of that drug.

The evidence for such potentiation has been presented by Lampkin and her co-workers (11). In a group of 21 patients with acute myeloblastic leukemia, she was able to induce remission in 19 patients by synchronization of the leukemic myeloblasts following an injection of cytosine arabinoside and subsequent administration of that same drug over a longer period of time when the maximal increase of cells in the drug-sensitive DNA synthesis phase of the cell cycle had been achieved. It was found in that study that there was variability from patient to patient in the time at which recovery and release of the cells from the cytosine arabinoside block had occurred. Therefore, in similar studies designed to take advantage of synchronization, it may be necessary to determine in the individual patient the characteristics of response of the malignant cell population.

SIMULTANEOUS AND SEQUENTIAL DRUG ADMINISTRATION

Not all attempts to increase therapeutic effectiveness by drug scheduling may be related to the potentiation by synchronization. Edelstein and his co-workers (12) have demonstrated that in some animal systems two drugs which act maximally on one phase of the cell cycle might be more effective if given in sequence rather than together. The proposition to support this increased effectiveness was that a greater number of cells in the sensitive phase of the cycle would be exposed to the drugs if they were given in sequence rather than together. A clinical trial of this proposition has been underway at the St. Jude Children's Research Hospital.[4] Patients failing continuation therapy for acute lymphoblastic leukemia have been randomized to receive cytosine arabinoside and methotrexate either simultaneously or sequentially (cytosine arabinoside was given followed [in 48 hours] by methotrexate). Before remission induction, preliminary cell kinetic studies have been done in order to determine the effect of the drug combination on the cell kinetic pattern of the bone marrow leukemic cells. Although the administration of cytosine arabinoside has not achieved a significant synchronization of cells in DNA synthesis at 48 hours, at which time the methotrexate has been given, the sequential method of administration has provided a median remission duration twice that of the patients given simultaneous cytosine arabinoside and methotrexate. This difference is significant ($P < 0.025$). Therefore, it would seem that the biochemical changes induced by the cytosine arabinoside within the cell might have greatly sensitized the cell to the subsequent administration of methotrexate. Thus, cell kinetic patterns are not the only determining factor for chemotherapeutic effectiveness.

REFERENCES

1. SAUNDERS EF, and MAUER AM. Reentry of nondividing leukemic cells into a proliferative phase in acute childhood leukemia. J Clin Invest 48:1299–1305, 1969.
2. GABUTTI V, PILERI A, TAROCCO RP, ET AL. Proliferative potential of out-of-cycle leukaemic cells. Nature 224:375–376, 1969.
3. SAUNDERS EF, LAMPKIN BC, and MAUER AM. Variation of proliferative activity in leukemic cell populations of patients with acute leukemia. J Clin Invest 46:1356–1363, 1967.
4. PANTAZOPOULOS N, and SINKS LF. Morphological criteria for prognostication of acute lymphoblastic leukaemia. Br J Haematol 27:25–30, 1974.
5. MURPHY SB, BORELLA L, ET AL. Lack of correlation of lymphoblast cell size with presence of T-cell markers or with outcome in childhood acute leukaemia. Br J Haematol 31:95, 1975.
6. MAUER AM, LAMPKIN BC, EVERT CF, ET AL. Cell kinetic patterns in human acute leukemia—evidence for control mechanisms. Bibl Haematol 39:1014–1021, 1973.
7. HAYES AV, and MAUER AM. Cell kinetics and chemotherapy in neuroblastoma. J Natl Cancer Inst 57:697–699, 1976.
8. LAMPKIN BC, NAGAO T, and MAUER AM. Synchronization and recruitment in acute leukemia. J Clin Invest 50:2204–2214, 1971.
9. ERNST P, and KILLMANN SA. Perturbation of generation cycle of human leukemic myeloblasts in vivo by methotrexate. Blood 38:689–705, 1971.

[4] Rivera G, and Murphy S. Unpublished observations.

10. KLEIN HO, LENNARTZ KJ, ET AL. Cytostatic treatment of partially synchronized tumor cells in animals and men. *In* Proceedings of the 7th International Congress of Chemotherapy, Prague, 1971.

11. LAMPKIN BC, MCWILLIAMS NB, and MAUER AM. The advantage of cell synchronization in therapy of myeloid leukemias in children. Blood 38:802, 1971.

12. EDELSTEIN M, VIETTI T, and VALERIOTE F. Schedule-dependent synergism for the combination of 1-β-D-arabinofuranosylcytosine and daunorubicin. Cancer Res 34:293–297, 1974.

Synchronization With Phase-Specific Agents in Leukemia and Correlation With Clinical Response to Chemotherapy [1]

William R. Vogler,* William B. Kremer, William H. Knospe, George A. Omura, and Karl Tornyos [2]

SUMMARY

Mitotic indices, labeling indices (LI), and tritiated thymidine incorporation into DNA of marrow cells were conducted in patients with leukemia to determine if correlations existed between kinetic measurements, clinical features, and response to chemotherapy. Higher proliferative activity was observed in chronic granulocytic leukemia (CGL) and blastic phase of CGL than in acute leukemia. In acute myelogenous leukemia there was no correlation with various clinical features studied. Those patients demonstrating > 60% reduction in circulating leukemia cells within 7 days had a higher initial LI than those with < 60% reduction. Cytosine arabinoside, methotrexate, and hydroxyurea were investigated to determine their synchronizing capability; cytosine arabinoside and methotrexate were superior to hydroxyurea. In a cycle-sensitive schedule specifically designed to synchronize cells, responses occurred more frequently in patients who increased their LI 48 hours after priming doses of cytosine arabinoside. In an intensive-chemotherapy schedule which produced more remissions than the cycle-sensitive schedule, there was no relationship between initial kinetic measurements and response. Kinetic values increased as patients achieved remissions.

[Cancer Treat Rep 60:1845–1859, 1976]

Numerous studies have been reported indicating that leukemic cells are not rapidly proliferating and in fact are less efficient than normal cells in their ability to replicate DNA and divide (1–8). The mean generation time and DNA-synthesis phase are prolonged (6,9,10). Furthermore, fewer cells appear to be in the mitotic cycle when compared to proliferating normal bone marrow cells (6,9).

Since most of the chemotherapeutic drugs effective in acute leukemia are cycle-active agents, one would expect that the proportion of cells killed by these agents at any given time would be small and a function of the growth fraction and the duration of lethal intracellular drug concentration. The fact remains that these drugs are effective and do kill leukemic cells. In the process, one would expect a greater proportion of normal proliferating cells to be killed, thus, it would seem that the exploitable kinetic difference between the normal and leukemic population is the rate of recovery. If the leukemic population behaved kinetically similar to the normal population, no exploitable differences would exist and unless factors other than growth kinetics were operative, therapy would be ineffective. However, if the proliferating fraction of leukemic cells was extremely small, cycle-active agents would kill a very small fraction of cells and prolonged treatment would be required. This would result in severe toxicity to the normal population. In the group of patients with small leukemic growth fraction, efforts are underway to increase the proportion of cells in cycle, which should make them more suscep-

[1]Supported by the American Cancer Society grant CI-40; and Public Health Service grants (CA) from the National Cancer Institute, National Institutes of Health, Department of Health, Education, and Welfare. The following institutions participated in this study: Emory University School of Medicine, Atlanta, Ga (*W. R. Vogler*, CA-03227); Veterans' Administration Hospital and Duke University Medical Center, Durham, NC (*W. B. Kremer*, CA-05634); Rush-Presbyterian-St. Luke's Hospital, Chicago, Ill (*W. H. Knospe*, CA-12640); University of Alabama, Birmingham (*G. A. Omura*, CA-03013); and Veterans' Administration Hospital, New Orleans, La (*K. Tornyos*, CA-13209).

[2]We wish to thank Dr. Donald P. Growth, Department of Biochemistry, Emory University, for developing the procedure for measuring DNA specific activity.

**Reprint requests to:* W. R. Vogler, MD, Emory University School of Medicine, 718 Woodruff Memorial Bldg, Atlanta, Ga 30322.

tible to chemotherapy. This might be done by recruitment, bringing more "resting" cells into the mitotic cycle, or by synchronization, putting more cells simultaneously into a sensitive phase of the cycle at the time chemotherapy is given. Thus, there would seem to be an optimal growth fraction in which a sufficient number of leukemic cells would be in cycle to be killed by lethal concentrations of cycle-active drugs and yet kinetically different from the normal cell population in rate of recovery, resulting in a differential effect on cell-kill. More remissions might be achieved if the growth fraction could be manipulated into this optimal range.

The purposes of this investigation were: (*a*) to define the kinetic characteristics in various human leukemias; (*b*) to correlate the kinetic characteristics in acute myelogenous leukemia with the response to chemotherapy; (*c*) to test various methods of recruiting cells into the mitotic cycle; and (*d*) to determine if a therapeutic advantage is achieved by recruitment.

MATERIALS AND METHODS

Methods of radioautography and measurement of the DNA synthesis rates in bone marrow.—The rate of tritiated thymidine incorporation in bone marrow and radioautography were done as previously described (11). In essence, triplicate samples of marrow were incubated at 37.5°C under oxygen with tritiated thymidine (specific activity 6.2 curies/mmol) for 10, 20, and 30 minutes. Aliquots were removed for radioautography and the DNA was extracted, measured by the diphenylamine reaction (12), and the specific activity determined by scintillation counting (efficiency 25%) and expressed as cmp/μmol DNA/minute. The labeling index (LI) was determined by counting the number of labeled cells per 1000 mononuclear cells. A cell was considered labeled if five or more grains were present.

Mitotic index (MI).—The MI was determined by counting the number of mitotic figures seen per 2000 nucleated cells on a Wright's stained preparation of a bone marrow aspirate.

Serum lysozyme.—Serum lysozyme was measured by the method of Zucker et al (13). Normal values ranged from 7 to 15 μg/ml.

Patient selection.—Kinetic studies were done in consenting patients with the following diagnoses: acute myelogenous leukemia (AML), which included myeloblastic, myelomonocytic, acute monocytic, and erythroleukemia; acute lymphoblastic leukemia (ALL); chronic granulocytic leukemia (CGL) and blastic transformation (crisis) (BLCr) of CGL.

Timing of clinical studies.—Marrow aspirations were performed prior to and at varying times after the introduction of chemotherapy. The majority of patients were treated with one of two treatment schedules. Some patients were treated with various agents and kinetic studies were done on several occasions over a period of 1 week to determine which agents might be the most effective in recruiting or synchronizing cells.

The chemotherapy schedules were as follows:

Schedule 1.—This program consisted of a course of cycle-active drugs given after a preliminary or priming dose of cytosine arabinoside administered for the purpose of increasing the growth fraction as described by Lampkin et al (14). Cytosine arabinoside was given either as a single iv injection of 100 mg/m^2 (schedule 1A) or three rapid iv injections of 100 mg/m^2/day × 3 days (schedule 1B). Forty-eight hours after the last dose of cytosine arabinoside all patients received methotrexate orally at a dose of 75 mg/m^2 every 6 hours for four doses followed by citrovorum factor (CF) at a dose of 5 mg every 6 hours for nine to 15 doses depending upon the creatinine clearance. In addition, vincristine (1 mg/m^2) was given during the methotrexate therapy. These courses were repeated at intervals of every 7–10 days.

Schedule 2.—This treatment schedule was designed to obtain a hypocellular marrow using cytosine arabinoside (100 mg/m^2) by rapid iv injection) and 6-thioguanine (100 mg/m^2 orally every 12 hours for ten doses) as described by Gee et al (15) or the same schedule with the addition of daunorubicin (10 mg/m^2/day × 5 days) (16). Courses were repeated every 10–14 days unless marrow hypoplasia was present.

Recruitment schedules.—Agents used to synchronize cells were: cytosine arabinoside (100 mg/m^2 given by rapid iv injection × 1 or 3 days); cytosine arabinoside infusion (100 mg/m^2/day × 24 or 48 hours); methotrexate (75 mg/m^2 every 6 hours for four doses) followed in 18 hours by CF (5 mg every 6 hours for nine to 15 doses); and hydroxyurea (4–16 g over a 24–60-hour period). These studies were conducted at five institutions. Slides were interchanged and LI determinations were compared. There was good agreement between institutions. Six studies were done at the Rush-Presbyterian-St. Luke's Hospital, eight at the Veterans' Administration Hospital, Durham, NC, four at the University of Alabama, one at the Veterans' Administration Hospital, New Orleans, La, and the remainder at Emory University.

Criteria for response.—Patients were judged as to response to chemotherapy by criteria previously described (17). In addition to complete and partial remissions, those showing a reduction in marrow infiltration from > 30% leukemic blast cells to < 5%

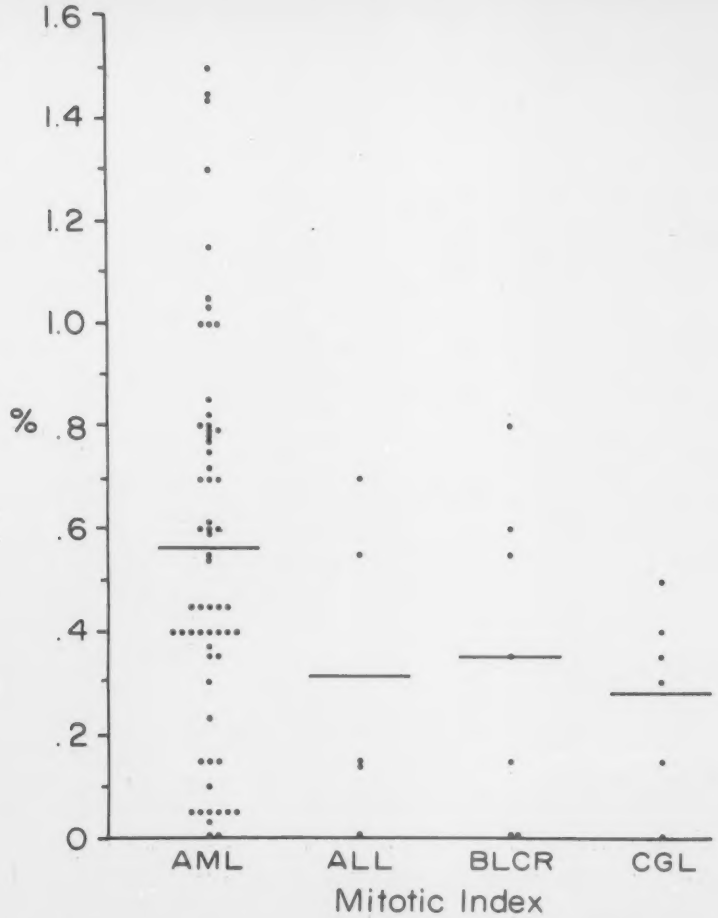

FIGURE 1.—Scattergram of MI for all studies grouped by diagnosis. Horizontal line = the mean.

associated with disappearance of hepatosplenomegaly (when present) and clearance of leukemic cells from the blood were considered to have an antileukemic effect, although remission was not achieved.

Statistical considerations.—For comparisons of samples of enumeration data a chi-square test with Yates corrections was employed. For comparisons of relationships between groups of measurements a Student's "t" test was used. A P value of < 0.05 was considered statistically significant and a P value of < 0.10 was suggestive of a difference.

RESULTS

A summary of the mean MI, LI, and DNA-synthesis rates of 62 untreated leukemic patients is given in table 1. These data have been previously reported (18). The MI was significantly higher in AML when compared to ALL and to CGL ($P < 0.05$). The latter difference can be explained because of the presence of more nondividing cells in the marrow aspirates of the CGL patients. If these cells are excluded the MI averaged $0.73\% \pm 0.19\%$. There is no obvious explanation for the differences between AML and ALL. The LI was significantly higher ($P < 0.05$) in CGL than in AML with BLCr falling in between. The DNA-synthesis rates tended to parallel the LI, but because of the large standard errors the differences were not statistically significant.

Scattergrams of the data are presented in figures 1–3. The horizontal bars illustrate the means; as can be seen, considerable variations are observed in each diagnostic category. These variations raise several questions. Are there any clinical features which correlate with the kinetic variations? Are these variations of predictive value in determining

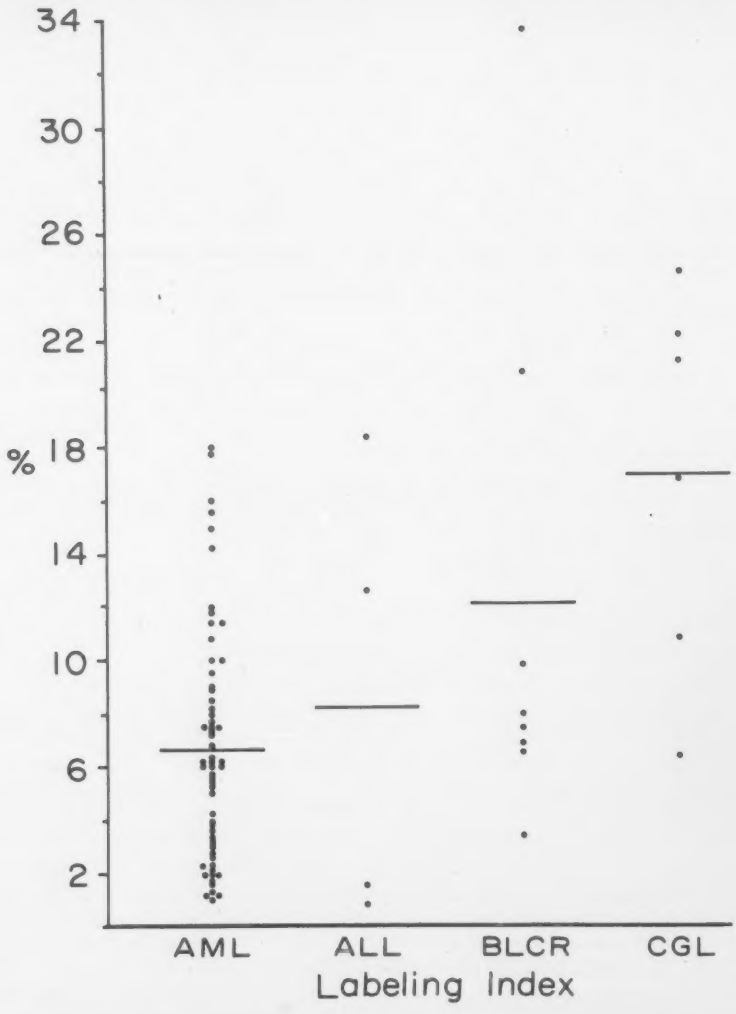

FIGURE 2.—Scattergram of 30-min LI for all studies grouped by diagnosis. Horizontal line = the mean.

the response to chemotherapy? Can they predict survival? Can the values be altered by any techniques? Are alterations helpful or of no consequence? To answer the first three questions detailed analyses were carried out in 43 AML patients seen at Emory University. This included subclassifications of myeloblastic, myelomonocytic, acute monocytic, and erythroleukemia. No consistent differences were observed in kinetic measurements among these subclassifications.

Correlation of clinical features with kinetic data.—Attempts to correlate the major clinical features with the initial kinetic values in untreated AML patients failed to show any effect of sex or age (table 2); thus, all sexes and ages were pooled. The following clinical variables bore no relationship to the kinetic variables under study: initial leukocyte and platelet counts, presence of infection, percentage of myeloblasts in the marrow, and serum lysozyme levels. The rate of clearance of leukemic cells from the blood after chemotherapy might reflect the proportion of cells in cycle. Thus, higher initial kinetic values might be present in those patients who had a greater reduction in circulating cells. The data are given in table 3. Those with $> 60\%$ reduction in circulating leukemic blast cells 7 days after initiation of chemotherapy had a significantly higher LI and DNA-synthesis rate than those with a $< 60\%$ reduction ($P < 0.05$).

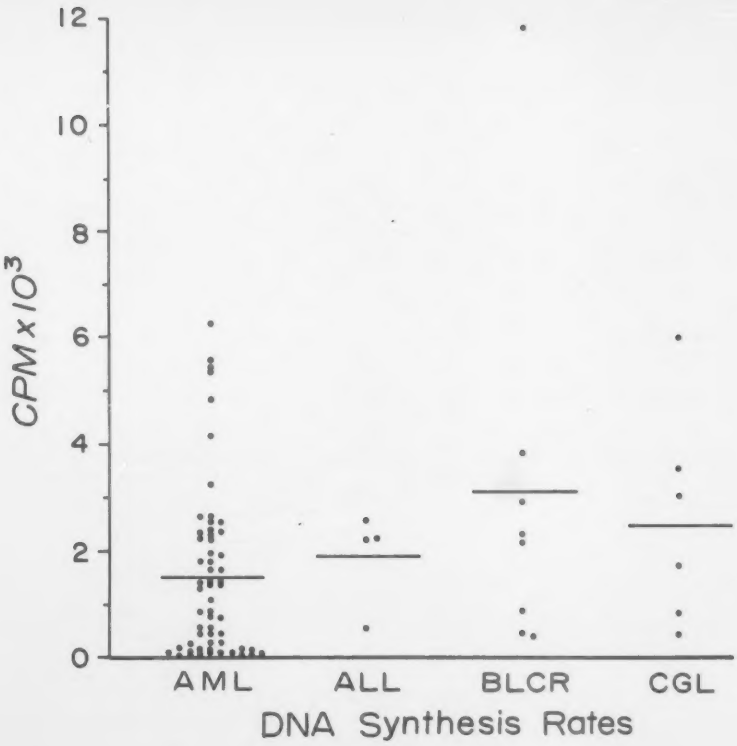

FIGURE 3.—Scattergram of DNA synthesis rates expressed as cpm/μmol DNA/min computed from triplicate samples at 2–3 time points per incubation period by the least squares method. Horizontal line = the mean.

TABLE 1.—Mean MI, LI, and DNA-synthesis rate in untreated leukemia*

Diagnosis	No. of patients	MI (%)†	LI (%)†	DNA-synthesis rate† (cpm/μmol DNA/min)
AML	43	0.62 ± 0.06	7.4 ± 0.71	1633 ± 259
ALL	5	0.31 ± 0.13	8.3 ± 4.3	1898 ± 451
BLCr	8	0.35 ± 0.12	12.1 ± 3.6	3134 ± 1323
CGL	6	0.28 ± 0.07	17.0 ± 3.0	2611 ± 839

*From ref No. 18.
†Mean ± SE.

Correlation of response to therapy and clinical variables.—To compare the various clinical features and the response to therapy the patients were grouped into response categories. An initial comparison of complete remissions to nonresponses failed to show any differences in sex, age, prior therapy, presence of infection, or wbc and platelet counts prior to initiation of treatment. Significantly more patients ($P < 0.05$) failing to respond to chemotherapy had > 90% leukemic blast cells in the bone marrow at the beginning of therapy than those responding to chemotherapy (complete remission, partial remission, or antileukemic effect). Serum lysozyme levels were > 20 μg/ml in 74% of the nonresponders and 46% of the responders ($P < 0.05$). The major factor influencing responses was

TABLE 2.—Effect of sex and age on LI, MI, and DNA-synthesis rate in AML

Category	No. of patients	MI (%)*	LI (%)*	DNA-synthesis rate* (cpm/μmol DNA/min)
Sex				
M	27	0.60 ± 0.07	7.0 ± 0.76	1906 ± 340
F	16	0.65 ± 0.11	8.2 ± 1.4	1161 ± 376
Age				
< 20	4	0.40 ± 0.13	7.7 ± 3.7	728 ± 364
21–40	7	0.54 ± 0.13	5.6 ± 0.93	1006 ± 349
41–60	13	0.76 ± 0.10	8.7 ± 1.4	2383 ± 613
> 60	19	0.62 ± 0.09	7.2 ± 1.0	1621 ± 381

*Mean ± SE.

TABLE 3.—Relationship of % reduction in leukemia cells after 1 wk of chemotherapy and initial MI, LI, and DNA-synthesis rate

% fall in circulating blast cells	No. of patients	MI (%)*	LI (%)*	DNA-synthesis rate* (cpm/μmol DNA/min)
0–40	9	0.55 ± 0.08	5.4 ± 0.88	1169 ± 520
41–60	7	0.63 ± 0.13	5.7 ± 1.8	448 ± 323
61–80	9	0.59 ± 0.13	7.9 ± 1.3	2518 ± 568
81–100	18	0.69 ± 0.10	8.9 ± 1.3	1832 ± 439

*Mean ±SE.

TABLE 4.—Initial kinetic values and response to chemotherapy in previously untreated AML patients

	MI (%)*	LI (%)*	DNA-synthesis rate* (cpm/μmol DNA/min)
Complete remission (13 patients)	0.60 ± 0.10	7.3 ± 1.2	1765 ± 500
No remission (18 patients)	0.66 ± 0.09	7.1 ± 1.1	1252 ± 337
P value	> 0.10	> 0.10	> 0.10

*Mean ± SE.

the chemotherapy schedule. Of 19 patients entered on schedule 1, 57% responded and 21% had complete remissions. Of 24 patients entered on schedule 2, 63% responded and 54% had complete remissions. Comparison of complete remissions with no remissions yielded significant differences between schedules 1 and 2 ($P < 0.05$).

Correlation of response to therapy and initial kinetic measurements.—Comparison of the initial kinetic values in 13 previously untreated patients who obtained a complete remission with 18 patients failing to obtain even an antileukemic effect revealed no differences (table 4). This analysis included patients treated on both schedules. Comparison of the kinetic factors by schedules and response is presented in table 5. There were no statistically significant differences between responders and nonresponders. However, on schedule 1 there was a tendency for responders to have a higher MI, LI, and DNA-synthesis rate when compared to the nonresponders. No similar trend was apparent on schedule 2. LI measured after 10, 20, and 30 minutes of incubation showed significant differences between responders and nonresponders on schedule 1 for 10 and 20 minutes ($P < 0.05$) and a suggestive difference at 30 minutes but no difference on schedule 2 (table 6).

TABLE 5.—Kinetic variables by schedule and response

Schedule No.	Responders: No. of patients	Responders: Variable (mean ± SE)	Nonresponders: No. of patients	Nonresponders: Variable (mean ± SE)	P value
		MI%			
1	9	0.66 ± 0.15	10	0.47 ± 0.09	NS*
2	15	0.55 ± 0.08	9	0.88 ± 0.13	NS
		LI%			
1	9	8.7 ± 1.5	10	5.3 ± 0.73	< 0.10
2	15	6.7 ± 1.3	9	9.1 ± 1.8	NS
		DNA-synthesis rate (cpm/μmol DNA/min)			
1	9	2351 ± 633	10	1623 ± 570	NS
2	14	1076 ± 279	8	1039 ± 396	NS

*NS = not significant.

TABLE 6.—Relationship of the initial LI (%) and response to therapy by schedule and incubation time

Schedule No.	Incubation time (mins)	Responders: No. of patients	Responders: LI% (mean ± SE)	Nonresponders: No. of patients	Nonresponders: LI% (mean ± SE)	P value
1	10	7	5.6 ± 1.2	6	2.6 ± 0.60	< 0.05
	20	7	6.7 ± 1.2	6	3.5 ± 0.71	< 0.05
	30	9	8.7 ± 1.5	10	5.3 ± 0.73	< 0.10
2	10	15	3.8 ± 1.0	9	4.1 ± 0.88	NS*
	20	15	5.4 ± 1.2	9	6.8 ± 1.4	NS
	30	15	6.7 ± 1.3	9	9.1 ± 1.8	NS

*NS = not significant.

Correlation of survival and initial kinetic measurements.—Comparisons were made concerning the LI and survival by schedules. On schedule 1 no differences were observed. On schedule 2 significantly more ($P < 0.05$) patients who lived > 100 days had a LI of < 8%.

Recruitment and synchronization.—A series of patients with AML were treated with priming doses of cycle-active drugs in an effort to increase the growth fraction of the leukemic population and kinetic measurements were made prior to and for varying periods of time after priming. The data are given in tables 7–10. We were unable to obtain marrows daily on any patients and thus tried to determine trends by averaging all of the LIs. Sufficient numbers of observations were made for statistical analysis for patients receiving cytosine arabinoside and methotrexate and the means are shown in figure 4. Synchronization was not observed in 22 of 65 patients (34%) as no subsequent LI exceeded the initial value. However, 66% of the patients did show some increase. As shown in figure 4, the mean LI showed an increase at 48 hours over the initial value and this was the most pronounced after methotrexate and CF. Of 30 patients receiving cytosine arabinoside by rapid injection, an increased LI was observed in 21 (table 7) (19). The highest LI occurred at 24 hours in eight patients and at 48 hours in 13. Of the 19 patients receiving methotrexate, 12 demonstrated an increase in LI over the initial value. Four patients peaked at 24 hours, five at 48 hours, three at 72 hours, and one later (table 10). Greater

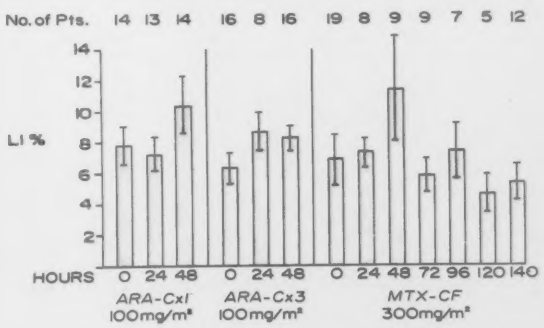

FIGURE 4.—Mean LI after pulse doses of cytosine arabinoside or methotrexate followed by CF.

TABLE 7.—LI following different dose schedules of cytosine arabinoside*

LI after dose of—							
100 mg/m², single dose				100 mg/m²/day × 3 days			
Patient No.	0 hr	24 hrs	48 hrs	Patient No.	0 hr	24 hrs	48 hrs
1	3.9	2.3	9.0	1	8.9	13.0	11.2
2	7.5	8.9	13.6	2	5.7	10.9	11.0
3	18.0	7.3	31.6	3	2.6	6.8	4.4
4	11.4	15.7	15.2	4	4.5	—	2.4
5	9.7	12.0	10.7	5	1.8	—	5.5
6	6.6	—	6.3	6	8.2	—	11.1
7	3.6	6.5	6.1	7	6.2	5.2	10.6
8	6.3	7.0	4.2	8	0.5	—	11.8
9	8.0	2.3	6.0	9	13.9	12.2	12.2
10	10.0	6.5	7.2	10	9.4	—	12.4
11	1.6	5.0	6.7	11	6.3	10.2	5.5
12	14.3	6.9	13.1	12	1.7	—	6.8
13	5.4	6.3	4.7	13	9.8	—	6.9
14	3.2	7.0	11.5	14	8.5	4.2	8.0
				15	10.0	7.3	6.9
				16	1.9	—	5.7
Mean ± SE	7.82 ± 1.22	7.21 ± 0.99	10.42 ± 1.88	Mean ± SE	6.24 ± 0.96	8.72 ± 1.16	8.28 ± 0.80

*From ref No. 19.

TABLE 8.—LI following infusions of cytosine arabinoside

Patient No.	LI at—				
	0 hr	48 hrs	72 hrs	96 hrs	120 hrs
	24-hr infusion (100 mg/m²)				
1	6.2	—	—	6.4	—
2	1.9	12.7	7.2	—	—
3	5.4	—	—	7.3	—
	48-hr infusion (100 mg/m²/day)				
1	16.0	2.2	1.6	7.0	14.0
2	18.6	4.5	14.0	6.0	2.0
3	2.6	2.6	12.5	2.9	3.7
4	13.7	7.7	9.8	6.0	5.7

TABLE 9.—LI following hydroxyurea given orally in divided daily doses

Patient No.	Total dose (g)	LI at—						
		0 hr	24 hrs	48 hrs	72 hrs	96 hrs	120 hrs	144 hrs
		1-day treatment						
1	4	9.5	—	8.0	12.0	—	—	9.9
2	4	0.5	1.5	1.8	0.9	—	—	2.3
		2-day treatment						
3	8	4.6	—	0.2	—	—	3.0	—
4	12	4.9	—	2.4	13.3	8.6	3.8	—
5	9	—	—	1.1	2.1	3.3	—	3.6
6	16	11.0	17.7	11.0	2.7	2.0	—	—
7	12	5.7	3.2	11.8	6.7	3.8	—	—
		2.5-day treatment						
9	10	14.9	—	3.3	—	—	—	2.3

TABLE 10.—LF following methotrexate-CF*

Patient No.	LI at—						
	0 hr	24 hrs	48 hrs	72 hrs	96 hrs	120 hrs	144 hrs
1	7.5	13.2			10.0		11.0
2	5.2		5.1			3.5	
3	8.2	10.2		8.6			12.0
4	12.0		10.7			6.3	
5	7.2				3.4		
6	7.5	9.2	2.5	4.4			5.9
7	16.0		36.1		15.3		4.1
8	10.0		17.0		10.2		
9	7.3	4.5		5.8			6.3
10	9.0			4.0		7.5	
11	1.2		3.8			2.1	
12	1.7	2.7		3.5			2.0
13	3.1		4.6		1.6		3.0
14	7.5	11.8		10.0			10.8
15	6.8			11.7		7.8	
16	14.2		10.2		4.6		3.7
17	2.1	4.3		1.8			1.0
18	1.3		12.8		6.1		2.8
19	1.9	1.5		2.7			1.5
Mean ± SE	6.83 ± 1.61	7.25 ± 0.93	11.5 ± 3.5	5.83 ± 1.16	7.31 ± 1.8	4.6 ± 1.2	5.32 ± 1.14

*Methotrexate given orally in doses of 75 mg/m² q6hrs × 4 doses. CF given orally at 5 mg q6hrs × 9–15 doses begun 36 hrs after the first dose of methotrexate.

variations were seen with cytosine arabinoside infusions and hydroxyurea but in some patients these procedures appeared to be effective (tables 8 and 9). It is apparent that in most instances the changes in LI occurred within 72 hours after the synchronizing agent. Figure 5 illustrates the temporal relationship of LI and MI in patients synchronized with methotrexate. At 24 hours there was a significant reduction in MI with no change in LI consistent with a delay of cells through S. The peak LI occurred at 48 hours and was followed 24 hours later by an increase in MI indicating that some synchronization had occurred.

Recruitment and response to chemotherapy.—Fourteen patients were treated with schedule 1A. Two patients died within 21 days and one was inevaluable. Of the remaining 11 patients two achieved complete remissions, three demonstrated an antileukemic effect, and the remainder failed to respond. Two of 16 patients who were treated with schedule 1B were inevaluable. Of the remaining patients six achieved complete remissions and four demonstrated an antileukemic effect. Analysis of variance of the LI revealed that there was no significant difference in the initial LI between schedules, but the LI at 48 hours was significantly different from the LI at 0 hour. The increment in LI from 0 to 48 hours was not different between schedules, but differed significantly between responders and nonresponders. As shown in table 11 (19), the mean increment in LI at 48 hours was 4.03% ± 0.17% in the responders as opposed to 0.13 ± 0.96% in the nonresponders ($P < 0.02$). Table 12 shows the relationship between those showing at least a 2% increment in LI and clinical response. Eleven of 14 patients responding to treatment increased the LI, whereas only four of 11 failing to increase LI achieved a response. In a group of 15 patients including 12 of those patients described above

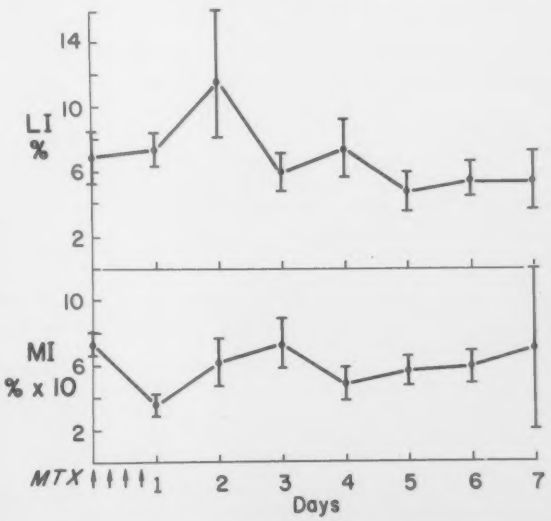

FIGURE 5.—Effect of methotrexate on MI and LI in AML patients prior to institution of chemotherapy.

TABLE 11.—Relationship of clinical response with mean LI in patients treated on schedule 1*

	LI% (mean ± SE)			
	Responders		Nonresponders	
	0 hr	48 hrs	0 hr	48 hrs
Schedule 1A	10.10 ± 2.09	16.00 ± 3.62	6.02 ± 1.13	6.08 ± 0.38
Schedule 1B	6.17 ± 1.22	9.26 ± 1.10	6.58 ± 1.54	6.80 ± 0.44
Increment at 48 hrs	4.03 ± 1.07		0.13 ± 0.96	

**From* ref No. 19.

TABLE 12.—Correlation of recruitment and clinical response in patients treated on schedule 1

	No. of patients with—	
Response	> 2% increase in LI	No increase in LI
Remission	6	2
Antileukemic effect	5	2
None	3	7

treated with schedules 1A or 1B and three patients treated by a 24-hour infusion of 100 mg/m² of cytosine arabinoside used as a recruiting agent followed 48 hours later by methotrexate, CF, and vincristine, the LI, MI, and DNA-synthesis rates were determined in responders and nonresponders. The data presented in table 13 indicate that LI and DNA-synthesis rates were significantly higher initially in responders when compared to nonresponders. The MI was significantly different at 48 hours. Kinetic studies were repeated in subsequent courses of treatment in three responders (one with antileukemic effect) and three nonresponders. In general, the initial increment pattern occurred with repeated studies. Those who responded had significant and consistent increments at 48 hours, whereas those who failed to respond had erratic or no increments. Examples of the two types of responses are shown in figures 6 and 7. Patients treated on schedule 2 failed to show any significant correlation between initial kinetic values and response to treatment. The mean LI in seven patients who obtained complete remission was 6.15% ± 1.79% and in six patients failing to achieve remission was 6.93% ± 2.45%. Figure 8 illustrates a patient treated on schedule 2 who obtained a remission after two courses of chemotherapy. Note the increment in LI as the marrow was repopulated with normal cells. Marrows were done on a number of patients between 10 and 25 days after a 5-day course of chemotherapy on schedule 2. The numbers are too small for statistical consideration, but the mean and range of values for LI are given in figure 9. Note that the mean LI began to increase after 14 days although considerable variations persist.

TABLE 13.—Mean kinetic values in 12 patients treated on schedule 1 (A and B) and 3 patients primed with a 24-hr infusion of cytosine arabinoside*

	Responders (6 patients)	Nonresponders (9 patients)	*P* value
LI (%)†			
0 hr	8.2 ± 1.4	4.0 ± 0.9	< 0.05
48 hrs	13.5 ± 2.5	6.1 ± 0.4	< 0.05
DNA-synthesis rate (cpm/μmol DNA/min)			
0 hr	3071 ± 661	743 ± 242	< 0.01
48 hrs	4431 ± 770	1307 ± 448	< 0.01
MI (%)†			
0 hr	0.79 ± 0.12	0.49 ± 0.14	> 0.10
48 hrs	0.78 ± 0.17	0.23 ± 0.10	< 0.05

**From* ref No. 11.
†Mean ± SE.

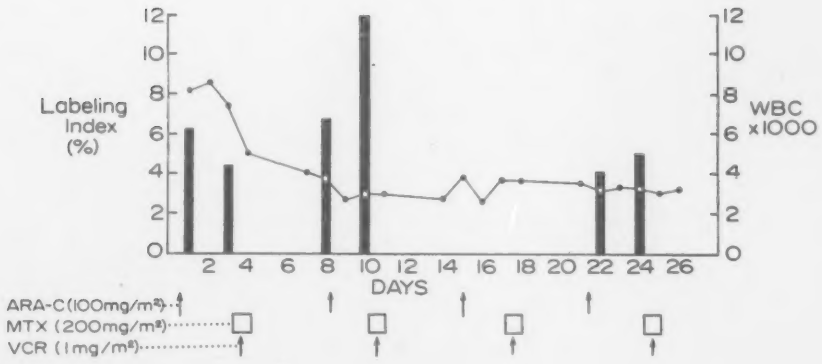

FIGURE 6.—Variable response to recruitment by cytosine arabinoside in a patient failing to achieve remission on the schedule 1A treatment. Subsequent remission obtained on schedule 2.

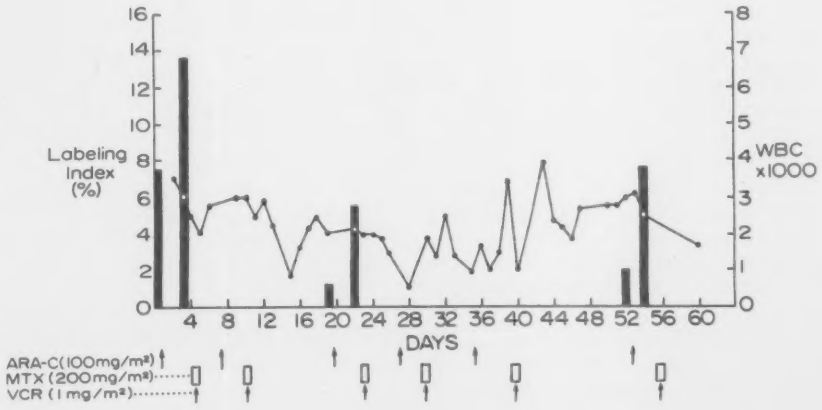

FIGURE 7.—Effective recruitment in patient obtaining a complete remission on schedule 1A.

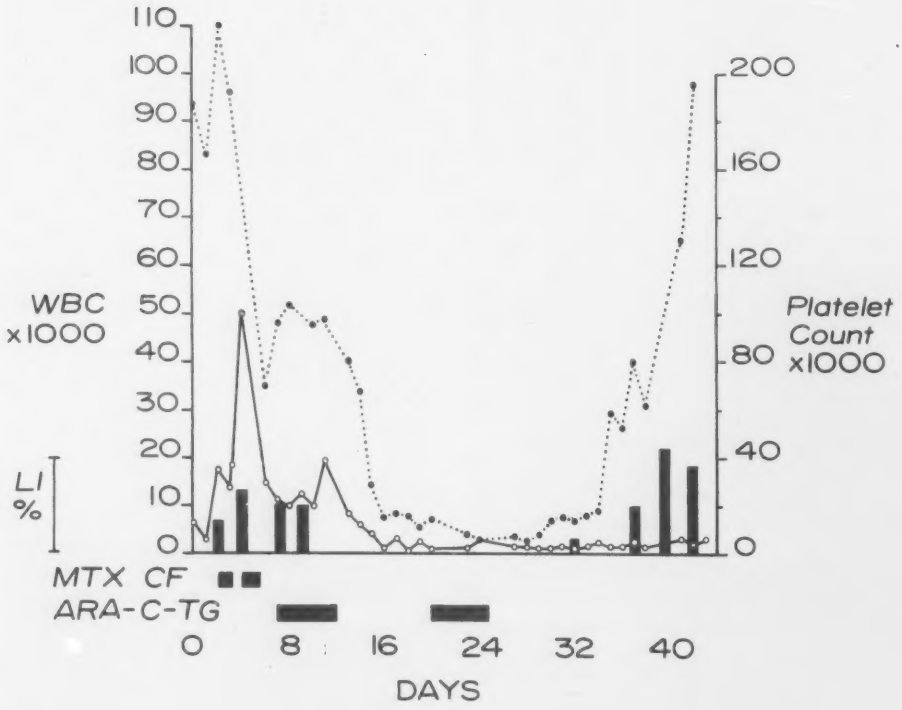

FIGURE 8.—Increase in LI in patient achieving remission treated on schedule 2.

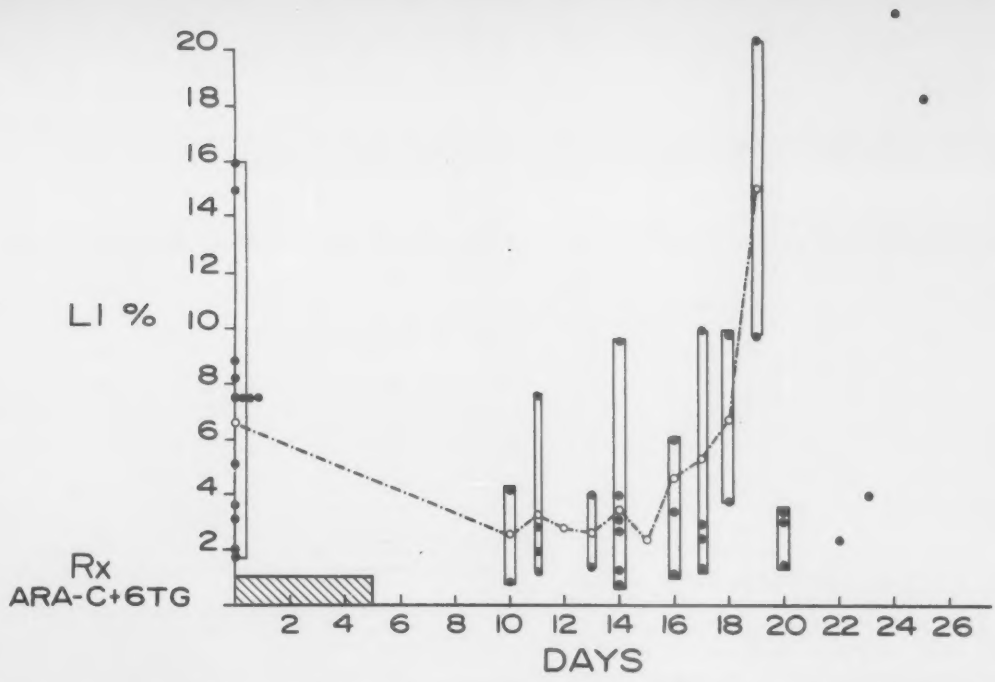

FIGURE 9.—Compilation of LI measurements in AML patient following chemotherapy. Vertical bars = ranges; horizontal line = the mean.

DISCUSSION

These data demonstrate that considerable variations in kinetic measurements occur among leukemic patients with identical morphologic diagnoses. These findings are consistent with the reports of others (2,4,20,21). The values in CGL and BLCr of CGL appear to approach the normal as summarized by Gavosto (22). If these cells behave similarly to normal marrow cells, no exploitable differences would be present. This may explain in part the difficulty in obtaining remissions in patients with BLCr.

It would appear from these data that the use of standard treatment procedures for all patients with AML would be inappropriate if growth patterns were of major importance in determining the outcome of the treatment. The facts are that increasing percentages of patients with AML are achieving remissions treated with intensive chemotherapy (15,23,24). Our data indicate that kinetic measurements in patients treated with such intensive therapy are of no value in predicting response. However, these remissions are obtained at the expense of extreme morbidity with prolonged hypoplasia of the marrow and require intensive supportive care. Even though our complete remission rate was low in patients treated on schedule 1, there appears to be a subset of patients who did have the appropriate kinetic values to respond to appropriately scheduled cycle-active agents. Identification of this group of patients might enable certain patients to be treated with less intensive chemotherapy schedules.

Most clinical variables investigated were of no prognostic value in predicting response to chemotherapy. Similar findings were noted by Clarkson et al (25). We found no correlation between the initial kinetic values and the clinical variables studied. When comparing initial kinetic values between those failing to demonstrate a significant reduction in marrow infiltration and those obtaining complete remission, no differences were observed. However, by adding those additional patients who demonstrated an antileukemic effect to the group with remissions, a greater number treated by schedule 1 had higher initial kinetic values. Similar results were observed by Zittoun et al (26) who found higher incorporation of tritiated thymidine into leukemic blast cells of responders when compared to nonresponders, all treated in a variety of ways. No

difference was found in schedule 2. It would appear that the therapeutic schedule introduces an additional variable.

Efforts to synchronize cells in one phase of the mitotic cycle in order to render cells more susceptible to cycle-active chemotherapeutic agents have been reported by other investigators (27–29). To date, with the exception of a report by Lampkin et al (30), the results of such efforts have not yielded remissions more frequently than those observed with more empiric therapy. However, in animal studies reported by Klein and Lennartz (31) and Young et al (32) it was found that it is possible to improve the therapeutic outcome after synchronization. Further studies are necessary in order to fully utilize this information for clinical benefit.

Numerous reports have appeared in the literature concerning efforts to synchronize cells by means of various chemotherapeutic agents (27,33–36). Ideally one would like a drug that is very rapidly eliminated, therefore having no delayed effect on the cells in cycle. Methotrexate and cytosine arabinoside seem to be effective and have these characteristics, however the degree of synchronization was not great and further efforts are necessary if a greater degree of synchronization is to be obtained.

Clinical application of the kinetic measurements has been hampered by the delay in obtaining results, particularly using radioautography. In acute leukemia we found a reasonable correlation between tritiated thymidine incorporation into DNA and the LI. This would provide the means of getting results within a few hours. However, even more rapid information might be obtained by the use of newer techniques such as pulse cytophotometry, which would make it possible to characterize the kinetic behavior of leukemic patients' cells prior to institution of therapy.

Exploitable kinetic differences between normal and tumor tissue do exist. Young et al (32) demonstrated that the peak tritiated thymidine incorporation into normal murine bone marrow and gastrointestinal mucosa preceded the peak incorporation into DNA of L1210 ascites tumor cells by approximately 48 hours. This lends support to the thesis that the more rapid recovery of the normal cell is an exploitable difference. From the incomplete data that we have obtained, our study would indicate that the schedule 2 treatment was poorly timed. Second courses were repeated after a 5–7-day interval at a time when the normal cells would be expected to recover and hence be more susceptible to cycle-active agents. The prolonged hypoplasia frequently seen with this regimen supports this concept.

In conclusion, the variability of growth patterns in human neoplasms is real. The identification of these patterns prior to treatment would be helpful and the techniques for doing so are at hand. Attempts to maximize the kinetic differences between normal and leukemic cells and the timing of chemotherapeutic administration are just beginning, but it is conceivable that with time, treatment schedules can be devised which will be less toxic and just as effective as current treatment which is complicated by severe toxicity.

LIST OF COMPOUNDS

Citrovorum factor: NSC-3590; CAS reg. No. 6055–86–5; glutamic acid, *N*-[*p*-[[(2-amino-5-formyl-5,6,7,8-tetrahydro-4-hydroxy-6-pteridinyl)methyl]amino]benzoyl]-, calcium salt

Cytosine arabinoside: NSC-63878; CAS reg. No. 69–74–9; cytosine, 1-β-D-arabinofuranosyl-, monohydrochloride

Daunorubicin: NSC-82151; CAS reg. No. 23541–50–6

Hydroxyurea: NSC–32065; CAS reg. No. 127–07–1

Methotrexate: NSC-740; CAS reg. No. 59–05–2; glutamic acid, *N*-[*p*-[[(2,4-diamino-6-pteridinyl)methyl]methylamino]benzoyl]-

6-Thioguanine: NSC-752; CAS reg. No. 1832–72–0; purine-6-thiol, 2-amino-

Vincristine: NSC-67574; CAS reg. No. 2068–78–2; leurocristine, sulfate (1:1)

REFERENCES

1. GAVOSTO F, MARAINI G, and PILERI A. Proliferative capacity of acute leukemia cells. Nature 187:611–612, 1960.
2. MAUER AM, and FISHER V. Comparison of the proliferative capacity of acute leukemia cells in bone marrow and blood. Nature 193:1085–1086, 1972.
3. ———. In vivo study of cell kinetics in acute leukemia. Nature 197:574–576, 1973.
4. CRADDOCK CG, and NAKAI GS. Leukemic cell proliferation as determined by in vitro deoxyribonucleic acid synthesis. J Clin Invest 41:360–369, 1972.
5. KILLMANN S-A, CRONKITE EP, ROBERTSON JS, ET AL. Estimation of phases of the life cycle of leukemic cells from labeling in human beings in vivo with tritiated thymidine. Lab Invest 12:671–684, 1973.
6. CLARKSON B, OHKITA T, OTA K, ET AL. Studies of cellular proliferation in acute leukemia. J Clin Invest 44:1035–1036, 1965.
7. CLARKSON B, OHKITA T, OTA K, ET AL. Studies of cellular proliferation in human leukemia. I. Estimation of growth rates of leukemic and normal hematopoietic cells in two adults with acute leukemia given single injections of tritiated thymidine. J Clin Invest 46:506–529, 1967.
8. CLARKSON B, STRIFE A, FRIED J, ET AL. Studies of cellular proliferation in human leukemia. IV. Behavior of normal hematopoietic cells in 3 adults with acute leukemia given continuous infusions of ^{3}H-thymidine for 8 or 10 days. Cancer 26:1–19, 1970.
9. GAVOSTO F, PILERI A, GABUTTI V, ET AL. Non-self-maintaining kinetics of proliferating blasts in human acute leukaemia. Nature 216:188–189, 1967.
10. LIN MS, and BOURONCLE BA. The size and transit time of nondividing subpool of precursor cells in acute leukemia. Blood 29:63–76, 1967.
11. VOGLER WR, COOPER LE, and GROTH DP. Correlation of cytosine arabinoside-induced increment in growth fraction

of leukemic blast cells with clinical response. Cancer 33:603–610, 1974.
12. BURTON K. A study of the conditions and mechanism of the diphenylamine reaction for the colorimetric estimation of deoxyribonucleic acid. Biochem J 62:315–323, 1956.
13. ZUCKER S, HANES DJ, VOGLER WR, ET AL. Plasma muramidase: a study of methods and clinical application. J Lab Clin Med 75:83–92, 1970.
14. LAMPKIN BC, NAGAO T, and MAUER AM. Drug effect in acute leukemia. J Clin Invest 48:1124–1130, 1969.
15. GEE TS, Yu KP, and CLARKSON B. Treatment of adult acute leukemia with arabinosyl cytosine and thioguanine. Cancer 23:1019–1032, 1969.
16. VOGLER WR, and CHAN Y-K. Prolonging remission in myeloblastic leukemia by Tice-strain *bacillus* Calmette-Guérin. Lancet 2:128–131, 1974.
17. VOGLER WR, HUGULEY CM, and RUNDLES RW. Comparison of methotrexate with 6-mercaptopurine-prednisone in treatment of acute leukemia in adults. Cancer 20:1221–1226, 1967.
18. VOGLER WR, GROTH DP, and GARWOOD FA. Cell kinetics in leukemia. Arch Intern Med 135:950–954, 1975.
19. KREMER WB, VOGLER WR, and CHAN Y-K. An attempt at synchronization of marrow cells in acute leukemia: relationship to therapeutic response. Cancer. In press.
20. MAUER AM, and FISHER V. Characteristics of cell proliferation in four patients with untreated acute leukemia. Blood 28:428–445, 1966.
21. KILLMANN S-A. Acute leukemia: the kinetics of leukemic blast cells in man. Ser Haematol 1:38–102, 1968.
22. GAVOSTO F. Granulopoiesis and cell kinetics in chronic myeloid leukaemia. Cell Tissue Kinet 7:151–163, 1974.
23. GLUCKMAN E, BASCH A, VARET IB, ET AL. Combination chemotherapy with cytosine arabinoside and rubidomycin in 30 cases of acute granulocytic leukemia. Cancer 31:487–491, 1973.
24. YATES JW, HOLLAND JF, WALLACE HJ, ET AL. Intensive induction treatment of acute myelocytic leukemia. Proc Am Assoc Cancer Res and ASCO 15:178, 1974.
25. CLARKSON BD, DOWLING MD, GEE TS, ET AL. Treatment of acute leukemia in adults. Cancer (Suppl) 36(2):775–797, 1975.
26. ZITTOUN R, BOUCHARD M, FACQUET-DANIS J, ET AL. Prediction of the response to chemotherapy in acute leukemia. Cancer 35:507–513, 1975.
27. BURKE PJ, and OWENS AH, JR. Attempted recruitment of leukemic myeloblasts to proliferative activity by sequential drug treatment. Cancer 28:830–836, 1971.
28. LAMPKIN BC, NAGAO T, and MAUER AM. Synchronization and recruitment in acute leukemia. J Clin Invest 50:2204–2214, 1971.
29. LEVI JA, VINCENT PC, and GUNZ FW. Combination chemotherapy of adult acute nonlymphoblastic leukemia. Ann Intern Med 76:397–403, 1972.
30. LAMPKIN BC, MCWILLIAMS NB, MAUER AM, ET AL. Manipulation of the mitotic cycle in treatment of acute myeloblastic leukemia. Blood 44:930, 1974.
31. KLEIN HO, and LENNARTZ KH. Chemotherapy after synchronization of tumor cells. Semin Hematol 11:203–227, 1974.
32. YOUNG RC, GOLDBERG D, and SCHEIN PS. Enhanced antitumor effect of cytosine arabinoside given in a schedule dictated by kinetic studies in vivo. Biochem Pharmacol 22:277–280, 1973.
33. SAUNDERS EF, LAMPKIN BC, and MAUER AM. Variation of proliferative activity in leukemic cell populations of patients with acute leukemia. J Clin Invest 46:1356–1363, 1967.
34. ERNST P, and KILLMANN S-A. Perturbation of generation cycle of human leukemic myeloblasts in vivo by methotrexate. Blood 38:689–705, 1971.
35. VERBIN RS, DILUISO G, LIANG H, ET AL. Synchronization of cell division in vivo through the combined use of cytosine arabinoside and Colcemid. Cancer Res 32:1489–1498, 1972.
36. ERNST P. Perturbation of generation cycle of human leukaemic blast cells in vivo by daunomycin. Scand J Haematol 11:13–22, 1973.

Resting Cells in L1210 and JB-1 Ascites Tumors With Special Emphasis on Recycling [1]

N. R. Hartmann, P. Dombernowsky,* and P. Bichel [2]

It has been known for about 20 years that cell populations in vivo in spite of morphologic homogeneity may consist of two populations, proliferating cells (P cells) and nonproliferating cells (Q cells). Mendelsohn (1) proposed the quantity growth fraction to denote the fraction of proliferating cells in a tumor.

The concept of resting cells was reviewed by Epifanova and Terskikh (2). They defined the resting period as an indefinite interval in which cells may stay without undergoing division or differentiation but retaining both of these potentials. When stimulated, such cells may enter into the cell cycle and divide or differentiate. Consequently, the resting cells in a tumor are defined as those of the Q cells which have retained their capacity of re-entering the P cell population when given proper conditions.

Figure 1 shows a model taking the above-mentioned concepts into account. Only rates which are generally accepted are recorded in the figure. K_b is the birth rate, K_L is the cell-loss rate, and M is the mitotic phase. The dotted arrow indicates the possible recycling of resting cells.

Lajtha et al (3,4) introduced the term G_0 phase for the bone marrow stem cell population. As shown in the model in figure 2, the G_0 phase is a nonproliferative stage the cells have to pass before entering into the G_1 phase of the cell cycle. According to this definition, the G_0 cells are much more restrictively defined than the Q cells in figure 1.

Only in recent years has attention been focused on the stages of the cell cycle at which cells may be transferred from P to Q cells. It has been suggested that a cell which has initiated DNA synthesis has already made the decision to divide (5). It has been proposed that the P cells enter the Q phase immediately after mitosis and consequently the nonproliferating cells have G_1 DNA content (Q_1 cells) (fig 3).

However, cells may also be arrested in the G_2 phase as first described by Gelfant (6). Thus, the next step so far in the analysis of nonproliferating cells in tumors was the introduction of Q cells with G_2 DNA content (Q_2 cells).

Detailed knowledge of resting cells in tumors is of importance since these cells play a role in the regrowth of tumors after treatment. Investigations of these cells in human tumors are presently limited for practical purposes and studies of experimental tumors, such as ascites tumors, are therefore necessary. Furthermore, in ascites tumors the experimental conditions can be closely controlled and manipulated. In this paper, investigations of resting

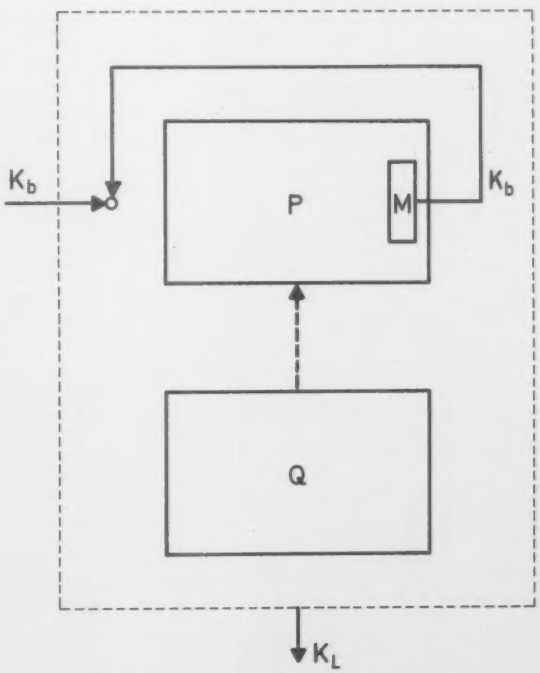

FIGURE 1.—A model for tumor growth dividing the cell population into P and Q cells.

[1]Supported by grants from the Daell Foundation, the Danish Cancer Society, the Danish Medical Research Council, the Hasselbalch Foundation, the Michaelsen Foundation, and the Irma Foundation (a bequest of Mr. and Mrs. Carl Schepler).

[2]Finsen Laboratory (Dr. Hartmann), Department of Internal Medicine (Dr. Dombernowsky), the Finsen Institute, Copenhagen, Denmark, and the Institute of Cancer Research (Dr. Bichel), Radiumstationen, Århus, Denmark.

*_Reprint requests to:_ Per Dombernowsky, MD, Department of Internal Medicine, the Finsen Institute, 49, Strandboulevarden, DK-2100, Copenhagen, Denmark.

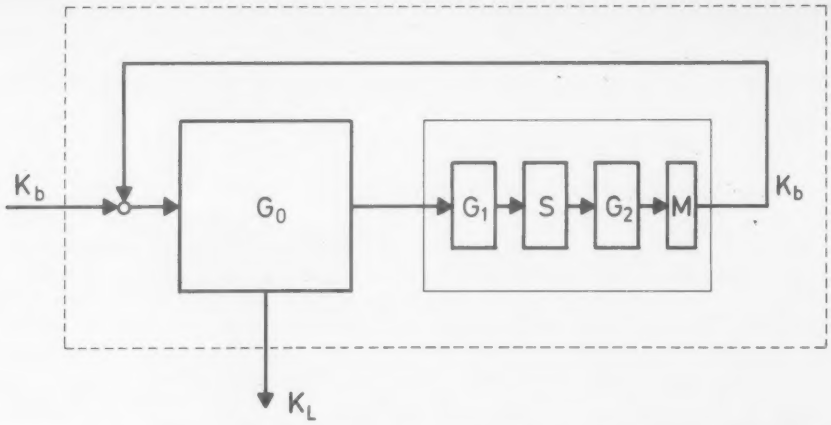

FIGURE 2.—A model for a bone marrow stem cell population with the nonproliferative G_0 stage before the G_1 phase.

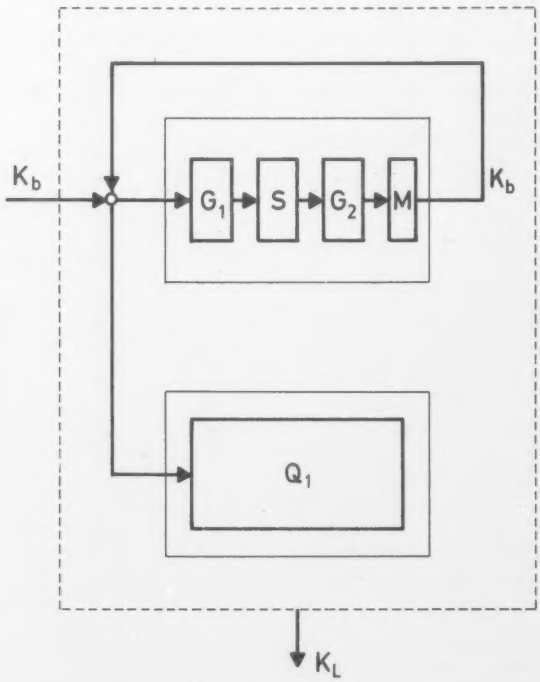

FIGURE 3.—A model for tumor growth in which the nonproliferating cells have G_1 DNA content (Q_1 cells).

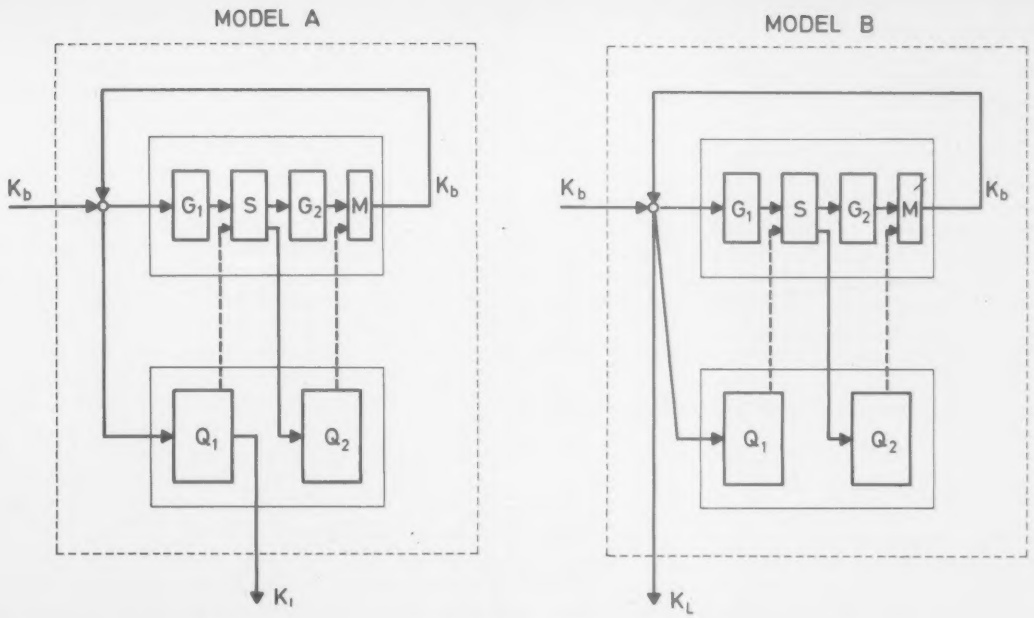

FIGURE 4.—Two models for the cell kinetics in the L1210 and JB-1 ascites tumors. The models differ with respect to the mode of cell loss. Q_1 and Q_2 are nonproliferative stages with G_1 and G_2 DNA content respectively.

cells in the L1210 and JB-1 ascites tumors are presented.

Accumulation of Q Cells

A model containing Q_1 and Q_2 cells has been used in the analysis of the cell kinetics of L1210 and JB-1 ascites tumors during undisturbed growth (7–10). The model has been used in two versions that differ with respect to the mode of cell loss (fig 4). In model A an age-specific cell loss occurs from Q_1 and in model B newly generated cells are lost. The dotted arrows indicate recycling of resting cells which can be achieved under appropriate conditions. On the assumption of exponential growth, a computer method has been developed for the analysis of the experimental data, ie, growth curves, percentage of labeled mitoses, and continuous labeling curves combined with cytophotometric determination of single-cell DNA content. The L1210 ascites tumor was analyzed on Days 5, 6, and 8 after ip inoculation of 10^5 cells and the JB-1 ascites tumor was analyzed on Days 4, 7, and 10 after inoculation of 2.5×10^6 cells. Furthermore, the JB-1 ascites tumor was investigated 24 hours after aspiration of the main part of the plateau tumors.

The estimated fractions of Q_1 and Q_2 cells are recorded in figure 5. The solid lines indicate the accumulation of Q_1 and Q_2 cells as a function of tumor age. These curves are estimated on the basis of model A which gave the best fit to the experimental data. It is seen that the fractions of Q_1 and Q_2 cells increase with increasing tumor age. The fraction of Q_1 cells is predominant, but even the fraction of Q_2 cells is of a certain magnitude in the JB-1 ascites tumor. These findings are in agreement with the flow microfluorometrically determined DNA distributions (11). The dotted lines in figure 5 show the drops in the fractions of Q_1 and Q_2 cells that occur after aspiration of the JB-1 ascites tumor as is discussed later. Results from the aspiration experiment are estimated on the basis of model B (fig 4). Consequently, a shift in the mode of cell loss was introduced by aspiration of the JB-1 ascites tumor.

The accumulation of Q_1 cells with increasing tumor age in ascites tumors is in accordance with previous observations (12–17). The present investigations on the L1210 and JB-1 ascites tumors also demonstrate an accumulation of Q_2 cells, an observation more rarely described (12–15).

Thus, our present knowledge of ascites tumor growth suggests that cells may pass into the Q-cell population not only after doubling their DNA content.

Recycling of Resting Cells

After demonstration of increasing fractions of noncycling cells with G_1 and G_2 DNA content with increasing number of L1210 and JB-1 ascites tumor cells, the question arises whether the noncycling cells represent true resting stages or are cells simply unable to proliferate because of irreversible damage to some process which is necessary for the continuation of the cell cycle. If some of the noncycling cells represent resting cells they should be expected to re-enter the cell cycle under proper conditions such as (*a*) in regenerative growth, (*b*) after retransplantation, or (*c*) after treatment with cytostatic agents.

The results of the above-mentioned conditions are described below.

Regenerative Growth

The regenerative growth was investigated after maximal percutaneous aspiration of 10-day plateau JB-1 ascites tumors (9,11,18). Figure 6 shows the normal growth curve (8) and in the same figure the growth curve for the aspirated tumor is shown. Investigations 24 hours after aspiration showed a pronounced decrease in the doubling time and a pronounced increase in the growth fraction. The latter observation is also illustrated in figure 5 by the decrease in the fractions of Q_1 and Q_2 cells.

Recycling of Q_1 cells during the first 24-hour period after aspiration was demonstrated by the combination of continuous labeling with ^{3}H-TdR and cytophotometric determination of single-cell DNA content (table 1). After 24 hours of prelabeling of plateau tumors with ^{3}H-TdR, all cycling cells in the tumor are labeled judging from the cell cycle parameters (8). Immediately on aspiration the histograms showed that 77% of the unlabeled cells had G_1 DNA content, 1% had intermediary DNA content (S phase), and 22% had G_2 DNA content (table 1). Four, 8, and 24 hours after aspiration the percentage of unlabeled cells with intermediary DNA content increased in parallel with a decrease in the fraction of unlabeled cells with G_1 DNA content, indicating a pronounced recycling of Q_1 cells.

Recycling of Q_2 cells was demonstrated by variations in the mitotic index (MI) and the percentage of labeled mitoses after 24 hours of continuous labeling with ^{3}H-TdR before aspiration (fig 7). It appears

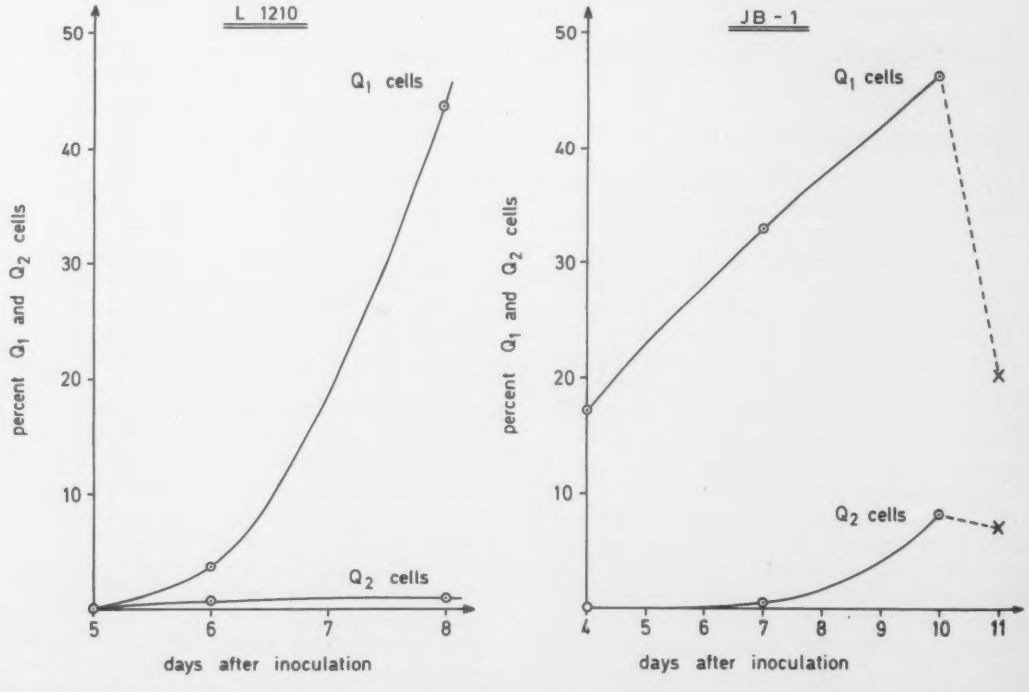

FIGURE 5.—Accumulation of Q_1 and Q_2 cells in the L1210 and JB-1 ascites tumors with an increasing number of tumor cells. The dotted lines show the decrease in the percentage of Q_1 and Q_2 cells after aspiration from a plateau JB-1 ascites tumor.

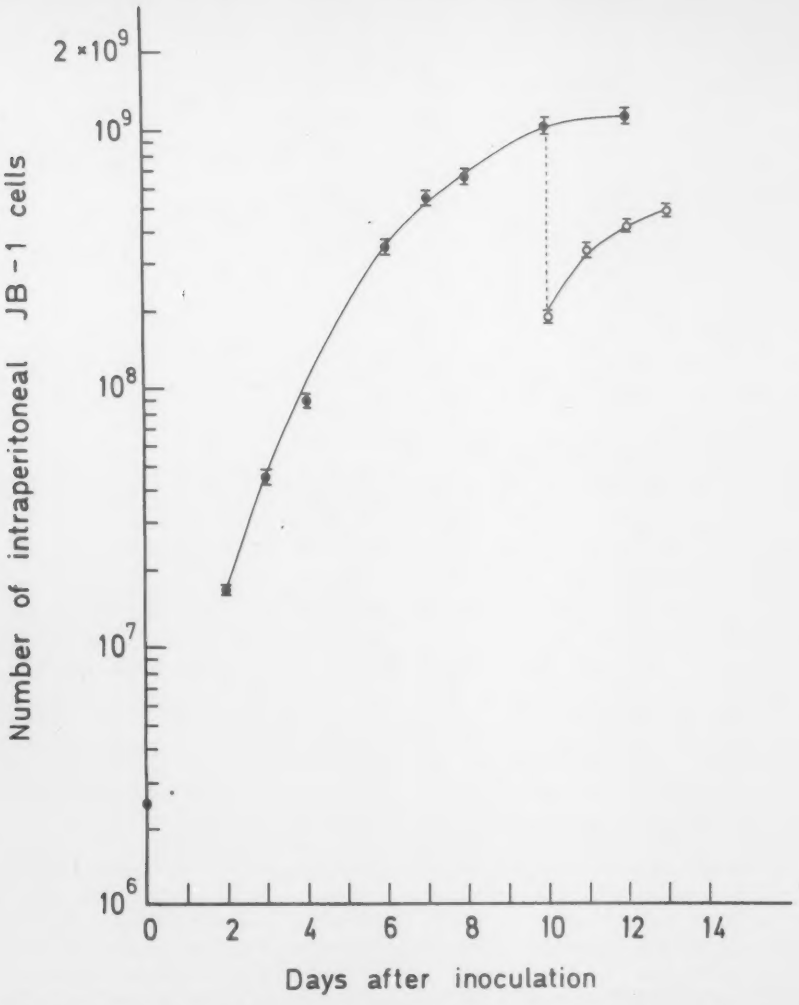

FIGURE 6.—Growth curve for the JB-1 ascites tumor (●) and growth curve for mice aspirated on Day 10 after the same inoculum (○). Each point represents the mean number of 4–12 mice. The vectors represent the standard error of the mean.

from the curve that the MI after a short latency period increased to a maximum value of about 3% at 8–10 hours after aspiration. The percentage of labeled mitoses decreased significantly ($P < 0.01$, Mann-Whitney rank-sum test) from the initial value of 93% to 82% at 4 hours after aspiration. At 10 hours the percentage of labeled mitoses had reached the initial value, and from 16 to 24 hours after aspiration a new decrease occurred. The shape of the curve indicates a short minor wave of cells released from Q_2 and a major wave released from Q_1.

As seen from figure 7 the recycling from Q_1 to S was considerable compared with the Q_2 recycling. This finding was confirmed by the data in table 1 in which the percentage of unlabeled cells with G_1 DNA content in continuously labeled plateau tumors decreased from 77% immediately on aspiration to 61% 24 hours later. In the same period, the percentage of unlabeled cells with S DNA content increased from 1% to 14% while the fraction of unlabeled cells with G_2 DNA content was nearly constant.

Figure 8 shows flow microfluorometric investiga-

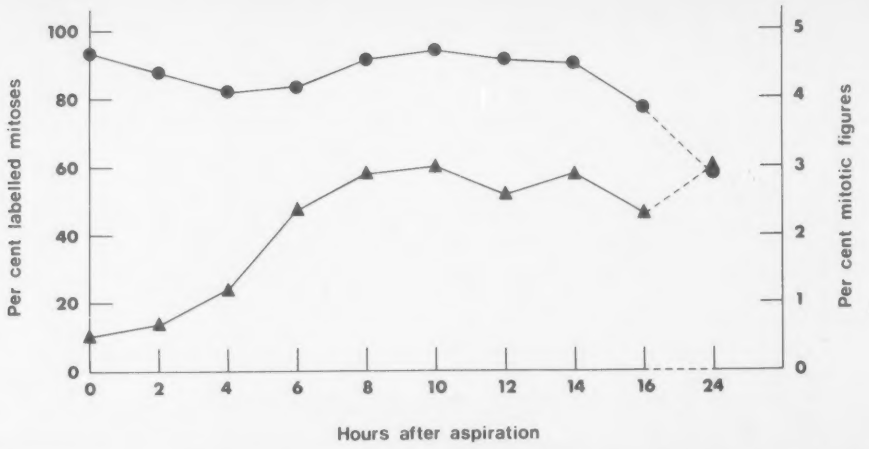

FIGURE 7.—Percentage of labeled mitoses (●) and MI (▲) after aspiration from mice of plateau JB-1 ascites tumors prelabeled with ^{3}H-TdR for 24 hrs at 4-hr intervals.

tions of the DNA distributions of JB-1 tumors after aspiration (11). Immediately on aspiration, 50% of the tumor cells had G_1 DNA content (G_1 + Q_1 cells), 31% had S DNA content, and 19% had G_2 DNA content (G_1 + Q_2 + mitotic cells). One and 2 days after aspiration the percentage of cells with S DNA content had increased while the percentages of cells with G_1 and G_2 DNA content had decreased. On Days 3 and 4 after aspiration the fraction of cells in S again decreased in parallel with an increase in the fraction of cells with G_1 DNA content, indicating renewed accumulation of cells with G_1 DNA content.

The flow microfluorometric results further support the earlier findings obtained by autoradiography and cytophotometry, thus indicating that the increase in the growth fraction after aspiration of the main part of plateau JB-1 tumors was due to recycling of resting cells with both G_1 and G_2 content.

Retransplantation

The transition of Q_1 and Q_2 cells to the proliferative compartment has been investigated after retransplantation of plateau JB-1 tumors to new hosts (18,19).

Table 2 shows the results of an experiment similar to that seen in table 1. By means of cytophotometry of unlabeled tumor cells after continuous labeling, it was shown that the number of unlabeled tumor cells with S DNA content increased significantly at the expense of unlabeled Q_1 cells. As seen from the table, the Q_1 recycling was most pronounced from 6 to 10 hours after transplantation.

The fate of the noncycling Q_2 cells after retransplantation was also studied. ^{3}H-TdR flash-labeled plateau tumors were pooled, transplanted to new hosts, and simultaneously injected with demecolcine[3] (fig 9). Three to 4 hours after retransplantation a burst of mitotic cells was noted, of which only a small number were labeled. The labeled cells were those which at the time of transplantation were in the S phase, while the unlabeled cells represented cells in G_2 + Q_2.

Evidence in support of recycling of Q_2 cells after retransplantation was obtained from an experiment similar to that in figure 7. Mice carrying JB-1 tumors at the plateau were repeatedly labeled with ^{3}H-TdR for 20 hours, pooled, and retransplanted to new hosts, and the percentage of labeled mitoses of total mitoses scored. From 1 to 3 hours after transplantation the percentage of labeled mitoses gradually decreased from 95% at 1 hour to 75% at 3 hours after transplantation ($P < 0.01$), thus indicating that some of the unlabeled noncycling Q_2 cells were ready to rapidly re-enter the cell cycle.

Other authors have also investigated the cell kinetics after transplantation of various ascites tumors in the plateau phase of growth to new host animals (16,17,20–24). They all observed an increase in the MI and the labeling index (LI) after transplantation. This was interpreted as an increase in the growth fraction due to recycling of resting cells. Lala and Patt (16) explained the increase in the MI after retransplantation of plateau tumors as being

[3]Demecolcine: NSC-3096; CAS reg. No. 477–30–5; colchicine, *N*-deacetyl-*N*-methyl-; Colcemid.

TABLE 1.—Percentage distribution of DNA content in unlabeled cells after aspiration of plateau JB-1 ascites tumors, prelabeled with ^{3}H-TdR for 24 hrs at 4-hr intervals before aspiration

Hrs after aspiration	No. of unlabeled cells measured	Percentage distribution of unlabeled tumor cells		
		$G_1 + Q_1$	S	$G_2 + Q_2$
0	102	77	1	22
4	99	78	2	20
8	103	72	9	19
24	102	61	14	25

TABLE 2.—Percentage distribution of DNA content in unlabeled cells after transplantation to new hosts of 100×10^6 plateau JB-1 ascites tumor cells, prelabeled every 4 hrs for 24 hrs with ^{3}H-TdR

Hrs after transplantation	No. of unlabeled cells measured	Percentage distribution of unlabeled tumor cells		
		$G_1 + Q_1$	S	$G_2 + Q_2$
0	369	84	3	13
1	100	82	2	16
3	132	80	5	15
6	122	62	19	19
10	120	61	26	13

due to a lag in the shortening of the mitotic phase relative to that of other stages during the initial readjustment of the cell cycle. Wiebel and Baserga (22) expressed the view that the increase in the MI was due to a transient delay of cells in G_2 followed by a rapid acceleration. Based on the variations in the MI, percentage of labeled mitoses, and cytophotometric data, Lala and Patt (16) concluded that recycling in their Ehrlich ascites tumor occurred only after the completion of mitosis and before DNA synthesis, ie, from the Q_1 stage.

Recycling After Cytostatic Treatment

Recycling of resting cells was also studied in plateau JB-1 ascites tumors after treatment with cytosine arabinoside[4] (Ara-C) (25). Ara-C has its main mechanism of action in the S phase and the lethal effect of the drug seems to be confined to cells synthesizing DNA (26,27).

Treatment with a single ip injection of Ara-C (200 mg/kg) to mice with plateau JB-1 tumors resulted in a significant reduction in the number of tumor cells 1 and 2 days later compared with untreated controls. As was the case after aspiration and retransplantation, recycling of Q_1 cells was demonstrated by the combination of continuous labeling with ^{3}H-TdR and cytophotometric determination of single-cell DNA content (experiments similar to the experiments in tables 1 and 2).

The recycling of Q_2 cells was demonstrated by variations in the MI and the percentage of labeled mitoses after 24 hours of continuous labeling with ^{3}H-TdR before Ara-C treatment (fig 10). Of all the mitoses, 95% were labeled after 24 hours of continuous labeling. The percentage of labeled mitoses had decreased significantly ($P < 0.005$) to 82% at 6 hours; it then increased to the initial value at 10 hours ($P < 0.02$) followed by a new decrease 16 hours after Ara-C.

Figure 11 shows the variations in the percentage of labeled mitoses and in the MI in tumors continuously labeled after Ara-C treatment also. A significant fall ($P < 0.01$) from 95% before Ara-C to 85% 8 hours later was again observed; then the percentage of labeled mitoses slowly increased to the initial value without a second decrease.

The first significant fall in the percentage of labeled mitoses 6–8 hours after Ara-C can be explained only by recycling of Q_2 cells (figs 10 and 11). The second significant fall in the percentage of

[4]Cytosine arabinoside: NSC-63878; CAS reg. No. 69-74-9; cytosine, 1-β-D-arabinofuranosyl-, monohydrochloride.

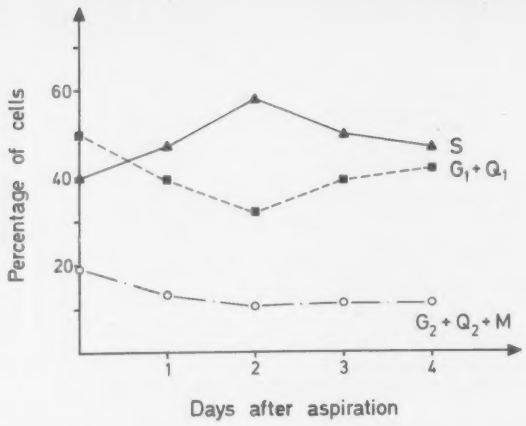

FIGURE 8.—Percentage of cells with G_1, S, and G_2 DNA content on Days 1–4 after aspiration of plateau JB-1 ascites tumors. Each point represents values from 10 to 13 mice.

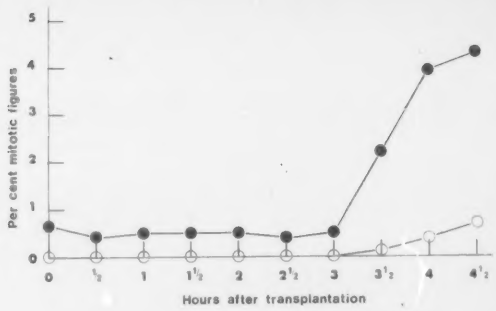

FIGURE 9.—Accumulation of mitotic figures after retransplantation of ^{3}H-TdR flash-labeled plateau JB-1 ascites tumors and demecolcine. ● = labeled + unlabeled mitoses; ○ = labeled mitoses.

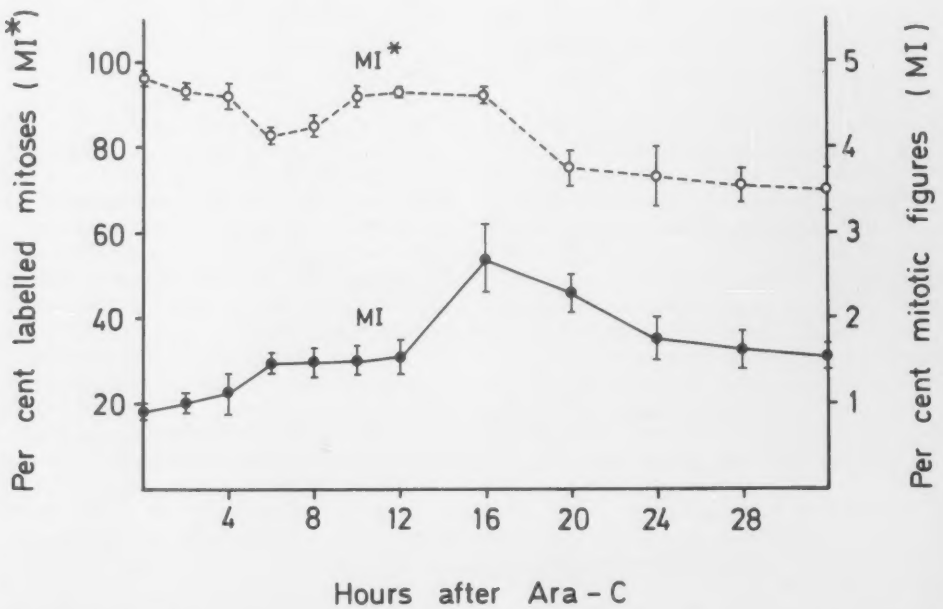

FIGURE 10.—Percentage of labeled mitoses (MI*) and MI after treatment of plateau JB-1 ascites tumors with Ara-C (200 mg/kg ip). The tumors were prelabeled with ^{3}H-TdR every 4 hrs for 24 hrs. Each point represents the mean of 6 mice. The vectors represent the standard error of the mean.

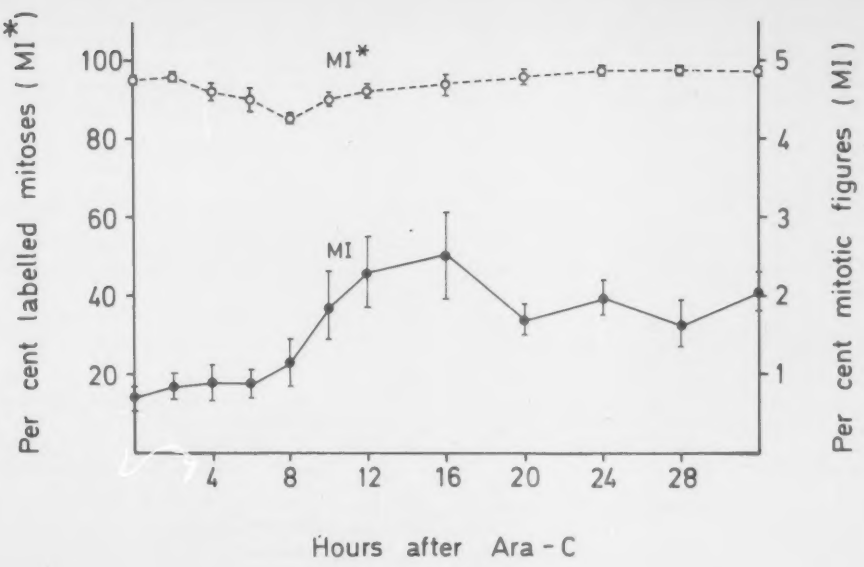

FIGURE 11.—Percentage of labeled mitoses (MI*) and MI after treatment of plateau JB-1 ascites tumors with Ara-C (200 mg/kg ip). The tumors were prelabeled with ^{3}H-TdR every 4 hrs for 24 hrs and the labeling was continued after Ara-C treatment. Each point represents the mean of 6 mice. The vectors represent the standard error of the mean.

labeled mitoses after 20 hours is probably due to recycling of Q_1 cells (fig 11). The first fall in labeled mitoses can be caused by recycling of Q_2 cells because of the following facts: (*a*) no or only one single unlabeled cell with intermediary (S) DNA content was observed by cytophotometry during the first 12 hours after Ara-C, but appeared after 16–20 hours (experiment similar to those in tables 1 and 2); and (*b*) continuous labeling with ^{3}H-TdR also after Ara-C, which labels recycling cells from Q_1, resulted in the disappearance of the second fall in the percentage of labeled mitoses (fig 11). As was the case in regenerative growth and after retransplantation, the recycling from Q_2 occurred first. The cytophotometric data, however, showed that the total amount of recycling from Q_2 was relatively small (a reduction in the fraction of cells with G_2 DNA content from 15% to 11% of the unlabeled population from 0 to 32 hours after Ara-C) compared with the massive recycling from Q_1 during the same period (a reduction from 84% to 62% for cells with G_1 DNA content).

The recycling observed results in an increase in the growth fraction which has also been observed in human tumors. After ip treatment with Ara-C in a patient with recurrent ovarian ascites carcinoma, Sheehy et al (28) demonstrated an increase in the growth fraction.

Indirect evidence of recycling after cytostatic treatment is provided by the variations in the flash LI and MI in acute leukemia and multiple myeloma in man after diminution of the tumor by treatment with single agents or by combination chemotherapy (29,30). By the combination of autoradiography and cytophotometry, recycling of resting cells with G_1 DNA content was observed in human acute leukemia after methotrexate treatment (31).

Recycling of resting cells with G_2 DNA content has been described in an autogeneous rat sarcoma after treatment with mechlorethamine (32), and in the ELD Ehrlich ascites tumor after the administration of antilymphocytic serum, hydrocortisone, or azathioprine (14,33). In these studies, recycling was demonstrated by the decrease in the percentage of labeled mitoses after continuous labeling with ^{3}H-TdR.

Recycling of resting cells has also been observed in human leukemia after leukopheresis (34) while our knowledge of recycling after incomplete surgical removal of solid tumors is modest.

The demonstration of resting cells in tumors and the recycling of these cells are of interest from a clinical point of view. Tumor cells, while in their resting stage, are refractory to most cytostatic agents, and after the withdrawal of the drug they contribute to renewed growth of the tumor (35). On

the basis of acquired knowledge of recycling, including the time schedule, observed in the JB-1 ascites tumor, it should be possible to devise a treatment program which gives maximum cell kill of both proliferating and recycling cells. Probably such a program will require both new experimental methods such as flow microfluorometry and new methods of analyzing cell kinetic data.

REFERENCES

1. MENDELSOHN ML. Autoradiographic analysis of cell proliferation in spontaneous breast cancer of C3H. III. The growth fraction. J Natl Cancer Inst 28:1015–1029, 1962.
2. EPIFANOVA OI, and TERSKIKH VV. On the resting periods in the cell life cycle. Cell Tissue Kinet 2:75–93, 1969.
3. LAJTHA LG, OLIVER R, and GURNEY CW. Kinetic model of a bone-marrow stem-cell population. Br J Haematol 8:442–460, 1962.
4. LAJTHA LG. On the concept of the cell cycle. J Cell Comp Physiol 62:143–145, 1963.
5. BASERGA R. The relationship of the cell cycle to tumor growth and control of cell division: a review. Cancer Res 25:581–595, 1965.
6. GELFANT S. Patterns of cell division: the demonstration of discrete cell populations. *In* Methods in Cell Physiology (Prescott DM, ed). New York, Academic Press, vol 2, 1966, pp 359–395.
7. DOMBERNOWSKY P, and HARTMANN NR. Analysis of variations in the cell population kinetics with tumor age in the L1210 ascites tumor. Cancer Res 32:2452–2458, 1972.
8. DOMBERNOWSKY P, BICHEL P, and HARTMANN NR. Cytokinetic analysis of the JB-1 ascites tumour at different stages of growth. Cell Tissue Kinet 6:347–357, 1973.
9. ———. Cytokinetic studies of the regenerative phase in the JB-1 ascites tumour. Cell Tissue Kinet 7:47–60, 1974.
10. HARTMANN NR, and DOMBERNOWSKY P. Autoradiographic and cytophotometric analyses of the resting stages of the L1210 ascites tumor. Cancer Res 34:3296–3302, 1974.
11. DOMBERNOWSKY P, and BICHEL P. Cytokinetic variations during ageing and regenerative growth in the JB-1 ascites tumour studied by impulse cytophotometry. Acta Pathol Microbiol Scand [A] 83:222–228, 1975.
12. ANDERSSON GKA, and KJELLSTRAND PTT. A cytophotometric study of the DNA distribution in Ehrlich ascites tumour populations at different stages of development. Virchows Arch B Cell Path 16:311–318, 1974.
13. DECOSSE J, and GELFANT S. Demonstration of subpopulations in ascites tumor cells. Proc Am Assoc Cancer Res 7:17, 1966.
14. ———. Noncycling tumor cells: mitogenic response to antilymphocytic serum. Science 162:698–699, 1968.
15. FRINDEL E, VALLERON AJ, VASSORT F, ET AL. Proliferation kinetics of an experimental ascites tumour of the mouse. Cell Tissue Kinet 2:51–65, 1969.
16. LALA PK, and PATT HM. A characterization of the boundary between the cycling and resting states in ascites tumor cells. Cell Tissue Kinet 1:137–146, 1968.
17. PEEL S, and FLETCHER PA. Changes occurring during the growth of Ehrlich ascites cells in vivo. Eur J Cancer 5:581–589, 1969.
18. BICHEL P, and DOMBERNOWSKY P. Resting stages of the JB-1 ascites tumour in the irradiated mouse. Eur J Cancer 11:425–431, 1975.
19. ———. On the resting stages of the JB-1 ascites tumour. Cell Tissue Kinet 6:359–367, 1973.
20. BASERGA R, and GOLD R. The uptake of tritiated thymidine by newly transplanted Ehrlich ascites tumor cells. Exp Cell Res 31:576–585, 1963.
21. BURNS ER. Initiation of DNA synthesis in Ehrlich ascites tumor cells in their plateau phase of growth. Cancer Res 28:1191–1196, 1968.
22. WIEBEL F, and BASERGA R. Cell proliferation in newly transplanted Ehrlich ascites tumor cells. Cell Tissue Kinet 1:273–280, 1968.
23. HARRIS JW, MEYSKENS F, and PATT HM. Biochemical studies of cytokinetic changes during tumor growth. Cancer Res 30:1937–1946, 1970.
24. SCHIFFER LM, and MARKOE AM. Earliest cytokinetic response after stimulation from G_0 and prolonged G_1. Proc Am Assoc Cancer Res and ASCO 15:7, 1974.
25. DOMBERNOWSKY P, and BICHEL P. Recycling of resting cells in the JB-1 ascites tumour after treatment with 1-β-D-arabinofuranosylcytosine (Ara-C). Cell Tissue Kinet 9:9–18, 1976.
26. BHUYAN BK, FRASER TJ, GRAY LG, ET AL. Cell-kill kinetics of several S-phase-specific drugs. Cancer Res 33:888–894, 1973.
27. YATAGANAS X, STRIFE A, PEREZ A, ET AL. Microfluorimetric evaluation of cell kill kinetics with 1-β-D-arabinofuranosylcytosine. Cancer Res 34:2795–2806, 1974.
28. SHEEHY PF, FRIED J, WINN R, ET AL. Cell cycle changes in ovarian cancer after arabinosylcytosine. Cancer 33:28–37, 1974.
29. LAMPKIN BC, NAGAO T, and MAUER AM. Synchronization and recruitment in acute leukemia. J Clin Invest 50:2204–2214, 1971.
30. SALMON SE. Expansion of the growth fraction in multiple myeloma with alkylating agents. Blood 45:119–129, 1975.
31. GABUTTI V, PILERI A, TAROCCO RP, ET AL. Proliferative potential of out-of-cycle leukaemic cells. Nature 224:375–376, 1969.
32. POST J, SKLAREW RJ, and HOFFMAN J. Immediate and delayed effects of nitrogen mustard on cell replication in an autogenous rat sarcoma. J Natl Cancer Inst 52:1897–1903, 1974.
33. DECOSSE JJ, and GELFANT S. Effect of hydrocortisone on cell division of tumor cells. Surg Forum 18:80–81, 1967.
34. HOELZER D, KURRLE E, DIETRICH M, ET AL. The effect of continuous cell removal on blast cell kinetics in acute leukaemia. Scand J Haematol 12:311–320, 1974.
35. SKIPPER HE, and PERRY S. Kinetics of normal and leukemic leukocyte populations and relevance to chemotherapy. Cancer Res 30:1883–1897, 1970.

Introduction to Session on Status of Human Tumor Cell Kinetics

E. P. Cronkite [1]

It was an exciting time to be at Brookhaven in the late 1950s after tritiated thymidine was synthesized, and such distinguished individuals as the late Henry Quastler and Taylor, Woods, and Hughes applied this material to the study of chromosomal replication. The initial studies were performed in the mouse and rat, and then a series of studies were done in the medical department with the participation of Drs. Killmann, Feinendegen, Johnson, Bond, Stryckmans, Schiffer, Greenberg, Odartchenko, and others. It was exciting to be able to characterize for the first time the sequence of events in normal erythropoiesis and normal granulocytopoiesis. Some initial studies were done in multiple myeloma, acute myelocytic and monocytic leukemia, glioblastoma multiforme, and breast tumors. We had great expectations and were excited to see these studies go on throughout the world and see the application of this material in the study of human and animal disease, and in the regulation of cell proliferation in general. However, nearly 20 years later, I must ask the question: Have our great expectations of the late 1950s been fulfilled? Certain things are evident. Drs. Mauer, Baserga, and Mendelsohn and their groups have made solid and substantial contributions to the understanding of human leukemia and the growth fraction in solid tumors of the mouse. There were substantial studies made by Lala and Patt on granulopoiesis and the influence of cell density on growth rates in the ascites tumor.

But where do we go from there? Briefly, I observed during the previous session some very small differences in labeling and mitotic indices that are called significant, and a cause and effect relationship has been imputed. Are these parameters that are being measured, including DNA content, biologically constant or do they cycle with time? If, in fact, they do cycle with time, a point-to-point analysis is utterly futile. One has to integrate over an entire cycle before one can impute any cause and effect relationship.

Without belaboring the obvious I would like to point out again that one determines a labeling index by autoradiography. Does one really consider adequately the physical factors that influence autoradiographic efficiency, the constant thickness of material overlying the nucleus, the self-absorption of the tritium, and the background corrections? Does one then ask the question: Is in fact DNA synthesis really time constant? If not, there is a built-in variation in the labeling index that has to be considered. What is the relative efficiency of the incorporation of tritiated thymidine via the de novo pathway and the salvage pathways? This makes a tremendous difference in the intensity of the labeling and, hence, the labeling index. I really do question whether these factors are being adequately controlled and/or considered.

Another problem of potential biologic importance is the outgrowth of the initial studies that Killmann made at Brookhaven on multiple myeloma. From the determination of the generation times and tumor masses, it is quite obvious that there is a tremendous spontaneous death rate. Otherwise, within a very short period of time a mass of myeloma cells would be produced that would be equivalent to body mass. What are the factors that determine whether a cell recycles or is destined to die without recycling? Perhaps we have grown too accustomed to thinking that cell proliferation is the important parameter; perhaps the biologic factors that determine whether a cell cycles or is destined to die are the important ones, just as they are in normal cells.

The papers presented by the participants in this session will address themselves to these questions that have been raised.

[1]Brookhaven National Laboratory, Upton, NY.

Role of Radioautographic Studies in Clinical Investigative Oncology and Chemotherapy

Stanley E. Shackney [1,*]

SUMMARY

Three clinical areas are identified in which radioautographic studies may be of practical usefulness. First, human tumors can be classified according to the predominant pattern of DNA synthesis in the slowly proliferating cell fraction. This classification scheme groups carcinoma of the breast and ovary together, melanoma and carcinoma of the lung together, and places acute adult leukemia in a separate class. If there are correlations between kinetic characteristics and drug response behavior, this classification scheme may simplify the clinical study of new drugs and drug combinations. Second, changes in the labeling index (LI) and/or cell labeling intensity may serve as useful guides in drug scheduling. There are circumstances where changes in cell labeling intensity may be more reliable than changes in the LI. Third, cell morphology, population kinetics, and clinical course may all be correlated in certain human tumors, particularly the lymphomas. Supporting evidence in Sézary's syndrome is presented.

[Cancer Treat Rep 60:1873–1886, 1976]

Despite the difficulties involved in carrying out radioautographic studies employing tritiated thymidine (^{3}H-TdR) administered in vivo in man, such studies are capable of providing important kinetic information which cannot be obtained in any other way. I would like to focus on three clinical areas in which such radioautographic information may contribute to the design of therapeutic regimens and guide their application in individual patients. These areas are: (*a*) the kinetic classification of human tumors, (*b*) the monitoring of the kinetics of drug response in normal and neoplastic tissues in man, and (*c*) the exploration of kinetic-histopathologic correlations.

In figure 1, the percent labeled mitosis (PLM) curves in two patients with adult acute leukemia (1) are compared with three PLM curves in malignant melanoma (2,3). You will note that there are similarities among the PLM curves of patients with the same tumor, and what appear to be consistent differences between the two malignancies. In particular, the first wave in leukemia approaches 100% peak labeling and exhibits steep ascending and descending limbs. In melanoma, a maximum of 70%–90% of the mitoses are labeled and the ascending and descending limbs of the first wave are less steep than in leukemia. In leukemia the trough occurs at 24–32 hours. In melanoma, if there is a trough, it occurs at 48–72 hours. In leukemia there is a lightly labeled second wave which peaks at 48–72 hours and is spent for the most part by 120 hours. In melanoma, there is a broad second wave which extends far beyond 120 hours. There is one other difference which is not often utilized in kinetic analyses, ie, in the leukemia study there were cells with grain counts exceeding 100 grains/cell (1), whereas in the melanoma study the most heavily labeled 10% of the population had a mean grain count of about 70 grains/cell (2). One would be hard put to explain all of the observed differences on the basis of differences in radioautographic technique.

Obviously, it would be preferable to do more than just catalog these differences; one would like to interpret them in some meaningful and cohesive way. The classic approach has been to obtain estimates of cell-cycle time and cycle-phase durations from the data by any one of several methods that were developed for this purpose. Cell-cycle time (T_c) and S-phase (T_s) durations obtained in these studies

[1]Division of Cancer Treatment (DCT), National Cancer Institute (NCI), Bethesda, Md.

Reprint requests to: Stanley E. Shackney, MD, DCT, NCI, Bldg 10, Rm 6N113, National Institutes of Health, Bethesda, Md 20014.

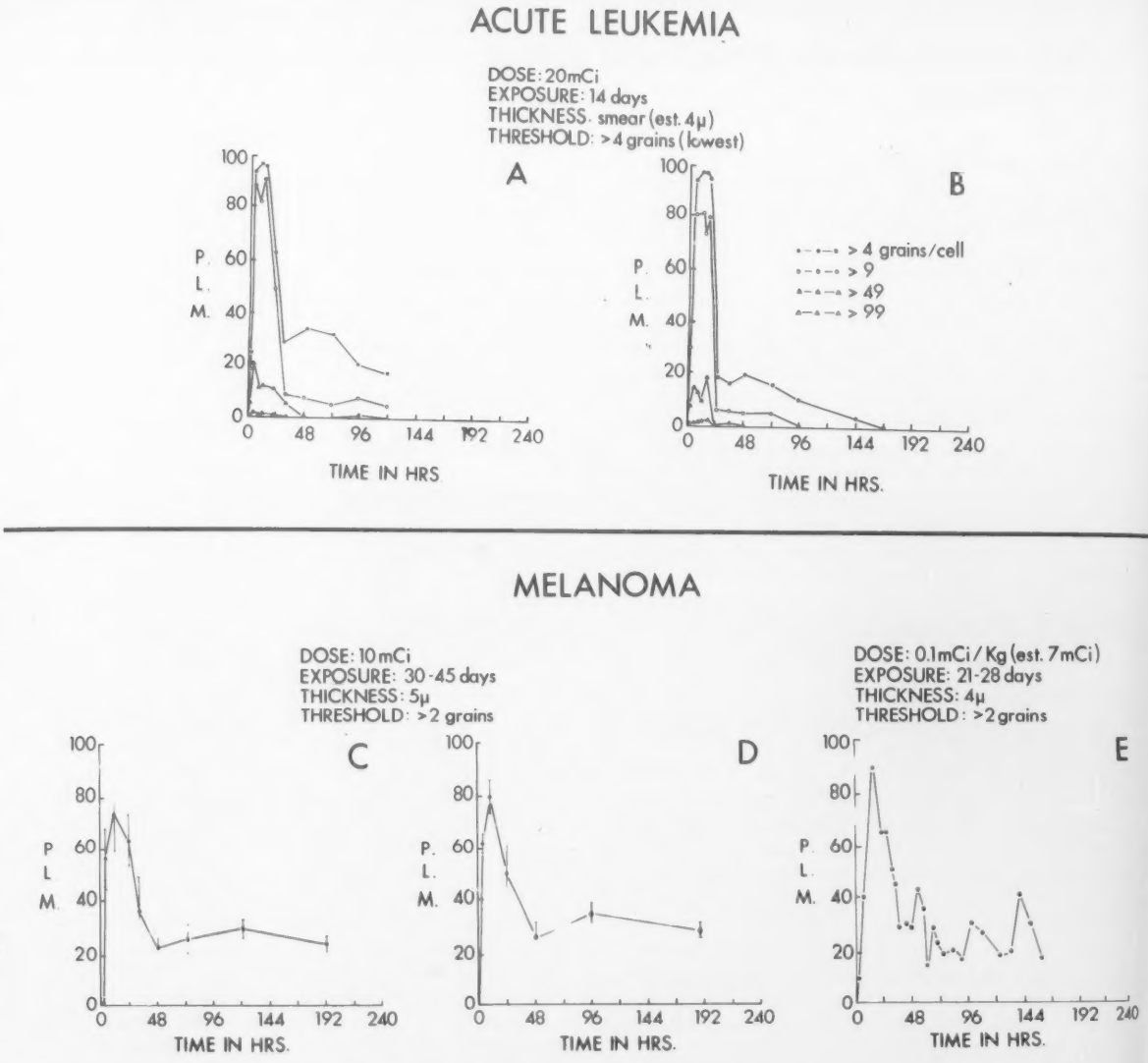

FIGURE 1.—(A,B) PLM curves in adult acute leukemia (1). (C–E) PLM curves in melanoma (2,3).

are given in table 1. In this instance, computed cycle time and cycle-phase durations simply do not reflect the differences that are readily discernible in the raw data.

Another approach to quantitative evaluation of the data is that of computer simulation. The computer simulation system that I have used has been described elsewhere in detail (4,5). For the present discussion, I would like to simply mention some of its basic features. Provision is made for a cell-cycle time distribution whose mean and variance change with population size. The cell-cycle time distribution is divided into discrete classes for computational purposes (fig 2A). Each cell-cycle time class is further compartmentalized and cells are distributed not only among cycle-time classes but throughout each cycle-time class as well (fig 2G). The rate of DNA synthesis, as reflected by radioautographic

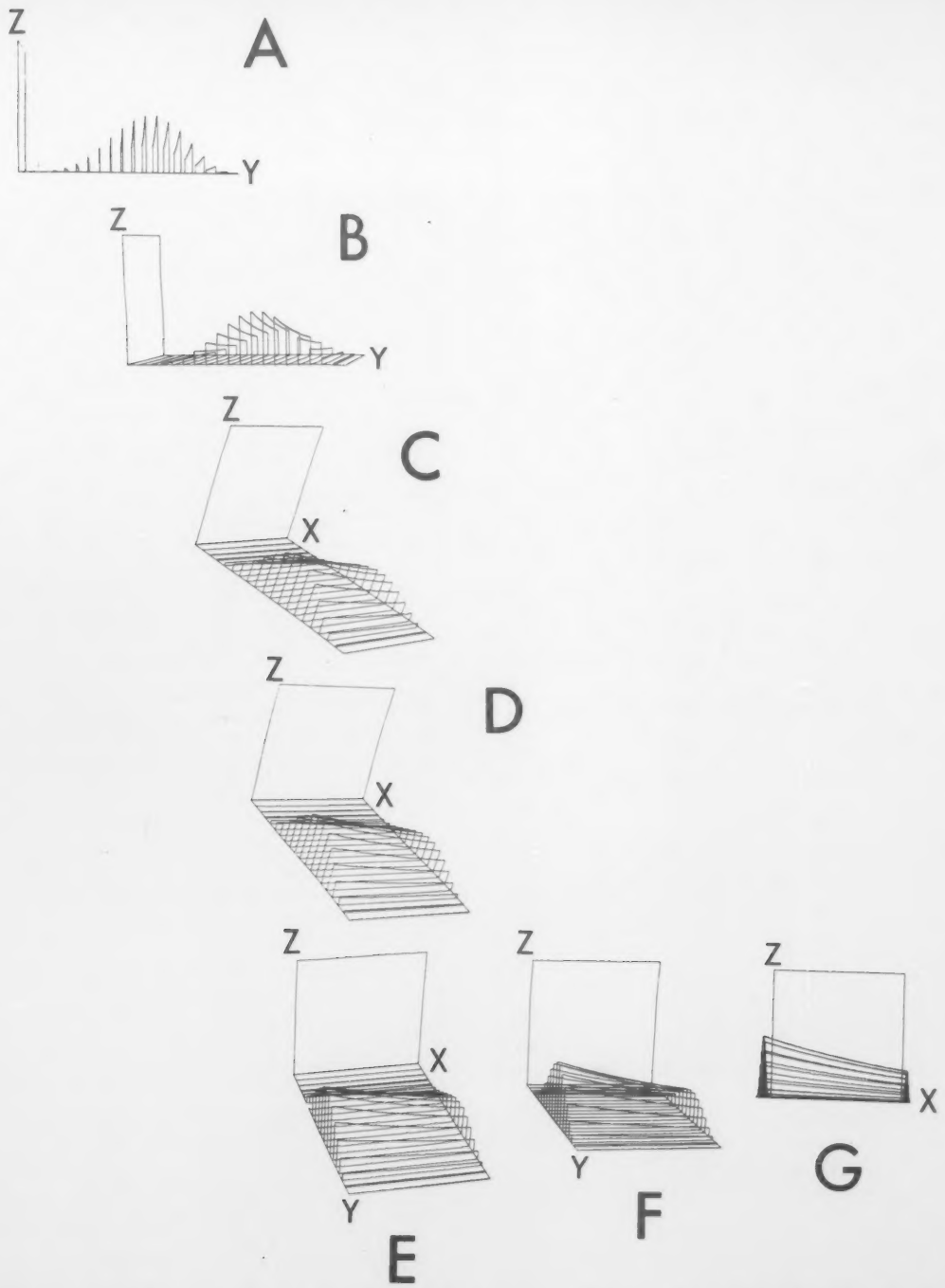

FIGURE 2.—Bivariate distribution of cells among cell-cycle time classes and within the cell cycle shown in different projections. x-Axis = fraction of cell cycle completed; y-axis = cell-cycle time class; x-axis = cell frequency. (A) Projection showing the cell-cycle time distribution. (G) Projection showing the relative cell-age distribution. (B–F) Projections showing the bivariate distribution.

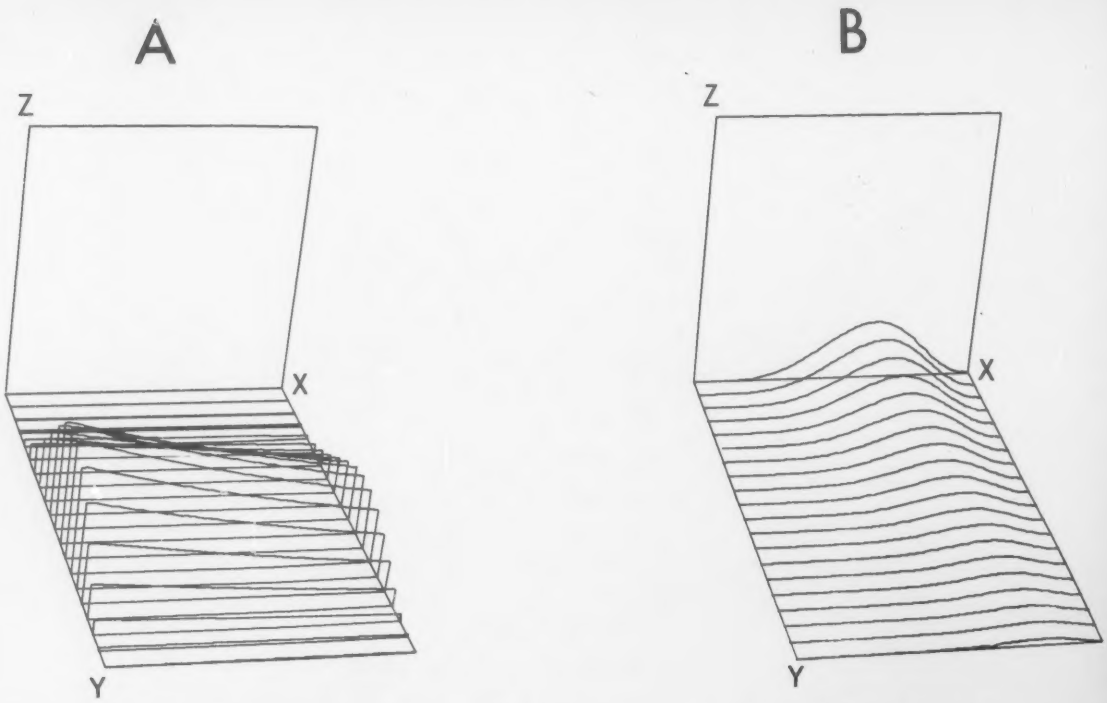

FIGURE 3.—Comparison of the cell-age/cell-cycle time distribution and the DNA synthesis rate function. (3A) Cell-age/cell-cycle time distribution. x-Axis = fraction of cell cycle completed; y-axis = cell-cycle time class; z-axis = cell frequency. (3B) DNA synthesis rate function. x-Axis = fraction of cell cycle completed; y-axis = cell-cycle time class (longest cell cycles are closest to the observer); z-axis = relative rate of DNA synthesis. The highest rates of DNA synthesis are in the shortest cell cycles, and the fraction of the cycle occupied by active DNA synthesis is greatest in the shortest cell cycles.

TABLE 1.—Estimates of cell-cycle time and S-phase duration obtained by various methods

Disease	Patient	Average S-phase duration (hrs)	Method	Average cell-cycle time duration (hrs)	Method	Ref No.
Leukemia	R.R. M.T.	22 19	Half-height method, PLM curve	49 (42–60) 83 (70–102)	Grain-count halving, most heavily labeled interphase cells	1
Melanoma	L.L. G.H.	Median, 21 Mean, 25	Barrett analysis, PLM curve	Median, 72	Barrett analysis, PLM curve	2
Melanoma	A.P.	21	Half-height method, PLM curve	42	Interval between half heights of ascending limbs, PLM curve	3

labeling intensity in pulse labeling studies, is assumed to vary, depending on where the cells are in the cycle and whether they are rapidly or slowly proliferating cells (fig 3B). There are also provisions in the model for loss of reproductive capacity and the eventual removal of nonreproductive cells from the population.

With this model it is possible to simulate multiple kinetic parameters in a given population including growth curves, PLM curves, pulse LIs, the LI as a function of time following pulse-^{3}H-TdR exposure, mitotic and interphase cell grain-count distributions as a function of time following pulse-^{3}H-TdR exposure, mitotic and interphase labeling curves during continuous ^{3}H-TdR exposure, DNA content distributions, and combined DNA content-radioautographic studies.

Given a constant cell-cycle time distribution (fig 4A), three DNA synthesis patterns can be distinguished in the simulations which I have designated as type I (fig 4B), intermediate (fig 4C), and type II (fig 4D). The type II pattern is equivalent to a constant S + G_2 with prolongation of G_1 as cell-cycle time lengthens. In the type I pattern low rates of DNA synthesis are spread over a prolonged period during long cell cycles. The type I and intermediate patterns do not have satisfactory equivalents in the classic model since the detection of light label and, therefore, the duration of S phase are highly dependent on relative radioautographic exposure.

Distinctive multithresholded PLM curves are obtained for the type I (fig 4E), intermediate (fig 4F), and type II (fig 4G) DNA synthesis patterns. The type I pattern produces a PLM curve which has no demonstrable second wave. The first wave is generally broad; it may or may not reach 100% labeling. The majority of mitoses are generally more lightly labeled than in intermediate or type II curves. The first wave in type II PLM curves lies close to the origin, approaches 100% labeling, has steep ascending and descending limbs, and includes a significant fraction of heavily labeled mitoses. There is a deep trough which occurs early and separates the first wave from a low, broad, relatively lightly labeled second wave. Intermediate curves exhibit intermediate features; the most prominent second waves are generated by intermediate DNA synthesis patterns. PLM curves exhibiting distinctive patterns comparable to those produced in the simulations are, in fact, observed in human tumors (fig 5).

Of course, one would like some independent corroborative evidence that these distinctions are real and that they are indeed attributable to differences in DNA synthesis rate patterns. Paired simulated mitotic and interphase labeling curves during long-term ^{3}H-TdR infusions are shown in figure 6 for each of the three DNA synthesis patterns. You will note that in the type II population, mitoses label rapidly in comparison with the interphase cells. In the type I population the mitotic labeling rate is lower, tending to approach the interphase labeling rate. Thus, a comparison of mitotic and interphase labeling rates in the same population should provide useful information regarding the patterns of DNA synthesis in the population.

Distinctive mitotic and interphase labeling patterns are, in fact, discernible in long-term infusion studies in human tumors (fig 7). The labeling curves in breast cancer suggest a type I pattern. The available PLM curve data in breast cancer exhibit relatively broad single first waves, supporting its classification as a type I population (3,6,7). In melanoma and leukemia, both the PLM curves and long-term infusion data confirm their classification as intermediate (2) and type II populations (8–10) respectively. The computer simulation studies that I have described here are considered in greater detail in a separate paper (see footnote 2).

The above distinctions are reflected in other measurements as well. If the pulse LI is high, but labeling intensity is low, a type I pattern is suggested. Again, breast cancer appears to fit this pattern (3). A low pulse LI with high grain counts among the labeled cells would be consistent with a type II pattern. Again, adult leukemia falls into place in this respect (1).

A grouping of human tumors by DNA synthesis pattern is shown in table 2. I have included only those tumors that could be classified according to this scheme with reasonable certainty. For example, there are abundant data for head and neck tumors (11–13), but in many cases the data were particularly noisy and/or relative radioautographic exposure appeared to be insufficient for a clear pattern to be discerned. Labeling intensity data would be highly useful for purposes of kinetic classification, but such data are hard to come by in the literature.

As for the tumors that do appear in table 2, a better grouping could not have been hoped for. One might expect that anatomic and histologic tumor classifications would be ideal for diagnosis and prognosis, but that a functional classification might be more useful for therapeutic purposes. The grouping shown in table 2 is very much in keeping with that expectation. Cancer of the breast and ovary exhibit similar spectra of response to single drugs. The DNA synthesis pattern assigned to acute leukemia is consistent with the high-dose, intermittent, S-phase drug therapy which appears to be most effective in this disease. Historically, both melanoma and carcinoma of the lung have been relatively unresponsive to chemotherapy; their apparent kinetic similarities would suggest that chemotherapeutic

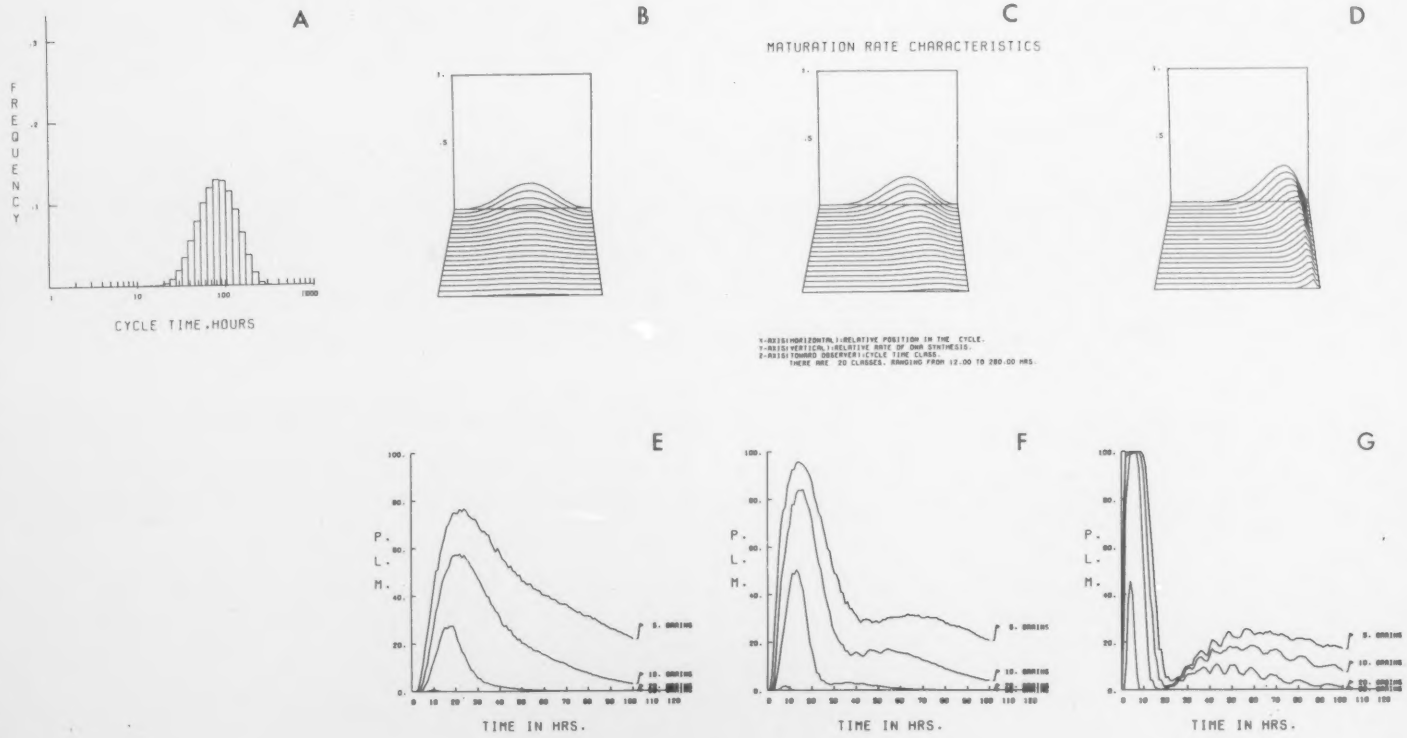

FIGURE 4.—Simulated multithresholded PLM curves at constant cell-cycle time (A) but with different DNA synthesis rate patterns. Type I DNA synthesis pattern (B) produces a type I PLM curve (E). Intermediate DNA synthesis pattern (C) produces an intermediate PLM curve (F). Type II pattern (D) produces a type II PLM curve (G).

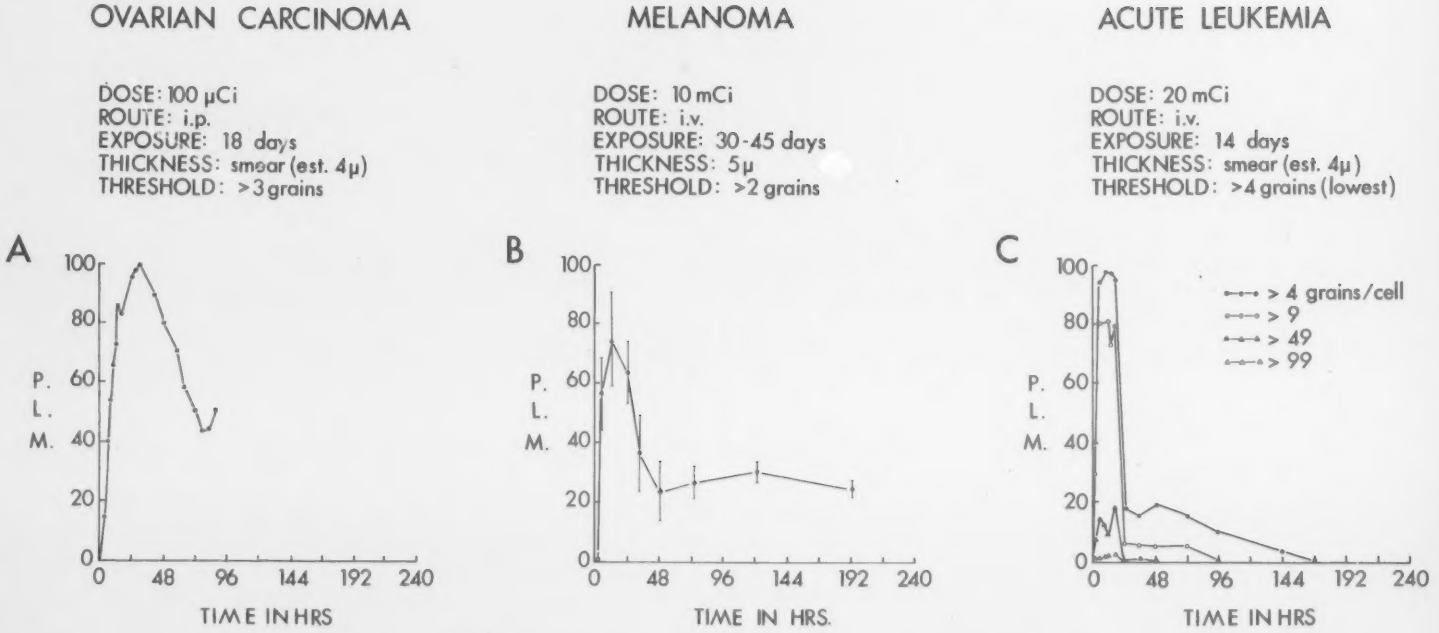

FIGURE 5.—PLM curves in human tumors which exhibit type I, intermediate, and type II patterns. (A) PLM curve in ovarian carcinoma (17). (B) PLM curve in melanoma (2). (C) PLM curve in adult acute leukemia (1).

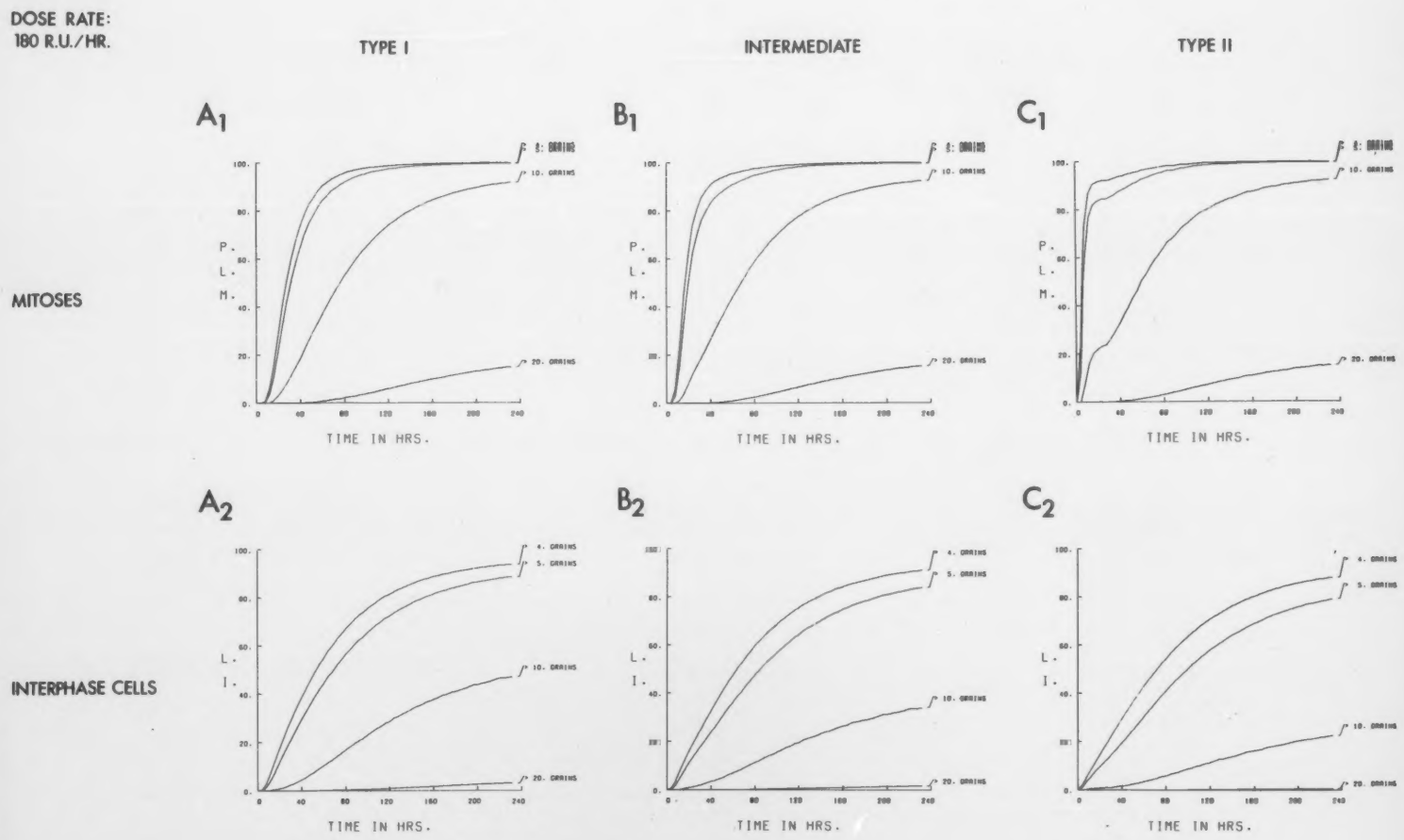

FIGURE 6.—Simulated multithresholded long-term ^{3}H-TdR labeling curves of mitoses and interphase cells for type I, intermediate, and type II DNA synthesis patterns. (A_1) Type I mitotic and (A_2) interphase labeling curves. (B_1) Intermediate mitotic and (B_2) interphase curves. (C_1) Type II mitotic and (C_2) interphase curves.

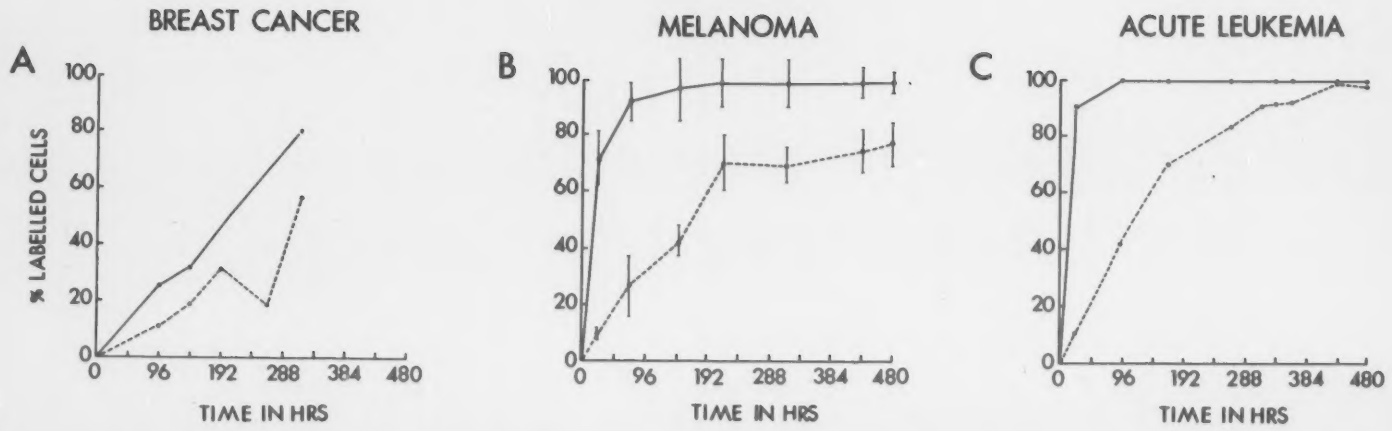

FIGURE 7.—Mitotic (solid lines) and interphase (broken lines) long-term ^{3}H-TdR infusion curves in human tumors. (A) Breast cancer (13), (B) melanoma (2), (C) acute adult leukemia (8).

TABLE 2.—Grouping of human tumors by DNA synthesis pattern*

Type I	Intermediate	Type II
Breast carcinoma (3,6,7,13)	Melanoma (2,3)	Adult acute leukemia (1,8–10)
Ovarian carcinoma (17)	Bronchogenic carcinoma (11)	

*Ref Nos. in parentheses.

strategies that prove to be effective in one tumor might be worth pursuing in the other.

If it is borne out that tumors with similar kinetic characteristics can also be grouped together with respect to their response to chemotherapeutic manipulation, it may be possible in the future to simplify the clinical study of new drugs and drug combinations considerably.

When labeling intensity information is taken into account, information may also be obtained regarding the frequencies of the various cell-cycle time classes in the population. Using the simulation system described above, it has been possible to show that mean cell-cycle time is of the order of 72 hours in leukemia and 100 hours in melanoma.[2] What is more important, however, is that the range of cell-cycle times spans well over several hundred hours in both tumor types. Given this degree of population heterogeneity it would not seem worthwhile to pursue therapeutic strategies that would rely on differences in *average* cycle time and cycle-phase durations, since these average values might be expected to apply to only a small fraction of the population.

Whatever alternative therapeutic approaches might be tried, if the choices are to be rational ones they must be dictated by quantitative data on the kinetics of response to therapy. Among the various radioautographic measurements that are available, serial in vitro labeling studies would appear to be the most suitable for monitoring transient kinetic changes in man. Here too, changes in labeling intensity may prove to be no less important than changes in the LI itself. I would like to illustrate this point with data obtained in our laboratory in Sarcoma 180 in vitro. In the study shown in figure 8, cells were harvested after a half-hour exposure to ^{3}H-TdR given at various times before and after a 2-hour exposure to hydroxyurea.[3] Mean grain count/cell fell sharply during the 2-hour exposure to drug, remained low for several hours, and rebounded at 6–10 hours. The LI did not change significantly during and shortly after drug exposure, and rose only slightly between 6 and 10 hours. If it weren't for the changes in labeling intensity, the magnitude and time course of the kinetic effects of hydroxyurea might not have been fully appreciated.

In parallel flow microfluorometric studies we have been able to show that the changes in labeling intensity during recovery from drug effects are correlated with changes in the rate of DNA synthesis (manuscript in preparation). This would suggest that we may have to consider drug effects in terms of the modulation of the rate of cell-cycle traverse, in addition to, or perhaps instead of, the imposition of all-or-none blocks at discrete points in the cell cycle.

The consideration of labeling intensity may raise certain problems with regard to the collection and interpretation of serial in vitro labeling data in man. There is no way to insure that labeling conditions in vitro will be comparable to those in vivo. In cell suspensions, such as those obtained from bone marrow or peripheral blood, experimental conditions may be adjusted so that in vitro LIs correspond to those observed in vivo. It is hoped that in vivo and in vitro grain-count distributions would then correspond as well, but this remains to be shown. In the case of solid tumor fragments one cannot count on uniform ^{3}H-TdR delivery to all cells. The peripheral zones of such fragments tend to be

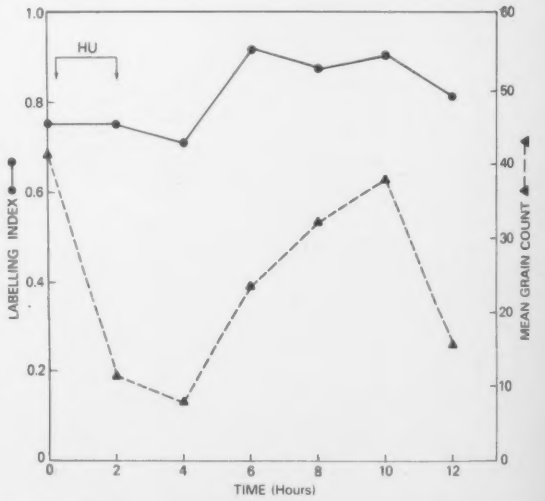

FIGURE 8.—LI (solid line) and mean grain count (broken line) as functions of time in Sarcoma 180 in vitro in relation to a 2-hr exposure to hydroxyurea (HU).

[2]Shackney SE. A cytokinetic model for heterogeneous mammalian cell populations. III. Tritiated thymidine studies: correlations among multiple kinetic parameters in human tumors. J Theor Biol. In press.

[3]Hydroxyurea: NSC-32065; CAS reg. No. 127-07-1.

heavily labeled in vitro while their centers may not be labeled at all (14). Such spatial distribution patterns of labeling are different from those found in in vivo labeling studies (14); it is not altogether clear just how one might relate them to tumor population growth and drug response in vivo. Cell-dispersal techniques may obviate this problem for solid tumors (15), but one must be concerned that such manipulations might affect the labeling characteristics of the cells. Again, this is an area that needs to be explored.

Another important area where cell kinetics may have useful patient-care applications is that of kinetic-cytologic correlations. We might take as our point of departure the classification scheme for the lymphomas recently proposed by Lukes and Collins (16), which attempts to interpret lymphocyte morphology as a reflection of functional immunologic state. These authors have suggested that the large cells in what were previously classified as histiocytic lymphomas or reticulum cell sarcomas present all of the morphologic features of transformed lymphocytes. Now, the morphologic changes that occur during lymphocyte transformation are associated with the induction of active DNA synthesis and cell division. Does this imply that these lymphomatous histiocytes are, in fact, cells that are engaged in active DNA synthesis? Does an increase in the fraction of large cells with large round nuclei in a lymphoma imply an increase in the T_s/T_c ratio? Given a high T_s/T_c ratio, can we differentiate between long T_s and T_c and short T_s and T_c? Radioautographic studies can provide answers to many of these questions. If lymphoid cells with large round nuclei are, in fact, comparable to transformed lymphocytes, they should appear labeled in radioautographic studies. If both T_s and T_c are long, the rate of DNA synthesis in individual cells may be expected to be low, and radioautographic labeling may be expected to be relatively light. Conversely, if T_s is short, the radioautographic grain count over individual cells may be expected to be heavy.

Our laboratory has been studying the kinetics of Sézary's syndrome in collaboration with the Dermatology Branch at the National Cancer Institute. In this disease there is an infiltration of abnormal lymphocytes in the skin and there are abnormal lymphocytes circulating in the peripheral blood. The disease may remain indolent for many years before entering an aggressive preterminal phase with extensive lymph node and visceral involvement.

The 2 hour pulse LIs of circulating Sézary cells are shown for three different patients in figure 9. A local background correction was applied to each cell which ranged from 0 to 3 grains in most instances. Patients 1 and 2 were in the chronic, indolent stage

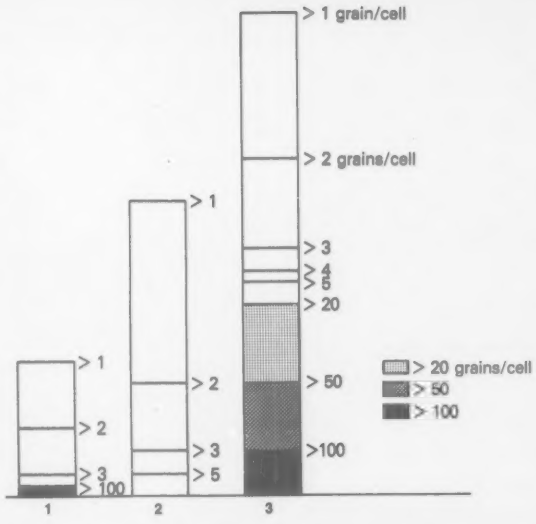

FIGURE 9.—Multithresholded LIs of circulating Sézary cells in patients 1–3.

of disease. Patient 3 had extensive visceral involvement at the time of study and died with extensive disease several months afterward. His circulating Sézary cells had the highest LI at 2 hours and many of the labeled cells exhibited very high grain counts.

The morphologic appearance of the circulating Sézary cells correlated well with the kinetic observations. The cells of patients 1 and 2 showed relatively little variation in nuclear size. The cells of patient 1 are shown in figures 10A–C. In patient 3 the variation in size and shape was considerable (figs 10D–F). Heavy labeling was observed primarily in cells with intermediate-to-large nuclei.

It would seem that at least certain aspects of the Lukes and Collins' proposal (16) are supported by these observations. Large cells with large nuclei are indeed the ones most likely to be engaged in active DNA synthesis, and the presence of such cells in increased numbers does seem to correlate with aggressive tumor behavior. The relatively high LI in patient 3 and the abundance of heavily labeled cells are suggestive of a higher T_s/T_c ratio and shorter T_s and average T_c than in the other two patients. PLM-curve studies on skin biopsy material are currently in progress and should provide more definitive kinetic information in these patients.

It is impossible to say whether the kinetic and morphologic features that accompany an aggressively malignant clinical course are due specifically to immunologic factors as Lukes and Collins (16) suggest, or to some other underlying mechanism. Regardless, it should be recognized that the func-

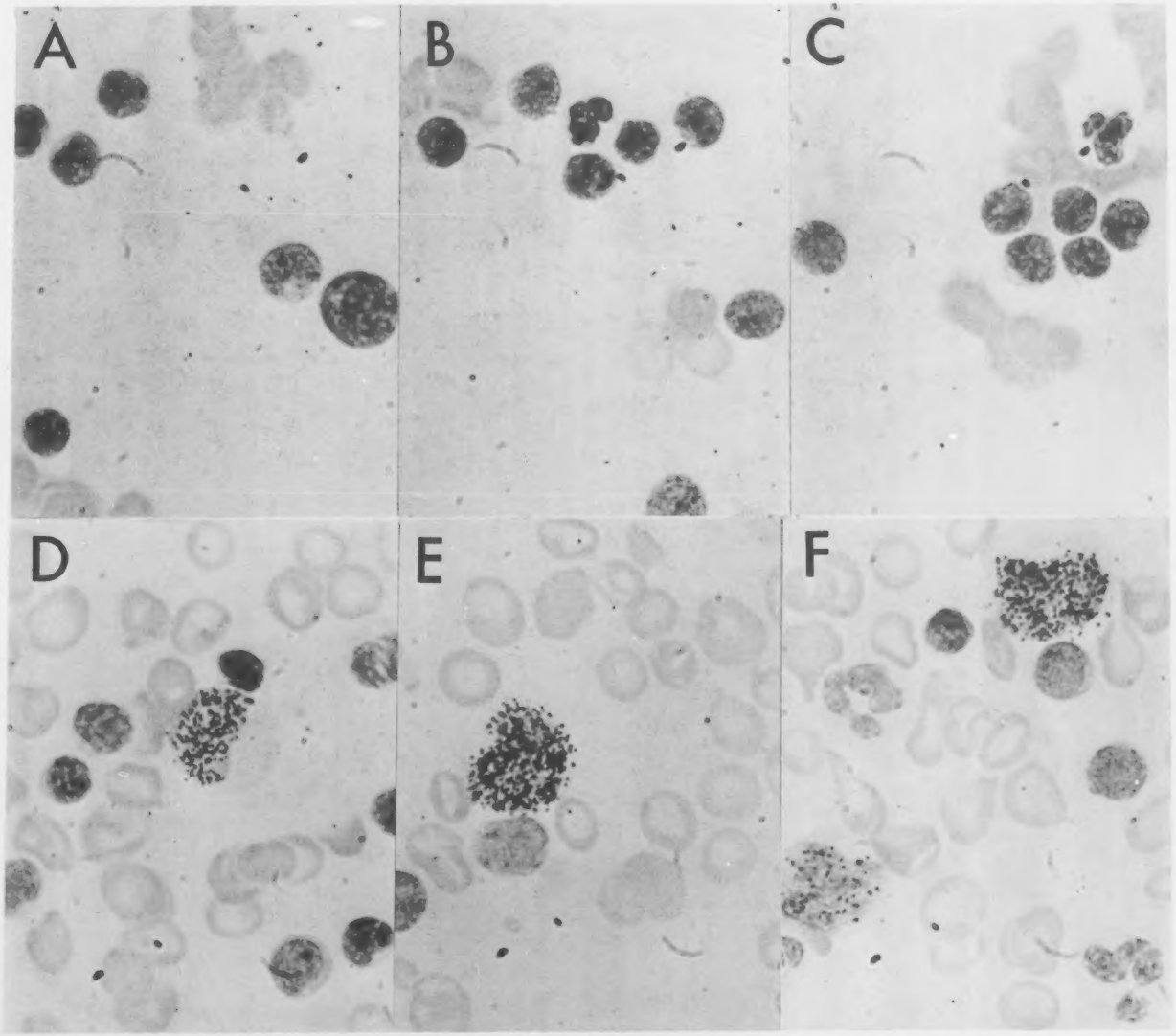

FIGURE 10.—(A–C) Radioautographs of circulating Sézary cells in patient 1, 2 hrs after ^{3}H-TdR administration. Note absence of label and predominance of small Sézary cells. (D–F) Radioautographs of circulating Sézary cells in patient 3, 2 hrs after ^{3}H-TdR administration. Note greater variation in cell and nuclear size and heavy labeling predominantly in the larger cells.

tional classification proposed by these authors represents a novel approach to histopathologic material with far-reaching implications. The notion that morphologic appearance is inherited from a specific progenitor cell through some fixed differentiational sequence seems to have given way to the assumption that morphologic appearance may vary among members of the same cell population, depending on the various metabolic activities in which the cells were engaged at the time of fixation. This is hardly new to the cell kineticist who has long since recognized that cells undergo sequential changes as they traverse the cell cycle. However, this approach is relatively new to the discipline of histopathology and undoubtedly its full impact on histopathology over the long term will be profound.

To conclude, the available evidence indicates that radioautographic studies are useful in the kinetic classification of human tumors and that patterns of kinetic behavior may correlate with patterns of tumor response to chemotherapy. The proposed classification scheme makes a virtue of heterogeneity in cell-cycle times inasmuch as it depends on the demonstration of distinctive DNA synthesis rate patterns among the more slowly proliferating cells in the population. For this reason, it is particularly well suited for the kinetic analysis of human cell populations. In contrast, if one relies on methods of analysis which do not distinguish between slowly proliferating and nonproliferating cells, the kinetic distinctions among tumors may not be appreciated.

Radioautographic kinetic classification studies are tedious and time consuming. They provide necessary basic information, but they are not likely to affect the clinical management of the individual patients under study. Hopefully, once definitive studies are performed in a sufficient number of patients with a given tumor type, these studies will not have to be repeated. For example, I believe that we now have a basic set of kinetic data in human adult acute leukemia that is quite adequate for purposes of kinetic classification. I think it is unlikely that the study of additional patients with adult acute leukemia using ^{3}H-TdR will yield much more information than we now have regarding population cell-age structure and DNA synthesis patterns in advanced disease. Before too long we may be able to say the same for malignant melanoma and human breast cancer.

In vitro labeling studies for the monitoring of drug response should be viewed somewhat differently from the kinetic classification studies. It is conceivable that in vitro labeling studies could achieve the status of routine laboratory tests, and play an important role in the management of individual patients. What is more, as the human kinetic data base is broadened, the demonstration of kinetic-morphologic correlations may permit limited but potentially valuable inferences regarding population kinetic behavior in individual patients from cell morphology alone.

The theme that ties together the three areas dealt with in this paper is the importance of information on cell labeling intensity in individual cells in radioautographic studies. When labeling intensity is considered together with LI data, a new dimension is added to the analysis of cell population kinetic behavior.

REFERENCES

1. CLARKSON B, OHKITA T, OTA K, ET AL. Studies of cellular proliferation in human leukemia. I. Estimation of growth rates of leukemic and normal hematopoietic cells in two adults with acute leukemia given single injections of tritiated thymidine. J Clin Invest 46:506–529, 1967.
2. SHIRAKAWA S, LUCE JK, TANNOCK I, ET AL. Cell proliferation in human melanoma. J Clin Invest 49:1188–1199, 1970.
3. TERZ JJ, CURUTCHET HP, and LAWRENCE W, JR. Analysis of the cell kinetics of human solid tumors. Cancer 28:1100–1110, 1971.
4. SHACKNEY SE. A cytokinetic model for heterogeneous mammalian cell populations. I. Cell growth and cell death. J Theor Biol 38:305–331, 1973.
5. SHACKNEY SE. A cytokinetic model for heterogeneous mammalian cell populations. II. Tritiated thymidine studies. The percent labelled mitosis (PLM) curve. J Theor Biol 44:49–90, 1974.
6. YOUNG RC, and DEVITA VT, JR. Cell cycle characteristics of human solid tumors in vivo. Cell Tissue Kinet 3:285–290, 1970.
7. POST J, SKLAREW RJ, and HOFFMAN J. Replication kinetics of human breast cancer cells in vivo and in vitro. Proc Am Assoc Cancer Res and ASCO 16:34, 1975.
8. CLARKSON BD. Review of recent studies of cellular proliferation in acute leukemia. Natl Cancer Inst Monogr 30:81–119, 1969.
9. CLARKSON B, FRIED J, STRIFE A, ET AL. Studies of cellular proliferation in human leukemia. III. Behavior of leukemic cells in three adults with acute leukemia given continuous infusions of ^{3}H-thymidine for 8–10 days. Cancer 25:1237–1260, 1970.
10. CLARKSON B, TODO A, OGAWA M, ET AL. Consideration of the cell cycle in chemotherapy of acute leukemia. Recent Results Cancer Res 36:88–118, 1971.
11. FRINDEL E, MALAISE E, and TUBIANA M. Cell proliferation kinetics in five human solid tumors. Cancer 22:611–620, 1968.
12. FRIEDMAN M, NERVI C, CASALE C, ET AL. Significance of growth rates, cell kinetics, and histology in the irradiation and chemotherapy of squamous cell carcinoma of the mouth. Cancer 31:10–16, 1973.
13. TERZ JJ, and CURUTCHET HP. Cell kinetics of human solid tumors following continuous infusion of ^{3}H-TdR. *In* The Cell Cycle in Malignancy and Immunity, Conf. 731005. Springfield, Va, National Technical Information Center, US Energy Research and Development Administration, 1975, pp 323–329.
14. IVERSEN OH, IVERSEN U, ZIEGLER JL, ET AL. Cell kinetics in Burkitt lymphoma. Eur J Cancer 10:155–163, 1974.
15. LIVINGSTON RB, AMBUS U, GEORGE SL, ET AL. In vitro determination of thymidine-^{3}H labelling index in human solid tumors. Cancer Res 34:1376–1380, 1974.

16. LUKES RJ, and COLLINS RD. Immunologic characterization of human malignant lymphoma. Cancer (suppl)34:1488–1503, 1974.

17. SHEEHY PF, FRIED J, WINN R, ET AL. Cell cycle changes in ovarian cancer after arabinosylcytosine. Cancer 33:28–37, 1974.

Comparison of Cell Proliferation Kinetics in Human and Experimental Tumors: Response to Irradiation

M. Tubiana* and E. Malaise [1]

SUMMARY

Available data on the parameters of cell kinetics in human solid tumors were reviewed. The mean duration of the cell cycle is 2 days; for G_1 it is 1 day, for S it is 18 hours, and for G_2 it is 6 hours. G_1 has the greatest variability from tumor to tumor. The cell cycle and its phases are shorter in animal tumors but the relative durations and variabilities are similar. The labeling index (LI) and the growth fraction vary widely among human tumors, but they are correlated with the histologic type of the tumor. There is a correlation between the mean doubling time and the mean LI of the various histologic types of tumors. Cell loss is considerable in all human tumors, but it is more important in tumors with a high LI. Metastases and recurrence appear to have shorter doubling and cell cycle times than the primary tumor. There seems to be in patients with metastases a correlation between the survival and the growth rate of the metastases. There does not seem to be any correlation between the LI and the probability of dissemination. The depression of LI after irradiation is more important in human tumors than in experimental tumors and varies widely among human tumors. After irradiation, the depopulation seems more important in tumors with a high LI. The histologic groups of tumors with a high mean LI are on the average more radiosensitive and more sensitive to drugs.

[Cancer Treat Rep 60:1887–1895, 1976]

The aim of this paper is to review briefly some of the data available on the cell kinetics of human solid tumors before and after irradiation and to compare them with what is known about experimental tumors. We shall first consider the main parameters of the kinetics of tumor cell proliferation: cell cycle time, growth fraction, and cell loss. Subsequently we shall discuss how this information could be correlated with clinical data, that is, the course of the disease and the response to treatment. Such a review of the information obtained mainly with autoradiography might be useful at a time when new techniques such as microfluorometry are introduced in clinical investigations.

[1]Institut Gustave-Roussy, Villejuif, France.

*Reprint requests to: M. Tubiana, Institut Gustave-Roussy, 94 Villejuif, France.

PRIMARY TUMORS BEFORE IRRADIATION

Cell Cycle Time

The difficulties met in studying the duration of the cell cycle (T_c) of human solid tumors are well known. For ethical reasons, the activity per unit of weight of tritiated thymidine injected into patients is ten to 20 times lower than in animals. Moreover, these investigations are permissible only in patients with a short life expectancy. On the other hand, since a percent labeled mitoses (PLM) curve requires a large number of samples, such investigations are performed only on large tumors which are easily accessible, and they are used only for tumors with a high mitotic index (1). These difficulties explain why the number of human tumors which were investigated with the PLM method is relatively small; furthermore, such investigations could introduce a bias since the tumors studied are proba-

bly not a representative sample of human solid tumors.

The PLM curves obtained from human tumors are similar to those obtained from animals, although the second peak is often very low and sometimes absent. This makes the interpretation difficult and frequently it is necessary to use a computer program to calculate the duration of the phases of the cycle (2). However, we did not limit our review to those tumors for which adequate information had been obtained with computers. In fact, the exclusion of the tumors for which a fit was not obtained could introduce a bias. Most available programs are based on assumptions such as a unimodal distribution of the duration of the phases of the cell cycle and of the total cell cycle, the absence of a correlation between the various phases of the cell cycle in each cell, and the stationarity of the cell population during the investigation (3). The exclusion of the tumors which were not fitted could result in the absence of the class of tumors for which these assumptions are not valid.

Other methods have been used: double labeling for the duration of the S phase (T_s), rate of reduction of mean grain count (MGC) per labeled mitoses after continuous labeling, and stathmokinetic methods (*see* ref 4). However, in spite of the difficulties linked to the use of the PLM method, it appears that until now most of our knowledge on the generation time of human solid tumors has been obtained with this method (4).

We have been able to collect from the literature and from our own data PLM curves obtained for 31 human solid tumors (fig 1). The median T_c is about 2 days, 90% of the values being between 15 hours and 5 days. However, these results might have been biased by the choice of the tumors which were often large superficial tumors. In order to answer this objection, a study was performed on a group of 16 squamous cell carcinomas of the mouth floor.[2] The method used was the rate of reduction of the MGC per labeled mitoses. It can be seen on figure 1 that there is no statistical difference between these two sets of values. This allows us to pool them. For these 53 tumors, a median value of T_c of 2 days was also found.

With respect to the duration of the phases of the cell cycle, we have information for 30 tumors. T_{G_2} has a median duration of about 6 hours and is the shortest one, for T_s it is about 18 hours, and for T_{G_1} it is about 1 day (table 1). The respective distributions of the duration of these various cell phases in human tumors differ very much.[3] The least variable

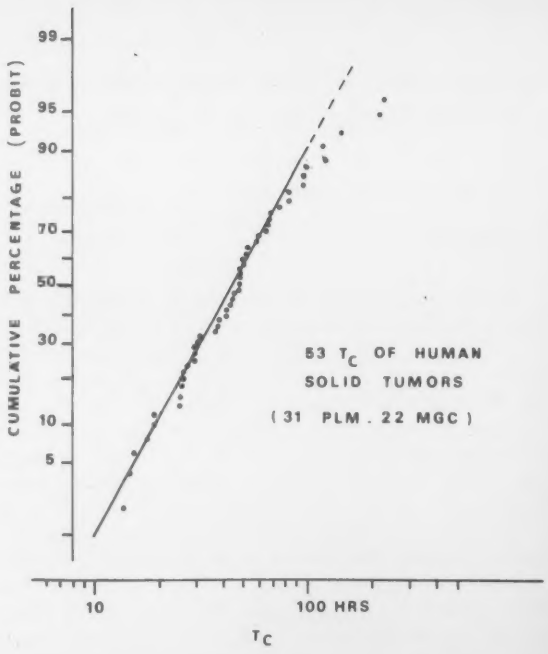

FIGURE 1.—Range of the mean T_c durations in human tumors. 53 values of T_c were collected from the literature or from our own unpublished results. For 31 patients T_c was obtained with the PLM technique and for 22 patients by the halving of the MGC. These 2 sets of data were pooled in this chart because the 2 distributions are identical.

is T_s with only a factor of 3 between the extreme values of the confidence interval; for T_{G_2} the ratio of the extreme values is 6. The most variable is T_{G_1} for which the ratio is 67 (table 1).

A correlation, that might however be a spurious correlation, was found between T_c and T_s by Mendelsohn (4) for all tissues—normal and malignant, human and animal. We observed it also in human tumors.[3] This statistically significant relation shows that the ratio of T_s/T_c varies from 0.5 when T_c is equal to 1 day, from 0.3 for a T_c of 2 days and from 0.2 for a T_c of 5 days.

T_c and T_s do not appear to vary with the histologic type of the tumor; however this conclusion is only tentative since the number of tumors studied is small. On the other hand, we shall see later that the labeling index (LI) and the doubling time (DT) correlate with the histologic type (5).

The distribution of T_c within a tumor was computed for some tumors, with various computer programs and similar results being obtained (3). The spread of T_c appears more important in some tumors (6), but the most obvious fact is that the

[2]Malaise EP, et al. Unpublished data.
[3]Focan C, Malaise EP, et al. Unpublished data.

TABLE 1.—Distribution of durations of cell-cycle phases

Tumor type†	Cell-cycle phase* T_c $\bar{m} \pm 2\sigma$ (hrs)	T_c Dispersion‡	T_{G_1} $\bar{m} \pm 2\sigma$ (hrs)	T_{G_1} Dispersion‡	T_s $\bar{m} \pm 2\sigma$ (hrs)	T_s Dispersion‡	T_{G_2} $\bar{m} \pm 2\sigma$ (hrs)	T_{G_2} Dispersion‡
All animal tumors (46)	20.74 (8.11 ≷ 53.00)	6.53	8.25 (1.57 ≷ 43.43)	27.66	8.83 (4.52 ≷ 17.24)	3.81	2.23 (0.91 ≷ 5.48)	6.02
Transplanted (32)	19.86 (7.80 ≷ 50.55)	6.48	7.41 (1.40 ≷ 39.20)	28	8.75 (4.92 ≷ 15.57)	3.16	2.25 (0.85 ≷ 5.68)	6.68
Spontaneous (14)	21.40 (7.52 ≷ 60.85)	8.09	9.32 (1.71 ≷ 50.80)	29.70	8.61 (3.48 ≷ 21.27)	6.11	2.07 (0.79 ≷ 5.39)	6.82
Human tumors (30)	49.91 (16.17 ≷ 154.10)	9.52	22.61 (2.76 ≷ 184.80)	66.95	17.77 (9.67 ≷ 32.62)	3.37	5.83 (1.19 ≷ 15.59)	13.1
$\frac{\bar{m}\text{ (human)}}{\bar{m}\text{ (animal)}}$	2.40		2.74		2.01		2.61	

*$\bar{m}$ = geometric mean obtained by regression analysis.
†Nos. in parentheses indicate the No. of tumors collected for analysis.
‡Dispersion is equal to the ratio of the 2 limits 97.5% and 2.5%.

spread of the T_c in a tumor is generally wider in human solid tumors than in experimental ones (7,8). The choice of an experimental tumor-model system should take into account the spread of the duration of T_c and of the phases. On the other hand, it should be underlined that ascitic tumors have different cell-kinetic characteristics, such as the lengthening of the cell cycle during the growth of the tumor (*see* ref 8). The use of these tumors as a model for human solid-tumor therapy is therefore open to discussion.

Other comparisons can be made between human and experimental tumors. The cell cycle and the phase durations are longer in human than in animal tumors. For the various phases, the ratios between the mean durations of a phase in human and animal tumors are comparable: 2.7 for T_{G_1}, 2.0 for T_s, 2.6 for T_{G_2}, and 2.4 for T_c (table 1). It can be concluded that when extrapolating from experimental to human tumors, a mean value of 2.5 appears adequate. On the other hand, the range of the mean durations of T_s and T_{G_2} in the various tumors to another is also comparable. In the animal and in man, the least variable is T_s with a ratio of 3 between the extreme values of the confidence interval and the most variable is G_1 with ratios of 28 and 67 respectively between the extreme values (table 1); for this phase the range is greater in man. It should be remembered that T_s and T_{G_1} do not differ in normal and tumor cells (4); on the other hand, T_{G_2} is longer in tumors (4).

GROWTH FRACTION

The concept of growth fraction (GF) was defined by Mendelsohn (4) as the quotient of the proliferating cells (P) by the total number of cells (P/P+Q where Q is the number of non-proliferating or quiescent cells). This concept has been criticized mainly because it is impossible to identify quiescent cells. Furthermore, the concept of quiescent cells is ambiguous as these cells could correspond to cells with a long T_{G_1} when the distribution of G_1 is bimodal, to differentiated tumor cells that can not proliferate or to damaged cells which have become unable to divide, and finally to quiescent cells that could be triggered into cycle, which could be called G_0 cells (if there are such cells in a human tumor). In spite of these ambiguities, the concept remains useful because it is convenient to refer to a parameter characterizing the size of the proliferating pool in a tumor.

Unfortunately it is difficult to measure the GF in human tumors with the methods advocated by Mendelsohn (4). This explains why there are only a few measurements of the GF (1,6). Furthermore, the risk of bias is even greater than in the measurement of T_c since the tumors studied have been highly selected. A few measurements of GF have been carried out in experimental solid tumors. They suggest first that when the growth rate slows down during the growth of a tumor, the GF diminishes slightly (9), and second, that the GF is smaller in slowly growing tumors (10). However, there are no data which allow us to extrapolate these observations to human solid tumors. Furthermore, nothing is known about the biologic factors which influence the GF.

Other methods are therefore required for studying the distribution of the GF among human tumors. We shall discuss two of them.

Continuous Labeling

If a cell population is continuously labeled during a time interval equal to T_c minus T_s, all the cycling cells should be labeled. A detailed analysis of the time course of the LI under continuous labeling requires a mathematic model (4) in order to take into account the spread of the values of T_c, the division of labeled cells, the cell loss which may concern both the proliferating and the quiescent cells (4), and the flow of cells from the proliferating compartment to the quiescent compartment and eventually from the quiescent to the proliferating compartment. However, the value of the LI after a few days of continuous labeling should give some indication about the GF although it is not a direct measure of the GF. A few investigators have reported results of continuous labeling of human solid tumors, ie, Breur (11), Bresciani et al (6), Shirakawa et al (12), and Terz et al (13). These studies have shown that in solid tumors there is a fraction of cells which do not enter into synthesis during the observation time. For instance, Terz and Curutchet injected 2 millicuries/day of tritiated thymidine intra-arterially during 6–20 days; in one rectal carcinoma they observed that after 20 days of continuous labeling, 40% of the cells were not labeled (13).

With this technique, Malaise et al[4] studied 16 squamous cell carcinomas of the floor of the mouth. After one pulse, the mean LI was 15% (fig 2). After 40 hours of continuous labeling, the mean LI increased up to 57% with values of the cumulative LI in individual tumors ranging from 25% to 97% which shows that the proportion of proliferating cells is higher than expected in many of these tumors. In all tumors the PLM was about 100% and remained at this value 2 days after the end of the labeling which means that almost all the cycling cells were labeled and suggests that the flux from Q to P compartment during this time interval is small if any.

During the 2 days after the end of the labeling period, the LI did not change while the MGC per labeled mitoses and per labeled cells decreased twofold. The decrease in MGC of the labeled mitoses suggests that the time interval between the two biopsies is about equal to the mean cycle time. The parallel decrease of the MGC per labeled cells and the similarity of the distribution of the grain count per cell in labeled mitoses and labeled cells 2 days after the end of the continuous labeling shows that there are no Q cells resting in G_2 and that the flux of cells from P to Q compartments is probably very small during this time interval. These facts and the lack of increase during the same period of the LI of the whole population suggest that the cell loss occurs mainly in the proliferative compartment that is around mitosis.

Evaluation Based on Pulse LI

The LI varies widely among human tumors from $< 0.1\%$ to $> 50\%$ (5). On the other hand, we have already shown that for human tumors, the extreme values of the ratio of T_s/T_c are 0.5 and 0.2 with a mean value of 0.3.[5] A calculation of GF based on the assumption that T_s/T_c is equal to 0.3 may therefore overestimate the proportion of proliferating cells in the tumors with a short T_c and underestimate it in tumors with a long T_c. These inaccuracies are small relative to the wide variations of the LI. Furthermore, the histologic type of the tumor does not seem to influence this ratio since T_c is probably not correlated with histologic type. The errors involved in the in vitro measurement of the LI have been discussed elsewhere[4] and are also relatively small.

We have been able to collect from the literature and our own data > 300 LIs of human solid tumors (5). These tumors were divided into five histologic groups and the results are shown in figure 3 and table 2. Three main conclusions can be drawn.

(*A*) The geometric means of the LI in the various pathologic groups are significantly different. They vary from 1.5% for the adenocarcinomas to 27% for the embryonal tumors. These differences are much greater than the inaccuracies due to the technique. Furthermore, the errors occur in all of the groups so that the differences in mean LI between the groups might be not much influenced.

(*B*) The spread of the LI is different in the five groups shown in figure 3; the ratios between the extreme values are respectively 1000, 100, 50, and < 10. The range of the individual values appears to be wider in the groups in which the mean LI is small.

(*C*) The mean LI is smaller in the groups with a long DT. There is a significant correlation between the geometric means of the LI and the geometric means of the DT (table 2). This suggests that the variation in DT from one histologic type to another is mainly due to changes in the GF (5).

In an attempt to get some information about the relationship between DT and LI within the same histologic group, we measured the DT for 15 breast cancers before mastectomy, and subsequently for the same tumors we measured the LI by an in vitro

[4]*See* footnote 2.

[5]*See* footnote 3.

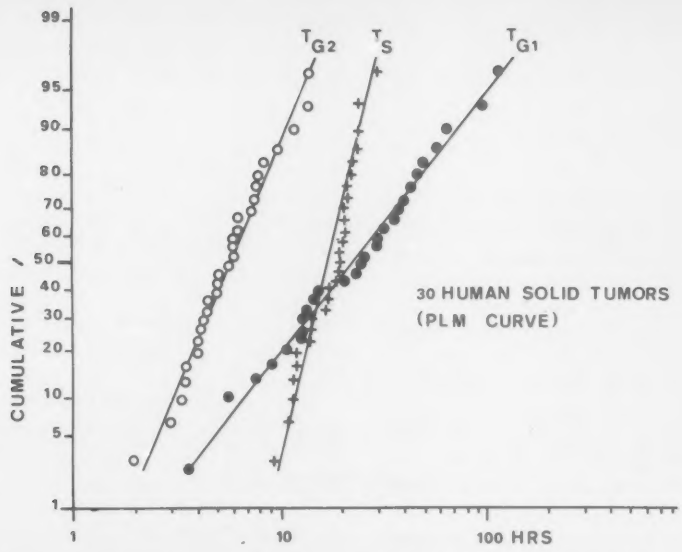

FIGURE 2.—Range of the mean duration of the 3 phases of the cell cycle in human tumors (*see* footnote 3). 30 values were collected from the literature and were obtained by the PLM method. S appears to be the phase in which duration is the least variable from patient to patient, while T_{G_1} is the most variable from patient to patient.

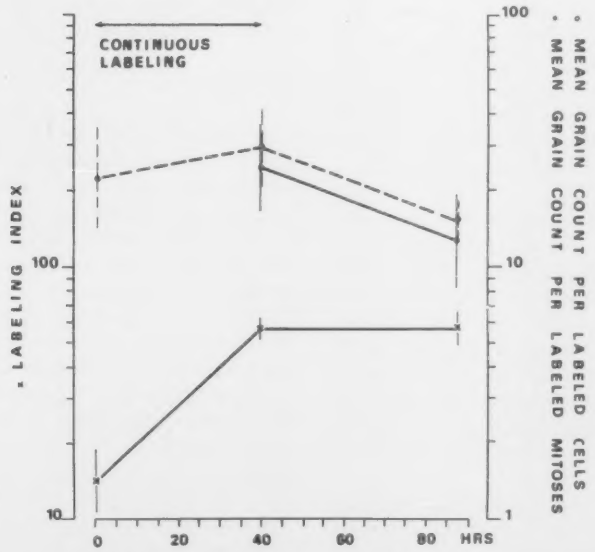

FIGURE 3.—Results obtained with continuous labeling by intra-arterial perfusion in 16 patients with tumors of the floor of the mouth (*see* footnote 2). The lower curve shows the time course of the average LI of the tumors during and after continuous labeling (left scale). The 2 upper curves show the variations in the average MGC per labeled cells and per labeled mitoses. The 2 curves appear to be parallel (right scale).

incubation. In those tumors, a correlation at the border line of significance was found between DT and LI, a long DT corresponding to a small LI.

Cell Loss

Of the three parameters of cell proliferation, the cell loss is generally the most difficult to evaluate. In man the cell-loss factor has generally been calculated by comparing the actual DT to the potential DT (14). The cell-loss factor has been found high in most human tumors studied. However, other methods of expression of the loss can be more relevant, for instance the percentage of the total number of cells that disappear from the tumor per unit time. It is easily calculated since it is equal to birth rate times cell-loss factor. When the LI is known, the birth rate can be computed by assuming a mean T_s of 18 hours. The results are given in table 2.

In man, the daily cell loss seems to be the smallest in those tumors of histologic type where the growth is the slowest and the LI the lowest. It appears that the probability of cell death is the greatest when the proliferation is most intense. However, we must ask ourselves whether this correlation observed between the mean value of various histologic groups of tumors remains valid within a histologic group for individual tumors. This is why we analyzed the group of breast cancers previously mentioned in which the DT and LI were measured for each patient. Assuming for T_s a duration of 18 hours, we found that the discrepancy between potential DT and the actual DT increases with the LI, showing again that the higher the LI the higher the cell loss (15).

On the whole, the cell loss reduces the spread of growth rates produced by the differences of GF in the various types of tumors. Hence it appears that the behavior of human tumors with respect to cell death is different from that observed in experimental tumors. In the latter, the cell-loss factor is small at the beginning of the growth of a solid tumor when the DT is short. Later it increases when the DT becomes longer and cell loss appears to be the parameter which contributes most to the prolongation of the DT (9).

In conclusion, the cell losses from human solid tumors are considerable and help to explain why the DTs are on the average 30–90 times longer than the duration of the cell cycle but they do not explain the differences between the mean durations of the DTs in different histologic groups which are mainly due to differences in GF. Differences in GF also explain why the DTs of human tumors are much longer than the DTs of experimental tumors.

COMPARISON BETWEEN THE PARAMETERS OF CELL KINETICS OF PRIMARY TUMORS, METASTASES, AND RECURRENCE

A few studies have compared the cell kinetics of primary tumors and of metastases. For instance, for breast cancers the mean DT of the primary tumors measured on sequential mammography is about 105 days (16), whereas the DT of pulmonary metastases is about 70 days (17) and that of skin metastases 40 days (18). For all the adenocarcinomas studied, the mean DT is 166 days in the primary tumors and 82 days in the lung metastases. For the squamous cell carcinomas the respective values are 82 and 58 days (17).

In three patients with cancer of the larynx, the LIs of the lymph node metastases were higher than the LIs of the primary tumor (respectively, 11.7% and 6%) (19).

Bresciani et al (6) compared the PLM curves of the primary and local recurrence in two patients. The mean T_c was shorter in the recurrences and the distribution of T_c less wide.

These data suggest that in human metastases or recurrences there is a selection of the cells with the shortest T_c and/or the greatest proliferative capacity.

CORRELATION BETWEEN TUMOR-CELL KINETICS AND CLINICAL DATA

Survival

Several studies have demonstrated that the growth rate of a tumor provides a valuable prognostic indicator (20). From a study of 203 patients with pulmonary metastases (21), we demonstrated that the survival is significantly correlated to the growth rate of the tumor and is shorter when the tumor progresses more rapidly. This relationship is found in each of the histologic groups defined previously. The distribution of survival of the patients is also log-normal and the spread of individual values is in practice comparable to those of the DT. Nevertheless, there is no simple proportionality between the tumor growth rate and survival (table 3). For example, the adenocarcinomas in this series had a mean DT four times longer than the embryonic tumors while the mean survival was only twice as long. It looks as if one or several factors prevent the patient bearing a tumor with a slow growth rate from obtaining all the benefits from this slow evolution.

Probability of Metastases

In breast cancers, Kusama et al (20) were unable

TABLE 2.—Mean kinetic parameters of various histologic types of human tumors*·†

Histologic type	DT (days)	LI (%)	GF‡ (%)	Cell-loss factor§ (%)	Absolute cell loss/10^9 cells/day¶	Cell renewal rate** (%/day)	Radiosensitivity (mean tumor control dose in rads)	Chemosensitivity††
Embryonal tumors	27 (76)	30 (6)	90	93	420–10^6	42	2500–3000	++
Malignant lymphoma	29 (41)	29 (15)	90	94	510–10^6	51	3500–4000	++
Mesenchymal sarcoma	41 (87)	15 (68)	15	76	55–10^6	5.5	8500	–
Squamous cell carcinoma	58 (51)	8 (68)	25	89	100–10^6	10	6000–7000	+
Adenocarcinoma	83 (134)	2 (121)	6	56	11–10^6	1	6000–8000	±

*See refs 5 and 17.
†Nos. in parentheses indicate the No. of patients for whom data were available.
‡Calculated from LI, assuming $T_r/T_s = 3$.
§Calculation based on DT and LI, as defined by Steel (ref 6) assuming $T_s = 15$ hrs and $\lambda = 0.7$.
¶Equal to the product: birth rate × cell-loss factor.
**Equal to absolute cell loss/No. of cells.
††++ = most sensitive; – = least sensitive.

TABLE 3.—Survival time of patients, DT of lung metastasis, distribution of the values of the survival time (log survival time = a. log DT + b), and correlation coefficient between DT and survival time (*from* ref 21)

Pathologic group	No. of patients	Survival time of patients* (mos)	DT of lung metastasis† (days)	Correlation coefficient between DT and survival time	Level of significance	Coefficient of multiplication
Embryonal tumors	16	9.5 (6.7–13.6)	19.5	0.45	0.10 (NS)	13.3 2.
Hematosarcomas	12	10.5 (6.2–17.8)	29.5	0.87	0.01	11.0 2.
Mesenchymal sarcomas	41	15.5 (11.8–20.4)	35.6	0.51	0.01	12.4 2.
Squamous cell carcinomas	30	15.6 (10.9–22.2)	51.0	0.45	0.01	9.0 2.
Adenocarcinomas	82	20.4 (16.3–25.7)	90.4	0.64	0.01	6.6 2.
Fibrosarcomas	22	35.7 (22.2–57.6)	64.9	0.49	0.01	16.5 2.

*Geometric mean and confidence interval.
†Geometric mean.

to find any correlation between the growth rate of the primary tumor and the probability of metastases to lymph nodes. Conversely, other investigators observed that more rapidly growing breast cancers are more likely to metastasize (22).

In a prospective study carried out at Villejuif (16), the LI was measured in vitro in 98 breast cancers. No correlation was observed between the LI and the probability of lymph node involvement. On the other hand, 2 years after treatment, the mean LI of the primary tumor in patients with relapses was higher than the mean LI in the patients without recurrences. If there is no link between the LI and the probability of dissemination, this finding is probably due to a correlation between the growth rate of metastases and the LI of the primary tumor.

EFFECT OF TREATMENT ON THE CELL KINETICS OF HUMAN TUMORS

Response to Radiotherapy

It is of interest to notice that the histologic groups of human tumors that have the most rapid mean growth rate and the highest GF and cell turnover rate are those that are most radiosensitive (table 2).

There is also a correlation between the growth rate, the LI, or the cell loss, and the response to chemotherapy (table 2).

Effect on the Growth Rate—Repopulation and Recruitment

An acceleration of the growth rate of the clonogenic cell population was observed by Barendsen et al (23) in an experimental rat tumor after 2000 rads. However, Guichard and Malaise,[6] studying the EMT6 mouse tumor, found that the growth rate of the clonogenic cell population was not modified by 2000 rads.

T_c, GF, and LI were measured after irradiation in a few experimental tumors. The results are conflicting. In some tumors, but not in all, a reduction of T_c and an increase of GF were observed. The effects of irradiation on the kinetics of cell proliferation of experimental tumors appear therefore to vary from tumor to tumor (8). The situation is similar for human tumors and here also there is a wide range of response to irradiation (24).[7] It would be of great interest to understand the causes of these differences, because they raise the problem of the control of cell proliferation in human tumors. Many factors have been discussed such as greater availability of nutrients, decrease in inhibiting factors, or appearance of stimulating factors. Obviously more investigations are required both in vivo and in vitro. For instance the presence of inhibiting factors has been shown in the fluid of ascitic tumors by an in vitro technique (25) and it would be interesting to study the influence of irradiation on its concentration.

The depression of the LI after irradiation appears to be more important and of a longer duration in human tumors than in experimental tumors. Whether or not this is linked with the longer cell cycle in human tumors remains to be demonstrated. A comparison of the variations of the LI during a course of radiotherapy shows that the depression is more important in laryngeal cancers than in rectal adenocarcinomas whose LIs are lower before irradiation.[7] Within a series of URDT tumors the LI was measured before two sessions of 850 rads and 2 weeks after. A decrease of the LI was observed which was more important in patients whose initial LI was higher. In those patients a significant correlation was found between the LI before irradiation and the decrease in the number of tumor cells per unit of volume (*see* preliminary data in ref 24). It should be remembered that Breur (11,26), Van Peperzeel (27), and Malaise et al (28) observed after radiotherapy of human lung metastases a greater volume reduction in those tumors with a short DT and that Hermens (29) observed in a review of all available data that for experimental tumors the specific growth delay caused by irradiation is longer for those tumors with a high GF. The meaning of such relationships between growth rate and apparent radiosensitivity is not clear (24) and deserves further study.

[6]Guichard M, and Malaise EP. Unpublished data.

[7]*See* footnote 2.

REFERENCES

1. FRINDEL E, MALAISE E, and TUBIANA M. Cell proliferation kinetics in five human solid tumors. Cancer 22:611–620, 1968.
2. STEEL GG. The cell cycle in tumours: an examination of data gained by the technique of labelled mitoses. Cell Tissue Kinet 5:87–100, 1972.
3. HARTMANN NR, GILBERT CW, JANSSON B, ET AL. A comparison of computer methods for the analysis of fraction labelled mitoses curves. Cell Tissue Kinet 8:119–124, 1975.
4. MENDELSOHN ML. The cell cycle in normal and malignant tissues. *In* The Cell Cycle in Malignancy and Immunity. ERDA Symposium Series, 1975, pp 293–314.
5. MALAISE E, CHAVAUDRA N, and TUBIANA M. The relationship between growth rate, labelling index and histological type of tumours. Eur J Cancer 9:305–312, 1973.
6. BRESCIANI F, PAOLUZI R, BENASSI M, ET AL. Cell kinetics and growth of squamous cell carcinoma in man. Cancer Res 34:2405–2415, 1974.
7. LAMERTON LF. Cell proliferation and the differential response of normal and malignant tissues. Br J Radiol 45:161–170, 1972.
8. TUBIANA M, and MALAISE EP. Cinétique de prolifération cellulaire des tumeurs et traitement des cancers. Pathol Biol 21:647–664, 1973.
9. FRINDEL E, MALAISE E, ALPEN E, ET AL. Kinetics of cell proliferation of an experimental tumor. Cancer Res 27:1122–1131, 1967.
10. STEEL GG, ADAMS K, and BARRETT JC. Analysis of the cell population kinetics of transplanted tumours of widely differing growth rate. Br J Cancer 20:784–800, 1966.
11. BREUR K. Effectiveness of radiation in relation to growth characteristics of tumors and normal tissues. *In* The Clinical and Biological Basis of Radiosensitivity (Friedman M, ed). Springfield, Charles C. Thomas, 1974, pp 502–520.
12. SHIRAKAWA S, LUCE JK, TANNOCK IF, ET AL. Cell proliferation in human melanoma. J Clin Invest 49:1188–1199, 1970.
13. TERZ JJ, and CURUTCHET H. Cell kinetics of human solid tumors following continuous infusion of ^{3}H-TdR. *In* The Cell Cycle in Malignancy and Immunity. ERDA Symposium Series, 1975, pp 323–329.
14. STEEL GG. Cell loss as a factor in the growth rate of human tumours. Eur J Cancer 3:381–387, 1967.
15. MALAISE EP, CHAUVEL P, CHAVAUDRA N, ET AL. La cinétique des cancers du sein. Gazette Med Fr 80:5391–5400, 1973.
16. TUBIANA M, CHAUVEL P, RENAUD A, ET AL. Vitesse de croissance et histoire naturelle du cancer du sein. Bull Cancer. In press, 1975.
17. CHARBIT A, MALAISE E, and TUBIANA M. Relation between the pathological nature and the growth-rate of human tumours. Eur J Cancer 7:307–315, 1971.
18. PHILIPPE E, and LE GAL Y. Growth of 78 recurrent mammary cancers. Quantitative study. Cancer 21: 461–467, 1968.
19. FABRIKANT J. The kinetics of cell proliferation in normal tissues and malignant tumors of the upper air passage. *In*

The Clinical and Biological Basis of Radiosensitivity (Friedman M, ed). Springfield, Charles C. Thomas, 1974, pp 274–313.
20. KUSAMA S, SPRATT JS, DONEGAN WL, ET AL. The gross rates of growth of human mammary carcinoma. Cancer 30:594–599, 1972.
21. MALAISE E, CHAVAUDRA N, CHARBIT A, ET AL. The relationship between the growth rate of human metastases survival and pathological type. Eur J Cancer 10:451–459, 1974.
22. SLACK NH, BLUMENSON LE, and BROSS IDJ. Therapeutic implications from a mathematical model characterizing the course of breast cancer. Cancer 24:960–971, 1969.
23. BARENDSEN GW, and BROERSE JJ. Experimental radiotherapy of a rat rhabdomyosarcoma with 15 MeV neutrons and 300 kV X-rays. I. Effects of single exposure. Eur J Cancer 5:373–391, 1969.
24. TUBIANA M, RICHARD JM, and MALAISE E. Kinetics of tumor growth and of cell proliferation in URDT cancers; therapeutic implications. Laryngoscope 85:1039–1052, 1975.
25. MALAISE E, and TUBIANA M. Etude in vitro de certains facteurs susceptibles d'influencer la croissance d'une ascite expérimentale. CR Acad Sci 270D:539–542, 1970.
26. BREUR K. Radiosensitivity of human tumours. Eur J Cancer 2:173–188, 1966.
27. VAN PEPERZEEL HA. Effects of single doses of radiation on lung metastases in man and experimental animals. Eur J Cancer 8:665–675, 1972.
28. MALAISE E, CHARBIT A, CHAVAUDRA N, ET AL. Changes in volume of irradiated human metastases. Br J Cancer 26:43–52, 1972.
29. HERMENS AF. Variations in the cell kinetics and the growth rate in an experimental tumor during natural growth and after irradiation. Publication of the Radiobiological Institute; TNO Rijswijk (ZH), The Netherlands, 1973.

Introduction to Session on Drug Scheduling—Experimental Studies

L. M. van Putten [1]

The field of development and evaluation of drug schedules and sequences in experimental models has traditionally been dominated by the idea that exploration of experimental models would be helpful in improving clinical combination therapy. The methodology by which this could be achieved has rarely been formulated explicitly. Two approaches are possible. The empiric approach says "a schedule which is effective for treatment of a model tumor may be good for clinical tumor treatment," or stated in a somewhat more sophisticated way, "whatever schedule is found to be uniformly effective when tested on a wide spectrum of model tumors should be effective in clinical tumors."

The alternative analytic approach says "when we know the mechanisms by which certain drug sequences show enhanced effectiveness in model tumors we will know how to construct optimal drug sequences for clinical treatment." Keeping these approaches in mind we can now try to see how close we have come to our goal of effectively producing better treatment schedules.

Many reports have indicated that a drug sequence is considered "useful" if more than additive effects (potentiation) are demonstrated in a model. Others have indicated usefulness only if potentiation is found in a tumor system but not in a similarly treated normal system. Of course, every step in analyses of this type should be considered useful, but at the present I am rather worried about the fact that many of the sequences found useful in one tumor model are not effective in another model. This would call for a more systematic approach in which fewer sequences are tested in a wider spectrum of models. The empiric approach may be very useful if we find uniform responses in many models.

The analytic approach emphasizes not so much the models as the mechanisms: the cytostatic mechanisms of synchronization and recruitment or, alternatively, the mechanism of drug-induced enhancement of uptake into the cell of the second drug may separately or simultaneously be responsible for enhanced effectiveness of some schedules. Unfortunately, it has thus far not been possible to analyze with complete confidence which of these mechanisms are operative in many of the drug sequences tested. Most importantly, the prediction of effectiveness of mechanisms is so far not possible, and the time at which predictability is realized seems remote. In this respect I may remind you of the biochemical terminology used to explain effectiveness of drug combinations a few years ago: sequential blockade, concurrent blockade, and complementary inhibition of enzyme systems were terms put forward to explain some mechanisms of potentiation. These terms indicate concepts of mechanisms of action which may or may not be relevant to certain drug combinations. Although they are relevant to a number of drug-combination effects in some models, their relevance is at present unpredictable; some combinations are effective and others are not. Rules are hard to give; some combinations are effective on normal immunocompetent cells but not on normal bone marrow cells and variably effective on tumor cells. In other words these terms denote concepts of unpredictable mechanisms. If our experimental studies are to have any relevance for clinical application we need predictable mechanisms and more emphasis should be given to the study of the predictability of our favorite cell kinetic mechanisms: recruitment and synchronization. If these mechanisms are not predictably operative, it will be better first to go back to the tedious and uninspired empiric testing of some sequences in many models in order to identify whether predictable responsiveness can be identified. It is clear that the absence of uniformity of response will limit the effectiveness of our studies markedly and that it emphasizes the importance of individualized treatment based on individual monitoring of each tumor's kinetic responses, an approach which may have only limited clinical applicability.

[1] Radiobiological Institute TNO, Rijswijk, The Netherlands.

Mathematic Models of Cell Synchrony and Drug Scheduling [1]

A-j. Valleron [2,3,*]

The most important aim of biomathematicians working in cancer is probably to participate in the development of treatment protocols and, specifically, drug scheduling.

The first direction of research is the modeling of drug pharmacokinetics and of dose repartition after irradiation in tumors and in normal tissues. The second one is the modeling of the synchronizing effects of treatments on cell kinetics in order to propose optimal scheduling of drugs or combinations of radiotherapy and chemotherapy. This paper will be devoted to this second point.

The four major steps in drug scheduling modeling are: (*a*) to define the age distributions of cell populations in the absence of treatment; (*b*) to discuss the biologic validity of underlying hypotheses which are currently used in mathematic models; (*c*) to define precisely synchrony and to propose specialized mathematic models of the various effects which lead to synchrony; and (*d*) to derive a mathematic method which makes it possible to group the above notions and to be able to draw the maximum information from experimental data after treatment or to simulate protocols. These four steps will be sequentially discussed.

BASIC METHODOLOGIC DEFINITIONS AND RESULTS

Chronologic Age of Cells

The time elapsed since the birth of a cell is the chronologic age. Two cells with the same physiologic age (eg, at the beginning of S phase) generally do not have the same chronologic age (in this example because of the variability of the duration of the G_1 phase).

Age Distribution

The age distribution of a cell population at a given time is the repartition of the cells of the population into the different classes of chronologic age. Experimentally such distributions usually cannot be directly observed. Cell fluorometry, for instance, gives the repartition of the cells in different classes of physiologic age (expressed in units of DNA content).

Stationarity

A stationary process of evolution for a cell population is a process in which all parameters (except the number of cells) remain constant with time. In a stationary process, means and standard deviations of cell-phase durations, probabilities of cell death, loss, differentiation, growth-fraction, etc, are assumed to be constants.

The branching-process theory leads to numerically manageable results only when this assumption is made. This is the very practical reason which explains why many probabilists make this assumption, which is sometimes unrealistic from a biologic point of view. However, some general nonstationary tumor-growth models have been devised (1,2).

In many cases however, it is possible to use valid mathematic results for stationary processes if the cell-population parameters do not vary during the particular study (for example, to model a percentage labeled mitosis [PLM] experiment, it is generally reasonable to assume that the cell-population parameters do not vary during a time of the order of the duration of the experiment).

Stable Limit Age Distribution (SLAD)

In a stationary process, if we start from an arbitrary age distribution at time 0, it can be demonstrated (3) that after a sufficient amount of time, the age distribution of the cells is always the same: the SLAD. This SLAD depends only on the characteristics of the model and the parameters of the process of the cell population and not on the initial age distribution.

Two SLAD which are commonly used are the exponential age distribution (fig 1a) which is obtained in a cell population with exponential growth

[1] Supported by contract 74/01105, INSERM.

[2] Unité de Recherches Statistiques de l'INSERM, et Laboratoire de Biostatistique de l'Université de Paris VII, France.

[3] The author gratefully acknowledges Madeleine Mallet for her technical assistance.

[*] *Reprint requests to:* A-j. Valleron, Laboratoire de Biostatistique, Institut Gustave Roussy, 16 bis, Ave Paul Vaillant Couturier, 94800 Villejuif, France.

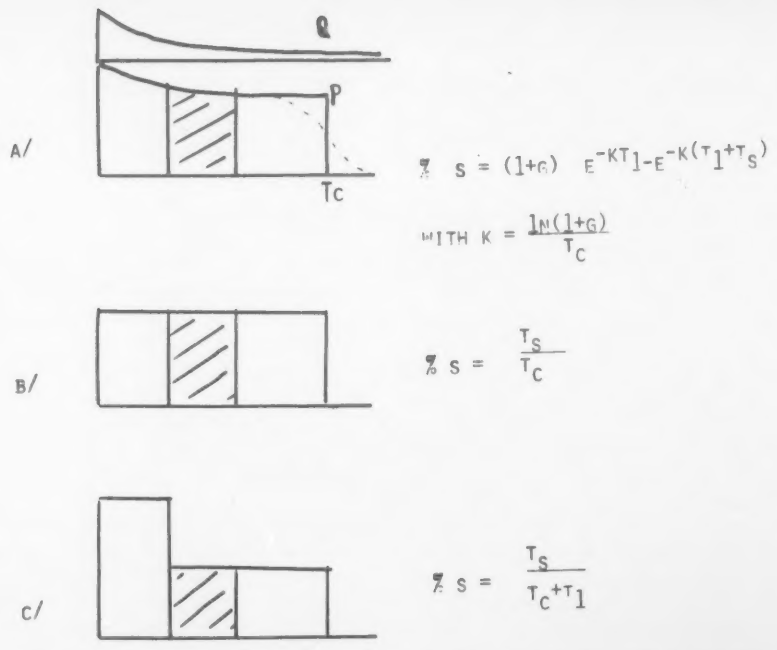

FIGURE 1.—3 SLAD. (1a): at mitosis, cells enter the Q compartment with probability (1+g)/2; (1b): at mitosis half of the cells escape from the population; (1c) at the end of G_1, half of the cells escape from the population. The growth of the first population is exponential, with growth fraction g; the No. of cells of the 2 other populations remain constant with time.

and the rectangular age distribution (fig 1b) which is obtained in a cell population where, at mitosis, or randomly during the whole cell cycle, one of the two daughter cells escapes (by cell loss, death, or differentiation); in this case, the total number of cells remains constant. Reciprocally, if the total number of cells remains constant, it is important to note that the SLAD is not necessarily rectangular as commonly assumed. If we suppose that 50% of the cells escape from the cell population at the end of G_1, the age distribution will not be rectangular (*see* fig 2c) (and the S percentage will not be $\frac{T_s}{T_c}$).

The mathematic methods for automatically analyzing the PLM experiment use the assumption of SLAD. They *cannot* be used after treatment when the age distribution of the cell population is different from the SLAD (*see* fig 2 for a hypothetic example where cells are supposed to be blocked in a large proportion in G_2 [70%]) at time 0.

The rapidity of the return to the SLAD after, for example, selective killing of cells depends on the variability of the duration of the cell phases.

We have studied in detail (fig 3) the hypothetic case where, at time 0, the whole cell population is synchronized at the beginning of G_1. If the coefficient of variation of the phase durations is 100%, the return to the SLAD is obtained within a time shorter than a cell cycle; if the coefficient of variation is 10%, the return to the SLAD is not obtained until after five cell cycle times. A practical consequence of these results is that since the cell-cycle durations are less variable in animal tumors than in human tumors, it is probably easier in practice to use the synchronizing effects of treatments in experimental rather than clinical studies.

Variable Limit Age Distributions: Chronobiology

While stationarity implies that if no treatment is used the age distribution remains stable, it is well known that in many tissues the S and M percentages of cells vary dramatically throughout the day. Many experimental studies have been done in normal tissues, particularly on hamster cheek-pouch epithelium (4–7).

Some studies show a variation of the mitotic activity in bone marrow, both in man (8) and in rats and mice (9). In tumors, spontaneous mammary cancer in specially bred mice exhibits diurnal rhythm (10).

Special attention should be paid to these variable age distributions both from a practical and a theoretic point of view: the possible differences of time

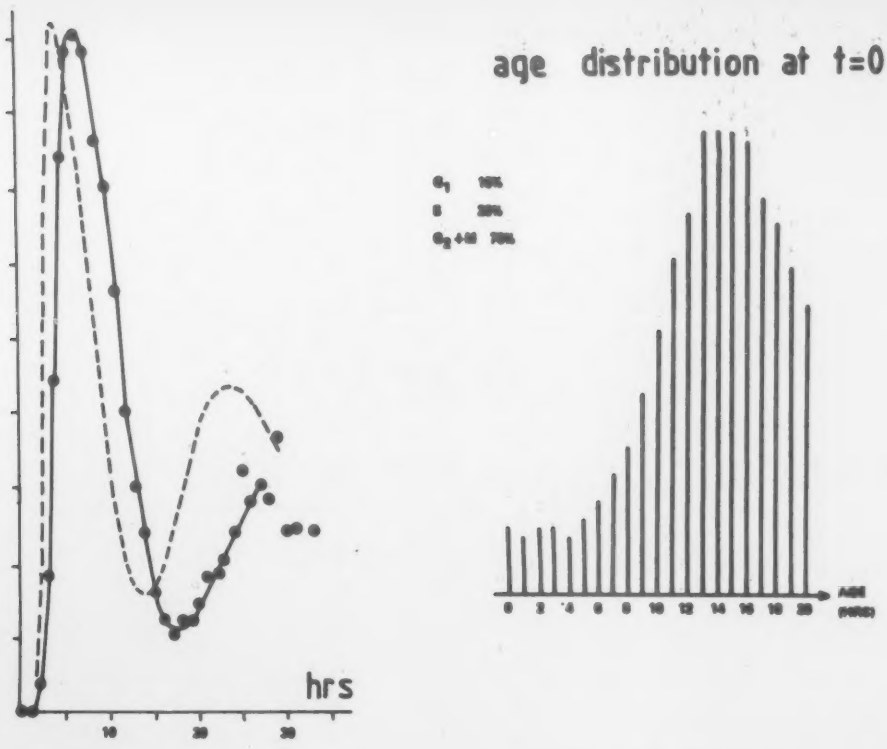

FIGURE 2.—Assuming that after a hypothetic treatment, the age distribution of the cell population is at time 0 as shown on the right side of the figure, the simulated PLM curve (solid line) is very different from the theoretic curve obtained under usual assumption of SLAD (dotted line); in both cases mean durations of G_1, S, G_2, and M were assumed to be 10, 7, 2, and 1 hr respectively; coefficients of variations were assumed to be 50%.

variation of the age distributions between normal and tumoral tissues could be used to set treatment protocols. Such a possibility has been investigated experimentally; the mean survival time of mice treated with L1210 depends on the repartition of the total dose of cytosine arabinoside throughout the day (11). From a methodologic point of view, it is interesting to devise mathematic methods making it possible, for instance, to compute the age distributions when the SLAD hypothesis is obviously wrong. We are presently (12) involved in the generalization of the cell-cycle compartmental model (13) to describe biologic rhythms; we recently used a simplified version (14) of this model in which the rate of entry from G_1 to S phase was dependent upon the time of the day to interpret experimental data from hamster cheek-pouch epithelium (6). Brockwell (15) is developing similar techniques.

USUAL ASSUMPTIONS IN CELL KINETIC MODELING

We shall first discuss some of the basic assumptions that are currently used to devise models in cell kinetics particularly for simulation of treatment protocols.

Independence Between Cell-Cycle Durations in Progeny

In most of the models, it is assumed that the durations of the cell cycle of the different cells of a progeny are not correlated. In particular, it is assumed that the cell-cycle times of two sister cells or the cell-cycle times of a cell and of its two daughters are not correlated. This assumption is useful when one uses the branching-process approach which is

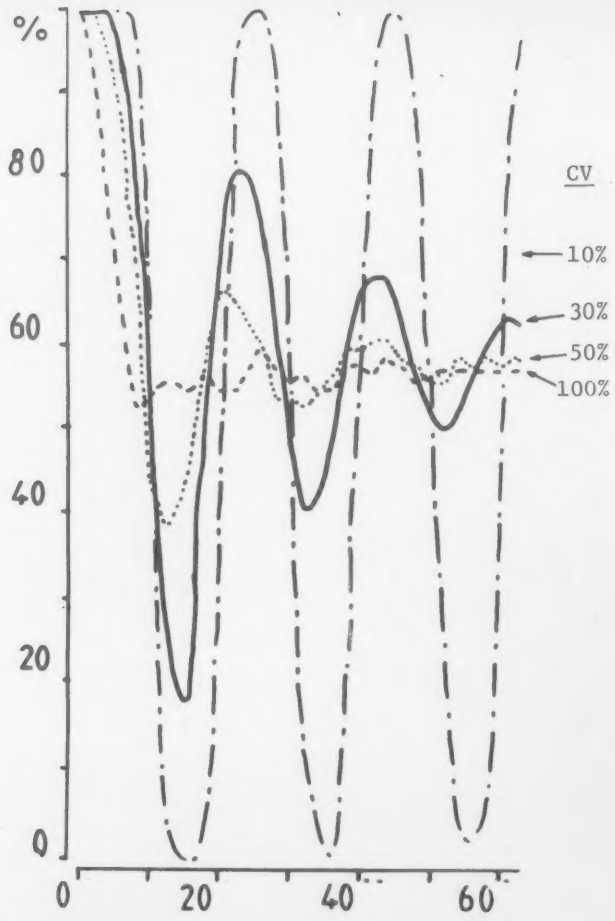

FIGURE 3.—After perturbation of the age distribution of a cell population, the rapidity of the return to the SLAD depends on the variability of the phase durations: at time 0, 100% of the cells are assumed to be in the beginning of G_1; the mean durations of the phases are as indicated in fig 1; the coefficients of variation are indicated on the figure.

not adapted to other situations. Even with our simulation method where we are not technically obliged to do so, we were faced with the lack of experimental data and we have been forced, at present, to the same assumption.

The assumption of independence between cell-cycle durations in a progeny is probably misleading: we have recently analyzed (16) data concerning 44 pedigrees of EMT-6 cells observed by microcinematography for up to ten generations. The preliminary results indicate that, under our experimental conditions, mean cell-cycle and mitosis times vary significantly from one generation to another; total cell-cycle and mitosis times of sister cells are strongly correlated, and mother and daughter mitotic times are surprisingly highly correlated, whereas cell-cycle times are poorly correlated. Table 1 summarizes these preliminary results. The discussion of the role of environmental factors to explain these correlations will be given in a forthcoming paper.

Independence Between Cell-Phase Durations

Here also, the assumption of independence between cell-phase durations is usually made because it is easier to do so from a technical point of

TABLE 1.—Correlations between cell cycle and mitotic durations in progeny: preliminary results

Generation	Correlation between T_c and T_c-T_M: $r(T_m,T_c-T_m)$	Similarity between sisters of this generation		Correlation with daughter parameters	
		$s(T_c,T_c)$	$s(T_m,T_m)$	$r(T_c,T_c^o)$	$r(T_m,T_m^o)$
II	0.11 (81)	0.69 (41) +++	0.10 (37)	0.02 (82)	0.20 (77)
III	0.10 (157)	0.90 (79) +++	0.30 (72) ++	0.44 (144) +++	0.27 (137) ++
IV	0.15 (282) +	0.89 (138) +++	0.33 (130) +++	0.35 (230) +++	0.28 (209) +++
V	0.53 (403) +++	0.74 (214) +++	0.44 (175) +++	0.33 (253) +++	0.15 (202) ++
VI	0.50 (370) +++	0.91 (214) +++	0.54 (147) +++	0.54 (148) +++	0.32 (112) +++
VII	0.35 (149) +++	0.86 (82) +++	0.62 (61) +++	0.54 (23)	0.71 (19) +++

*T_c = the mean cell cycle time and T_m = the mean mitosis time; T_c^o and T_m^o = the corresponding daughter parameters. Correlation coefficients cannot be used to express the relation between sister parameters (because of the symmetry between sisters). The similarity coefficients are Nos. between 0 and 1: 0 would mean that the similarity between 2 sisters is the same as that between any 2 cells; 1 would mean that the 2 sister parameters are exactly the same. Nos. in parentheses are the No. of observations; +, ++, and +++ indicate that the quantity is significantly different from 0 with $P < 0.05$, $P < 0.01$, and $P < 0.001$, respectively. Definite results can be found in ref 18.

view and, more seriously, because of the lack of data.

Macdonald (17) devised a maximum likelihood method for analyzing PLM experiments which makes it possible, theoretically, to estimate the possibility of a correlation between cell-phase durations.

In the pedigrees described previously, we also found correlations between intermitotic and mitotic times at some generations (*see* table 1).

Probabilistic Models for Cell-Phase Durations

Commonly, cell-phase durations are assumed to be log-normally distributed (18,19); γ distributed (13,20); or normally distributed (17) [Hartmann and Pederson (21)]. Kubitschek (22) studied experimental cell-cycle distributions and compared different probabilistic models. All these distributions are skewed. In the pedigrees we analyzed (16), we also found that the cell-cycle and mitotic time distributions were clearly skewed. Thus, it is probably not proper to use normal distributions to model the cell-phase distributions (because since the sum of four normal distributions is a normal distribution, the cell cycle should be normally distributed which is experimentally wrong). A recent intercomparison of six very different methods for PLM modeling (23) has shown very similar results when these methods were used to interpret the same data. In the specific problem of treatment modeling, Steward (24) compared the optimal treatment schedules obtained by using two different mathematic models on the same experimental data (25) and found that there was practically no difference. These results seem to indicate that the choice of a particular probability-density function of the cell-cycle times is not practically important in treatment modeling.

SYNCHRONY AFTER TREATMENT

Synchrony After Treatment: Definition

Let us assume that a cell population is treated at time 0 with a given treatment, T. The observed age distribution of the cells at time t is noted, AD_t. The age distribution of the cells at time t if no treatment was used is noted, $\widehat{AD}_t$. If AD_t is different than $\widehat{AD}_t$ (fig 4), we can say that the treatment induces a synchrony. It is important to note that in this definition we do not precisely know the importance of the difference between AD_t and $\widehat{AD}_t$. Of course, the interesting cell population to be considered in the computation and observation of age distributions should be only the clonogenic cell population.

Index of Synchrony for S-Specific Agents

We define synchrony as a modification of the age distribution at time t as compared to the theoretic age distribution which would be obtained if no treatment was used. However, if we

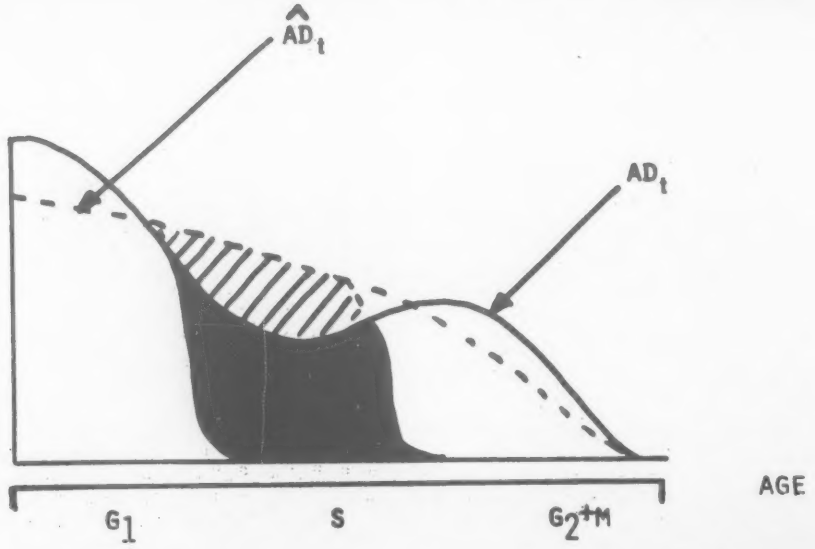

FIGURE 4.—At time t after treatment, cell population is synchronized because AD_t (observed age distribution) is different from $\hat{AD}_t$ (expected age distribution if no treatment is given); the index of synchrony for an S-specific drug (*see* text) would be negative (fewer S cells than expected if no synchronizer).

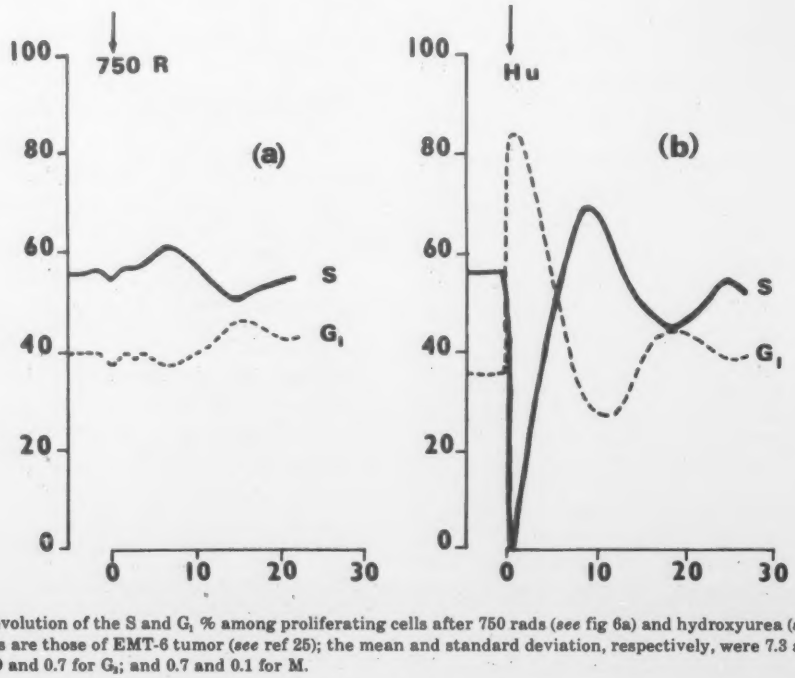

FIGURE 5.—Time evolution of the S and G_1 % among proliferating cells after 750 rads (*see* fig 6a) and hydroxyurea (*see* fig 6b). The cell-cycle parameters are those of EMT-6 tumor (*see* ref 25); the mean and standard deviation, respectively, were 7.3 and 10.2 for G_1; 11.9 and 3.6 for S; 1.9 and 0.7 for G_2; and 0.7 and 0.1 for M.

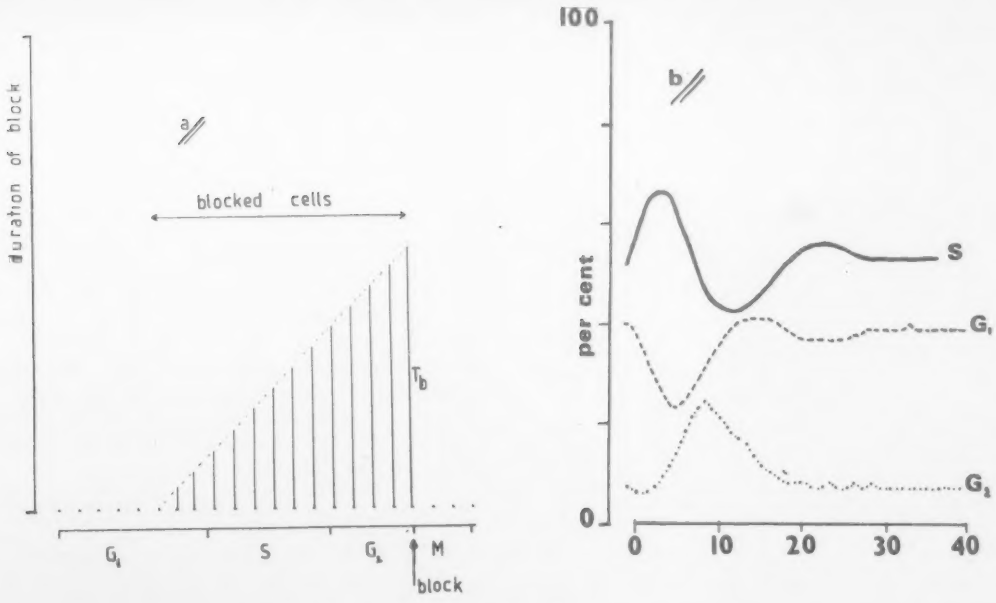

FIGURE 6.—*a*. Model of block: an 8-hr block is assumed to occur at the G_2-M border; abscissa, position of the cell at treatment time; ordinate, duration of the block for the considered cell; late G_2 cells are blocked by 8 hrs, late-S cells will be blocked by 4 hrs; G_1 cells will not be blocked. *b*. Application of the model to the simulation of an 8-hr G_2-M block after irradiation; cell-cycle parameters same as fig 5; ordinate, % of S cells among proliferating cells.

use at time t a second treatment (for instance, for simplicity of presentation, an S-specific drug) we have only in practice to consider the modification of the percentage of S cells instead of considering the modification of the whole age distribution. Let $\hat{p}_s(t)$ be the expected percentage of S cells if no treatment would have been used at time 0 and $p_s(t)$ be the observed percentage of S cells after treatment. We define as index of synchrony the quantity

$$I(t) = \frac{p_s(t) - \hat{p}_s(t)}{\hat{p}_s(t)}.$$

This index is zero if the first treatment does not synchronize the cell population in S phase at time t. It is positive when after the first treatment (or synchronizer) administered at time 0 the percentage of cells in S phase is larger than the control value (without synchronizer) $\hat{p}_s(t)$. The computation of this index would make it possible to compare quantitatively two synchronizers.

Lethal and nonlethal effects of treatment may induce synchrony on a cell population.

Selective Cell Killing

If the probability of death after treatment depends on the age of the cell, the age distribution of the viable population is modified and the synchrony is induced.

In the case of phase-specific drugs, selective killing may induce in the next few hours after treatment an important synchrony; in the other cases, and especially with irradiation, it will be negligible. This is demonstrated in figure 5 where we compare the synchronizing effect of a single dose of 750 rads and of a hypothetic S-specific drug on an EMT-6 tumor whose cell-cycle parameters have been previously described (25).

Blocks After Treatment

Independently of cell death, it is well known that many treatments may "block" the progression of cells through the cell cycle. After irradiation, this is commonly referred to as division delay. In chemotherapy, blockings have been reported for many drugs: for example, vinblastine blocks cells at the G_2-M border and actinomycin D blocks cells at the G_1-S and G_2-M borders.

Blocks may be modeled in different ways which correspond to different biologic concepts. We use the block model described in figure 6a; this model has been previously discussed and used to interpret experimental data (26). Basically it is assumed that, at treatment time, any cell present

has to "repair" during a time T_b to be allowed to pass through the block (eg, G_2-M). One consequence of that model is shown in figure 6a, in which the cells immediately before the G_2-M transition are those which exhibit the largest division delay. This is relevant to many experimental observations. We have simulated the joint effect of a 5-hour S-G_2 block and of an 8-hour G_2-M block in the evolution of the age distribution of a cell population with EMT-6 tumor cell-cycle parameters, assuming that there is no cell death. Results, shown in figure 6b, indicate that the consequent synchrony is more important than the one deduced from the selective killing effect (fig 5a); the particular values of the blocks which we show here were chosen because they are used to interpret the kinetics of nonclonogenic EMT-6 tumor cells after 250 rads. Another example is shown in figure 8b where an 8-hour block is assumed to occur at the G_1-S border.

Recruitment

Recruitment after treatment is a rather imprecise word, although commonly used. A general definition could be: quiescent cells are "recruited" after treatment if they synthesize DNA earlier than they would have done without treatment.

One can imagine that there are as many recruitment models as there are models of quiescent cells. We use two models of recruitment which correspond to two extreme models of quiescent cells. In the first one, following Mendelsohn (27), we assume that before treatment, cells at birth enter Q compartment and remain quiescent indefinitely. After treatment, the model specifies that a proportion, a, of the quiescent cells initiates DNA synthesis T_a hours later. In the second model, which is an adaptation from that of Burns and Tannock (28), quiescent cells are randomly released in the cycling compartment with a flux, γ, per unit of time.

With the first recruitment model, we interpreted data concerning proliferation of hemopoietic stem cells after hydroxyurea[4] (29) and, more recently,[5] data concerning the proliferation of the clonogenic cells in EMT-6 tumors after hydroxyurea with the second model and data concerning the proliferation of the nonclonogenic cells (30). Figure 8c shows the simulated age distribution of this tumor calculated on the hypothesis that the only effect of hydroxyurea was recruitment. Thus, by itself, recruitment synchronizes (ie, induces variations of percentage of cells in S after treatment).

Modification of Cell-Cycle Parameters After Treatment

Many investigators have shown that different treatments of various tumors lead to modifications of cell-kinetic parameters (for example, the duration of cell cycle). Such situations would, of course, induce synchrony because they would modify the age distribution. However, it is extremely difficult to derive a general law and to build any model because the observations appear to be extremely variable and, at times, contradictory. Moreover, we suspect that many of the observed variations in the cell-phase durations could be due to bias. For instance, as shown in figure 2, the PLM curves before and after treatment can be different simply because the age distributions are different (and not because of differences in cell-cycle durations).

SIMULATION OF TREATMENT PROTOCOLS

We shall present our simulation method for the modeling of treatment protocols.

Method

Our simulation method makes it possible to simulate the effects of up to ten treatments on the evolution of a cell population during up to 12 generations. Basically, this method uses the general simulation method described earlier (19) whose main characteristics are the following. The method makes it possible to simulate *forward* the progenies of N_0 cells present at time 0. Family trees originating from each of the N_0 cells and associated events (labeling, cell death, etc) are simulated iteratively. In figure 7 such a family tree is represented. It is drawn with the assumption that there is no cell death or cell loss. Each branch of the tree represents a cell and is divided into four segments which correspond to each of the four phases of the cell cycle.

A two-dimensional array Y(J;K) is defined by the following equations:

(*i*) Y(J;K) = time necessary to reach the end of the Kth($k \leq 4$) phase of cell J (*see* identification numbers in fig 9).

(*ii*) the mother of the Jth cell is the J_1th cell, where $J_1 = \left[\frac{1}{2} J\right]$ (= the largest integer smaller than $\frac{1}{2}$ J): this is due to our choice of cell identification system; it makes it easy to compute the parenthood of any two cells of the family tree, for instance, J_2 is the grandmother

[4]Hydroxyurea: NSC-32065; CAS reg. No. 127-07-1.

[5]Rockwell S. Demeestère M, Frindel E, et al. Cell proliferation in EMT6 tumors treated with single doses of X rays or hydroxyurea—comparison in clonogenic and nonclonogenic populations. In preparation, 1977.

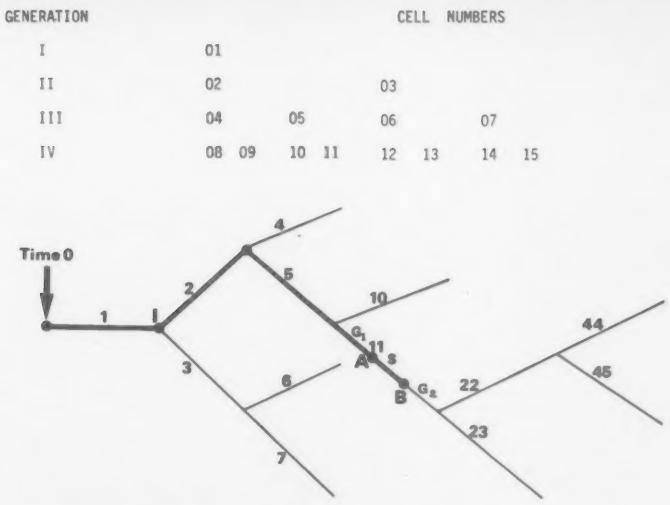

The mother of cell no.45 is cell no. .45 = 22.5 = 22.

(b) Representation of the cell population in the computer :

I = G_1 II = S III = G_2 IV = M

Examples:

Y(I,IV) = time elapsed between time 0 and time I (mitosis);

Y(II,I) = time elapsed between time 0 and time A
= Y(5,IV) + G_1(end of the G_1 phase of cell no.11);

Y(II,II)= time elapsed between time 0 and time B
= Y(II,I) + S (end of the S phase of cell no.11);

FIGURE 7.—*a.* Principle of identification of the cells in each family tree. *b.* Principle leading to the recurrence equations (*see* text).

method of J when $J_2 = \left[\frac{1}{2}\left[\frac{1}{2}J\right]\right]$.

(*iii*) $Y(J,1) = Y(J_1,4) + Ph_1(J)$, $Y(J,K) = Y(J;K-1) + Ph_k(J)(K \neq 1)$, where $Ph_k(J)$ is the duration of the Kth phase of the Jth cell.

In practice, the array Y(J,K) is completed by using the recurrence relations in (*iii*) where the numbers $Ph_k(J)$ are pseudo-random numbers from suitable distributions. We generally use log-normal distributions although, as stated above, we do not think that the choice of the distribution is very important in treatment modeling. To simulate nonstationary cell populations, mean and standard deviations are chosen to depend on other parameters, eg, time.

The array Y(J,K) is stored and may be used, for instance to compute how many cells are present in each phase at time t. For instance, the cell J is present in S at time t if

$$Y(J,1) < t < Y(J,2).$$

It is possible to simulate cell loss or death in proportion p by defining a new array D(J) as follows:

(*iv*) D(J) = 1 if cell J is dead or does not exist.

(*v*) D(J) = 1 if $D(J_1) = 1$, where $J_1 = \frac{1}{2}J$.

Condition (*v*) expresses the fact that daughters of a dead cell do not exist. If we assume that a proportion p of the cells present at time t die, we let D(J) = 1 with probability p for the cell J present at time t; p may be time dependent. This method makes it easy to follow (within a family tree) the progeny of a particular cohort of cells.

In the adaptation of this method to simulate treatment protocols, several subprograms are used to simulate the various effects of treatments (cell killing, block, recruitment, etc).

The entry parameters of the program are:

(*a*) the characteristics of the cell population: mean and standard deviations of cell-phase duration, percentage of proliferating cells, and eventually, age distribution before treatment;

(*b*) the scheduling of the treatments;

(*c*) the characteristics of each treatment: age-response curve, position(s) and duration(s) of the block(s), model, and corresponding param-

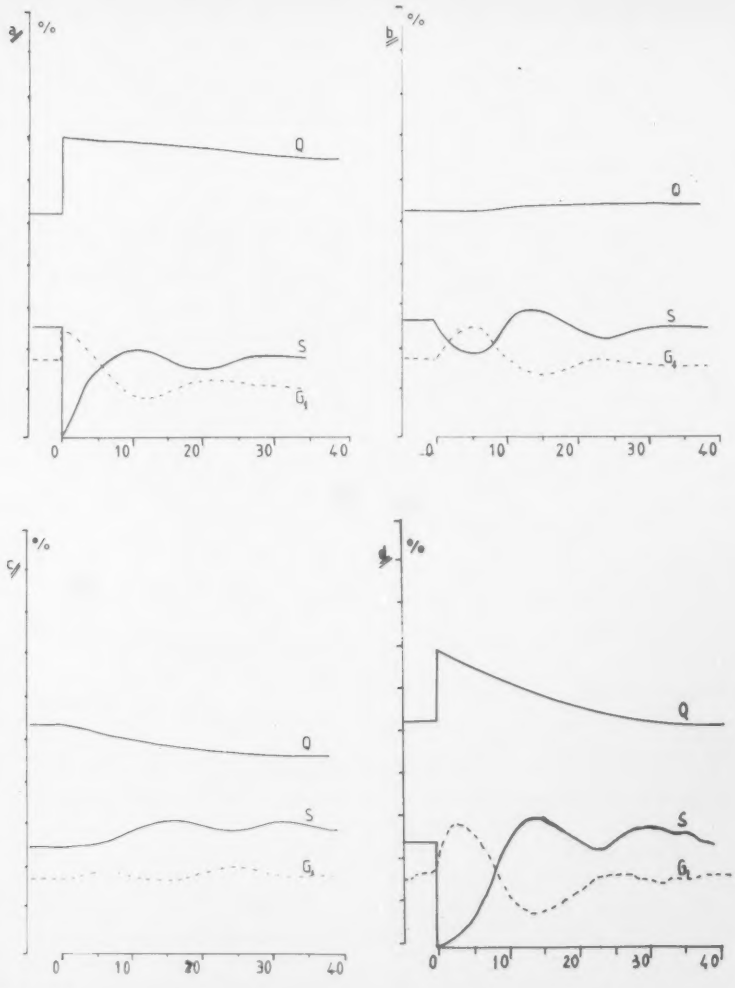

FIGURE 8.—Synchronies after hydroxyurea in nonclonogenic EMT-6 tumor cells; selective killing (*a*), G_1-S block (*b*), recruitment (*c*); and joint effect of these 3 factors (*d*).

eters of recruitment, and modification of cell-cycle parameters after treatment (if any).

The output of the program is the evolution of the age distribution and of the number of cells of the population during and after the treatments.

This simulation method probably requires a larger amount of computer time than analytic mathematic methods (at least in the more simple cases). However, the "cost" of a model cannot be evaluated only—as many mathematicians do—by considering the computing time. One has also to consider the "mathematician's time" which is expensive also.

Second, to make effective the collaboration between modelers and experimentalists, it seems very important to us to have a short delay between the elaboration of a hypothesis and the response of the model. This is why we generally prefer the simulation approach.

Application to Interpretation of Experimental Data

We have used our model to analyze experimental data on the EMT-6 tumor, labeling and mitotic indices observed at various times after hydroxyurea and irradiation, and percent of clonogenic cells in S phase after hydroxyurea, and irradiation obtained from an in vitro assay. Here we will only

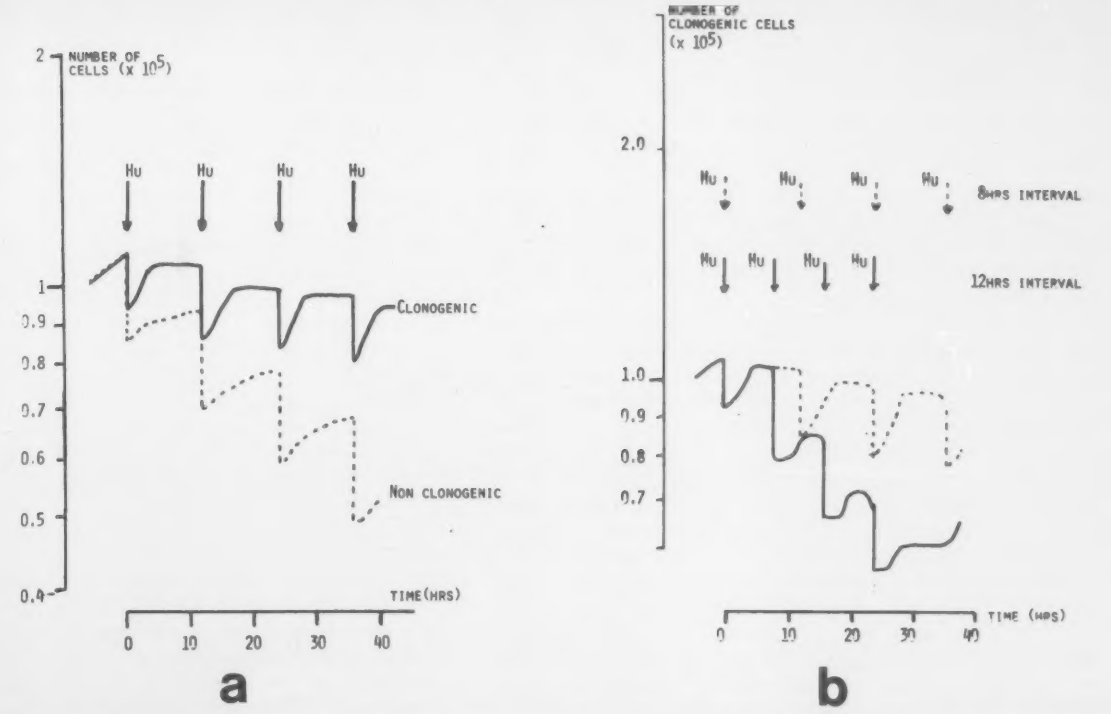

FIGURE 9.—Effect of 12-hr (*a*) protocols on clonogenic and nonclonogenic cells of EMT-6 tumor. Effect of 12-hr and 8-hr protocols on clonogenic cells (*b*). Clonogenic and nonclonogenic cell-cycle parameters of model were computed in another paper (*see* footnote 5).

present partial, preliminary results. The full results will appear in a forthcoming paper.[6]

The very preliminary results obtained in the interpretation of data after hydroxyurea:

(*a*) the cell cycle of clonogenic cells (17.8 hours) was shorter than the cell cycle of nonclonogenic cells (21.8 hours) (this appears to be in accordance with Steward [24] who noted that this EMT-6 tumor could be composed of two such subpopulations because of the lack of sensitivity of the PLM experiment to heterogeneous cell populations);

(*b*) all S cells are immediately killed after hydroxyurea;

(*c*) there is a G_1-S block after hydroxyurea (whose duration is approximately 5 hours in clonogenic and 8 hours in nonclonogenic cells);

(*d*) about 15% of the quiescent clonogenic cells are recruited 4 hours after hydroxyurea while 25% of the quiescent nonclonogenic cells are recruited with a flux from the Q to the P compartment of approximately 1%/hour.

The results concerning the evolution of the percent of nonclonogenic S-phase cells after hydroxyurea treatment are shown in figure 8d; figures 8a, b, and c show what the expected time variations would be if hydroxyurea had only killed S cells, blocked cells at the G_1-S border, or recruited cells. Thus, the overall synchrony (fig 8d) cannot be analyzed as based only on the selective cell killing (fig 9a) but also based on the block (fig 8b) and, somewhat less importantly, on the recruitment (fig 8c).

Application to Drug Scheduling

Many authors have described application of models to drug scheduling (*see* ref 31). Various mathematic methods make it possible to simulate treatment protocols. The most difficult and exciting work is, in fact, to classify precisely the various effects of treatments, to discuss the relative importance of the commonly used mathematic and biologic hypotheses, and finally, to devise mathematic methods which make it possible to analyze the drug mechanisms.

The other task is, of course, to get enough experimental data. As an example, we shall again use the previous EMT-6 tumor. The maximum experimental labeling index is observed 12 hours after hydroxyurea. It seems that good scheduling would be to use

[6] *See* footnote 5.

a 12-hour interval treatment. Based on known cell-cycle parameters, and assuming that hydroxyurea acts as described in the previous section, we have simulated effects of this 12-hour protocol on the total cell population. In this particular case, we get additional data on the clonogenic subpopulation and thus are able to estimate the effect of the 12-hour interval treatment on the subpopulation. The results are shown in figure 9a. The protocol is ineffective on the clonogenic subpopulation while it is apparently effective against the total population; figure 9b indicates that an 8-hour protocol treatment would be more effective against the clonogenic cell subpopulation while it would be less effective against the nonclonogenic cell population. However, treatment should be directed against the relevant clonogenic cells.

It is also important to note that it is probably unrealistic to devise standard treatment protocols based on the maximization of killing of tumor cells since the variability of tumor cell-cycle parameters from patient to patient is important. In the same direction, the lack of precision of tumor parameters has to be taken into account in modeling of drug scheduling. This is only possible if one uses methods utilizing the standard deviation of the computed parameters corresponding to the experimental variability in PLM experiments (17,32).

The minimization of killing of normal cells whose parameters are probably much less variable from one patient to another could be better investigated if more quantitative data on the kinetics of normal tissues and on the precise action of treatments were known.

CONCLUSION

We have focused on four main points.

A. The stationary principle very often used in the modeling of cell populations before treatment has to be questioned. In particular, it is interesting to develop mathematic models of diurnal rhythms: the dramatic spontaneous variations in percentages of the S and M cells in the hamster cheek pouch which are observed throughout the day are more important than those which could be expected after most of the drugs. The question is how to go from this experimental evidence to a practical clinical conclusion.

B. Other hypotheses currently made in cell-kinetic modeling were also discussed: correlations between cell-cycle parameters of sister cells and also between mother and daughter cell-cycle parameters have been reported for in vitro EMT-6 cells. Probably any skewed distribution of probability can be used to model treatment protocols.

C. Models of cell-cycle blocks and of recruitment were proposed.

D. Finally, a Monte-Carlo simulation method of a cell population undergoing chemotherapy (or irradiation) treatments was described. Two examples of its application were given. First, the interpretation of experimental data after treatments to give a detailed description of the mechanisms of these treatments was discussed, and second, the modeling of treatment protocols was discussed. In this last example, we have shown the importance of the lack of experimental data on clonogenic tumor cells in the computing of "optimized" treatment protocols.

We have also described some of the functions of mathematic models in cell kinetics.

A. Clarification of definitions and hypothesis.—One cannot make mathematic models with hazy definitions; the development of definitions, notions, and criticism of hypotheses is probably the more interesting, from a biologic point of view.

B. An a priori theoretic examination of the interest of further experiments.—Models can be used to prepare experiments and to select those which can be expected to lead to the more interesting results. For example, one can think to the a priori criticism of clinical trials; in order to clarify the point, assume that we wonder whether or not it is beneficial to start a clinical trial to compare treatment protocol A with treatment protocol B. Assume that all but one of the parameters of the cell population and of treatments A and B are known. We can vary that parameter and check whether the advantage of A versus B does not depend on the particular value of this unknown. If it does, we cannot begin this experiment before knowing this unknown or we have to choose another experiment. The same procedure can be used if we do not know several model parameters.

C. Acquisition of the maximum amount of information from the experimental data.—This can be done by making it possible to analyze quantitatively the 44 pedigrees and to compute all the possible parental correlations and all the possible distributions. As another example of this, the use of our method of treatment simulation made it possible for us to describe the G_1-S blocks and the recruitment after hydroxyurea. This could not have been hypothesized from the experimental data without the model.

REFERENCES

1. JANSSON B, and REVESZ L. Analysis of the growth of tumor cell populations. Mathemat Biosci 19:131–143, 1975.
2. SHACKNEY SE. A cytokinetic model for heterogeneous mammalian cell populations. I. Cell growth and cell death. J Theor Biol 38:305–333, 1973.

3. HARRIS TE. The Theory of Branching Processes. Berlin, Springer-Verlag, 1963.
4. BROWN JM, and BERRY RJ. The relationship between diurnal variation of the number of cells in mitosis and the number of cells synthesizing DNA in the epithelium of the hamster cheek pouch. Cell Tissue Kinet 1:23–33, 1968.
5. IZQUIERDO JN, and GIBBS SJ. Circadian rhythms of DNA synthesis and mitotic activity in hamster cheek pouch epithelium. Exp Cell Res 71:402–408, 1972.
6. IZQUIERDO JN, and GIBBS SJ. Turnover of cell renewing populations undergoing circadian rhythms in cell proliferation. Cell Tissue Kinet 7:99–111, 1974.
7. MOLLER U, LARSEN JK, and FABER M. The influence of injected tritiated thymidine on the mitotic circadian rhythm in the epithelium of the hamster cheek pouch. Cell Tissue Kinet 7:251–257, 1974.
8. MAUER AM. Diurnal variation of proliferative activity in the human bone marrow. Blood 26:1–7, 1965.
9. CLARK RH, and KORST DR. Circadian periodicity of bone marrow mitotic activity and reticulocyte counts in rats and mice. Science 166:235–236, 1969.
10. ROSENE GL, and HALBERG F. Circadian and ultradian mitotic rhythms in liver breast cancer and Ehrlich ascites tumors of mice. Bull All India Inst Med Sci 4:77–94, 1970.
11. HAUS E, HALBERG F, PAULY JE, ET AL. Increased tolerance of leukemic mice to arabinosyl cytosine with schedule adjusted to circadian system. Science 177:80–82, 1972.
12. KLEIN B, and VALLERON A-j. A compartment model for study of diurnal rhythms in cell proliferation. J Theor Biol, 1977.
13. TAKAHASHI M. Theoretical basis for cell cycle analysis. I. Labelled mitosis wave method. J Theor Biol 13:202–211, 1966.
14. KLEIN B, and VALLERON A-j. Mathematical modelling of cell cycle and chronobiology: preliminary results. Biomedicine 23:214–217, 1975.
15. BROCKWELL P. Random walks, diffusion processes and diurnal rhythm in cell populations. *In* Mathematical Models in Cell Kinetics (Valleron A-j, ed). Ghent, European Press, 1975, pp 24–25.
16. COLLYN M, VALLERON A-j, and MALAISE E. Statistical analysis of 44 family trees of EMT 6 cells observed by microcinematography. Exp Cell Res. In press, 1977.
17. MACDONALD PDM. Statistical inference from the fraction labelled mitoses curve. Biometrika 57:489–503, 1970.
18. BARRETT JC. Optimized parameters for the mitotic cycle. Cell Tissue Kinet 3:349–353, 1966.
19. VALLERON A-j, and FRINDEL E. Computer simulation of growing populations of cells. Cell Tissue Kinet 6:69–79, 1973.
20. HAHN GM. A formalism describing the kinetics of some mammalian cell populations. Mathemat Biosci 6:295–304, 1970.
21. HARTMANN NR, and PEDERSEN T. Analysis of the kinetics of granulosa cell populations in the mouse ovary. Cell Tissue Kinet 3:1–13, 1970.
22. KUBITSCHEK HE. The distribution of cell generation times. Cell Tissue Kinet 4:113–122, 1971.
23. HARTMANN NR, GILBERT CW, JANSSON B, ET AL. Comparison of computer methods for FLM curve analysis. Cell Tissue Kinet 8:119–124, 1975.
24. STEWARD PC. The Cell Cycle in Malignancy and Immunity. US Energy Research and Development Administration, 1975, p 443.
25. ROCKWELL S, KALLMAN RF, and FAJARDO LF. Characteristics of a serially transplanted mouse mammary tumor and its tissue-culture-adapted derivative. J Natl Cancer Inst 49:735–747, 1972.
26. VALLERON A-j. A method of computer simulation used to study some sublethal effects of irradiation on cell kinetics. *In* Mathematical Models in Biology and Medicine. Amsterdam, North-Holland Publishing Co, 1974, pp 111–131.
27. MENDELSOHN ML. Autoradiographic analysis of cell proliferation in spontaneous breast cancer of C3H mouse. III. The growth fraction. J Natl Cancer Inst 28:1015–1029, 1962.
28. BURNS TJ, and TANNOCK IF. On the existence of a G-phase in the cell cycle. Cell Tissue Kinet 3:321–334, 1970.
29. VASSORT F, WINTERHOLER M, FRINDEL E, ET AL. Kinetics parameters of bone marrow stem cells using in vivo suicide by tritiated thymidine or by hydroxyurea. Blood 41:789–796, 1973.
30. DEMEESTERE M, MARY J, and VALLERON A-j. A general program for simulation of lethal and non-lethal effects of treatments. *In* Mathematical Models in Cell Kinetics (Valleron A-j, ed). Ghent, European Press, 1975, pp 84–88.
31. STEWARD PC, and HAHN GM. The application of age response functions to the optimization of treatment schedules. Cell Tissue Kinet 4:279–291, 1971.
32. VALLERON A-j, MARY JY, and FRINDEL E. Méthode d'analyse sur ordinateur des courbes de mitoses marqées. Biomedicine 18:118–123, 1973.

Rapid Methods for Utilizing Cell Kinetics for Treatment in the C3H/He Spontaneous Mammary Tumor: Effects of Vincristine [1,2]

Lewis M. Schiffer,* Paul G. Braunschweiger, and Lawrence Poulakos [3]

For many years oncologists have been frustrated by the apparent lack of progress in obtaining clinically useful cell kinetic measurements of human solid tumors. The technique of in vivo administration of tritiated thymidine (^{3}H-TdR) followed by multiple biopsies, to determine the fraction of labeled mitoses, has largely remained unchanged during the past 15 years, and the limitations of this procedure are well known and do not need reemphasis. Although in vitro measurement of ^{3}H-TdR-labeling indices (LI) and in vitro estimation of DNA synthesis times (T_S) have been practiced for many years, there have been few controlled studies to determine whether the in vitro results are really comparable to those found in vivo. In addition, only indirect measurements of growth fraction (GF) have been possible. It was with these problems in mind that our laboratory began investigations into rapid techniques with clinical applicability for measuring cytokinetic parameters. From the start it was understood that our results probably would not detect the nuances and would be a pragmatic approach to the problem.

The model chosen for the development of techniques was the spontaneous mammary tumor of the C3H/He mouse. The spontaneous tumor model was chosen because of its relatively well differentiated histology, low GF, and potential variation in growth rates, and because the vascular patterns are far different from transplantable tumors. The limitation of this model is primarily that of relatively few tumor animals.

This report will describe the comparison between in vitro and in vivo studies of the measured cytokinetic parameters which include: number of cells in DNA synthesis, T_S, estimate of GF, and the derived parameters of cell-cycle time (T_C) and potential doubling time (T_{pot}). Since these in vitro studies are applicable at the point-in-time of the biopsy, the perturbations of the tumor cytokinetics by drug or radiation therapy can be experimentally determined. A recent study in our laboratory (1) showed that a time-sequenced course of vincristine (VCR) and cyclophosphamide[4] (CYT) would cure an otherwise lethal transplantable T1699 tumor guided by the methods described in this paper; this study will be described in detail later. This report will include initial studies of the effects of VCR on the C3H/He spontaneous mammary tumor and a comment about some of the potential uses to which these techniques may be put.

MATERIALS AND METHODS

Animals

C3H/He retired breeders (JAX) (ten to 15 per cage) were kept until they developed tumors; they were then housed five to a cage.

In Vivo ^{3}H-TdR Labeling

Tumor-bearing animals were injected ip with 2 microcuries/g body weight of ^{3}H-TdR (14–17 curies/mmol) in 0.5 ml of saline. Sixty minutes later the animals were killed by cervical dislocation and the tumors were excised and minced with fine scissors in McCoy's medium with 20% fetal calf serum (FCS). Tissue fragments were further disaggregated with a Pasteur pipette and the suspension was filtered through a stainless steel screen. The cells were suspended in 0.1 M citric acid for 1 minute at 4°C. Drop preparations were made by resuspending the cells in Clarke's fixative for 5 minutes at 4°C and then applying one or two drops of the suspension to acid-cleaned slides. The slides were air dried, washed for 20 minutes in running water, and air dried again (3).

[1]Supported by Breast Cancer Task Force contract N01-CB-43899 and Clinical Radiation Therapy Research Center grant CA-10438 from the National Cancer Institute, National Institutes of Health, Department of Health, Education, and Welfare.

[2]Vincristine: NSC-67574; CAS reg. No. 2068-78-2; leurocristine, sulfate (1:1).

[3]Cancer Research Unit, Division of Radiation Oncology, Allegheny General Hospital, Pittsburgh, Pa.

Reprint requests to: Lewis M. Schiffer, MD, Cancer Research Unit, Division of Radiation Oncology, Allegheny General Hospital, 320 E North Ave, Pittsburgh, Pa 15212.

[4]Cyclophosphamide: NSC-26271; CAS reg. No. 6055-19-2; 2*H*-1,3,2-oxazaphosphorine, 2-[bis(2-chloroethyl)amino]tetrahydro-, 2-oxide, monohydrate.

In Vitro ^{3}H-TdR Labeling

In vitro labeling was done by a modification of the method of Livingston et al (2). Single-cell suspensions were prepared from solid tumors by mincing at room temperature as described for in vivo labeling. After the suspension was filtered through the stainless steel screen, 3-ml suspensions ($3–5 \times 10^7$ cells/ml) were incubated for 1 hour at 37°C in fresh media with 2.5 microcuries/ml of ^{3}H-TdR. Labeling was terminated on ice and the suspension centrifuged at 1200 rpm in a clinical centrifuge. The cells were resuspended in cold calcium-free Eagle's Minimal Essential Media, applied to a Hypaque-Ficoll gradient, and spun at 400 g for 20 minutes at 4°C. Cells confined to the gradient-media interface were collected with a Pasteur pipette and diluted in seven to eight volumes of fresh media. Samples were taken for viability determinations (trypan blue exclusion) and the suspension was centrifuged at 1200 rpm for 5 minutes in a clinical centrifuge. The cells were resuspended in 0.1 M citric acid and drop preparations were made as described above (3).

In Vivo /In Vivo Double Labeling

Tumor-bearing animals were injected ip with 40 microcuries of ^{3}H-TdR (14–17 curies/mmol) and 60 minutes later were similarly injected with 2.5 microcuries of ^{14}C-TdR (54 millicuries/mmol). Thirty minutes later the animals were killed by cervical dislocation and the tumors quickly excised and placed on ice. The tumors were then minced with fine scissors in McCoy's media with 20% FCS and filtered through a stainless steel screen to remove large tissue fragments. The cells were washed with cold media and drop preparations prepared as described above (3).

In Vitro/In Vitro Double Labeling

Single-cell suspensions for in vitro double labeling were prepared in a manner similar to that described above and the cells resuspended ($3–5 \times 10^7$ cells/ml) in fresh media. Three-ml aliquots were incubated at 37°C with 2.5 microcuries/ml of ^{3}H-TdR for 60 minutes at which time ^{14}C-TdR was added to a final concentration of 0.25 microcurie/ml. The reactions were terminated on ice 30 minutes later, the suspension was centrifuged, and the cells were resuspended in calcium-free Eagle's Minimal Essential Media. The suspensions were applied to Hypaque-Ficoll gradients with cells collected and prepared as before (3).

In Vivo/In Vitro Double Labeling

Tumor-bearing animals were injected ip with 40 microcuries of ^{3}H-TdR and killed 60 minutes later. Single-cell suspensions were prepared as described above and the cells were incubated for 30 minutes at 37°C with ^{14}C-TdR (0.25 microcurie/ml). The reactions were terminated on ice and the suspensions were applied to Hypaque-Ficoll gradients. After centrifugation for 20 minutes at 400 g drop preparations were made.

In Vivo Estimate of GF

This estimate was made by the method of Mendelsohn (4) in which the fraction

$$\frac{\text{labeled cells}}{\text{total cells}} \Big/ \frac{\text{labeled mitoses}}{\text{total mitoses}}$$

was determined after the desynchronization phase of the labeled-mitoses curve. A total of 16 tumors were studied after the ip administration of 20 microcuries of ^{3}H-TdR. The animals were killed at 5 days, and the tumors removed, bisected, and fixed. After histologic preparation and autoradiography the above parameters were determined.

In Vitro Estimate of GF

This laboratory has previously utilized a new autoradiographic technique to demonstrate the proportion of cells whose unfixed nuclei contain endogenous DNA primer-template and DNA-dependent DNA polymerase (PDP index) (5). It has now been shown that the PDP index estimates the proportion of cells in the replication cycle (GF) in at least ten mouse and rat tumor systems (6,7).[5]

Unlabeled tumors were excised and bisected, and tumor imprints were made on acid-cleaned slides and air dried. Previous studies have shown the equivalence of tumor imprints and disaggregated tumor cells for the PDP indices, and tumor imprints were preferred because of simplicity.

The unfixed smears were dipped in 0.125% agar and again air dried. This process appears to disrupt the cytoplasmic membrane leaving only nuclei adherent to the slide. Chambers were made by affixing a glass ring to each slide and 0.5 ml of incubation medium was added. This medium contained 8.3×10^{-5} M deoxycytidine-5′-triphosphate, deoxyguanosine-5′-triphosphate, and deoxyadenosine-5′-triphosphate, 10^{-2} M $MgCl_2$ and 10^{-2} M KCl in 8.3×10^{-2} M tris-HCl buffer (pH 8.0 at 25°C). Prior to use the

[5]Other studies done by this group.

medium was supplemented with 400 mg of Ficoll and 10 microcuries of tritiated deoxythymidine-5′-triphosphate (^{3}H-TTP) per ml of incubation medium; β-mercaptoethanol was added at a final concentration of 10^{-3} M. The slides were incubated at 37°C for 45 minutes. After incubation the medium and rings were removed and the slides were fixed and processed for autoradiography. The developed slides were stained with hematoxylin and the fraction of labeled nuclei was determined microscopically. In this system, all of the requisite materials for DNA synthesis are provided to the nuclei with the exception of DNA polymerase and DNA capable of acting as primer-template. If these two essentials are available in the nucleus, DNA synthesis is forced and the ^{3}H-TTP will be incorporated into insoluble DNA. The uptake of ^{3}H-TTP is not contingent upon cells being in S phase when the slides are prepared.

Rapid Autoradiography

Kodak NTB-2 liquid emulsion was applied by dipping at 45°C. The autoradiograms were dried at room temperature for 1 hour and exposed in light-tight boxes at 4°C from 6 hours to 10 days.

Gold activation autoradiography (GARG) was utilized wholly after initial studies provided equivalence with normal autoradiography (3). Studies have indicated a fourfold to fivefold decrease in exposure time necessary to provide equivalent gains in both single- and double-emulsion autoradiograms. A solution of gold salts was used to activate the latent image produced in the photographic emulsion prior to development. The gold solution was prepared by dissolving 75.6 mg of $KAuCl_4$ and 100 mg of KSCN in 20 ml of triple distilled water. This solution was then heated to 50°C and 300 mg of KBr was added. When the solution had cooled the volume was brought to 500 ml with triple distilled water. Since the shelf life of this solution is very short it was prepared just before use to ensure greatest activity and lowest background.

Autoradiograms processed by the GARG procedure were incubated at 15°C for 20 minutes in the gold solution, washed briefly in three changes of triple distilled water, and developed at 15°C in a Kodak amidol developer. The slides were fixed in acid fixer for 10 minutes, washed in tap water for 30 minutes, and air dried.

VCR Experiments

VCR was given ip at a dose of 2.5 mg/kg of body weight. This is less than an LD10 dose of VCR for the C3H/He mouse. The drug was given at 9:00 AM to animals carrying tumors of approximately 1 cm^3 in volume. Tumors were excised at predetermined times for the in vitro studies previously mentioned. Several animals were used to calculate the growth curve after VCR using a three-dimensional caliper measurement

$$\frac{L \times W \times H}{2}$$

Calculations

The ^{3}H-TdR LI and PDP index represent direct measurements of labeled fractions of a total population. The T_S is calculated from:

$$T_S = \frac{Ta \times {}^{14}C\text{-labeled cells}}{{}^3H\text{-only labeled cells}} \quad (1)$$

where Ta is the time between administration of ^{3}H-TdR and ^{14}C-TdR. The T_{pot} is calculated from:

$$T_{pot} = \frac{\lambda \times T_S}{{}^3H\text{-TdR LI}} \quad (2)$$

where the initial λ (correction factor for nonlinear distribution) is 0.75 and iteration is made between formulas 2 and 3.

$$\lambda = \frac{T_{pot}}{T_S}\left(e^{0.693\,\frac{T_S + T_{G_2}}{T_{pot}}} - e^{0.693\,\frac{T_{G_2}}{T_{pot}}}\right). \quad (3)$$

T_{G_2} is assumed to be 2 hours. The T_C is calculated from:

$$T_C = \frac{\lambda \times T_S \times \text{PDP index}}{{}^3H\text{-TdR LI}} \quad (4)$$

where the PDP index is assumed to be equal to the GF.

RESULTS AND DISCUSSION

Comparison of In Vivo and In Vitro Results

Table 1 shows the comparison of in vivo- and in vitro-measured cytokinetic data for the C3H/He spontaneous tumor. The data show little or no difference between in vivo and in vitro results for ^{3}H-TdR LI, T_S, and GF. Results indicate that completely in vitro studies can be performed in the C3H/He system without compromising reliability.

Table 2 shows cytokinetic parameters for spontaneous mammary tumors calculated from labeling and growth data. Where possible these parameters were determined for individual tumors so that sta-

tistical analysis could be made. The T_{pot} was calculated for individual animals and although considerable variation was observed between tumors, the mean values for in vitro and in vivo determinations were quite similar.

The T_C was determined for individual tumors studied in vitro utilizing the PDP index as an estimate of GF. For tumors studied in vivo an average T_C was calculated from the mean in vivo T_{pot} and GF as determined by the desynchronization method. The T_C in vivo (24.1 hours) was similar to that observed in vitro (21.7 ± 7.3 hours). One aspect not readily recognized in vivo is the large variation observed for T_C. In vitro values ranged from 16 to 44 hours. For example, table 3 shows cytokinetic parameters for 17 consecutive C3H/He tumors performed by the in vitro methodologies and GARG. Although the T_S values were relatively constant, the ^{3}H-TdR LI and PDP index varied by a factor of about two.

TABLE 1.—Comparison of in vivo and in vitro cell kinetic data for C3H/He spontaneous mammary tumors

	In vivo: $\bar{x}$ ± 1 SD (No.)	In vitro: $\bar{x}$ ± 1 SD (No.)
LI	0.069 ± 0.033 (70)	0.070 ± 0.023 (76)
T_S (hrs)*	10.6 ± 1.5 (25)	10.4 ± 0.6 (53)
GF†	0.179 ± 0.044 (16)	0.166 ± 0.037 (91)

*Calculated from $T_S = \frac{Ta \times {}^{14}C}{{}^{3}H}$

†For in vivo studies: calculated from desynchronization $\frac{L_C/T_C}{L_M/T_M}$. For in vitro studies: determined by the PDP index.

TABLE 2.—Calculated cytokinetic parameters for C3H/He spontaneous mammary tumors

	In vivo: $\bar{x}$ ± 1 SD (No.)	In vitro: $\bar{x}$ ± 1 SD (No.)
λ*	0.72	0.72
T_{pot}	134.5 ± 59.5 (25)	134.7 ± 53.9 (53)
T_C	24.1	21.7 ± 7.3 (36)
T_M	0.8	0.8
T_{G_2}	2.0	2.0
T_{G_1}	10.6	8.4 ± 4.8 (36)
θ	0.593 ± 0.300 (25)	0.572 ± 0.400 (53)

*Calculations described in the text.

TABLE 3.—Cytokinetic parameters in 17 consecutive C3H/He tumors: rapid technique

^{3}H-TdR LI	T_S (hrs)	GF (PDP)	T_C (hrs)
0.079	11.0	0.159	15.9
0.070	10.0	0.157	16.1
0.075	9.5	0.183	16.7
0.055	10.6	0.135	18.7
0.088	10.7	0.214	18.7
0.045	9.8	0.125	19.6
0.037	10.0	0.101	19.7
0.069	10.5	0.182	19.9
0.057	10.3	0.160	20.8
0.054	9.9	0.159	21.0
0.047	11.1	0.125	21.2
0.046	9.3	0.153	22.2
0.053	11.3	0.148	22.8
0.038	9.9	0.122	22.9
0.051	9.6	0.172	23.3
0.045	11.7	0.125	23.4
0.048	10.5	0.180	28.4
0.037–0.088	9.3–11.7	0.101–0.214	15.9–28.4

Cell loss factor (θ), determined by the method of Steel (8), was also quite variable within each experimental group. Individual values ranged from 0.03 for the most rapidly growing tumor to 1.5 for a tumor showing spontaneous regression at the time of study.

The results from these preliminary experiments strongly suggest that the in vitro techniques for determining ^{3}H-TdR LI, T_S, and GF are applicable to solid tumor systems. These methodologies together with GARG permit determination of cytokinetic profiles for individual tumors from single biopsy samples in a relatively short period of time.

Cytokinetic Effects of VCR

VCR causes a reduction of tumor volume which reaches a nadir of 75% of its original volume at 3 days. Figure 1 shows the effects of VCR on the ^{3}H-TdR LI and PDP index. There was an initial decline of the ^{3}H-TdR LI followed by two peaks in labeling activity at 36 and 60 hours. At 72 hours the ^{3}H-TdR LI was significantly greater than control values, but by Day 7 the LI was similar to that of untreated control tumors. The PDP index decreases immediately after VCR; however, starting at 24 hours, a progressive rise in the PDP activity resulting in a peak of 85% at 60 hours was observed. If the assumption is correct that the PDP index represents the GF in the perturbed state as well as it seems to in the unperturbed state, the results would seem to suggest that the fraction of proliferating cells has increased from about 20% to nearly 85% by 60 hours after a single dose of VCR. The sudden drop and failure to rise after 72 hours may be an artifact of insufficient sampling after that time, or it may be significant.

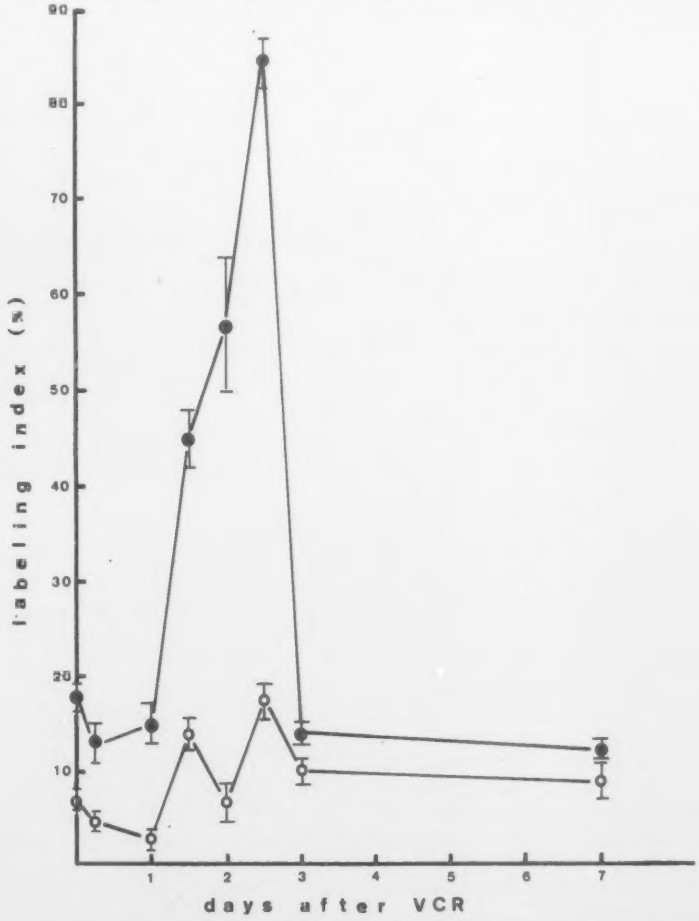

FIGURE 1.—Response of PDP index (●) and ^{3}H-TdR LI (○) after 2.5 mg/kg of VCR in C3H/He tumor. ⊥ = 1 SEM.

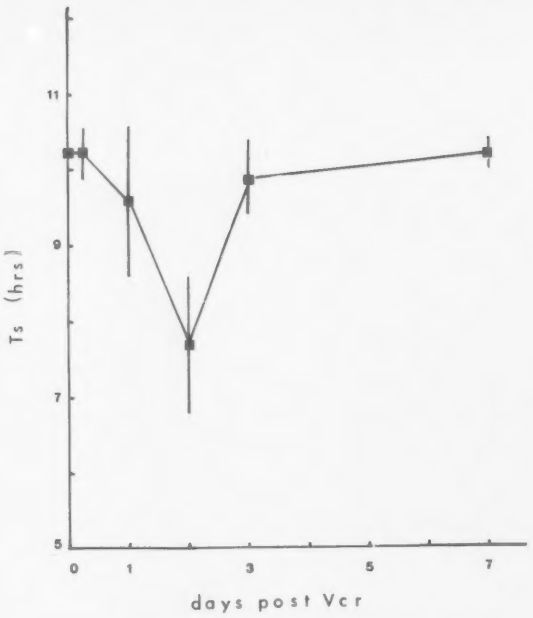

FIGURE 2.—Response of T_S after 2.5 mg/kg of VCR in C3H/He tumor. ▮ = 1 SEM.

Figure 2 shows the effect of a single dose of VCR on the T_S of the C3H/He tumor. There is a progressive shortening of T_S beginning 24 hours after treatment resulting in approximately a 25% reduction by 48 hours. By 72 hours T_S was observed to be within normal limits.

Table 4 is a compilation of the calculated and measured cytokinetic parameters at various intervals after a single dose of VCR. The λ factor does not change by > 10%. The T_{pot} increases to a maximum at 24 hours which is primarily the result of a decrease in the ^{3}H-TdR LI. At 60 hours the T_{pot} is nearly equivalent to the T_C as the large increase in the PDP index becomes the most significant feature. The T_C fluctuates before the ^{3}H-TdR LI, however, and maximal values were reached at 48 hours when the PDP index was still increasing and most of the cycling cells were probably in G_1. The T_C shortens markedly after 60 hours and the great majority of cycling cells are in S phase. The θ, measured by doubling time (T_D) changes and T_C values, peaks at 24 hours. The volumetric T_D showed a decrease from 14 days to a minimum of −9.3 during regression. The T_D between Days 4 and 7 increased, however, it remained approximately one third of that observed for these animals before treatment.

Figure 3 is a graphic version of the above with the

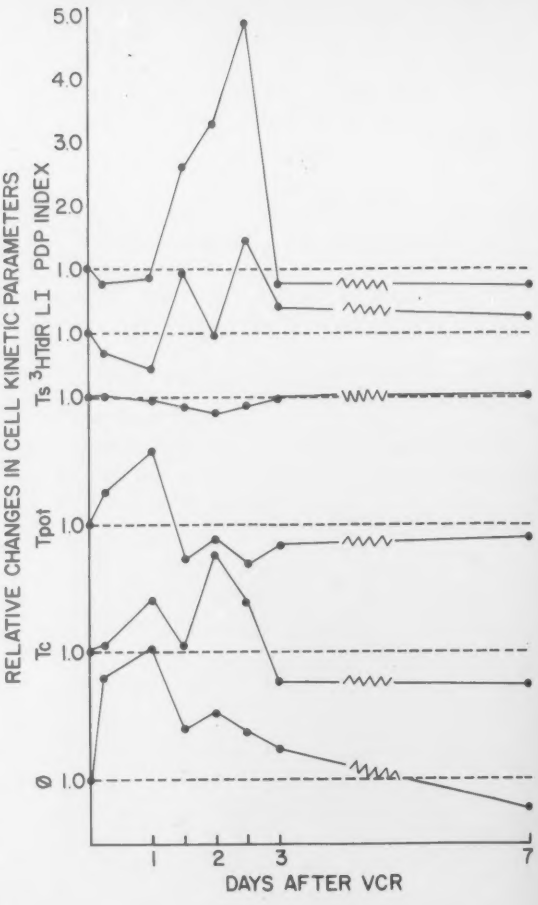

FIGURE 3.—Relative changes in cell kinetic parameters using time 0 as denominator after 2.5 mg/kg of VCR in C3H/He tumor.

Y-axis representing the relative change in parameters using time 0 as the control values.

Figure 4 is a description of the total compartment sizes of the C3H/He tumor, taking into account the measured change in tumor volume over the 7-day period. The change in tumor volume is represented by the upper line. The 0–24-hour period is obviously not corrected for the change in the mitotic compartment that would be expected from the administration of VCR; this parameter was not measured. Looking at figures 3 and 4 the effects on S phase can be summarized as probably being a result of cell death in S, a shortening of S phase with a nadir at 48 hours, and partial synchronization of the population reflected by the cells in S phase at 36 and 60 hours. We suspect that the PDP changes are a reflection of a change in G_0 and G_1 status, from the

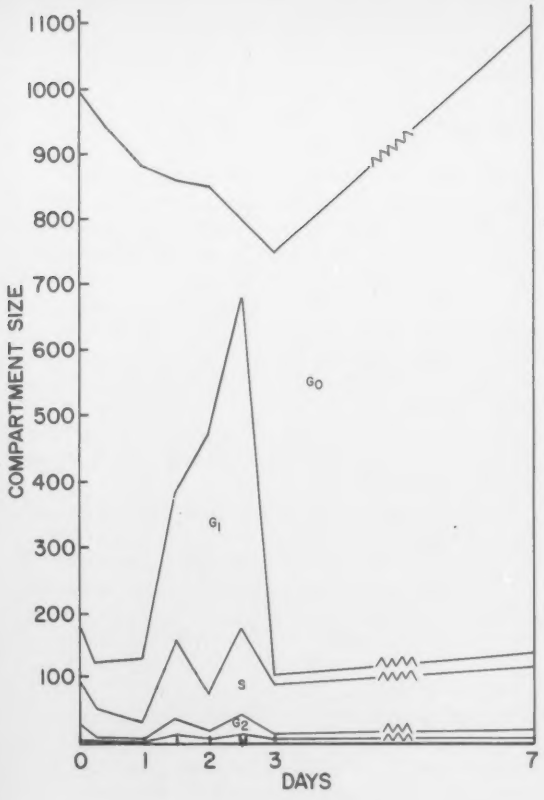

FIGURE 4.—Cell-cycle compartment size using 1000 cells as a starting base after 2.5 mg/kg of VCR in C3H/He tumor. Corrected for change in tumor volume.

noncycling to cycling state. If that is so, then the effects on G_1 appear to be an immediate G_1/S block which is released by 24 hours, a kill of cells in G_1, and a recruitment of G_0 cells into G_1 from 24 to 72 hours with a sharp peak at 60 hours. From 3 to 7 days the compartment is very small. The effect on the G_0 compartment is a kill of cells and a recruitment out of G_0 into G_1. The sudden increase in G_0 cells at 60–72 hours, manifested by the drop in the PDP index, is not completely explainable. Perhaps future points at 12- or 24-hour intervals will make it clearer but at the present one of two explanations seems most plausible. The mass of G_1 cells at 60 hours could rush through the cycle and revert to noncycling cells once through mitosis. If this were so one might expect a higher ^{3}H-TdR LI at 72 hours. Another explanation might be that cells continue to die in G_1, or that the G_1 cells revert back into a G_0 state without going through S and the rest of the cycle. This latter semi-heretical option is, as yet, not substantiated by fact.

What is apparent from dissection of these results is that both synchronization and recruitment do occur. The recruitment is so intense and exquisitely time-sensitive that attempts at treatment with cycle-active and S-active agents at and around 60 hours becomes imperative. These studies are now in progress.

The reason for believing that time-sequenced drug therapy after VCR may be effective on the C3H/He tumor is based on the favorable results seen with the T1699 tumor. This transplantable mammary tumor of the DBA/2J (JAX) mouse was studied with the same techniques as the spontaneous tumor. Figure 5 shows the effect of VCR, with time, on the tumor volume, PDP index, and ^{3}H-TdR LI. The marked depression and overshoot of the PDP index prompted the introduction of a second drug, CYT, at early times (6 hours, 1 and 2 days) after VCR and at late times (3–7 days) after VCR. The expectation

TABLE 4.—Perturbation of cytokinetic parameters after 2.5 mg/kg of VCR in the C3H/He spontaneous mammary tumor

	Time after VCR (hrs)							
	0	6	24	36	48	60	72	7 days
PDP index (GF)	0.175	0.130	0.150	0.450	0.565	0.850	0.135	0.125
^{3}H-TdR LI	0.070	0.045	0.028	0.140	0.065	0.170	0.098	0.088
T_S (hrs)	10.3	10.3	9.6	8.6*	7.7	8.8*	9.9	10.2
λ	0.75	0.72	0.69	0.76	0.73	0.78	0.74	0.73
T_{pot} (hrs)	110	165	237	46.8	86.5	40.4	75	85
T_C (hrs)	19.3	21.4	35.5	21.0	48.9	34.3	10.1	10.6
T_D (days)	14	−9.3	−9.3	−9.3	−9.3	−9.3	—	5
θ	0.67	1.74	2.06	1.21	1.39	1.18	1.00	0.29

*Estimated *from* fig 2.

was that CYT, presumably a cycle-active drug, would prove most effective at times when the PDP index, presumably an indicator of GF, was elevated. Figure 6 shows the change in tumor volume with each of these drugs alone. Neither drug cured any of the animals. Figure 7 shows the combined drug regimens, and it can be noted that the total tumor volume was significantly more affected by the late rather than the early CYT. This is reflected even more strikingly by figure 8 which is the survival curve. Although early CYT did show an increased median survival, the late CYT was better and, furthermore, the late CYT resulted in a 20% cure rate of these animals. The implication was that VCR caused recruitment of G_0 cells into G_1 where they were more effectively treated by CYT.

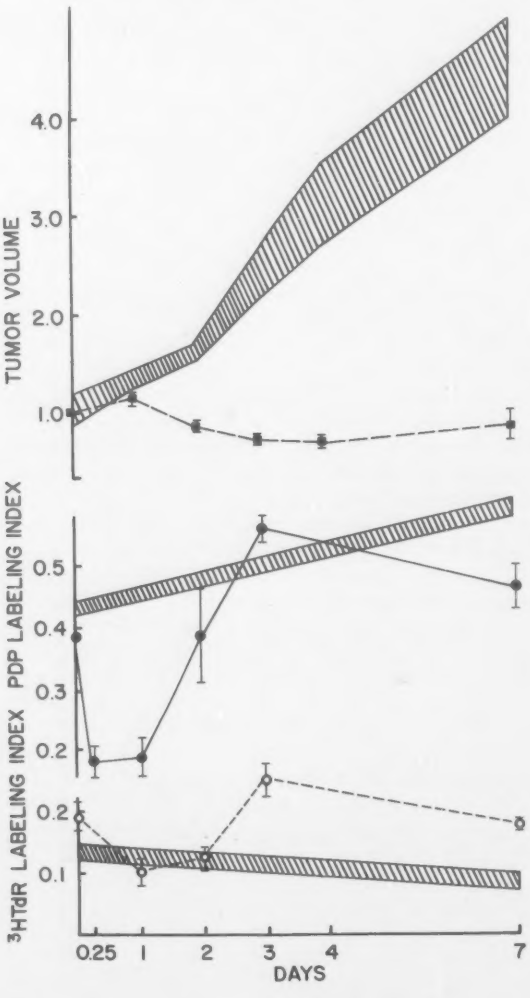

FIGURE 5.—Response of PDP index (●), ^{3}H-TdR LI (○), and tumor volume (■) after 2.5 mg/kg of VCR in 14-day T1699 tumor of DBA/2J mouse. ▮ = 1 SEM. Hatched areas are age-matched control values.

COMMENT

Although clinicians have long realized that VCR was cytocidal in cell-cycle phases other than mitosis, the problem of defining the details has only recently been attempted. Much of the experimentation has occurred in different tumor systems and with different dosages of the drug. The issue is still quite muddled, although low-dose VCR is thought to produce synchronization and high-dose VCR a degree of cell kill (9–11). Not all investigators are in agreement however (11,12). Using a high dose of VCR in our system, the C3H/He spontaneous solid mouse mammary tumor, synchronization, recruitment, and cell kill are apparent.

However, in the context of this conference it is appropriate to comment on the potentials of our set of techniques and how cell kinetics may possibly be used in the clinical situation. We must show that human tumor in vitro studies are equivalent to the in vivo studies before we can safely utilize the in vitro studies. This is in progress and the results are quite encouraging.

Assuming that the comparisons will be adequate, one method of utilization would be to estimate the unperturbed cytokinetics of a large quantity of primary and metastatic tumors and to build a data bank. Predictions and clinical correlations, if any exist, could be made on the basis of retrospective studies. If we become truly clever at this, learn our pharmacokinetics and cancer biology well, and begin to predict the effects of drugs on tumors, then we can attempt to design cytokinetically oriented therapy without biopsying individual tumors.

Most likely, however, we will have the patient's own tumor to work with. Since our techniques are designed to produce information rapidly, within 1 week or less, it is certain that we can have individual cytokinetic data available after biopsy. Of great importance, moreover, is the problem of differential cytokinetics between primary and metastatic lesions. This information on individual cytokinetics can be used to design therapy for the patient.

After initial treatment with single or multiple agents, as this paper demonstrates, the kinetics of the tumor will change markedly. The cytokinetics of the tumor can be followed by repeated biopsy of large tumors or small tumor nodules that are available. A historical compilation of these data will guide us in the design of time-sequencing subsequent drugs. It is even conceivable that the cytoki-

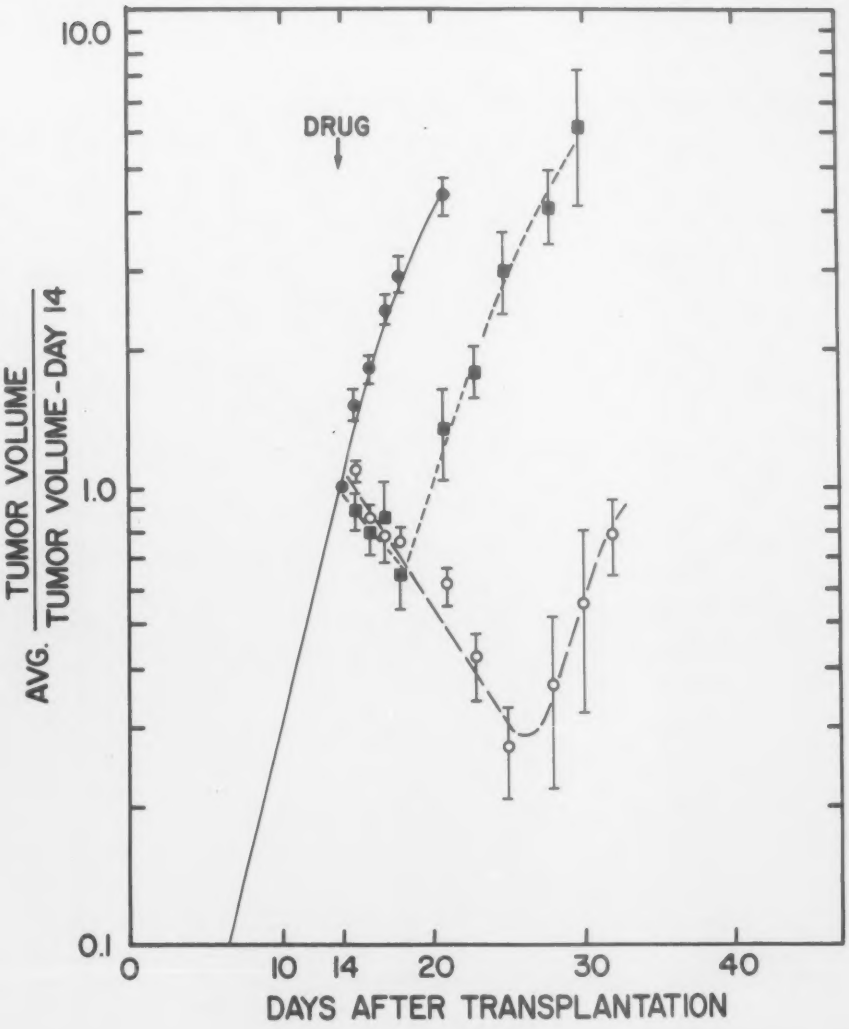

FIGURE 6.—Effect on average tumor volume of T1699 tumor, corrected to Day-14 values, of VCR (2.5 mg/kg) and CYT (170 mg/kg). ● = controls; ■ = VCR; ○ = CYT; I = 1 SEM.

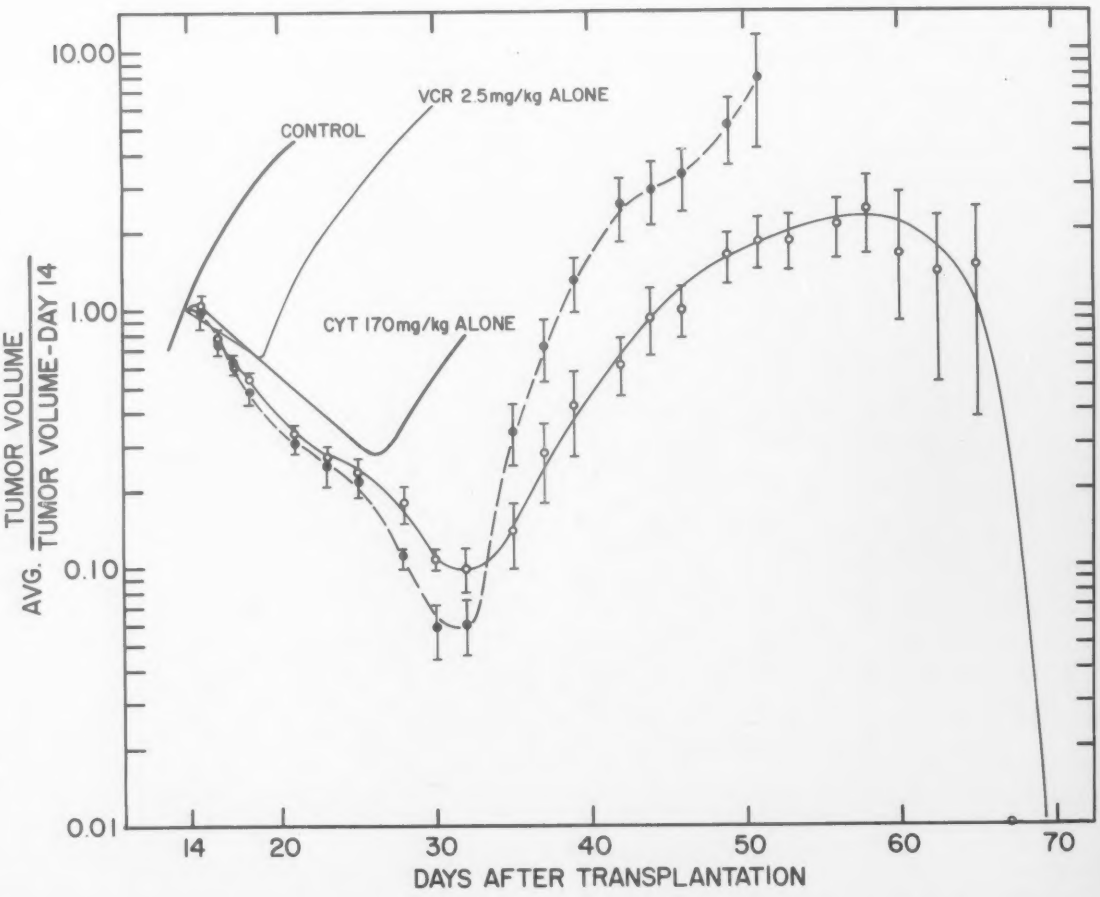

FIGURE 7.—Effect on average tumor volume of T1699 tumor corrected to Day-14 values, of VCR (2.5 mg/kg) followed by CYT (170 mg/kg) at 6 hrs, 1 or 2 days (●) (early CYT) and the same combination given at Days 3, 4, 5, 6, or 7 (○) (late CYT). ● = 1 SEM.

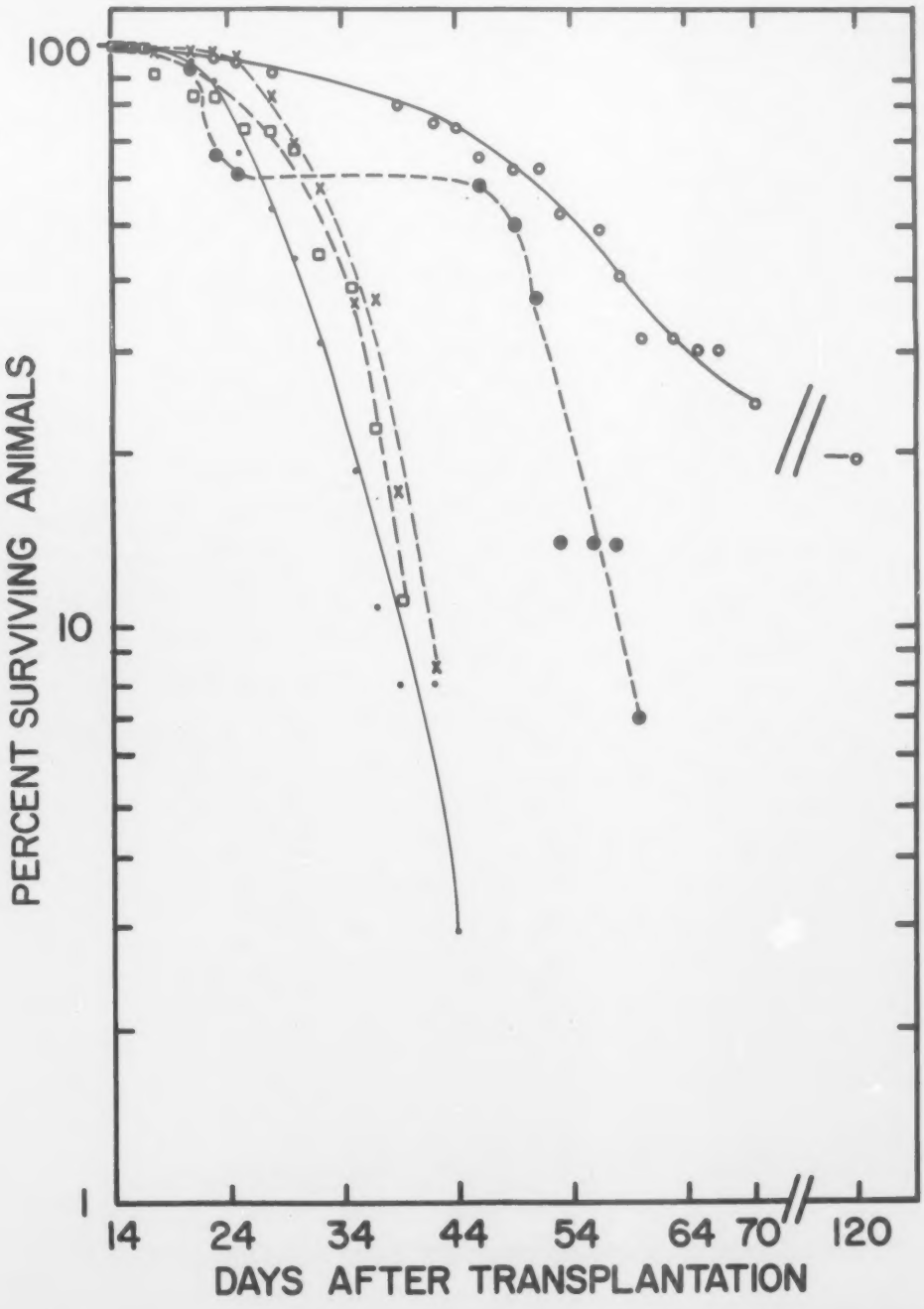

FIGURE 8.—Survival curves for animals with T1699 tumors treated with VCR (2.5 mg/kg) (□), CYT (170 mg/kg) (X), early CYT combination (●), late CYT combination (○), and controls (•).The early combination may, in fact, be toxic early.

netic evaluation of the patient's tumor can be made rapidly enough to direct his own therapy.

Collection of cytokinetic data on human tumors is already in progress. It is becoming apparent that these studies will be successful in helping to define human tumor cytokinetics. This information can reach the clinician rapidly, and it is clear that in the future the design of tumor therapy, with particular emphasis on time-sequencing of drugs, will be at least partially dependent upon information of this type.

ADDENDUM

The formula for $T_C = \lambda\ T_S$ (GF or PDP) $\div$ ^{3}H-TdR LI should be $T_C = \lambda \times T_S$ [ln (1 + GF or PDP) $\div$ ln 2] $\div$ ^{3}H-TdR LI. This would increase the cell cycle and G_1 time.

REFERENCES

1. SCHIFFER LM. Prediction of drug time-sequencing in-vitro. Proc Am Assoc Cancer Res and ASCO 16:15, 1975.
2. LIVINGSTON R, AMBUS V, GEORGE S, ET AL. In vitro determination of thymidine-^{3}H labeling index in human solid tumors. Cancer Res 34:1376–1380, 1974.
3. BRAUNSCHWEIGER PG, POULAKOS L, and SCHIFFER LM. In vitro labeling and gold activation autoradiography for determination of labeling index and DNA synthesis times of solid tumors. Caneer Res 36:1748–1753, 1976.
4. MENDELSOHN ML. Autoradiographic analysis of cell proliferation in spontaneous breast cancer of C3H mouse. III. The growth fraction. J Natl Cancer Inst 28:1015–1029, 1962.
5. NELSON JSR, and SCHIFFER LM. Autoradiographic detection of DNA polymerase containing nuclei in Sarcoma 180 ascites cells. Cell Tissue Kinet 6:45–54, 1973.
6. SCHIFFER LM, MARKOE AM, and NELSON JSR. Evaluation of the PDP index as a monitor of growth fraction during tumor therapy. *In* The Cell Cycle in Malignancy and Immunity. US Energy Research and Development Administration, 1975, pp 459–472.
7. SCHIFFER LM, MARKOE AM, and NELSON JSR. Estimation of tumor growth fraction in murine tumors by the primer-available DNA-dependent DNA polymerase assay. Cancer Res 36:2415–2418, 1976.
8. STEEL GG. Cell loss as a factor in the growth rate of human tumors. Eur J Cancer 3:381–387, 1967.
9. KLEIN HO, and LENNARTZ KJ. Chemotherapy after synchronization of tumor cells. Semin Hematol 11:203–227, 1974.
10. LAMPKIN BC, NAGAO T, and MAUER AM. Synchronization and recruitment in acute leukemia. J Clin Invest 50:2204–2214, 1971.
11. STRYCKMANS PA, LURIE PM, MANASTER J, ET AL. Mode of action of chemotherapy in vivo on human acute leukemia. II. Vincristine. Eur J Cancer 9:613–620, 1973.
12. MAIDHOF R, JELLINGHAUS W, SCHULTZE B, ET AL. Experimentelle und Theoretische Untersuch ungen zur Erzeugung einer teilsynchron proliferierenden Zellpopulation mit Vincristin in vivo. Dtsch Med Wochenschr 100:54–56, 1975.

Combined Effect of Cytosine Arabinoside and Thiopurines [1,2]

Fred Valeriote,* Teresa Vietti, and Mark Edelstein [3,4]

SUMMARY

Dose and time survival curves for leukemic colony-forming units (LCFU) and normal hematopoietic colony-forming units (NCFU) were obtained after the administration of either 6-mercaptopurine (6-MP) or 6-thioguanine (TG). Survival decreased to a plateau level with increasing doses as expected with phase-specific agents. Time survival curves demonstrated increased killing of LCFU after administration of 2 mg of 6-MP/mouse or 0.1 mg of TG/mouse reaching a minimum by 3–8 hours with repopulation thereafter. Cytosine arabinoside (Ara-C) (1 mg/mouse) was combined with each agent, and the effects of sequence and interval were examined in terms of LCFU and NCFU survival. When Ara-C and either thiopurine were administered together, fractional survival was less than additive. However, as the interval was increased for either sequence and for both combinations, survival decreased to synergistic levels. Variation in dose of Ara-C and TG showed an inhibitory effect to be dependent upon the Ara-C dose. A correlation between results from the colony assay for LCFU and survival of treated tumor-bearing mice was demonstrated for Ara-C plus TG. The results of these experiments are interpreted in terms of the proliferation kinetics of L1210 and the cellular effects of the agents; their clinical implications are discussed.

[Cancer Treat Rep 60:1925–1934, 1976]

Clinical investigators are increasingly demonstrating that combination chemotherapy is superior to single-agent therapy with respect to both remission induction and duration rate. Combinations of cytosine arabinoside (Ara-C) and thiopurines, especially 6-thioguanine (TG),[5] have been found to be effective in the treatment of acute myelogenous leukemia (1–4) and acute lymphocytic leukemia (5). We consider here, in some detail, the theoretic, experimental, and clinical aspects of combination chemotherapy with the S-phase specific agents Ara-C, 6-mercaptopurine (6-MP),[6] and TG. All of these agents probably exert their cytotoxic effect specifically on cells in the DNA synthetic phase of the cell cycle (6–8). Therefore, it might be expected that any combination of these agents, when administered within short intervals, would not have an increased toxicity to proliferating cells; however, proper scheduling of these agents in combination should increase their effectiveness (9).

MATERIALS AND METHODS

Mice

Six- to 8-week-old CD_2F_1(BALB/c × DBA/2) mice were supplied by the NCI and maintained for a minimum of 2 weeks before being used in these

[1]Supported by Public Health Service grant CA-13053 and contract CM-43731 from the National Cancer Institute (NCI), National Institutes of Health, Department of Health, Education, and Welfare.

[2]Cytosine arabinoside: NSC-63878; CAS reg. No. 69–74–9; cytosine, 1-β-D-arabinofuranosyl-, monohydrochloride; Ara-C. Purchased from The Upjohn Co, Kalamazoo, Mich.

[3]Division of Radiation Oncology, Mallinckrodt Institute of Radiology (F. Valeriote), and Division of Hematology and Oncology, Mallinckrodt Department of Pediatrics (T. Vietti and M. Edelstein), Washington University School of Medicine, St. Louis, Mo.

[4]The authors wish to thank Ms. Kathy Atwood and Mr. Dean Coulter for their technical assistance.

[5]6-Thioguanine: NSC-752; CAS reg. No. 1832–72–0; purine-6-thiol, 2-amino-. Supplied by the Drug Development Branch (DDB), Developmental Therapeutics Program (DTP), Division of Cancer Treatment (DCT), NCI.

Reprint requests to: Dr. F. Valeriote, Section of Cancer Biology, Department of Radiology, Washington University School of Medicine, 510 S Kingshighway, St. Louis, Mo 63110.

[6]6-Mercaptopurine: NSC-755; CAS reg. No. 6112–76–1; purine-6-thiol, monohydrate. Supplied by DDB, DTP, DCT, NCI.

experiments. DBA/2J mice from the Jackson Laboratory (Bar Harbor, Me) were used for passaging the leukemia.

Leukemic Cells

L1210 cells, originally obtained from the NCI, were passaged from the spleens of DBA/2J mice which had received 10^5 leukemic cells iv 7 days previously. The spleens were passed through a stainless-steel screen with alpha-MEM (Flow Laboratories, Rockville, Md) as previously described (10). Appropriate dilutions were then made in alpha-MEM to bring the final concentration of cells to 4×10^6/ml, and 0.5-ml fractions were injected iv into male CD_2F_1 mice weighing between 20 and 24 g. Four days later, when these mice had advanced leukemia, experimental studies were done on groups of four mice each.

Assay for Leukemic Colony-Forming Units (LCFU)

LCFU were quantitated by the spleen colony assay as previously described (10). A mono-dispersed suspension of cells was prepared from the pooled femoral marrows of the donor mice and 0.5 ml of an appropriate dilution of this suspension was injected into groups of eight CD_2F_1 recipients. The recipient mice were killed 8 days later, their spleens were fixed in Bouin's solution, and the macroscopic colonies were counted. The number of colonies has been shown to be proportional to the number of LCFU originally present in the marrow suspension. We determined that the femoral marrow of an untreated leukemic mouse contains approximately 2.5×10^4 or 1.6×10^5 LCFU 4 and 5 days, respectively, after the animal receives 2×10^6 leukemic cells. For all dose survival and combination studies, the data obtained were normalized to an untreated control assayed at 5 days. The time survival studies were normalized to a 4-day control.

Assay for Normal Hematopoietic Colony-Forming Units (NCFU)

NCFU were assayed by a modification of the technique used for LCFU, and differed only in that the donors were not leukemic. Groups of 15 recipients received 900 rads of whole-body radiation prior to the injection of the appropriate cell suspension; the colonies were counted 10 days thereafter (10). The femoral marrow of an untreated CD_2F_1 mouse contains approximately 2×10^3 NCFU. The data obtained were normalized to an untreated control and expressed in terms of fractional survival.

Anticancer Agents

Ara-C, 6-MP, and TG were dissolved in distilled water, diluted in saline, and administered iv in a volume of 0.5 ml.

RESULTS

Dose and Time Survival Curves for 6-MP and TG

In order to determine the appropriate dose of agent for the combination studies, dose survival curves were obtained for 6-MP and TG. Studies for Ara-C have already been reported (11). Increasing dose levels of each drug were administered iv; colony-forming units (CFU) were assayed 24 hours later. The results are shown in figures 1 and 2.

After increasing doses of 6-MP, survival of LCFU decreased to about 3×10^{-2} for 2 mg/mouse. Thereafter, the fractional survival decreased slowly with increasing dose, reaching a level of 6×10^{-3} by 12 mg/mouse. As previously discussed (11), we chose a dose of agent which yields a surviving fraction of between 10^{-1} and 10^{-2} for combination studies; therefore, we chose a dose of 2 mg of 6-MP/mouse.

The lethal effect on LCFU was more marked with increasing dose levels of TG. At 0.6 mg of TG/mouse, the fractional survival decreased to 3×10^{-4}, after which there was little further cell killing with doses up to 2 mg/mouse, although there was considerable scatter of the data at higher doses. We chose a dose of 0.1 mg of TG/mouse for the combination studies.

Dose survival curves for NCFU were similar for both agents in that survival decreased to 40%–50% of control values for 2 mg of 6-MP/mouse and 0.1 mg of TG/mouse and remained at that level for increasing dose levels of the agents.

The dose survival results for 6-MP and TG were as expected for phase-specific agents (12,13); that is, the fractional survival decreased with increasing dose and reached a plateau. Such curves indicate that the agent exerts its cytotoxic effect during some specific portion of the cell cycle. The fact that the dose survival curve plateaus at a surviving fraction of about 10^{-4} for TG and 10^{-2} for 6-MP and Ara-C suggests that (*a*) the sensitive portion of the cell cycle is longer for TG than for 6-MP or Ara-C; (*b*) that TG remains at cytotoxic levels longer than 6-MP or Ara-C; or (*c*) that Ara-C and 6-MP block cells from entering the drug-sensitive phase of the cell cycle more effectively than TG. Drugs can inhibit the progression of cells from one phase of the cell cycle to another. Those that prevent movement into the specific drug-sensitive phase have been termed "self-limiting" agents. It is likely that more than

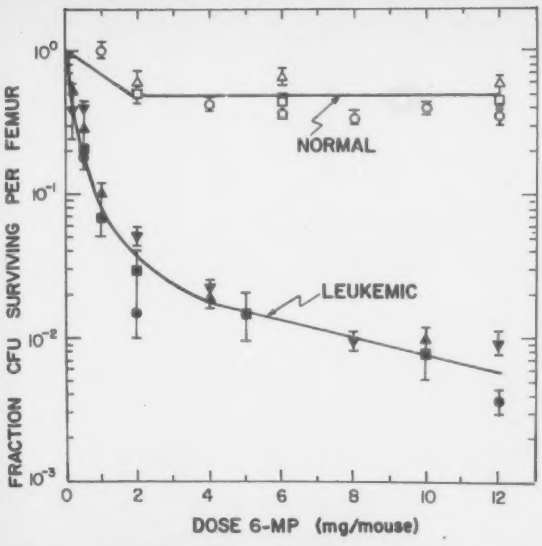

FIGURE 1.—Survival of LCFU and NCFU after increasing doses of 6-MP. Different symbols represent different experiments. Errors are ±1 SE.

one of the above possibilities are involved in the explanation.

While the age-response for cytotoxicity to cells of 6-MP and TG has not been reported, we assume that both of these agents kill cells selectively in S phase, as do Ara-C and other inhibitors of DNA synthesis (6). This may not be the case, however, as 6-MP and TG are also extensively incorporated into RNA and therefore may kill cells in other phases of the cycle. Thus, the difference in the extent of killing among these three agents for both the dose and time survival curves may also reflect cytotoxicity in phases of the cell cycle other than the S phase.

Time survival curves were next obtained for both 6-MP and TG. Similar studies for Ara-C have already been reported (11). Single doses of 2 mg of 6-MP/mouse or 0.1 mg of TG/mouse were administered and LCFU were assayed at different times thereafter. The results are shown in figures 3 and 4. After either drug, survival decreased with time to a minimum level, followed by repopulation of the marrow. After 6-MP, there was a continuous decrease in LCFU survival for about 3 hours, reaching a minimum value of about 10^{-1}. After TG administration, an initial decrease in LCFU to about 3×10^{-1} occurred within 15 minutes followed by a more gradual decrease to a minimum survival of about 10^{-2} by 8 hours, after which repopulation occurred.

These results are not at variance with the contention that cells in the sensitive (S) phase of the cell cycle are destroyed within about 2 hours after drug

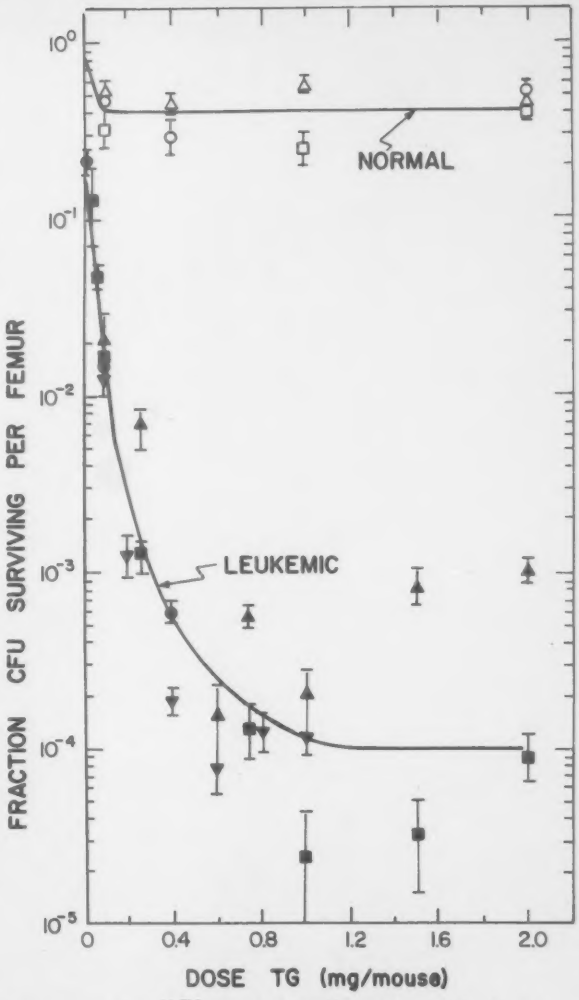

FIGURE 2.—Survival of LCFU and NCFU with increasing doses of TG. (Symbols are same as in fig 1.)

administration. About 85% of L1210 cells are in this phase (14). A further decrease in survival, as observed for 0.1 mg of TG, probably indicates persistence of cytocidal concentrations of drug for a period of time which allows progression of the cells into a sensitive phase of the cell cycle or other reasons previously mentioned. In any event, following the doses employed here, cell killing and progression-delay effects appear to be complete within 8 hours after drug administration.

Combined Effect of Ara-C and 6-MP

Leukemic mice received either 1 mg of Ara-C or 2 mg of 6-MP, and at different times thereafter re-

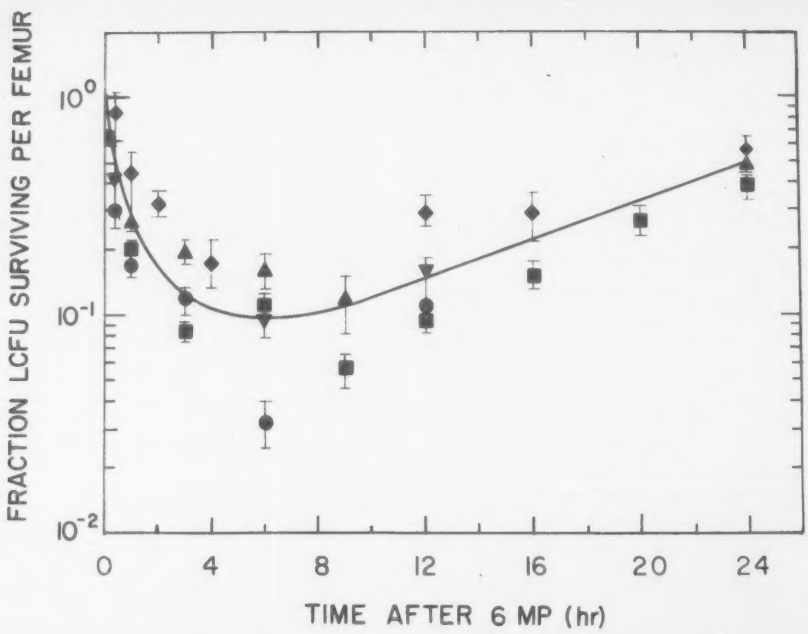

FIGURE 3.—Survival of LCFU as a function of time after 2 mg of 6-MP/mouse. (Symbols are same as in fig 1.)

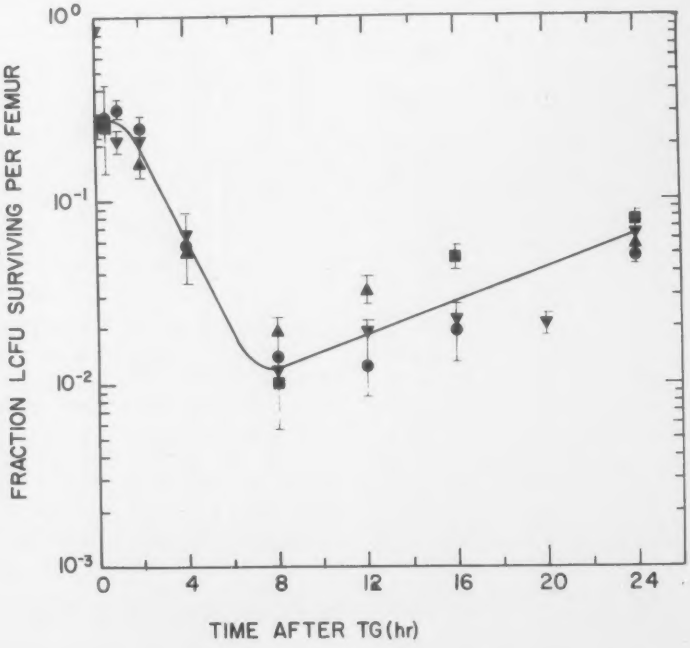

FIGURE 4.—Survival of LCFU as a function of time after 0.1 mg of TG/mouse. (Symbols are same as in fig 1.)

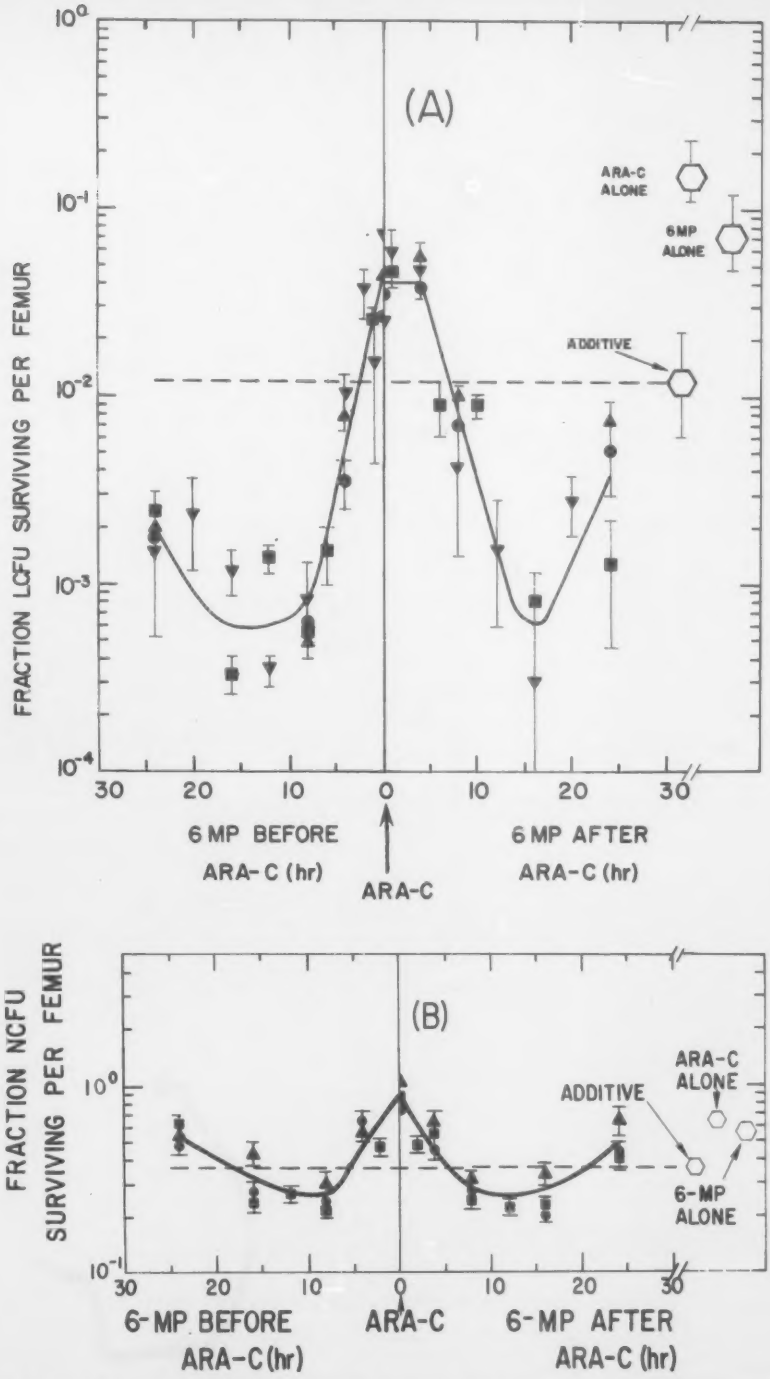

FIGURE 5.—Survival of (A) LCFU and (B) NCFU as functions of sequence and interval between the administration of Ara-C (1 mg/mouse) and 6-MP (2 mg/mouse). The survival for either agent alone is the geometric mean of 4 experiments. (Symbols other than hexagons represent separate experiments; errors are ±1 SE.)

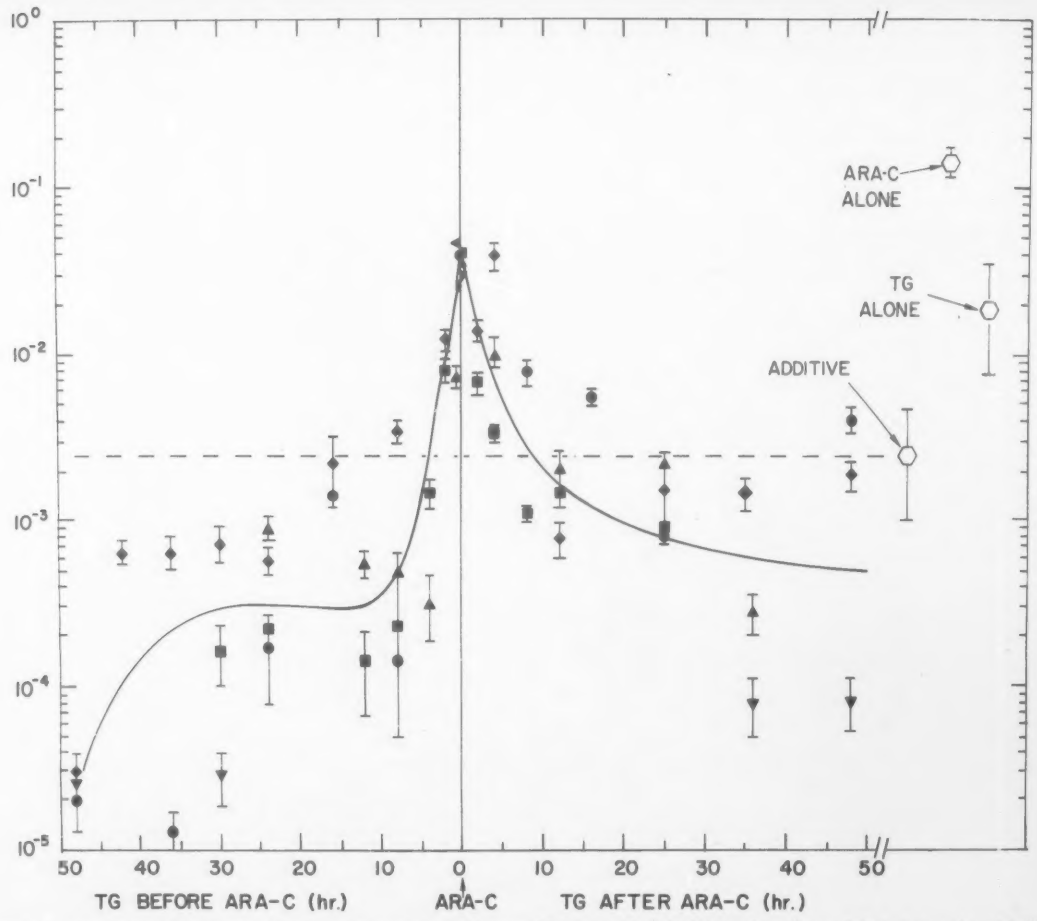

FIGURE 6.—Survival of LCFU as a function of sequence and interval between the administration of Ara-C (1 mg/mouse) and 6-MP (2 mg/mouse). (Symbols are same as in fig 5.)

ceived the second agent; femoral marrow was assayed for LCFU 24 hours after the second agent. The results, presented in figure 5A, include corrections for proliferation of LCFU before administration of the second agent. This correction was made for intervals > 12 hours when Ara-C was given first and 10 hours when 6-MP was given first.

The geometric mean and range of the fractional survival values for LCFU after either agent alone are shown by open hexagons in figure 5. The "additive" survival level (1.2×10^{-2}) is the geometric mean of the products of the survival of the single agents alone and is shown by both a hexagon and by a horizontal dashed line. The standard error shown represents the range of the products obtained. This additive level is that expected when two agents act independently of one another with regard to cytotoxicity.

When Ara-C and 6-MP were administered within 5 minutes of one another, the surviving fraction of LCFU was about 4×10^{-2}; that is, the killing was less than additive. As the time interval between the administration of 6-MP and Ara-C was increased, there was a rapid decrease in fractional survival of LCFU to less than additive within 5 hours. For the reverse administration there was an initial plateau followed by a fall in fractional survival to less than additive within 10 hours. Possibly this results from the progression-delay effect of Ara-C (15,16) which prevents cells from entering the 6-MP-sensitive phase of the cell cycle. At the 16-hour interval for both sequences, survival reached a minimum of about 6×10^{-4}. Thus, an approximately 50-fold increase in cell killing can be obtained by the appropriate scheduling of two doses of these agents. After this, there is an increasing survival with an increasing interval towards the additive level.

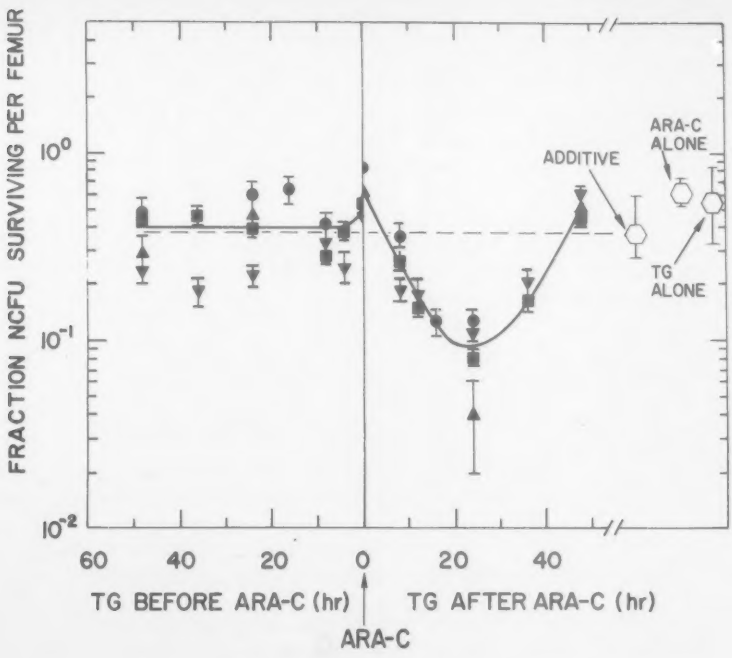

FIGURE 7.—Same as fig 6 except survival is for NCFU.

Combined Effect of Ara-C and 6-MP on NCFU

The effect of varying the sequence and interval of Ara-C and 6-MP on NCFU survival was examined in normal mice using the same dose levels and intervals as above for LCFU. The results are shown in figure 5B. When the two agents were administered together, cell killing was not greater than that found for either agent alone. Maximum killing of NCFU occurred when the interval was 8–10 hours for either sequence; cytotoxicity was slightly greater than additive.

Combined Effect of Ara-C and TG

Leukemic mice received either 1 mg of Ara-C or 0.1 mg of TG and then, at different times thereafter, received the second agent. LCFU were assayed and the survival fraction was determined as above for Ara-C and 6-MP. The results presented in figures 6 and 7 are similar to those in figure 5. When either agent was administered within 5 minutes of the other, fractional survival was about 4×10^{-2}, a level higher than that found for TG alone. As the interval increased, survival of LCFU decreased for either sequence, reaching the additive level by 8 hours when TG was administered after Ara-C and by 4 hours when TG preceded Ara-C. As the interval increased further to 48 hours, for either sequence, survival continued to decrease. Unlike the Ara-C plus 6-MP combination, the data for Ara-C plus TG were quite scattered at longer intervals.

Combined Effect of Ara-C and TG on NCFU

The effect of varying the sequence and interval of Ara-C and TG on NCFU survival was examined in normal mice using the same dose levels and intervals as indicated for LCFU. The results are shown in figure 7. The surviving fraction of NCFU was similar irrespective of the interval when TG was given before Ara-C. When TG was given after Ara-C, survival decreased with an increasing interval, reaching a minimum of about 10^{-1} at about 24 hours. Thereafter survival increased to the level obtained for either agent alone.

Cellular Model for Combined Effect of Ara-C and Thiopurines

Our explanation for the results obtained above is made strictly on a cell-cycle basis. The initial dose of Ara-C or thiopurine destroys those cells in the S phase of the cell cycle and has little or no effect on cells in other phases of the cycle. Thus, the administration of both agents together yields no increased

cell killing. However, as the interval between the agents increases, the surviving fraction decreases as cells enter the drug-sensitive phase and are killed. The extent of killing eventually falls significantly below the indicated additive level. The magnitude of this cell killing depends upon the degree of synchrony produced by the first drug and the variation in the distribution of cell-cycle phase transit times. Obviously, if the killed cells constituted the major portion of the cell cycle, and there was no transit time variation, the second drug should *completely* destroy the cell population. That this is not found is probably because even at the doses employed, not *all* cells are killed in the drug-sensitive phase because (*a*) there is a significant variation in the transit times; and (*b*) the agents produce progression delay which acts to desynchronize rather than to sharpen the synchrony. Finally, as the interval is increased further, the surviving fraction increases due both to movement of the partially synchronized cells out of the sensitive phase and to increased desynchronization.

The term "additive" as used here must be redefined when using combinations of agents such as phase-specific agents since their actions are *not* independent. In fact, they probably have their cytotoxic effects on the same cell population. Thus, "additive" must now mean the achievement of the survival level expected when the two agents are administered at an interval sufficient to allow desynchronization of the population after treatment with the first agent. At long intervals, for the combinations examined here, this appears to be the situation.

Examination of Different Drug Dosages

In the combination studies described above, only one dose level of each agent was used. To determine whether the same effect was obtained irrespective of dose, three dose levels of both Ara-C and TG were studied at two different time intervals. The agents were administered together, or TG was administered 16 hours before Ara-C. The actual survival results obtained are shown in table 1 together with the synergy index. The synergy index is the ratio of the expected survival value and the experimental value obtained. The expected survival is the product of the fractional survivals obtained for either agent alone.

When the agents were given together, the ratio was always < 1, that is, the full effect of one agent was interfered with by the second. For low doses of Ara-C, this effect was not very apparent, since low survival levels were obtained with the combination; for example, 0.1 mg of Ara-C plus 1 mg of TG/mouse resulted in a surviving fraction of 6.5×10^{-4} with a synergy index of 0.33. However, for the high dose of Ara-C, marked inhibition occurred and the survival was not much less than that found for Ara-C alone. This is not entirely unexpected since it is known that Ara-C inhibits the incorporation of TG into DNA (17) and any therapeutic synergism obtained for simultaneous drug administration probably reflects a decreased toxicity to bone marrow (18) while TG is allowed to destroy Ara-C-resistant cells (19).

When Ara-C followed TG by 16 hours, however, the results were close to additive for all dose levels studied, showing this schedule to be much more effective than simultaneous administration in terms of leukemic cell killing.

Increased Lifespan Studies

Since many experimental drug combination studies are examined in terms of increase in lifespan of tumor-bearing mice, we carried out one small study to examine the predictions from the above data. We expected that Ara-C and TG would yield better results if not administered simultaneously. Time intervals of 5 minutes and 24 and 48 hours were studied in tumor-bearing mice. The results are shown in table 2. The increased survival time correlates well with the results obtained for LCFU if one considers that a 1-day increase correlates approximately to a sixfold reduction in LCFU survival. Thus, Ara-C and TG given together yielded a survival of 4×10^{-2} for LCFU (fig 6) which should result in a 1–2-day increase in animal lifespan. The 24- and 48-hour intervals yielded surviving fractions of between 10^{-4} and 10^{-5} and should result in about a 5-day increase in lifespan, as we in fact observed.

DISCUSSION

The data generated for Ara-C combined with the thiopurines 6-MP and TG provide experimental verification of the theoretic and cellular results of combinations of S-phase specific agents. If one agent kills the majority of cells in a phase of the cell cycle, then a second agent with the same age-response would not provide any therapeutic advantage if administered shortly after the first drug. However, significant cell killing would be expected from the second agent if it were administered at a time after the first agent when the sensitive phase of the cell cycle was "refilled."

There are two major difficulties in trying to compare our results with the literature. First, we are studying effects of drug combinations mainly in terms of cell survival rather than animal survival. We believe that we can obtain more fundamental

TABLE 1.—Fractional survival and synergy index of LCFU after different drug combinations of Ara-C and TG*

TG (mg/mouse)	Ara-C → TG: 5-min interval				TG → Ara-C: 16-hr interval		
	Ara-C (mg/mouse)				Ara-C (mg/mouse)		
	0	0.01	0.1	1.0	0.01	0.1	1.0
0	1.0	3.5×10^{-1}	1.3×10^{-1}	4.8×10^{-2}	3.5×10^{-1}	1.3×10^{-1}	4.8×10^{-2}
0.1	1.3×10^{-2}	2.5×10^{-2} (0.18)	3.8×10^{-2} (0.4)	5.1×10^{-2} (0.012)	6.9×10^{-3} (0.66)	1.6×10^{-3} (1.1)	5.7×10^{-4} (1.1)
0.5	1.4×10^{-4}	5.7×10^{-4} (0.09)	6.7×10^{-4} (0.03)	1.7×10^{-2} (0.0004)	6.3×10^{-5} (0.78)	1.6×10^{-4} (0.11)	9.3×10^{-5} (0.07)
1.0	1.3×10^{-4}	1.4×10^{-4} (0.33)	6.5×10^{-4} (0.03)	1.8×10^{-2} (0.0003)	3.4×10^{-5} (1.3)	1×10^{-4} (0.17)	6.4×10^{-5} (0.39)

*Nos. in parentheses = synergy index (*see* Results for explanation).

TABLE 2.—Lifespan of tumor-bearing mice after Ara-C and TG*

Treatment group	Median survival time† (days)	ILS‡ (%)
Control	6.5	0
Ara-C (1 mg/mouse)	7.0	8
TG (0.1 mg/mouse)	8.5	31
Ara-C → TG: 5-min interval	8.0	23
Ara-C → TG: 24-hr interval	10.5	62
TG → Ara-C: 48-hr interval	11.0	69

*Mice received 10^6 L1210 cells 1 day before initiation of treatment.

†10 mice/group (survival time determined from time of cell inoculation).

‡Increase in lifespan.

information concerning drug combinations or predictions by administering two single injections of different drugs and analyzing the effects of interval in detail. Most investigators administer multiple injections of the agents. For example, in the first animal studies on Ara-C and 6-MP (20,21), the agents were given together daily for many days after tumor inoculation. The results were indeed additive and even greater than additive for some of the combinations (21). Although we indicated previously that simultaneous drug administration is not optimal, one might expect that repeating the combination in 24 hours would provide the increased effectiveness found in the earlier studies. It is, however, doubtful, on the basis of our data, that such would be an optimal schedule.

Animal studies have also been carried out previously with Ara-C and TG. Schabel (18) has recently summarized and reported studies with Ara-C and TG administered simultaneously but on a schedule of every 3 hours for 24 hours against early L1210 leukemia and has reported therapeutic synergism. He similarly showed that this combination did not have additive toxicity. Although it is difficult to compare his schedule with our simple system of two single injections, we confirmed our prediction as to the expected efficacy of two injections separated by an optimal time interval on lifespan as shown in table 2. We are presently examining whether less complicated schedules in terms of number of drug administrations (single injection, multiple injections, or infusions) can yield results as good as, if not better than, those reported by Schabel (18).

While one experimental study indicated a synergistic effect of Ara-C and TG when given simultaneously (22), it is difficult to interpret since some of the mice were cured of their leukemia with the single drugs alone.

Clinical studies were established from the early animal results and the combination of Ara-C and TG has been shown to be effective for acute myelogenous leukemia (1,2) and acute lymphocytic leukemia (5). In one protocol (2), the agents are administered 12 hours apart "since both drugs are probably only lethal to cells in S." Few studies have been done with Ara-C and 6-MP, since the dose of TG does not have to be modified when xanthine oxidase inhibitors are included in the therapy. However, the combination of Ara-C with either thiopurine seems to yield similar remission results (3).

Other clinical results indicate that Ara-C plus TG is not more effective than Ara-C alone when there is a 6-hour interval with TG given first (23). This possibly reflects the pharmacokinetics of oral TG in that peak drug levels are not achieved until many hours after drug administration (24). This would then be comparable to simultaneous administration, where we observed little difference from administration of either agent alone. This question would be answerable by administering TG iv clinically; however, in the only study of this (4), Ara-C and TG were given simultaneously every 12 hours and were reported to be no more effective than oral TG. Even for low doses of each agent below that necessary for

extensive killing of S-phase cells, we might expect little additive effect, on biochemical grounds, since Ara-C inhibits DNA polymerase, thus inhibiting incorporation of TG (17).

REFERENCES

1. GEE TS, YU K-P, and CLARKSON B. Treatment of adult leukemia with arabinosylcytosine and thioguanine. Cancer 23:1019–1032, 1969.
2. CLARKSON BD. Acute myelocytic leukemia in adults. Cancer 30:1572–1582, 1972.
3. BUCHANAN JG, MATHEWS JRD, DAVISON JG, ET AL. Treatment of acute myeloid leukemia of adults with cytosine arabinoside in combination with 6-mercaptopurine. Cancer 32:789–795, 1973.
4. CLARKSON BD, DOWLING MD, GEE TS, ET AL. Treatment of acute leukemia in adults. Cancer 36:775–795, 1975.
5. BRYAN JH, HENDERSON ES, and LEVENTHAL BG. Cytosine arabinoside and 6-thioguanine in refractory acute lymphocytic leukemia. Cancer 33:539–544, 1974.
6. BHUYAN BK, SCHEIDT LG, and FRASER TJ. Cell cycle phase specificity of antitumor agents. Cancer Res 32:398–407, 1972.
7. BARRANCO SC, and HUMPHREY RM. The effect of β-2-deoxythioguanosine on survival and progression in mammalian cells. Cancer Res 31:583–586, 1971.
8. PATERSON ARP, and TIDD DM. 6-Thiopurines. *In* Antineoplastic and Immunosuppressive Agents, II (Sartorelli AC, and Johns DJ, eds). New York, Springer-Verlag, 1975, pp 384–403.
9. VALERIOTE F, STEWARD P, VIETTI T, ET AL. Cellular quantitation of the cytotoxic effects of combinations of anticancer agents. *In* Proceedings of the 11th International Cancer Congress, 1975, vol 5, pp 217–221.
10. VALERIOTE F, VIETTI T, and TOLEN S. Kinetics of the lethal effects of actinomycin D on normal and leukemic cells. Cancer Res 33:2658–2661, 1973.
11. EDELSTEIN M, VIETTI T, and VALERIOTE F. Schedule-dependent synergism for the combination of 1-β-D-arabinofuranosylcytosine and daunorubicin. Cancer Res 34:293–297, 1974.
12. WHEELER GP, BOWDON BJ, ADAMSON DJ, ET AL. Comparison of the effects of several inhibitors of the synthesis of nucleic acids upon the viability and progression through the cell cycle of cultured H. Ep. No. 2 cells. Cancer Res 32:2661–2669, 1972.
13. BRUCE WR, and VALERIOTE FA. Normal and malignant stem cells and chemotherapy. *In* The Proliferation and Spread of Neoplastic Cells. Baltimore, The Williams and Wilkins Co, 1968, pp 409–420.
14. YANKEE RA, DEVITA VT, and PERRY S. The cell cycle of leukemia L1210 cells in vivo. Cancer Res 27:2381–2385, 1967.
15. TOBEY RA, and CRISSMAN HA. Use of flow microfluorometry in detailed analysis of effects of chemical agents on cell cycle progression. Cancer Res 32:2726–2732, 1972.
16. KARON M, and SHIRAKAWA S. Effect of 1-β-D-arabinofuranosylcytosine on cell cycle passage time. J Natl Cancer Inst 45:861–867, 1970.
17. LEPAGE GE, and KANEKO T. Effective means of reducing toxicity without concomitant sacrifice of efficacy of carcinostatic therapy. Cancer Res 29:2314–2318, 1969.
18. SCHABEL FM, JR. Synergism and antagonism among antitumor agents. *In* Pharmacological Basis of Cancer Chemotherapy. Baltimore, The Williams and Wilkins Co, 1975, pp 596–623.
19. LEPAGE GE, and WHITE SC. Scheduling of arabinosylcytosine and 6-thioguanine therapy. Cancer Res 33:946–949, 1973.
20. EVANS JS, MUSSER EA, BOSTWICK L, ET AL. The effects of 1-β-D-arabinofuranosylcytosine hydrochloride on murine neoplasms. Cancer Res 24:1285–1293, 1964.
21. BURCHENAL JH, and DOLLINGER MR. Cytosine arabinoside (NSC-63878) in combination with 6-mercaptopurine (NSC-755), methotrexate (NSC-740), or 5-fluorouracil (NSC-19893) in L1210 mouse leukemia. Cancer Chemother Rep 51:435–438, 1967.
22. KREIS W. Studies on drug resistance. V. Combination chemotherapy with cytosine arabinoside (NSC-63878) plus 6-thioguanine (NSC-752) in cytosine arabinoside-sensitive and -resistant P815 mouse neoplasms. Cancer Chemother Rep 57:349–351, 1973.
23. EORTC LEUKAEMIA AND HAEMATOSARCOMA COOPERATIVE GROUP. A second cooperative trial of remission induction (by cytosine arabinoside given every 12 hours, or C. A. R. and thioguanine, or C. A. R. and daunorubicin) and maintenance therapy (by C. A. R. or Methylgag) in acute myeloid leukemia. Eur J Cancer 10:413–418, 1974.
24. LEPAGE GA, and WHITECAR JP, JR. Pharmacology of 6-thioguanine in man. Cancer Res 31:1627–1631, 1971.

Introduction to Session on Drug Scheduling—Clinical Studies

Emil Frei [1]

Cytokinetic concepts and data are increasingly influencing our thinking and approaches to drug scheduling. Historical approaches to drug scheduling were largely based on empirical studies. Dr. Abraham Goldin first demonstrated, initially with methotrexate and subsequently with cyclophosphamide, that the schedule of an antitumor agent may markedly affect the therapeutic index (therapeutic effect per unit cost in host toxicity) in experimental in vivo systems. In spite of this, it was a number of years before this impacted upon the clinic. In the mid-1960s the Acute Leukemia Group B, following pilot studies at the National Cancer Institute, demonstrated unequivocally in a quantitative study, that intermittent high doses of methotrexate were superior to daily methotrexate in the treatment of acute lymphocytic leukemia in remission. Subsequently, there has developed substantial evidence indicating, in man as well as in experimental systems, that the therapeutic effect of a given agent may be substantially influenced by the schedule of administration.

Today, cytokinetic considerations are involved in the construction of most clinical cancer chemotherapeutic trials. Such considerations include: (1) knowledge as to the effect of the agent on the mitotic cycle; (2) knowledge as to the effect of the agent on cycling as compared to resting (G_0) cells; (3) knowledge as to the clinical cytokinetic effect of the agent on normal tissues, most particularly the bone marrow and gastrointestinal tract; (4) knowledge as to the cytokinetics of the particular tumor category under treatment; and (5) knowledge as to the biochemical pharmacology of the agent in question. Definitive information in the above areas is usually incomplete but available technology is decreasing this information gap. Parenthetically, this meeting which brought together persons representing disciplines ranging from basic through clinical cytokinetics will, of itself, decrease this gap. Finally, it is becoming increasingly possible to perform cytokinetic analyses with autoradiography, flow microfluorometry, and the various colony-forming techniques on target, tumor, and host tissues prospectively as a component of formal clinical trials. One can look forward with reasonable certainty to the fact that such studies will: (1) provide strategic and tactical optimization of clinical trials, (2) provide basic information and leads for further clinical and basic studies, and (3) decrease the empirical to rational ratio of input in the clinical trials which always renders clinical research more exciting and heuristic.

Relatively new concepts with respect to drug scheduling including such phenomena of synchronization and recruitment will most certainly impact in a major way on the construction of clinical trials in the immediate future.

ARCHIVE http://Archivebeta.Sakhrit.com

Kinetic Response of Human Leukemic and Lymphoma Cells In Vivo to Combination Chemotherapy Using Flow Microfluorometry [1]

Jerrold Fried,* Zalmen Arlin, Agnes Alikpala, Charlotte T. C. Tan, and Bayard Clarkson [2,3]

SUMMARY

Two patients with acute leukemia and one with a presumptive diagnosis of diffuse histiocytic lymphoma were treated with vinca alkaloids (vincristine or the new chemotherapeutic agent desacetyl vinblastine amide [vindesine]); two patients were also given prednisone and one received adriamycin. Kinetic responses of the tumor cells to treatment were measured by sampling bone marrow or peripheral blood prior to and at intervals after the administration of the drugs. Differential counts, mitotic and ^{3}HTdR pulse-labeling indices, and the distribution of cells among the phases of the mitotic cycle by flow microfluorometry were determined. In the patient diagnosed as having lymphoma there was an initial increase in the mitotic index and in the percentage of S-phase cells, but these decreased after prednisone administration. The patient subsequently went into remission. Another patient (with acute myelomonocytic leukemia), who received vincristine together with prednisone and adriamycin, showed little apparent kinetic or clinical response to the treatment except for a small increase in the percentage of cells in G_2 and a moderate decrease in the percentage of blast cells. Although his leukemic cells were affected by subsequent administration of cytosine arabinoside, remission was not achieved. The third patient, who had acute lymphoblastic leukemia and who had been treated extensively with other drugs prior to the present study, was given vindesine in a single iv injection. There was a transient increase in the mitotic index and a decrease in the percentage of S-phase cells, but the changes were not striking.

[Cancer Treat Rep 60:1937–1946, 1976]

A promising application of flow microfluorometry (FMF) to human leukemia is the determination of the kinetic status of the leukemic cells and their early response to therapy. If such information can be obtained rapidly enough, it may be possible to evaluate the response or lack thereof to a particular drug or drug combination earlier than by ordinary clinical observation.

While a considerable amount of knowledge has been accumulated concerning the mechanisms of action of many of the drugs used in cancer chemotherapy, including their cell cycle specificities, it is generally recognized that the in vivo effects of many drugs are dependent on several factors. These include relative sensitivity of tumor vs normal tissue, differences in the metabolism, transport, degradation, and excretion of drugs by different patients, ability of the normal hematopoietic cells to recover from the effects of the disease itself and from the drugs used, immunologic factors, etc, and these factors cannot often if ever be explained solely in terms of cell kinetics. Nevertheless, there may be many cases in which cell kinetics considerations play an important or even decisive role. We believe that prior to making a major effort to direct chemotherapy on the basis of inferences derived from an FMF observation of cell kinetics, a certain minimum body of data should be accumulated. By comparing FMF data with clinical results using the most effec-

[1]Supported in part by Public Health Service grants CA-08748 and CA-16757 from the National Cancer Institute, National Institutes of Health, Department of Health, Education, and Welfare, and grant ACS-ET-2C from the American Cancer Society.

[2]Memorial Sloan-Kettering Cancer Center, New York, NY.

[3]We wish to thank Ms. Jean Campbell for carrying out the autoradiographic procedures and for determining the labeling and mitotic indices and differential counts. We also thank Drs. Monroe Dowling and Timothy Gee for their kindness and cooperation in arranging for the participation of their patients in this investigation, and Ms. Lana Hart for typing the manuscript.

*_Reprint requests to:_ Dr. Jerrold Fried, Box 381, Sloan-Kettering Institute, 1275 York Ave, New York, NY 10021.

tive current modes of treatment for various types of leukemia, it may be possible to judge whether the two are correlated, and whether FMF is likely to help in guiding treatment or in indicating whether or not a specific drug is effective.

In the present investigation, three patients were studied. One patient had a presumptive diagnosis of diffuse histiocytic lymphoma and had previously been untreated; another had acute myelomonocytic leukemia and had been treated prior to the present study without achieving remission; and the third had acute lymphoblastic leukemia and had been in remission but had relapsed prior to the study. All three patients were given vinca alkaloids immediately after the first bone marrow sample. In two patients the drug was vincristine (VCR), and in the third patient it was a new drug, desacetyl vinblastine amide (vindesine or DVA), which is believed to have a mechanism of action similar to vincristine but which appears to exhibit less neurotoxicity to normal tissue and which may be more potent (1,2). The first two patients also received prednisone, one 12 hours after VCR and the other simultaneously (the latter also received adriamycin concurrently).

One of our principal objectives in using FMF is to determine whether the kinetic and clinical responses to chemotherapeutic agents can be related to observed changes in the FMF histograms as well as to the labeling and mitotic indices.

The staining method employed is that recently proposed by Krishan (3), which is much faster and entails less cell loss than previous methods we have used (eg, the acriflavine-Feulgen technique [4,5] and the ethidium bromide method [6]).

CASE REPORTS

Patient No. 1

This patient is a 29-year-old man who was asymptomatic until a few days prior to admission when he experienced fatigue and anterior chest pain. His physical examination was normal except for an enlarged spleen and bilateral axillary adenopathy. There was no mediastinal adenopathy. Although a biopsy of an enlarged axillary node showed an infiltration compatible with leukemia, no definite histologic diagnosis could be made.

The wbc count was 8500 cells/mm^3 with 90% blast cells, some of which had monocytoid features, the platelet count was 15,000 platelets/mm^3, and the Hgb was 9.6 g/100 ml. The bone marrow aspirate was very hypercellular and showed replacement with predominantly blast and immature monocytoid cells.

The patient was given an iv dose of 1.4 mg/m^2 of VCR; 12 hours later treatment with prednisone was begun (60 mg/m^2/day orally divided into three doses daily).

Bone marrow samples were obtained for differential counts, for analysis by FMF, and for determination of mitotic indices (MIs) and labeling indices following pulse labeling with tritiated thymidine (^{3}HTdR). Samples were obtained prior to therapy and at 7, 24, 48, and 96 hours after treatment was begun.

Seven days after beginning therapy, the patient was given an additional dose of VCR (1.4 mg/m^2 iv) and was in remission a week later. He has remained in remission and is currently being given maintenance therapy with a combination of cytotoxic drugs.

Although there was uncertainty as to whether the diagnosis was acute monocytic leukemia or diffuse histiocytic lymphoma, the latter was believed to be more likely in view of the subsequent rapid response to VCR and prednisone.

Patient No. 2

This is a 16-year-old boy who was well until April of 1975 when he presented with epistaxis, cervical adenopathy, and a high wbc count. A bone marrow aspirate was diagnosed as acute myelomonocytic leukemia and he began therapy with AAFC (anhydro-ara-5-fluorocytidine) and 6-thioguanine. He was given two courses of therapy without achieving remission. He also subsequently failed to respond to a combination of daunorubicin and a continuous infusion of cytosine arabinoside (Ara-C). He was then treated with a combination of four drugs (adriamycin, cyclophosphamide, methotrexate, and 5-fluorouracil), again without response.

On September 22, 1975, with an increasing wbc count consisting entirely of blast cells, the patient was treated with a regimen similar to that described by McCredie et al (7). It began with adriamycin (40 mg/m^2 iv); VCR (1.4 mg/m^2 orally); and prednisone (60 mg/m^2 orally in three divided doses daily). A bone marrow aspirate was obtained just prior to this therapy, and 7, 24, 48, and 72 hours later. These were analyzed for determination of differential counts, MIs, ^{3}HTdR pulse-labeling indices, and the percentages of cells in the G_1, S, and G_2+M phases by FMF.

Immediately after obtaining the 72-hour bone marrow aspirate, a continuous iv infusion of Ara-C was begun (200 mg/m^2/24 hrs). Within 24 hours his wbc count decreased from 190,000 to 33,000 cells/mm^3. Ara-C was discontinued after 4 more days. The marrow became hypoplastic and remained so for

about 2 weeks, at which time the regenerating cells were all leukemic. The patient was then treated with several other drugs in a further attempt to induce remissions but thus far without success.

Patient No. 3

This patient was a 9-year-old girl who had been healthy until February of 1975 when she developed hematomas and ecchymoses. Her wbc count was 240,000 cells/mm^3, her platelet count was 45,000 cells/mm^3, and her Hgb level was 8.0 g/100 ml. A chest roentgenogram revealed a mediastinal mass. A diagnosis of acute lymphoblastic leukemia was made from a marrow aspirate at another hospital, and she was treated with four weekly doses of VCR and daily prednisone. She entered remission and was placed on maintenance therapy consisting of a combination of 6-mercaptopurine, cyclophosphamide, and methotrexate.

In June of 1975 her bone marrow showed signs of early relapse and she was again given VCR (six weekly doses) plus prednisone, but she failed to achieve remission. Before she was transferred to this hospital, she had received additional doses of adriamycin, VCR, and cyclophosphamide without response. Upon admission to this hospital on October 1, 1975, she was lethargic; she had marked enlargement of the liver and spleen and cranial nerve palsies. Her wbc count was 998,000 cells/mm^3, her platelet count was 10,000 platelets/mm^3, and her Hgb was 7 g/100 ml. That evening she received an iv dose of vindesine of 4 mg/m^2.

A bone marrow aspirate was taken prior to the vindesine injection. Because of the packed marrow, only a minute amount of cellular material was obtained in the aspirating needle; this was processed for FMF. Peripheral blood was also obtained for comparison with the bone marrow DNA histogram. After therapy, we were unable to obtain additional bone marrow aspirates because of the packed marrow, but we took peripheral blood samples at intervals for analysis.

The patient died from an intracerebral hemorrhage on October 4, 1975, 3 days after admission.

MATERIALS AND METHODS

Preparation of Cells for FMF

Heparinized bone marrow or blood samples were treated by a method described previously (8) to remove erythrocytes and mature myeloid cells. After filtering the cells through a nylon-mesh filter to remove bone marrow spicules and cell clumps, they were stained with a 0.05-mg/ml solution of propidium iodide (Calbiochem, San Diego, Calif) in 0.1% sodium citrate (3). The relative fluorescence of the cells was measured in a Cytofluorograf Model 4802 (Bio/Physics Systems, Inc, Mahopac, NY) using an argon ion laser at 488 nm. Data were stored on a Northern Model NS-602 pulse height analyzer (Tracor-Northern Scientific, Inc, Middleton, Wisc), recorded on a teletype printer and paper tape punch (Model ASR 33), and analyzed on an IBM digital computer. The fractions of cells in the G_1, S, and G_2+M phases of the cell cycle were determined by a mathematic method described previously (9–11).

Labeling Procedure and Autoradiography

Each sample consisting of about 0.3 ml of bone marrow was aspirated from either the sternum or the anterior or posterior iliac crest and added to a 5-ml glass centrifuge tube containing 0.6 ml of McCoy's 5a medium (modified), 0.05 ml of heparin, and 2 microcuries of 3HTdR (specific activity 6 curies/mM). The sample was then incubated at room temperature for 1 hour and centrifuged; smears were made of the buffy coat. Peripheral blood specimens were treated similarly except that 10 ml of blood was incubated with 20 microcuries of ^{3}HTdR. Ten to 15 smears were made of each specimen and immediately dried with a hair dryer. The slides were then fixed in methanol for 15 minutes, dried in air, and stored until the experiment was completed.

Slides were processed together using Kodak NTB2 emulsion. The emulsion was liquefied at 40°C–42°C; the slides were dipped and were then placed in the dark at room temperature for 24 hours. The slides were then refrigerated for 1 week. After this, the slides were developed and stained with Jenner-Giemsa stain at pH 5.4 for 1 hour, dried in air, and counted.

One thousand cells were counted for determination of labeling index; cells with five grains or more overlying the nucleus were considered labeled. The average background grain count was usually less than one grain per nucleus.

Differential Counts and MIs

Portions of the bone marrow samples were stained with tetrachrome Giemsa for determination of the differentials and MIs. Two hundred cells were usually counted for the former and 5000 for the latter. All stages of mitosis were included except for early prophase (unless otherwise indicated).

RESULTS

Patient No. 1

Figure 1 shows the therapy administered during the first 4 days of treatment together with the wbc count, the fraction of blast cells in the bone marrow, and the results of FMF analysis. Table 1 presents some of these data in numerical form, together with the available MIs and ^{3}HTdR pulse-labeling indices.

After the initial VCR injection, the percentage of cells in mitosis increased dramatically (albeit transiently) and the wbc count dropped significantly. Although the MIs could not be determined accurately in the later samples because of decreased cellularity, no mitoses were found in the 24-, 48-, or 96-hour samples. After an initial increase, the FMF-derived estimates of G_2+M remained at about 10% for 1 day and then decreased below the initial value. The relative number of cells in the S phase also increased transiently, but had dropped below the starting value by 24 hours, which was 12 hours after prednisone treatment had begun. The blast cells in the marrow disappeared very rapidly. By 24 hours the marrow was already markedly hypocellular, and the percentage of blast cells had decreased from 99% to 53% (the other cells remaining were almost all small lymphocytes). Since the patient later went into complete remission after another dose of VCR, treatment with VCR and prednisone was highly effective even though no striking changes occurred in the distribution of cells in the cell cycle (except for a transient increase in mitoses after the first dose of VCR). These results are compatible with the death of most cells in G_1, presumably due largely to prednisone but possibly to the combined effects of the two drugs.

Patient No. 2

Figure 2 displays selected data concerning treatment and response of the patient during the first 3 days of the treatment regimen which began on September 22, 1975. Table 2 lists numerical values of selected parameters, including FMF-derived distributions of cells among the phases of the cycle, ^{3}HTdR pulse-labeling indices, and MIs.

TABLE 1.—Kinetic parameters of marrow cells of patient No. 1*

	Time (hrs)				
Parameter	0	7	24	48	96
MI (%)	0.6 (0.6)	2.3 (2.3)†	0‡	0§	0§
LI (%)¶	7.2 (7.2)	1.4 (1.4)	4.7 (2.5)	0.4 (0.2)	—
G_1	82.6	71.8	83.6	90.3	93.4
S	11.7	18.6	6.5	7.2	4.9
G_2+M	5.7	9.6	9.9	2.5	1.6
Blast cells (%)	99	98	53	45	56

*Nos. without parentheses refer to blast cells only; Nos. within parentheses represent total population.
†3.2% if prophase is included.
‡Because of low bone marrow cellularity, only 500 cells were scanned.
§Only 1000 cells were examined in these samples.
¶LI = labeling index.

TABLE 2.—Kinetic parameters of leukemic cells in marrow of patient No. 2*

	Time (hrs)				
Parameter	0	7	24	48	72
MI (%)	0.4 (0.3)	0.2 (0.1)	0.2 (0.1)	0.2 (0.1)	0.1 (0.03)
LI (%)	8.5 (7.2)	1.8 (1.2)	1.0 (0.8)	2.8 (1.5)	2.4 (0.9)
G_1	90.5	91.7	86.7	84.2	89.6
S	6.1	4.5	6.6	9.8	9.6
G_2+M	3.4	3.8	6.7	6.0	0.8
Leukemic cells† (%)	92	86	81	86	74

*See footnote 1 of table 1.
†These include blast cells, promonocytes, and monocytes.

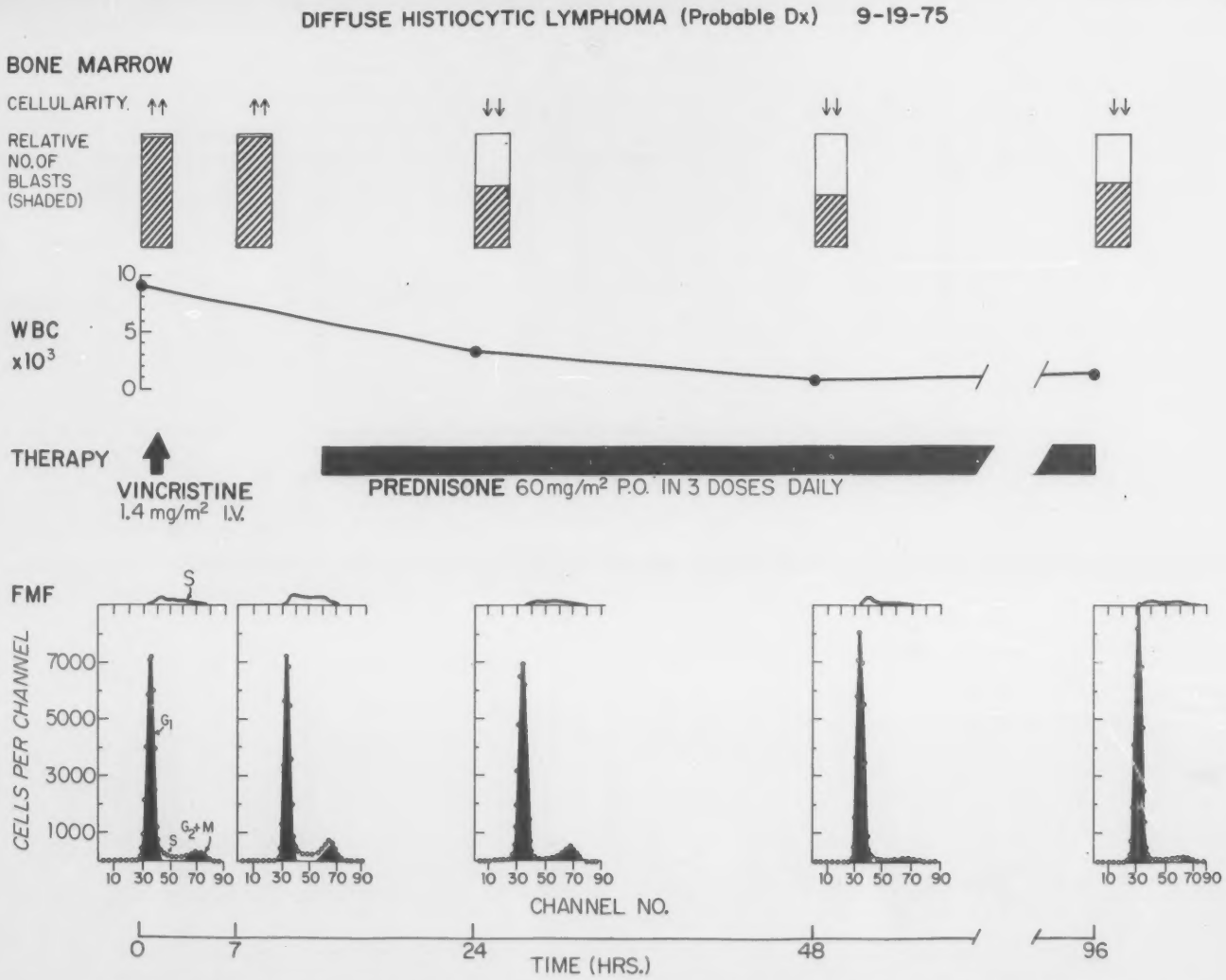

FIGURE 1.—Relative bone marrow cellularity, fraction of blast cells in the bone marrow, wbc count, chemotherapy, and FMF histograms of patient No. 1 just prior to treatment and at 7, 24, 48, and 96 hrs after beginning treatment. The date given on the top of the figure corresponds to time O. FMF histograms show the data points (○) and the results of mathematic analysis of the data by the method of Fried (refs 9–11). In these histograms, the shaded areas are proportional to the percentages of cells in G_1 and G_2+M, as indicated. The unshaded areas between those components correspond to S-phase cells and are redrawn in the upper portions of each histogram. All data were normalized to 50,000 cells to facilitate comparison between samples.

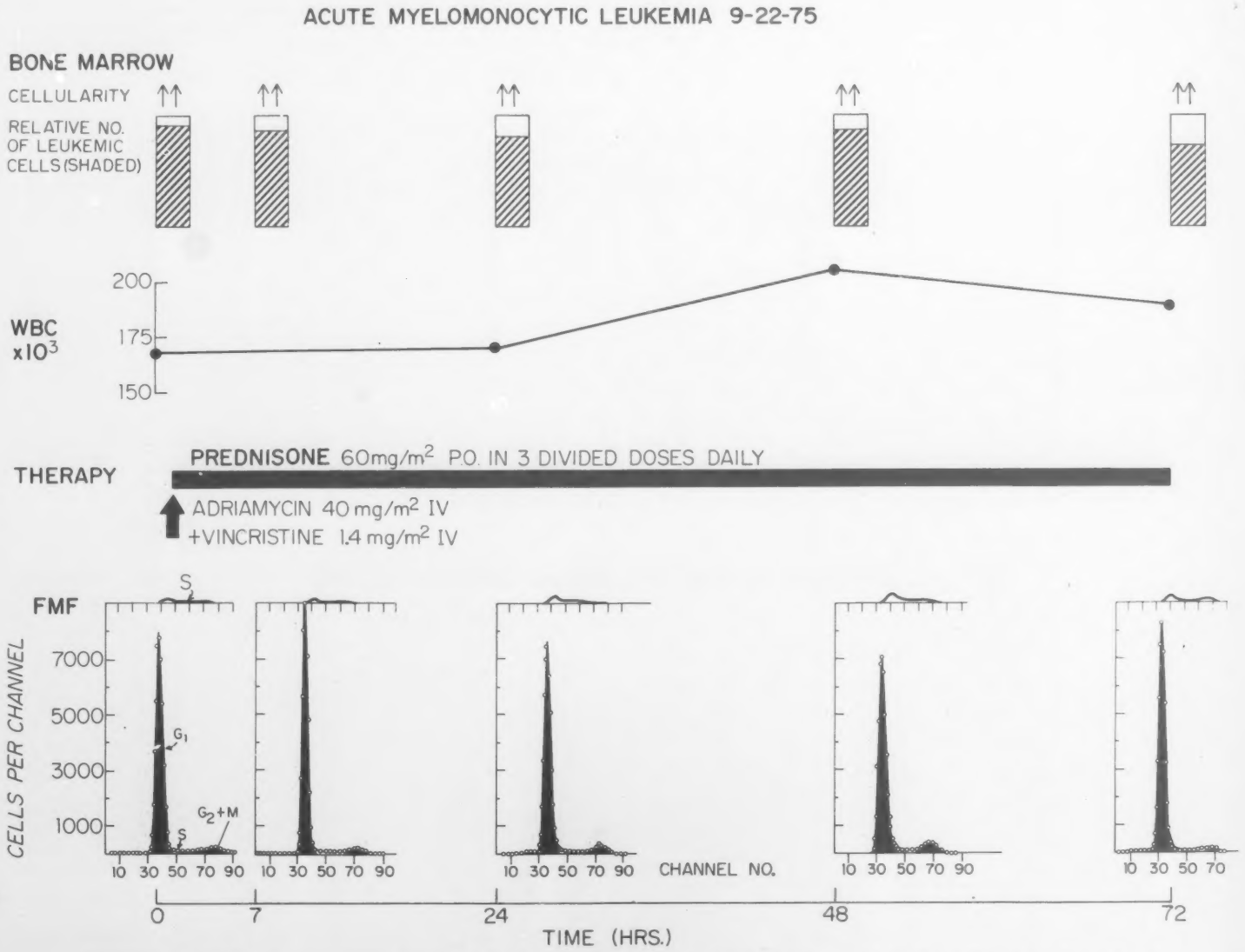

FIGURE 2.—Selected bone marrow and blood characteristics of patient No. 2 prior to therapy indicated, and at 7, 24, 48, and 72 hrs thereafter, as in fig 1. Explanation of FMF histograms is given in fig 1.

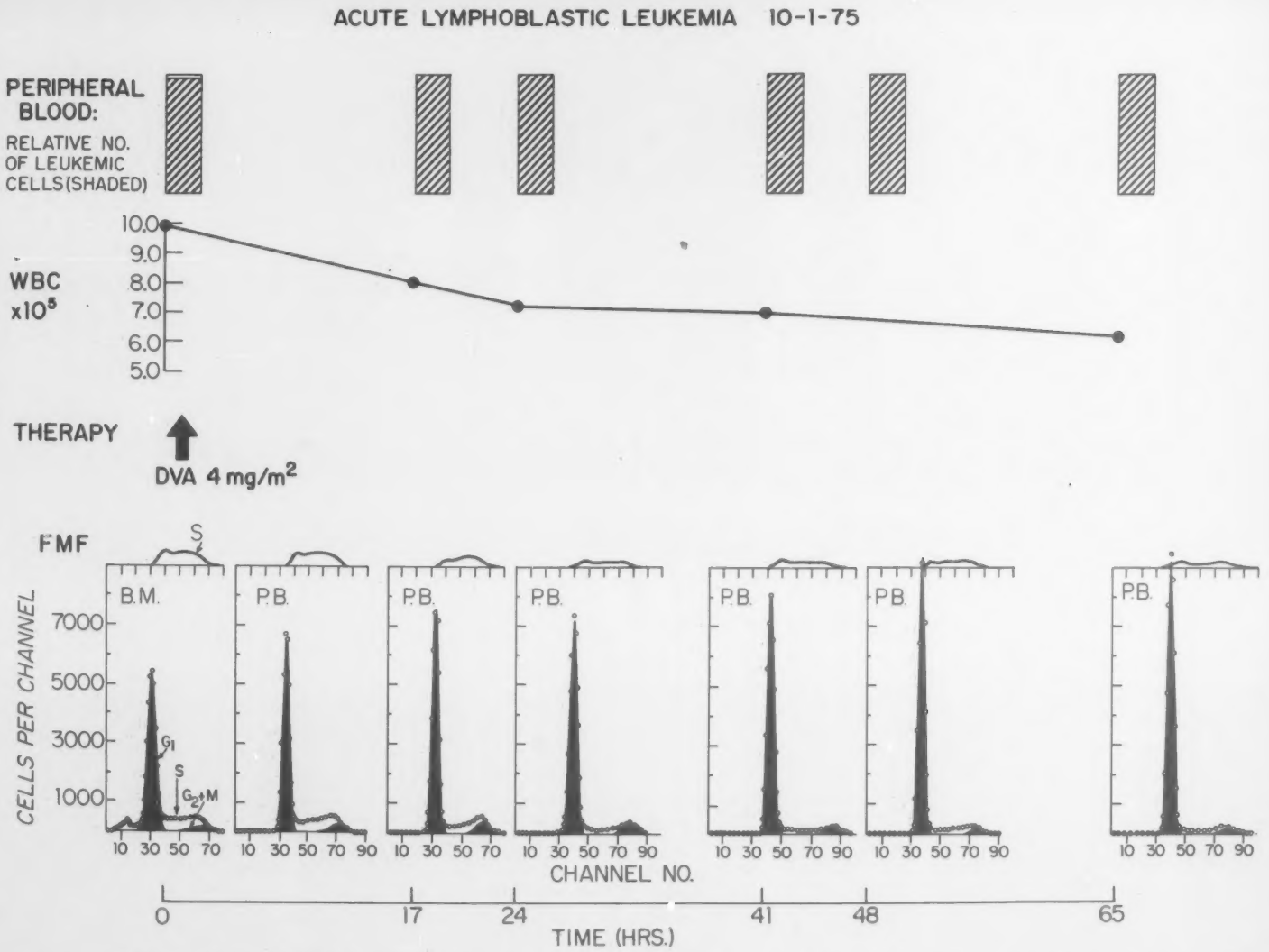

FIGURE 3.—% of leukemic cells in peripheral blood, wbc, and FMF histograms prior to and at 17, 24, 41, 48, and 65 hrs after iv injection of vindesine (DVA) in patient No. 3. Both bone marrow (BM) and peripheral blood (PB) samples were obtained for FMF prior to DVA; only peripheral blood samples were obtained subsequently as explained in Results. Explanation of FMF histograms is given in fig 1.

TABLE 3.—Kinetic parameters of blast cells in peripheral blood and marrow of patient No. 3*

Parameter	Time (hrs)						
	0	0	17	24	41	48	65
MI (%)	—	0.18†	0.48‡	0	0	0.08	0
LI (%)	—	—	6.0	10.0	1.0	1.4	1.0
G_1	69.9	68.2	77.0	82.4	85.3	86.9	89.9
S	26.4	26.4	15.6	10.5	11.4	10.2	8.1
G_2+M	3.6	5.4	7.4	7.0	3.3	2.9	2.0
Wbc ($\times 10^3$)	—	998	802	726	701	—	620
Leukemic blast cells in blood (%)	—	98	99	99	99	99	99

*All data refer to peripheral blood except 1st 0-hr column which refers to bone marrow (*see* footnote 1 of table 1).

†Includes prophase (about ½ were in this category).

‡Almost all of these were in prophase.

According to the results shown in figure 2 and table 2, relatively few significant changes occurred in the observed parameters after treatment. About 90% of the cells were in the G_1 phase, with about 6% in S phase and 0.3% in mitosis. At 24 hours there was a small increase in the percentage of cells in G_2 which persisted for an additional 24 hours. However, by 72 hours most of these cells had been eliminated, presumably due to death of the G_2-arrested cells. The wbc count remained fairly stable at nearly 200,000 cells/mm^3, and the percentage of cells classified as leukemic declined only slightly during the first 2 days and decreased to 74% by the third day. Accompanying this was a moderate decrease in the percentage of leukemic blast cells relative to more mature monocytoid forms.

The FMF results in this patient appear consistent with most of the other observed parameters; this suggests that this treatment had little significant effect on the patient's leukemic cells. An infusion of Ara-C was begun after 72 hours which caused rapid cell kill, and thus, while a delayed response to the prior therapy with adriamycin, VCR, and prednisone cannot be excluded, this seems unlikely since most patients in whom this latter combination is effective have already shown marked cell kill before 72 hours.

Patient No. 3

As with the two preceding patients, figure 3 and table 3 show the principal treatment and response characteristics prior to and following drug administration. Since this patient had previously received VCR, prednisone, adriamycin, and cyclophosphamide without achieving remission, she appeared to be a good candidate for a therapeutic trial with the new drug vindesine.

Because of the packed bone marrow, we were unable to obtain marrow aspirates for analysis, except for one sample analyzed by FMF prior to the vindesine injection. Subsequent samples were of peripheral blood, which we believe in the present case may adequately represent the behavior of cells in the marrow. This belief is supported by a comparison of analyses of the FMF data from the initial blood and bone marrow specimens.

After administration of the drug, the percentage of cells in S phase decreased from 26% to 10% while those in G_2+M increased from 3.6% to 7% within 1 day. Although the MI had also increased considerably by 17 hours, mitoses accounted for only a small fraction of the cells in G_2+M. Furthermore, the MI had dropped to 0 by 24 hours even though the G_2+M component remained the same. The wbc count decreased progressively during the 3 days of the study, but was still > 600,000 cells/mm^3 at the end of this time. The percentage of leukemic blast cells in the blood remained at nearly 100% throughout.

Thus, although some minor kinetic changes occurred after drug administration, they were not dramatic and it appeared likely that, even had clinical improvement occurred, it would have been transient.

DISCUSSION

One of our objectives in this study was to investigate whether certain drugs having known (or suspected, in the case of vindesine) cell cycle specificities would have the predicted kinetic effects when used for the treatment of patients. In conjunction with this, we were interested in whether the administration of additional drugs either concurrently or subsequently would significantly affect the kinetic response of the tumor cells to the first drug. Finally,

we wished to obtain data bearing on the question of whether kinetic changes occurring in response to drugs could be correlated with the patient's clinical behavior.

Major limitations in the present study were that only three patients were studied; they did not have the same disease and two of them were treated prior to the reported investigations. While these factors restrict the conclusions that we can justifiably make, we believe that the data nevertheless provide information relevant to the above questions, and can be helpful as well in guiding future kinetic studies using FMF.

After the administration of VCR to patient No. 1 (previously untreated), there was a marked but brief rise in the MI. By the time of the 24-hour sample, the bone marrow cellularity had decreased considerably, and only 53% were blast cells. Furthermore, no mitoses were found in this or later samples. This decrease in the percentage of mitoses at 24 hours was unexpected in view of the fact that at least in acute lymphoblastic leukemia, prednisone appears to inhibit the entry of cells into S but not their progression through this phase (12,13). We would have expected a decreased MI only after cells initially in S phase had progressed into mitosis.

These observations, together with the discrepancy between the ^{3}HTdR labeling indices and the FMF-derived percentages of cells in the S phase in the 7-hour and later samples (table 1), suggest that in this patient, VCR and prednisone may have inhibited either the incorporation of thymidine or DNA synthesis itself. The rapidity with which the blast cells disappeared from the marrow also implies that a significant number of G_1 cells must have been killed by prednisone, VCR, or both. This interpretation is consistent with results reported previously by Ernst and Killmann (13) and by Stryckmans et al (14).

The qualitative observations of initial increases and then decreases (by 24 hours) in the MIs and labeling indices are similar to the response we previously observed in a patient with acute lymphoblastic leukemia treated by the same protocol (8); in the latter case, however, the MI decreased only slightly by 24 hours.

Although the interpretation of the later FMF samples is complicated by the fact that only about half of the cells were blast cells, the remainder were almost all lymphocytes in G_0, which were presumably included within the G_1 compartment.

Patient No. 2, who received VCR, adriamycin, and prednisone simultaneously, exhibited no significant changes in either his clinical status or in the number of leukemic cells in the marrow or blood. However, the later marrow samples showed proportionally fewer blast cells and more promonocytes and partially mature monocytoid forms. There were no significant changes in the distribution of the cells among the phases of the cell cycle, except for a small increase in G_2 cells which occurred at 24 hours and which persisted for at least an additional 24 hours. It is likely that the failure of cells to accumulate in mitosis was due at least in part to the effects of adriamycin in inhibiting DNA synthesis and perhaps in arresting cells in G_2. This hypothesis is supported by comparison of the FMF with the autoradiographic results, since both yielded similar estimates of S-phase fraction in the pretreatment sample, but the ^{3}HTdR labeling indices were much lower than the equivalent FMF-derived values in the later samples. Adriamycin, an antitumor antibiotic which intercalates into DNA, probably has a mechanism of action similar to that of daunorubicin. Ernst (15) found that DNA synthesis of leukemic blast cells in some patients with acute myeloblastic leukemia and acute lymphoblastic leukemia was inhibited by the latter drug, and Stryckmans et al (16) and Arlin et al (17) showed that daunorubicin could also arrest leukemic blast cells in the G_2 phase.

Although the patient had not been given either VCR or prednisone previously and had been exposed only briefly to adriamycin prior to the present study, the kinetic and clinical results imply that his leukemic cells were refractory to this drug combination. Although VCR has been found to kill leukemic cells even in G_1 in unusually sensitive populations (14), it appears unlikely that patient No. 2's cells were in this category. Subsequent treatment with the S-phase specific drug Ara-C caused a precipitous drop in the wbc count and in the bone marrow cellularity although remission was not attained.

Interpretation of data from patient No. 3 in our study was complicated both by the prior treatment with VCR and other drugs, and by our inability to obtain bone marrow aspirates (other than a small sample just prior to vindesine). The question naturally arises as to the accuracy with which the peripheral blood samples represent the behavior of the cells in bone marrow. The fact that the blood cells had an S-phase component almost identical to the marrow cells, together with the presence of a moderate percentage of mitotic cells in the early samples, suggests that the usual control mechanisms inhibiting the release of dividing cells from the bone marrow may have been ineffective in this patient. Furthermore, quantitative results from the blood and bone marrow samples prior to vindesine were in very close agreement with respect to the FMF histograms, and the percentage of leukemic blast cells in the blood was virtually 100%, as expected. We believe that no contamination of the bone marrow sample with blood occurred in this

case, for reasons discussed previously. We have observed the kinetic parameters of leukemic cells in marrow and blood to be similar in several patients studied previously who had very high wbc counts.

The observed decrease in the MI to 0 by 24 hours after vindesine injection was unexpected. A possible explanation might be that the mitotic cells were severely damaged by the drug and were rapidly removed from the circulation by the liver and spleen.

In conclusion, we note that the interaction of some of the drug combinations used may have been antagonistic rather than synergistic. Such possible effects with respect to both tumor and normal tissue require further exploration, together with the possible use of the autoradiographic labeling index in comparison with the FMF-derived fraction of cells in S as a measure of drug-induced suppression of DNA synthesis or thymidine incorporation.

REFERENCES

1. SWEENEY MJ, CULLINAN GJ, POORE GA, ET AL. Experimental antitumor activity of vinblastine amides. Proc Am Assoc Cancer Res and ASCO 15:37, 1974.
2. OCHS S, and WORTH R. Comparison of the block of fast axoplasmic transport in mammalian nerve by vincristine, vinblastine and desacetyl vinblastine amide sulfate (DVA). Proc Am Assoc Cancer Res and ASCO 16:70, 1975.
3. KRISHAN A. Rapid flow cytofluorometric analysis of mammalian cell cycle by propidium iodide staining. J Cell Biol 66:188–193, 1975.
4. VAN DILLA MA, TRUJILLO TT, MULLANEY PF, ET AL. Cell microfluorometry: a method for rapid fluorescence measurement. Science 163:1213–1214, 1969.
5. TOBEY RA, CRISSMAN HA, and KRAEMER PM. A method for comparing effects of different synchronizing protocols on mammalian cell cycle traverse. J Cell Biol 54:638–645, 1972.
6. GÖHDE W, and DITTRICH W. Simultane impulsfluorimetrie des DNS-und Proteingehaltes von Tumorzellen. Z Anal Chem 252:328–330, 1970.
7. MCCREDIE KB, HESTER JP, GUTTERMAN JU, ET AL. Survival of adults with acute leukemia. Proc Am Assoc Cancer Res and ASCO 16:141, 1975.
8. FRIED J, ARLIN Z, and CLARKSON B. Flow microfluorometry of bone marrow cells from a patient with acute lymphocytic leukemia during chemotherapy. *In* Proceedings of the 2nd International Symposium on Pulse Cytophotometry (Schumann J, Göhde W, and Büchner T, eds). Ghent, European Press. In press, 1976.
9. FRIED J. Mathematical analysis of flow microfluorometric data and its application to the determination of cell cycle parameters. *In* Mathematical Models in Cell Kinetics (Valleron A-j, ed). Ghent, European Press, 1975, pp 68–70.
10. FRIED J. Method for the quantitative evaluation of data from flow microfluorometry. Comput Biomed Res 9:263–276, 1976.
11. FRIED J, YATAGANAS X, KITAHARA T, ET AL. Quantitative analysis of flow microfluorometric data from asynchronous and drug-treated cell populations. Comput Biomed Res 9:277–290, 1976.
12. LAMPKIN BC, NAGAO T, and MAUER AM. Drug effect in acute leukemia. J Clin Invest 48:1124–1130, 1969.
13. ERNST P, and KILLMANN S-A. Perturbation of generation cycle of human leukemic blast cells by cytostatic therapy in vivo: effect of corticosteroids. Blood 36:689–696, 1970.
14. STRYCKMANS PA, LURIE PM, MANASTER J, ET AL. Mode of action of chemotherapy in vivo on human acute leukemia. II. Vincristine. Eur J Cancer 9:613–620, 1973.
15. ERNST P. Perturbation of generation cycle of human leukaemic blast cells in vivo by daunomycin. Scand J Haematol 11:13–22, 1973.
16. STRYCKMANS PA, MANASTER J, LACHAPELLE F, ET AL. Mode of action of chemotherapy in vivo on human leukemia. I. Daunomycin. J Clin Invest 52:126–133, 1973.
17. ARLIN Z, FRIED J, and CLARKSON B. Effects of daunomycin on human leukemic cells in vivo as studied by flow microfluorometry. Proc Am Assoc Cancer Res and ASCO 16:180, 1975.

Kinetic Aids to Proper Chemotherapeutic Scheduling: Labeled Nucleoside Incorporation Studies In Vivo

Robert C. Young [1,*]

Cancer chemotherapists have long sought techniques for determining proper drug sequences. Considerable time and effort have been expended in such studies because of the observation that variation in drug sequencing in animal models has frequently brought about enhanced antitumor effect. Unfortunately, in general, kinetic investigations have found limited applicability in the design of cancer treatment in man. Many studies have provided invaluable information concerning growth kinetics, mechanisms of drug action, site of cell-cycle action, etc, but have been unsuccessful in fulfilling the requirements most necessary for direct application to cancer treatment in man. Kinetic techniques most valuable to the clinician are those which (*a*) are performed in vivo; (*b*) simultaneously study the effect of chemotherapy on both the tumor and the normal host tissues ordinarily injured by such chemotherapy; (*c*) can be performed rapidly and conveniently without an extensive lag time so that data generated can be applied to the patient being studied; and (*d*) allow opportunity for repeated study so that the alterations and perturbations induced by drug therapy can be studied.

Studies from this laboratory have employed a technique which satisfies some of these requirements by monitoring the incorporation of labeled nucleoside into DNA in both normal and tumorous tissues in vivo after administration of a chemotherapeutic agent (1–4). The technique is comparatively easy to perform, allows results to be obtained rapidly, and allows repeated kinetic study after perturbation by chemotherapy. For chemotherapeutic agents such as cytosine arabinoside (ara-C) (1), cyclophosphamide (CTX) (3,5), 5-fluorouracil (5-FU) (6), and the nitrosoureas (2), drug schedules based on the differential recovery patterns of host tissues and tumor have produced reduced toxicity to normal animals and have increased the survival of tumor-bearing animals. With the use of short-term in vitro incubations of labeled nucleosides, such studies can be modified for application to man.

[1]Medicine Branch, Clinical Oncology Program (COP), Division of Cancer Treatment (DCT), National Cancer Institute (NCI), Bethesda, Md.

**Reprint requests to:* Robert C. Young, MD, Medicine Branch, COP, DCT, NCI, Bldg 10, Rm 12N226, National Institutes of Health, Bethesda, Md 20014.

MATERIALS AND METHODS

Detailed descriptions of the methods of toxicity and survival studies, labeling-index and colony-forming unit studies, and methotrexate (MTX) assays have been previously published (1–7).

Labeled Nucleoside Incorporation Studies (dpm/μg DNA)

Labeling was achieved with ip doses of 100 microcuries of ^{3}H-thymidine (^{3}H-TdR) (specific activity 6.7 curies/mmol) or 100 microcuries of ^{3}H-deoxyuridine (^{3}H-UdR) (specific activity 10 curies/mmol) (New England Nuclear Corp, Boston, Mass) and mice were killed 1 hour later. The ascites tumor was aspirated from the peritoneal cavity, the proximal duodenum was removed, and the mucosa was dispersed in iced phosphate-buffered 0.85% NaCl, pH 7.4 (PBS). The bone marrow was removed from the tibias and dispersed in iced PBS. Separate samples of ascites tumor, duodenal mucosa, and bone marrow from each of six mice were pooled into two groups of three. The DNA of each specimen was extracted by a modification of the Schneider method (8). A 0.5-ml aliquot of the final supernatant was added to 15-ml Aquasol (New England Nuclear Corp) and counted by liquid scintillation. A 0.5-ml aliquot of the final supernatant was processed by the Burton method (9) for DNA determination. The results were then expressed as cpm/μg of DNA and graphed as percent of control over time (%C/T), or were corrected using a standard quench curve for tritium. The efficiency of the tritium counting was 22%–29% and the results were expressed as dpm/μg of DNA and graphed as %C/T. Variation in the incorporation of ^{3}H-TdR or ^{3}H-UdR among the control groups was 10%–15%.

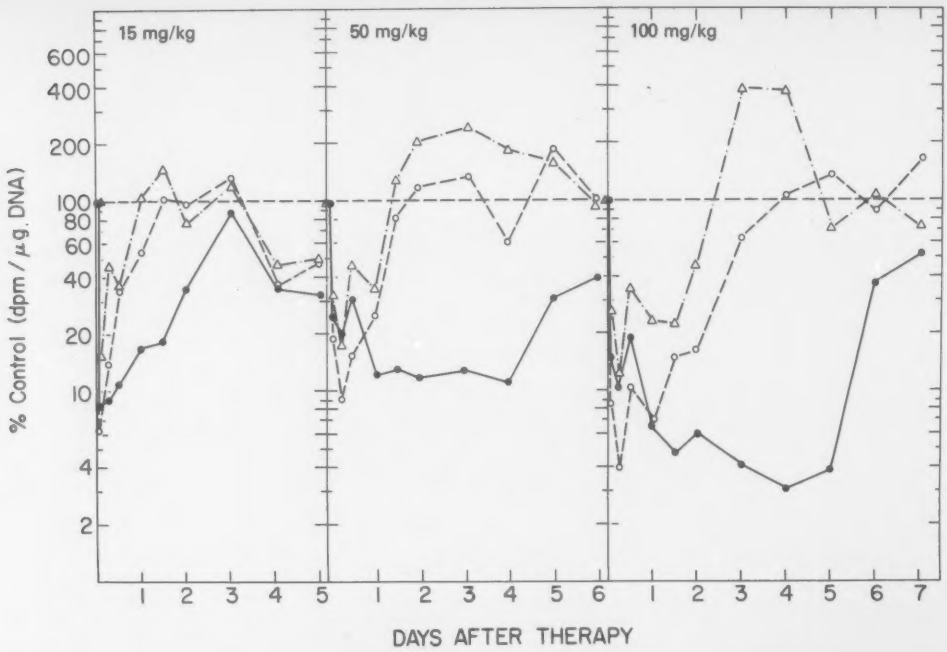

FIGURE 1.—Alterations in ^{3}H-UdR incorporation induced in ascites tumor (●---●), GI mucosa (△---△), and bone marrow (○---○) in CDF$_1$ mice after exposure to 15, 50, and 100 mg/kg of 5-FU ip.

RESULTS

Alterations Induced in Normal and Tumorous Tissue by 5-FU

The kinetic effect of 5-FU on P1534 ascites tumor as well as on normal bone marrow and intestinal epithelium was evaluated by following ^{3}H-UdR incorporation into the DNA of these tissues after 15, 50, and 100 mg/kg ip (fig 1). 5-FU inhibits thymidylate synthetase and interferes with conversion of dUMP to dTMP impairing incorporation of ^{3}H-UdR as shown in figure 1. The magnitude and duration of suppression of ^{3}H-UdR incorporation into DNA was directly related to drug dose for both the normal and tumorous tissues. However, the recovery pattern for the tumor cells clearly differed from the normal tissues in that recovery of the tumor was delayed, especially at doses of 50 and 100 mg/kg. Maximal differential inhibition occurs with 100 mg/kg. Normal tissues recover by 2–3 days but the tumor remains inhibited, only beginning recovery on Days 5–6.

Alterations Induced by 5-FU in a Less Sensitive Tumor Model (fig 2)

The duration of suppression of ^{3}H-UdR incorporation appears to correlate with the sensitivity of the tumor to drug therapy. When an Ehrlich ascites tumor less sensitive to 5-FU therapy was investigated (fig 2) following a dose of 50 mg/kg, suppression of ^{3}H-UdR incorporation into DNA of gastrointestinal (GI) mucosa, bone marrow, and Ehrlich ascites tumor was maximal within 1 hour after drug administration. Although the magnitude of the depression was greater for the tumor than for the normal tissues, the time course of suppression and recovery was similar in all three tissues and no exploitable difference in recovery between normal and tumorous tissues was seen.

Nucleoside Incorporation Patterns and Normal Tissue Toxicity

5-FU is known to be most toxic to rapidly proliferating cells and therefore a second dose of 5-FU

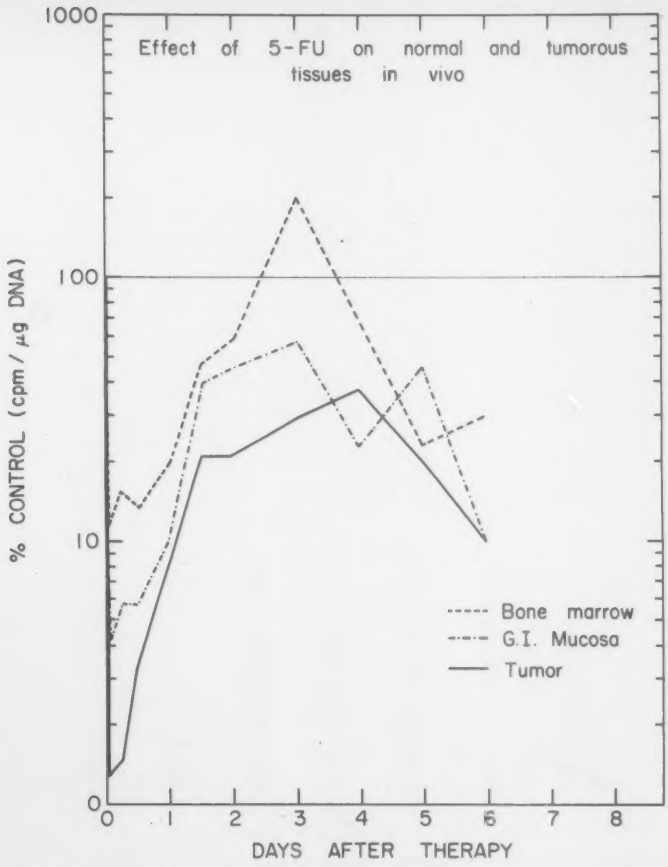

FIGURE 2.—Alterations in ^{3}H-UdR incorporation induced by 50 mg/kg of 5-FU in GP mice bearing Ehrlich ascites tumor of intermediate sensitivity.

might be expected to have maximum toxicity in normal tissues during the recovery phase when DNA synthesis achieves a maximal rate. This hypothesis was tested by studying second doses of 100 mg/kg of 5-FU at specified intervals after the first dose (fig 3). During the first 6 hours, when incorporation of ^{3}H-UdR into DNA of bone marrow and duodenal mucosa was maximally suppressed, repetition of 5-FU caused little toxicity (< LD10). However, during the period of rapid recovery (Days 2–6) ^{3}H-UdR incorporation into the normal tissues increased to a maximum and a second dose was associated with severe toxicity to otherwise normal animals (LD80–100). From Days 6 through 8, ^{3}H-UdR incorporation into DNA began to return toward baseline levels and a second dose of 5-FU at that time was associated with progressively less toxicity.

Nucleoside Incorporation Patterns and Antitumor Effect

In order to determine whether the relationship observed above between the ^{3}H-UdR incorporation rate and the effects of a second 5-FU dose could provide information about proper sequences of therapy in tumor-bearing animals, CDF_1 mice bearing P1534 ascites tumor had 5-FU doses repeated at various times after the first dose (fig 4). A single dose of 100 mg/kg of 5-FU resulted in a 20% prolongation in the median survival time. Second doses of 5-FU fail to enhance survival if given in the first 4 days, presumably because of excessive toxicity (fig 3). From Days 4 through 7, the second dose of 5-FU increased survival to a maximum of 60% greater than control.

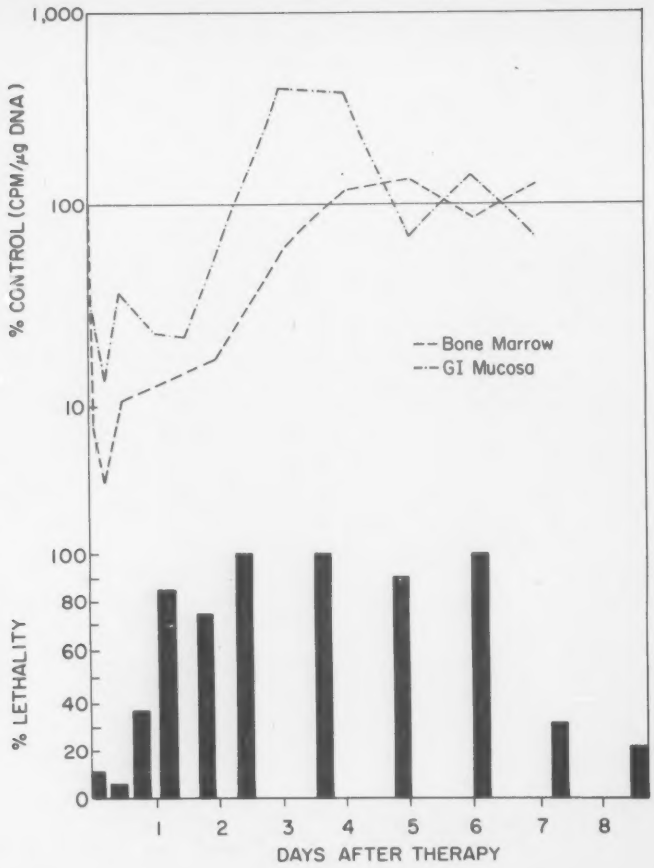

FIGURE 3.—Alterations induced by 5-FU in ^{3}H-UdR incorporation into normal tissues. Lower panel charts the lethality of a second identical dose of 5-FU given at various times after the first dose.

Nucleoside Incorporation Alterations Induced by CTX

While it is hardly surprising that drugs which specifically inhibit some step in nucleoside incorporation (ie, 5-FU, ara-C, or MTX) can be monitored in this manner, it was of interest to see if agents not possessing such inhibitory effects could be similarly studied. CTX was investigated and the simultaneous changes in DNA synthesis, as reflected by ^{3}H-TdR incorporation in the tumor (ascites) and host target tissue (bone marrow and GI mucosa) after a single dose of CTX of either 50, 100, or 200 mg/kg ip are presented in figure 5.

After each of these doses, the incorporation of ^{3}H-TdR into bone marrow-DNA shows a significant depression and reaches a nadir by 12 hours. The GI mucosa also showed a marked depression in ^{3}H-TdR incorporation following CTX therapy, although recovery was complete at all these doses by 36 hours. DNA synthesis in the ascites tumor was suppressed by CTX within 1 hour at the 100- and 200-mg/kg doses and by 6 hours at the 50-mg/kg dose. Recovery was not noted during the 3 days of study at the 50- and 100-mg/kg doses and had only begun by Days 6–8 (14% of control) at 200 mg/kg. Thus, a clear difference between the recovery pattern of the host target tissue (bone marrow and GI mucosa) and the tumor was seen.

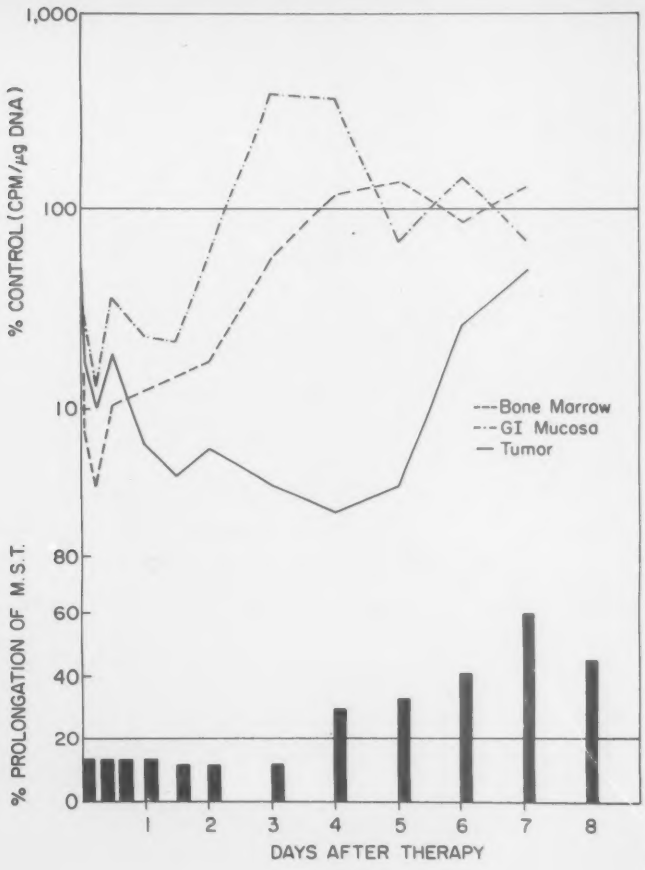

FIGURE 4.—Alterations induced by 5-FU in ^{3}H-UdR incorporation in normal and tumorous tissues (upper panel) compared with the prolongation of survival induced by identical second doses of 5-FU given at various times after the first dose (lower panel).

Nucleoside Incorporation Compared With Serial Labeling Index (LI) Studies in Normal and Tumorous Tissues In Vivo

Injury and recovery of tumor and normal tissues induced by a single dose of CTX were studied by the conventional kinetic techniques of the LI and compared to the results obtained using inhibition and recovery of DNA synthesis (fig 6). The two techniques gave slightly discordant results only during the first few hours of the study. After the initial 24-hour period the results obtained with the two techniques were comparable.

Simultaneous Alterations in the Peripheral Wbc Count, Bone Marrow Cellularity, Colony-Forming Units in Culture, and ^{3}H-TdR Incorporation

Figure 7 compares the simultaneous effects of CTX on a number of the commonly used parameters for assessing bone marrow injury.

After a single dose of CTX, granulocyte colony production became markedly depressed by 1 hour and remained essentially unmeasurable for the next 30 hours. Recovery started between 30 and 48 hours after therapy, overshot control from Days 2 to 5, and returned to control levels between Days 5 and 6.

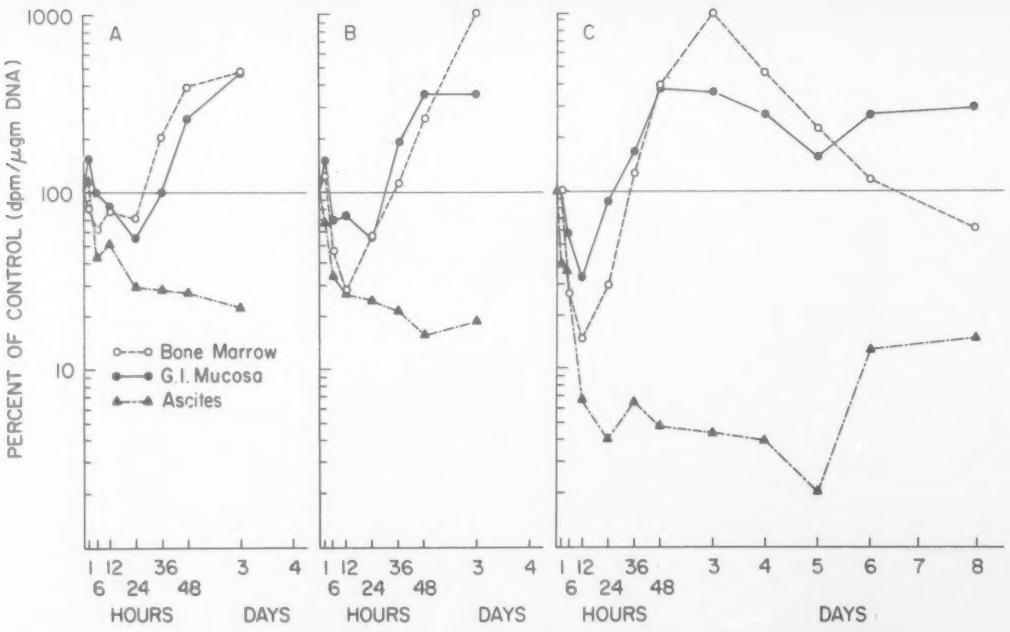

FIGURE 5.—Effect of a single dose of CTX on the ^{3}H-TdR incorporation into L1210 ascites tumor, bone marrow, and GI mucosa. Panel A (50 mg/kg CTX ip); panel B (100 mg/kg CTX ip); panel C (200 mg/kg CTX ip). (*From* ref 5.)

The timing of suppression and recovery of DNA synthesis in the bone marrow roughly parallels the changes seen in the colony-forming ability of bone marrow precursor cells with the notable exception that DNA synthesis in the bone marrow can be seen to recover 24 hours sooner than the colony-forming ability.

Following CTX therapy, the fall in bone marrow cellularity and the peripheral wbc count followed the pattern of bone marrow suppression and recovery, but was delayed significantly. These manifestations of CTX injury occurred much later than the alteration in DNA synthesis in the bone marrow.

Correlation of Plasma-MTX Concentration With Inhibition of ^{3}H-UdR Incorporation Into DNA

Because accurate assay techniques for determining precise plasma MTX concentrations are available, it is possible to determine the relationship of plasma concentration of MTX to the in vivo inhibition of nucleoside incorporation into the normal target tissues.

Inhibition of ^{3}H-UdR incorporation was virtually complete in host tissues when the concentration of MTX in plasma was $> 10^{-8}$ M for all doses of MTX studied (fig 8). ^{3}H-UdR incorporation in bone marrow recovered to 50% of pretreatment levels only when plasma antifolate concentration fell to $< 10^{-8}$ M.

The foregoing studies indicate that an important relationship exists between extracellular concentration of MTX and its inhibitory effect on DNA synthesis in host tissues. Over a 70-fold range of MTX dosage, recovery of DNA synthesis in host tissues is found only when plasma-MTX concentration is $\leq 10^{-8}$.

Similar studies can be performed in patients who have assessible tumors such as ovarian cancer where a large percentage of free-floating ascites cells are tumorous. Serial studies of short-term in vitro ^{3}H-UdR incorporation into bone marrow and ovarian tumor after iv administration of 25 mg/m^2 MTX in vivo have demonstrated a rapid and marked decrease in the incorporation of ^{3}H-UdR into DNA by both ovarian tumor cells and normal human bone marrow (10). In patients showing no clinical response to MTX, ascites cells recovered to control levels of nucleoside incorporation within 6 hours of drug administration and at ascites MTX levels one to two logs higher than those at which the bone marrow of the same patient recovered. A

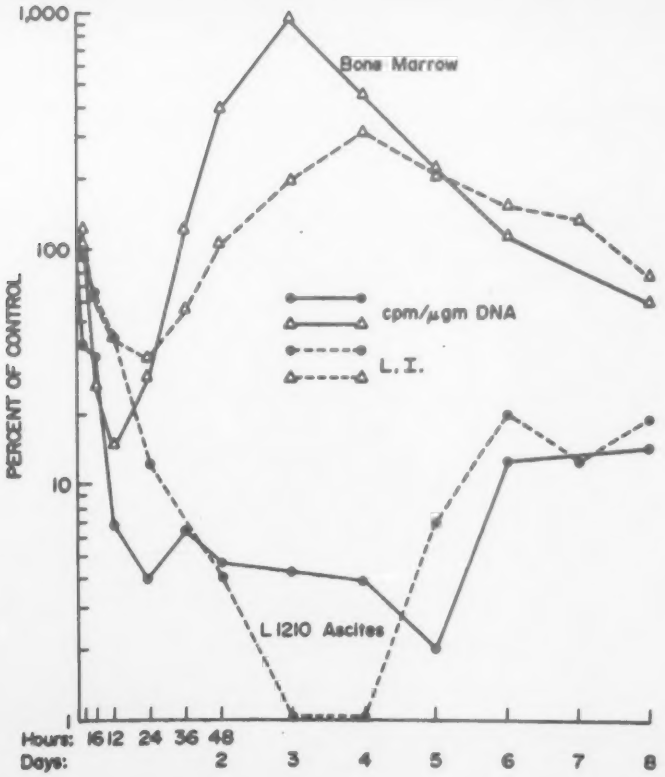

FIGURE 6.—Alterations in ^{3}H-TdR incorporation induced by 200 mg/kg of CTX in ascites tumor (●——●) and bone marrow (△——△) compared with alterations induced in the LI of ascites tumor (●---●) and bone marrow (△---△). (*From* ref 3.)

single patient studied who had a partial response to MTX displayed a more delayed recovery of the tumor cells after MTX exposure. Such studies serve to demonstrate that an important relationship exists between free-MTX levels in plasma and ascites. The inhibition of ^{3}H-UdR incorporation into DNA in human bone marrow was closely correlated with the prolonged retention of low concentrations of MTX in plasma, with full recovery becoming manifest only when plasma concentration fell into the range of 10^{-8}–10^{-9} M. In contrast to the human marrow, the ovarian tumor cells were in general far more resistant to MTX and recovered at ascites concentrations as high as 10^{-7} M.

Nucleoside Incorporation Studies in a Solid Tumor Model—B16 Melanoma

Application of such a technique to a solid tumor system is more difficult because of the lack of homogeneity in solid tumors as well as the irregular clearance of dead or dying cells from the tumor. Nevertheless, such an analysis may be employed under certain specific instances to estimate proper sequences of chemotherapy and provide information about the onset and character of drug resistance. The simultaneous changes that occur in ^{3}H-TdR incorporation into DNA in B16 melanoma, duodenal mucosa, and bone marrow after 4-, 16-, and 32-mg/kg doses of methyl-CCNU (meCCNU) are shown in figure 9.

Although the 32-mg/kg dose appeared to produce the optimal differential effect between the tumor and normal tissues, it is nevertheless still too toxic to normal tissues and is a lethal dose to approximately 100% of $BD2F_1$ male mice. The dose producing the greatest differential effect between tumor and normal tissues but still acceptable toxicity to the normal tissues was 16 mg/kg.

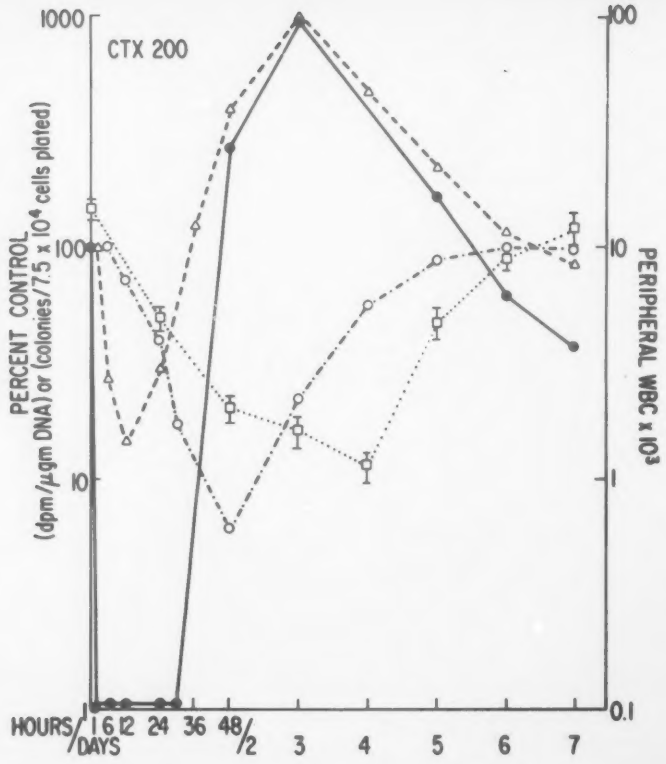

FIGURE 7.—Comparison of alterations induced by CTX therapy on ^{3}H-TdR incorporation (Δ---Δ); colony-forming units in culture (●——●); bone marrow cellularity (O–·–O); and peripheral wbc count (□···□).

Survival and Kinetic Studies After Two Doses of MeCCNU Given 6 Days Apart in Tumor-Bearing Animals

On the basis of the preceding studies, it appeared that the toxicity of a second dose of meCCNU could be minimized by giving it either on Days 1 or 6 following the initial dose. However, the potential for antitumor effect would theoretically be better on Day 6 since ^{3}H-TdR incorporation into DNA in the tumor had largely recovered by that time.

The mean survival time of untreated animals bearing B16 melanoma was 12 days. A mean survival time of 32 days was noted after the administration of either a single dose of meCCNU (16 mg/kg ip) on Day 12 of tumor growth or doses of meCCNU (16 mg/kg ip) on Days 12 and 18 of tumor growth. The failure of a properly spaced second dose to prolong survival suggested an altered sensitivity of the B16 melanoma to meCCNU.

Studies to Determine the Persistence of Altered Sensitivity Induced in B16 Melanoma by MeCCNU In Vivo

Tumor-bearing mice were treated with meCCNU at a dose of 16 mg/kg ip and again 6 days later at the same dose. Kinetic studies were performed as previously described. The studies in figure 10 are contrasted to identical studies carried out after meCCNU (16 mg/kg ip) with mice bearing tumors previously unexposed to meCCNU shown in the previous figure.

Tumors previously exposed to meCCNU showed only a modest reduction in ^{3}H-TdR incorporation into DNA and recovery paralleled that of the normal tissues. The differential recovery pattern seen in figure 9 after 16 mg/kg of meCCNU had been lost.

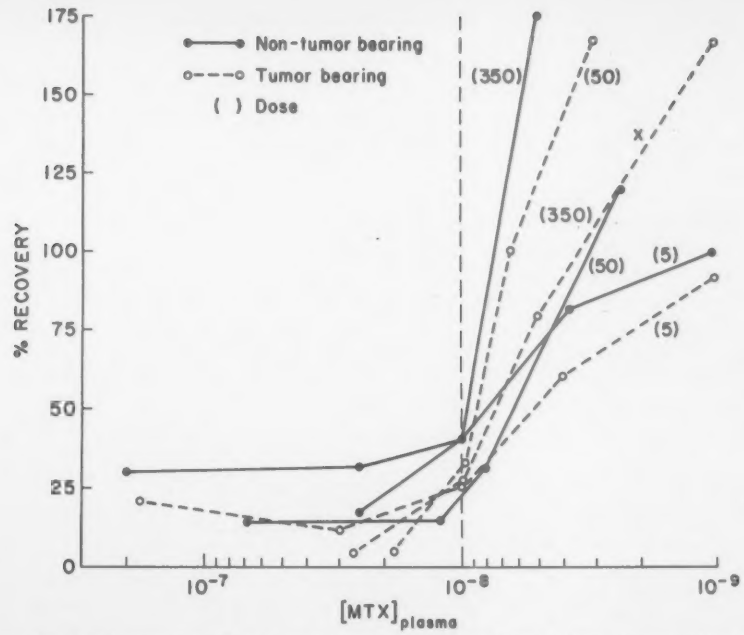

FIGURE 8.—Recovery of ^{3}H-UdR incorporation into bone marrow as a function of the plasma concentration of MTX. Doses ranging from 5 to 350 mg/kg of MTX ip in both tumor-bearing and tumor-free CDF_1 mice.

DISCUSSION

Many chemotherapeutic agents exert an increased cytotoxic effect on rapidly proliferating tissues regardless of type. As a consequence, considerable cytotoxic effect is unfortunately sustained by normal tissues such as the GI mucosa and the bone marrow which undergo constant cell proliferation (11). Thus, chemotherapeutic agents are two-edged swords from a kinetic point of view, exerting significant antitumor effect but at a cost governed by the extent of injury to normal proliferating tissues.

In a real sense, successful chemotherapy must always be based upon a differential effect upon the tumor and normal tissues. Agents with profound antitumor effect with correspondingly high toxicity to normal proliferative tissues will be far less clinically useful than an agent with less antitumor effect but with minimal impact on normal proliferating cell systems. The former drug would appear far more impressive in in vitro assays in which only antitumor effect was analyzed.

Explanations of the cause of differential injury sustained by normal and tumorous tissues may be quite varied and in part related to intrinsic cell sensitivity, cellular transport, drug-activation mechanisms, pharmacokinetics, and drug degradation. Proper assay of such a myriad of effects can only be expected to be accurately reflected in an in vivo system where each exerts its effect and the final common pathway is the success or failure of the drug and schedule in a tumor-bearing host.

There are several systems for assaying the proliferative capacity of a tissue and the impact of such proliferation on chemotherapeutic effect. All have attributes and drawbacks and no currently available kinetic technique affords both the laboratory researcher and clinician a totally satisfactory study system.

Our studies have monitored in vivo incorporation of labeled nucleoside into DNA in both normal and tumorous tissues after in vivo administration of chemotherapy. This technique and its modification using in vitro incubation satisfies some of the requirements for application to the scheduling of chemotherapeutic agents in a clinical setting.

Testing the assumption that a drug which disrupts DNA synthesis should have its greatest effect during a period when DNA is being actively produced, we were able to demonstrate differential suppression and recovery of DNA synthesis between normal and tumorous tissues in vivo. If cells are exposed to therapy when DNA synthesis is rapid, they should be more profoundly affected than

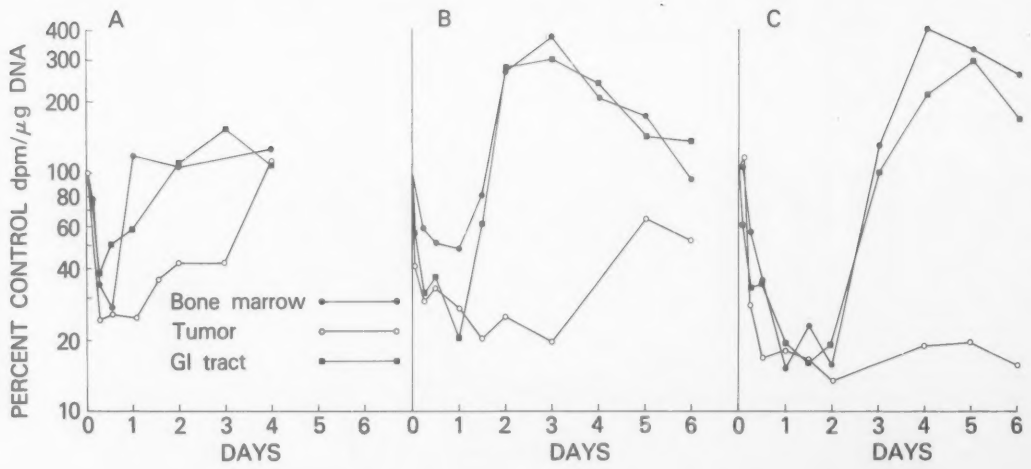

FIGURE 9.—Alterations in ^{3}H-TdR incorporation induced by meCCNU in bone marrow, GI mucosa, and B16 melanoma after 4 mg/kg of meCCNU (panel A), 16 mg/kg of meCCNU (panel B), and 32 mg/kg of meCCNU (panel C).

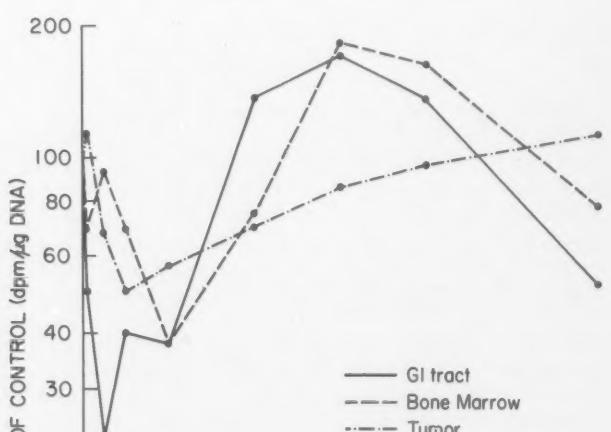

FIGURE 10.—Alteration in ^{3}H-TdR incorporation into bone marrow, GI mucosa, and B16 melanoma after previous treatment with meCCNU administered 6 days previously.

during periods of low DNA synthesis. Second doses administered at a time of recovery of DNA synthesis in normal proliferative tissues would be expected to produce excessive toxicity to normal tissues. Conversely, if the second dose of chemotherapy is delayed until the tumor is recovering but normal tissues have returned to baseline rates of DNA synthesis, more antitumor effect will be sustained at a minimal cost of normal tissue toxicity.

Initial studies presented here with 5-FU and others with MTX (7), ara-C (1), BCNU (2), meCCNU (12), and 5-azacytidine (13) have been able to demonstrate that in sensitive ascites tumors in vivo and in one solid tumor system in vivo (4) there is a differential suppression and recovery pattern induced in the tumor which is different in magnitude and duration from that in the normal proliferative tissues. The differential pattern favoring earlier recovery of normal tissues than tumor is a phenomenon of a sensitive tumor system and is not seen in the Ehrlich ascites tumor line which was partially resistant to 5-FU (fig 2). Similar observations have been made with meCCNU (12) and 5-azacytidine (13) in partially resistant tumor cell lines and suggest that this difference provides a clinically exploitable therapeutic differential. Studies presented here with 5-FU (figs 3 and 4) indicate that second doses administered when the normal tissues are recovering are associated with enhanced host toxicity and reduced survival even in non-tumor-bearing animals. In contrast, second doses administered when the tumor is recovering are associated with enhanced therapeutic efficacy shown here with 5-FU and also demonstrated with ara-C (1), BCNU (2), meCCNU (12), 5-azacytidine (13), and CTX (5) in previous studies with sensitive tumors.

The most precise studies can be performed on chemotherapeutic agents which directly inhibit DNA synthesis. Nevertheless, many other chemotherapeutic agents disrupt DNA synthesis as a secondary effect of lethal or sub-lethal cell injury and are generally dependent upon the proliferative state of the injured tissues. These so-called phase-specific and/or cycle-specific agents may also be studied using similar techniques. Studies reported here with CTX (fig 5) indicate a similar differential toxicity for increasing doses.

Comparisons were made of the technique of ^{3}H-nucleoside incorporation with conventional LI studies and figure 6 indicates a high correlation between the two techniques as well as the lack of accuracy of a single post-therapy study of LI in determining response to therapy. The ease, speed, and simplicity favors the use of the nucleoside incorporation rather than the more complex serial LI technique.

Comparisons were also made between alterations induced in ^{3}H-TdR incorporation and bone marrow or peripheral wbc count recovery. As shown in figure 7, the recovery of peripheral wbc count and bone marrow cellularity were out of phase with the recovery of DNA synthesis in the bone marrow and failed to accurately reflect the sensitivity of the bone marrow to subsequent chemotherapeutic injury. Comparison of this technique (fig 7) with the technique of granulocyte colony formation in vitro demonstrated the two techniques to be relatively similar except that the ^{3}H-TdR incorporation preceded the recovery of colony formation. Colony-forming ability would not have precisely defined the time for the markedly reduced toxicity of a second dose of CTX nor predicted the increasing toxicity of a second dose of CTX 24 or 36 hours after the first dose.

Accurate assay techniques are available to study the pharmacokinetics of MTX and to relate the in vivo alterations in DNA synthesis to the extracellular concentration of the drug in fluids bathing the target tissues. Using these techniques, the threshold concentration for inhibition of normal and tumorous tissue in vivo can be defined. Figure 8 indicates that normal murine bone marrow remains inhibited until the plasma concentration of MTX falls to $\leq 1 \times 10^{-8}$. Such techniques allow definition of important relationships between the pharmacokinetics of a chemotherapeutic agent and its in vivo kinetic effect.

Under certain well-defined and controlled circumstances, such studies can be performed in patients. Studies in patients with ovarian carcinoma in ascites form have been performed along with plasma and ascites pharmacokinetics related to the in vivo alterations in DNA synthesis in ovarian carcinoma and human bone marrow. Patients showing no response to MTX had tumor recovery at two logs higher concentration than the marrow. The single patient having a partial response to MTX had more delayed recovery of DNA synthesis in the ovarian tumor. Such studies have demonstrated that an important relationship exists between free-MTX levels in plasma and ascites and the pharmacologic effects of this agent on bone marrow and neoplastic tissues in patients.

Applications of this technique to the alterations induced by chemotherapy in solid tumors are more difficult because of the heterogeneity of the tumor, the persistence of lethally injured cells in the tumor, and the variable perfusion of the tumor. In spite of such limitations, certain observations may be made. Studies employing meCCNU in B16 melanoma have shown the differential recovery patterns between the solid tumor and the normal proliferative tissues

as well as the induction of drug resistance after a single sub-curative dose of meCCNU (fig 10).

It would appear that the technique for following ^{3}H-nucleoside incorporation into DNA simultaneously in tumorous and normal host tissues has the combined virtues of being comparatively easy to perform and of defining therapeutically important recovery intervals. Also for the first time, such techniques have allowed simultaneous correlation of plasma drug concentration and pharmacokinetics with in vivo kinetic effects both in animals and man. These attributes may recommend this technique as a kinetic tool of potential clinical utility.

LIST OF COMPOUNDS

5-Azacytidine: NSC-102816; CAS reg. No. 320-67-2; *s*-triazin-2(1*H*)-one, 4-amino-1-β-D-ribofuranosyl-

BCNU: NSC-409962; CAS reg. No. 154-93-8; urea, 1,3-bis(2-chloroethyl)-1-nitroso-

Cyclophosphamide: NSC-26271; CAS reg. No. 6055-19-2; 2*H*-1,3,2-oxazaphosphorine, 2-[bis(2-chloroethyl)amino]tetrahydro-, 2-oxide, monohydrate

Cytosine arabinoside: NSC-63878; CAS reg. No. 69-74-9; cytosine, 1-β-D-arabinofuranosyl-, monohydrochloride

5-Fluorouracil: NSC-19893; CAS reg. No. 51-21-8

Methotrexate: NSC-740; CAS reg. No. 59-05-2; glutamic acid, *N*-[*p*-[[(2,4-diamino-6-pteridinyl)methyl]methylamino]benzoyl]-

Methyl-CCNU: NSC-95441; CAS reg. No. 33073-59-5; urea, 1-(2-chloroethyl)-3-(4-methylcyclohexyl)-1-nitroso-

REFERENCES

1. YOUNG RC, GOLDBERG D, and SCHEIN PS. Enhanced antitumor effects of cytosine arabinoside given in a schedule dictated by kinetic studies in vivo. Biochem Pharmacol 22:227–280, 1973.
2. ROSENOFF SH, BOSTICK F, and YOUNG RC. Alterations induced by 1,3-bis(2-chloroethyl)-1-nitrosourea (BCNU) in deoxyribonucleic acid synthesis in normal and tumorous tissues. Biochem Pharmacol 33:3097–3106, 1974.
3. ROSENOFF SH, BULL JM, and YOUNG RC. The effect of chemotherapy on the kinetics and proliferative capacity of normal and tumorous tissues in vivo. Blood 45:107–118, 1975.
4. BRERETON HD, BRYANT T, and YOUNG RC. Inhibition and recovery of DNA synthesis in host tissues and sensitive and resistant B-16 melanoma after methyl CCNU. A predictor of clinical efficacy. Cancer Res 35:2420–2425, 1975.
5. ROSENOFF SH, BOSTICK F, and YOUNG RC. Recovery of normal hematopoietic tissue and tumor following chemotherapeutic injury from cyclophosphamide (CTX): comparative analysis of biochemical and clinical techniques. Blood 45:465–475, 1975.
6. MYERS CE, OLIVERIO VT, and YOUNG RC. Kinetic alterations induced by 5-FU in vivo: the simultaneous effect of chemotherapy on bone marrow, intestinal mucosa and Ehrlich's ascites tumor. Proc Am Assoc Cancer Res 14:42, 1973.
7. CHABNER BA, and YOUNG RC. Threshold methotrexate concentration for in vivo inhibition of DNA synthesis in normal and tumorous tissues. J Clin Invest 52:1804–1811, 1973.
8. SCHNEIDER WC. Phosphorus compounds in animal tissues. I. Extraction and estimation of deoxypentose nucleic acid and of pentose nucleic acid. J Biol Chem 161:293–303, 1945.
9. BURTON K. A study of the conditions and mechanism of the diphenylamine reaction for the colorimetric estimation of deoxyribonucleic acid. Biochem J 62:315–323, 1956.
10. YOUNG RC, and CHABNER BA. An in vivo method for monitoring differential effects of chemotherapy on target tissues in animals and man. J Clin Invest 52:92A, 1973.
11. GOSS RJ. The strategy of growth. *In* Control of Cellular Growth in Adult Organisms (Teir H, and Rytomaa T, eds). New York, Academic Press, 1967, pp 3–27.
12. YOUNG RC, GOLDBERG D, and GROTZINGER KR. Alterations in ^{3}H-thymidine incorporation into DNA induced by methyl CCNU in normal and tumorous tissues in vivo. Cell Tissue Kinet. In press.
13. MCGUIRE WP, GROTZINGER KR, and YOUNG RC. Alterations in ^{3}H-thymidine incorporation into DNA and ^{3}H-uridine incorporation into RNA induced by 5-azacytidine in vivo. Proc Am Assoc Cancer Res and ASCO 16:87, 1975.

Investigations on Pharmacologic Induction of Partial Synchronization of Tumor Cell Proliferation: Its Relevance for Cytostatic Therapy [1]

H. O. Klein,* D. Adler, M. Doering, P. J. Klein, and K. J. Lennartz [2,3]

During the past few years we tested experimentally and clinically whether pharmacologic induction of partial synchronization of tumor cell proliferation using vincristine[4] (VCR) enhances the cytocidal effect of cell-phase-specific drugs (1–5). An essential requirement for such a therapy concept is knowledge of the proliferation pattern of tumor cells.

The purpose of this paper is to present: (*a*) further investigations on kinetic data and on the reproducibility concerning the pharmacologic modification of the Ehrlich ascites tumor (EAT) cell proliferation after administration of VCR; (*b*) new animal experiments on a sequential combination of hydroxyurea[5] (HU) and VCR attempting to enhance the degree of cell synchrony; and (*c*) a summary of clinical results (6) of a cooperative phase II study in patients with lymphoreticular tumors by the so-called synchronization therapy with VCR and cyclophosphamide[6] (CPH). The results confirm and complete earlier findings in the EAT tumor model system (1,4) and in patients with Hodgkin's disease as well as non-Hodgkin's lymphoma (3,4).

MATERIALS AND METHODS

Animal Experiments

The investigations were performed in male NMRI mice (20–30 g) bearing a diploid EAT. All experiments were carried out during the log-phase growth of the tumor cells (Days 4–7 after inoculation of 15–17 $\times$ 10^6 tumor cells). Kinetic data on EAT cells (Day 5 after inoculation) are as follows: T_c min, 19 hours; T_S, about 12 hours; T_{G2} + M/2, about 3 hours; size of the growth fraction, about 70% (4).

Induction of Partial Synchronization In Vivo

VCR (0.025 μg/g of body weight ip) and HU (0.25 mg/g of body weight ip) were used as inducers of partial synchronization of tumor cell proliferation. In a special set of experiments both drugs were sequentially combined in order to induce a higher degree of cell synchronization. The criteria to prove synchronization after either VCR or HU alone or a combination of both were as follows: (*a*) mitotic index (fraction of mitotic cells/1000 tumor cells on Feulgen-stained smears); (*b*) ^{3}H-thymidine (^{3}H-TdR) labeling index (4); (*c*) the rate of ^{3}H-TdR incorporation in tumor cells, measured by means of a liquid scintillation spectrometer (Packard, Model No. 3390) (7); and (*d*) the relative DNA content of tumor cells (flow microfluorometry).

Flow Microfluorometry

The relative DNA content per cell was measured by means of flow microfluorometry (ICP 11, Phywe) (8–10). Preparations of samples were as follows: tumor cells were collected by trypsin (1% solution, 5 minutes at 37°C), washed twice with saline (0.9% NaCl), and fixed in suspension by dropwise addition of absolute alcohol and rigorous shaking. Ethidium bromide was used for fluorochromy of DNA (11): cells fixed in suspension were washed twice in Tris-buffer (pH 7.5) and then incubated in RNase (1 mg/ml Tris-buffer, 1 hour at 37°C). After another wash in buffer, cells were suspended in ethidium bromide (10 mg/l Tris-buffer, pH 7.5) and incubated for 20 minutes (cell concentration approximately 10^6 cells/ml). Another procedure for collection and staining of tumor cells was as follows: 1 ml of the ascites tumor was collected in an edetic acid tube and added dropwise to a 0.5% pepsin solution (10 ml). After 2–5 minutes the cell suspension was filtered through a membrane with gap sizes of 70 μm and a 0.1% ethidium bromide solution was added. Tumor cells suspended in dye solution were sucked through an 80-μm aperture of the ICP 11. The fluorescence of DNA-bound dye per cell was measured and stored

[1]Supported by Deutsche Forschungsgemeinschaft.

[2]Medical Clinic (Dr. H. O. Klein), Institute of Radiology (Dr. Adler), and Institute of Pathology (Drs. Doering, P. J. Klein, and Lennartz), University of Cologne, West Germany.

[3]We would like to thank very much E. Christian for her skillful technical assistance in performing these experiments.

[4]Vincristine: NSC-67574; CAS reg. No. 2068–78–2; leurocristine, sulfate (1:1).

[5]Hydroxyurea: NSC-32065; CAS reg. No. 127–07–1.

[6]Cyclophosphamide: NSC-26271; CAS reg. No. 6055–19–2; 2*H*-1,3,2-oxazaphosphorine, 2-[bis(2-chloroethyl)amino]tetrahydro-, 2-oxide, monohydrate.

**Reprint requests to:* Dr. H. O. Klein, Medical Clinic, University of Cologne, Cologne, West Germany.

automatically according to the intensity of fluorescence signals being proportional to DNA content (filters: GG 550, BG 38, and BG 3).

Liquid Scintillation Counting

Measurements were performed according to the technique of Byfield and Scherbaum (7).

Combined Autoradiography and Cytophotometry

A combination of single-cell cytophotometry and autoradiography (double labeling with ^{3}H-TdR and ^{14}C-TdR) was chosen to study the flux rates of cells as a function of time after VCR at different border lines of the generation cycle (12). Figure 1 shows the time schedule and the dosages of ^{3}H-TdR. At the start of the experiments tumor-bearing animals received ^{3}H-TdR (specific activity: 2.000 millicuries/mM; dose: 2 microcuries/g of body weight) ip. Forty minutes later they got VCR (0.025 μg/g of body weight). At different time intervals after VCR animals were injected with ^{14}C-TdR (specific activity: 25–30 millicuries/mM; dose: 0.2 microcuries/g of body weight) and 30 minutes later they were killed and smears of tumor ascites were prepared. After drying in air and fixation for 1 minute in 96% methanol the cells were stained according to Feulgen. First, tumor cells were photographed and labeled with a number. Thereafter, photometric measurements of the relative cellular DNA content were performed by means of a UMSP I (Zeiss) at a wave length of 560 μm.

The same smears were used for preparing autoradiograms with a double layer of a K2 emulsion after removal of Eukitt. At first, a thin K2 emulsion (Ilford, London, England) was exposed in the dark for 28 days and then developed and fixed. Cells were stained by hematoxylin. The second cover with a thick K2 emulsion was exposed for 10 days. On the slides the photographed cells were assessed whether they were unlabeled, double labeled by ^{14}C- and ^{3}H-TdR, or labeled by either ^{3}H- or ^{14}C-TdR alone.

This procedure makes it possible to determine at various times after administration of VCR: (*a*) the flux rate of tumor cells into S phase (^{14}C-labeled cells); (*b*) the fraction of only ^{3}H-TdR-labeled cells located in the various phases of the cell cycle; and (*c*) the fraction of double-labeled cells (S-phase cells).

Cytostatic Treatment After Induction of Partial Synchronization by a Combination of HU and VCR

The experiments were performed in tumor (EAT)-bearing mice between Days 4 and 7 after tumor cell inoculation. Partial synchronization of cell proliferation was induced by sequential ip administration of HU (0.25 mg/g of body weight) and 12 hours later VCR (0.025 μg/g of body weight). CPH (0.1 mg/g of body weight) was used as a cytocidal drug and administered during DNA synthesis of partially synchronized cells. A followup of the mitotic and labeling indices showed that between the 50th and 55th hour after a sequential HU-VCR combination a large and statistically significant higher fraction of cells than observed in control animals was synthesizing DNA and, beginning the 60th hour after HU, entering mitosis. The start of therapy was on Day 4 after tumor cell inoculation. The therapeutic effect was assessed by counting the whole number of tumor cells in the abdominal cavity (Coulter Counter, Model DN) as a function of time after the start of therapy (4,13).

The following treatment protocols were tested: (*a*) therapy with HU on Day 4 after inoculation; (*b*) therapy with VCR on Day 4 after inoculation; (*c*) therapy with CPH on Day 4 after inoculation; (*d*) combination therapy, beginning on Day 4 after inoculation, with HU and 12 hours later with VCR; (*e*)

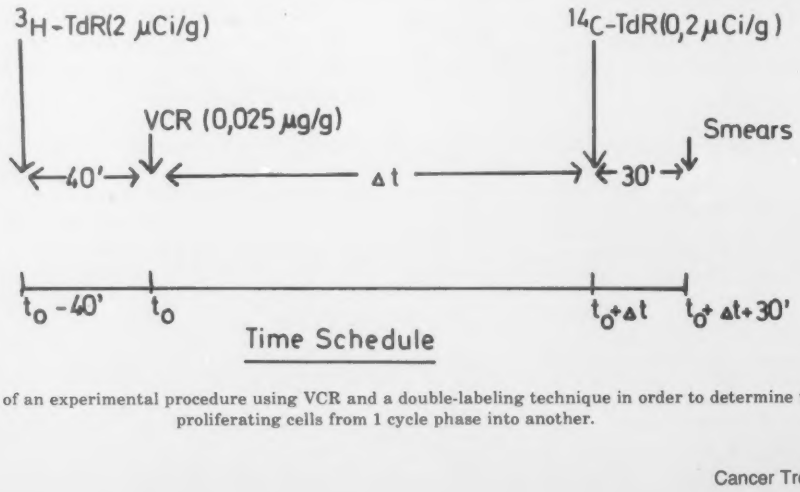

FIGURE 1.—Outline of an experimental procedure using VCR and a double-labeling technique in order to determine the flux rates of proliferating cells from 1 cycle phase into another.

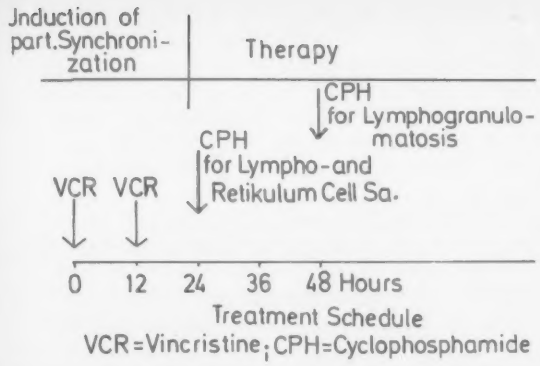

FIGURE 2.—Therapy protocol for the so-called synchronization therapy of lymphoreticular tumors in man.

combination therapy, beginning on Day 4 after inoculation, with HU and followed 55 hours later by CPH; (*f*) combination therapy, beginning on Day 4 after inoculation, with simultaneous administration of HU, VCR, and CPH; and (*g*) combination therapy (so-called synchronization therapy), beginning on Day 4 after inoculation, with HU followed 12 hours later by VCR and 55 hours after HU by CPH.

Investigations in Patients

Cytostatic Treatment After Induction of Partial Synchronization of Tumor Cell Proliferation

A cooperative phase II study (6) was carried out to determine whether cytostatic treatment based on cell kinetic data as well as on partial synchronization of tumor cell proliferation may induce a high rate of complete remission in patients with lymphoreticular tumors. Besides the University Clinic of Cologne, clinics in Hannover, Bonn, Wuppertal, and Dortmund, West Germany, also participated in this trial.

The treatment protocol is schematically outlined in figure 2. This protocol was established during earlier experimental investigations concerning the modification of tumor cell proliferation in man by means of one or two low doses of VCR (0.025 mg/kg) (2–4). CPH (plasma half-life in man, 6.5 hours) (14,15) was used as a cytocidal drug (30–50 mg/kg) at the time when partially synchronized cells were expected to enter the S phase. On the average, each patient received four such treatment courses. In general, the time interval between single courses was 14–18 days according to the leukocyte level in the peripheral blood.

A detailed description of methods and results of this phase II study is published elsewhere (6). Briefly, a total of 88 patients (33 women and 55 men) with advanced Hodgkin's disease and lymphosarcoma as well as reticulum cell sarcoma were treated. The age of the patients ranged from 13.5 to 78 years (mean value, 47 years). More than half of the patients were pretreated with X-ray therapy and/or cytostatic combination chemotherapy. In all cases diagnosis was based on histologic examinations. In the case of Hodgkin's disease histologic classification was performed according to Lukes and co-workers (16,17).

Non-Hodgkin's lymphoma was subdivided histologically into lymphosarcoma and reticulum cell sarcoma. The stage of disease was established by means of clinical examination, chest roentgenograms (tomography of mediastinum included), scintigraphy of spleen and liver, as well as abdominal lymphography. In some cases of Hodgkin's disease an explorative laparotomy with splenectomy was performed. The staging of Hodgkin's disease corresponded to the criteria set by the Rye conference (18). The following parameters were continuously determined in all patients during the course of their disease: erythrocyte sedimentation rate, total amount of blood protein and electrophoresis, activity of transaminases, alkaline phosphatase and lactate dehydrogenase, and examinations of peripheral blood and bone marrow smears. Further parameters for evaluating disease activity were weight, body temperature, and roentgenographic and scintigraphy results.

The criteria used for evaluating the therapy results were published earlier (4). The duration of complete remission was calculated from the start of therapy (19). Remission maintenance therapy consisted of CPH (3 mg/kg/day) and methylprednisolone[7] (3 × 6 mg/day) given orally.

RESULTS AND DISCUSSION

Further Investigations on the Synchronizing Effect of VCR

As previously demonstrated in our laboratory VCR induces a modification of cell proliferation in a diploid EAT similar to partial synchronization (1–4) (fig 3). VCR was administered ip in a low (0.025 μg/g) and non-cytocidal dose.

We tried to determine whether our earlier results could be reproduced. As figure 4 shows, variations, induced by one injection of VCR (0.025 μg/g), of the mitotic and labeling indices correspond to those seen in earlier experiments (fig 3). Also the incorporation rate of ^{3}H-TdR into DNA of tumor cells as a

[7] Methylprednisolone: NSC-19987; pregna-1,4-diene-3,20-dione, 11β,17,21-trihydroxy-6α-methyl-.

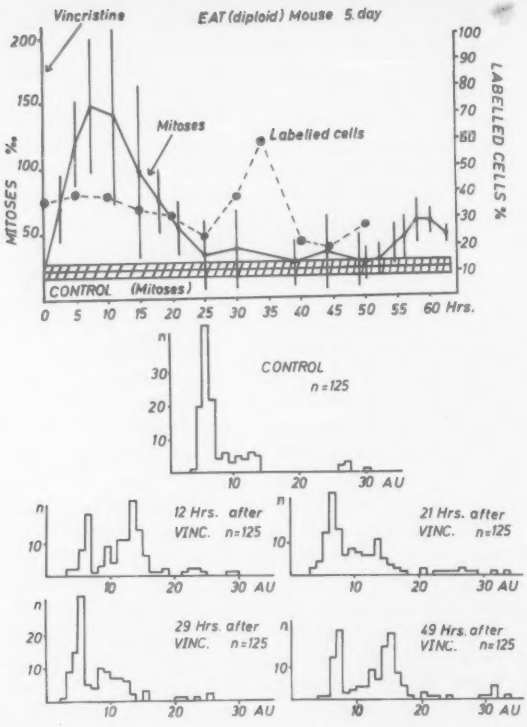

FIGURE 3.—Mitotic and labeling indices as well as relative nuclear DNA content of diploid EAT cells in mice as a function of time after 1 injection of VCR.

function of time after VCR fits well with the labeling index (fig 5a). Flow microfluorometric measurements of variations of cellular DNA content (fig 5b) also agree well with earlier observations obtained by means of single cell cytophotometry (fig 3). Obviously, according to these results the observed increased incorporation rate of ^{3}H-TdR into EAT cells between the 35th and 42nd hour after VCR is due to a large fraction of cells in S phase.

In further experiments using the percent labeled mitoses (PLM) method the fate of this cohort of S-phase cells was followed up. After a single ip injection of ^{3}H-TdR at the 42nd hour after VCR (peak of labeled cells) the first labeled mitotic cells appear at the 43rd hour, ie, by the time the mitotic index after VCR is rising (fig 6). The further temporal course of both curves is approximately congruent. Hence, it can be supposed that those cells in S phase at the time ^{3}H-TdR is injected will be labeled and proceed through S and G_2 and enter mitosis. These labeled mitoses should be, according to earlier findings (2), identical with the mitotic figures which form the second mitotic peak of the mitotic index curve.

According to the PLM curve (fig 7) the mean duration of G_2 phase and M/2 of these VCR-treated EAT cells is about 5–6 hours, ie, a prolongation by a factor of two to three compared with untreated controls. Cell loss was not observed after administration of VCR as can be seen from the growth curve in figure 8. This is in agreement with previous observations (4).

These results obtained with different methods show that in this tumor model VCR induces partial synchronization of cell proliferation if the drug is administered in a low and non-cytocidal dose, and that this phenomenon can be reproduced. From these experiments it is also clear that VCR causes not only a temporary block in mitosis at the metaphase stage but in addition a marked prolongation of G_2 phase which is still recognizable 40–50 hours after VCR. Further investigations were performed in order to prove whether there are still other cell-cycle phases being influenced by VCR. A combination of single-cell cytophotometry and autoradiography was used. Methodologic details are described in Materials and Methods.

Figure 9 shows frequency distribution patterns of differently labeled cells as a function of time after one injection of VCR. Six hours after VCR the percentage of only ^{14}C-labeled tumor cells, ie, the relative frequency of cells having entered S phase recently, amounts to only about 6% of the whole cell population in S. This is, in absence of cell loss, strong evidence for a reduced cell flux rate from G_1 in S. The calculated flux rate is about 10‰ per hour and markedly lower than in controls (about 33‰ per hour).

McWilliams and co-workers (20) observed similar results in PHA stimulated lymphoblasts in which at high doses (1.0–10.0 μg/ml) VCR inhibits RNA synthesis and prevents entry of cells in S and M phases. At low doses the cells proceed through the cycle phases but are unable to complete mitosis.

In our experiments the flux rate from G_2 in M is also reduced to 10‰ per hour. This is in good agreement with the results calculated from the increase of the mitotic index during the first 6 hours after VCR (fig 3). This effect of VCR on G_1 phase is rapidly reversible as the results show which are obtained at the 12th hour after VCR (fig 9). By this time, there is a striking increase of only ^{14}C-labeled cells in S phase. The mean calculated flux rate from G_1 to S is now about 65‰ per hour, ie, a marked elevation above normal. However, at the same time, the flux rate from G_2 to M is still low (10‰ per hour) corresponding well with data calculated from the mitotic index curve (fig 3). As mentioned earlier this prolongation of G_2 lasts until the 50th hour after VCR (fig 7).

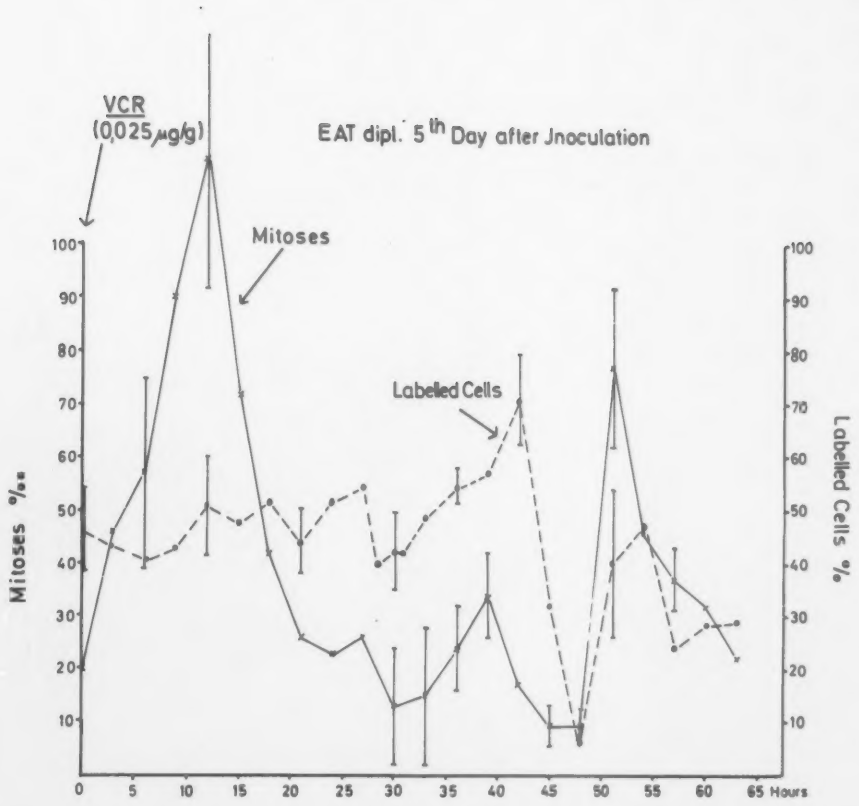

FIGURE 4.—Control experiment: variations of the mitotic and labeling indices in diploid EAT cells as a function of time after 1 injection of VCR. Each point represents the average value of 7–12 tumor-bearing mice ± standard deviation.

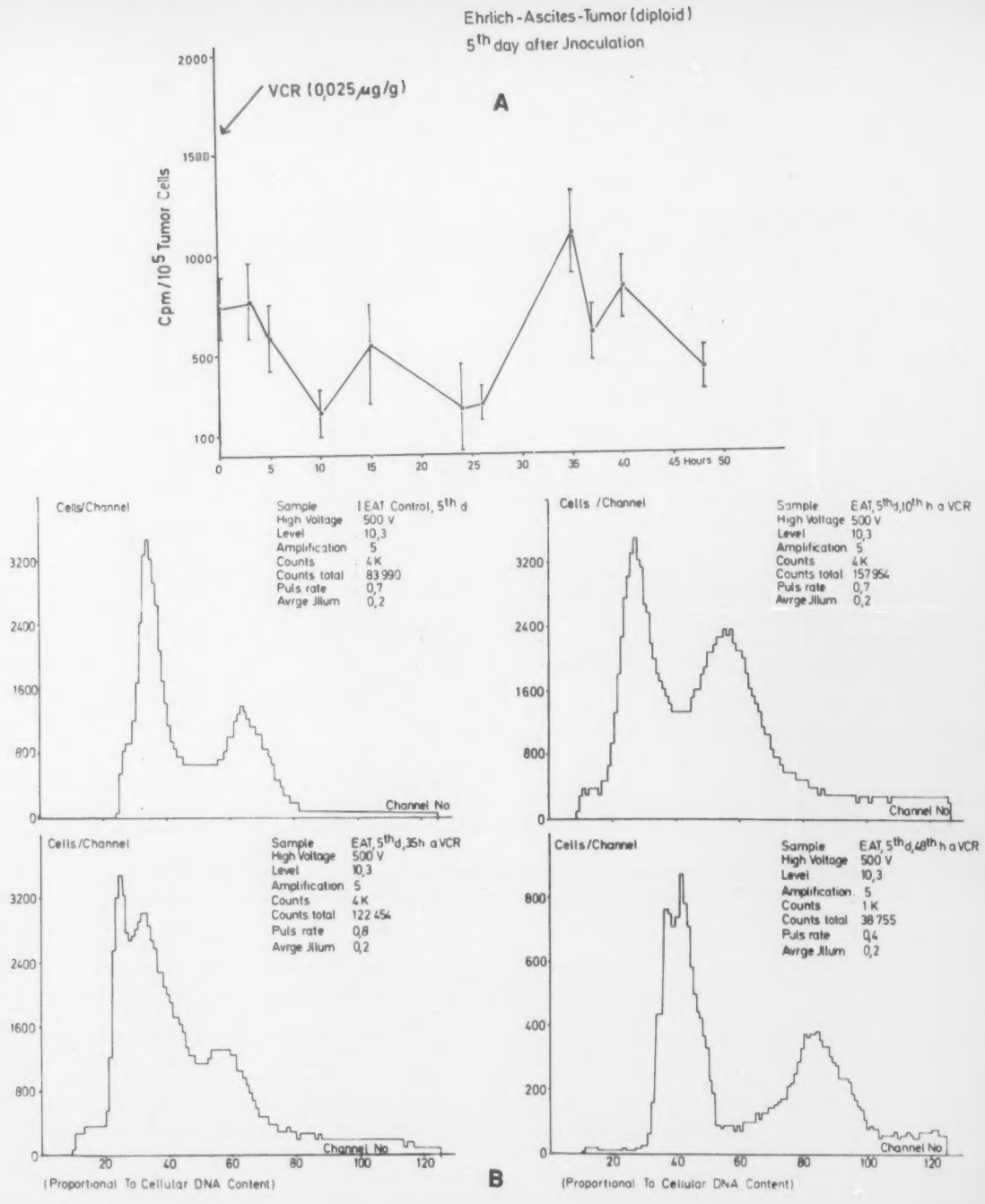

FIGURE 5.—(A) Variations of the incorporation of ^{3}H-TdR (CPM) into diploid EAT cells as a function of time after 1 injection of VCR. (B) Variations of the relative nuclear DNA content in diploid EAT cells, measured by means of the ICP 11 (Phywe), as a function of time after 1 injection of VCR.

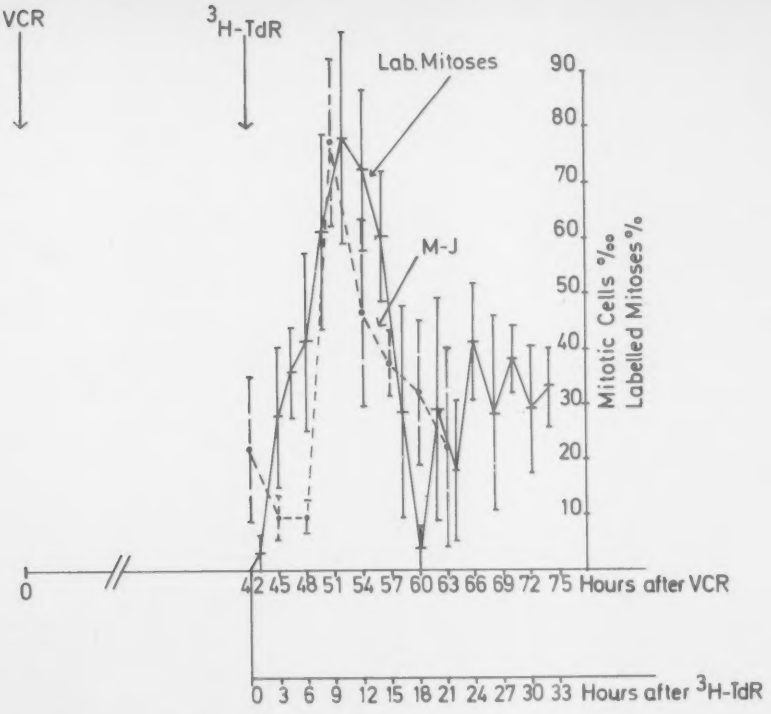

FIGURE 6.—Comparison between the mitotic index curve and the PLM curve as a function of time after 1 injection of VCR. ^{3}H-TdR was administered 42 hrs after VCR.

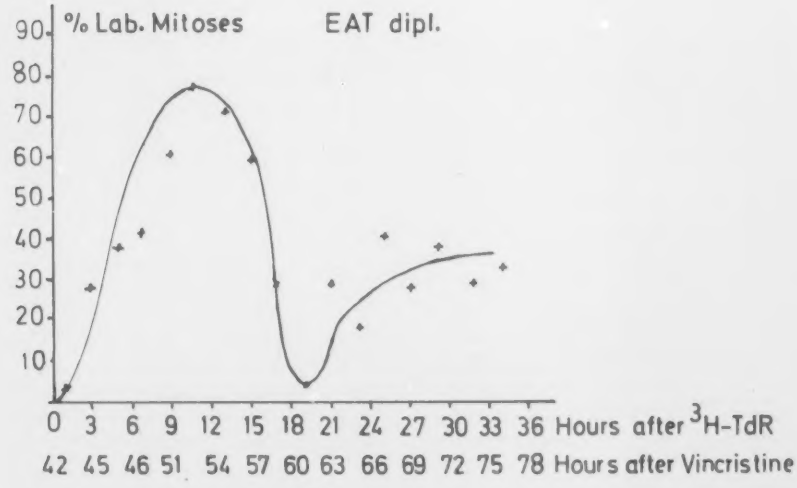

FIGURE 7.—PLM as a function of time after 1 injection of VCR. ^{3}H-TdR was administered 42 hrs after VCR.

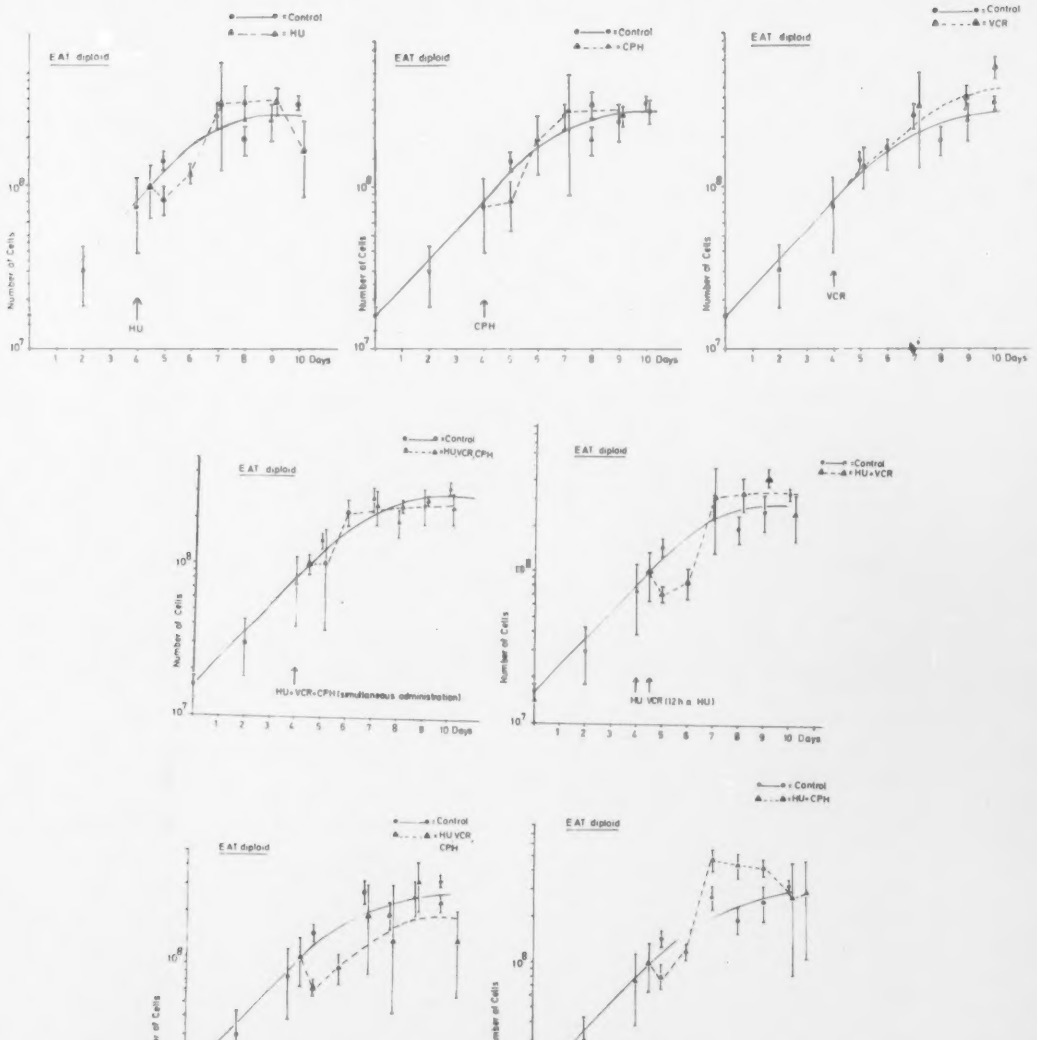

FIGURE 8.—Influence of different cytostatic treatment protocols on the growth curve of diploid EAT cells.

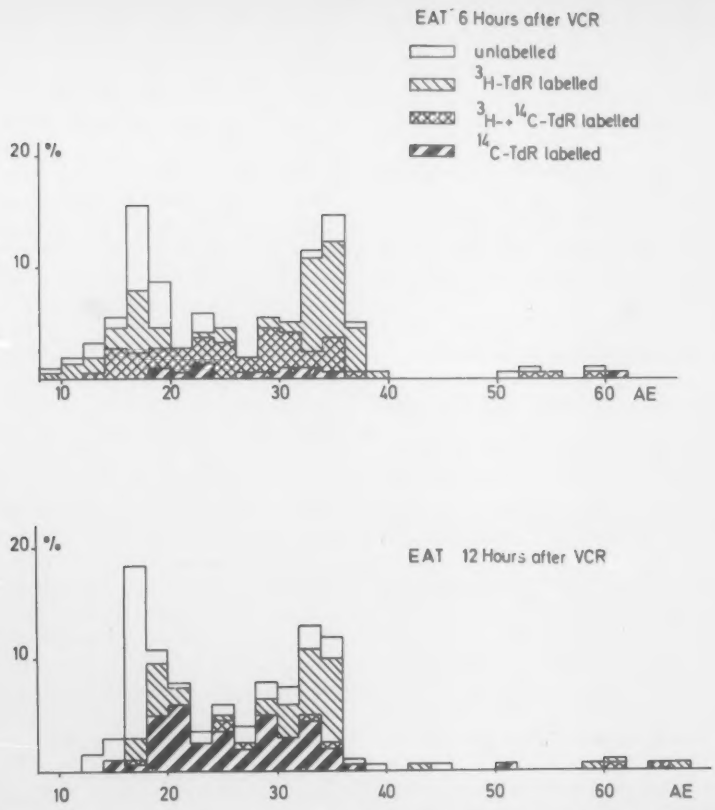

FIGURE 9.—DNA histograms of ^{3}H-, ^{14}C-, and double-labeled cells as well as unlabeled cells 6 and 12 hrs after 1 injection of VCR.

Obviously, the influence of VCR on the single cycle phases of this diploid EAT differs: in G_1 it is of short duration, in G_2 it is long lasting. Preliminary results do not show any essential prolongation of the duration of S.

These data are in good agreement with our earlier findings (1,3–5). It has always been striking that only a mitotic peak of about 130‰ was observed after a single injection of VCR, although the flux rate of the untreated tumor cells (about 33‰ per hour) should have led to an amount of approximately 350‰. Our explanation at that time was that either the flux rate from G_2 into mitosis is reduced or that numerous tumor cells located in G_2 or mitosis will become necrotic instantly after VCR administration. The latter was improbable because by means of a supravital staining method no elevated number of necrotic cells was observed (4). The new findings confirm our earlier assumption that only the flux rate is reduced.

In addition, the appearance of a second mitotic peak between the 50th and 65th hour after VCR (figs 3 and 4) may be better understood now in the light of the earlier and new data. From a theoretic point of view there are two possibilities to explain the high mitotic index by that time: (*a*) Partial synchronization of cell proliferation lasts for a long time. This fact is supported by the good temporal congruence of the PLM curve with the mitotic index curve (fig 6) as well as by an earlier observation, made with an autoradiographic double-labeling procedure, that the mitotic cells of the second peak are daughter cells of those cells which have been held up by VCR previously (2,4). (*b*) Theoretically, a late mitotic peak might also occur in case a cell population shows a high degree of desynchronization already a few hours after the administration of VCR. To provide this effect it is necessary that VCR shows a long-lasting action in the cells which causes a marked reduction of the cell flux rate in G_2 and mitosis compared to the normal flux rate in the preceding phases. Hence, cells coming from S and entering G_2 phase would accumulate in this phase. There is some experimental evidence that these

considerations are right. As could be demonstrated (figs 6 and 7) the G_2 phase is prolonged by a factor of two to three for the bulk of partially synchronized cells synthesizing DNA between the 35th and 42nd hour after administration of VCR. An accumulation of tumor cells in G_2 was also observed by means of cytophotometry (figs 3 and 5b). Furthermore, long-lasting toxic effects of VCR were also evident by the appearance of pathologic mitotic figures (ball and c-mitoses) between the 50th and 65th hour after VCR. Likewise, these mitoses were recorded for determination of the mitotic index.

According to the data it must be assumed that under our experimental conditions both possibilities account for the statistically significant increase of the mitotic index between the 50th and 65th hour after VCR.

Other investigators (21–23) did not observe such a striking modification of cell proliferation after administration of VCR. The investigations were performed in an EAT and in an L1210 leukemia. The authors used different high VCR doses. They did not report on studies concerning VCR-induced cell loss. Therefore, it cannot be excluded that cells arrested in mitosis as well as cells synthesizing DNA were killed (24,25). A large cell loss might be an explanation for the fact that after a first high mitotic peak no second mitotic peak and no large fraction of cells synthesizing DNA were observed. However, it must also be discussed that in these tumors VCR-resistant cell lines might have been present which have the ability to repair toxic effects quickly (26,27).

Maurer and co-workers (22,23) stated that VCR is not a suitable agent to induce partial synchronization of cell proliferation. This statement was derived from calculations and a schematic drawing which shows the frequency distribution of L1210 leukemia cells over the generation cycle as a function of time after administration of VCR. Two assumptions were made by the authors which were not proven experimentally: (*a*) the duration of the generation cycle and its subphases is not altered by VCR, and (*b*) the size of the growth fraction is not influenced by VCR.

Our own results and those of Schiffer, published in this issue, show the contrary however. Besides induction of partial synchronization by VCR, a prolongation of G_1 and G_2 phases and a triggering of cells from the non-growth fraction into cycle were also observed after VCR. This is again in good agreement with findings of other authors who showed that colchicine and vinca alkaloids also affect interphase as well as mitotic cells (20,28–35).

Cytostatic Treatment After Partial Synchronization With HU and VCR

The importance of partial synchronization of cell proliferation for cytostatic therapy with CPH at the time when synchronized EAT cells are synthesizing DNA was demonstrated in earlier publications (fig 10) (1,3,4). A similar therapeutic effect was observed after administration of cytosine arabinoside or adriamycin (5).

We questioned whether a combination of VCR and HU (with both drugs partial synchronization of cell proliferation can be induced) may increase the degree of synchrony and, consequently, enhance the therapeutic effect of CPH in a diploid EAT at an advanced stage of the disease. In recent years it was shown by several investigators (36–39) that administration of HU in a dose range between 0.2 and 0.5 mg/g induces partial synchronization of cell proliferation in tumors as well as in normal intestinal crypt cells in vivo. HU inhibits ribonucleotide reductase (40) and, in this way, temporarily blocks DNA synthesis as well as holds up and accumulates cells at the G_1/S boundary (38,41–47). After metabolism of the drug, cells nonlethally damaged continue their progression through the following cell-cycle phases in a more or less partially synchronized way.

With VCR and HU as single agents only about 30% of the proliferating cells can be partially synchronized in vivo for a short period of time. The aim of our investigations was to prove: (*a*) whether knowledge of the proliferation pattern of tumor cells modified by either drug alone may give information on how to combine both drugs (ie, how to administer them in the right sequence and at the optimum time in order to increase the synchronization effect); and (*b*) whether such a theoretically possible enhancement of synchronization may influence the killing effect of phase-specific drugs if administered at the time when most of the synchronized cells are in the cycle phase sensitive for the drug.

EAT (diploid) Mice	Number of Tumor Cells at the 8^{th} day after inoculation	Number of Tumor Cells at the 9^{th} day after inoculation
Control	$4{,}29 \pm 0{,}55 \cdot 10^8$	—
Cyclophosphamide	$4{,}21 \pm 0{,}36 \cdot 10^8$ (48 hrs. after therapy)	—
Vincristine and Cyclophosphamide (during DNA Synth. Phase)	$2{,}77 \pm 0{,}49 \cdot 10^8$ (48 hrs. after Cyclophosphamide)	$3{,}09 \pm 0{,}22 \cdot 10^8$ (72 hrs. after Cyclophosphamide)
Vincristine and Cyclophosphamide (combined application at the same time)	$3{,}56 \pm 0{,}5 \cdot 10^8$ (48 hrs. after therapy)	—

FIGURE 10.—Influence of different cytostatic treatments on the number of diploid EAT cells in mice at the 8th and 9th day after inoculation. Comparison with a control group.

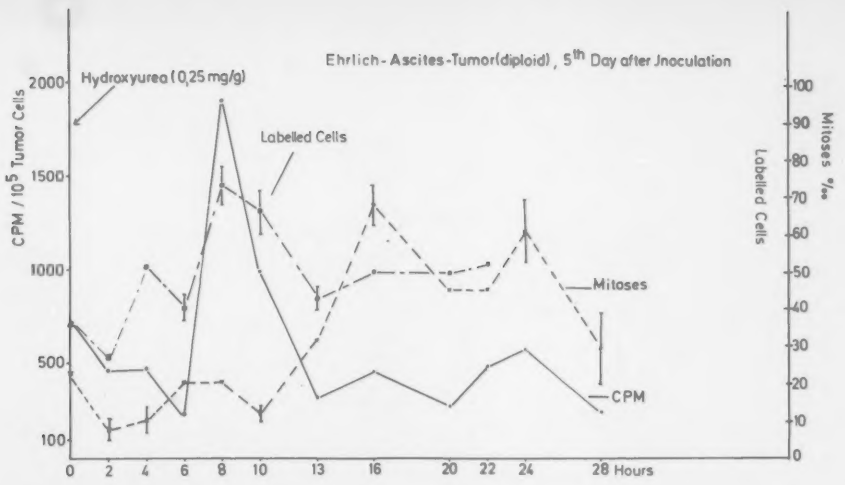

FIGURE 11.—Variations of the mitotic and labeling indices as well as of the incorporation values (CPM) of ^{3}H-TdR in EAT cells as a function of time after 1 injection of HU.

Figure 11 shows the effect of a single ip injection of HU (0.25 mg/g) on the proliferation pattern of diploid EAT cells. In the first 2 hours after HU administration the labeling index and the mitotic index as well as the incorporation rate of ^{3}H-TdR fall to low values. Thereafter, the labeling index rises continuously and reaches a peak at the 8th hour. At that time the incorporation rate of ^{3}H-TdR into tumor cells is also at its maximum. During this period of time the mitotic index is still below normal. However, about the 12th hour after HU it also begins to increase markedly. A first peak of mitoses (about 70‰, normal = about 20‰) is observed at the 16th hour and a second peak at the 24th hour. During this period of time the labeling index and the rate of ^{3}H-TdR incorporation fall again in the normal and subnormal range respectively. Further observation did not show any new significant increase of the labeling index up to the 65th hour after HU.

These results are confirmed by flow microfluorometric measurements of variations of the relative DNA content in diploid EAT cells as a function of time after a single injection of HU (fig 12). At the 10th hour after HU a large fraction of cells are in S phase according to the DNA content per cell. This is in good agreement with the high labeling index. At the 16th hour after HU a marked increase of cells with tetraploid DNA values is observed. It corresponds well to the high mitotic index at this time.

Instant cytocidal effects of HU could not be observed. However, a marked cell loss occurs around the 24th hour after HU (fig 8). After a few hours an overshooting cell production can be measured. According to these results HU induces a certain modification of cell proliferation in a diploid EAT during log-phase growth which may be regarded as partial synchronization. The effect is small and short-lasting.

We questioned how to combine HU with VCR in order to get a higher degree of partial synchronization. From a theoretic point of view both drugs should be sequentially combined. This means that VCR, mainly a mitotic poison, should be administered in a low and non-cytocidal dose (fig 8) by the time after HU when the mitotic index is rising, because by means of a temporary block of the cell division process a large fraction of cells could be accumulated which, after metabolism of VCR, would pass nearly synchronously through the following cycle phases. The 12th hour after HU was chosen as the time for administration of VCR (0.025 μg/g) because by this time the mitotic index is already increasing (fig 11).

Figure 13 shows variations of the mitotic and labeling indices as well as of incorporation rates of ^{3}H-TdR in diploid EAT cells as a function of time after sequential administration of HU and VCR. The main result is the appearance of a cycling proliferation pattern of these tumor cells. The labeling index shows two peaks, the first at the 10th hour and the second around the 55th hour after HU. The curve of the ^{3}H-TdR incorporation rate fits well with these variations of the labeling index. Also the curve of the mitotic index displays two distinct peaks, the first at the 24th hour and the ascending limb of a second peak at the 65th hour. The flux rate

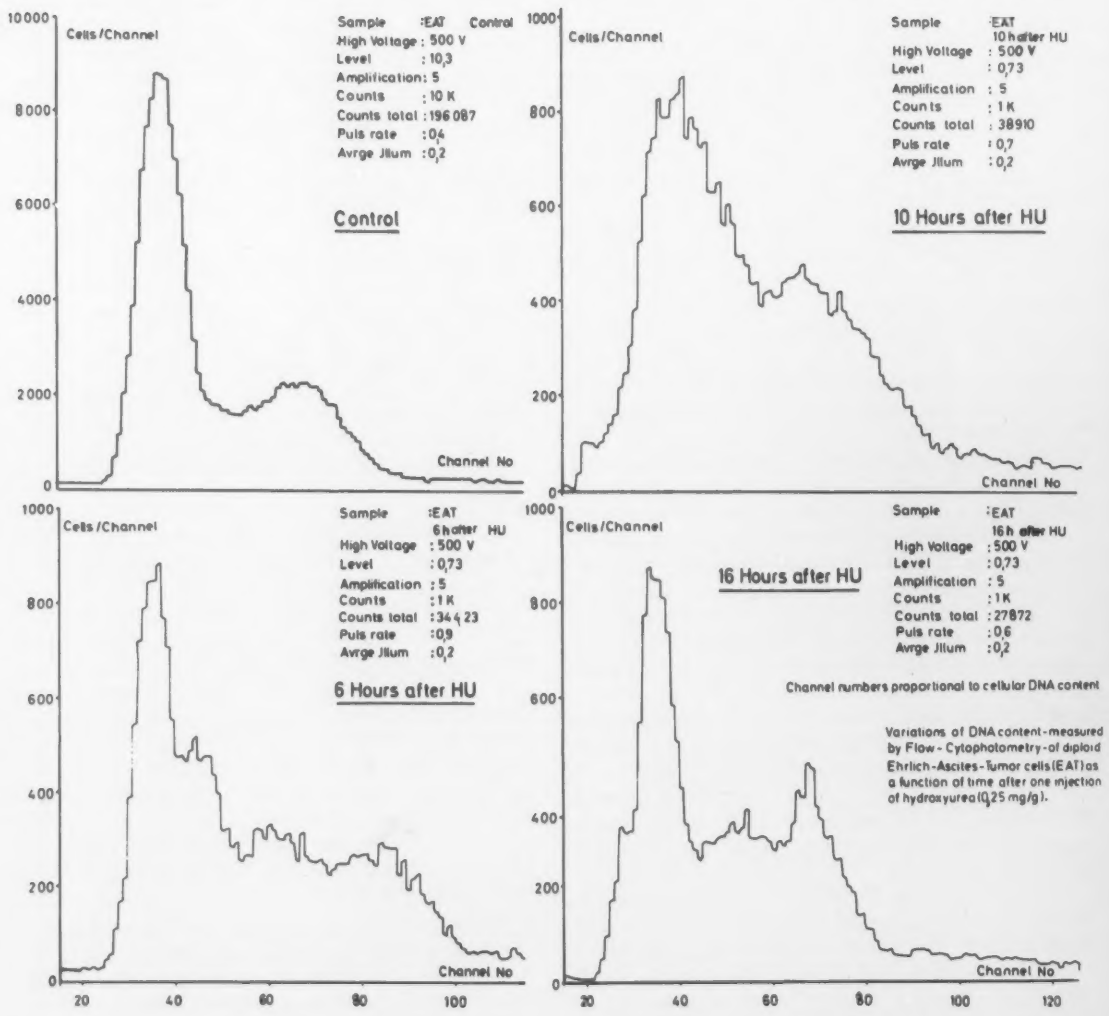
Cells/Channel
Sample :EAT Control
High Voltage : 500 V
Level : 10,3
Amplification: 5
Counts : 10 K
Counts total : 196 087
Puls rate :04
Avrge Jllum :0,2
Control
Channel No
Sample :EAT
10 h after HU
High Voltage : 500 V
Level : 0,73
Amplification : 5
Counts : 1 K
Counts total : 38910
Puls rate : 0,7
Avrge Jllum : 0,2
10 Hours after HU
Sample :EAT
6 h after HU
High Voltage : 500 V
Level : 0,73
Amplification : 5
Counts : 1 K
Counts total : 34423
Puls rate : 0,9
Avrge Jllum : 0,2
6 Hours after HU
Sample :EAT
16 h after HU
High Voltage : 500 V
Level : 0,73
Amplification : 5
Counts : 1 K
Counts total : 27872
Puls rate : 0,6
Avrge Jllum : 0,2
16 Hours after HU
Channel numbers proportional to cellular DNA content
Variations of DNA content - measured by Flow - Cytophotometry - of diploid Ehrlich-Ascites-Tumor cells (EAT) as a function of time after one injection of hydroxyurea (0,25 mg/g).
Mitoses ‰

FIGURE 12.—Variations of the DNA content, measured by flow cytophotometry, of diploid EAT cells as a function of time after 1 injection of HU (0.25 mg/g).

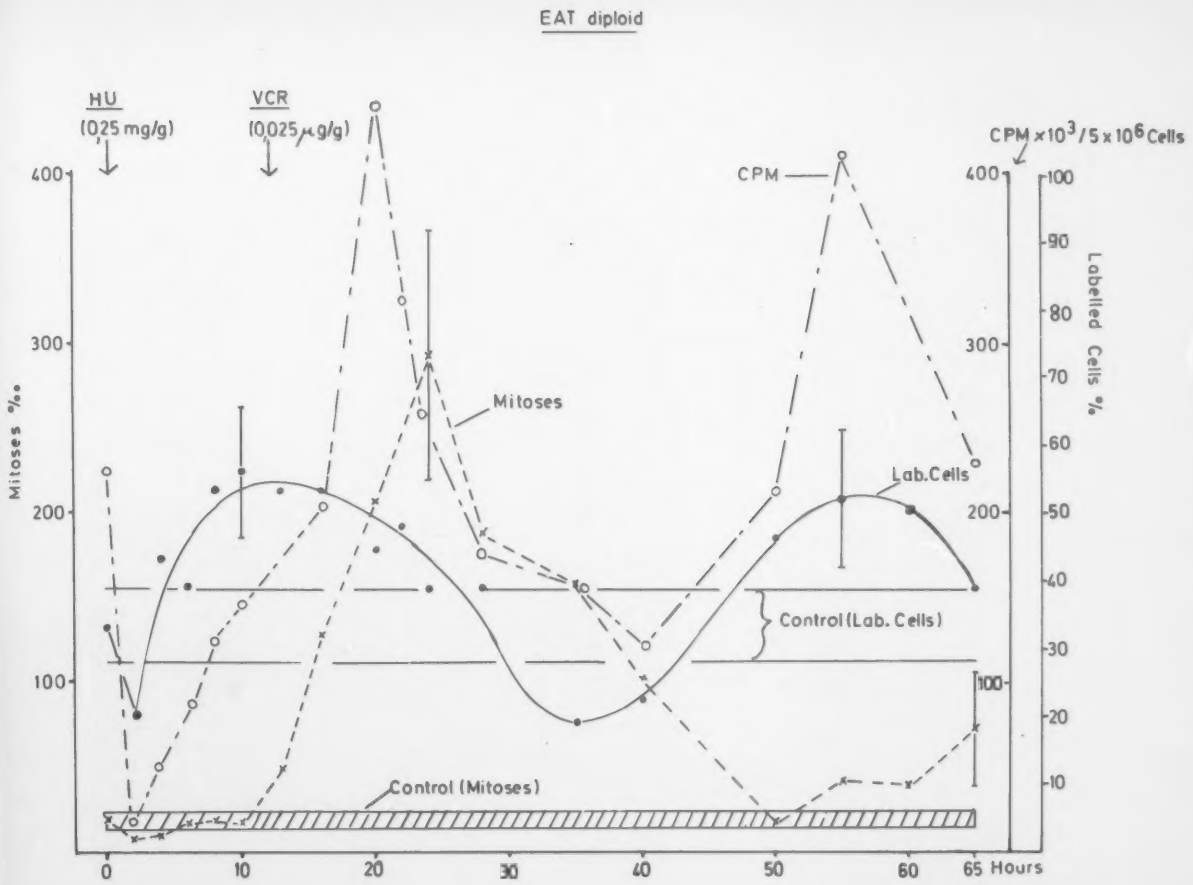

FIGURE 13.—Mitotic and labeling indices as well as ^{3}H-TdR incorporation values (CPM) of diploid EAT cells as a function of time after sequential administration of HU and VCR. Each point is the average value of 4–9 tumor-bearing mice. Confidence limits for $P = 5\%$. Experiments were started on the 4th day after tumor cell inoculation.

of cells into mitosis is about 20‰ per hour. This is a lower value than observed in untreated controls (about 32‰ per hour). From the 24th until the 50th hour the mitotic index decreases slowly to normal value (flux rate, 11‰ per hour).

These kinetic results are confirmed by flow microfluorometric measurements of the relative cellular DNA content as a function of time after this drug combination (fig 14). An exciting finding is the appearance of a diploid and tetraploid subpopulation in this model (at the 65th hour after HU).

Cell loss after administration of both drugs is not greater than observed after administration of HU alone (fig 8). Apparently, sequential administration of HU and VCR with precise timing of the mitotic poison according to kinetic data induces a high degree of partial synchronization of cell proliferation in this diploid EAT (mitotic index after HU alone, about 70‰; mitotic index after HU and VCR, about 300‰). However, this high degree of synchrony (48) lasts only for a short period of time. Due to cell loss (fig 8) and decay of synchrony (49) the second peak of labeled cells is not higher than the first peak.

Whether this phenomenon of partial synchronization, induced by sequential administration of HU and VCR, can be used for cytostatic treatment was proven by a set of quantitative experiments. As a cytostatic drug, CPH was chosen because it is mainly effective during DNA synthesis and G_2 phase (4). The therapeutic effect was evaluated by counting the total number of tumor cells in the abdominal cavity of the mice. Therapy regimens were started at Day 4 after tumor cell inoculation.

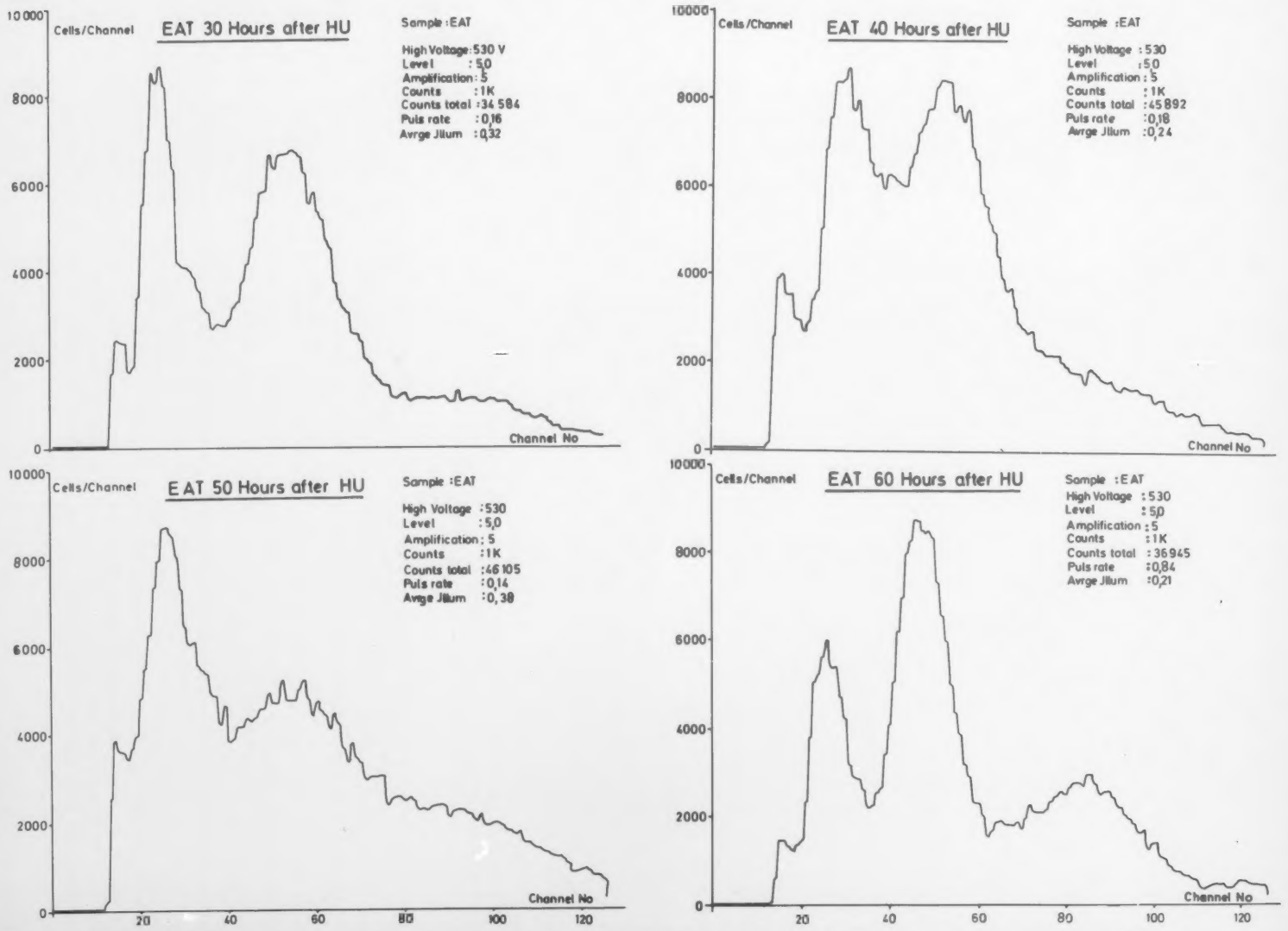

FIGURE 14.—Variations of the DNA content, measured by flow cytophotometry, of diploid EAT cells as a function of time after sequential administration of HU and VCR (12 hrs after HU).

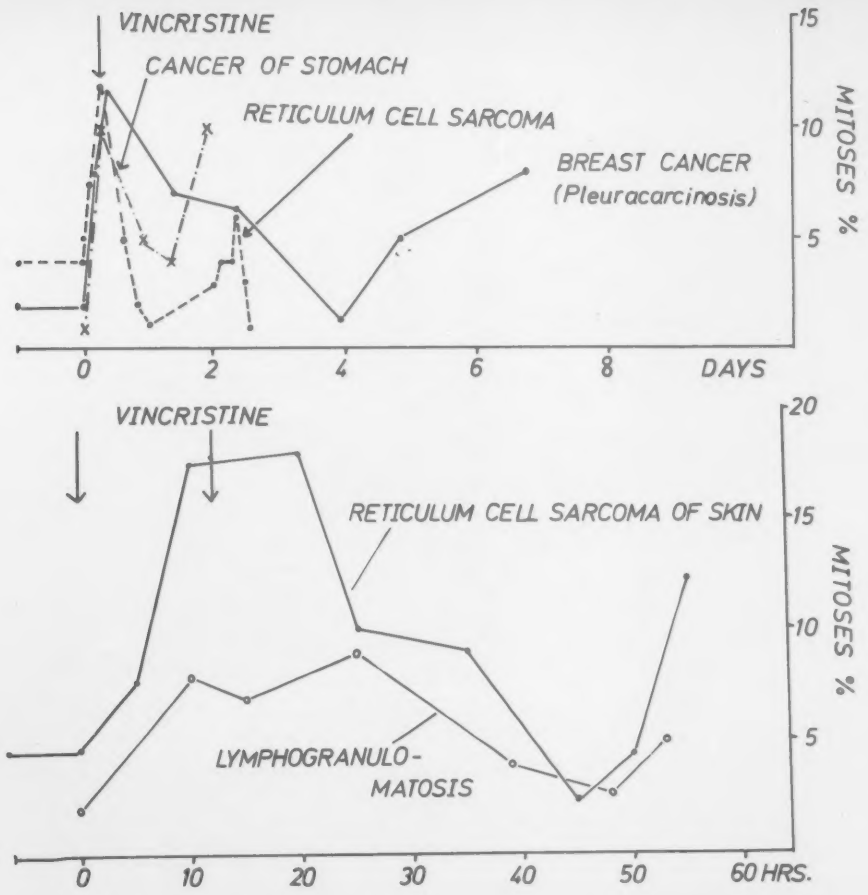

FIGURE 15.—Percentage of mitoses of malignant cells in reticulum cell sarcoma, breast cancer, cancer of the stomach, and lymphogranulomatosis of man as a function of time after 1 or 2 injections of VCR.

The essential finding is that only a sequential administration of HU, VCR, and CPH leads to a significant cell loss during > 5 days (fig 8). In this scheme VCR was administered 12 hours and CPH 55 hours after HU. Simultaneous injection of HU, VCR, and CPH or sequential administration of HU and CPH (at the 55th hour after HU) does not cause any significant effect compared with the controls or single-drug therapy.

It is still not known why CPH, administered 55 hours after HU and VCR, induces such a long-lasting growth depression. This effect cannot be explained by kinetic data alone. Probably, the large tetraploid subpopulation which appeared after sequential administration of HU and VCR is very sensitive to alkylation and/or possesses an impaired repair mechanism.

Further experiments were carried out to determine whether the administration of CPH at the time when the first cohort of labeled cells appears after injection of HU (10th hour) may cause a significant reduction of the number of tumor cells. It was found that cell loss was not higher than observed after administration of HU alone and was lower than after the sequential combination of HU, VCR, and CPH. This indicates that many of the cells synchronized by HU are due to die (fig 8) and that there is no further therapeutic gain by an additional attack with CPH at this time.

In conclusion, in this model system it is again shown that knowledge of modification of proliferation kinetics of tumor cells after perturbation by cytostatic drugs plays a role in planning cytostatic treatment.

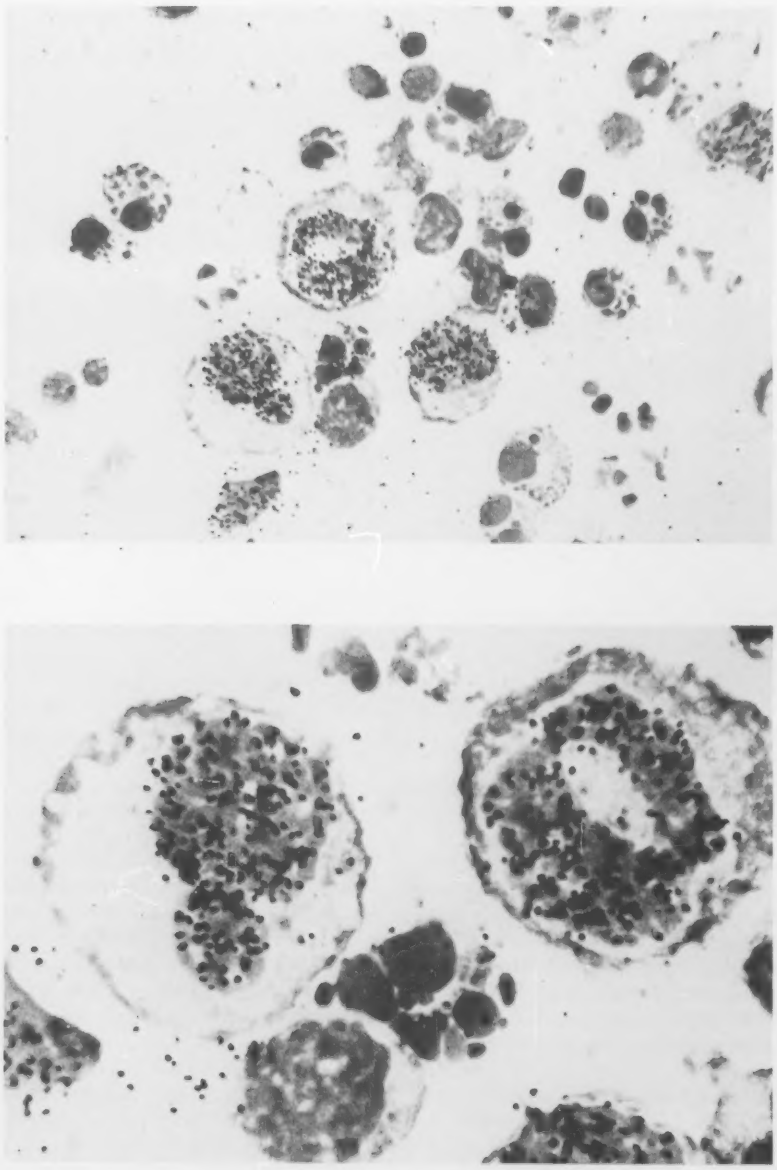

FIGURE 16.—Autoradiograms of 2 patients with lymphosarcoma. In vitro incubation of tumor specimen during 2 hrs with ^{3}H-TdR and ^{14}C-TdR according to the double-labeling technique.

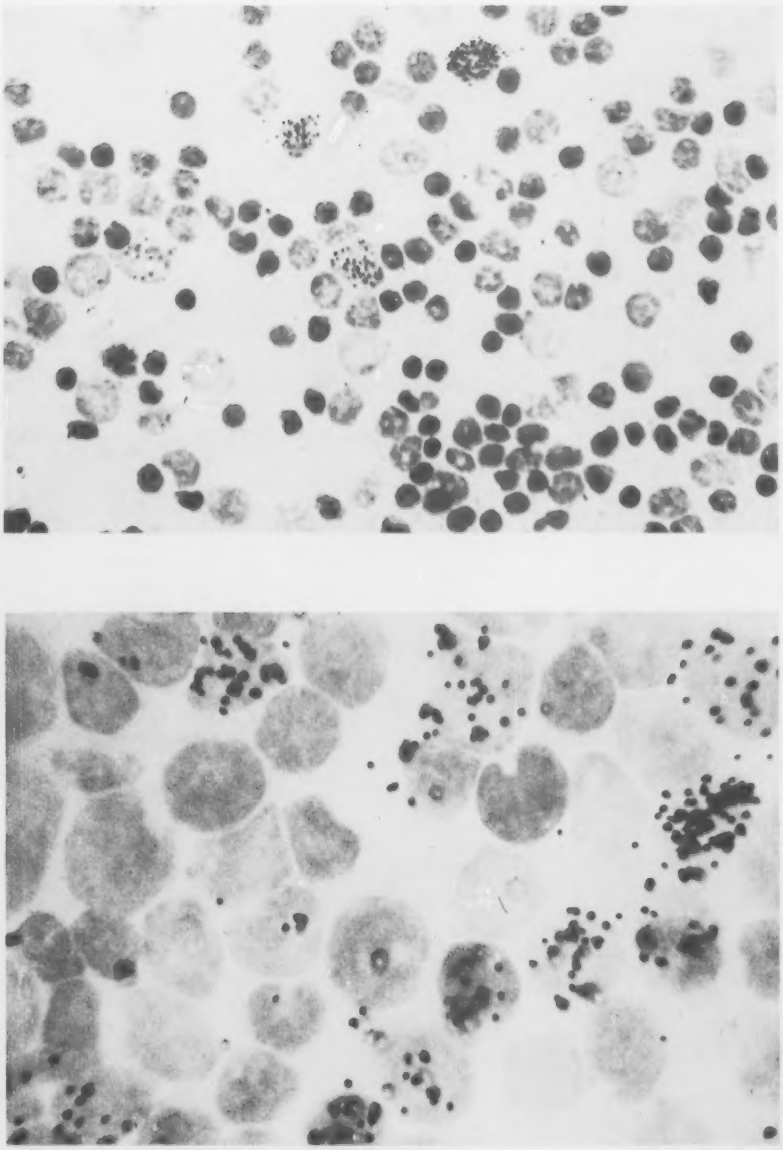

FIGURE 17.—Autoradiogram of a patient with lymphogranulomatosis. Two magnifications. In vitro incubation of a tumor specimen during 2 hrs with ^{3}H-TdR and ^{14}C-TdR according to the double-labeling technique.

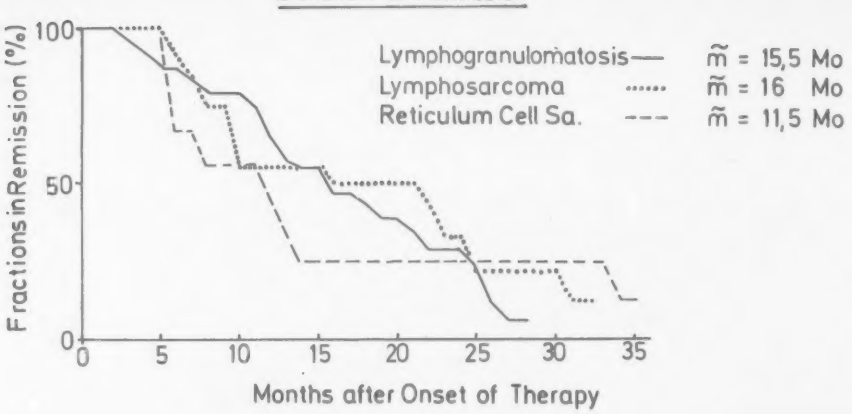

Diagnosis		Number of Patients	Remission Complete	Remission Partial	No Response
Lymphogranulomatosis	III B	19	14 (73,7 %)	4 (21,1%)	1 (5,2 %)
	IV	23	9 (39,1%)	9 (39,1%)	5 (21,8%)
Reticulum Cell Sarcoma (advanced)		15	9 (60,0%)	6 (40,0%)	0
Lymphosarcoma (advanced)		30	13 (43,3%)	13 (43,3%)	4 (13,4%)

FIGURE 18.—Therapeutic results in patients with lymphoreticular tumors after treatment with VCR and CPH according to the synchronization protocol. Cooperative study of medical clinics in Cologne, Bonn, and Hannover.

INVESTIGATIONS IN PATIENTS

Chemotherapy After Partial Synchronization in Hodgkin's Disease and Non-Hodgkin's Lymphoma

As was recently demonstrated in human tumors also, the induction of partial synchronization can be achieved in vivo by one or two low doses of VCR (fig 15) and, in analogy to the animal experiments, this phenomenon may be used for an effective chemotherapy with CPH during the S phase of the partially synchronized tumor cells (2–4). For the timing of CPH, knowledge of proliferation kinetics of the cells is an essential prerequisite. Kinetic data were obtained by means of a radioautographic in vitro method using the double-labeling technique (3,4). Tumor cells in granulomas of Hodgkin's disease and in non-Hodgkin's lymphoma (figs 16 and 17) seem to proliferate rapidly as the high labeling indices, the short DNA synthesis times, and as the mean generation times show (3,4). In most of the cases tumor

cells did not show marked variations of the kinetic parameters. Our findings agree with data published by other authors (50–52).

Based on the in vitro data of proliferation kinetics a therapy scheme (fig 2) for lymphoreticular tumors was established (3,4). Because of technical reasons, each patient treated in this trial could not be investigated completely with regard to synchronization or proliferation kinetics. Therefore, the following assumptions were made: (*a*) human tumor cells proliferate asynchronously; (*b*) in man, partial synchronization of cell proliferation can be induced; (*c*) a higher degree of synchronization can be obtained by two injections of VCR; and (*d*) in analogy to the animal experiments the generation time of human tumor cells is lengthened by VCR.

Recently it was found that lymphoreticular tumors respond especially well to this therapy protocol (3,4). In a cooperative phase II trial conducted in several clinics these results were confirmed (6). Figure 18 shows the remission rates and the remission duration. Most of these patients were ambulatory. Severe side effects were not observed.

It should be pointed out that, compared with other effective multiple-drug combination protocols, our concept of synchronization therapy is, in fact, single-drug therapy because only one drug is administered in a cytocidal dosage. Similar therapeutic results using synchronization therapy were obtained by Pouillart et al (53, 54) in human solid tumors, by Lampkin and co-workers (55) in acute leukemia of children, as well as by Vadlamudi and Goldin (56) in the L1210 leukemia in mice.

CONCLUSIONS

It was shown that under certain experimental conditions a modification of cell proliferation like partial synchronization can be induced by low, noncytocidal doses of VCR or HU. Both drugs which display their toxic effects mainly in one certain phase of the cell cycle may also be administered sequentially in order to enhance the degree of synchrony (4,34,38,41–47,57). Obviously, this phenomenon of partial synchronization of tumor cell proliferation can be used for an effective therapy with cell-phase-specific cytostatic drugs in animal as well as in human tumors. The best results were obtained in human lymphoreticular tumors which for the most part appear to have diploid and slightly hyperdiploid numbers of chromosomes without a shift of modal DNA content and are composed of rapidly proliferating cells (50–52). Our results are comparable with the best results obtained by multiple-drug chemotherapy protocols (6). However, the rate of side effects seems to be much lower in patients treated by the so-called synchronization therapy than by other treatments.

Our therapy concept might also be supported by the work of Razek and co-workers (58). They reported on a synergistic therapeutic effect of VCR and CPH only if CPH was administered 8 hours after VCR. They speculate that this could be due to a synchronization effect induced by VCR or by an increased permeability of the malignant cells for CPH. The latter assumption was made by analogy to experiments with VCR and methotrexate (59–61).

Despite our good results in lymphoreticular tumors, a critical consideration of experimental data shows that concerning other solid tumors this therapy concept might eventually not really be effective because of: (*a*) numerous heteroploid cell clones with different proliferation behavior (4,30,62,63); (*b*) varying fractions of non-proliferating cells in large tumors; and finally (*c*) poor vascularization of large tumor nodules (4). Therefore, further experience with the so-called synchronization therapy is needed before it can be concluded that synchronization techniques will permit major improvements of therapeutic results induced by cytostatic drugs (63).

REFERENCES

1. KLEIN HO, LENNARTZ KJ, HABICHT W, ET AL. Synchronisation von Ehrlich-Aszites-Tumorzellen und ihre Bedeutung bei der Anwendung eines alkylierenden Cytostaticum. Klin Wochenschr 48:1001–1005, 1970.
2. KLEIN HO, LENNARTZ KJ, TEICHMULLER W, ET AL. Cytostatic treatment of partially synchronized tumor cells in animals and man. *In* Advances in Antimicrobial Antineoplastic Chemotherapy. München, Urban and Schwarzenberg, 1972, pp 431–433.
3. KLEIN HO, LENNARTZ KJ, GROSS R, ET AL. In-vivo- und In-vitro-Untersuchungen zur Zellkinetik und Synchronisation menschlicher Tumorzellen. Dtsch Med Wochenschr 97:1273–1282, 1972.
4. KLEIN HO, and LENNARTZ KJ. Chemotherapy after synchronization of tumor cells. Semin Hematol 11:203–227, 1974.
5. KLEIN HO. Relevance of chemically induced synchronization of cell cycle to chemotherapy of human solid tumors. *In* Proceedings of the 11th International Cancer Congress, Florence, Oct 20–26, 1974, vol 5, p 208.
6. KLEIN HO, GERECKE D, BORBERG H, ET AL. Ergebnisse der Synchronisationstherapie mit Vincristin und cyclophosphamid bei Lymphogranulomatose, Retikulumzell- und Lymphosarkom. Eine Phase-II-Studie. Dtsch Med Wochenschr 100:1719–1726, 1975.
7. BYFIELD JE, and SCHERBAUM OH. A rapid radioassay technique for cellular suspensions. Anal Biochem 17:434–443, 1966.
8. DITTRICH W, and GÖHDE W. Impulsfluorometrie bei Einzelzellen in Suspension. Z Naturforsch 246:360–361, 1969.
9. ———. Phase progression on two dose response of Ehrlich ascites tumor cells. Atomkernenergie 15:174–176, 1970.
10. GÖHDE W, and DITTRICH W. Impulszytophotometrie, ein neuartiges Durchflussverfahren zur ultraschnellen Mengenbestimmung von Zellinhaltsstoffen. Acta Histochem (suppl) 10:429–437, 1972.

11. LE PECQ SB, and PAOLETTI C. A fluorescent complex between ethidium bromide and nucleic acids. J Mol Biol 27:87–106, 1967.
12. ADLER D, DOERING M, and LENNARTZ KJ. Cell kinetic investigations by single cell cytophotometry and double labeling autoradiography. *In* Molecular Base of Malignancy (Deutsch E, Moser K, Rainer H, et al, eds). Thieme, 1976, pp 273–278.
13. TILLMANN B, LENNARTZ KJ, and EDER M. Quantitative Untersuchungen zum Wachstumsverhalten eines diploiden Ehrlich- und MCa 1-Aszitestumors der Maus. Z Krebsforsch 70:295–302, 1968.
14. BAGLEY CM, BOSTICK FW, and DEVITA VT. Clinical pharmacology of cyclophosphamide. Cancer Res 33:226–233, 1973.
15. HILL DL. A Review of Cyclophosphamide. Springfield, Ill, Charles C. Thomas, 1975, p 225.
16. LUKES R, CRAVER LF, HALL TC, ET AL. Report of the nomenclature committee. Cancer Res 26:1311, 1966.
17. LUKES R, BUTLER JJ, and HICKS EB. Natural history of Hodgkin's disease as related to its pathologic picture. Cancer 19:317–344, 1966.
18. ROSENBERG SA. Report of the committee on the staging of Hodgkin's disease. Cancer Res 26:1310, 1966.
19. CUTTLER SJ, and EDERER F. Maximum utilization of the life table method in analyzing survival. J Chronic Dis 8:699–712, 1958.
20. MCWILLIAMS NB, MAUER AM, and LAMPKIN BC. Dose dependent vincristine effects. Clin Res 19:494, 1971.
21. HARTENSTEIN R, ERHART H, and HOFFMANN K. Zellkinetische Untersuchungen beim Ehrlich-Aszites-Tumor unter Vincristin. Z Krebsforsch 79:213–220, 1973.
22. JELLINGHAUS W, MAIDHOF R, SCHULTZE B, ET AL. Experimentelle Untersuchungen und zellkinetische Berechnungen zur Frage der Synchronisation mit Vincristin in vivo (Mäuseleukämie L1210, Kryptenepithelien der Maus). Z Krebsforsch 84:161–176, 1975.
23. MAIDHOF R, JELLINGHAUS W, SCHULTZE B, ET AL. Experimentelle und theoretische Untersuchungen zur Erzeugung einer teilsynchron proliferierenden Zellpopulation mit Vincristin in vivo. Dtsch Med Wochenschr 100:54–56, 1975.
24. FREI E III, WHANG J, SCOGGINS RB, ET AL. The stathmokinetic effect of vincristine. Cancer Res 24:1918–1925, 1964.
25. MAURO F, and MADOC-JONES H. Age responses of cultured mammalian cells to cytotoxic drugs. Cancer Res 30:1397–1408, 1970.
26. GRANZOW C, and GRANZOW V. Eine Fehlerquelle bei Synchronisationsversuchen mit malignen Tumoren in vivo. Z Krebsforsch 81:15–22, 1974.
27. HASHOLT L, and KELD D. Cytogenetic investigations on an Ehrlich ascites tumor, and four sublines resistant to daunomycin, adriamycin, vincristine, and vinblastine. Hereditas 77:303–310, 1974.
28. ERBE W, PREISS J, SEIFERT R, ET AL. Increase in RNase and DPNase activities in ascites tumor cells induced by various cytostatic agents. Biochem Biophys Res Commun 23:392–397, 1966.
29. JOHNSON JS, WRIGHT HF, SVOBODA GH, ET AL. Antitumor principles derived from *Vinca rosea* Linn. I. Vincaleukoblastine and leurosine. Cancer Res 20:1016–1022, 1960.
30. KILLMANN S-A. Effect of cytostatic drugs on the kinetics of leukemic blast cells in man. Schweiz Med Wochenschr 104:278–284, 1974.
31. PETERSEN DF, TOBEY RA, and ANDERSON EC. Synchronously dividing mammalian cells. Fed Proc 28:1771–1779, 1969.
32. ROBBINS E, and GONATAS NK. Histochemical and ultrastructural studies on HeLa cell cultures exposed to spindle inhibitors with special reference to the interphase cell. J Histochem Cytochem 12:704–711, 1964.
33. STUBBLEFIELD E, and KLEVECZ R. Synchronization of Chinese hamster cells by reversal of colcemid inhibition. Exp Cell Res 40:660–667, 1965.
34. STUBBLEFIELD E, and BRINKLEY BR. Cilia formation in Chinese hamster fibroblasts in vitro as a response to colcemid treatment. J Cell Biol 30:645–652, 1966.
35. WAGNER EK, and ROIZMAN B. Effect of the vinca alkaloids on RNA synthesis in human cells in vitro. Science 162:569–570, 1968.
36. DETHLEFSEN LA, SORENSEN SP, and RILEY RM. Effects of double and multiple doses of hydroxyurea on mouse duodenum and mammary tumors. Cancer Res 35:694–699, 1975.
37. GILLETTE EL, WITHERS HR, and TENNOCK JF. The age sensitivity of epithelial cells of mouse small intestine. Radiology 96:639–643, 1970.
38. MADOC-JONES H, and MAURO F. Age responses to X-rays, vinca alkaloids, and hydroxyurea of murine lymphoma cells synchronized in vivo. J Natl Cancer Inst 45:1131–1143, 1970.
39. RAJEWSKY MF. Synchronization in vivo: kinetics of a malignant cell system following temporary inhibition of DNA synthesis with hydroxyurea. Exp Cell Res 60:269–276, 1970.
40. BROCKMAN RW. Biochemical aspects of drug combinations. Cancer Chemother Rep Part 2, vol 4(1):115–129, 1974.
41. BACCHETTI S, and WHITMORE GF. The action of hydroxyurea on mouse L cells. Cell Tissue Kinet 2:193–211, 1969.
42. BHUYAN BK, FRASER TJ, GRAY LG, ET AL. Cell kill kinetics of several S-phase-specific drugs. Cancer Res 33:888–894, 1973.
43. BOSMANN HB. Antineoplastic drug activity in the mitotic cycle—effects of six agents on macromolecular synthesis in synchronous mammalian leukemic cells. Biochem Pharmacol 21:1977–1988, 1972.
44. KIM JH, GELBARD AS, and PEREZ AG. Action of hydroxyurea on the nucleic acid metabolism and viability of HeLa cells. Cancer Res 27:1301–1305, 1967.
45. SINCLAIR WK. Hydroxyurea: differential lethal effects on cultured mammalian cells during the cell cycle. Science 150:1729–1731, 1965.
46. WHEELER GP, BOWDON BJ, ADAMSON DJ, ET AL. Comparison of the effects of several inhibitors of the synthesis of nucleic acids upon the viability and progression through the cell cycle of cultured H. Ep. No. 2 cells. Cancer Res 32:2661–2669, 1972.
47. YATAGANAS X, and CLARKSON B. Flow microfluorometric analysis of cell killing with cytotoxic drugs. J Histochem Cytochem 22:651–659, 1974.
48. SINCLAIR WK, and MORTON RA. X-ray and ultraviolet sensitivity of synchronized Chinese hamster cells at various stages of the cell cycle. Biophys J 5:1–25, 1965.
49. TERASIMA T, and TOLMACH LJ. Growth and nucleic acid synthesis in synchronously dividing populations of HeLa cells. Exp Cell Res 30:344–362, 1963.
50. COOPER EH, PECKHAM MJ, MILLARD RE, ET AL. Cell proliferation in human malignant lymphomas. Analysis of labeling index and DNA content in cell populations obtained by biopsy. Eur J Cancer 4:287–296, 1968.
51. SCHIFFER LM. Human lymphocyte proliferation: DNA synthesis time. Cell Tissue Kinet 4:585–595, 1971.
52. SHEEHY PF, FRIED JF, DOWLING MD, ET AL. Studies of cellular proliferation in human leukemia. VIII. The generation time and growth fraction in lymphosarcoma in a leukemic phase during advanced and early relapsing disease. Cancer 36:203–210, 1975.
53. POUILLART P, SCHWARZENBERG L, MATHÉ G, ET AL. Essai clinique de combinaisons chimiotherapeutiques basées sur la notion de tentative de synchronisation cellulaire. Administration première d'un antimitotique suivie de l'application

de produit(s) cycle on phase dépendent(s). Nouv Presse Méd 1:1757–1762, 1972.

54. POUILLART P, MATHÉ G, and SCHWARZENBERG L. Essai de recrutement cellulaire par synchronisation partielle pour l' établissement d'une combinaison chimiothérapique. Bull Cancer 60:187–196, 1973.
55. LAMPKIN BC, MCWILLIAMS NB, and MAUER AM. Cell kinetics and chemotherapy in acute leukemia. Semin Hematol 9:211–223, 1972.
56. VADLAMUDI S, and GOLDIN A. Influence of mitotic cycle inhibitors on the antileukemic activity of cytosine arabinoside in mice bearing Leukemia L1210. Cancer Chemother Rep 55:547–555, 1971.
57. BRUCHOVSKY N, OWEN AA, BECKER AJ, ET AL. Effects of vinblastine on the proliferative capacity of L cells and their progress through the division cycle. Cancer Res 25:1232–1237, 1965.
58. RAZEK A, VIETTI T, and VALERIOTE F. Optimum time sequence for the administration of vincristine and cyclophosphamide. Cancer Res 34:1857–1861, 1974.
59. FYFE MJ, and GOLDMAN JD. Characteristics of the vincristine induced augmentation of methotrexate uptake in Ehrlich ascites tumor cells. J Biol Chem 248:5067–5073, 1973.
60. GOLDMAN JD, and FYFE MJ. The mechanism of action of methotrexate. II. Augmentation by vincristine of inhibition of DNA synthesis by methotrexate in Ehrlich ascites tumor cells. Mol Pharmacol 10:275–282, 1974.
61. POUILLART P, HOANG THY HUONG T, and L'HERITIER J. La leucémie L 1210, modèle experimental pour la potentialisation des drogues applicables aux leucémies aigües. Bull Cancer 61:509–526, 1974.
62. FRINDEL E, and TUBIANA M. Radiobiology and the cell cycle. *In* The Cell Cycle and Cancer (Baserga R, ed). New York, Marcel Dekker, Inc, 1971, pp 391–447.
63. VAN PUTTEN LM. Are cell kinetic data relevant for the design of tumor chemotherapy schedules? Cell Tissue Kinet 7:493–504, 1974.

Abstracts From the Flow Microfluorometry Workshop

In Vivo Effects of Cyclophosphamide and Adriamycin on Mouse Tumor Cell Cycle Parameters Using Flow Microfluorometry Analysis

David S. Alberts and Joe Gray

Section of Hematology-Oncology, College of Medicine, University of Arizona, Tucson, Ariz 85724, and Lawrence Livermore Laboratory, The Biomedical Division, University of California, Livermore, Calif 94550.

Flow microfluorometry assisted by DNA histogram synthesis computer analysis was used to determine the in vivo effects of adriamycin (NSC-123127) or cyclophosphamide (NSC-26271) on P388 ascites tumor cell cycle progression. Male DBA_2 mice were given single ip doses of either adriamycin or cyclophosphamide 48 hours after the ip transplantation of 10^6 P388 leukemia cells. Animals were killed at 2-hour intervals from 0 to 24 hours after drug injection. Ascites tumor cells were removed and the red blood cells were lysed with tris-ammonium chloride buffer and suspended in 10% formalin. The Lawrence Livermore flow microfluorometer was used to generate the DNA histograms of 10^6 acriflavin-stained tumor cells from each of the time points. Analysis of the DNA histogram sequence revealed that there was a build-up with time between 4 and 16 hours after drug injection of P388 cells in the G_2 + M region, indicating a G_2 or M block by both adriamycin and cyclophosphamide. In addition, cyclophosphamide caused a possible early S phase partial block.

Perturbation of Cell Cycle Progression With Melphalan In Vitro

B. Barlogie and B. Drewinko

University of Texas System Cancer Center, M. D. Anderson Hospital and Tumor Institute, Houston, Tex 77030.

Melphalan (NSC-8806) was tested for its effects on the cell cycle progression of a long-term human lymphoma cell line (T_1 cells) in vitro utilizing sequential DNA histograms obtained by pulse cytophotometry. Mithramycin was used as a DNA-specific fluorescent dye on ethanol-fixed cells. The influence of drug concentration (0.05, 0.25, 0.5, 1.0, 2.5, and 5.0 μg/ml) and exposure time (1, 3, 12, 24, and 48 hours) was analyzed in asynchronous cell populations. Block of the mitotic cycle in G_2 phase is the major kinetic response. Magnitude and duration of G_2 accumulation are positively correlated to concentration and exposure time with a maximum achieved after treatment with > 2.5 μg/ml for > 12 hours. There is an inverse correlation between recovery from the G_2 block and drug concentration and incubation time. Treatment with > 0.5 μg/ml for > 24 hours induces a transient prolongation of S-phase transit, the extent of which is concentration and exposure time dependent. Thus, the onset of G_2 accumulation is delayed. The $G_{1/0}$ compartment evacuates promptly indicating no block in G_1 or at the G_1-S boundary. The influence of cell age on the kinetic response to melphalan was analyzed in thymidine-synchronized cells. When T_1 cells are treated with 2.5 μg/ml for 1 hour in selected stages of the cycle, delay in G_2 phase is most pronounced after initiation of treatment in G_1 phase; in this case, the G_2 block becomes manifest during the immediate life cycle. When cells are treated in S and G_2 phases, G_2 delay is evidenced after cell division in the subsequent life cycle and is less pronounced.

Determination of Sensitivity and Resistance of L1210 Leukemia to Cytosine Arabinoside, In Vivo, Using Flow Microfluorometric Cell-Cycle Analysis

Oliver Alabaster and Bill Bunnag

Laboratory of Pathology, Division of Cancer Biology and Diagnosis, National Cancer Institute, Bethesda, Md 20014.

Sensitive L1210 and resistant L1210/cytosine arabinoside (NSC-63878) ascites cells in CDF_1 mice were exposed to 750 mg/kg of cytosine arabinoside ip (one dose). Cell samples were obtained from each of five mice at timed intervals from 0 to 72 hours. These cells were stained with the DNA-specific stoichiometric fluorochrome, mithramycin (NSC-24559). Labeling and mitotic indices were concurrently obtained. Sequential DNA histograms obtained with a flow microfluorometer were integrated and the components of the cell cycle were defined in terms of DNA content by approximating the S-phase value to the labeling index in the L1210 controls. The G_2 value was obtained by subtracting the mitotic index from the G_2 + M value.

Cell-cycle analysis indicated that in L1210, cytosine arabinoside killed cells mostly in S phase and produced a G_1 block which persisted for 72 hours. The depressed labeling index transiently increased between 4 and 16 hours as a subpopulation of cells entered early-S phase prior to their death. Mitosis was inhibited for 48 hours.

In the L1210/cytosine arabinoside population there was an increase in S-phase cells at 8 and 32 hours associated with an increased labeling index. Relatively few cells were killed in S phase. A G_1

block was absent. Mitosis was incompletely inhibited. Recovery occurred by 48 hours.

Comparison of the DNA histograms between 24 and 72 hours clearly distinguished the two cell populations raising the possibility of using flow microfluorometric cell-cycle analysis as a monitor or predictor of tumor response in the clinical setting.

Flow Microfluorometric Determinations of DNA, Protein, and Cell Volume: Analysis of Tumor Cell Kinetics

H. A. Crissman, P. L. Wanek, and J. A. Steinkamp

Biophysics and Instrumentation Group, Los Alamos Scientific Laboratory, University of California, Los Alamos, N Mex 87545.

Cellular DNA- and protein-content analyses were made on cell populations of mouse L1210 ascites and solid (sc) B16 melanoma and Lewis lung carcinoma tumors grown in vivo using flow microfluorometric techniques. Tumors were dispersed, fixed in 70% ethanol, and treated with RNase prior to staining for both DNA and protein, respectively, with propidium iodide (red) and fluorescein isothiocyanate (green). Simultaneous analyses of DNA, protein, and cell volume were performed using the Los Alamos multiparameter analysis and cell-sorter system. DNA content analyses of cells from both the L1210 ascites and B16 melanoma specimens showed these tumors to be composed of proliferating populations having G_1 cells with a 2C-DNA content, based on the distributions obtained from normal spleen (diploid) cells. Analysis of the DNA distribution patterns obtained from samples of L1210 ascites cells on Days 3, 4, 6, and 7 after ip implantation of 10^5 cells revealed changes in cell-growth kinetics associated with tumor age or cell density. DNA distributions of Lewis lung carcinoma cell populations contained a 2C peak and a cell proliferation pattern extending between 4C and 8C. Cells sorted from the 2C and the 4C–8C content of the DNA spectrum were morphologically identified as normal and tumor cells, respectively. Analysis of pulmonary metastases from the primary Lewis lung carcinoma also revealed trimodal DNA distribution patterns with peaks at 2C, 4C, and 8C. The protein contents of normal and tumor cells contained in the primary Lewis lung carcinoma were analyzed using gated analysis techniques.

Tumor cells were found to have a greater protein mass compared to normal cells; however, tumor cells were quite heterogeneous with respect to cell size and morphology. Analysis of cellular DNA and protein in these and other tumor systems permits characterization of the growth kinetics during the various stages of tumor development. Such information has predictive value in chemotherapeutic treatment and regimen scheduling. (This work is being performed under a joint agreement between the US Energy Research and Development Administration and the National Cancer Institute.)

Study of In Vivo Tumor State and Response to Therapy by Analysis of DNA Distribution

Yosh Maruyama, M. R. Raju, Elvira Bain, and James H. Jett

Department of Radiation Medicine, A. B. Chandler Medical Center, Lexington, Ky 40506.

A model in vivo tumor system and its characteristics with tumor growth were studied. This tumor system offers an intermediate system useful for the study of tumor cells in the intact animal but does not have the complexities of solid tumors. DNA distribution was studied and correlated with macromolecular DNA synthesis. H^3TdR uptake was active during the early stages of tumor growth and correlated with flow microfluorometric distribution curves of numerous S-phase cells. Mechlorethamine (NSC-762), BCNU (NSC-409962), hydroxyurea (NSC-32065), and radiation were studied and produced perturbation in stationary phase cell kinetics. There was a redistribution of cell ages consistent with induced cycling activity with most, but not all, of the above agents. These indicated a recruitment from a stationary phase by cancer therapeutic agents although subsequent cell cycle traverse may also be greatly perturbed. A number of considerations important to the interpretation of this type of data are discussed. (Supported in part by Public Health Service grants R01-CA-13849 and P01-CA-17786 from the National Cancer Institute, National Institutes of Health, Department of Health, Education, and Welfare.)

Dissociation of Mammary Tumors and the Characterization of Cells by Electronic Volume Analysis, Velocity Sedimentation, Density Gradients, Morphology, and Chemotherapy

R. M. Zucker, J. Harari, J. Finley, and J. Noel

Papanicolaou Cancer Research Institute at Miami, Inc, PO Box 6188, Miami, Fla 33123.

Four tumors, R3230AC mammary adenocarcinoma, C3H mammary adenocarcinoma, 13762 papillary adenocarcinoma, and B16 melanoma, were optimally dissociated into single cells using a combination of enzymatic and mechanical methods. The dissociation medium was Ca^{++}-free M199 containing collagenase II, crystalline trypsin, DNase, and bovine serum albumin. The dissociated cells

were separated by velocity sedimentation and density gradients and then characterized by electronic volume distributions, light and electron microscopy, and [^{3}H]thymidine uptake. The 13762 papillary adenocarcinoma tumor cells' response to melphalan (NSC-8806), melphalan + 5-FU (NSC-19893), and 5-FU and the B16 tumor cells' response to methyl-CCNU (NSC-95441), cyclophosphamide (NSC-26271), and palm-O-ara-C (NSC-135962) were studied by combined methodology. The different interactions of drugs against tumor cells were monitored with the cell-separation procedures combined with electronic volume distributions, light and electron microscopy, and [^{3}H]thymidine uptake.

Quantitative Comparison of Measurements With Different Fluorochromes of DNA

Walfried A. Linden and Heinz Baisch

Institut für Biophysik und Strahlenbiologie der Universität Hamburg, Martinistrasse 52, D-2000 Hamburg 20, Germany.

Pulse cytophotometric DNA distribution patterns of mouse fibroblasts, L-929, were measured after staining with ethidium bromide, mithramycin (NSC-24559), and a benzimidazol derivative, Hoechst-33258 (Berkhan E. Pulse-cytophotometry as a method for rapid photometric analysis of cells. *In* Pulse-Cytophotometry, Part I [Haanen CAM, Hillen HFP, and Wessels JMC, eds]. Ghent, European Press Medikon, 1975, pp 15–21). The fractions of cells in the different phases of the cell cycle were calculated using a computer program (Baisch H, Göhde W, and Linden WA. Analysis of PCP-data to determine the fraction of cells in the various phases of cell cycle. Radiat Environ Biophys 12:31–39, 1975). The results are given in table 1. A t test proved that the differences in the fractions of cells as determined using the different fluorochromes are within the frame of statistical error for $P = 0.05$. Since staining with mithramycin and Hoechst-33258 respectively is simpler and faster than staining with ethidium bromide, these two fluorochromes are recommended for routine use.

TABLE 1.—Fractions of L-cells (%) in the various phases of the cell cycle and coefficient of variation (CV) 48 hrs after subcultivation determined by using different fluorochromes (mean ± SE of 20 samples each)

Fluorochrome	Cell-cycle phases G_1	S	G_2 + M	CV (%)
Ethidium bromide	58.2±0.6	30.5±0.3	11.3±0.5	3.5
Mithramycin	56.8±0.6	30.6±0.4	12.6±0.3	7.7
Hoechst-33258	56.5±0.8	31.3±0.5	12.2±0.5	5.0
Hoechst-33258 + ethidium bromide	58.0±0.9	30.5±0.6	11.5±0.4	6.3

Evaluation of Two-Parameter Pulse-Cytophotometric Data From Cells Stained With DNA- and Protein-Specific Dyes

Heinz Baisch

Institut für Biophysik und Strahlenbiologie der Universität Hamburg, Martinistrasse 52, D-2000 Hamburg 20, Germany.

Simultaneous measurements of DNA and protein content are very interesting for cells progressing through the cell cycle, especially after treatment with drugs having a different effect on the various phases. With the two-parameter pulse cytophotometer, a fluorescence flow-through device, measurements of this type can be accomplished (Göhde, 1975). This paper deals with the evaluation of two-parameter pulse cytophotometric data which yield the fraction of cells in the G_1, S, and G_2 + M phases and distributions of protein content of the cells in all phases of the cell cycle.

Ehrlich ascites cells were stained with ethidium bromide and fluorescein-isothiocyanate binding to DNA and protein respectively. The fluorescence signals proportional to DNA and protein content were stored in a two-dimensional array of a multichannel analyzer.

A projection of the data of the array on the horizontal axis yielded the DNA distribution which was analyzed as described previously (Baisch H, et al, Radiat Environ Biophys 12:31–39, 1975). Taking normal distributions for the DNA content of G_1 and G_2 + M cells and a Gaussian integral for the S-phase distribution, fractions of cells in the various phases were obtained by a computer fit. With the calculated DNA distributions the data of the array were sorted according to the phases in the cell cycle. Thus, separate arrays of data were obtained for G_1, S, and G_2 + M phases. A projection on the vertical axis now yielded protein distributions for the cells of every phase.

For untreated cells the protein distributions can be fitted by a normal distribution. From the fit, the relative mean protein content for the phases was derived. We obtained a continuous increase of protein content from G_1 to G_2 + M, but taking into account that the G_2 + M phase is shorter than the other phases, the protein-synthesis rate in G_2 + M was found to be 2.5 times higher than in G_1 or S phase.

Flow-Microfluorometric Analysis of Nuclei Isolated From Brain and Brain Tumors

T. Hoshino, K. T. Wheeler, J. W. Gray, and K. Nomura

Brain Tumor Research Center, University of California, San Francisco, Calif 94143.

Small pieces (50–100 mg) of rat cerebellum, rat cerebrum, rat brain tumor, and several human brain tumors were homogenized in a Dounce tissue grinder and filtered through a 15-μm NITEX. The isolated nuclei were then collected by centrifugation through 40% sucrose (15 minutes at 4000 rpm in an IEC-PR6), fixed with 10% formalin, and stained with Acriflavin-Feulgen. Flow-microfluorometry profiles of cerebrum revealed one prominent double peak at the 2C DNA position and a few nuclei in the 4C DNA position. The 4C nuclei were shown to be primarily doublets. The profile of cerebellum showed a sharp peak at the 2C DNA position with 5%–6% of the population with an apparent 4C DNA composition. The 4C nuclei were also determined to be doublets. Both profiles contained essentially no nuclei in the position corresponding to S phase. The rat brain tumor profile contained a more prominent 4C DNA peak and many nuclei in the position corresponding to S phase. The same technique was used to analyze human brain tumors (meningioma, glioblastoma, and astrocytoma). The profiles gave results that agree with the biologic behavior of each tumor type. (Supported by NIH grant CA-13525.)

Cell Cycle Studies of Isoproterenol-Stimulated Transplantable Salivary Gland Carcinoma of the BALB/c Mouse

W. E. Delaney, I. R. Toth, P. Basuk, E. C. Wu, D. Lehane, and P. J. McKenna

St. Vincent's Hospital Center, 153 West 11th St, New York, NY 10011.

The responses of three lines of transplantable salivary gland carcinoma of BALB/c mice were studied after a single ip injection of isoproterenol followed at 20 hours by ^{3}H-thymidine iv. Portions of host salivary gland and of tumor were studied at hourly intervals between 21 and 32 hours; tissue was analyzed biochemically for total protein (Folin-phenol assay) and total nucleic acid (ethidium bromide technique) with and without either ribonuclease or deoxyribonuclease digestion. Parallel autoradiography was performed. Thymidine indices of tumor showed a sharp increase in synthesis (initially below control levels) at 30–32 hours although biochemical DNA synthesis in both normal salivary gland and tumor peaked at 27 hours. A significant quantitative increase in DNA synthesis and ^{3}H-thymidine uptake over the amounts resulting from non-isoproterenol-induced activity was observed. The findings indicate that a substantial proportion of cells in this continuously dividing system can respond to a single chemical stimulus with the initiation of cell division.

Differential Effects of Chemotherapeutic Agents on Labeling Index, Incorporation of Radiolabeled DNA-Precursors, and Colony Formation of Human Lymphoma Cells

Pamela Roper

Department of Clinical Chemistry and Laboratory Medicine, the University of Texas System Cancer Center, M. D. Anderson Hospital and Tumor Institute, Houston, Tex 77030.

In proliferating cell populations, inability to reproduce is the only relevant criterion to assess cell lethality. The in vitro colony-formation technique used to determine reproductive death is, however, too slow to be used in routine clinical studies. To find suitable, more rapid techniques that assess drug-induced cell killing, a human lymphoma cell line was exposed in vitro to increasing concentrations of adriamycin (NSC-123127), bleomycin (NSC-125066), and BCNU (NSC-409962) for 1 hour. Survival was assayed immediately after treatment and at regular intervals thereafter. Data from the colony-formation technique were compared with those obtained from determinations of the labeling index and the rate of incorporation of ^{3}H-TdR. The labeling index and ^{3}H-TdR values demonstrated temporal fluctuations insensitive to changes in drug concentrations, grossly overestimating or underestimating killing activity. Only colony-formation technique results exhibited a clear dose-dependent decline in survival. Failure to demonstrate correlation with colony formation implies that these in vitro methods determining metabolic dysfunctions should not be used as criteria to predict loss of proliferative capacity.

Double-Emulsion Autoradiography for Analysis of a Possible G_0 Phase in Rat Epidermis

Fredric J. Burns

Institute of Environmental Medicine, New York University Medical Center, 550 First Ave, New York, NY 10016.

The properties of the G_0 phase in rat epidermis were investigated by determining how frequently G_1 cells enter the S phase in response to a wound stimulus. At time 0, rats were injected with 0.15 microcurie/g of C^{14}-thymidine and then 18 hours later, when the C^{14}-labeled cells were in the G_1 phase, the skin was stripped with cellophane tape to stimulate the movement of cells out of G_1. At the same time, some of the rats were irradiated with 1000 and 2500 rads to determine whether radiation affects the G_1 to S transition. At various times after stimulation, small biopsies of skin were removed and incubated in 10 microcuries/ml of H^3-thymidine. Sections were dipped in Ilford K-5, diluted 1:1 with water, exposed for 2 weeks, and then developed. The slides were then dipped in a 4.5% solution of nitrocellulose in order to provide about 2 microns of absorber and then into undiluted liquid emulsion and exposed for 6 weeks.

Cells labeled with H^3 only, C^{14} only, and both isotopes were clearly distinguishable and were counted. The results indicated that in controls about 2% of the basal cells were in S phase but stimulation by stripping increased the percentage to about 12% although irradiation held the increase to about 6%. The proportion of C^{14}-labeled cells entering S phase was about the same as the proportion of all cells entering the S phase which indicated that all cells in G_1 were available on a more or less random basis for responding to a proliferative stimulus, a result consistent with the existence of a G_0 phase.

Thymidine Incorporation During Aging of Normal Human Diploid Cell Cultures: Quantitative Autoradiographic Analysis Using Scanning Microdensitometry

G. L. Grove, E. D. Kress, and V. J. Cristofalo

The Wistar Institute of Anatomy and Biology, 36th St at Spruce St, Philadelphia, Pa 19104.

Human diploid cells have a finite lifespan in vitro and are currently being used in our laboratory as a model of cellular senescence. Autoradiographic studies have shown that the fraction of cells able to incorporate ^{3}H-thymidine during a 30-hour labeling period decreases with advancing age. This relationship has proven to be extremely useful in providing a relatively accurate and reproducible index of biologic age in this system.

Quantitative grain counts using a Vickers M-85 scanning microspectrophotometer revealed that under these conditions early-passage cells on the average incorporated more ^{3}H-thymidine than late-passage cells. Cytokinetic analysis by the percent-labeled-mitoses method indicated that the average generation times of early- and late-passage cells were approximately 18 and 30 hours, respectively. The median duration of the S phase remained relatively constant during aging while G_1 became progressively longer, accounting for the bulk of the increase in generation time. Thus, re-entry of cells into S could account for the observed differences in labeling intensity. However, a slight but consistent shift to the lower labeling classes was also observed after a 2-hour pulse. It was also found that the reduced rate of incorporation of ^{3}H-thymidine in late-passage cells can lead to an underestimate of the number of labeled cells if proper consideration is not given to choice of counting threshold and exposure duration. Additional studies are currently underway in an attempt to resolve the nature of these apparently age-related changes in ^{3}H-thymidine metabolism.

Studies on the Kinetics of "Nonproliferating" Cells in Solid Tumors Aided By Autoradiography

Milan Potmesil and Anna Goldfeder

Cancer and Radiobiological Research Laboratory, Department of Biology, New York University, and the City of New York Health and Hospitals Corporation, New York, NY.

The problem of "nonproliferating" cells, that is, cells apparently not participating in progression through the cell cycle, is becoming increasingly important. Since it is strongly suggested that nonproliferating cells of solid tumors constitute a heterogeneous population, close characterization of their various subpopulations according to age, drug sensitivity, repair potential, or clonogenicity would be of significant value. Studies using the demonstration of nucleoli and autoradiographic labeling of cells have revealed that nucleolar morphology is also applicable for classification of proliferating and nonproliferating cells in normal tissue and for studies of their kinetics (Potmesil and Goldfeder, J Cell Biol 53:823, 1972; Exp Cell Res 77:31, 1973). Quantitative data on the proliferating and the nonproliferating pool of parenchymal tumor cells assessed in vivo have been presented (Potmesil and Goldfeder, Cancer Res 31:789, 1971). In the present study, paren-

chymal cells of isogenic mouse mammary carcinomas were identified by their different nucleolar morphology. Depending on the tumor line, 20%–46% of cells of the first pool with large dense nucleoli incorporated a pulse label of ^{3}H-TdR. Cells of the second pool had either trabeculate or ring-shaped nucleoli. Autoradiographically, these cells showed no incorporation of ^{3}H-TdR in pulse-label experiments. Trabeculate and ring-shaped nucleoli on one side and dense nucleoli on the other not only had a distinctly different structure, but also differed in their size. Size-distribution curves suggest that this morphologic distinction can be utilized in semiautomatic or automatic screening techniques. Before the completion of cell division, nucleoli were re-organized and could be identified either as trabeculate and ring shaped, or as large nucleoli with a net of trabecules. Nucleoli of the latter type were gradually transformed, in intermitotic cells, to dense nucleoli. This indicated that cells with trabeculate and ring-shaped nucleoli were present at the beginning of G_1 phase as products of symmetric or asymmetric divisions. Means of silver grain counts increased with prolonged exposure of the autoradiographic emulsion only above cells with dense nucleoli, pulse labeled with ^{3}H-TdR, but remained unchanged above cells with trabeculate or ring-shaped nucleoli. Different threshold levels of grain counts in autoradiographs exposed for 1–9 weeks did not reveal any tritium uptake in cells with trabeculate or ring-shaped nucleoli. Thus, even low levels of DNA synthesis, which would indicate residency of cells with trabeculate and ring-shaped nucleoli in S phase, were not demonstrable.

When ^{3}H-TdR was injected repeatedly at 4-hour intervals into tumor-bearing mice, labeled progenitor cells would divide and newly generated daughter cells with trabeculate or ring-shaped nucleoli would share the label. In the course of repeated ^{3}H-TdR injections, all cells with dense nucleoli became labeled at 36–60 hours, depending on the tumor line. At this time, all mitotic figures were also labeled and only cells with trabeculate or ring-shaped nucleoli constituted the unlabeled population. Based on the aforementioned observations, it can be concluded that parenchymal cells with dense nucleoli represent the proliferating pool, and that cells with trabeculate or ring-shaped nucleoli are derived from proliferating cells, with at least part of them confined in a G_1-like phase. These cells appear to be replaced steadily with an average transit time of 84 hours and longer. Such data indicate that a considerable portion of cells with trabeculate or ring-shaped nucleoli are not lost rapidly via cell death, metastases, or transformation into cells of a different type. The demonstration of nucleoli and autoradiographic labeling has been currently applied in studies of cell kinetics in therapeutically treated tumors (Potmesil et al, Cell Tissue Kinet 8:369, 1975). (This investigation was supported by Public Health Service grant R01 CA-12076-04A2 from the National Cancer Institute, National Institutes of Health, Department of Health, Education, and Welfare.)

Semi-Automated Cell and Grain Counting

P. A. Bunn, S. S. Ford, and S. E. Shackney

Division of Cancer Treatment, National Cancer Institute, Bethesda, Md 20014.

A commercially available bacterial colony counter has been adapted for the counting of radioautographic grains over individual cells in smears and for counting cells in histologic sections. For the counting of radioautographic grains the variation between the visual counts of two observers, the variation between two instrument counts, and the variation between the visual and instrument counts were compared. The correlation coefficient for the two instrument counts ($r = 0.974$), the two visual observations ($r = 0.999$), and the instrument and visual counts ($r = 0.998$) were quite similar. It was concluded that the instrument was as consistent and accurate as the visual observations. The instrument counts were obtained more rapidly than the visual counts and were associated with less operator fatigue. The performance of the instrument in counting cells in mouse bone marrow sections was less accurate than in counting radioautographic grains, but results were quite acceptable. The correlation coefficient between instrument and visual counts was 0.968. Data on bone marrow cellularity were obtained far more rapidly than with existing quantitative methods.

Lymphocyte PHA and PPD Stimulation as an In Vitro Model for Recruitment: Proliferation Kinetics of the System

J. L. Bernheim, R. Dorian, M. Djobadze, and J. Mendelsohn

Department of Medicine M-013, University of California, San Diego, La Jolla, Calif 92093.

The kinetics of DNA synthesis and cell proliferation of lymphocytes stimulated by mitogens and antigens are incompletely understood. Although after in vitro PHA stimulation logarithmic growth in dilute culture conditions has been observed (1,2), most studies have reported little or no net increase

in cell numbers (4,5) or total culture DNA content (3) despite high labeling indices (6). Also, three laboratories have reported selective secretion of newly synthesized DNA into the culture medium (5,7,8). The latter phenomenon was felt not to be attributable to cell death although this could not be measured accurately. In both cases, the DNA synthesis rate would be expected to exceed the mitotic rate. This study attempts to clarify the apparent discrepancies by measuring the number of cells entering the DNA synthesis phase (S)

$$= \frac{\text{Labeling index} \times \text{cell number}}{\text{Duration of S} + \text{duration of } ^3\text{H-TdR pulse}},$$

the number of cells dividing

$$= \frac{\text{Mitotic index} \times \text{cell number}}{\text{Duration of colcemid block}},$$

and cell death, as defined by the difference between expected and observed cell number.

PHA stimulation is shown to cause a steep initial rise in the numbers of cells in cycle and the incorporation of ^{3}H-thymidine, representing polyclonal activation. These numbers decrease after the fourth day, as cell death increases. The percent labeled mitosis curve shows S to be 9 hours, G_2, 5 hours, and G_1 + M, 3–4 hours.

Cell death was evaluated by whole population kinetics. For example, in an experiment with an initial cell number of 2.30×10^5 cells/ml, the final cell number after 7 days of culture in the presence of PHA was 3.12×10^5 cells/ml, and the total number of mitoses was 2.43×10^5 cells/ml. Hence, total cell death was calculated as 1.61×10^5 cells/ml. The consecutive percentages of trypan-blue positive cells were measured over the culture period; these data plus the total dead cell number were used to calculate a disintegration time of 12 hours for trypan-blue positive cells. This type of actuarial analysis is valid if the whole cell population has only one unvariable disintegration time for dead cells. Subsequent work has revealed subpopulations with long and short disintegration times, with a weighted mean of 22 hours. These data make more complex analyses necessary but lead to the same overall conclusion (9). This is in fair agreement with experimental data on cell death in which cell-disintegration time after KCN or irradiation was computed (9). Assuming a T_S of 9 hours, no deficit of mitoses significantly higher than attributable to cell death between S and M was demonstrated, leaving no room for a population synthesizing non-premitotic DNA.

The secondary antigen response to PPD is characterized by logarithmic increase of ^{3}H-thymidine counts and labeled cell number from Day 2 onward, with a doubling time between 7 and 16 hours, yielding measurable increases in cell numbers from Day 6 onward. Assuming a T_S of 6 or 7 hours, as inferred from cinematographic observation (10), of cells stimulated with PPD, the comparison of mitotic and S rate would yield a deficit of proliferation, 20%–40% of the cells which enter S not going on to mitosis. However, if a significant number of cells had a longer T_S with a mean of about 10 hours, and if there were recruitment of other cells by the originally reactive clones, there would be no deficit and all DNA synthesis would be premitotic. These questions are under continued investigation. (Supported by Public Health Service grants CA-11971 and CA-70891 from the National Cancer Institute, National Institutes of Health, Department of Health, Education, and Welfare, and Fonds voor Geneeskundig Wetenschappelijk Onderzoek 30024.75.)

REFERENCES

1. BERNHEIM JL, and MENDELSOHN J. Clin Res 23:401A, 1975.
2. STEWART CC, CRAMER SF, and STEWARD PG. Cell Immunol 16:237, 1975.
3. SCHELLEKENS PTA, and EIJSVOOGEL VP. Clin Exp Immunol 3:571, 1968.
4. POLGAR PR, and KIBRICK S. Nature 225:857, 1970.
5. ROGERS JC, BOLDT D, KORNFELD S, ET AL. Proc Natl Acad Sci USA 69:1685, 1972.
6. SÖREN L. Exp Cell Res 79:350, 1973.
7. SARMA DSR, and ZUBROFF J. Immunol Commun 2:277, 1973.
8. HÖSSLI D, and WAKSMAN B. Fed Proc 34:1011, 1975.
9. BERNHEIM JL, MENDELSOHN J, KELLEY M, ET AL. Submitted for publication.
10. MARSHALL WH, VALENTINE FT, and LAWRENCE HS. J Exp Med 130:327, 1969.

Subject Index

A

ABDV (adriamycin, bleomycin, DTIC, and vinblastine)
alternating with MOPP (mechlorethamine, vincristine, procarbazine, and prednisone) and radiotherapy for advanced Hodgkin's disease, 1217
versus MOPP (mechlorethamine, vincristine, procarbazine, and prednisone) in the treatment of Hodgkin's disease, 205
Acrolein, biologic activity in vitro compared to other derivatives and possible metabolites of cyclophosphamide, 373
Actinomycin D (NSC-3053)
combined with cyclophosphamide and vincristine in the treatment of advanced sarcomas: a comparative clinical trial with other single-agent and combination therapy, 1385
combined with cytosine arabinoside: use of cell-cycle information in the preparation of drug combinations, 1813
combined with DTIC and BCNU in the treatment of advanced malignant melanoma, 33
combined with DTIC and BCNU in the treatment of malignant melanoma, 205
in vitro response of mammalian cells to drug-induced potentially lethal and sublethal damage, 1799
Limulus amebocyte lysate assay used to detect the presence of bacterial endotoxin in various lots of, 9
single-dose, pharmacokinetically based phase I–II study of, 289
Adenocarcinoma 755 (*see also* Tumor systems in animals)
effects on macromolecular synthesis in cell culture and evidence for alkylating activity, 1317
studies with 2,5-piperazinedione, 3,6-bis(5-chloro-2-piperidyl)-, dihydrochloride: kinetic and biologic effects in cultured cells, 1307
Adrenalectomy *see* Surgery
Adriamycin (NSC-123127)
activity of anthracyclines, particularly cinerubin A, against a subline of P388 leukemia resistant to, 99
alone and combined with DTIC in the treatment of various sarcomas, 199
alone versus 5-FU combined with cyclophosphamide in the treatment of metastatic prostate cancer, 115
amelioration of toxicity by α-tocopherol (vitamin E), 961
arrested and cycling CHO cells as a kinetic model: studies with, 1829
cardiotoxicity, echocardiographic evaluation of, in children, 1281
cardiotoxicity, noninvasive monitoring of, by "Sphygmo-Recording" of the pulse wave delay (QK_4 interval), 1239
and CCNU in advanced breast cancer, 1687
combined with bleomycin and vinblastine for advanced testicular tumors, 953
combined with bleomycin, vinblastine, and DTIC (ABVD) in the treatment of Hodgkin's disease, 205
combined with CCNU and hexamethylmelamine in the treatment of lung cancer, 269
combined with *Corynebacterium parvum* in experimental tumor systems, 823
combined with cyclophosphamide, methotrexate, and procarbazine (CAMP) in the effective treatment of metastatic non-oat cell lung carcinoma, 1225
combined with DTIC against B16 melanoma and C3H mammary adenocarcinoma, 135
combined with DTIC and vincristine in the treatment of advanced sarcomas: a comparative clinical trial with other single-agent and combination therapy, 1385
combined with DTIC in the treatment of soft tissue sarcomas, 205
combined with vinblastine and procarbazine in a phase II study of small cell carcinoma of the lung, 1263
compared to activity of cinerubin A against transplanted animal tumors, 99
in vitro response of mammalian cells to drug-induced potentially lethal and sublethal damage, 1799
Limulus amebocyte lysate assay used to detect the presence of bacterial endotoxin in various lots of, 9
phase II trials, combined with cyclophosphamide in the treatment of various solid tumors, 77
phase II trial of, combined with methotrexate and 5-FU in the treatment of lung adenocarcinoma, 623
pigmentation of the tongue after treatment with, 1402
prevention by coenzyme Q_{10} of the inhibition of coenzyme Q_{10} enzymes by, 223
proliferative character and growth modes of neoplastic disease in animals as determinants of chemotherapeutic efficacy, 1761
rapid analytic method for, and metabolites in human plasma by a thin-film fluorescence scanner, 1611
response of metastatic malignant carcinoid tumor to, 273
studies of, using a weekly regimen demonstrating its clinical effectiveness and lack of cardiac toxicity, 813
in the treatment of far-advanced lung cancer, 939
used sequentially with cyclophosphamide, vincristine, bleomycin, methotrexate, and methyl-CCNU in the treatment of advanced, recurrent, squamous cancer of the head and neck, 103
plus vincristine and bleomycin compared to ICRF-159 alone in non-small cell lung cancer, 947
plus vincristine and bleomycin compared to VP-16-213 alone and vincristine plus cyclophosphamide and methotrexate for advanced small cell cancer, 949

Adverse reactions *see* Toxic reactions in man
Aldophosphamide
pharmacokinetics of, in vivo, 415
synthesis, characterization, and comparison with "Hohorst's aldophosphamide," 317
Aminopterin (NSC-739), competitive dehydrofolate reductase binding assay of, 615
Anhydro-ara-5-fluorocytidine (2,2′-anhydro-1-β-D-arabinofuranosyl-5-fluorocytosine) (NSC-166641)
compared to cytosine arabinoside in the treatment of murine brain tumor, 875
effects on ultrastructure of submaxillary salivary glands from mice treated with, compared to effects of cytosine arabinoside and cyclocytidine, 881
phase I study of weekly administration of, 281
Antibiotics (*see also* specific drugs), yeast mutants with distorted cell membranes as tests in the screening for, 637
5-Arylpyrimidine antifolates (*see* DDMP)
L-Asparaginase (NSC-109229)
activity in acute nonlymphocytic leukemia, 966
combined with vincristine and prednisone, in a study of cytosine arabinoside synchronization of leukemic cells, for remission induction in advanced acute leukemia in children, 591
comparative experimental evaluation of immunodepressive and toxic effects of, from *Escherichia coli* and from *Erwinia carotovora*, 255
Limulus amebocyte lysate assay used to detect the presence of bacterial endotoxin in various lots of, 9
L-Asparagine synthetase, inhibitors of, in vitro, 1493
5-Azacytidine (NSC-102816)
dihydro-5-azacytidine hydrochloride, a biologically active and chemically stable analog of, 1671
Limulus amebocyte lysate assay used to detect the presence of bacterial endotoxin in various lots of, 9
symptomatic hypophosphatemia secondary to therapy for acute nonlymphocytic leukemia, 1400

B

Bacillus Calmette-Guérin
plus BACON in the treatment of head and neck cancer, 535
immunotherapy in combination with DTIC in the treatment of malignant melanoma, 177
as treatment for malignant melanoma, 159
BACON (bleomycin, adriamycin, CCNU, vincristine, and mechlorethamine), alone versus BACON plus Bacillus Calmette-Guérin in the treatment of head and neck cancer, 535
BCNU (NSC-409962)
in combinations with DTIC plus vincristine and DTIC plus hydroxyurea in the treatment of metastatic malignant melanoma, 601
combined with DTIC and actinomycin D in the treatment of malignant melanoma, 205
combined with DTIC and vincristine, and actinomycin D and DTIC in the treatment of advanced malignant melanoma, 33
combined with DTIC in the treatment of malignant melanoma, 193
combined with DTIC and vincristine in the treatment of malignant melanoma, 205
combined with DTIC and vincristine in the treatment of metastatic cutaneous malignant melanoma, 1381
combined with 5-FU, DTIC, and vincristine in the treatment of advanced colorectal cancer, 29
combined with procarbazine in the treatment of malignant brain tumors, 243
combined with vincristine and DTIC, review of activity in malignant melanoma, 1141
effects on transcription in Ehrlich cells compared with cyclophosphamide and mechlorethamine, 471
intracarotid toxicity study of, in rhesus monkeys, 541
liposomal activation of, against Ehrlich ascites tumor and L1210 leukemia, 617
in malignant lymphomas, 739
phase II study of, combined with DTIC and hydroxyurea with or without vincristine in the treatment of disseminated melanomas, 189
phase II study of, combined with DTIC and vincristine with or without chlorpromazine in the treatment of disseminated melanomas, 189
proliferation character and growth modes of neoplastic disease in animals as determinants of chemotherapeutic efficacy, 1761
pulmonary toxicity in long-term administration of, 1691
size dependence of the response of Lewis lung tumors to, 1743
studies with 2,5-piperazinedione, 3,6-bis(5-chloro-2-piperidyl)-, dihydrochloride; biochemical and therapeutic effects in L1210 leukemias sensitive and resistant to alkylating agents: comparison with melphalan and cyclophosphamide, 1325
in the treatment of advanced Hodgkin's disease: remission induction and maintenance, 761
use in the LSA tumor model to study the growth characteristics of tumor cells by analysis of DNA distribution, 579
plus vincristine versus DTIC alone in the treatment of metastatic malignant melanoma, 595
1,2-Bis diazoacetyl ethane, antitumor activity of, in animals, 1601
Bladder cancer *see* Cancer, bladder
Bleomycin (NSC-125066)
alone followed by a combination of cyclophosphamide, vincristine, methotrexate, and 5-FU in the treatment of non-oat cell lung cancer, 61
as a cause of soft tissue metastatic calcification after treatment for lymphoma, 963
combined with adriamycin and vinblastine for advanced testicular tumors, 953
combined with adriamycin, vinblastine, and DTIC (ABVD) in the treatment of Hodgkin's disease, 205
combined with CCNU and vincristine in the treatment of stage III melanoma, 1273
combined with vinblastine and *cis*-dichlorodiammineplatinum(II) in the treatment of various cancers, phase I study, 91
dose fractionation does not prevent repair of potentially lethal damage induced by, in vivo, 259

Limulus amebocyte lysate assay used to detect the presence of bacterial endotoxin in various lots of, 9
recovery of mammalian cells in culture from induced, potentially lethal damage, 1791
used sequentially with cyclophosphamide, vincristine, methotrexate, adriamycin, and methyl-CCNU in the treatment of advanced, recurrent, squamous cancer of the head and neck, 103
plus vincristine and adriamycin compared to ICRF-159 alone in non-small cell lung cancer, 947
plus vincristine and adriamycin compared to VP-16-213 alone and vincristine plus cyclophosphamide and methotrexate in advanced small cell lung cancer, 949
B16 melanoma *see* Tumor systems in animals
Brain cancer *see* Cancer, brain
Breast cancer *see* Cancer, breast
Bronchogenic carcinoma *see* Cancer, lung
Bruceantin (NSC-165563)
a new plant-derived tumor inhibitor; mechanism of action, 1115
pharmacology of, 1127
Butocin (NSC-172755), results of testing against tumors in animals, 215

C

Calusterone (NSC-88536), in advanced breast cancer, 220
CAMP (cyclophosphamide, adriamycin, methotrexate, and procarbazine), for metastatic non-oat cell lung carcinoma, 1225
Camptothecin (NSC-100880), pharmacology of, 1127
Cancer (nonhematologic)
bladder, advanced, *cis*-dichlorodiammineplatinum(II) in, 917
brain
clinical studies with the nitrosoureas, 713
development of acute nonlymphocytic leukemia associated with previous nitrosourea therapy in 2 patients with, 1257
malignant, BCNU combined with procarbazine in the treatment of, 243
nitrosoureas in the treatment of, 719
role of surgery in, 717
breast
adrenalectomy and oophorectomy plus limited-term chemotherapy (cyclophosphamide, vincristine, methotrexate, and 5-FU) in the treatment of, 857
advanced, adriamycin and CCNU in the treatment of, 1687
advanced, comparison of tamoxifen and conventional hormone therapy (diethylstilbestrol) in patients with, 1461
advanced, evaluation of tamoxifen dose in, 1451
advanced, overview of EORTC clinical trials with tamoxifen in patients with, 1463
advanced, phase II evaluation of VP-16-213 and cytembena in, 633
advanced, phase II study of 5-FU combined with methotrexate, vincristine, cyclophosphamide, and prednisone in the treatment of: 2 years' followup, 107
advanced, phase II trial of cytembena in, 1655
advanced, therapeutic use of tamoxifen in: correlation with biochemical parameters, 1437
disseminated, 5-FU, cyclophosphamide, vincristine, and methotrexate, followed by citrovorum factor in the treatment of, combined with hormonal therapy, 85
evaluation of an intermittent schedule of dibromodulcitol in, 1593
interaction of antiestrogens with, in long-term tissue culture, 1421
isophosphamide in the treatment of, 955
metastatic, response to medroxyprogesterone acetate as secondary hormone therapy for, in postmenopausal women, 251
review of Cooper regimen in the treatment of, 1141
review of vincristine in the treatment of, 1141
role of radioautographic studies in clinical investigative oncology and chemotherapy in, 1873
stage IV, phase II study of tamoxifen in 74 patients with, 1431
stage IV, tamoxifen-induced remissions in, 1445
cervical, squamous cell, porfiromycin in the treatment of, 907
colon, hepatic artery infusion of 5-FUDR after prior systemic 5-FU in patients with, 1277
colorectal
advanced, 5-FU, BCNU, DTIC, and vincristine in the treatment of, 29
advanced, 5-FU, methyl-CCNU, and vincristine in: phase II study utilizing weekly 5-FU, 1597
advanced, methyl-CCNU in the treatment of, after 5-FU therapy, 235
metastatic, phase II study of ICRF-159 in patients with, previously exposed to systemic chemotherapy, 1395
phase II studies of dianhydrogalactitol and VP-16-213 in, 1247
staging, is there a role for liver biopsy?, 295
treated with methyl-CCNU and β-2'-deoxythioguanosine, 965
gastrointestinal
advanced, 5-FU alone compared to 5-FU and methyl-CCNU in the treatment of, 733
advanced, nitrosoureas in the treatment of, 769
advanced, phase II study using methyl-CCNU, 285
advanced, randomized comparison of melphalan and 5-FU in the treatment of, 1267
combination chemotherapy with mitomycin C, 5-FU, and cytosine arabinoside, 1373
hydrazine sulfate in, 933
nitrosoureas alone and in combination in the treatment of, 729
head and neck
randomized study of BACON versus BACON plus bacillus Calmette-Guérin in the treatment of, 535
squamous advanced recurrent, sequential combination chemotherapy for, 103
squamous cell, porfiromycin in the treatment of, 907
large intestine, adenocarcinoma, evaluation of daunorubicin in, 1667

lung
adenocarcinoma and large cell, methyl-CCNU, 5-FU, and vincristine in the treatment of, 1393
adenocarcinoma, phase II trial of 5-FU, adriamycin, and methotrexate in the treatment of, 623
advanced small cell, VP-16-213 versus polychemotherapy (vincristine plus cyclophosphamide and methotrexate; vincristine plus bleomycin and adriamycin) in, 949
CCNU combined with hexamethylmelamine and adriamycin in the treatment of, 269
chemotherapy for, with various drugs, 1479
combined surgery and chemotherapy for, 1489
cytologic diagnosis of, 1467
far-advanced, adriamycin in the treatment of, 939
general principles of surgical treatment of, 1473
heparin and cyclophosphamide in the treatment of, 575
histologic classification of, 1469
hydrazine sulfate in, 933
inoperable squamous and large cell, mechlorethamine plus CCNU in the treatment of, 625
isophosphamide in the treatment of, 955
metastatic non-oat cell, combination of cyclophosphamide, adriamycin, methotrexate, and procarbazine (CAMP) in the effective treatment of, 1225
nitrosourea combinations in, 757
nitrosoureas as single agents in, 753
non-oat cell, bleomycin alone followed by cyclophosphamide, vincristine, methotrexate, and 5-FU in the treatment of, 61
non-small cell, ICRF-159 versus vincristine plus bleomycin and adriamycin in, 947
occurrence of, according to stage and determination of its dissemination, 1471
phase II evaluation of *cis*-dichlorodiammineplatinum(II) in, 1679
prerequisites for effective radiotherapy for, 1475
small cell anaplastic, vincristine in the treatment of, 239
small cell and adenocarcinoma, cyclophosphamide plus CCNU compared to cyclophosphamide alone in the treatment of, 925
small cell, conservative treatment of, 1483
small cell, phase II study of vinblastine, adriamycin, and procarbazine in the treatment of, 1263
squamous cell, porfiromycin in the treatment of, 907
undifferentiated, combination chemotherapy and radiotherapy for, 1487
lymphoreticular, summary of clinical results of phase II study in patients with, using the so-called synchronization therapy with vincristine and cyclophosphamide, 1959
oat cell, extensive, prolonged survival in patients treated with radiotherapy combined with methotrexate, vincristine, and cyclophosphamide, 221
ovarian
adenocarcinoma, advanced, phase II study of *cis*-dichlorodiammineplatinum(II) in, 55
advanced, phase II trial of cytembena in, 1655
epithelial, disseminated, phase I and II study of cytembena in the treatment of, 1389
isophosphamide in the treatment of, 955
methotrexate plus citrovorum factor rescue, alone and combined with cyclophosphamide, in the treatment of, 527
role of radioautographic studies in clinical investigative oncology and chemotherapy, 1873
pancreas, advanced phase II study of methyl-CCNU in, 1659
prostate, metastatic, adriamycin versus 5-FU and cyclophosphamide in the treatment of, 115
squamous cell, various sites, porfiromycin in the treatment of, 907
testicular, advanced, evaluation of bleomycin, adriamycin, and vinblastine in combination therapy for, 953
transitional cell, porfiromycin in the management of, a phase II study, 907
Carboxycyclophosphamide, qualitative and quantitative investigations by field-desorption mass spectrometry, 501
Carboxyphosphamide, permeation into animal tumor cells, 423
Carcinoid tumors, metastatic malignant, response to adriamycin, 273
Carcinoma *see* Cancer, type of
CCNU (NSC-79037)
and adriamycin in advanced breast cancer, 1687
in combination with DTIC and vincristine in the treatment of metastatic malignant melanoma, 601
combined with adriamycin and hexamethylmelamine in the treatment of lung cancer, 269
combined with mechlorethamine in the treatment of inoperable squamous and large cell carcinoma of the lung, 625
combined with vincristine and bleomycin in the treatment of stage III melanoma, 1273
plus cyclophosphamide compared to cyclophosphamide alone in the treatment of inoperable small cell carcinoma and adenocarcinoma of the lung, 925
in vitro response of mammalian cells to drug-induced potentially lethal and sublethal damage, 1799
Cell kinetics
age-dependent survival and cell-cycle progression of cultured cells exposed to chemotherapeutic drugs, 1707
arrested and cycling CHO cells as a kinetic model: studies with adriamycin, 1829
and cancer therapy: history, present status, and challenges, 1699
combined effects of cytosine arabinoside combined with either 6-thioguanine or 6-mercaptopurine; dose and time survival curves for leukemic colony-forming units and normal hematopoietic colony-forming units in mice, 1925
comparative chemosensitivity of exponential- versus plateau-phase cells in both in vitro and in vivo model systems, 1719
comparison of cell proliferation kinetics in human and experimental tumors: response to irradiation, 1887
computer simulation of leukemia therapy: combined pharmacokinetics, intracellular enzyme kinetics, and cell kinetics of the treatment of L1210 leukemia by cytosine arabinoside, 1723
cytotoxic damage and repair, 1777

effects of surgery on cell kinetics of residual tumors in animals, 1749
effects of tumor bearing on the dynamics of host hemopoietic cells, 1781
evidence for recruitment and synchronization in leukemia and solid tumors, 1841
investigation on pharmacologic induction of partial synchronization of tumor cell proliferation: its relevance for cytostatic therapy, 1959
in vitro responses of mammalian cells to drug-induced potentially lethal and sublethal damage, 1799
kinetic aids to proper chemotherapeutic scheduling: labeled nucleoside incorporation studies in vivo, 1947
kinetic response of human leukemic and lymphoma cells in vivo to combination chemotherapy using flow microfluorometry, 1937
mathematic models of cell synchrony and drug scheduling, 1899
physical-chemical characterization of living cells by laser-flow microfluorometry, 1819
proliferative character and growth modes of neoplastic disease as determinants of chemotherapeutic efficacy, using cyclophosphamide, BCNU, and adriamycin, 1761
rapid methods for utilizing cell kinetics for treatment in the C3H/He spontaneous mammary tumor: effects of vincristine, 1913
recovery of cells from induced, potentially lethal damage, 1791
resting cells in L1210 and JB-1 ascites tumors with special emphasis on recycling, 1861
role of radioautographic studies in clinical investigative oncology and chemotherapy, 1873
size dependence of the response of Lewis lung tumors to BCNU, 1743
synchronization with phase-specific agents in leukemia and correlation with clinical response, 1845
use of cell-cycle information in the preparation of drug combinations: results with cytosine arabinoside plus actinomycin D, 1813
Central nervous system, nitrosourea pharmacodynamics in relation to the, 725
Cephalotaxus, source of homoharringtonine and related anticancer alkaloids, 1157
Cervical cancer *see* Cancer, cervical
C3H/He *see* Tumor systems in animals
Chinese hamster ovary (CHO) cells
arrested and cycling cells as a kinetic model: studies with adriamycin, 1829
in vitro response to drug-induced potentially lethal and sublethal damage, 1799
Chlorambucil (NSC-3088), aspects of the teratology of, compared to cyclophosphamide, 477
Chloroplatinic acid (NSC-4958), nephrotoxicity of, in animals, 1675
Chlorozotocin, pharmacology of, 801
Chlorpromazine, combined with DTIC, BCNU, and vincristine versus the 3 drugs alone in the treatment of disseminated melanoma, 189
C3H mammary carcinoma *see* Tumor systems in animals
Chondrosarcoma *see* Tumor systems in animals
Chromomycin A_3 (NSC-58514), phase I alternate-day dose study of, 1251
CI-628, interaction with human breast cancer in long-term tissue culture, 1421
Cinerubin A (NSC-18334), activity of, against an adriamycin-resistant subline of P388 leukemia, 99
Citrovorum factor (NSC-3590)
plus 5-FU, cyclophosphamide, vincristine, and methotrexate and combined with hormonal therapy in the treatment of disseminated breast carcinoma, 85
plus methotrexate alone or with cyclophosphamide in the treatment of ovarian carcinoma, 527
preliminary studies of toxicity and responsiveness of Sarcoma 180 to DDMP combined with, 547
Clomiphene citrate, interaction with human breast cancer in long-term tissue culture, 1421
Coenzyme Q_{10} (NSC-140865), used to prevent the inhibition by adriamycin of coenzyme Q_{10} enzymes, 223
Colon cancer *see* Cancer, colon
Colorectal cancer *see* Cancer, colorectal (*see also* other individual sites)
Corynebacterium parvum, alone and in combination with adriamycin in experimental tumor systems, 823
Cyclocytidine (NSC-145668)
cardiovascular effects of, 1663
effects on ultrastructure of submaxillary salivary glands from mice treated with, compared to effects of cytosine arabinoside and anhydro-ara-5-fluorocytidine, 881
myelotoxicity and orthostatic hypotension of, 215
phase I–II study of, combined with DTIC in disseminated malignant melanoma, 1369
Cyclophosphamide (NSC-26271)
alone compared to cyclophosphamide and CCNU in the treatment of inoperable small cell carcinoma and adenocarcinoma of the lung, 925
approaches to the pharmacokinetics of, quantitation of metabolites, 403
aspects of the teratology of, compared to chlorambucil, 477
biologic activity in vitro of 2 derivatives and 6 possible metabolites of, 373
characterization of metabolites and related derivatives of, by field-desorption and electron-impact mass spectrometry, 509
combined with actinomycin D and vincristine in the treatment of advanced sarcomas: a comparative clinical trial with other single-agent and combination therapy, 1385
combined with adriamycin, methotrexate, and procarbazine (CAMP) in the effective treatment of metastatic non-oat cell lung carcinoma, 1225
combined with citrovorum factor rescue and methotrexate in the treatment of ovarian cancer, 527
combined with 5-FU versus adriamycin alone in the treatment of metastatic prostate cancer, 115
combined with heparin in the treatment of lung cancer, 575
combined with radiotherapy for undifferentiated lung cancer, 1487
combined with radiotherapy, vincristine, and metho-

trexate in the treatment of extensive oat cell carcinoma, 221
combined with surgery for lung cancer, 1489
combined with vincristine and methotrexate in the treatment of soft tissue sarcomas, 205
combined with vincristine, methotrexate, and 5-FU following bleomycin alone in the treatment of non-oat cell lung cancer, 61
combined with vincristine, summary of clinical results of phase II study in patients with lymphoreticular tumors by the so-called synchronization therapy, 1959
comparative pharmacologic study in vitro and in vivo with, and its metabolites and plain nitrogen mustard compounds, 301
disposition of, in tumor-bearing mice by means of gas chromatography-chemical ionization-mass fragmentography, 493
effects of, alone or combined with vincristine and prednisone on some hepatic oxidations and conjugations, 1285
effects of, in the treatment of metastatic prostate adenocarcinoma in germfree rats, 619
effects on transcription in Ehrlich cells compared with mechlorethamine and BCNU, 471
plus 5-FU, vincristine, and methotrexate and combined with adrenalectomy and oophorectomy in patients with breast cancer, 857
plus 5-FU, vincristine, methotrexate, and citrovorum factor and combined with hormonal therapy in the treatment of disseminated breast cancer, 85
importance of pharmacokinetic studies on, in understanding its cytotoxic effect, 395
Limulus amebocyte lysate assay used to detect the presence of bacterial endotoxin in various lots of, 9
metabolites, deactivation of, by sulfhydryl compounds, 355
metabolites, identification and pharmacokinetics of, in vivo, 415
permeation of metabolites of, into animal tumor cells, 423
phase II study with, combined with 5-FU, methotrexate, vincristine, and prednisone in the treatment of advanced breast cancer: 2 years' followup, 107
phase II trials, combined with adriamycin in the treatment of various solid tumors, 77
pretreatment, sparing effect of, on animals lethally treated with γ-irradiation, 409
problem of oncostatic specificity of: studies on reactions that control the alkylating and cytotoxic activity, 309
proliferative character and growth modes of neoplastic disease in animals as determinants of chemotherapeutic efficacy, 1761
qualitative and quantitative investigations of cyclophosphamide, cyclophosphamide metabolites, and related compounds by field-desorption mass spectrometry, 501
related phosphoramide mustards—recent advances and historical perspective, 337
some studies on the distribution and effects of, in normal and neoplastic tissues, 459
2 stable Fenton oxidation products of, as precursors of 4-hydroxycyclophosphamide under physiologic conditions, 369
studies on 4-hydroperoxycyclophosphamide: a simple preparation method and its application for the synthesis of a new class of "activated" sulfur-containing derivatives of, 429
studies on the enhancement of artificial lung metastasis after labeled cell inoculation, 465
studies on the in vivo formation of acrolein: 3-hydroxypropylmercapturic acid as an index of activation of, 327
studies on the selective action of: inactivation of the hydroxylated metabolite by tissue-soluble enzymes, 321
studies with 2,5-piperazinedione, 3,6-bis(5-chloro-2-piperidyl)-, dihydrochloride; biochemical and therapeutic effects in L1210 leukemias sensitive and resistant to alkylating agents: comparison with BCNU and melphalan, 1325
synthesis and structure-activity relationships of preactivated analogs of, tested against L1210 leukemia, 381
used sequentially with vincristine, bleomycin, methotrexate, adriamycin, and methyl-CCNU, in the treatment of advanced recurrent squamous cancer of the head and neck, 103
use of deuterated analogs in qualitative and quantitative investigations of the metabolism of, 483
plus vincristine and methotrexate compared to VP-16-213 alone and vincristine plus bleomycin and adriamycin in advanced small cell lung cancer, 949
X-ray crystallographic studies of derivatives of, 517
Cytembena (NSC-104801)
phase II evaluation of, with VP-16-213 in advanced breast cancer, 633
phase I and II study of, in disseminated epithelial ovarian cancers and sarcomas, 1389
phase II trial of, in advanced ovarian or breast cancer, 1655
Cytosine arabinoside (NSC-63878)
combined with actinomycin D: use of cell-cycle information in the preparation of drug combinations, 1813
combined with daunorubicin, 6-thioguanine, and pyrimethamine and compared to daunorubicin alone in the treatment of acute nonlymphocytic leukemia, 41
combined with 5-FU and mitomycin C in P815 ascites and solid mouse neoplasms, 1399
combined with 5-FU and mitomycin C in the treatment of gastrointestinal cancer, 1373
combined with 5-FU, 6-thioguanine, 6-mercaptopurine, 6-methylmercaptopurine riboside, and methotrexate, development of resistance to, in mice with L1210 leukemia, 23
combined with 6-mercaptopurine or 6-thioguanine; dose and time survival curves for leukemic colony-forming units and normal hematopoietic colony-forming units in mice, 1925
combined with vinblastine and procarbazine for reinduction of childhood acute myelocytic leukemia, 1683
compared to anhydro-ara-5-fluorocytidine in the treatment of murine brain tumor, 875
computer simulation of leukemia therapy: combined

pharmacokinetics, intracellular enzyme kinetics, and cell kinetics of the treatment of L1210 leukemia by, 1723
effects on ultrastructure of submaxillary salivary glands from mice treated with, compared to effects of cyclocytidine and anhydro-ara-5-fluorocytidine, 881
Limulus amebocyte lysate assay used to detect the presence of bacterial endotoxin in various lots of, 9
maintenance of remission in adult acute nonlymphocytic leukemia using intermittent courses of, with 6-thioguanine, 585
in sequence with daunorubicin in the treatment of acute myelogenous leukemia, 629
synchronization with, in patients with leukemia and correlation with clinical response, 1845
used to synchronize leukemic cells followed by vincristine, prednisone, and L-asparaginase for remission induction in advanced acute leukemia in children, 591

D

Daunorubicin (NSC-82151)
alone or combined with cytosine arabinoside, 6-thioguanine, and pyrimethamine in the treatment of acute nonlymphocytic leukemia, 41
evaluation of, in adenocarcinoma of the large intestine, 1667
Limulus amebocyte lysate assay used to detect the presence of bacterial endotoxin in various lots of, 9
in sequence with cytosine arabinoside in the treatment of acute myelogenous leukemia, 629
DDMP (pyrimidine, 2,4-diamino-5-(3,4-dichlorophenyl)-6-methyl-; NSC-19494), preliminary studies of toxicity and responsiveness of Sarcoma 180, used alone and combined with citrovorum factor, 547
3-Deazauridine (NSC-126849), synergistic interaction of, with D-galactosamine: enzyme pattern-directed chemotherapy, 835
4-Demethoxydaunorubicin (NSC-256439), synthesis and antitumor activity of, and 4-demethoxy-7,9-diepidaunorubicin and their β anomers, 829
4-Demethoxy-7,9-diepidaunorubicin, synthesis and antitumor activity of, and 4-demethoxydaunorubicin and their β anomers, 829
β-2′-Deoxythioguanosine (NSC-71261), combined with methyl-CCNU for advanced solid tumors, 965
Dianhydrogalactitol (NSC-132313)
phase I evaluation of, 611
phase II study in colorectal cancer, 1247
phase II study of, versus VP-16-213 in metastatic malignant melanoma, 1681
phase I trial of, administered iv in a weekly schedule, 895
preclinical toxicologic evaluation of, in dogs and monkeys, 1585
Dibromodulcitol (NSC-104800), evaluation of an intermittent schedule of, in breast cancer, 1593
***cis*-Dichlorodiammineplatinum(II) (NSC-119875)**
in advanced bladder cancer, 917
combined individually with 11 other drugs in vitro in a search for synergistic pairs, 1619
combined with bleomycin and vinblastine in the treatment of various cancers, phase I study, 91
nephrotoxicity of, in animals, 1675
phase II evaluation of, in lung cancer, 1679
phase II study of, in patients with advanced adenocarcinoma of the ovary, 55
Diethylstilbestrol (NSC-3070), compared with tamoxifen in advanced breast cancer, 1461
Dihydro-5-azacytidine hydrochloride (NSC-264880), a biologically active and chemically stable analog of 5-azacytidine, 1671
Dihydrofolate reductase, comparison of 4 antifolates as inhibitors of, 615
DON cells (Chinese hamster fibroblast line), in culture, use of cell-cycle information in the preparation of drug combinations: results with cytosine arabinoside plus actinomycin D, 1813
DTIC (NSC-45388)
alone or combined with methyl-CCNU or BCNU in the treatment of malignant melanoma, 193
alone or combined with adriamycin in the treatment of various sarcomas, 199
antitumor activity of, in animals, 135
clinical studies with, in various malignancies, 213
combined with adriamycin and vincristine in the treatment of advanced sarcomas: a comparative clinical trial with other single-agent and combination therapy, 1385
combined with adriamycin, bleomycin, and vinblastine (ABVD) in the treatment of Hodgkin's disease, 205
combined with adriamycin in the treatment of soft tissue sarcomas, 205
combined with bacillus Calmette-Guérin immunotherapy in the treatment of malignant melanoma, 177
combined with BCNU and actinomycin D in the treatment of malignant melanoma, 205
combined with BCNU and vincristine in the treatment of malignant melanoma, 205
combined with BCNU and vincristine in the treatment of metastatic cutaneous malignant melanoma, 1381
combined with 5-FU, BCNU, and vincristine in the treatment of advanced colorectal cancer, 29
combined with vincristine and BCNU, review of activity in malignant melanoma, 1141
combined with vincristine and BCNU, vincristine and hydroxyurea, and actinomycin D and BCNU in the treatment of advanced malignant melanoma, 33
experimental studies at Southern Research Institute with, 125
history and development of, 123
Limulus amebocyte lysate assay used to detect the presence of bacterial endotoxin in various lots of, 9
mechanism of action and pharmacology studies with, 149
phase I evaluation of, in the treatment of malignant melanoma, 183
phase I–II study of, combined with cyclocytidine in disseminated malignant melanoma, 1369
phase II study, combined with BCNU and hydroxyurea

with or without vincristine in the treatment of disseminated melanoma, 189
phase I study with, 189
phase II study in the treatment of Hodgkin's disease and other lymphomas, 189
phase II study of, combined with vincristine and BCNU with or without chlorpromazine in the treatment of disseminated melanomas, 189
randomized prospective trial of, alone versus BCNU plus vincristine in the treatment of metastatic malignant melanoma, 595
a review of its use in malignant melanoma, 165
studies on the mechanism of action of, 141
toxicity of, in man, 219
used alone and in various combinations with BCNU, CCNU, vincristine, and hydroxyurea in the treatment of metastatic malignant melanoma, 601

E

EARAD-1 leukemia *see* Tumor systems in animals
Echocardiography, evaluation of adriamycin cardiotoxicity in children, 1281
Ehrlich ascites tumor cells, inhibitors of hypoxanthine metabolism in, in vitro, 1567
Ehrlich carcinoma *see* Tumor systems in animals
Elephantin, a new plant-derived tumor inhibitor, mechanism of action, 1115
Elephantopin and derivatives, a new plant-derived tumor inhibitor, mechanism of action, 1115
Endotoxin, *Limulus amebocyte* lysate assay to detect the presence of, in chemotherapeutic agents, 9

F

Fluorescence scanner, thin-film, rapid analytic method for adriamycin and metabolites in human plasma, 1611
5-Fluorouracil (NSC-19893; 5-FU)
alone and compared to 5-FU and methyl-CCNU in advanced gastrointestinal cancer, 733
combined with cyclophosphamide versus adriamycin alone in the treatment of metastatic prostate cancer, 115
combined with cyclophosphamide, vincristine, and methotrexate following bleomycin alone in the treatment of non-oat cell lung cancer, 61
combined with DTIC, BCNU, and vincristine in the treatment of advanced colorectal cancer, 29
combined with 6-mercaptopurine, 6-thioguanine, 6-methylmercaptopurine riboside, cytosine arabinoside, and methotrexate, development of resistance to, in mice with L1210 leukemia, 23
combined with methyl-CCNU and vincristine in the treatment of adenocarcinoma and large cell carcinoma of the lung, 1393
combined with mitomycin C and cytosine arabinoside in P815 ascites and solid mouse neoplasms, 1399
combined with mitomycin C and cytosine arabinoside in the treatment of gastrointestinal cancer, 1373
combined with radiotherapy for undifferentiated lung cancer, 1487
compared to ftorafur; quantitative and qualitative differences in toxicity to mice, 1335
compared to ftorafur; therapeutic response and development of resistance in murine tumors, 1347
plus cyclophosphamide, vincristine, methotrexate, and citrovorum factor and combined with hormonal therapy in the treatment of disseminated breast cancer, 85
dissociation of uptake of, from intracellular pH in Walker 256 carcinosarcoma, 867
failure of, in the treatment of advanced colorectal carcinoma, followed by methyl-CCNU, 235
plus 5-FU, vincristine, and methotrexate and combined with adrenalectomy and oophorectomy in patients with breast cancer, 857
hepatic artery infusion of 5-FUDR after prior systemic treatment with, 1277
neurotoxicity from administration of, reproduced by mitomycin C, 293
phase II study with, combined with methotrexate, vincristine, cyclophosphamide, and prednisone in the treatment of advanced breast cancer: 2 years' followup, 107
phase II trial of, combined with adriamycin and methotrexate in the treatment of lung adenocarcinoma, 623
physiologic disposition of, compared to 5-FUDR in mice bearing solid L1210 lymphocytic leukemia, 845
serpentine supravenous hyperpigmentation, 639
randomized comparison with melphalan in the treatment of advanced gastrointestinal cancer, 1267
use of, in an elemental diet in animals during treatment with, 17
weekly, combined with methyl-CCNU and vincristine in advanced colorectal carcinoma, 159
Flow microfluorometry
abstracts from Workshop on Flow Microfluorometry, part of Proceedings of the Symposium on Cell Kinetics and Cancer Chemotherapy, 1981
kinetic response of human leukemic and lymphoma cells in vivo to combination chemotherapy using, 1937
laser, physical-chemical characterization of living cells by, 1819
Ftorafur (NSC-148958)
compared to 5-FU; quantitative and qualitative differences in toxicity to mice, 1335
compared to 5-FU; therapeutic response and development of resistance in murine tumors, 1347
5-FUDR (NSC-83097)
hepatic artery infusion of, after prior systemic 5-FU, 1277
physiologic disposition of, compared to 5-FU in mice bearing solid L1210 lymphocytic leukemia, 845

G

D-Galactosamine, synergistic interaction with 3-deazauridine: enzyme pattern-directed chemotherapy, 835

Gardner 6C3HED lymphosarcoma *see* Tumor systems in animals
Gastrointestinal cancer *see* Cancer, gastrointestinal (*see also* other individual sites)
Glioma, malignant *see* Cancer, brain
Glioma 261 *see* Tumor systems in animals
Gross leukemia *see* Tumor systems in animals
Guérin carcinoma *see* Tumor systems in animals

H

Harding-Passey melanoma *see* Tumor systems in animals
Head and neck cancer *see* Cancer, head and neck
Hemopoietic cells, effects of tumor bearing on the dynamics of, in animals, 1781
Heparin, combined with cyclophosphamide in the treatment of lung cancer, 575
Hepatic artery infusion, of 5-FUDR after prior systemic 5-FU, 1277
Hepatoma 72 *see* Tumor systems in animals
Hexamethylmelamine (NSC-13875), combined with CCNU and adriamycin in the treatment of lung cancer, 269
Hodgkin's disease
advanced, BCNU in the treatment of, remission induction and maintenance, 761
advanced, 8-drug combination chemotherapy (MOPP alternating with ABDV) and local radiotherapy in the treatment of, 1217
hydrazine sulfate in, 933
mechlorethamine, vincristine, prednisone, and procarbazine (MOPP) versus adriamycin, bleomycin, vinblastine, and DTIC (ABVD) in the treatment of, 205
nitrosoureas in, 781
phase II study of DTIC in the treatment of, 189
review of vinblastine and vincristine in the treatment of, 1141
sequential laparoscopy and laparotomy combined with bone marrow biopsy in staging, 1231
Homoharringtonine, and related *Cephalotaxus* alkaloids, antitumor activity, isolation, structural characterization, synthesis, biogenesis, and mechanism of action of, 1157
Hormones, therapy with, combined with combination chemotherapy in disseminated breast carcinoma, 85
Human epidermoid No. 2 tumor
comparison of cytotoxic and DNA synthesis inhibitory effects of 2,5-piperazinedione, 3,6-bis(5-chloro-2-piperidyl)-, dihydrochloride and 2,5-piperazinedione, 3,6-bis(1-azabicyclo[3.1.0]hex-2-yl)- in, 1317
studies with 2,5-piperazinedione, 3,6-bis(5-chloro-2-piperidyl)-, dihydrochloride: kinetic and biologic effects in cultured cells, 1307
Hydrazine sulfate (NSC-150014)
clinical data on the activity of, 933
clinical trial of, in solid tumors, 959
in the treatment of cancer, 964
4-Hydroperoxycyclophosphamide (NSC-181815)
biologic activity in vitro compared to other derivatives and possible metabolites of cyclophosphamide, 373
cytostatic and chemical properties of, compared to 4-hydroxycyclophosphamide, 369
permeation into animal tumor cells, 423
studies on, a simple preparation method and its application for the synthesis of a new class of "activated" sulfur-containing cyclophosphamide derivatives, 429
X-ray crystallographic studies of, 517
4-Hydroperoxyisophosphamide (NSC-227114)
stereochemistry, metabolism, and antitumor activity of, and its stereoisomer, 361
X-ray crystallographic studies of stereoisomers of, 517
4-Hydroxycyclophosphamide (NSC-196562)
anhydro-dimer, biologic activity in vitro compared to other derivatives and possible metabolites of cyclophosphamide, 373
anhydro-dimer, cytostatic and chemical properties of, compared to 4-hydroxycyclophosphamide, 369
characterization of, by field-desorption and electron-impact mass spectrometry, 509
deactivation of, by sulfhydryl compounds, 355
pharmacokinetics of, in vivo, 415
qualitative and quantitative investigations by field-desorption mass spectrometry, 501
synthesis and activity of in vitro, 429
3-Hydroxypropylmercapturic acid, as an index of cyclophosphamide activation, studies on the in vivo formation of acrolein, 327
Hydroxylamine mustard, biologic activity in vitro compared to other derivatives and possible metabolites of cyclophosphamide, 373
Hydroxyurea (NSC-32065)
combined with DTIC and vincristine in the treatment of advanced malignant melanoma, 33
combined with DTIC plus BCNU in the treatment of metastatic malignant melanoma, 601
phase II study, combined with BCNU and DTIC with or without vincristine in the treatment of disseminated melanomas, 189
synchronization with, in patients with leukemia and correlation with clinical responses, 1845
used sequentially with vincristine to enhance the degree of cell synchrony in animal tumors, 1959
use in the LSA tumor model to study the growth characteristics of tumor cells by analysis of DNA distribution, 579
Hyperthermia, used sequentially with irradiation, recovery of mammalian cells in culture from induced potentially lethal damage, 1791
Hypoxanthine metabolism, inhibitors of, in Ehrlich ascites tumor cells in vitro, 1567

I

ICRF-159 (NSC-129943)
phase II study of, in patients with metastatic colorectal carcinoma previously exposed to systemic chemotherapy, 1395
in the treatment of Kaposi's sarcoma, 111
versus vincristine plus bleomycin and adriamycin in non-small cell lung cancer, 947

Immunotherapy *see* Bacillus Calmette-Guérin and *Corynebacterium parvum*
Inosine dialdehyde (NSC-118994)
pharmacologic disposition of, in mice, rats, dogs, and monkeys, 555
protein cross-linking properties of, 563
Isophosphamide (NSC-109724)
biologic activity in vitro compared to other derivatives and possible metabolites of cyclophosphamide, 373
further experience with, in man, 955
studies on the clinical pharmacology and toxicology of, 445
studies on the human pharmacokinetics of, 451
studies on the metabolism of, in man, 437
synthesis and structure-activity relationships of preactivated analogs of, tested against L1210 leukemia, 381

J

Jatrophone, a new plant-derived tumor inhibitor: mechanism of action, 1115
JB-1 ascites tumor *see* Tumor systems in animals

K

Kaposi's sarcoma *see* Sarcoma, Kaposi's
4-Ketocyclophosphamide, biologic activity in vitro compared to other derivatives and possible metabolites of cyclophosphamide, 373

L

La leukemia *see* Tumor systems in animals
Lapachol (NSC-11905), pharmacology of, 1127
Laparoscopy, used sequentially with laparotomy combined with bone marrow biopsy in staging Hodgkin's disease, 1231
Laparotomy, used sequentially with laparoscopy combined with bone marrow biopsy in staging Hodgkin's disease, 1231
Large intestine cancer *see* Cancer, large intestine
Laser differential light-scattering bioassay, for methotrexate, 225
Leo-1031 (NSC-134087), study of, in the treatment of lymphocytic lymphoma and chronic lymphocytic leukemia, 277
Leukemia
acute
childhood, advanced, cytosine arabinoside synchronization of leukemic cells followed by vincristine, prednisone, and L-asparaginase for remission induction in, 591
childhood, late-stage, VM-26 in a phase I–II trial in the treatment of, 265
myelocytic, childhood, vinblastine, procarbazine, and cytosine arabinoside combined for reinduction of, 1683
myelogenous, sequencing of cytosine arabinoside and daunorubicin in, 629
nonlymphocytic
in adults, maintenance of remission, using intermittent courses of cytosine arabinoside and 6-thioguanine, 585
L-asparaginase activity in, 966
daunorubicin alone or combined with cytosine arabinoside, 6-thioguanine, and pyrimethamine in the treatment of, 41
developing in patients previously treated with nitrosoureas, 1257
symptomatic hypophosphatemia secondary to 5-azacytidine therapy of, 1400
role of radioautographic studies in clinical investigative oncology and chemotherapy in, 1873
VP-16-213 in the treatment of, 967
chronic lymphocytic, study of Leo-1031 in the treatment of, 277
evidence for recruitment and synchronization in, 1841
kinetic response of human cells in vivo to combination chemotherapy using flow microfluorometry, 1937
L1210 cells in culture, use of cell-cycle information in the preparation of drug combinations: results with cytosine arabinoside plus actinomycin D, 1813
synchronization with phase-specific agents in patients with, and correlation with clinical response, 1845
Levamisole (NSC-177023)
in clinical immunotherapy, 217
modulating effects of, on human lymphocyte response in vivo, 571
in a phase I trial, 963
Lewis lung carcinoma *see* Tumor systems in animals
Limulus amebocyte, used in an assay to detect the presence of bacterial endotoxin in chemotherapeutic agents, 9
Liposomal potentiation, of the antitumor activity of BCNU and mechlorethamine against Ehrlich ascites tumor and L1210 leukemia, 617
L1210 leukemia (*see also* Tumor systems in animals), amino acid-conferred resistance to melphalan: structure-activity relationship in cultured cells, 1363
LSA tumor model (a lymphoblastic lymphoma syngeneic for the C57BL mouse), growth characteristics of tumor cells by analysis of DNA distribution using mechlorethamine, BCNU, radiation, and hydroxyurea, 579
Lung cancer *see* Cancer, lung
L5178Y leukemia *see* Tumor systems in animals
Lymphocytes, in culture, modulating effects of levamisole on cell response, 571
Lymphoma
correlation of cell morphology, population kinetics, and clinical course as a guide to the study of new drugs and combinations, 1873
human cells in culture, age-dependent survival and cell-cycle progression of cells exposed to chemotherapeutic drugs, 1707
human cells in culture, *cis*-dichlorodiammineplat-

inum (II) combined individually with 11 other drugs in a search for synergistic pairs, 1619
human cells in culture, survival and cycle-progression delay of, with Yoshi 864, 1637
kinetic response of human cells in vivo to combination chemotherapy using flow microfluorometry, 1937
lymphocytic, study of Leo-1031 in the treatment of, 277
malignant, BCNU in the treatment of, 739
survival and cycle-progression delay of human cells in vitro exposed to VP-16-213, 1295
Lymphoreticular tumors *see* Cancer, lymphoreticular

M

Mass fragmentography, disposition of cyclophosphamide in tumor-bearing mice by means of gas chromatography-chemical ionization-mass fragmentography, 493
Mass spectrometry
characterization of cyclophosphamide derivatives and metabolites by field-desorption and electron-impact, 509
field-desorption, qualitative and quantitative investigations of cyclophosphamide, cyclophosphamide metabolites, and related compounds by, 501
Maytansine (NSC-153858)
pharmacology of, 1127
and related maytansinoids, new plant-derived tumor inhibitors; mechanism of action, 1115
Mechlorethamine (NSC-762)
combined with CCNU in the treatment of inoperable squamous and large cell carcinoma of the lung, 625
combined with prednisone, vincristine, and procarbazine (MOPP) in the treatment of Hodgkin's disease, 205
effects on transcription in Ehrlich cells compared with cyclophosphamide and BCNU, 471
liposomal activation of, against Ehrlich ascites tumor and L1210 leukemia, 617
recovery of mammalian cells in culture from induced potentially lethal damage, 1791
use in the LSA tumor model to study the growth characteristics of tumor cells by analysis of DNA distribution, 579
Medroxyprogesterone acetate (NSC-26386), response to, as secondary hormone therapy for metastatic breast cancer in postmenopausal women, 251
Melanoma
advanced malignant, comparative evaluation of DTIC, vincristine, and BCNU; DTIC, vincristine, and hydroxyurea; and DTIC, actinomycin D, and BCNU in the treatment of, 33
disseminated malignant, phase I–II study of DTIC and cyclocytidine in, 1369
disseminated, nitrosoureas in the management of, 747
disseminated, phase II study; DTIC, BCNU, and hydroxyurea with or without vincristine in the treatment of, 187
disseminated, phase II study of DTIC, BCNU, and vincristine with or without chlorpromazine in the treatment of, 189
malignant, bacillus Calmette-Guérin immunotherapy combined with DTIC in the treatment of, 177
malignant, DTIC alone and combined with methyl-CCNU or BCNU in the treatment of, 193
malignant, DTIC, BCNU, and either actinomycin D or vincristine in the treatment of, 205
malignant, natural history of, as related to therapy, 153
malignant, phase I evaluation of DTIC, 183
malignant, review of activity of DTIC, BCNU, and vincristine in, 1141
malignant, a review of the activity of "standard" and investigational agents in, 165
malignant, a review of DTIC in, 165
malignant, surgical treatment of, 159
metastatic cutaneous malignant, combination cytotoxic chemotherapy with DTIC, BCNU, and vincristine, 1381
metastatic malignant, phase II study of VP-16-213 versus dianhydrogalactitol, 1681
metastatic malignant, randomized prospective trial of DTIC alone versus BCNU plus vincristine in the treatment of, 595
metastatic malignant, DTIC alone and in various combinations with BCNU, CCNU, vincristine, and hydroxyurea in the treatment of, 601
role of radioautographic studies in clinical investigative oncology and chemotherapy in, 1873
stage III, combination of CCNU, vincristine, and bleomycin in the treatment of, 1273
Melphalan (NSC-8806)
amino acid-conferred resistance to; structure-activity relationship in cultured murine L1210 leukemia cells, 1363
randomized comparison with 5-FU in the treatment of advanced gastrointestinal cancer, 1267
studies with 2,5-piperazinedione, 3,6-bis(5-chloro-2-piperidyl), dihydrochloride; biochemical and therapeutic effects in L1210 leukemias sensitive and resistant to alkylating agents: comparison with BCNU and cyclophosphamide, 1325
6-Mercaptopurine (NSC-755)
combined with cytosine arabinoside; dose and time survival curves for leukemic colony-forming units and normal hematopoietic colony-forming units in mice, 1925
combined with 6-thioguanine, 6-methylmercaptopurine riboside, methotrexate, 5-FU, and cytosine arabinoside; development of resistance to, in mice with L1210 leukemia, 23
Methasquin (NSC-122870), competitive dihydrofolate reductase binding assay of, 615
Methotrexate (NSC-740)
plus citrovorum factor rescue alone or with cyclophosphamide in the treatment of ovarian carcinoma, 527
combined with cyclophosphamide, adriamycin, and procarbazine (CAMP) in the effective treatment of metastatic non-oat cell lung carcinoma, 1225
combined with cyclophosphamide and vincristine in the treatment of soft tissue sarcomas, 205
combined with cyclophosphamide, vincristine, and 5-FU following bleomycin alone in the treatment of non-oat cell lung cancer, 61

combined with 6-mercaptopurine, 6-methylmercaptopurine riboside, 5-FU, 6-thioguanine, and cytosine arabinoside; development of resistance to, in mice with L1210 leukemia, 23
combined with radiotherapy, cyclophosphamide, and vincristine in the treatment of extensive oat cell carcinoma, 221
compared to triazinate, methasquin, and aminopterin as inhibitors of dihydrofolate reductase, 615
device for constant sc infusion of; plasma results in mice, 889
plus 5-FU, cyclophosphamide, vincristine, and citrovorum factor and combined with hormonal therapy in the treatment of disseminated breast cancer, 85
inhibition of transport of, from cerebrospinal fluid by probenecid, 913
laser differential light-scattering bioassay for, 225
phase II study with, combined with 5-FU, vincristine, cyclophosphamide, and prednisone in the treatment of advanced breast cancer: 2 years' followup, 107
phase II trial of, combined with 5-FU and adriamycin in the treatment of lung adenocarcinoma, 623
synchronization with, in patients with leukemia and correlation with clinical responses, 1845
used sequentially with cyclophosphamide, vincristine, bleomycin, adriamycin, and methyl-CCNU in the treatment of advanced recurrent squamous cancer of the head and neck, 103
plus vincristine and cyclophosphamide compared to VP-16-213 alone and vincristine plus bleomycin and adriamycin in advanced small cell lung cancer, 949
plus vincristine, cyclophosphamide, and 5-FU and combined with adrenalectomy and oophorectomy in patients with breast cancer, 857
Methoxsalen (NSC-45923), bis-chloroethyl derivatives of, potential agents against malignant melanoma, 217
Methyl-CCNU (NSC-95441)
combined with β-2′-deoxythioguanosine for advanced solid tumors, 965
combined with DTIC in the treatment of malignant melanoma, 193
combined with 5-FU and compared to 5-FU alone in advanced gastrointestinal cancer, 733
combined with 5-FU and vincristine in the treatment of adenocarcinoma and large cell carcinoma of the lung, 1393
combined with vincristine and weekly 5-FU in advanced colorectal carcinoma, 1597
in vitro responses of mammalian cells to drug-induced potentially lethal and sublethal damage, 1799
phase II study of, in the treatment of advanced gastrointestinal cancer, 285
phase II study of, in the treatment of advanced pancreatic carcinoma, 1659
preclinical toxicologic evaluation of a single iv infusion in dogs and monkeys, 1559
in the treatment of advanced colorectal cancer after failure of 5-FU therapy, 235
in the treatment of advanced sarcomas: a comparative clinical trial with two 3-drug combinations, 1385
used sequentially with cyclophosphamide, vincristine, bleomycin, methotrexate, and adriamycin in the treatment of advanced, recurrent, squamous cancer of the head and neck, 103
6-Methylmercaptopurine riboside (NSC-40774), combined with 6-thioguanine, 6-mercaptopurine, methotrexate, 5-FU, and cytosine arabinoside; development of resistance to, in mice with L1210 leukemia, 23
Methylmethane sulfonate, recovery of mammalian cells in culture from induced potentially lethal damage, 1791
Mitomycin C (NSC-26980)
combined with 5-FU and cytosine arabinoside in P815 ascites and solid mouse neoplasms, 1399
combined with 5-FU and cytosine arabinoside in the treatment of gastrointestinal cancer, 1373
neurotoxicity from 5-FU administration reproduced by, 293
oral, phase I study of, 1633
MOPP (mechlorethamine, vincristine, prednisone, and procarbazine)
alternating with ABDV (adriamycin, bleomycin, DTIC, and vinblastine) in radiotherapy for advanced Hodgkin's disease, 1217
outline of original clinical study with, 1141
versus adriamycin, bleomycin, vinblastine, and DTIC (ABVD) in the treatment of Hodgkin's disease, 205
Myeloma, multiple, nitrosoureas in, 789

N

Nafoxidine, interaction with human breast cancer in long-term tissue culture, 1421
Nitrogen mustards (*see also* mechlorethamine), pharmacologic study in vitro and in vivo compared with cyclophosphamide and cyclophosphamide metabolites, 301
Nitrosoureas (*see also* specific agents)
chemistry and structure-activity studies of, 651
clinical studies in malignant gliomas, 713
clinical schedules and toxic effects, 709
clinical studies in various solid tumors, 795
combinations of, in lung cancer, 757
development of acute nonlymphocytic leukemia associated with previous therapy with, 1257
early history and development of, 647
future studies with, based on review of past studies, 807
in the management of disseminated malignant melanoma, 747
mechanism of action of, 699
in multiple myeloma, 789
pharmacodynamics of, in relation to the central nervous system, 725
pharmacology of, 703
review of experimental antitumor activity, 665
as single agents in the treatment of lung cancer, 753
therapy for gastrointestinal cancer, used alone and in combination, 729
in the treatment of advanced gastrointestinal cancer, 769
in the treatment of Hodgkin's disease, 781
in the treatment of primary malignant gliomas, 719
***Nor*-nitrogen mustard (NSC-10873)**
biologic activity in vitro compared to other derivatives and possible metabolites of cyclophosphamide, 373

permeation into animal tumor cells, 423
qualitative and quantitative investigations by field-desorption mass spectrometry, 501
NSC-739 *see* Aminopterin
NSC-740 *see* Methotrexate
NSC-752 *see* 6-Thioguanine
NSC-755 *see* 6-Mercaptopurine
NSC-762 *see* Mechlorethamine
NSC-3053 *see* Actinomycin D
NSC-3061 *see* Pyrimethamine
NSC-3070 *see* Diethylstilbestrol
NSC-3088 *see* Chlorambucil
NSC-3590 *see* Citrovorum factor
NSC-4958 *see* Chloroplatinic acid
NSC-6396 *see* ThioTEPA
NSC-8806 *see* Melphalan
NSC-10023 *see* Prednisone
NSC-10873 *see* *Nor*-nitrogen mustard
NSC-11905 *see* Lapachol
NSC-13875 *see* Hexamethylmelamine
NSC-18334 *see* Cinerubin A
NSC-18786 *see* Probenecid
NSC-19494 *see* DDMP [pyrimidine, 2,4-diamino-5-(3,4-dichlorophenyl)-6-methyl-]
NSC-19893 *see* 5-Fluorouracil
NSC-26271 *see* Cyclophosphamide
NSC-26386 *see* Medroxyprogesterone acetate
NSC-26980 *see* Mitomycin C
NSC-32065 *see* Hydroxyurea
NSC-40774 *see* 6-Methylmercaptopurine riboside
NSC-42076 *see* SPG-827
NSC-45388 *see* DTIC
NSC-45923 *see* Methoxsalen
NSC-49842 *see* Vinblastine
NSC-56410 *see* Porfiromycin
NSC-58514 *see* Chromomycin A_3
NSC-63878 *see* Cytosine arabinoside
NSC-67574 *see* Vincristine
NSC-68075 *see* Thalicarpine
NSC-69945 *see* Phosphoramide mustard
NSC-69947 *see* Phosphoramide mustards
NSC-71047 *see* Trioxsalen
NSC-71261 *see* β-2′-Deoxythioguanosine
NSC-72274 *see* SPI-77
NSC-72505 *see* Phosphoramide mustards
NSC-72510 *see* Phosphoramide mustards
NSC-77213 *see* Procarbazine
NSC-79037 *see* CCNU
NSC-82151 *see* Daunorubicin
NSC-82623 *see* Vitamin E
NSC-83097 *see* 5-FUDR
NSC-85998 *see* Streptozotocin
NSC-88536 *see* Calusterone
NSC-91523 *see* Propranolol
NSC-95441 *see* Methyl-CCNU
NSC-100880 *see* Camptothecin
NSC-102627 *see* Yoshi 864
NSC-102816 *see* 5-Azacytidine
NSC-104800 *see* Dibromodulcitol
NSC-104801 *see* Cytembena
NSC-109229 *see* L-Asparaginase
NSC-109723 *see* Trophosphamide
NSC-109724 *see* Isophosphamide
NSC-112907 *see* Tetrahydrouridine
NSC-118994 *see* Inosine dialdehyde
NSC-119875 *see* *cis*-Dichlorodiammineplatinum(II)
NSC-122819 *see* VM-26
NSC-122870 *see* Methasquin
NSC-123127 *see* Adriamycin
NSC-125066 *see* Bleomycin
NSC-126849 *see* 3-Deazauridine
NSC-129943 *see* ICRF-159
NSC-132313 *see* Dianhydrogalactitol
NSC-134087 *see* Leo-1031
NSC-135758 *see* 2,5-Piperazinedione, 3,6-bis(5-chloro-2-piperidyl)-, dihydrochloride
NSC-139105 *see* Triazinate
NSC-104865 *see* Coenzyme Q_{10}
NSC-141540 *see* VP-16-213
NSC-145668 *see* Cyclocytidine
NSC-148958 *see* Ftorafur
NSC-150014 *see* Hydrazine sulfate
NSC-153858 *see* Maytansine
NSC-165563 *see* Bruceantin
NSC-166641 *see* Anhydro-ara-5-fluorocytidine
NSC-172755 *see* Butocin
NSC-176986 *see* 4-Peroxycyclophosphamide
NSC-177023 *see* Levamisole
NSC-178248 *see* Chlorozotocin
NSC-180512 *see* Platinum uracil blue
NSC-180973 *see* Tamoxifen
NSC-181815 *see* 4-Hydroperoxycyclophosphamide
NSC-196562 *see* 4-Hydroxycyclophosphamide
NSC-201424 *see* 2,5-Piperazinedione, 3,6-bis(1-azabicyclo[3.1.0]hex-2-yl)-
NSC-224964 *see* Platinum, (1,2-cyclohexanediamine-*N*,*N*′)[propanedioato-(2-)-*O*,*O*′]-, (*SP*-4-2)-
NSC-227114 *see* 4-Hydroperoxyisophosphamide
NSC-239851 *see* Platinum, (1,2-cyclohexanediamine-*N*,*N*′)bis(nitrato-*O*)-, (*SP*-4-2)-
NSC-250427 *see* Platinum, (1,2-cyclohexanediamine-*N*,*N*′)[sulfato(2-)-*O*,*O*′]-, (*SP*-4-2)-
NSC-256439 *see* 4-Demethoxydaunorubicin
NSC-264880 *see* Dihydro-5-azacytidine hydrochloride
NSC-409962 *see* BCNU

O

Oat cell cancer *see* Cancer, oat cell
Oophorectomy *see* Surgery
Ovarian cancer *see* Cancer, ovarian

P

Pancreatic cancer *see* Cancer, pancreas
P388 leukemia *see* Tumor systems in animals
P815 ascites and solid mouse neoplasms *see* Tumor systems in animals
4-Peroxycyclophosphamide (NSC-176986), activity against L1210 leukemia, Lewis lung carcinoma, and C3H mammary tumor, 381

Phase I studies
alternate-day dose study of chromomycin A_3, 1251
of dianhydrogalactitol, 611
of dianhydrogalactitol administered iv in a weekly schedule, 895
of DTIC, 189
of DTIC in the treatment of malignant melanoma, 183
of levamisole, 963
of oral mitomycin C, 1633
of an oral solution of VP-16-213, 943
and phase II study of cytembena in disseminated epithelial ovarian cancers and sarcomas, 1389
and phase II study of DTIC and cyclocytidine in disseminated malignant melanoma, 1369
and phase II study of single-dose actinomycin D, pharmacokinetically based, 289
and phase II trial of VM-26 in the treatment of children with late-stage leukemia, 265
of vinblastine combined with bleomycin and *cis*-dichlorodiammineplatinum(II) in the treatment of various cancers, 91
of weekly administration of anhydro-ara-5-fluorocytidine, 281
Phase II studies
of *cis*-dichlorodiammineplatinum(II) in lung cancer, 1679
of *cis*-dichlorodiammineplatinum(II) in patients with advanced adenocarcinoma of the ovary, 55
of cyclophosphamide and adriamycin in the treatment of various solid tumors, 77
of cytembena in advanced ovarian or breast cancer, 1655
of dianhydrogalactitol and VP-16-213 in colorectal cancer, 1247
of DTIC combined with BCNU and hydroxyurea with or without vincristine in the treatment of disseminated melanomas, 189
of DTIC combined with vincristine and BCNU with or without chlorpromazine in the treatment of disseminated melanomas, 189
of DTIC in the treatment of Hodgkin's disease and other lymphomas, 189
of 5-FU, adriamycin, and methotrexate in the treatment of lung adenocarcinoma, 623
of 5-FU, methotrexate, vincristine, cyclophosphamide, and prednisone in the treatment of advanced breast cancer: 2 years' followup, 107
of ICRF-159 in patients with metastatic colorectal carcinoma previously exposed to systemic chemotherapy, 1395
of methyl-CCNU in advanced pancreatic carcinoma, 1659
of methyl-CCNU in the treatment of advanced gastrointestinal cancer, 285
and phase I study of cytembena in disseminated epithelial ovarian cancers and sarcomas, 1389
and phase I study of DTIC and cyclocytidine in disseminated malignant melanoma, 1369
and phase I study of single-dose actinomycin D, pharmacokinetically based, 289
and phase I trial of VM-26 in the treatment of children with late-stage leukemia, 265
of porfiromycin in the management of epidermoid and transitional cell cancer, 907
of tamoxifen: report of 74 patients with stage IV breast cancer, 1431
using methyl-CCNU, vincristine, and weekly 5-FU in advanced colorectal cancer, 1597
of vinblastine, adriamycin, and procarbazine in small cell carcinoma of the lung, 1263
vincristine combined with cyclophosphamide; summary of clinical results of a study in patients with lymphoreticular tumors by the so-called synchronization therapy, 1959
of VP-16-213 and cytembena in advanced breast cancer, 633
of VP-16-213 versus dianhydrogalactitol in metastatic malignant melanoma, 1681
Phenylalanine ammonia-lyase, in vivo effects of, in animals, 261
Phosphoramide mustard (NSC-69945)
characterization of, by field-desorption and electron-impact mass spectrometry, 509
derivatives of amino acids and peptides, 347
quantitation of, in human serum and urine using gas chromatography-chemical ionization-mass spectrometry, 403
synthesis and structure-activity relationships of preactivated analogs of, tested against L1210 leukemia, 381
Phosphoramide mustards, antitumor activity of NSC-69945 compared to other active phosphoramide mustards (NSC-69947, NSC-72595, and NSC-72510), 337
2,5-Piperazinedione, 3,6-bis(1-azabicyclo[3.1.0]hex-2-yl)- (NSC-201424), comparison with 2,5-piperazinedione, 3,6-bis(5-chloro-2-piperidyl)-, dihydrochloride: cytotoxic and DNA synthesis inhibitory studies in human epidermoid No. 2 cells, 1317
2,5-Piperazinedione, 3,6-bis(5-chloro-2-piperidyl)-, dihydrochloride (NSC-135758)
cell kinetic and biologic effects in cultured L1210, human epidermoid No. 2, and Adenocarcinoma 755 cells, 1307
effects on macromolecular synthesis in cell culture and evidence for alkylating activity, 1317
studies with; biochemical and therapeutic effects in L1210 leukemias sensitive and resistant to alkylating agents: comparison with melphalan, cyclophosphamide, and BCNU, 1325
Plant products
bioassay of extracts for antitumor activity, 1007
in clinical cancer chemotherapy, 1141
distribution of anticancer activity in, 1081
folklore, a tool for predicting sources of antitumor activity, 979
history of the National Cancer Institute's screening program for, 975
isolation and chemical characterization of antitumor agents from, 1011
novel plant-derived tumor inhibitors and their mechanisms of action, 1115
oncogenic and tumor-promoting spermatophytes and pteridophytes and their active principles, 1171
pharmacology of 9 antitumor agents from, 1127

preparation of extracts for antitumor screening, 999
procurement of, for antitumor screening, 987
as a source of anticancer drugs, 1069
types of anticancer agents isolated from, 1031
Platinum, (1,2-cyclohexanediamine-*N,N'*)bis(nitrato-*O*)-, (*SP*-4-2)- (NSC-239851), nephrotoxicity of, in animals, 1675
Platinum, (1,2-cyclohexanediamine-*N,N'*)(propanedioate-(2)-*O,O'*)-, (*SP*-4-2)- (NSC-224964), nephrotoxicity of, in animals, 1675
Platinum, (1,2-cyclohexanediamine-*N,N'*)(sulfato(2-)-*O,O'*)-, (*SP*-4-2)- (NSC-250427), nephrotoxicity of, in animals, 1675
Platinum uracil blue (NSC-180512), nephrotoxicity of, in animals, 1675
P388 leukemia *see* Tumor systems in animals
Podophyllotoxins (*see also* VP-16-213 and VM-26), compounds isolated from *Podophyllum* species, 1141
Porfiromycin (NSC-56410), in the management of epidermoid and transitional cell cancer: phase II study, 907
Prednisone (NSC-10023)
combined with mechlorethamine, vincristine, and procarbazine (MOPP) in the treatment of Hodgkin's disease, 205
combined with vincristine and L-asparaginase in a study of cytosine arabinoside synchronization of leukemic cells, for remission induction in adv[illegible] acute leukemia in children, 591
effects of, alone or combined with c[illegible]mide and vincristine on some hepatic oxida[illegible]ons and conjugations, 1285
phase II study with, combined with 5-FU, methotrexate, cyclophosphamide, and vincristine in the treatment of advanced breast cancer: 2 years' followup, 107
Probenecid (NSC-18786), inhibition of methotrexate transport from cerebrospinal fluid by, 913
Procarbazine (NSC-77213)
combined with adriamycin and vinblastine in a phase II study of small cell carcinoma of the lung, 1263
combined with BCNU in the treatment of malignant brain tumors, 243
combined with cyclophosphamide, adriamycin, and methotrexate (CAMP) in the effective treatment of metastatic non-oat cell lung carcinoma, 1225
combined with mechlorethamine, vincristine, and prednisone (MOPP) in the treatment of Hodgkin's disease, 205
combined with vinblastine and cytosine arabinoside for reinduction of childhood acute myelocytic leukemia, 1683
Propranolol (NSC-91523), bis-chloroethyl derivatives of, potential agents against lung cancer, 217
Prostatic cancer *see* Cancer, prostate
Pteridophytes, identification of oncogenic and tumor-promoting principles of, 1171
Purines, analogs and derivatives tested for ability to inhibit parameters of purine metabolism in Ehrlich ascites tumor cells, 1567
P815X2 mastocytoma *see* Tumor systems in animals
Pyrimethamine (NSC-3061), combined with daunorubicin, cytosine arabinoside, and 6-thioguanine and compared to daunorubicin alone in the treatment of acute nonlymphocytic leukemia, 41

R

Radiation therapy
combined with chemotherapy for small cell lung cancer, 1483
combined with cyclophosphamide, vincristine, and methotrexate in the treatment of extensive oat cell carcinoma, 221
combined with 8-drug chemotherapy (MOPP alternating with ABDV) in the treatment of advanced Hodgkin's disease, 1217
combined with 5-FU or cyclophosphamide for undifferentiated lung cancer, 1487
prerequisites for effective treatment of lung cancer, 1475
recovery of mammalian cells in culture from induced potentially lethal damage, 1791
response to, comparison of cell proliferation kinetics in human and experimental tumors, 1887
use in the LSA tumor model to study the growth characteristics of tumor cells by analysis of DNA distribution, 579
Rebuck skin window, as a guide in cancer chemotherapy, 903
Respiration, of tumor cells, effects and specificity of anticancer agents on, 1
Retinoids, inhibition of growth and regression of a transplantable rat chondrosarcoma by Ro 10–1670, Ro 10–9359, and Ro 11–1430, 1647

S

Saponin P, a new plant-derived tumor inhibitor; mechanism of action, 1115
Sarcoma
adriamycin and DTIC (used alone or as a combination) in the treatment of, 197
advanced, a comparative clinical trial evaluating the combination of adriamycin, DTIC, and vincristine, the combination of actinomycin D, cyclophosphamide, and vincristine, and methyl-CCNU alone in the treatment of, 1385
Kaposi's, ICRF-159 in the treatment of, 111
phase I and II study of cytembena in the treatment of, 1389
soft tissue, cyclophosphamide, vincristine, and methotrexate versus adriamycin and DTIC in the treatment of, 205
Sarcoma 45 *see* Tumor systems in animals
Sarcoma 180 *see* Tumor systems in animals
Schweitz erythromyelosis *see* Tumor systems in animals
Spermatophytes, identification of oncogenic and tumor-promoting principles of, 1171
SPG-827 (NSC-42076), review of clinical responses with, 1141
"Sphygmo-Recording," noninvasive monitoring of adria-

mycin cardiotoxicity by; technique to record the pulse wave delay (QK_d interval), 1239
SPI-77 (NSC-72274), review of activity and toxic effects in man, 1141
Squamous cell cancer *see* Cancer, squamous cell
Streptozotocin (NSC-85998), *Limulus amebocyte* lysate assay used to detect the presence of bacterial endotoxin in lots of, 9
Surgery
adrenalectomy and oophorectomy plus limited-term chemotherapy (cyclophosphamide, vincristine, methotrexate, and 5-FU) in the treatment of breast cancer, 857
combined with chemotherapy for lung cancer, 1489
effects of, on the cell kinetics of residual tumor in animals, 1749
general principles in the treatment of lung cancer, 1473
in the treatment of malignant gliomas, 717
treatment of malignant melanoma, 159

T

Tamoxifen (NSC-180973)
antiestrogenic and antitumor properties of, in laboratory animals, 1409
comparison with conventional hormone therapy (diethylstilbestrol) for advanced breast cancer, 1461
evaluation of dosage in advanced breast cancer, 1451
interaction of, with human breast cancer in long-term tissue culture, 1421
overview of EORTC clinical trials with, in patients with advanced breast cancer, 1463
phase II study of, in 74 patients with stage IV breast cancer, 1431
remissions in stage IV breast cancer, 1445
therapeutic use in advanced breast cancer: correlation with biochemical parameters, 1437
TA-3(St) tumor *see* Tumor systems in animals
Testicular cancer *see* Cancer, testicular
Tetrahydrouridine (NSC-112907), distribution of, in experimental animals, 1627
Thalicarpine (NSC-68075)
pharmacology of, 1127
plasma decay and excretion of, in man, 69
6-Thioguanine (NSC-752)
combined with cytosine arabinoside; dose and time survival curves for leukemic colony-forming units and normal hematopoietic colony-forming units in mice, 1925
combined with daunorubicin, cytosine arabinoside, and pyrimethamine and compared to daunorubicin alone in the treatment of acute nonlymphocytic leukemia, 41
combined with 6-mercaptopurine, methotrexate, 6-methylmercaptopurine riboside, 5-FU, and cytosine arabinoside; development of resistance to, in mice with L1210 leukemia, 23
maintenance of remission in adult acute nonlymphocytic leukemia using intermittent courses of, with cytosine arabinoside, 585
Thiopurines *see* 6-Mercaptopurine and 6-thioguanine
ThioTEPA (NSC-6396)
analogs, spin-labeled; toxicity, antitumor activity, and pharmacokinetics of, 1605
combined with surgery for lung cancer, 1489
α-Tocopherol *see* Vitamin E
Toxic reactions: observations in animals
cardiovascular effects of cyclocytidine, 1663
comparative nephrotoxicity of various platinum cancer chemotherapeutic agents, 1675
Toxic reactions: observations in man
amelioration of toxicity of adriamycin by α-tocopherol (vitamin E), 961
echocardiographic evaluation of adriamycin cardiotoxicity in children, 1281
neurotoxicity from 5-FU administration reproduced by mitomycin C, 293
noninvasive monitoring of adriamycin cardiotoxicity by "Sphygmo-Recording" of the pulse wave delay (QK_d interval), 1279
pigmentation of the tongue after treatment with adriamycin, 1402
pulmonary toxicity in long-term administration of BCNU, 1691
Rebuck skin window as a clinical test to evaluate risk for infection in neutropenic patients receiving chemotherapy, 903
serpentine supravenous 5-FU hyperpigmentation, 639
soft tissue metastatic calcification after bleomycin therapy for lymphoma, 963
studies on adriamycin using a weekly regimen demonstrating its clinical effectiveness and lack of cardiac toxicity, 813
symptomatic hypophosphatemia secondary to 5-azacytidine therapy of acute nonlymphocytic leukemia, 1400
Transitional cell cancer *see* Cancer, transitional cell
Triazinate (NSC-139105), competitive dihydrofolate reductase binding assay of, 615
Triazine derivatives, effects and specificity of, on the respiration and energy metabolism of tumor cells, 1
Trioxsalen (NSC-71047), bis-chloroethyl derivatives of, potential agents against malignant melanoma, 217
Triptolides, new plant-derived tumor inhibitors, mechanism of action, 1115
Trophosphamide (also triphosphamide) (NSC-109723)
biologic activity in vitro compared to other derivatives and possible metabolites of cyclophosphamide, 373
synthesis and structure-activity relationships of preactivated analogs of, tested against L1210 leukemia, 381
X-ray crystallographic studies of, 517
Tumor systems in animals
Adenocarcinoma 755, antitumor activity of 1,2-bis diazoacetyl ethane in, 1601
B16 melanoma
antitumor activity of DTIC combined with adriamycin against, 135
comparison of activity of adriamycin and cinerubin A against, 99
comparison of 5-FU and ftorafur; therapeutic response and development of resistance in, 1347

comparison of phosphoramide mustards against, 337
effects of *Corynebacterium parvum* alone and in combination with adriamycin in, 823
in vivo effects of phenylalanine ammonia-lyase, 261
C3H/He spontaneous mammary tumor, rapid methods for utilizing cell kinetics for treatment in; effects of vincristine, 1913
C3H mammary carcinoma
antitumor activity of DTIC combined with adriamycin against, 135
comparison of activity of 4-peroxycyclophosphamide and cyclophosphamide against, 381
Chondrosarcoma, transplantable, inhibition of growth and regression of, by three retinoids, 1647
EARAD-1 leukemia, in vivo effects of phenylalanine ammonia-lyase, 261
Ehrlich carcinoma
ascites, effects of tumor bearing on the dynamics of host hemopoietic cells, 1781
ascites, investigations on kinetic data and reproducibility concerning the pharmacologic modification of cell proliferation after vincristine, 1959
liposomal activation of mechlorethamine and BCNU against, 617
Gardner 6C3HED lymphosarcoma, comparison of 5-FU and ftorafur; therapeutic response and development of resistance in, 1347
Glioma 261, comparison of anhydro-ara-5-fluorocytidine and cytosine arabinoside in the treatment of, 875
Gross leukemia, antitumor activity of 4-demethoxydaunorubicin, 4-demethoxy-7,9-diepidaunorubicin, and their β anomers in, 829
Guérin carcinoma
antitumor activity of 1,2-bis diazoacetyl ethane in, 1601
toxicity, antitumor activity, and pharmacokinetics of spin-labeled thioTEPA analogs, 1605
Harding-Passey melanoma, antitumor activity of 1,2-bis diazoacetyl ethane in, 1601
Hepatoma 72, antitumor activity of 1,2-bis diazoacetyl ethane in, 1601
JB-1 ascites tumor, resting cells in; with special emphasis on recycling, 1861
La leukemia, antitumor activity of 1,2-bis diazoacetyl ethane in, 1601
Lewis lung carcinoma
comparison of activity of adriamycin and cinerubin A against, 99
comparison of activity of 4-peroxycyclophosphamide and cyclophosphamide against, 381
comparison of phosphoramide mustards against, 337
disposition of cyclophosphamide in mice bearing, by gas chromatography-chemical ionization-mass fragmentography, 493
effects of *Corynebacterium parvum* alone and in combination with adriamycin, 823
effects of surgery on cell kinetics of residual tumors in, 1749
size dependence of the response of, to BCNU, 1743
L1210 leukemia
activity of some *Cephalotaxus* alkaloids against, 1157
antitumor activity of 1,2-bis diazoacetyl ethane in, 1601
antitumor activity of 4-demethoxydaunorubicin, 4-demethoxy-7,9-diepidaunorubicin, and their β anomers in, 829
antitumor activity of DTIC alone and combined with adriamycin against, 135
comparison of activity of adriamycin and cinerubin A against, 99
comparison of 5-FU and ftorafur; therapeutic response and development of resistance in, 1347
comparison of phosphoramide mustards against, 337
computer simulation of leukemia therapy: combined pharmacokinetics, intracellular enzyme kinetics, and cell kinetics of the treatment of, by cytosine arabinoside, 1723
development of resistance to combination of 6-mercaptopurine, 6-thioguanine, 6-methylmercaptopurine riboside, methotrexate, 5-FU, and cytosine arabinoside, 23
dose regimen studies with DTIC, 125
liposomal activation of mechlorethamine and BCNU against, 617
resting cells in, with special emphasis on recycling, 1861
solid, comparative physiologic dispositions of 5-FUDR and 5-FU in mice bearing, 845
structure-activity relationships of analogs of cyclophosphamide (especially 4-peroxycyclophosphamide), isophosphamide, trophosphamide, and phosphoramide mustard tested against, 381
studies with 2,5-piperazinedione, 3,6-bis(5-chloro-2-piperidyl)-, dihydrochloride; biochemical and therapeutic effects in L1210 leukemias sensitive and resistant to alkylating agents: comparison with melphalan, cyclophosphamide, and BCNU, 1325
studies with 2,5-piperazinedione, 3,6-bis(5-chloro-2-piperidyl)-, dihydrochloride: kinetic and biologic effects in cultured cells, 1307
L5178Y leukemia, in vivo effects of phenylalanine ammonia-lyase, 261
P815 ascites and solid neoplasms, combination therapy with mitomycin C, 5-FU, and cytosine arabinoside, 1399
P388 leukemia
activity of anthracyclines against an adriamycin-resistant subline of, with special emphasis on cinerubin A, 99
activity of some *Cephalotaxus* alkaloids against, 1157
comparison of 5-FU and ftorafur; therapeutic response and development of resistance in, 1347
comparison of phosphoramide mustards against, 337
effects of *Corynebacterium parvum* alone and in combination with adriamycin in, 823
prostatic adenocarcinoma, effects of cyclophosphamide in the treatment of, 619
P815X2 mastocytoma, proliferative character and growth modes of neoplastic disease as determinants of chemotherapeutic efficacy, using cyclophosphamide, BCNU, and adriamycin, 1761
Sarcoma 45, antitumor activity of 1,2-bis diazoacetyl ethane in, 1601

Sarcoma 180
preliminary studies of toxicities and responsiveness of, to DDMP alone and combined with citrovorum factor, 547
solid and ascitic, antitumor activity of 4-demethoxy-daunorubicin, 4-demethoxy-7,9-diepidaunorubicin, and their β anomers in, 829
Schweitz erythromyelosis, toxicity, antitumor activity, and pharmacokinetics of spin-labeled thioTEPA analogs, 1605
TA-3(St) tumor, effects of tumor bearing on the dynamics of host hemopoietic cells, 1781
Walker 256 carcinosarcoma
antitumor activity of 1,2-bis diazoacetyl ethane in, 1601
dissociation of 5-FU uptake from intracellular pH in, 867
toxicity, antitumor activity, and pharmacokinetics of spin-labeled thioTEPA analogs, 1605
Yoshida sarcoma, carcinostatic activity of yemenimycin in, 937

V

Vernolepin, and derivatives, a new plant-derived tumor inhibitor; mechanism of action, 1115
Vernomenin, a new plant-derived tumor inhibitor; mechanism of action, 1115
Vinblastine (NSC-49842)
combined with adriamycin and bleomycin for advanced testicular tumors, 953
combined with adriamycin, bleomycin, and DTIC (ABVD) in the treatment of Hodgkin's disease, 205
combined with adriamycin and procarbazine in a phase II study of small cell carcinoma of the lung, 1263
combined with bleomycin and *cis*-dichlorodiammineplatinum (II) in the treatment of various cancers, phase I study, 91
combined with procarbazine and cytosine arabinoside for reinduction of childhood acute myelocytic leukemia, 1683
Limulus amebocyte lysate assay used to detect the presence of bacterial endotoxin in various lots of, 9
pharmacology of, 1127
plant product in clinical cancer chemotherapy, 1141
Vincristine (NSC-67574)
plus BCNU versus DTIC alone in the treatment of metastatic malignant melanoma, 595
plus bleomycin and adriamycin compared to ICRF-159 alone in non-small cell lung cancer, 947
in combinations with DTIC plus CCNU and DTIC plus BCNU in the treatment of metastatic malignant melanoma, 601
combined with adriamycin and DTIC or actinomycin D and cyclophosphamide in the treatment of advanced sarcomas: a comparative clinical trial with methyl-CCNU alone, 1385
combined with BCNU and DTIC in the treatment of metastatic cutaneous malignant melanoma, 1381
combined with cyclophosphamide and methotrexate in the treatment of soft tissue sarcomas, 205
combined with cyclophosphamide, methotrexate, and 5-FU following bleomycin alone in the treatment of non-oat cell lung cancer, 61
combined with cyclophosphamide; summary of clinical results of a phase II study in patients with lymphoreticular tumors by the so-called synchronization therapy, 1959
combined with DTIC and BCNU in the treatment of malignant melanoma, 205
combined with DTIC and BCNU; review of activity in malignant melanoma, 1141
combined with DTIC and BCNU, and DTIC and hydroxyurea in the treatment of advanced malignant melanoma, 33
combined with DTIC, BCNU, and hydroxyurea versus the 3 drugs alone in disseminated melanomas, 189
combined with 5-FU, DTIC, and BCNU in the treatment of advanced colorectal cancer, 29
combined with mechlorethamine, prednisone, and procarbazine (MOPP) in the treatment of Hodgkin's disease, 205
combined with methyl-CCNU and 5-FU in the treatment of adenocarcinoma and large cell carcinoma of the lung, 1393
combined with methyl-CCNU and weekly 5-FU in advanced colorectal cancer, 1597
combined with prednisone and L-asparaginase in a study of cytosine arabinoside synchronization of leukemic cells, for remission induction in advanced acute leukemia in children, 591
combined with radiotherapy, cyclophosphamide, and methotrexate in the treatment of extensive oat cell carcinoma, 221
plus cyclophosphamide, 5-FU, and methotrexate and combined with adrenalectomy and oophorectomy in patients with breast cancer, 857
plus cyclophosphamide and methotrexate compared to VP-16-213 alone and vincristine plus bleomycin and adriamycin for advanced small cell lung cancer, 949
effects of, alone or combined with cyclophosphamide and prednisone on some hepatic oxidations and conjugations, 1285
effects of: rapid methods for utilizing cell kinetics for treatment in the C3H/He spontaneous mammary tumor, 1913
plus 5-FU, cyclophosphamide, methotrexate, and citrovorum factor and combined with hormonal therapy in the treatment of disseminated breast cancer, 85
investigations on kinetic data and reproducibility concerning the pharmacologic modification of Ehrlich ascites tumor cell proliferation after, 1959
Limulus amebocyte lysate assay used to detect the presence of bacterial endotoxin in various lots of, 9
pharmacology of, 1127
phase II study of, combined with DTIC and BCNU with or without chlorpromazine in the treatment of disseminated melanomas, 189
phase II study with, combined with 5-FU, methotrexate, cyclophosphamide, and prednisone in the treatment of advanced breast cancer: 2 years' followup, 107
plant product in clinical cancer chemotherapy, 1141

in the treatment of small cell anaplastic lung cancer, 239
used sequentially with cyclophosphamide, bleomycin, methotrexate, adriamycin, and methyl-CCNU in the treatment of advanced, recurrent, squamous cancer of the head and neck, 103
used sequentially with hydroxyurea to enhance the degree of cell synchrony in animal tumors, 1959
Vitamin E (α-tocopherol) (NSC-82623)
amelioration of toxicity of adriamycin by, 961
bis-chloroethyl derivatives of, as potential agents against cancer, 217
VM-26 (NSC-122819)
phase I–II trial in the treatment of children with late-stage leukemia, 265
plant product in clinical cancer chemotherapy, 1141
pharmacology of, 1127
VP-16-213 (NSC-141540)
comparison of the biologic activity of, given iv and orally in capsules or drink ampules, 1377
oral solution, phase I clinical trial of, 943
pharmacology of, 1127
phase II evaluation of, with cytembena in advanced breast cancer, 633
phase II study of, versus dianhydrogalactitol in metastatic malignant melanoma, 1681
phase II study in colorectal cancer, 1247
plant product in clinical cancer chemotherapy, 1141
survival and cycle-progression delay of human lymphoma cells in vitro exposed to, 1295
in the treatment of acute leukemia, 967
versus polychemotherapy (vincristine plus cyclophosphamide and methotrexate; vincristine plus bleomycin and adriamycin) in advanced small cell lung cancer, 949

W

Walker 256 carcinosarcoma *see* Tumor systems in animals

X

X-ray crystallographic studies, of cyclophosphamide derivatives, 517

Y

Yeast mutants, with distorted cell membranes, as tests in the screening for antitumor antibiotics, 637
Yemenimycin, carcinostatic activity of, in animal tumors, 937
Yoshi 864 (1-propanol, 3,3'-iminodi-, dimethanesulfonate [ester], hydrochloride; NSC-102627), survival and cycle-progression delay of cultured human lymphoma cells treated with, 1637
Yoshida sarcoma *see* Tumor systems in animals

Author Index

A

Abbasi MM, 1671
Abbott BJ, 1007
Adams K, 1743
Adams T, 269
Adamson DJ, 1307
Adamson RH, 217, 555, 563, 1127
Adler D, 1959
Ahmann DL, 633, 747, 1385, 1681
Aisner J, 41
Alabaster O, 1981
Alarcon RA, 327
Alberto P, 281
Alberts DS, 1981
Alikpala A, 1937
Allen LM, 69, 445, 451
Amery WK, 217
Anderson T, 761, 801
Andrews NC, 269
Arcamone F, 829
Arlin Z, 1937
Armitage JO, 585
Aroesty J, 1723
Asal NR, 857
Ashby R, 477
Aungst CW, 277
Avadhani NG, 471, 617
Azzarelli A, 205

B

Bain E, 579, 1982
Baisch H, 1983
Bajetta E, 205
Bakemeier RF, 739
Baker LH, 91, 199, 733, 1369, 1389, 1633
Balcerzak S, 199
Band PR, 1431
Barclay AS, 1081
Barlogie B, 1295, 1637, 1707, 1981
Barlow JJ, 527
Barranco SC, 1799
Bartolucci A, 781
Bartošek I, 395
Baserga R, 1811, 1819
Basler GA, 875
Basuk P, 1984
Bateman JR, 953, 1251
Bear RA, 1400
Bearden JD III, 1679
Beazley RW, 1437
Beisler JA, 1671
Bellet RE, 595, 1395
Belvedere G, 493
Benckhuysen C, 369
Benjamin RS, 199, 289
Bennett JM, 625, 739, 925, 939
Beretta G, 33, 205, 1231
Bergevin PR, 293
Bernardi L, 829
Bernath AM, 1393
Bernheim J, 1273
Bernheim JL, 1986
Bhuyan BK, 1813
Bichel P, 1861
Bick RL, 269
Billings A, 1225
Bingel AS, 1171
Bird GG, 1267
Bisel HF, 633, 1385, 1681
Bitran JD, 221, 1225
Blanco M, 1
Block JB, 295
Blom J, 1593
Bloomfield CD, 1683
Blumenschein GR, 199, 289
Bodey GP, Sr, 199
Bodurtha AJ, 595
Bolan G, 1421
Boldrey EB, 243
Bollag W, 281
Bonadonna G, 33, 205, 1231
Bono VH, Jr, 141, 699, 1307
Bottomley RH, 199, 857
Bounous G, 17
Bowdon BJ, 1307
Boyle LE, 61
Brambilla G, 255
Braunschweiger PG, 1913
Brereton HD, 1239
Brindley C, 575
Brock N, 301
Brockman RW, 1307, 1317, 1325
Brodovsky HS, 925
Brodsky I, 625
Brooks JC, 965
Brown AK, 1402
Brown GJA, 1267
Brundrett R, 403
Brunner KW, 1377
Bryan JH, 591
Buck MJ, 1647
Bull F, 953

Bull JM, 1451, 1593
Bullen BR, 1267
Bunch GA, 1267
Bunn PA, 1986
Bunnag B, 1981
Burgess MA, 103, 177, 199, 289
Burns CP, 585
Burns FJ, 1985
Buroker TR, 91, 1277

C

Camerman A, 517
Camerman N, 517
Canetta R, 1231
Cantor RI, 1667
Carbone PP, 193, 625, 739, 925, 939, 1659
Carmo-Pereira J, 107, 1381
Carr DT, 947, 949
Carter G, 1723
Carter RD, 601
Carter SK, 645, 807, 1141
Casazza AM, 829
Cascinelli N, 33
Case DC, Jr, 1217
Catalano RB, 285, 1395
Cavalli F, 1377
Cavanna M, 255
Cedermark BJ, 235
Celle G, 255
Chabner BA, 615
Chadwick DP, 1663
Chadwick M, 845
Chan KK, 1611
Chang C, 845
Charest MC, 881
Chen FP, 1627
Christenson GM, 1171
Clarkson BD, 1217, 1819, 1937
Coccia PF, 1683
Cohen MH, 445, 1393
Cohen RJ, 1257
Coles DT, 947
Colman M, 221, 1225
Colombo T, 395
Colsky J, 925, 939
Coltman CA, Jr, 199, 1679
Colvin M, 403
Comis RL, 165
Coon FB, 999
Cooney DA, 1493
Cooper MR, 1687
Correa J, 1277
Costa FO, 107
Costanzi JJ, 189
Costello W, 193
Cox PJ, 299, 321, 483
Crafts DC, 243, 541
Creagan ET, 1385
Creaven PJ, 69, 445, 451
Creech RH, 285, 625, 925, 1395
Crissman HA, 1729, 1982
Cristofalo VJ, 1985
Cronkite EP, 1871
Crooke ST, 1633
Culliton P, 1285
Cummings FJ, 625
Cysyk RL, 555, 563

D

Dalcq JM, 85
Danova LA, 933
Dar'yalova SL, 1487
Davis L, 477
Davis RD, 1493, 1675
Day KJ, 1813
De Jager RL, 1373
De Lena M, 205
De Wasch G, 1273
Dedrick RL, 889
Deinard A, 903
Delaney WE, 1984
Derriks R, 85
de Ruiter J, 465
Desaive C, 1819
Desner MR, 571
Desser RK, 221, 1225
Devos JM, 91
Dewhurst BB, 477
DeMeester TR, 1225
DeVita VT, Jr, 153, 761
Di Marco A, 829
Didolkar MS, 235
Djachkovskaya RF, 1601, 1605
Djobadze M, 1986
Dodero M, 255
Doering M, 1959
Dombernowsky P, 239, 943, 1263, 1861
Donaldson MH, 265
Donelli MG, 395, 493
Dorfman RF, 781
Dorian R, 1986
Dorick DM, 547
Douglass HO, Jr, 769, 965, 1659
Douros JD, 1069
Draeger U, 309, 355, 423, 509
Drewinko B, 1295, 1619, 1637, 1707, 1981
Driscoll JS, 1493, 1671
Durant JR, 781
Durie BGM, 77

E

Eagan RT, 115, 633, 947, 949, 1385
Edelstein M, 1925
Edlis HE, 575
Edmonson JH, 625, 633, 925, 1385, 1681

Einhorn LH, 103
El Dareer SM, 1627
El-Aaser AA, 937
El-Merzabani MM, 937
Elashoff RM, 243
Elias EG, 235
Eliot HM, 615
Elkind MM, 1777
Emanuel NM, 1601, 1605
Engstrom PF, 285, 1395
Enot KJ, 243
Espinal R, 477
Ethier MF, 1559
Evans R, 1225
Ezdinli EZ, 739, 925

F

Falkson G, 220, 955, 1593, 1655
Falkson HC, 220
Farmer PB, 299, 483
Farnsworth NR, 1171
Farquhar D, 149
Fauvie KA, 1675
Fenselau C, 403
Filov VA, 933
Finley J, 1982
Fisher JI, 1251
Fisher RI, 153
Fleischman RW, 1559
Fletcher WS, 601, 813
Folk RM, 1585
Folkers K, 223
Fong HHS, 1171
Ford SS, 1986
Forrest APM, 1461
Fortner C, 41
Fortuny IE, 903
Fossieck BE, 1393
Foster AB, 483
Fraile R, 1277
Fraser TJ, 1813
Frei E, 1935
Frelick RW, 269
Fried J, 1819, 1937
Friedman OM, 337
Frigerio A, 493
Frytak S, 633, 947, 949, 1681

G

Galvão Teles A, 107
Gams RA, 781
Gang M, 1347
García-Cañero R, 1
Garibjanian BT, 1335, 1347
Garvey MB, 1400
Gaston MR, 823, 1335
Gause GF, 637
Gehan EA, 713, 733
Gennari L, 1231
Germano G, 281
Gershanovich ML, 933
Gerulath AH, 149
Gessner T, 1285
Giardino P, 829
Gilby ED, 483
Giles GR, 1267
Golbey RB, 1373
Gold J, 964
Goldfeder A, 1985
Goldin A, 99, 823, 1335, 1347
Golomb FM, 601
Golomb HM, 221, 1225
Gonzalez-Vitale JC, 917
Gorshein D, 963
Gosálvez M, 1
Gottlieb JA, 103, 177, 199, 215, 289
Goudsmit A, 575
Grabstald H, 917
Grage TB, 601, 813
Gray JW, 1981, 1984
Greco FA, 1239
Green C, 1619
Greenberg SD, 1691
Greenspan EM, 925
Griem M, 1225
Grove GL, 1985
Guaitani A, 395
Guarino AM, 1675
Gurtoo HL, 1285
Gurucharri-Lloyd C, 1
Gutterman JU, 177, 535

H

Haas CD, 611
Hahn GM, 1705, 1791
Hahn RG, 115, 633, 729, 1247, 1385, 1681
Hainau B, 239
Hall R, 1267
Hall SW, 289
Hamilton T, 1461
Hamlin R, 293
Hanjura GL, 277
Hanley J, 1659
Hansel J, 617
Hansen HH, 239, 943, 1263
Hansen R, 1647
Harada M, 361
Harari J, 1982
Hartmann NR, 1861
Hartwell JL, 1031
Hayes FA, 1841
Henderson JF, 1567
Henderson M, 1633
Herman EH, 1663
Hersh EM, 177, 535

Heuson JC, 1463
Hill DL, 1627
Hill GJ II, 183, 601
Hilton J, 725
Hirte WE, 251
Ho M, 1400
Hoge AF, 857
Hohorst H-J, 309, 355, 415, 423, 429, 509
Hollister M, 611
Holmquist JP, 1749
Holoye PY, 61, 1681
Hoogstraten B, 199, 215, 611
Horton J, 625, 925, 939
Hoshino T, 1984
Hoth D, 1437
Houchens DP, 823, 1335
Houghton PJ, 459
Housholder GE, 149
Hrushesky WJ, 639, 966
Hudspith BN, 409
Huff K, 1421
Hult RL, 867
Hutchison DJ, 23

I

Ihde DC, 1393
Israel L, 625, 925, 939, 1431
Iwata T, 361
Izbicki RM, 91, 1369, 1389

J

Jackson RC, 835
Jacobs EM, 953
Jacobs P, 967
Jardine I, 403
Jarman M, 299, 483
Jayaram HN, 1493
Jenkins DE, 1691
Jensen PA, 1251
Jett JH, 579, 1982
Johnson RK, 99, 823, 1335, 1347
Johnson RO, 183
Jones SE, 77
Jordan VC, 1409

K

Kaplan S, 1281
Kardinal CG, 953
Karon M, 9
Kas'yanenko IV, 1483
Kaufman JH, 277, 965
Kendall F, 1819
Kenis Y, 1273
Killmann S-A, 1839
Kiseleva VS, 1487
Kishi T, 223
Kisner DF, 1597
Klaassen DJ, 251
Klein HO, 1959
Klein PJ, 1959
Kline I, 1335, 1347
Knight EW, 939
Knospe WH, 1845
Kondratyev VB, 933
Konovalova NP, 1601, 1605
Korfhagen J, 1281
Kraevskii NA, 1469
Krakoff IH, 1373
Kreis W, 1399
Krementz ET, 183, 601
Kremer WB, 1845
Kress ED, 1985
Krivit W, 1683
Kroner T, 55
Kupchan SM, 1115

L

Lagakos SW, 625, 925, 939
Laiko AV, 637
Lala PK, 1781
Lamerton LF, 1741
Lane M, 907
Langlands AO, 1461
Lanzotti VJ, 61
Larsen V, 29, 943
Larson RE, 867
Laster WR, Jr, 1325
Laucius JF, 595
Laurent C, 85
Lavin PT, 769
Lee BJ III, 1217
Lee RE, 949
Lehane D, 1984
Leimbrock S, 9
Lejeune F, 1273
Lelieveld P, 373
Lenhard RE, Jr, 739
Lennartz KJ, 1959
Lerner HJ, 959, 1431
Leung BS, 1431
Levin VA, 243, 541, 719
Levitt M, 925
Lichtenfeld JL, 41, 571, 963
Lincoln T, 1723
Linden WA, 1983
Lippman M, 1421, 1437, 1451, 1593
Liss RH, 881
Livingston RB, 103, 535, 757, 1141
Lloyd RE, 77
Loo TL, 149, 1619
Lowitz BB, 623
Luckert PH, 619

Luthra YK, 1559
Lutz W, 1461

M

Macdonald JS, 1437, 1597
Maestracci D, 17
Magill GB, 1373
Maksimov IA, 1471
Malaise E, 1887
Malhotra A, 1267
Malyugina LL, 933
Mannes P, 85
Manni A, 1445
Mansour EG, 625, 925
Mardiney MR, Jr, 571
Marmorshtein SIa, 1471
Marshall JS, 1445
Martini A, 395, 493
Maruyama Y, 579, 1982
Masaba JP, 111
Mastrangelo MJ, 595, 1395
Matsumoto S, 361
Matthews MJ, 1393
Mauer AM, 1841
Mavligit GM, 177
McCracken RJ, 973
McFadyen IJ, 1461
McGuire W, 961
McKenna PJ, 1984
McMahon LJ, 77
Mead JAR, 881, 1127
Medenica R, 281
Meiselbaugh D, 219
Mellett LB, 225, 1627
Mendelsohn J, 1986
Metter GE, 183, 601, 813
Meyer RA, 1281
Michel J, 1273
Mikolajczak KL, 1157
Millar JL, 409
Milman HA, 1493
Minna JD, 1393
Minow RA, 215
Minton JP, 601
Mittelman A, 277
Moccio DM, 547
Modica R, 395
Moens R, 85
Moertel CG, 729, 769, 1247, 1659
Montgomery JA, 125, 381, 651
Moon TE, 199
Moore GE, 219
Moore MR, 895
Morabito A, 33
Morgan LR, Jr, 1437
Morgan SK, 591
Morrison P, 1723
Muggia FM, 925
Murphy GP, 277
Murphy SB, 1841
Murphy WK, 289
Muss HB, 1687
Myers CE, 615, 961, 1451
Myers RP, 115
Myles A, 337

N

Nachum R, 9
Nealon TF, 269
Nelson RL, 445, 451
Nesbit ME, 1683
Nichols M, 293
Nicolini C, 1819
Nielsen S, 541
Niemetz J, 575
Nisce L, 1217
Nissen NI, 943
Nivinskaya MM, 1487
Noel J, 1982
Nomura K, 1984
Norpoth K, 437

O

O'Bryan RM, 199, 215
O'Connell MJ, 41, 633, 1681
Oka MS, 1729
Oliveira Costa F, 1381
Oliverio VT, 703
Olweny CLM, 111
Omura GA, 629, 1845
Otter GM, 23
Ovejera AA, 99, 823

P

Pacciarini MA, 395
Pajak TF, 953, 1251
Panasci L, 801
Panettiere FJ, 907
Pannacciulli I, 255
Pantarotto C, 493
Patelli B, 829
Patterson FK, 273
Pavkov KL, 1585
Pearson OH, 1445
Pedersen H, 29
Penn RN, 477
Perdue RE, Jr, 979, 987, 1081
Perevodchikova NI, 1479
Perlia CP, 625, 925, 939
Perlin E, 1593
Perry MC, 1247

Perry S, 1699
Peter G, 309, 355, 429, 509
Peterson SYe, 1473
Petrova AS, 1467
Phelan RS, 1559
Phillips BJ, 321
Picciotto A, 255
Pilch Y, 295
Pimentel P, 107, 1381
Pinedo HM, 889
Pirogov AI, 1471, 1489
Pischer TL, 243
Pittillo RF, 225
Piver MS, 527
Pollard M, 619
Posey LE, 1437
Potmesil M, 1985
Potnis AV, 1402
Poulakos L, 1913
Powell RG, 1157
Pratesi G, 829
Przybylski M, 509
Pullen J, 591

Q

Quagliana JM, 199

R

Rabinovitz M, 1363
Raju MR, 579, 1982
Ramirez G, 813
Ramos A, 1281
Ramsay NKC, 1683
Ransohoff J, 717
Rao SP, 1402
Rapp EF, 251
Ratanatharathorn V, 1369
Reed R, 177
Regelson W, 625, 939, 959
Reggiani P, 829
Reitemeier RJ, 729, 1247
Reynolds RD, 1251
Rice LS, 225
Richards F II, 1687
Richman SP, 535
Rilke F, 1231
Ringsdorf H, 509
Ritter CA, 617
Rivkin SE, 199
Roberts J, 261
Roberts MM, 1461
Rodbard D, 1239
Rodriguez V, 199
Roper P, 1984
Rosenberg SA, 159
Rosenbloom B, 295
Rosenstock JG, 265
Rossof AH, 1679
Rubenstein L, 1225
Rubin J, 947, 949
Ruderman AI, 1475, 1487
Rutman RJ, 471, 617
Ryssel HJ, 1377

S

Saiki JH, 199
Sakurai Y, 937
Saleh AA, 1171
Salmon SE, 77, 789
Samson MK, 91, 1277, 1369, 1389, 1633
Samuels ML, 61
Sanford AH, 1749
Saufferer SM, 1171
Saunders PH, 149
Schabel FM, Jr, 665, 1325
Schaeppi U, 1559
Schein PS, 801, 1437, 1597
Schenken LL, 1761
Schepartz SA, 123, 647, 975
Schiffer CA, 41
Schiffer LM, 1913
Schimpff SC, 41
Schmid FA, 23, 261
Schulten H-R, 501
Schultz MJ, 243
Schutt AJ, 729, 1247
Seager M, 243
Seitz JF, 933
Selawry OS, 925
Selesneva TI, 637
Shackney SE, 1697, 1873, 1986
Shaddix SC, 1317, 1325
Shapiro C, 1225
Shapiro WR, 875
Shaw MT, 857
Shimi IR, 937
Shiratori O, 361
Shnider BI, 625
Sieber SM, 217, 1127
Siegel SE, 9
Sikyewunda W, 111
Simon RM, 1451
Simpson-Herren L, 1749
Sinkovics JG, 199
Sirotnak FM, 547
Slavik M, 213, 795
Smink T, 465
Smith CM, 1567
Smith CR, Jr, 1157
Smith HW, 517
Smith L, Jr, 1597
Smith TL, 61
Smythe T, 1597
Sobrinho TC, 1402
Sohner S, 895

Solomon A, 273
Sonntag RW, 1377
Sonoda T, 273
Sørensen PG, 239
Sörenson S, 1263
Spanjersberg EJ, 369
Sparks FC, 601
Spector R, 913
Spinelli P, 1231
Spjut RW, 979
Spurr CL, 1687
Stanley J, 1743
Starichkov MS, 1487
Starinskii VV, 1471
Statz D, 999
Steel GG, 1743
Steinkamp JA, 1982
Stephens RL, 611
Steuber CP, 591
Stewart HJ, 1461
Stock CC, 23
Stolbach L, 625, 925, 939
Struck RF, 317, 381, 1317
Stukov AN, 933
Suen JY, 535
Sullivan P, 199
Sutow WW, 591
Syrkin AB, 1335
Szekerke M, 347

T

Takai K, 261
Takamizawa A, 361
Talley RW, 907
Tan CTC, 1937
Tancini G, 205, 1231
Taylor DM, 459
Taylor H, 1011
Tew KD, 459
Thake DC, 1585
Theologides A, 903
Thigpen T, 199
Thomas DR, 61, 591
Thomas P, 321
Toal JN, 1363
Tobey RA, 1829
Tochino Y, 361
Tormey DC, 1451, 1593
Tornyos K, 1845
Torres J, 907
Toth IR, 1984
Toya T, 111
Trader MW, 1325
Trakhtenberg AKh, 1489
Trown PW, 1647
Trujillo J, 1445
Tubiana M, 1887
Twentyman PR, 259, 1719

U

Upshall DG, 477

V

Vadlamudi S, 1347
Vaitkevicius VK, 91, 733, 1277
Valeriote F, 1925
Valleron A-j, 1899
Vats T, 591
Velez-Garcia E, 781
Venditti JM, 135, 215, 1347
Veronesi U, 33, 205
Vietti T, 1925
Vistica DT, 1363
Voelcker G, 309, 415, 509
Vogel CL, 895
Vogler WR, 1845
Vyas AC, 293

W

Wagner T, 415, 429
Walker MD, 713, 725, 1257
Wall ME, 1011
Wampler G, 925
Wanek PL, 1982
Wani MC, 1011
Ward JM, 1675
Wasserman TH, 709, 807
Watson E, 1611
Watson RC, 917
Weber G, 835
Weiss AJ, 813, 1667
Wheeler GP, 1307
Wheeler KT, 1984
Wheeler WL, 289
White DR, 1687
White V, 1627
Whitmore WF, 917
Wiernik PH, 41, 571, 963, 1257
Williams JC, 835
Williams M, 1317
Wilson CB, 243, 719
Wilson WL, 183, 269, 813
Wiltshaw E, 55
Winton EF, 895
Wodinsky I, 337
Wolf J, 753
Wolpert MK, 1675
Wong KY, 1281
Woolley C, 225
Woolley PV, 801, 1437, 1597
Wu EC, 1984
Wyatt PJ, 225

Y

Yagoda A, 917
Yamaguchi K, 361
Young CW, 1217
Young DM, 1675
Young RC, 761, 961, 1947

Z

Zaharko DS, 889
Zombor G, 1567
Zucker RM, 1982

Reviewers

We wish to thank the following Reviewers who participated in evaluating the manuscripts submitted to *Cancer Treatment Reports* during the past year:

Martin D. Abeloff
David Abraham
Richard H. Adamson
Khalil Ahmed
Joseph Aisner
Tom Anderson
Fred J. Ansfield
Frederick R. Appelbaum
James I. Ausman
Nicholas R. Bachur
Richard F. Bakemeier
Pierre R. Band
William G. Banfield
Joseph J. Barlow
Sam C. Barranco
Sam P. Battista
William H. Beierwaltes
J. George Bekesi
Robert E. Bellet
Richard A. Bender
Robert S. Benjamin
John M. Bennett
Daniel E. Bergsagel
Joseph R. Bertino
Bijoy K. Bhuyan
Werner A. Bleyer
Jerome B. Block
Johannes Blom
H. J. G. Bloom
Ronald H. Blum
Avrum Bluming
Gerald P. Bodey, Jr.
Arthur E. Bogden
Werner Bollag
Gianni Bonadonna
Vincent H. Bono
Robert S. Bourke
Robert L. Bowman
Laurence A. Boxer
Matthews O. Bradley
Karen Brandt
Harmar D. Brereton
Michael J. Brescia
Robert W. Brockman
W. R. Bruce
Howard W. Bruckner
Steven Brynes
Donald R. Buhler
Joan M. Bull
Paul A. Bunn, Jr.
Philip J. Burke
Haydn Bush
Keith H. Byington
Daniel Byrd
Ritchard G. Cable
Blake Cady
Edward J. Cafruny
George P. Canellos
Robert Capizzi
Paul P. Carbone
Stephen K. Carter
Walter H. Carter, Jr.
Marjory Chadwick
Paul Chang
Ting-Chao Chou
Colin F. Chignell
Dennis L. Citrin
Bayard Clarkson
Arthur M. Cohen
Martin H. Cohen
Philip Cohen
Ronald J. Cohen
Seymour S. Cohen
Charles E. Coltman, Jr.
T. A. Connors
Edmund S. Copeland
D. H. Cowan
G. W. Crabtree
James C. Cradock
William A. Creasey
Patrick J. Creaven
Esteban Cvitkovic
Richard L. Cysyk
David S. Dale
Giulio J. D'Angio
J. Paul Davignon
Hugh L. Davis, Jr.
Paul J. Davis
Thomas E. Davis
Ronald C. DeConti
Robert L. Dedrick
E. Paul Denine
Eugene R. DeSombre
Vincent T. DeVita
Charles Diggs
Aurelio Di Marco
Henry W. Dion
Robert L. Dixon
Sarah Donaldson
John D. Douros
Benjamin Drewinko
John S. Driscoll
Robert T. Eagan
Sandor Eckhardt
Mark B. Edelstein
Frederick R. Eilber
Lawrence H. Einhorn
Ronald J. Elin
Gertrude B. Elion
Rose Ruth Ellison
Robert J. Esterhay
Geoffrey Falkson
Alvan R. Feinstein
Joseph D. Fenstermacher
Isaiah J. Fidler
Jerry Z. Finklestein
Bernard Fisher
Richard I. Fisher
Roger M. Folk
Thomas P. Fondy
George F. Fritch
Ruth A. Fugmann
David Fukushima
Glen R. Gale
Robert E. Gallagher
Timothy S. Gee
Beppino C. Giovanella
Robert I. Glazer
John H. Glick
Joseph Gold
Abraham Goldin
Harvey Golomb
Paul E. Gormley
Mario Gosalvez
Harvey R. Gralnick
Theodore E. Gram
F. Anthony Greco
Linda D. Green
William H. Greene
Ezra M. Greenspan
Gerald B. Grindey
Daniel P. Griswold, Jr.
Pietro M. Gullino
Jordan U. Gutterman
Zareh Hadidian
Davis Hahn
Fred E. Hahn
Peter Hahn
Richard G. Hahn
Harry Handelsman
L. J. Hanka
Corwin Hansch
Harold Harder
Chava T. Hardesty
Jules E. Harris
Jacqueline S. Hart
Charles M. Haskell
Charles Heidelberger
Samuel Hellman
Edward S. Henderson
I. Craig Henderson
J. Frank Henderson
Fred J. Hendler
Jane E. Henney
David W. Henry
Eugene H. Herman
Evan M. Hersh
J. C. Heuson
Donald J. Higby
George A. Higgins
Russell Hilf
Dah Hsi Wang Ho
Thomas E. Hobbins
Louis Hodes

H. J. Hohorst
James F. Holland
Antoinette F. Hood
Barth Hoogstraten
H. F. Hope-Stone
David P. Houchens
Susan P. Hubbard
David H. Huffman
Ronald M. Humphrey
Dorris J. Hutchison
Daniel C. Ihde
James N. Ingle
Lowell E. Irwin
William H. Isacoff
Zafar H. Israili
Samuel A. Jacobs
Norman Jaffe
Hiremagalur N. Jayaram
P. H. Jellinck
Ralph E. Johnson
Randall K. Johnson
Stephen E. Jones
Thomas K. Jones, Jr.
C. Ronald Kahn
Karl Karrer
Richard J. Kaufman
Robert J. Keehn
Cecil Kelly
Diane E. Kelson
B. J. Kennedy
David Kessel
Jean Klastersky
Michael D. Klein
Ira Kline
Geraldine S. Konior
John S. Kovach
Irwin H. Krakoff
Willi Kreis
A. Krishan
William Krivit
M. Eugene Lahey
W. R. Laster, Jr.
John Laszlo
Dennis B. Leeper
Sewa Legha
Luigi Lenaz
Raymond E. Lenhard, Jr.
Gerald A. LePage
Howard E. Lessner
Brigid G. Leventhal
John Levi
Bernard Levin
Victor A. Levin
Arthur S. Levine
Brian J. Lewis
J. Leonard Lichtenfeld
Peter Lim
Charles L. Litterst
Robert B. Livingston
Harris H. Lloyd
Jacob J. Lokich
John P. Long
Ti Li Loo
James K. Luce
David B. Ludlum
Ian T. Magrath
H. George Mandel
David A. Margileth
Barry J. Maron
Alvin M. Mauer
Harold M. Maurer
Kenneth B. McCredie
J. Patrick McGovren
William L. McGuire
Philip C. Merker
Claude E. Merrin
Enrico Mihich
Irvin Miller
Rodney R. Million
John Minna
Malcolm S. Mitchell
Arnold Mittelman
Edward J. Modest
Charles G. Moertel
Leon A. Moore
Roy Morris
Franco M. Muggia
Sharon Murphy
Charles E. Myers
Larry Nathanson
Gary L. Neil
Mark E. Nesbit
P. Nettisheim
Manuel Ochoa, Jr.
Michael J. O'Connell
Takao Ohnuma
Vincent T. Oliverio
Stanley E. Order
C. Kent Osborne
Martin W. Oster
Artemio A. Ovejera
Lawrence C. Panasci
Leroy M. Parker
Robert E. Parks, Jr.
John W. Pearson
Olaf H. Pearson
Carlos A. Perez
Theodore P. Pincus
Herbert Pinedo
Barry J. R. Pitts
Philip A. Pizzo
Carl W. Porter
Carol D. Portlock
Charles B. Pratt
David J. Prieur
George R. Prout, Jr.
Lawrence Prutkin
Marco Rabinovitz
Kanti R. Rai
Nathan Rakieten
Donald J. Reed
Richard C. Reed
Steven D. Reich
John J. Rinehart
DeWayne Roberts
M. Maureen Roberts
Victorio Rodriguez
W. R. Rose
Gerald Rosen
Barnett Rosenberg
Saul A. Rosenberg
Steven A. Rosenberg
Robert H. Roth
Sheldon P. Rothenberg
Marcel Rozencweig
John C. Ruckdeschel
Philip A. Salem
Sydney E. Salmon
Melvin L. Samuels
Alan C. Sartorelli
Frank M. Schabel, Jr.
Philip S. Schein
Leonard Scherlis
Charles A. Schiffer
Lewis M. Schiffer
Lowell Schnipper
Robert J. Schnitzer
Alberta M. Schumacher
Allan J. Schutt
Allen D. Schwartz
Arnold Schwartz
Joel Schwartz
Albert Segaloff
Oleg S. Selawry
Lyle L. Sensenbrenner
Arthur A. Serpick
Stanley E. Shackney
William R. Shapiro
Michael T. Shaw
Branimir I. Sikic
Richard T. Silver
Richard M. Simon
Joseph V. Simone
Linda Simpson-Herren
Lucius F. Sinks
Roland T. Skeel
Norman E. Sladek
Julian Smith
A. Collier Smyth
Robert J. Speer
Michael B. Sporn
Federico Spreafico
H. Stahelin
Peter Steinherz
Robert L. Stolfi
David G. Stolinsky
Ronald G. Stoller
Thomas A. Strike
Robert F. Struck
Pierre Stryckmans
Herman D. Suit
John Sutherland
W. W. Sutow
D. Sweet
Robert W. Talley
Charlotte Tan
Martin H. N. Tattersall
D. Jane Taylor
Robert A. Tobey
Douglass C. Tormey
John E. Ultmann
Richard S. Ungerleider
V. K. Vaitkevicius
Frederick Valeriote
David Van Echo
L. M. van Putten
Eugene J. Van Scott
David T. Vistica
Charles L. Vogel
W. R. Vogler
Daniel D. Von Hoff
Peter E. Voytek
Michael D. Walker
Jerrold Ward

Todd H. Wasserman
Lawrence Weed
Eugene C. Weinbach
Howard D. Weiss
Glynn P. Wheeler
Peter H. Wiernik
Jordan Wilbur
Lee J. Wilkoff

Charles B. Wilson
E. Wiltshaw
Isidore Wodinsky
Mary K. Wolpert
Sheldon M. Wolff
Norma Wollner
Paul Woolley
Alan Yagoda

Jerome W. Yates
David W. Yesair
David M. Young
Lowell Young
Robert C. Young
Daniel S. Zaharko
Gerhard Zbinden
Marvin Zelen

☆U.S. GOVERNMENT PRINTING OFFICE: 1977 241-171/5 1-3

If your address has changed and you wish to continue receiving this publication, please send your new address and the mailing label from this copy to:

Cancer Treatment Reports
National Cancer Institute
8300 Colesville Rd
Blair Bldg, Rm 3A05
Silver Spring MD 20910

If you do not wish to continue receiving this publication, please notify us at the address noted above and enclose the mailing label from this copy.

A publication of the National Cancer Institute

DHEW Publication (NIH) 76-22